Defatting of donor transplant livers during normothermic perfusion and modulating extended-criteria donor graft tolerance to ischaemia-reperfusion injury

Syed Hussain Abbas

Green Templeton College

University of Oxford

A thesis submitted for the degree of

Doctor of Philosophy

Hilary 2025

Abstract

The limited availability of suitable donor livers remains a critical challenge in liver transplantation, necessitating the use of extended criteria donor (ECD) livers, including those from donation after circulatory death (DCD) donors and those exhibiting moderate-to-severe hepatic steatosis (HS). These livers, however, are more susceptible to ischemia-reperfusion injury (IRI), particularly when preserved using static cold storage (SCS). This thesis investigates the clinical application of normothermic machine perfusion (NMP) as a dynamic preservation strategy to mitigate the risk profile of steatotic and DCD livers and improve transplantation outcomes. Through a large-scale analysis of donor livers from the Quality in Organ Donation (QUOD) bioresource, I have characterised pre-retrieval predictors of donor HS severity and explored the use of digital image analysis (DIA) as a rapid and reproducible tool for quantifying HS, addressing limitations in macroscopic and histopathological assessments. The clinical application of these measures could facilitate early identification of steatotic livers and guide preservation strategies to improve utilisation. I further explored clinical outcomes of steatotic livers preserved using NMP compared to SCS through use of samples from a previous phase III multicentre randomised clinical trial. I demonstrated that NMP reduced IRI related complications in steatotic livers and demonstrated graft survival rates comparable to lean livers preserved with SCS. Despite these advances, metabolic challenges persisted (as assessed through biochemical perfusate measurements), highlighting the need for additional interventions beyond replacing SCS with NMP. Through proteomic analysis of this cohort, I demonstrated that while NMP enhanced mitochondrial function and lipid metabolism, it did not fully restore metabolic efficiency in steatotic livers. The potential to improve fat metabolism is therefore described in the context of an ongoing clinical trial 'The DeFat Study' which involves defatting of donor transplant livers during NMP. If the intervention proves effective, it could certainly expand the donor pool through utilisation of steatotic donor livers. To further optimise defatting protocols, I performed a series of pre-clinical perfusions in discarded human livers and explored the role of pharmacological modulation of hypoxia-inducible factors (HIFs) during NMP. This approach facilitated a reduction in HS and improved graft function, thereby offering an opportunity to further refine current defatting protocols. Finally, I investigated the removal of damage-associated molecular patterns (DAMPs) in an ex-situ porcine DCD model of liver transplant. Through use of a specialised column, I demonstrated effective removal of DAMPs, correlating with improved graft function and reduced microclot burden during whole blood allogenic reperfusion.

Dedication

In loving memory of my grandparents

Syed Abbas Shah
Saiyid Muhammad Rizvi
Ruqaiyya Abbas

My dear cousin who left this world too early

Dr Syed Arshad Abbas

To my parents, Professor Syed Akhtar (Papa) and Mrs Rana Rizvi (Umi), and to my older brother, Syed Faiz Abbas:

Papa and Umi, you have been my greatest sources of inspiration, thank you for your unconditional love, support and belief in me. From your tireless efforts to provide me with the best opportunities to your constant encouragement during life's toughest moments, I owe so much of who I am to you. The values of perseverance, compassion, and a commitment to excellence that you have instilled in me will guide me for the rest of my life. Faiz, my dear brother, you have been a pillar of strength and wisdom. Your faith in me has given me the courage to keep going, even when the road felt impossible to navigate.

To my loving wife, Dr Samira Farzadi:

Your unwavering love, encouragement and belief in me have been the foundation of this journey. Through the countless late nights, the challenges, and the long stretches of time spent away from home whilst running a clinical trial, you have been my source of strength. Your patience, understanding and quiet sacrifices have made this work possible. This thesis is as much a testament to your support as it is to my efforts. I could not have achieved this without you by my side. Thank you for walking this path with me, for standing steadfastly through the highs and lows and for being my greatest confidant.

Acknowledgments

I would like to thank my supervisors Professor Peter Friend, Professor Leanne Hodson and Professor Simon Knight.

Professor Friend, thank you for believing in me and for encouraging me to pursue an academic career in surgery. Your mentorship has been invaluable, providing steadfast support throughout the journey of completing this thesis, regardless of the challenges or circumstances. You have been a constant source of inspiration, a role model whose dedication to advancing the field of transplantation is truly remarkable. I am deeply grateful for your accessibility and willingness to provide guidance at any hour, even while managing the complexities of a clinical trial and perfusion experiments. Your commitment to excellence and generosity with your time have left a profound impact on me, for which I am sincerely thankful.

Professor Hodson, thank you for your patience and unwavering guidance as I navigated the complexities of laboratory experiments. I am deeply indebted to your wisdom and expertise, which have been instrumental in planning and executing my experimental work. Your mentorship has not only helped me overcome challenges but also enabled me to grow both as a clinician and a scientist. Your encouragement and insight have been invaluable throughout this journey, and I am grateful for the lasting impact you have had on my development.

Professor Knight, thank you for your rational guidance, steadfast support, and encouragement, which have been invaluable in maintaining momentum with the DeFat clinical trial. Your mentorship has been pivotal in many aspects of my development throughout the course of this thesis. In particular, your expertise and insight have been instrumental in helping me navigate the complexities of novel clinical trials in the field of transplantation. I am grateful for the significant role you have played in shaping both my professional growth and the progress of this work.

My gratitude is also extended to Mr Carlo Ceresa, Mr David Nasralla, Dr Sadr Shaheed and Professor Christopher Pugh who have supported and facilitated the research presented within this thesis.

Mr Carlo Ceresa and Mr David Nasralla, I am grateful to both of you for your unwavering encouragement and support in my pursuit of an academic career. Your early engagement with me was pivotal, and your guidance in planning perfusion studies provided a strong foundation for much of the work within this thesis. Your advice on securing research grants and your invaluable input in shaping the DeFat study have been instrumental in navigating the challenges of this journey. Beyond your professional support, I deeply appreciate the camaraderie, friendship and encouragement you have offered throughout this process.

Dr Sadr Shaheed, thank you for your friendship and invaluable guidance and support during the early phases of this thesis. I am deeply indebted to you for the countless hours you dedicated to training me in basic science research, laboratory techniques and the analysis of complex data. Your mentorship has been crucial to the success of these studies, and without your support, this work would not have been possible. The depth and richness of the mechanistic insights presented within this thesis are a testament to the high level of training you have provided me. I am sincerely grateful for your contributions and encouragement throughout this journey.

Professor Christopher Pugh, thank you for your support and engagement early in my journey. Your expert knowledge, particularly in the field of hypoxia biology has been invaluable. Your willingness to foster the cross-pollination of ideas and explore innovative solutions to address clinical challenges has significantly shaped the work presented within this thesis.

I would like to thank Mr Fungai Dengu, Mr Kumaran Shanmugrajah, Mr Hatem Sadik, Mr Faysal Elgilani, Miss Ann Ogbemudia, Dr Georg Ebeling and Mr Daniel Voyce for your friendship, support and encouragement along the way.

I am fortunate to have had the support of many colleagues and friends without whom the research presented within this thesis would not have been possible. Notably, I would like to extend my sincere gratitude to Dr Maria Letizia Lo Faro, Professor Rutger Ploeg, Dr Andrew Aswani and Dr Quin Wills.

From the Nuffield Department of Surgical Sciences, I would like to thank Mr Alexander Sagar, Mr Richard Dumbill, Dr Kazuyuki Gyoten, Mr John Fallon, Mr Mohamed Elzawahry, Mr John Gilbert, Mrs Katherine Gordon Quayle and Miss Aimee Stewart. From the Oxford Centre for

Diabetes, Endocrinology and Metabolism, I would like to thank Dr Elspeth Johnson. From the Oxford Transplant Centre, I would like to thank Mr Srikanth Reddy, Mr Venkatesha Udupa, Miss Isabel Quiroga, Mr Sanjay Sinha and Mr John Milton. From Ludwig Institute for Cancer Research and Target Discovery Institute, I would like to thank Dr Véronique Lafleur. At the Oxford Big Data Institute, I would like to thank Dr Nasullah Alham. From the Institute of Biomedical Engineering, I would like to thank Professor Constantine Coussios. From the Department of Clinical Biochemistry (Oxford), I would like to thank Dr Alireza Morovat and at the Department of Cellular Pathology (Oxford), I would like to thank Mrs Helen Euston-Meller. From the Department of Histopathology (Royal Free Hospital, London), I would like to thank Professor Alberto Quaglia. From the Department of Hepato-Pancreatico-Biliary Surgery (Oxford), I would like to thank Mr Michael Silva, Mr Zahir Soonawalla and Mr Alex Gordon-Weeks who have always supported me and facilitated my clinical and academic development.

I would like to thank the entire team at OrganOx Ltd. Particularly Mr Chris Morris and Mr Dan Fower who have provided technical guidance and supported perfusion innovation. At the University of Liverpool, I would like to thank Dr Jeremy Schofield, Dr Simon Abrams and Professor Cheng-Hock Toh.

I am grateful to the Transplant teams at the Royal Free, Addenbrooke's, King's College and Queen Elizabeth Hospital for their support and facilitating clinical trial research. In particular, I would like to thank Professor Joerg Pollok, Professor Christopher Watson, Mr Rohit Gaurav, Mr Satheesh Iype, Mr Wayel Jassem, Mr Aamir Nawaz, Mr Abdul-Hakeem, Professor Thamara Perera and the local perfusionist and transplant co-ordinators at each site.

Finally, I would like to extend my sincere gratitude to the NHSBT Clinical Trials Unit (NHSBT CTU), Quality in Organ Donation (QUOD) and the Consortium of Organ Preservation in Europe, donor and their families for making this research possible.

The research detailed in thesis has been funded by the National Institute for Health and Care Research (NIHR), Oxford Transplant Foundation (OTF), Royal College of Surgeons of Edinburgh and Oxfordshire Health Services Research Committee (OHSRC) alongside collaborators at OrganOx Ltd. (Oxford, UK), OchreBio Ltd. (Oxford, UK) and Santersus AG (Zurich, Switzerland).

Declaration

The research presented within this thesis is my own unless included for illustrative purposes or clearly stated otherwise. All porcine liver perfusions were performed by myself with assistance of other research fellows (in particular, Mr Fungai Dengu). Specialised assays and analyses that could not be conducted locally in Oxford were made possible through the invaluable support of collaborators at the Toh Lab, University of Liverpool.

Table of Contents

List of Figures

List of Tables

List of Abbreviations

ACAD11	Acyl-CoA dehydrogenase family member 11
ACLY	ATP-citrate synthase
ACOX1	Peroxisomal acyl-CoA oxidase 1
ACSL5	Long-chain-fatty-acid-CoA ligase 5
AI	Artificial Intelligence
AKI	Acute Kidney Injury
ALD	Alcohol-Associated Liver Disease
ALP	Alkaline Phosphatase
ALT	Alanine Aminotransferase
APEX1	DNA-(apurinic or apyrimidinic site) lyase, mitochondrial
APOB	Apolipoprotein B-100
APOC4	Apolipoprotein C-IV
AST	Aspartate Aminotransferase
ATP	Adenosine Triphosphate
ATP2A2	Sarcoplasmic/endoplasmic reticulum calcium ATPase 2
BMI	Body Mass Index
CBD	Common Bile Duct
CIT	Cold Ischaemia Time
CMV	Cytomegalovirus
CRP	C-Reactive Protein
CYP2E1	Cytochrome P450 2E1
DAAs	Direct-Acting Antivirals
DAMPs	Damage-Associated Molecular Patterns

DBD	Donation after Brain Death
DCD	Donation after Circulatory Death
DEPs	Differentially Expressed Proteins
DIA	Digital Image Analysis
EAD	Early Allograft Dysfunction
ECD	Extended Criteria Donor
ECMO	Extracorporeal Membrane Oxygenation
ELISA	Enzyme-Linked Immunosorbent Assay
FFPE	Formalin-Fixed Paraffin-Embedded
FGF-21	Fibroblast Growth Factor 21
FI	Fluorescence Intensity
FLI	Fatty Liver Index
FWIT	Functional Warm Ischaemia Time
GGT	Gamma-Glutamyl Transferase
GO	Gene Ontology
GUI	Graphical User Interface
H&E	Haematoxylin and Eosin
HAT	Hepatic Artery Thrombosis
HCC	Hepatocellular Carcinoma
HIF	Hypoxia-Inducible Factor
HLA-C	HLA class I histocompatibility antigen, C alpha chain
HMGB1	High-Mobility Group Box 1
HMOX1	Heme oxygenase 1
HS	Hepatic Steatosis

HSI	Hepatic Steatosis Index
Hb	Haemoglobin
Hct	Haematocrit
IC	Ischaemic Cholangiopathy
ICAM1	Intercellular Adhesion Molecule 1
ICG	Indocyanine Green
ICU	Intensive Care Unit
IHTG	Intrahepatic Triglyceride Content
IRI	Ischaemia-Reperfusion Injury
ITU	Intensive Therapy Unit
IVC	Inferior Vena Cava
L-GrAFT	Liver Graft Assessment Following Transplantation
Ld-MaS	Large Droplet Macrovesicular Steatosis
LT	Liver Transplantation
LiMAx	Maximum Liver Capacity
MASH	Metabolic Dysfunction-Associated Steatohepatitis
MASLD	Metabolic Dysfunction-Associated Steatotic Liver Disease
MEAF	Model of Early Allograft Function
MEGX	Monoethylglycinexylidide
MELD	Model for End-Stage Liver Disease
MRI	Magnetic Resonance Imaging
MaS	Macrovesicular Steatosis
MiS	Microvesicular Steatosis
NAS	Non-Anastomotic Biliary Strictures

NETs	Neutrophil Extracellular Traps
NMP	Normothermic Machine Perfusion
OPS	Organ Preservation Solutions
PAS	Periodic Acid-Schiff
PNF	Primary Non-Function
PRS	Post-Reperfusion Syndrome
QUOD	Quality in Organ Donation
ROI	Region of Interest
ROS	Reactive Oxygen Species
RRT	Renal Replacement Therapy
SCS	Static Cold Storage
SDHAF2	Succinate dehydrogenase assembly factor 2
SQSTM1	Sequestosome-1
TCA	Tricarboxylic Acid
TNF-α	Tumour Necrosis Factor Alpha
TPN	Total Parenteral Nutrition
UKELD	United Kingdom Model for End-Stage Liver Disease
UPR	Unfolded Protein Response
UW	University of Wisconsin Solution
VLDL	Very Low-Density Lipoproteins
WC	Waist Circumference
cNMP	Continuous Normothermic Machine Perfusion
pCO2	Partial Pressure of Carbon Dioxide
pO2	Partial Pressure of Oxygen

pRBCs	Packed Red Blood Cells
pSCS-NMP	Post-Static Cold Storage Normothermic Machine Perfusion
sd-MaS	Small Droplet Macrovesicular Steatosis

Chapter 1: Introduction

1.1 Liver transplantation

The clinical status of liver transplantation (LT) has transformed over the past five decades from a high-risk surgical procedure with debatable benefit to that of a standardised and definitive procedure for end-stage liver disease. Key factors contributing to this transformation include advances in organ preservation solutions (OPS), preservation technology, surgical approach, immunosuppression pharmacology and peri-operative care (1). This success has led to an expansion in LT indications, resulting in a significant shortage of donor organs and increased deaths on the waiting list in many countries of up to 20% (1,2). This has necessitated the use of extended criteria donor (ECD) livers including those procured from donation after circulatory death (DCD) donors, donors >65 years old and with liver grafts with evidence of moderate-severe hepatic steatosis (HS) (3). Traditionally, liver preservation has depended on static cold storage (SCS), the primary functions of which are to reduce cellular swelling and metabolic activity during storage and transport. However, the ever-present need to increase utilisation of ECD livers (in particular those with evidence of HS and DCD status) has prompted liver transplant teams to consider alternative dynamic (non-static) preservation methods to minimise the storage related cold-ischaemic injury and ischaemia-reperfusion injury (IRI) to which these livers are susceptible, in order to improve post-transplantation outcomes (1). These factors will be discussed within this chapter: the following sections (1.4.3, 1.5.2-4 and 1.6) have been replicated (verbatim) from a review article that I have published as first author, titled: Steatotic donor transplant livers: preservation strategies to mitigate against ischaemia-reperfusion injury (4).

1.2 Indications for liver transplantation

Liver transplantation is recommended for all patients with end-stage liver disease when it can extend life beyond the expected survival of the underlying condition (typically ≤ 1 year), or when liver disease significantly impairs quality of life. Indications for liver transplant include end-stage chronic liver disease, hepatocellular carcinoma (HCC) and acute liver failure (5). In adults, cirrhosis is the most commonest cause for end-stage liver disease and a common indication for LT, particularly when complications including variceal bleeding, ascites, hepatorenal syndrome or encephalopathy are present (5). Acute liver failure, often triggered by

viral infections (notably hepatitis A and B) or drug toxicity (such as from paracetamol), urgently necessitates transplantation (6). The indications for liver transplantation in Europe are detailed in Figure 1.1.

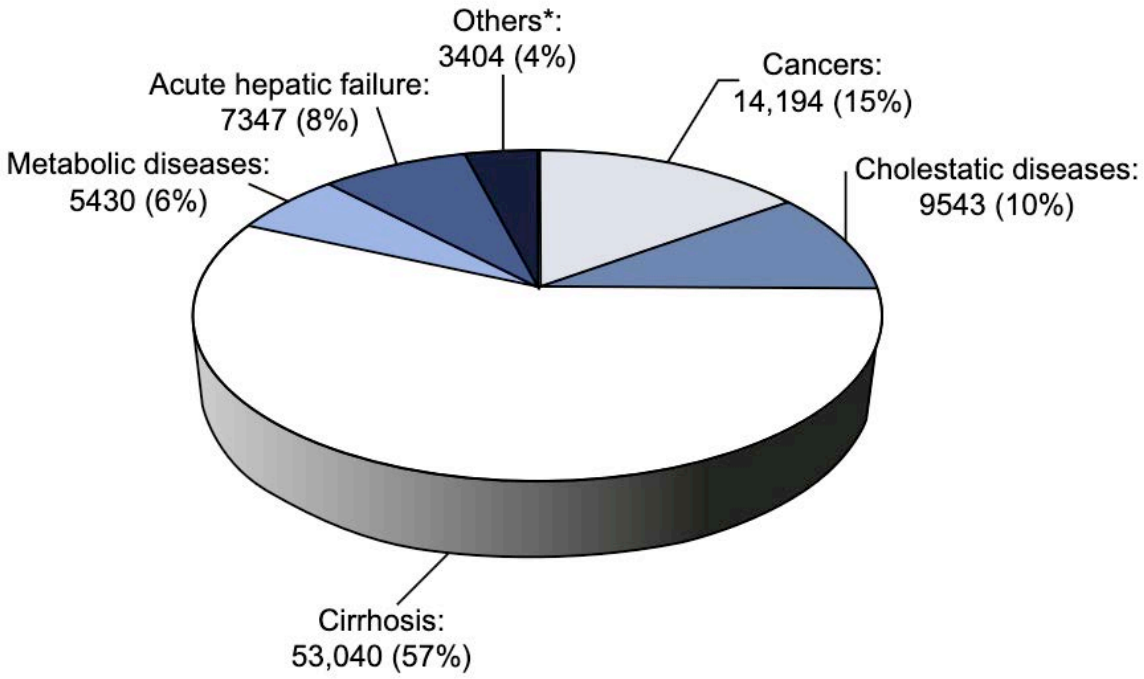

Figure 1.1. Primary indications for LT in Europe as reported by the European Association for Liver Disease in 2016. * Other liver diseases: *n* = 1304, benign liver tumours or polycystic diseases: *n* = 1228, Budd-Chiari: *n* = 792 and parasitic diseases: *n* = 80. Figure reproduced with permission from Elsevier (5).

Overall, the aetiologies of cirrhosis resulting in LT differ by geographical location and are changing over time. Despite advancements in treating hepatitis B and C, viral hepatitis continues to be the main cause of cirrhosis and liver cancer in Africa, Southeast Asia and East Mediterranean countries (7). Since 2014, when direct-acting antivirals (DAAs) became available, there has been a significant reduction in the number of liver transplants (LT) for hepatitis C virus (HCV) in the United States and Europe (8). Alcohol-related liver disease (ALD) remains the most common indication for LT in Europe and has also become the leading indication in the United States.

Hepatic steatosis is characterised by the accumulation of triglycerides within the hepatocyte cytoplasm. A new consensus on fatty liver disease (FLD) terminology has recently been established, following a Delphi process led by three pan-national liver associations: the

American Association for the Study of Liver Diseases (AASLD), the European Association for the Study of the Liver (EASL), and the Latin American Liver Association (ALEH). The new nomenclature is described in Table 1.1 (9). The global proportion of LT for Metabolic dysfunction-associated steatotic liver disease (MASLD, formerly referred to as Non-alcoholic fatty liver disease i.e. NAFLD) and the associated inflammatory sequalae i.e. Metabolic dysfunction-associated steatohepatitis (MASH, formerly referred to as Non-alcoholic steatohepatitis i.e. NASH) is currently lower than for viral hepatitis and ALD (7). However, MASLD is expected to become the predominant indication for LT within the next decade: this affects 38% of the global population, has strong association with features of metabolic syndrome (i.e. obesity and type 2 diabetes mellitus), and is an aetiological risk factor for development of HCC (7,10). The World Health Organization (WHO) has identified obesity, affecting 60% of adults and one-third of children in Europe, as a significant independent risk factor for MASLD (11).

This trend is evident amongst deceased donors in the United Kingdom (UK); the proportion of donors with a Body Mass Index (BMI) of ≥30 kg/m^2 has increased from 23% to 29% in the past decade (12). Similarly, in the United States, projections suggest that by 2030, approximately 49% of adults will be obese, with a BMI ≥30 kg/m^2 and 24% will be severely obese with a BMI ≥35 kg/m^2 (13).

A recent scientific registry study in United States including data from 31,209 LT candidates (≥65 years, listed for transplantation between 2002-2020) demonstrated that the proportion of MASH amongst elderly candidates increased from 13% (2002–2005) to 39% (2018–2020) (14). With the ongoing global obesity crises, MASLD (resulting in Metabolic-associated steatohepatitis, MASH) is likely to become the primary indication for LT and concurrently, HS will become more prevalent in the donor pool (15,16).

Table 1.1. Updated nomenclature for fatty liver disease (FLD) (9)

Previous Nomenclature	**Updated Nomenclature**
Fatty liver disease (FLD)	Steatotic liver disease (SLD)
Non-alcoholic fatty liver disease (NAFLD)	Metabolic dysfunction-associated steatotic liver disease (MASLD) with ≥1 cardiometabolic risk factor (out of 5): 1. Anthropometric measures (either of): • BMI ≥ 25 kg/m^2 (23 kg/m^2 Asia) • Waist circumference >94cm (males) and >80cm (females) OR ethnicity-adjusted 2. Glucose (either of): • Fasting serum glucose ≥ 5.6 mmol/L • 2-h post-load glucose levels ≥ 7.8 mmol/L • HbA1c ≥ 5.7% (≥39 mmol/L) • Treatment for T2DM 3. Blood pressure (either of): • Blood pressure ≥130/85 mmHg • Antihypertensive drug treatment 4. Plasma triglycerides: • ≥1.70 mmol/L • Lipid lowering treatment 5. Plasma HDL cholesterol • ≤ 1.0 mmol/L (males) and ≤1.3 mmol/L (females) • Lipid lowering treatment
Non-alcoholic steatohepatitis (NASH)	Metabolic dysfunction-associated steatohepatitis (MASH)
Alcohol-related liver disease (ALD)	Alcohol-associated liver disease (ALD) described as liver injury occurring in individuals with an average alcohol intake of >50 g/day (females) and >60 g/day (males)
New terms	1. MetALD i.e. MASLD with average alcohol intake ranging from 20–50 g/day (females) and 30–60 g/day (males) 2. Specific aetiology SLD i.e. related to drug-induced liver injury, monogenic diseases (Wilson's disease) and miscellaneous (HCV) 3. Cryptogenic SLD: • Steatosis without any cardiometabolic risk factors or other identifiable causes • In cases where metabolic dysfunction is highly suspected but no cardiometabolic risk factors are present, the term 'possible MASLD' may be used until further tests are performed

As the number of indications for LT expands, organ allocation systems have evolved to ensure that the prioritisation of recipients and timing of transplantation yield the best possible outcomes. This task is the manifestation of a global shortage of available donor livers (17). The Model for End-Stage Liver Disease (MELD) score (which relies on objective metrics) including creatinine, bilirubin, and international normalised ratio (INR), is employed in many countries in order to prioritise patients on the waiting list (18). Originally developed to predict three-month mortality in patients with end-stage liver disease, the MELD score does not fully account for the complications of liver disease (such as ascites and encephalopathy) or the risk associated with HCC in determining mortality without transplantation. Consequently, exceptions must be made to ensure that suitable patients receive access to LT (18,19).

1.3 Deceased donors

Transplantation critically depends on the availability of suitable donor organs, which remains a limiting factor in transplant activities and has introduced ethical considerations to the field, in particular the need to balance equity of access (i.e. 'fairness') with the need to make the best use of a scarce resource. Clearly this challenge would be greatly reduced if it were possible to increase the number of transplantable donor organs. Numerous strategies have been implemented to expand the donor pool, including varied definitions of death (20), the incorporation of living donors (21,22) and consideration of xenotransplantation (23). Furthermore, media campaigns and legislative amendments in various European nations, including the United Kingdom (UK) (24), have significantly enhanced organ donation rates (25,26).

1.3.1 Donation after brain death (DBD) donors

In the UK, Europe, and North America, the primary source of organ donors for deceased donor liver transplantation has been donation after brainstem death (DBD) (27,28). DBD donors are those who have sustained irreversible neurological injury that fulfils specific criteria confirming the absence of all brainstem functions (29). DBD donation has constituted the majority of organ donation for liver transplantation: DBD donors are generally considered to be of lower risk (compared to DCD donors) due to the absence of warm ischaemic injury during organ procurement (30,31).

Despite a notable increase in donor numbers, this has not been associated with a corresponding increase in transplant numbers, with levels plateauing or even declining just before the COVID-19 pandemic (32) (Figure 1.2). This is largely attributed to the increasingly high-risk characteristics of donor livers that are offered and retrieved for transplantation.

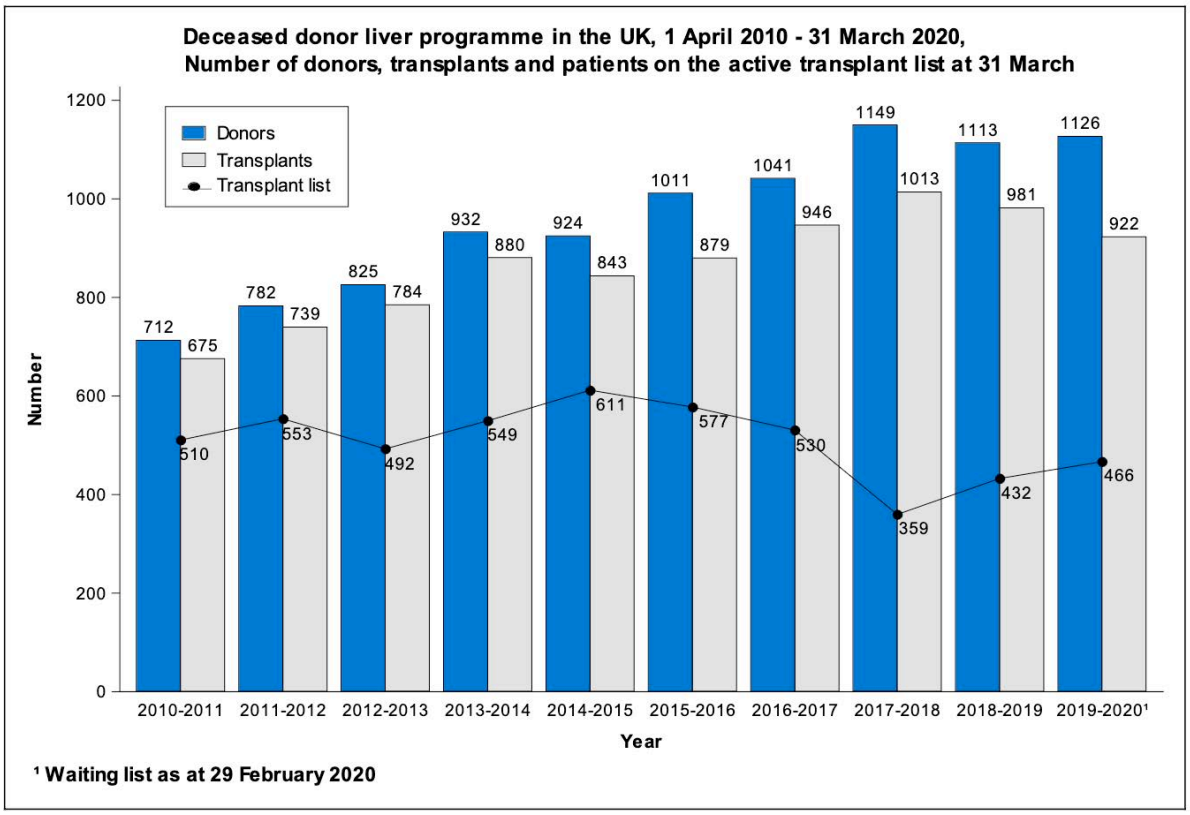

Figure 1.2. The 2019/20 NHSBT Annual Report covers liver transplant activity in the UK prior to the COVID-19 pandemic, including data on the waiting list and the number of donors available during that period (32).

1.3.2 Donation after circulatory death (DCD) donors

Donation after circulatory determination of death involves donors declared deceased based on cardiovascular (rather than neurological) criteria (20). DCD organ donation can be categorised as either: (i) controlled (Maastricht category III/IV), which occurs following the withdrawal of life-supporting care (in situations where this is deemed no longer in the best interest of the patient) or; (ii) uncontrolled, which follows an unexpected cardiac arrest and unsuccessful resuscitation attempts (27,33). The legal framework surrounding this type of donation varies in different countries, encompassing diverse regulations and protocols that dictate allowable actions before and after death. These include the precise criteria for determining death, and the duration of the mandatory 'no touch' period after death prior to the commencement of organ

retrieval (34). In this thesis, the term DCD is used to denote controlled Maastricht III/IV DCD, which is standard practice in the UK (27,35).

DCD livers experience an unavoidable period of warm ischemia prior to being cooled via in-situ perfusion during organ retrieval, and this has clinical consequences. Transplantation of DCD livers is associated with rates of graft loss and recipient mortality approximately twice as high compared to DBD transplants (36). In contrast to DCD, the functional warm ischaemia time, FWIT (defined as the time from hypoxia/hypoperfusion to in-situ cold perfusion) during DBD retrieval is minimal because the organ remains oxygenated until the point at which in-situ cold perfusion is commenced. For DCD retrieval, the FWIT commences when the systolic blood pressure falls (and is sustained) below 50 mmHg and extends up to the commencement of in-situ cold perfusion (37). The duration of FWIT is a critical determinant of LT outcomes and correlates with the risk of complications, including primary graft non-function, ischaemic cholangiopathy and recipient mortality. It is currently recommended to maintain a FWIT of under 20 minutes (38–40), although this recommendation is arbitrary and the decision to proceed is multifactorial. Consequently, DCD livers that are initially retrieved may be declined for LT after a thorough evaluation of various criteria.

Transplantation of DCD livers has been associated with inferior post-transplant outcomes, repeating some of the challenges experienced in earlier periods of LT (41–43). Whilst the donor pool has expanded in recent years due to an increase in the availability of DCD donors, this has not correspondingly enhanced the rate of DCD LT. This discrepancy underscores the need for strategies that safely optimise the use of available DCD livers. Such strategies must mitigate the inherent risks of DCD liver transplantation, and thereby improve recipient outcomes (28,35,43).

1.4 Extended criteria donor livers

1.4.1 Overview

Recent advancements in LT have significantly altered donor organ selection criteria i.e. beyond donor type alone (DBD vs. DCD). In attempts to increase organ utilisation, consideration is being given to the transplantation of extended criteria donor (ECD) livers (44,45). ECD livers are associated with a combination of 'non-modifiable' factors as well as 'modifiable' factors, Table 1.2. Donor livers exhibiting one or more of these non-modifiable characteristics are

frequently classified as ECDs (although no universally accepted definition currently exists) (3,35,46–50). ECD livers are associated with suboptimal post-transplant outcomes i.e. prolonged intensive care unit (ITU) admission, requirement for renal replacement therapy (RRT), further interventions (radiological and/or endoscopic) and re-transplantation (45,51,52). These outcomes affect surgical decision-making, are resource-intense (with cost implications) and result in non-utilisation of ECD livers. Therefore, when considering the transplantation of ECD livers, a number of recipient related factors (including MELD/UKELD scores) are carefully assessed alongside donor characteristics in order to mitigate risks associated with the transplantation of ECD livers, Table 1.2.

Table 1.2. Characteristics of ECD livers and recipient selection factors (3,35,46–50)

Non-modifiable factors	**Modifiable factors**	**Recipient factors**
Age (>65 years)	Cold-ischaemia time	MELD/UKELD score
DCD status	Donor hepatectomy time	Re-transplantation
Hepatic steatosis (>30%)	Anastomotic time	Size-mismatch
Deranged donor biochemistry		
Split liver grafts		

1.4.2 Susceptibility to ischaemia-reperfusion injury

Central to the assessment of donor liver suitability for LT is the pathophysiological process of ischemia-reperfusion injury (IRI). This process interconnects the stages of organ donation, preservation and transplantation in the recipient. A thorough comprehension of IRI and its influence on donor livers from the time of donation through to transplantation is imperative for maximising the potential of available donor livers to meet waiting list demands.

The susceptibility to severe IRI has conventionally been linked to ECD livers with aforementioned characteristics described in Table 1.2 that can amplify the magnitude of IRI (3,53–55). Clinically, the sequelae of IRI in LT encompass a wide range, from transient hemodynamic instability following reperfusion (which can typically be managed intraoperatively), or minor post-operative biochemical derangement, to more severe outcomes such as cardiac arrest upon reperfusion, post-reperfusion syndrome (PRS), early allograft dysfunction (EAD) and primary non-function (PNF).

IRI plays a pivotal role in liver transplantation, significantly influencing post-transplant outcomes. Efforts in liver preservation research have been directed towards reducing the harmful effects of IRI to enhance post-transplant outcomes. The pathophysiology of IRI involves a complex interplay of molecular and immunological processes, some of which are unique to solid organ transplantation. Initiation of IRI occurs during the donation phase with the onset of ischaemia and the cascade of events that characterise IRI ensue following reperfusion in the recipient.

1.4.3 Mechanism of ischaemia-reperfusion injury

IRI occurs following restoration of blood supply (circulation) following a period of ischaemia (56). The process is initiated in the mitochondria; during ischaemia, metabolism is switched to anaerobic glycolysis and the absence of oxygen results in the accumulation of succinate (57–59). Subsequent accumulation of lactate, compounded by adenosine triphosphate (ATP) depletion (with reliance of glycogen stores for energy generation) cause cellular acidosis and electrolyte imbalances. Following reperfusion in the recipient, the rapid restoration of oxygen results in a burst of reactive oxygen species (ROS) (due to the negative potential across the mitochondrial matrix generated during cold ischaemia) and reverse electron transfer with detachment of flavin mononucleotide from mitochondrial complex I (60). In addition, ROS initiate a sustained sterile pro-inflammatory immune response described in Figure 1.3 (61–63).

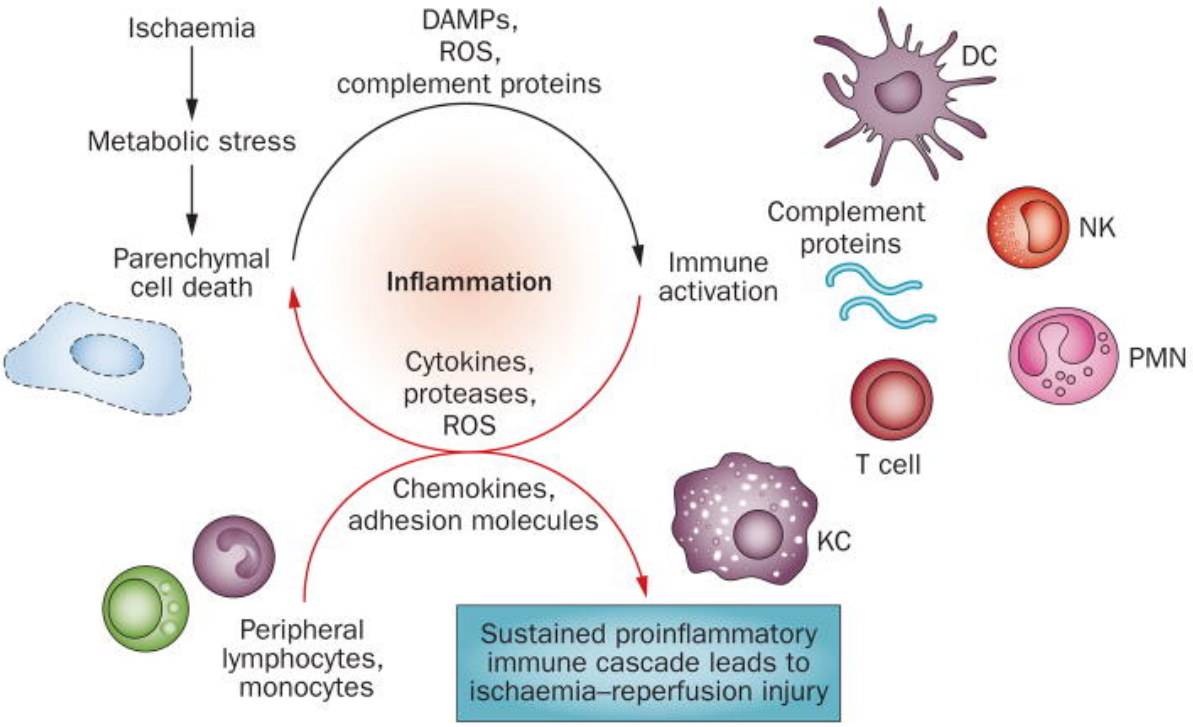

Figure 1.3. Liver ischemia-reperfusion injury unfolds through distinct phases. Initially, ischaemic injury emerges as a localised disruption of hepatic metabolism, characterised by the depletion of glycogen, a reduction in oxygen supply and subsequent ATP depletion. Following this, the cell death process releases damage-associated molecular patterns (DAMPs e.g. HMGB1) and the damage induces complement activation - part of the protein system involved in tissue injury and repair. There is also the production of mitochondrial reactive oxygen species (ROS) upon reoxygenation. Together, these factors trigger an immune response in the liver after reperfusion, engaging a variety of nonparenchymal liver cells such as Kupffer cells, dendritic cells, T cells, natural killer cells and neutrophils. The reperfusion phase is marked by a pro-inflammatory immune cascade that not only sustains itself by drawing peripheral immune cells from the circulation but also drives the severe inflammatory response responsible for extensive liver reperfusion damage and microcirculatory failure. Abbreviations: DAMPs, damage-associated molecular patterns; DC, dendritic cells; KC, Kupffer cells; NK, natural killer cell; PMN, polymorphonuclear cells; ROS, reactive oxygen species. Figure reproduced with permission from Macmillan Publishers Limited (56).

1.4.4 Clinical relevance of ischaemia-reperfusion injury

The immediate effects of IRI include intraoperative hemodynamic instability and biochemical disturbances. The condition known as post-reperfusion syndrome (PRS) has long been recognised in clinical transplantation and was formally categorised and defined by Hilmi et al. who linked PRS to dysrhythmias, decreased mean arterial pressure, lowered systemic vascular resistance, right heart strain (elevated pulmonary artery pressure, pulmonary wedge pressure, and central venous pressure), acidosis, hypothermia, hyperkalaemia and coagulation abnormalities such as hyperfibrinolysis (64,65). These observations are crucial for assessing the severity of IRI in the context of LT.

Severe IRI extends its impact beyond intraoperative cardiovascular instability, leading to immediate postoperative graft dysfunction. This condition, when followed by an eventual recovery of function, is termed early allograft dysfunction (EAD). The concept of EAD has undergone significant evolution; currently, the most accepted criteria, as defined by Olthoff et al. provide a binary differentiation between grafts with limited versus more severe injury (66). EAD is defined by specific biochemical markers: a bilirubin level of ≥10 mg/dL on post-operative day 7, an international normalised ratio (INR) of ≥1.6 on post-operative day 7 and an alanine aminotransferase (ALT) or aspartate aminotransferase (AST) level exceeding 2000 IU/L within the 7 days post-transplant (66). This classification has gained widespread acceptance.

More recent evolutions of the same concept have led to continuous scores, including the Model for Early Allograft Function (MEAF) and the Liver Graft Assessment Following Transplantation (L-GrAFT) model (67,68). The MEAF provides a graded score from 0 to 10, enhancing the assessment of EAD and enabling more accurate predictions (based on hazard ratios) of early post-transplant outcomes. This represents a significant improvement over the binary Olthoff classification (66). The L-GrAFT model, integrates clinical markers from the first ten days post-transplant, specifically focusing on serum AST levels as a marker of graft injury, alongside the INR and bilirubin levels as metrics of the graft's synthetic and metabolic functions. This model has proven highly predictive for three-month graft survival outcomes. The L-GrAFT7 model has been recently validated in the COPE liver normothermic machine perfusion (NMP) trial and has demonstrated improved predictive accuracy with an area under the receiver operating characteristic curve (AUROC) of 0.78 compared to the binary classification of EAD (AUROC 0.68, $P = 0.001$) and MEAF score (AUROC 0.72, $P < 0.001$) (69).

In its most extreme form, IRI leads to primary graft non-function (PNF), a critical condition where the liver lacks adequate function to support life, thereby necessitating an emergency re-transplant to save the life of the patient (70,71). The aetiology of PNF is often multi-factorial, yet the role of IRI is clearly significant and has profoundly affected donor selection strategies (72). Severe disorders of coagulation are also associated with IRI, manifest by a prothrombotic state that predisposes to hepatic artery thrombosis (HAT), also a reason for early emergency re-transplantation (73–75).

IRI is also a central factor in the development of non-anastomotic biliary strictures (NAS), which are alternatively referred to as ischaemic type biliary lesions (ITBL) or ischaemic cholangiopathy (IC) (52,76). This complication is particularly problematic in the context of DCD liver transplants, not only compromising graft survival, but also significantly restricting the utilisation of DCD livers. Patients who develop these biliary complications often require multiple endoscopic procedures, additional surgeries and are frequently listed for re-transplantation. These factors are associated with prolonged hospital admission, higher costs and considerable morbidity (76,77).

Liver IRI extends its effects to other organ systems, notably affecting the kidneys and often necessitating renal replacement therapy post-transplant. The origins of post-transplant acute kidney injury (AKI) are diverse and intricate, with IRI playing a significant but not exclusive role. It is well-documented that patients who develop AKI experience poorer long-term outcomes (78).

1.5 Hepatic steatosis in liver transplantation

Since the advent of LT, hepatic steatosis (HS) has been associated with poor outcomes including EAD, PNF and inferior graft/patient survival (79). Despite the impact of HS on LT outcomes, the quantification of HS has been heterogenous amongst liver transplant units (80–82), consequently, this is also reflected in the assessment and reporting of LT outcomes (83–85).

1.5.1 Quantification of hepatic steatosis

The standard method for the quantification of HS is the histopathologist's assessment of a haematoxylin and eosin (H&E) stained liver section. The severity of steatosis is dependent on the percentage of cells infiltrated by fat: no steatosis (<5%), mild steatosis (5-30%), moderate steatosis (30-60%) and severe steatosis (>60%) (86). In the clinical setting of LT, assessment of steatosis severity is performed by the macroscopic assessment of the surgeon and/or by histological evaluation of the donor liver biopsy. The macroscopic indicators of a severe HS steatotic liver include yellow liver parenchyma, rounded edges and a firm texture (87). Whilst histological analysis is regarded as the most definitive standard, it is not performed for all cases.

A transatlantic survey of surgeons in the UK and the United States demonstrated that donor liver biopsies were performed in only about 50% of instances where the liver showed macroscopic abnormalities (88). Literature on the concordance and correlation between histological and macroscopic assessments has yielded varied results. El Badry et al. reported that HS quantification on 46 liver sections by 4 different histopathologists varied significantly (i.e. was observer-dependent) and lacked reproducibility (80). Conversely, Hall et al. investigated the inter-observer concordance among 12 independent histopathologists assessing 20 liver biopsy sections and demonstrated substantial agreement in HS scoring (kappa = 0.64) (81). When determining the accuracy of macroscopic steatosis assessment, Yersiz et al. demonstrated that quantification of HS could be improved by consideration of liver texture characteristics (yellowness, absence of scratch marks, and round edges) (87). However, this is contradicted by several studies that have demonstrated a lack of concordance between the macroscopic assessment and histological degree of steatosis, with some livers deemed unsuitable for transplant based on surgical evaluation of steatosis, potentially leading to unnecessary discards in up to one in six cases (89,90).

Most histological analyses of liver biopsy sections (especially in the context of organ donation and LT) are performed on frozen-sections in order to provide urgent evaluation and minimise CIT. However, these frozen-sections typically suffer from poor quality, making it challenging to differentiate between fat vacuoles and tissue artefact (90,91). In addition, the accuracy of histological assessment is also compromised by the minimal amount of tissue sampled (approximately 1/50,000th of the total liver size) and the heterogeneity in sampling techniques i.e. operator dependent (92). It also remains uncertain whether steatosis observed in one section of the liver accurately reflects the condition of the entire organ (93).

The ideal methodology for assessing HS should be practical, cost-efficient, rapid and reproducible. Computational digital image analysis (DIA) offers a promising solution that could yield more accurate, unbiased and standardised quantification of HS. Research has shown a strong correlation between assessments by histopathologists and those derived from DIA software. However, histopathologists tend to overestimate steatosis relative to DIA (80,81,94,95). This must be considered prior to implementation into routine clinical practice especially when considering utilisation of severely steatotic livers that are at a high risk of graft failure. Despite its utility in steatosis quantification, DIA (in the setting of LT) does not detect

other critical pathologies (essential for evaluating the viability of high-risk grafts) including necrosis, fibrosis, malignancy and bile duct injury.

1.5.2 Banff consensus for reporting hepatic steatosis

In 2021, Neil et al. published the Banff consensus recommendations for reporting of donor HS into three categories (96): (i) Large droplet Macrovesicular Steatosis (ld-MaS) characterised by a single fat vacuole causing cellular distension, being larger than adjacent non-steatotic/minimally steatotic hepatocytes with nucleus displacement to the hepatocyte periphery; (ii) Small droplet Macrovesicular Steatosis (sd-MaS, previously described as microvesicular steatosis) characterised by presence of fat vacuoles that are not true ld-MaS i.e. less than half the size of the cell and does not cause displacement of the nucleus. and; (iii) True Microvesicular Steatosis characterised by multiple tiny droplets occupying hepatocytes with a signature foam like appearance which require a specialised 'fat' stain to confirm presence. Typically, these are either non-zonal aggregates or with diffuse liver involvement that typically present in the setting of acute liver failure rather than in liver grafts retrieved for transplantation (96). In the clinical setting of LT, sd-MaS has been historically described as microvesicular steatosis. Sd-MaS is known to increase during preservation and at reperfusion and is a transient short-lived process that indicates both liver stress/injury and recovery/regeneration from these processes. Despite efforts to standardise quantification of HS in the setting of clinical LT, the lack of uniformity in the histological assessment of HS should be considered when reporting outcomes (96).

1.5.3 Hepatic steatosis and liver transplantation

In general, ≥30% sd-MaS is considered to be safe with no overall impact on graft survival (96,97). However, the presence of moderate (30–60%) or severe (≥60%) ld-MaS is associated with reduced tolerance to static cold storage (SCS, the gold standard for organ preservation) and an increased sensitivity to the process of ischaemia-reperfusion injury (IRI), clinically manifesting as post-reperfusion syndrome (PRS), EAD, requirement for renal replacement therapy (RRT) and reduced graft/patient survival (83,84). Ld-MaS is widely acknowledged to be a negative prognostic factor in models that predict graft/patient survival following LT (97,98). Consequently, this is reflected by the reservation and caution of liver transplant units in utilising donor livers with evidence of moderate-severe steatosis (85,99–102) and in the UK, donor livers with evidence of HS account for 39% of organ discards (103). Recently, a large

study analysing data from the Scientific Registry of Transplant Recipients demonstrated that ld-MaS ≥31% was associated with lower odds of donor liver utilisation and the use of such livers was associated with an increased risk of graft failure by 53% (104).

1.5.4 Hepatic steatosis and ischaemia-reperfusion injury

Steatotic livers do not tolerate SCS well and have increased sensitivity to the process of IRI. In the clinical setting of LT, elevated hepatocellular injury markers including transaminases are associated with histological evidence of IRI (105,106) and this is evident in recipients transplanted with steatotic livers demonstrating higher early post-operative transaminase levels and EAD (99,101,107–113). Experimental models indicate that hepatocellular damage (as a result of IRI) is initiated within hepatic parenchymal cells and the presence of excess lipids within hepatocytes contribute to an amplified IRI response (114–116). Evidence from a hepatocyte IRI cell culture model suggests that the degree of hepatocellular injury (quantified by transaminase release) correlates with the degree of intrahepatic triglyceride (IHTG) content and a reduction in IHTG results in reduced hepatocellular injury. These findings suggest that HS is independently associated with IRI (115). The underpinning pathophysiological mechanisms are not completely understood but can be explained through a number of complex interlinked cellular processes and mechanisms: (i) mitochondrial oxidative stress; (ii) microcirculatory distortion and impaired sinusoidal blood flow; (iii) lipid peroxidation; (iv) pro-inflammatory environment; (v) hypoxia inducible factors (HIFs) and (vi) damage associated molecular patterns (DAMPs) and NETs. The described mechanisms below, while not yet fully elucidated, lay the foundational groundwork for devising strategies aimed at mitigating IRI injury in steatotic donor livers.

1.5.4.1 Mitochondrial oxidative stress

Experimental data point to a different inflammatory response to IRI in steatotic compared to lean livers (characterised by increased mitochondrial oxidative stress and reduced ATP restoration following SCS), as one reason for the increased vulnerability of steatotic livers to IRI (116–118). The deterioration in mitochondrial function is triggered by ROS production which results in altered energy metabolism, disrupted cellular bioenergetics and cellular function which results in cell death (119–122). Previous studies have demonstrated that mitochondrial proton adenosine triphosphate (ATPase) activity required for ATP synthesis and oxidative phosphorylation is rapidly reduced following 6 hours of SCS in steatotic compared

to lean livers (123–125). The lack of ATP restoration consequently results in ATP-dependant Na^+/K^+ pump failure contributing to cellular swelling and necrosis (rather than apoptosis which is ATP dependant) in steatotic livers (126,127).

Furthermore, the mitochondrial uncoupling protein-2 (UCP-2) required for the regulation of proton leakage across the inner membrane is paradoxically increased in steatotic livers in attempts to counteract oxidative stress and ROS production as well as prevent chronic hepatocellular lipid accumulation. However, due to dysregulation in ATP synthesis and diminished ATP levels, the overexpression in UCP-2 limits the capacity of hepatocytes to respond to increasing energy demands at reperfusion resulting in a mitochondrial permeability transition (MPT) and membrane potential failure (118,128).

Comparatively, in lean livers, cell death is mainly a result of apoptosis (an energy dependant process) and the ATP depletion in steatotic livers results in an inability to induce apoptosis resulting in other pathways of programmed cell death and necrosis. This is evident in increased iron overload, capase-1, capase-9, receptor-interacting kinase 1 (RIPK1) and receptor-interacting kinase 3 (RIPK3) expression observed in steatotic hepatocytes exposed to IRI, indicating ferroptosis, pyroptosis, necroptosis and MPT mediated necrosis mechanisms respectively (117,129–131).

1.5.4.2 Microcirculatory distortion and impaired sinusoidal blood flow

Lipid droplet accumulation in steatotic livers results in structural distortion and obstruction of microcirculation and sinusoidal blood flow compared to lean livers (132–136). Following graft reperfusion, impairment of microcirculation can be exacerbated by hepatocellular membrane rupture resulting in expulsion of lipid droplets into the extracellular space (lipopeliosis) causing obstruction of liver sinusoids and further compounding the issue (137,138). In addition, the microcirculatory distortion and impaired blood flow contribute to a chronic hypoxic state due to inadequate oxygenation. This results in exacerbated ischaemic injury upon reperfusion characterised by increased ROS production and Kupffer cell activation. The activated Kupffer cells produce endothelin-1 (ET-1, vasoconstrictor) in excess to inducible nitric oxide synthase (iNOS, vasodilator). This imbalance promotes microcirculatory damage due to sinusoidal vasoconstriction (and limited blood flow) during reperfusion (136,139,140). The consequent

injury impairs the role of the endoplasmic reticulum (ER) involved in hepatocellular lipid metabolism, protein synthesis and calcium storage. The increased ER stress can also be attributed to chaperonin downregulation (141) and results in activation of a signal transduction cascade (unfolded protein response, UPR) that promotes JUN N-terminal kinase (JNK), NF-κB, and caspase-12 activation (117).

1.5.4.3 Lipid peroxidation

Steatotic livers are more prone to lipid peroxidation, following ischaemia and post-reperfusion (115,142,143). Lipid peroxidation (oxidative degradation of lipids) is characterised by the reduction of hydrogen peroxide resulting in a hydroxyl radical involved in the destruction of polyunsaturated fats (144). These free radicals scavenge electrons from lipids located in cell membranes and aggravate cellular injury (145). In clinical LT, lipid peroxidation has been associated with oxidative injury induced by ROS during reperfusion (146).

1.5.4.4 Pro-inflammatory environment

Following implantation, the reperfusion of steatotic livers is associated with an exacerbated inflammatory response driven by pro-inflammatory mediators including TNF-a and neutrophils. Cytokine releases is associated with endothelial dysfunction, increased expression of adhesion molecules and the activation and migration of platelets and leukocytes (147–150). Kupffer cell activation results in sustained ET-1 production, lower phagocytic activity and increased ROS, IL-6 and IL-Iβ production in steatotic livers compared to lean livers (151,152). The ongoing activation of inflammatory cells further promote ROS and protease production thereby promoting hepatocellular injury (151).

1.5.4.5 Hypoxia inducible factors

Hypoxia has been attributed as a central instigator in the development and progression of hepatic steatosis due to structural distortion caused by hepatocyte swelling and fibrotic scar formation, increased metabolic demands, oxygen consumption and perturbation of lipid homeostasis (153). Hypoxia-inducible factors (HIFs) are cellular oxygen sensitive transcription factors which have been implicated as the ‘master regulators’ in response to hypoxia through activation of a number of hypoxia responsive genes. The HIF-1α isoform has demonstrated a

protective effect through reduction in lipid synthesis, *de novo* lipogenesis and lipid peroxidation as well as promotion of fatty acid β-oxidation (154). However, the HIF-2α isoform is reported to activate genes involved in fatty acid synthesis (Srebp1c and Fasn), fatty acid uptake (Cd36) and suppression of genes that regulate fatty acid β-oxidation resulting in progression of lipid accumulation and fibrosis (153,155). Pre-clinical murine studies have demonstrated the benefit of pre-treatment with HIF prolyl-hydroxylase inhibitors and other pharmacological agents including Mangafodipir (a contrast agent) in up-regulation of HIF-1α expression with improved liver graft tolerance to IRI during reperfusion (156,157). This effect has also been demonstrated in steatotic murine livers that received pre-treatment with trimetazidine (an anti-ischaemic drug) through activation of cytoprotective genes (heme-oxygenase associated with HIF-1α (157). In addition, a recent study by Dery et al. (158) has demonstrated carcinoembryonic antigen-related cell adhesion molecule 1 (CEACAM1) alternative splicing, mediated by HIF-1α in response to stress, significantly augments hepatic ischaemic tolerance in hepatic tissues of both mice and humans. The research delineates the mechanism of action, demonstrating HIF-1α 's direct association with the promoter region of the polypyrimidine tract-binding protein 1 (PTBP1) splicing enzyme. This interaction facilitates the induction of the CEACAM1-short isoform, thereby enhancing ischaemic tolerance with reduction in DAMPs including Histone H3 expression. Importantly, the findings from this study underscore a novel biomarker for assessing the viability of liver transplant donor livers.

1.5.4.6 Damage associated molecular patterns (DAMPs)

DAMPs typically originate from an intracellular source (cytoplasm, mitochondria and nucleus) and are associated with hepatocellular injury during reperfusion (159–162). More recently, attention has been drawn to DAMPs of nuclear origin that have significant potential to exacerbate injury during liver IRI. Nuclear DAMPs include nucleosomes as well as free nucleic acids and proteins such as cell-free (cfDNA), mitochondrial DNA, free histones, HMGB-1 that are released during unprogrammed cellular injury or death (163–165). The interaction of these molecules with Toll-Like-Receptors (TLR, in particular 2,4, 7 and 9), RAGE (Receptor for Advanced Glycation Endproducts) and pattern recognition receptors (PRRs) in the activation of innate immune and inflammatory responses (166–168) during reperfusion thereby propagating the magnitude of injury/inflammation which is already heightened in steatotic livers (159,169).

1.5.4.7 Neutrophils and NETosis

Neutrophils in circulation are mobilised to the site of tissue injury where they interact with activated endothelial cells, facilitating their adhesion and subsequent migration into the sub-sinusoidal spaces. This migration is mediated by the interaction between integrin αMβ2 (Mac1) on neutrophils and Intercellular Adhesion Molecule 1 (ICAM-1) on liver sinusoidal endothelial cells (LSECs), a process that is directed by chemokines from Kupffer cells and a chemotactic gradient originating from the site of injury (170–172). Upon reperfusion, neutrophils contribute to the exacerbation of tissue damage through the promotion of inflammatory responses (173). A key mechanism through which neutrophils augment liver injury during IRI involves the release of NETs—structures composed of extracellular DNA decorated with histones and granular proteins. The phenomenon of NET formation, or NETosis, represents a recently elucidated mode of neutrophil death, distinct from the caspase-dependent pathways of apoptosis. Unlike apoptosis, which leads to the generation of apoptotic bodies without subsequent inflammation, NETosis encompasses both lytic and non-lytic pathways that culminate in the dissemination of nuclear contents into the extracellular milieu. The lytic pathway of NETosis is marked by the disintegration of the nuclear envelope, cellular depolarisation, chromatin de-condensation and cell membrane rupture leading to the dispersion of extracellular chromatin fragments into circulation. Conversely, the non-lytic pathway of NETosis does not culminate in cellular death, but involves the expulsion of a mesh-like structure of decondensed chromatin, decorated with intracellular and granular proteins into the extracellular space. The formation of NETs triggers several processes that intensify the severity of IRI, including thrombosis and the amplification of inflammatory responses resulting in liver graft injury (167,168,174).

1.5.5 Hepatic lipid metabolism

1.5.5.1 Hepatic lipid metabolism

Fat accumulation in the liver typically results from an imbalance in fatty acid (FA) synthesis, intake, and clearance (disposal) (175). The liver acquires fats from three principal sources: (i) the uptake of circulating plasma non-esterified fatty acids (NEFA), which are released during lipolysis of subcutaneous and visceral adipose tissue; (ii) dietary sources and; (iii) *de novo* lipogenesis (DNL), the endogenous production of FAs from non-lipid precursors (176–178). FAs are removed from the liver primarily via secretion in very low-density lipoproteins

(VLDL) as triglycerides (TG) or by oxidation through the tricarboxylic acid (TCA) cycle and ketogenesis. FAs that are not cleared are esterified and stored predominantly as TG within the liver (178). The metabolism of FAs in the liver is a dynamic and rapidly evolving process, which, in a healthy state, is tightly regulated by hormonal factors and is closely linked to the overall metabolic and nutritional status. For a detailed representation of hepatic lipid metabolism, refer to Figure 1.4.

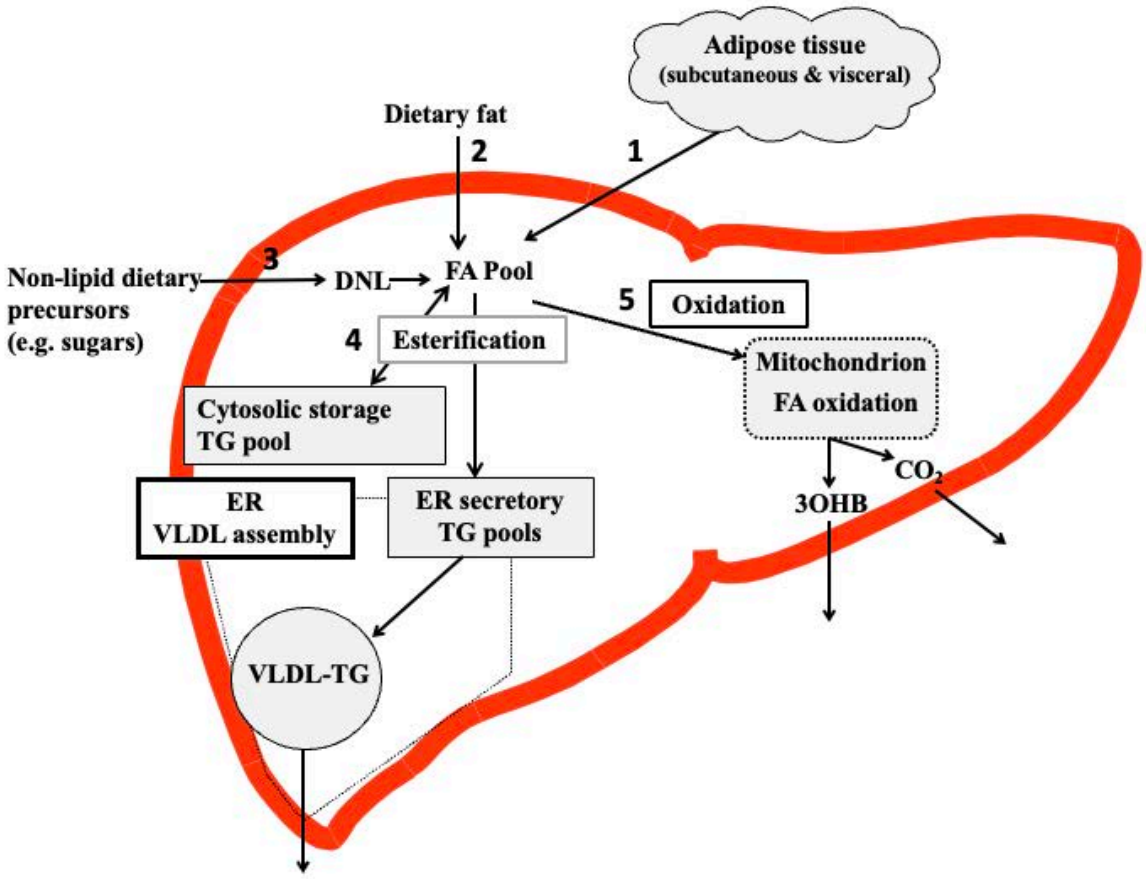

Figure 1.4. Overview of hepatic fatty acid (FA) input, synthesis and disposal in the postprandial state. FA input to the liver derives from (1) the lipolysis of adipose (subcutaneous and visceral) tissue triglyceride (TG), and (2) dietary fat, which enter the liver as either chylomicron remnants or chylomicron-derived spillover FAs. (3) FA synthesis occurs within the liver, via *de novo* lipogenesis (DNL) which involves the synthesis of FA from acetyl-CoA derived from non-lipid precursors, such as glucose. FAs enter a common pool and are broadly partitioning between two pathways for disposal: (4) the esterification pathway, where predominantly TG is produced which can then be either stored in the cytosol (as a lipid droplet) or can lipidate very-low density lipoprotein (VLDL) in the endoplasmic reticulum (ER) to form VLDL-TG and then secreted into the systemic circulation, or 5) oxidation either via the tricarboxylic acid (TCA) cycle to form CO2, or the ketogenic pathway where β-hydroxybutyrate (3OHB) is produced and enters the systemic circulation. Figure reproduced with permission from BioMed Central (179).

1.5.5.2 Lipid synthesis and esterification

Fatty acids (FAs) taken up by the liver are primarily esterified with glycerol-3-phosphate to form triglycerides (TG) along with other lipid molecules such as phospholipids and cholesterol esters (177). Additional contributions to the FA pool are from FAs are synthesised *de novo* from non-lipid precursors like glucose and amino acids through DNL (180). In this process, insulin and malonyl-CoA (an intermediate in the DNL pathway) regulate FA oxidation by inhibiting carnitine palmitoyltransferase-1 (CPT-1), thereby restricting the entry of FAs into mitochondria for oxidation. The esterification of fatty acyl-CoA with glycerol-3-phosphate is also insulin-dependent, aligning with insulin's role in promoting the storage of FAs as TG during the fed state, rather than directing these molecules towards oxidation pathways. In such states, the liver primarily meets its energy needs through the oxidation of amino acids (181).

The TGs stored are later used as substrates for the secretion of fat into the bloodstream in the form of very low-density lipoproteins (VLDL). VLDL particles, which contain a single molecule of apolipoprotein B100 (ApoB) that remains part of the particle throughout its lifespan, also include cholesterol esters and small quantities of apolipoproteins E and C. The surface of VLDL particles is coated with phospholipids and unesterified cholesterol (182).

1.5.5.3 Fatty acid oxidation

The liver primarily relies on mitochondrial β-oxidation of fatty acids (FAs) for energy production, supporting its extensive metabolic functions. FAs transition from glycerolipid synthesis to oxidation when fatty acyl-CoA is transported into the mitochondrion. However, as mitochondrial membranes are impermeable to fatty acyl-CoAs, these molecules must first transfer their acyl groups to carnitine. This transfer is facilitated by the enzyme carnitine CPT-1, which is regulated by malonyl-CoA. At the cellular level, malonyl-CoA regulates the activity of the enzyme carnitine CPT-1, serving as a critical intermediary that integrates carbohydrate and fat metabolism and plays a significant role in the DNL pathway (180). High concentrations of malonyl-CoA during carbohydrate surplus inhibit CPT-1, thus suppressing fat oxidation. This effect is complementary to the role of insulin in inhibiting FA release from adipose tissue. Consequently, during carbohydrate excess, the liver favours esterification of FAs over oxidation (177). Within the mitochondria, the acetyl CoA produced from oxidation enters the Krebs' cycle to be further oxidised to CO2, or it can proceed to ketogenesis. During

ketogenesis, two acetyl-CoA molecules combine (within the mitochondrion) to form acetoacetic acid, which is further converted to 3-hydroxybutyrate (3-OHB). This ketone body is then released into systemic circulation and is often used as an indicative marker of hepatic FA oxidation (183).

1.6 Liver preservation

The primary objective of liver preservation for transplantation is to reduce the magnitude of ischaemic injury (resulting from anaerobic metabolism and hypoxia) while maintaining structural and functional integrity (184,185). Post-transplant liver function is related to the pathophysiological process of brainstem/cardiac death and subsequent ischaemic injury (related to organ retrieval and the preservation environment). Therefore, optimisation of each stage of the donor pathway from retrieval to implantation is essential to ensure satisfactory outcomes in the recipient (186).

1.6.1 Static cold storage

The current standard for liver preservation is SCS, this involves rapid cooling of the liver to 4°C and is achieved by flushing of the liver with cold specialised organ preservation solution thereby effectively removing residual blood from the liver until the effluent is clear and the liver uniformly pale and cooled down. Subsequently, the liver is immersed and stored in preservation solution (0-4°C), enclosed in sterile bags and positioned on ice within an insulated organ transport ice-box. At this reduced temperature, the liver's metabolic rate is reduced to 10% of its normative rate at physiological body temperature. This reduction is facilitated by the application of organ preservation solutions (OPS), which prevent cellular swelling and lysis as the temperature drops and cellular membrane functions cease. Rapid execution of these steps, from the initial cold perfusion within the donor to the final packaging and placement in an ice-box, is crucial to sufficiently lower the temperature, diminish metabolic rate and preserve cellular energy stores (186).

Since the 1980s, various OPS have been adopted for LT (187). The University of Wisconsin (UW) solution is the most widely used OPS for preserving donor livers, followed by histidine-tryptophan-ketoglutarate (HTK) solution (187–193). The UW solution has enabled extended preservation times: Todo et al. reported successful LT after more than 15 hours of cold-

ischemia time (CIT), significantly enhancing the feasibility of transporting organs over long distances and thus revolutionising LT logistics (194).

However, prolonged CIT can exacerbate cellular injury during SCS and is characterised by the depletion of ATP, increased glycolysis, and accumulation of lactic acid. For this reason, the duration of CIT is restricted to less than 12 hours, with even stricter limitations for grafts classified as high-risk, such as DCD grafts and those exhibiting steatosis (186). These particular grafts are more vulnerable to hypoxia and the impacts of anaerobic metabolism, which includes the production of metabolites that serve as precursors for IRI upon transplantation into the recipient (184,185).

Despite the limitations of SCS and associated IRI, the use of OPS is associated with approximately 85% survival at 1 year and 75% at 5 years. Whilst organs from standard criteria donors usually have adequate physiological reserve to endure SCS related ischaemic injury, ECD livers often lack this capacity, thus restricting the effectiveness of cold storage for these organs (195).

1.6.2 Normothermic machine perfusion

The imperative to broaden the utilisation of donor organs (particularly those of the high-risk category) and reduce waiting list mortality rates have played a pivotal role in the evolution of NMP technology. NMP, which utilises a blood-based perfusate (packed red blood-cells, pRBCs) warmed to physiological temperature (37°C) enriched with oxygen and nutrients, is designed to keep the donor liver in a functional, near-physiological condition prior to LT. NMP can be applied in a continuous manner i.e. at the point of organ retrieval (device-to-donor or continuous NMP, cNMP) or after a period of SCS (back-to-base, end-ischaemic or post-SCS NMP). The benefits attributed to NMP in comparison to traditional preservation techniques encompass: (i) the capability to recover from acute injury (such as hypoxia) incurred before or during the organ retrieval process, particularly in DCD organs; (ii) the ability to objectively evaluate liver functionality prior to transplantation (through the assessment of metabolic or synthetic activities), facilitating the identification of high-risk organs that would otherwise be deemed unsuitable for transplantation (with criteria established through clinical research); (iii) enhancement of transplant logistics via prolonged preservation durations; (v) restoration of ATP levels and modulation of apoptosis, immune responses and enhancement of regenerative

pathways and; (vi) the prospect of administering therapeutic treatments to the donor liver prior to transplantation (as indicated by experimental research) (196–200).

A major advantage of NMP over SCS and other dynamic preservation methods is its capability to evaluate liver function parameters during perfusion. This enables the assessment of liver viability prior to exposing a recipient to the risks associated with LT. Researchers in Cambridge and Birmingham have identified criteria including metabolic indicators (such as lactate clearance), markers of organ injury (like perfusate transaminase levels), haemodynamic measurements (such as perfusion flow rates), and indicators of potential biliary complications (bile biochemistry), detailed in Table 1.3 and 1.4 (201,202). Additionally, the team in Groningen has identified histological indicators of bile duct injury (BDI) during NMP with a BDI scoring system (ranging from 0 to 7) based on stroma necrosis, damage or loss of extramural peribiliary glands, and vascular lesions. High BDI scores have been linked to poor biliary function predictors, including low bile pH and high levels of glucose and lactate dehydrogenase (LDH) (203).

Table 1.3. Cambridge NMP criteria for optimal NMP parameters associated with favourable post-transplant outcomes (201). Table reproduced with permission from MDPI (4).

NMP parameter	**Description**
Perfusate pH	The ability to maintain perfusate pH >7.2 (without bicarbonate supplementation exceeding >30mmol)
Bile pH	A minimum bile pH value >7.5
Clearance of perfusate lactate	Evidence of a peak reduction in perfusate lactate ≥ 4.4 mmol/l/kg/h
Metabolism of glucose (perfusate)	Evidence of a reduction in perfusate glucose following 2h of perfusion OR a glucose value of 10 mmol/l (that also subsequently falls following a challenge 2.5g of glucose)
Bile glucose concentration	A bile glucose concentration of ≤3 mmol/l OR ≥10 mmol/l less than the perfusate glucose concentration
Hepatocellular injury as demonstrated by perfusate alanine aminotransferase (ALT) level	A perfusate ALT <6000 IU/l at 2h of perfusion

Table 1.4. Birmingham NMP criteria as recommended in the 'VITTAL' trial (202). Table reproduced with permission from MDPI (4).

Mandatory NMP parameter	**Description**
Clearance of perfusate lactate	Evidence of reduction of perfusate lactate to ≤2.5 mmol/l
Two or more of the following NMP parameters at 4h of perfusion	
Perfusate pH	The ability to maintain perfusate pH ≥ 7.3
Glucose	Evidence of glucose metabolism during perfusion
Bile	Evidence of bile production during perfusion
Hepatic arterial (HA) flow and portal venous (PV) flow	Maintenance of HA flow ≥150ml/min and PV flow ≥500ml/min
Macroscopic assessment of donor liver during NMP	Homogenous macroscopic appearance of the liver parenchyma during perfusion

Initial evidence regarding the utility of NMP emerged from case studies in Birmingham (204) and Cambridge (205). The safety and efficacy of continuous NMP (cNMP) was first demonstrated by Ravikumar et al. from Oxford (206) confirming the feasibility of this preservation technique, but also demonstrating a substantial reduction in graft injury compared to SCS. The landmark multicentre randomised controlled trial (RCT) involving 220 liver transplant recipients, was carried out by Nasralla et al. in 2018 under the Consortium for Organ Preservation in Europe (COPE), comparing cNMP with SCS. NMP-treated livers showed a notable reduction in reperfusion-related injury, evidenced by a 49% decrease in peak postoperative AST levels, and a 50% reduction in the rate of organ discard, despite a 54% extension in mean preservation duration. The enhanced rate of organ utilisation, marked by the lower discard rate among cNMP-treated livers, was partly credited to the capacity for direct functional assessment of liver function for viability, thus offering surgeons increased confidence in utilising higher-risk donor livers (207). In a subset analysis of steatotic donor livers from this cohort, Ceresa et al. explored the impact of cNMP on histologically confirmed steatotic livers with matched lean controls preserved with cNMP. Steatotic livers demonstrated distinct variations in lipid metabolism during perfusion compared to lean livers, characterised by enhanced triglyceride mobilisation, increased mitochondrial fatty acid β-oxidation and greater hepatocellular injury (quantified by perfusate transaminase levels). Nonetheless, steatotic livers preserved with cNMP had comparable outcomes to lean livers preserved with SCS, suggesting a reduction in risk profile of these livers facilitated by enhanced preservation

during cNMP. In addition, when compared to steatotic livers with SCS there was no significant histological reduction in the degree of macrovesicular steatosis (MaS) during cNMP (208).

In 2021, Markmann et al., representing the OCS Liver 'Protect' Randomized Clinical Trial Group in the United States, shared findings from a multicentre RCT examining the impact of cNMP on transplant outcomes. This RCT compared NMP with SCS in 293 patients (per protocol population). Compared to the COPE trial, the PROTECT trial featured shorter average NMP durations, with a mean (SD) of 276.6 (117.4) minutes. The study highlighted that NMP was associated with a reduction in EAD and ischaemic bile duct complications (IBC), fewer histological features of IRI, reduction in ICU and hospital stay, improved utilisation of DCD livers and graft survival. The research design limited inclusion to livers with MaS of 40% or below, but it did not clearly detail the actual steatosis levels of the included livers (209).

The logistically more straightforward approach of conventional SCS, followed by connection of the donor liver to the normothermic perfusion device at the recipient centre ('back-to-base'), has also been explored by Ceresa et al. who reported a series of liver transplants preserved with pSCS-NMP. Adhering to the same recruitment criteria as a COPE trial, a total of 31 livers were transplanted using the back-to-base (pSCS-NMP) approach with no significant differences in graft injury indicators (peak AST in the first 7 postoperative days), graft and patient survival, or organ discard rates when compared to all transplanted cNMP livers ($n = 104$) from the COPE trial (210). However, out of the 31 livers included in the pSCS-NMP cohort, 3 (9.7%) were discarded. Of the discarded livers, one liver had histological evidence of 80% MaS with poor lactate clearance, glucose metabolism and lack of bile production during perfusion.

In the VITTAL study by the Birmingham group, previously declined livers were perfused. Those meeting pre-defined functional criteria were transplanted: 22 of 31 (71%) perfused organs were transplanted (all with immediate function) with a median preservation time of 18 hours (comprising both SCS and NMP components). The 90-day survival rate (graft and patient) was 100% (202). However, it was notable that there was a high rate of biliary strictures and the need for later re-transplantation, suggesting that the combination of relatively prolonged SCS followed by NMP may not be the optimal method in the context of ECD livers. Notably, the livers that did not meet viability criteria were heavier, with increased donor peak AST, longer CIT (550 vs. 452 mins) and a greater proportion (77.8% vs 40.9%) had MaS >30% (202). To achieve wider clinical adoption of this approach, specific acceptance and perfusion

criteria will be needed, possibly in association with specific interventions during NMP to reduce postoperative morbidity.

Patrono et al. further investigated the utilisation and outcomes of steatotic donor livers preserved with pSCS-NMP and MaS ≥ 30%: 10 out of 14 livers (71.4%) were transplanted, of which 2 livers (14%) developed PNF (211). This study highlights the challenges in determining the viability of livers with moderate-severe steatosis using existing viability criteria. The results indicate that an extended observation period (≥6 hours) may be necessary for these livers, emphasising that consistent lactate clearance is essential for their utilisation (211). To address the limitation of pSCS-NMP of steatotic donor livers, Patrono et al. further published a proof-of-concept case utilising device-to-donor (cNMP) on an HCV-positive DBD donor liver with 70% MaS (212). This case met the functional assessment benchmarks described by both the Birmingham and Groningen groups and was transplanted with 6-month graft and patient survival, normal post-operative graft function and the absence of any clinical or laboratory signs of ischaemic cholangiopathy (212).

Whilst pSCS-NMP has several advantages, this end-ischaemic approach may result in suboptimal results and discards of steatotic livers that are sensitive to even short periods of CIT and this is evident in aforementioned end-ischaemic (pSCS-NMP) studies that have included a small proportion of steatotic livers within the overall cohort. These data suggest steatotic donor livers may require active intervention beyond that of simply replacing SCS with NMP.

More recently, He et al. explored the advantages of preventing ischaemia and complete avoidance of cooling prior to LT i.e. ischemia-free liver transplantation (IFLT) which involves the procurement, preservation, and transplantation of the donor liver using continuous normothermic perfusion without interruption of blood flow (213). The authors described the successful transplantation of a steatotic DBD liver with 85-95% MaS (213). The clinical application of IFLT has been further described by Chen et al. in a study that included 26 steatotic livers (16 with moderate and 10 with severe steatosis) (214). Within this cohort, 6 livers (23.1%) underwent IFLT and demonstrated a reduction in a peak AST, GGT and creatinine post-transplant with a significant reduction in EAD (0% vs. 60%; $P = 0.001$) (214). These findings have also been further validated in a randomised clinical trial by Guo et al (215). Nonetheless, to fully assess the potential of NMP to enhance the viability of steatotic donor

livers for transplantation, a comparative analysis with livers preserved via post-SCS-NMP, cNMP, and IFLT is required.

In the current clinical setting, IFLT is a sophisticated technique carried out in a high-volume, single centre in China, making it less accessible globally. Continuous cNMP emerges as a practical alternative, navigating between the constraints of end-ischaemic NMP (pSCS-NMP) and the advantages of IFLT for the preservation of steatotic donor livers. Crucially, in the current era where IFLT is not widely available, ex-situ preservation (including pSCS-NMP and cNMP) may offer a platform for therapeutic interventions such as defatting therapies that target hepatocellular lipid metabolism during NMP as an alternative strategy to improve ex-situ function and the risk profile of livers with moderate-severe steatosis.

1.6.3 Ex-situ defatting of steatotic donor livers during normothermic perfusion

Attempts to improve post-transplant outcomes in steatotic livers have included treatments to attenuate the IRI to which these grafts are particularly susceptible. However, in experimental models, levels of injury remained higher in treated steatotic than in lean livers (179). Rather than identifying methods to reduce IRI, targeting the primary cause, accumulation of intra-hepatocellular triglyceride (IHTG), may yield improved transplantation outcomes. By eliminating the root of the problem, the associated complications may be avoided. Several groups have explored this approach, particularly using NMP as a method to enhance the quality of steatotic grafts by actively removing IHTG during preservation.

Preclinical studies have demonstrated that NMP can improve ex-situ liver function and reduce intrahepatic triglyceride content (IHTG) through the promotion of lipid metabolism and thereby potentiating the reversal of steatosis. Jamieson et al. (216) investigated the effect of NMP alone in steatotic porcine livers preserved over 48 hours. In this model, HS was induced through pre-treatment with streptozotocin and a high-fat diet, inducing hyperglycaemia and ketosis prior to organ retrieval for NMP. During perfusion, steatotic livers maintained perfusate base excess, factor V and bile production. In addition, the perfusion haemodynamics and hepatocellular injury markers were comparable to that of lean controls. Notably, these livers demonstrated elevated levels of glucose and urea in the perfusate. Following 48 hours of perfusion, there was a significant reduction in MaS from 28% to 15% and the size of lipid droplets, achieved without the use of defatting agents. This study demonstrated mobilisation

of fat from the liver into the perfusate. Indeed, one limitation of the study was the recirculation of secreted TGs in the circuit, thereby making the perfusate extremely lipaemic. It was thought that this might be a factor that limited the amount of fat that could be extracted by perfusion alone.

Nagrath et al. developed an experimental oxygenated normothermic model to study the impact of a 'defatting cocktail' on steatotic livers retrieved from Zucker rats during 3 hour perfusions (217). This cocktail was a combination of pharmacological compounds, including GW501516 (a PPARδ ligand), GW7647 (a PPARα ligand), forskolin (a cAMP activator), hypericin (a pregnane X receptor ligand), visfatin (an insulin-mimicking adipokine), and scorparone (a constitutive androstane receptor ligand), (Table 1.5). Following addition of the 'defatting cocktail' to the NMP perfusate, there was a 65% decrease in hepatic triglyceride levels and a 50% reduction in intracellular lipid content. In contrast, livers perfused without the 'defatting cocktail' demonstrated a 30% reduction in hepatic triglycerides (217). Raigani et al. (218) demonstrated comparable outcomes by incorporating L-carnitine (to enhance fatty acid β-oxidation) as a constituent of the 'defatting cocktail'. The interventions led to a reduction in MaS from 41.5% to 8.5%. Furthermore, there was a rise in ketone levels in the perfusate (indicative of enhanced fatty acid β-oxidation), as well as increased bile bicarbonate content and improved lactate clearance in the steatotic rat livers that received these interventions.

Table 1.5. Constituents of 'defatting cocktail' described by Nagrath et al (217).

Defatting agent	**Mechanism of action**
PPARδ ligand GW501516	PPARδ ligand that improves fatty acid β-oxidation
Peroxisome proliferator-activated receptor (PPAR) α ligand GW7647	PPARα ligand improves mitochondrial fatty acid oxidation
Forskolin, cyclic adenosine monophosphate (cAMP) activator (glucagon mimetic)	cAMP activator that increases lipolysis and improves fatty acid oxidation
Hypericin	Pregnane X receptor ligand that increases β-oxidation of very long chain fatty acids
Visfatin	Adipokine (insulin-memetic, role not completely understood)
Scorparone	Upregulates PPAR (androstane receptor ligand)

These preclinical studies demonstrate the potential of NMP as a platform to provide active intervention to treat donor HS. The findings indicate that both hepatic triglyceride levels and MaS can be altered during ex-situ preservation. However, the limited sample size and uniformity of the livers, where steatosis was experimentally induced, suggest caution when extrapolating these results to clinical settings involving a heterogenous group of steatotic human livers intended for transplantation.

The effect of defatting agents during NMP would be better investigated in a discarded steatotic human liver model. Initial results from a discarded human liver study involving NMP of steatotic donor livers for 24 hour did not demonstrate and overall reduction in MaS (219). However, Banan et al. reported outcomes from two human livers preserved with NMP and defatting agents (L-carnitine and exendin-4), with one liver demonstrating a 10% decrease in MaS after 8 hours of NMP (220).

More recently, Boteon et al. (221) explored the use of the 'defatting cocktail' developed by Nagrath et al. with the addition of L-carnitine in livers declined for transplantation due to advanced steatosis. These perfusion experiments comprised of 10 steatotic human livers perfused with either the modified 'defatting cocktail' during NMP ($n = 5$) and with NMP alone ($n = 5$). Discarded livers that were subjected to pharmacological defatting during NMP demonstrated improvement in metabolic function, decreased vascular resistance, reduction in hepatocellular injury and greater bile production. Mechanistic studies also demonstrated a reduction in oxidative damage, immune cell activation, inflammatory cytokine release and tissue triglycerides, achieving a 40% reduction in MaS after 6 hours of perfusion.

In addition, all 5 livers that received pharmacological defatting during NMP met the accepted viability criteria for transplantation, in contrast to only 2 out of 5 in the control group ($P = 0.04$). However, not all defatted livers demonstrated a clinically meaningful reduction in MaS of <30%. This raises questions about the relationship between histological steatosis and liver function during NMP. Mechanistically, these findings suggests that the benefits observed may not necessarily be due to fat removal alone. Instead, the activation of cytoprotective and vaso-protective pathways during NMP could be critical in making these organs suitable for transplantation, and the combined effects of NMP and defatting treatments may synergistically contribute to meeting ex-situ functional criteria for transplantation (222).

Although Boteon et al. demonstrated favourable outcomes, the pre-clinical nature of the study did not involve actual liver transplants (221). A thorough assessment of the safety profile for the suggested 'defatting cocktail' is essential before it can be adopted in clinical settings. Some components of the 'defatting cocktail' are yet to be fully evaluated for safety, despite some in vitro tests on cytotoxicity (151). Hypericin, found in St John's Wort, plays a role in enhancing the activity of the cytochrome P450 3A4 enzyme, which is crucial in metabolising drugs including cyclosporine and tacrolimus (223). Furthermore, the peroxisome proliferator-activated receptor agonists, GW501516 and GW7647, have yet to undergo human trials, with existing animal studies raising concerns about potential carcinogenic effects (224). A summary of early pre-clinical studies is provided in Table 1.6.

Table 1.6. Summary of defatting interventions and effect on MaS (216,217,219–222)

Ref.	Defatting interventions	Model	Total ex-situ perfusion time (h)	Absolute percentage (%) reduction in macrovesicular steatosis (MaS)
Nagrath et al, 2009	GW501516, GW7647, forskolin, hypericin, visfatin and scorparone	Zucker rats (*n* = 12)	3	50
Jamieson et al, 2011	NMP alone	Porcine (*n* = 8)	48	13
Raigani et al, 2019	GW501516, GW7647, forskolin, hypericin, visfatin, scorparone and L-carnitine	Zucker rats (*n* = 18)	6	33
Banan et al, 2016	L-carnitine and exendin-4	Discarded human livers (*n* = 2)	8	10
Liu et al, 2018	NMP alone	Discarded human livers (*n* = 10)	24	-
Boteon et al, 2019	GW501516, GW7647, forskolin, hypericin, visfatin, scorparone and L-carnitine	Discarded human livers (*n* = 10)	6 12	40 50

Ceresa et al. (225) have recently described outcomes of a study involving 18 human discarded steatotic livers subjected to 48 hours of NMP. Whilst designing the study the authors addressed some of the limitations of previous defatting studies with consideration of requirements of translation into a subsequent clinical trial. This included use of readily available pharmacological agents, licenced for human use (albeit off-label) and with avoidance of pharmacological agents that would require extensive testing and optimisation prior to use in the setting a clinical trial. The study involved three groups: NMP alone (n = 6), NMP plus a lipid apheresis filter (n = 6), and NMP with a lipid apheresis filter and the adjunct of defatting agents including L-carnitine, water soluble forskolin (NKH477), and glucose/insulin reduction (to reduce *de novo* lipogenesis), (n = 6). The use of the apheresis filter led to lowered triglyceride and cholesterol levels in the perfusate. Incorporating defatting agents promoted fatty acid β-oxidation and resulted in decreased steatosis, as evidenced by tissue triglyceride measurements and a significant reduction in the amount of fat within the liver by 45% at 48 hours. Whilst none of these livers were transplanted, structural and functional improvements were evident following 6 hours of perfusion. These improvements, reflected in enhanced perfusion and biochemical parameters that would have rendered these livers transplantable based on current functional criteria, suggest that these organs could meet the current criteria for transplantation. The results suggest a minimum of 6 hours of perfusion is necessary for functional assessment in order to assess suitability for transplantation. The logical next step following the discarded liver study above, is to test the same therapeutic combination in a clinical trial: this is part of the work described in this thesis (see Chapter 6) (179).

Further research on discarded steatotic human livers has been explored by Da Silva et al. (226) who have recently published on defatting ex-situ over multi-day perfusions. In this study, a total of 51 liver grafts were included (23 discarded liver grafts and 28 partial livers obtained from hepatic resections) and were subjected to NMP. Out of 51 liver grafts, 20 were steatotic with MaS up to 85% and were subjected to NMP for as long as 12 days. Of these, half showed a significant reduction in steatosis and the remaining half showed no change. The authors attributed defatting as a consequence of extended perfusion duration, regulated glucose levels, tailored nutrition and supplementation with L-carnitine and fenofibrate. The majority of liver grafts maintained their synthetic and metabolic functions throughout the perfusion period.

1.7 Adding objectivity to current functional liver assessment during NMP

Hepatic function assessment during NMP is dependent on monitoring of functional parameters during NMP such as lactate clearance and bile production. However, the effectiveness of these specific parameters is limited due to their inability to consistently differentiate between donor livers that function well and those that do not (227,228). Consequently, there is a vital need for more dependable functional assessments to evaluate liver functional capacity during NMP. Notably, the metabolic functional (as opposed to injury) assessment of NMP livers in current clinical practice is based on relatively uncontrolled measures of lactate clearance and glucose consumption. A more quantifiable assessment of hepatocellular function may provide a more consistent means to define a viable liver.

1.7.1 LiMAx

Assessing the activity of cytochrome p450 (CYP) enzymes might provide insights into core hepatocellular function. These enzymes are responsible for metabolising a variety of substances, including steroids, fatty acids and xenobiotics (229). The Maximum Liver Capacity (LiMAx test, Humedics GmbH) allows real-time monitoring of CYP1A2 (prominent in functional livers cells and less prominent in damaged cells) and is based on the metabolism of 13C-methacetin into $^{13}CO_2$ and paracetamol (acetaminophen). The $^{13}CO_2$ in exhaled air can be quantified and compared to $^{12}CO_2$. From this, a LiMAx value is derived based on the $^{13}CO_2$:$^{12}CO_2$ ratio (230). The technology has been used to measure functional liver capacity in patients with liver tumours and those undergoing major liver surgery/transplant in order to predict and monitor post-operative outcomes (230–233). A LiMAx value exceeding 315 µg/kg/h signifies normal hepatic function, while a score under 140 µg/kg/h reflects impaired liver function, associated with a 40% mortality risk following major liver resection (231).

In the context of NMP, the LiMAx test may provide useful point-of-care information to support functional assessment for transplantation (234). The LiMAx test utilises a substrate that is known to be metabolised by all segments of the liver thereby providing a more objective and global assessment of liver function during ex-situ perfusion: this contrasts with conventional liver function tests that only provide an indication of liver injury/damage. In the future, such a test could become standard of care during NMP and increase the number of safe and successful transplants. The use of this test in the context of NMP is described in Chapter 7.

1.7.2 MEGX

The hepatic conversion of lidocaine to monoethylglycinexylidide (MEGX) can be used as a dynamic liver function test to provide additional prognostic information, which can supplement existing static liver function assays. Historically, the MEGX test was used clinically for real-time assessment of liver function in transplantation and critical care medicine. However, this test is no longer widely used in clinical practice due to various factors including complex kinetics, potential drug interactions and insufficient data to support its prognostic value (235). Lidocaine undergoes primary metabolism in the liver through successive oxidative N-dealkylation, predominantly mediated by the liver cytochrome P450 system (specifically through CYP3A4 activity) (236). The major first metabolite in humans is known as MEGX. The liver function test is influenced by both the hepatic metabolic capacity and the hepatic blood flow due to the comparatively high extraction ratio of lidocaine. The majority of published research indicate that the MEGX test is a valuable tool that can enhance decision-making process when selecting liver transplant candidates. Patients who have a MEGX 15 or 30 minute test value below 10 μg/L are at risk of pre-transplant non-survival (236,237). There is a paucity in the literature regarding application of MEGX during NMP and its ability to supplement current functional tests therefore warrants further investigation (238). The use of this test in the context of NMP is described in Chapter 7.

1.7.3 ICG

Indocyanine green (ICG) is a non-toxic inert water soluble tricarbocyanine dye and is fluorophore that absorbs near-infrared light within the 790–805 nm range and emits fluorescence at 835 nm (239). The use of ICG was established as early as 1961 and the elimination rate has been used as a measure of liver function and hepatic blood flow. ICG is almost exclusively extracted by the hepatic parenchymal cells (independent of ATP) and excreted via an ATP-dependent transport system into the bile unconjugated (240,241). In the context of LT, the ICG clearance test can provide a quantitative measure of liver function prior to transplantation. Tang et al. identified that donor ICG retention rate at 15 minutes (ICGR15) before procurement was independently predictive of three-month post-transplant survival, with an optimal ICGR15 threshold of 11%/min to guide utilisation decisions (242). In a porcine DCD NMP model, Dondossola et al. measured ICG levels in perfusate and bile samples. A decrease in perfusate ICG and an increase in bile ICG correlated with less injury on histological evaluation (243). More recently, Lau et al. have assessed the use of ICG in discarded human

livers subjected to NMP for a median of 7.2 days and have demonstrated the ability of ICG plasma disappearance rate (PDR) to distinguish between short and long-surviving grafts over the course of perfusion (243). If translated into clinical practice, the ICG clearance test holds promise for future functional assessment due to its safety and ease of use. The use of this test in the context of NMP is described in Chapter 7.

1.8 Overview and aims

The success of liver transplantation is critically limited by the increasing disparity between the demand and supply of suitable donor livers. This shortage has necessitated the use of extended criteria donor (ECD) livers and in turn has catalysed the clinical implementation of normothermic machine perfusion (NMP) which aims to enhance liver preservation and mitigate the impact of cold ischaemic injury on graft viability. However, it remains uncertain if NMP alone is sufficient to reduce the risk profile of ECD livers which are particularly sensitive to the process of ischaemia-reperfusion injury (IRI). Within this thesis, I explore the utility of NMP as a platform for targeted therapeutic interventions and enhanced functional assessment to further optimise ECD livers (i.e. those with hepatic steatosis and DCD status) to meet functional criteria for transplantation. The aims of this thesis are to:

- Explore the utility of pre-retrieval donor predictors including anthropometric measures, clinical risk scores and biochemical tests in the early identification of livers with evidence of hepatic steatosis in order to guide preservation strategies (Chapter 3)
- Investigate clinical outcomes of recipients transplanted with steatotic livers preserved with NMP and SCS compared to lean counterparts and explore the impact of NMP on IRI (Chapter 4)
- Explore tissue proteomic signatures of steatotic livers preserved with NMP and SCS compared to lean counterparts and identify the impact of preservation technique on molecular, cellular and biological pathways (Chapter 5)
- Facilitate the clinical adoption of NMP as a therapeutic platform to optimise steatotic donor livers for transplantation by investigating the safety and assessing the efficacy of defatting during NMP in the setting of a multicentre randomised clinical trial (Chapter 6)

- Explore the role of hypoxia-inducible factor modulation as an adjunct to defatting during NMP in order to enhance ex-situ defatting and mitigate ischaemia-reperfusion injury (Chapter 7)
- To explore the role of ex-situ damage-associated molecular pattern (DAMP) removal to mitigate ischaemia-reperfusion injury in an ex-situ model of DCD liver transplant (Chapter 8)

Chapter 2: General Methods

The methods described in this chapter have been commonly used within the context of this thesis. Additional methods pertinent to individual chapters are described in the methods section of those chapters.

2.1 Normothermic machine perfusion (NMP)

2.1.1 The OrganOx *metra* for normothermic liver perfusion

All normothermic liver perfusions described within experimental chapters of this thesis were performed using the 2nd Generation OrganOx *metra* (OrganOx Ltd, Oxford, UK) NMP device (Figure 2.1). The commercially available OrganOx *metra* is a CE-marked device, licenced for use (up to 24 h) and is also FDA approved (for use up to 12 h) in the clinical setting of normothermic liver perfusion (206,207).

Figure 2.1. The OrganOx *metra* (2nd Generation) for normothermic machine perfusion (NMP) of the liver.

The device enables ex-situ normothermic perfusion of the liver in a closed automated system through cannulation of the hepatic artery (HA), portal vein (PV) and inferior vena cava (IVC). The core components of the device comprise of: (i) a centrifugal pump; (ii) heater/oxygenator; (iii) blood (perfusate) reservoir and; (iv) a blood gas analyser. Arterial flow is non-pulsatile, delivered continuously with automated pressure control between 60-75mmHg (244,245) (Figure 2.2).

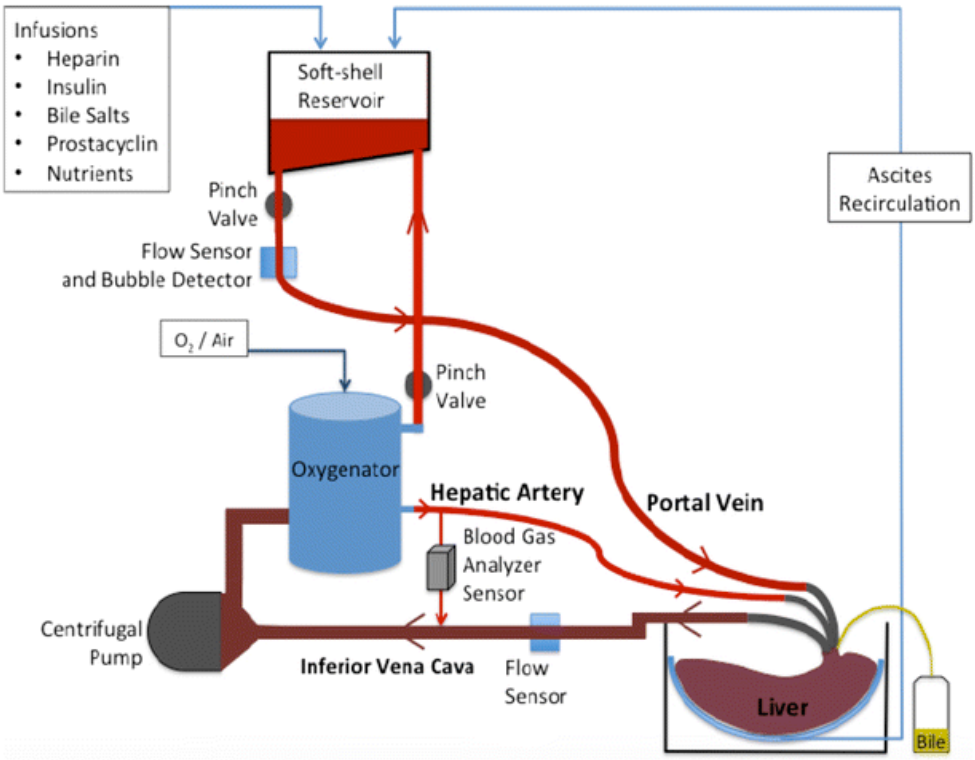

Figure 2.2. The OrganOx *metra* circuit: The liver is situated in the liver bowl and is cannulated via the hepatic artery (HA), portal vein (PV) and inferior vena cava (IVC). Blood (perfusate) exits the liver via the IVC cannula (traversing through a flow sensor) before reaching the centrifugal pump. Perfusate is pumped via the centrifugal pump to a disposable Extracorporeal Membrane Oxygenation (ECMO) oxygen concentrator within the disposable perfusion circuit. This is a stand-alone device (within the tower of the disposable perfusion circuit) that extracts oxygen from air and allows for the perfusate to be warmed to 37°C and oxygenated to a partial pressure of oxygen (pO2) between 12-18kPa . Perfusate inflow back to the liver is via two routes: (i) directly to the liver via the hepatic artery line/cannula (low flow and high pressure) and; (ii) to the soft-shell portal reservoir (via a line that has a variable-setting pinch valve to regulate arterial pressure) before flowing back to the liver (traversing through a flow sensor) via the portal vein line/cannula (at high flow and low pressure). Portal pressure is dictated by the height of the reservoir fluid level relative to the liver. A second portal pinch valve (non-variable) serves as a safety mechanism to prevent air entering the liver i.e. secondary to inadequate liver haemostasis causing the soft-shell portal reservoir to empty. Air detected by the portal flow sensor will cause this pinch valve to completely occlude, allowing the portal soft-shell reservoir to refill and preventing air entry into the liver. Any blood collected in the liver bowl (secondary to bleeding from the liver) is recirculated to the soft-shell portal reservoir via a roller pump at a rate of 120-140ml/min. The bile duct is also cannulated, and bile drains into a separate chamber within the liver bowl (passing through a flow sensor) with bile flow recorded in ml/h. Bile can also be collected manually without connection to the flow sensor. Real time blood gas monitoring (using an in-built Terumo shunt sensor)

is enabled via a shunt between the hepatic artery and inferior vena cava line. This allows for continuous monitoring of pO2, pCO2 and pH during perfusion. Figure reproduced with permission from Elsevier (206).

2.1.2 Perfusate solutions

The OrganOx *metra* is primed following device set-up and calibration of the blood gas analyser. This allows for optimal perfusate conditions to be met prior to commencement of perfusion i.e. temperature (37ºC), pO2 (12-18 kPa), pCO2 (4-6 kPa) and pH (7.25 – 7.35). Whilst in prime mode, the donor liver is benched and cannulated ready for connection to the device. Perfusate components are described below:

2.1.2.1 Blood

The circuit was primed with 3 units of donor/recipient-matched or group O packed red blood cells (pRBCs) as an oxygen carrier. Normalisation of haematocrit and osmolarity was achieved through addition of a colloid solution i.e. 500ml Gelofusine (B Braun, Sheffield, UK). For clinical normothermic liver perfusions within the context of randomised clinical trials pRBC units were sourced from blood banks at either the donor (Chapter 4) or recipient (Chapter 6) hospitals, respectively. For pre-clinical research human liver perfusions (Chapter 7), recently expired pRBC units were sourced from the blood bank at John Radcliffe Hospital, Oxford or purchased from non-clinical issue surplus (Filton, Bristol, UK).

2.1.2.2 Boluses

Boluses were administered directly to the soft-shell portal reservoir during priming of the circuit (before commencement of liver perfusion) and comprised of:

- 10% calcium gluconate (B Braun), 10mls for correction of calcium binding
- 10,000 IU unfractionated heparin sodium (Wockhardt UK Ltd, Wrexham, UK), for prevention of thrombosis
- 750mg of cefuroxime (Flynn Pharma Ltd, Dublin, Ireland) or 500mg Meropenem (Pfizer, Kent, UK) in porcine perfusions were administered for prevention of bacterial overgrowth. In Chapter 6, antibiotic and antifungal agents were delivered as per current local hospital protocols.
- 8.4% sodium bicarbonate (B Braun), 30mls for normalisation of perfusate pH prior to connection of the liver and commencement of perfusion

2.1.2.3 Continuous infusions during perfusion

Infusions solutions were delivered to the soft-shell portal reservoir at 1ml/h via automated integrated pumps (n = 4). All infusion solutions were made up to 30ml with 0.9% sodium chloride (B Braun):

- 25,000 IU unfractionated heparin sodium (Wockhardt UK Ltd) for prevention of thrombosis
- 200 units insulin (Actrapid) (Novo Nordisk, West Sussex, UK) for glucose control
- 4.5g sodium taurocholate (bovine bile salt) (OrganOx Ltd) to replace exogenous bile salts
- 0.5mg epoprostonol sodium (Flolan®) (Glaxo, Middlesex, UK) for optimisation of microperfusion

Total parenteral nutrition (TPN) (Nutriflex Special, B Braun), a source of glucose and amino acids for liver maintenance, was infused at a rate of 4ml/h when the perfusate glucose level fell below 10mmol/L.

2.1.2.4 Graphical user interface (GUI)

The graphical user interface (GUI) allows for real-time monitoring of the perfusion providing information on pressure and flow dynamics. The arterial flow is not directly measured and is derived as a difference between portal and IVC flow. Other GUI features include (Figure 2.3):

- pH and blood gas analyser values: updated every 10 seconds
- Glucose values: measured and inputted every 4h (manually) to regulate the TPN infusion
- Bile production: updated every hour

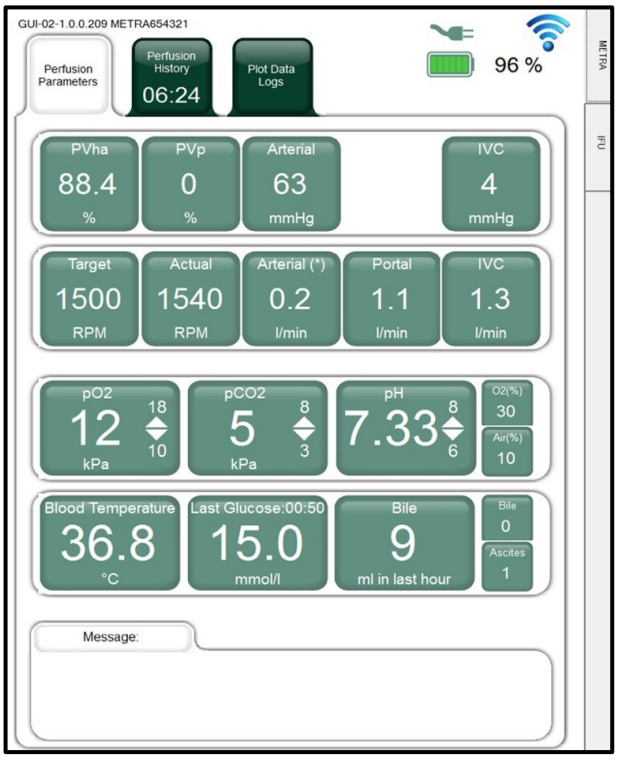

Figure 2.3. Graphical user interface (GUI) for real-time monitoring of perfusion metrics

2.2 Liver preparation and cannulation

During multi-visceral deceased donor organ retrieval (246), all donor livers were flushed (in-situ cold perfusion) with University of Wisconsin (UW) (Bridge to Life, London, UK) solution. On completion of donor hepatectomy, livers were benched and cannulated either at the donor hospital (device-to-donor) without cold-storage and placed on the OrganOx *metra* (Chapter 4) or transported on ice (static cold storage, in UW solution) back to the recipient hospital and there placed on the OrganOx *metra* (back-to-base, Chapter 6).

2.2.1 Liver bench-work

Donor livers were benched as described by Makowka et al (247) in preparation for liver cannulation. Briefly, the retro-hepatic IVC was dissected free from surrounding non-hepatic tissue and the adrenal vein was ligated. Tissue adherent to the posterior aspect of the liver was removed and the supra-hepatic IVC was dissected free from any diaphragm remnants. Following identification and ligation of phrenic vein orifices, the suprahepatic IVC was oversewn with a 4'0 prolene suture (Ethicon, Johnson & Johnson Medical Devices, Wokingham, UK). The portal vein was dissected free from surrounding tissue to demonstrate the portal bifurcation. Following initial inspection for any aberrant arterial anatomy, dissection

of the common hepatic artery and coelic trunk was performed to the level of the gastroduodenal artery (GDA) with suture ligation of small branches and any residual lymphatic tissue. Anomalous hepatic arteries were identified and preserved for arterial reconstruction prior to cannulation. Following closure of the gallbladder and cystic duct suture ligation, only minimal dissection to the common bile duct (CBD) was performed prior to cannulation.

2.2.2 Liver cannulation

A 2'0 prolene suture was used for a purse-string suture around the infra-hepatic IVC for placement of a 28 Fr bespoke IVC cannula (Sorin, Gloucester, UK). The portal vein and coelic trunk were cannulated with 20 and 10 Fr cannulae (Sorin, Gloucester, UK) respectively and secured with 2'0 vicryl ties (Ethicon). Depending on the diameter of the CBD, cannulation was performed using a 12-18 Fr T-tube (Summit Medical, Cheltenham, UK) and secured with a 2'0 vicryl tie (Ethicon). On completion of cannulation, the liver was primed (initially through the portal cannula followed by the arterial cannula) with 0.5-1L of Gelofusine (B Braun) in order to remove any residual air pockets prior to connecting the liver to the OrganOx *metra* (Figure 2.4).

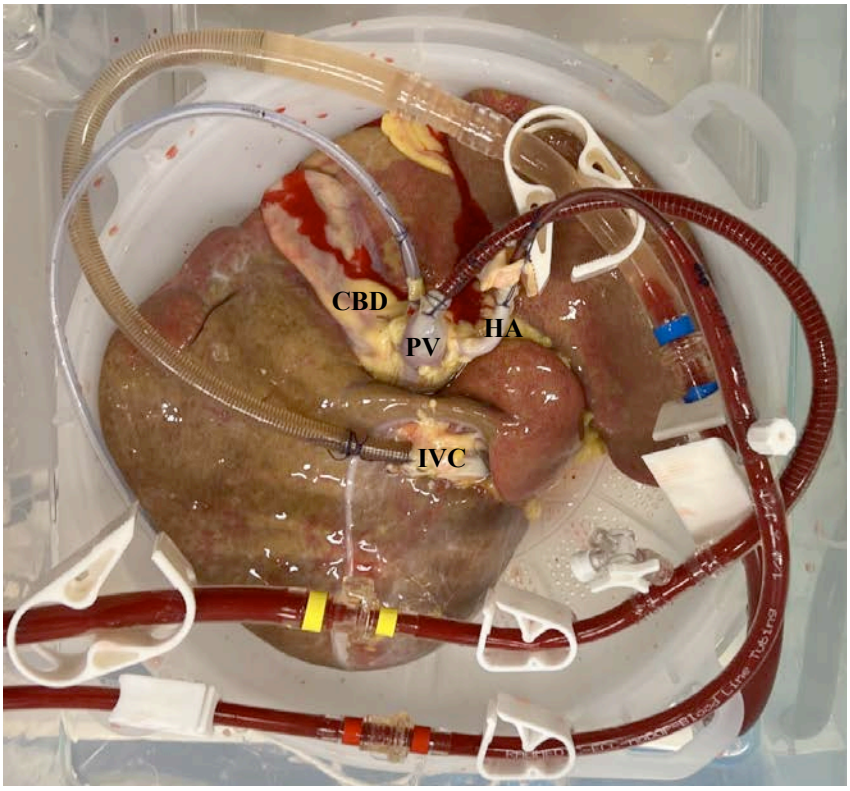

Figure 2.4. Prepared and cannulated liver prior to the commencement of NMP: The inferior vena cava (IVC), portal vein (PV) and hepatic artery and common bile duct (CBD) are cannulated.

2.3 Liver tissue preparation and staining

2.3.1 Tissue acquisition

The liver biopsies described in this thesis were obtained using a the Biopince™ Full Core Biopsy Instrument (Argon Medical Devices, Texas, USA). The instrument has a 33mm throw length which yields a 29mm specimen length. Following acquisition of biopsies, the specimens were fixed on 10% formalin and stored at 4^{o}C or snap frozen using liquid nitrogen with subsequent storage at -80^{o}C for use in mechanistic studies.

2.3.2 Paraffin-embedding of formalin-fixed tissue

Formalin-fixed biopsies were transferred to cassettes and washed in phosphate buffered saline (PBS) (Sigma-Aldrich, Dorset, UK) prior to being automatically processed through 70% to 100% methanol (VWR International Ltd, Leighton Buzzard, UK), xylene (Fisher Scientific UK Ltd, Loughborough, UK) and paraffin (VWR International Ltd) using a Leica TP1020 automatic tissue processor (Leica Biosystems, Newcastle, UK) in order to fix, dehydrate and infiltrate the biopsy specimens. Melted paraffin was used to embed the tissue into blocks and subsequently allowed to cool prior to storage.

2.3.3 Tissue sectioning

Formalin-fixed paraffin-embedded (FFPE) blocks were sectioned at 3µm thickness using a microtome (Leica Biosystems, Newcastle, UK) for general histological staining and at 4µm thickness for immunohistochemical (IHC) staining. The sections cut onto superfrost plus microslides (VWR International Ltd, Leighton Buzzard, UK).

2.3.4 Haematoxylin & Eosin (H&E) Staining

2.3.4.1 Principle

Haematoxylin is a deep blue stain (positively charged) which binds basophilic molecules, such as DNA/RNA, which are acidic and negatively charged. Eosin is a pink, acidic stain that binds to positively charged acidophilic components in tissue such as amino side chains (lysine and arginine) in the cytoplasm (248).

2.3.4.2 Method

Processing of slides was performed using the automated Leica ST 5020 Multistainer. Slides were processed through 2x2 min washes of xylene (Genta Medical Ltd, York, UK) to dewax specimens. Sections were rehydrated in 4x30 secs washes of Industrial Denatured Alcohol (IDA, 100%, 100%, 95% and 70%) (Genta Medical Ltd, York, UK). After rinsing the slides in water for 30 secs, they were placed in haematoxylin (Leica Biosystems, Newcastle, UK) for 8 minutes and subsequently rinsed in water for 30 secs. Acid Alcohol 1% (Atom Scientific, Cheshire, UK) was applied for 2 secs and the slides were rinsed in water for a further 30 secs followed by application of Scott's tapwater substitute (Atom Scientific, Cheshire, UK) for 1 min. Eosin (Atom Scientific, Cheshire, UK) was then applied for 5 mins and slides were rinsed in water for 30 secs. Sections were then dehydrated in ethanol with 4x30 secs washes (70%, 95%, 100% and 100%) and cleared in 2x30 secs washes of xylene (Genta Medical Ltd, York, UK). The H&E-stained sections were subsequently mounted under a coverslip using the Leica CV5030 Robotic Coverslipper.

2.3.5 Periodic acid-Schiff (PAS) Staining

2.3.5.1 Principle

Periodic acid-Schiff (PAS) is a staining technique used for identification of polysaccharides (macromolecules, consisting of monosaccharide units linked by covalent bonds). The primary polysaccharide identified using the PAS stain is glycogen (249). The initial reaction involves periodic acid as an oxidising agent that oxidises the carbon-to-carbon bonds between two adjacent hydroxyl groups resulting in Schiff-reactive aldehyde groups. In the subsequent reaction, tissue reacts with Schiff reagent (comprising of basic fuchsin, hydrochloric acid and sodium metabisulphite) (249). The reaction of basic fuchsin with the aldehyde groups results in a bright magenta colour, the intensity of which is proportionate to the hydroxyl group concentration originally present with in the monosaccharide units (249). Haematoxylin is employed as a counter-stain to facilitate the visualisation of other tissue components.

2.3.5.2 Method

Slides were manually processed through xylene (Genta Medical Ltd, York, UK) and IDA (Genta Medical Ltd, York, UK) using steps described in section 2.3.4.2. Slides were then immersed in periodic acid solution (Leica Biosystems, Newcastle, UK) for 5 min and rinsed

with distilled water prior to immersion in Schiff solution (TCS Biosciences Ltd, Buckingham, UK) for 10 min. After washing in in tap water, slides were placed in haematoxylin (Leica Biosystems, Newcastle, UK) for 2 min and dipped in acid alcohol 1% (Atom Scientific, Cheshire, UK) for 2 secs, rinsed in water for 30 secs followed by application of Scott's tapwater substitute (Atom Scientific, Cheshire, UK) for 1.5 min. Slides were then dehydrated, cleared in xylene (as described in section 2.3.4.2) and mounted under a cover slip with distyrene plasticizer xylene (DPX) (Sigma-Aldrich, Dorset, UK).

2.3.6 Masson's Trichome

2.3.6.1 Principle

The Masson's trichrome stain is used to specifically visualise connective tissues. It utilises Weigert's iron hematoxylin to stain cell nuclei, ponceau fuchsin to stain muscle, cytoplasm, and red blood cells, and methyl blue to stain collagen. Post fixation with Bouin's solution enhances the staining of collagen and muscle fibres by increasing selectivity of the dyes, particularly when the initial staining is insufficient.

2.3.6.2 Method

Slides were manually processed through xylene (Genta Medical Ltd, York, UK) and IDA (Genta Medical Ltd, York, UK) using steps described in section 2.3.4.2, then incubated in Bouin's solution (Atom Scientific, Cheshire, UK) at 60°C for 1 hour and washed in running tap water for 10 min (to remove yellow colour). Masson Trichome Kit (Atom Scientific, Cheshire, UK) was prepared by mixing equal volumes of Haematoxylin Weigerts - Part A and Haematoxylin Weigerts – Part B with incubation of slides for 30 mins. Slides were washed in running tap water and differentiated in 1% acid alcohol solution and then rinsed with distilled water prior to application of Ponceau Fuchsin Masson Solution for 5 min. Subsequently, slides were further rinsed with application Phosphotungstic Acid 1% Solution for 15 mins and transferred without rinsing to 2% Methyl Blue solution for 5 mins. Following this, slides were rinsed in water and then dehydrated, cleared in xylene (as described in section 2.3.4.2) and mounted under a cover slip with distyrene plasticizer xylene (DPX) (Sigma-Aldrich, Dorset, UK).

2.3.7 Picrosirius RED

2.3.7.1 Principle

The combination of yellow picric acid dye (a small anionic and marginally hydrophobic compound) and Sirius Red (a large hyrdophillic red acid dye, combined with a metal complex cationic dye) provide the mechanism for staining collagen fibres and related tissues.

2.3.7.2 Method

Slides were manually processed through xylene (Genta Medical Ltd, York, UK) and IDA (Genta Medical Ltd, York, UK) using steps described in section 2.3.4.2. Weigert's haematoxylin was applied for 8 mins to stain nuclei and slides washed in running tap for 10 min. Subsequently, slides were stained in Picorsirius red solution (Sigma-Aldrich, Dorset, UK) for 60 min and washed in two changes of acidified water. Following this, slides were rinsed in water and then dehydrated, cleared in xylene (as described in section 2.3.4.2) and mounted under a cover slip with distyrene plasticizer xylene (DPX) (Sigma-Aldrich, Dorset, UK).

2.3.8 Immunohistochemistry

Liver tissue sections (4μm thickness) from formalin-fixed, paraffin embedded blocks were tested for the presence of anti-HIF-1α (ab16066, Abcam), anti-HIF-2α (D9E3, Cell Signal), anti-MPO (EPR20257, Abcam), anti-Histone H3 (CITH3, 14955, Abcam) and anti-HMGB1 (EPR35047, Abcam), primary antibodies using Bond Polymer Refine Detection DAB (Leica Microsystem, Bannockburn, Illinois). This detection system utilises controlled polymerisation technology to prepare polymeric HRP-linked antibody conjugate system for the detection of tissue-bound primary antibodies. The antibody concentrations used for each immunohistochemical stain are described in Table 2.1:

Table 2.1. Immunohistochemical stain antibody concentrations

Antibody	Antibody concentration
HIF-1α: Mouse monoclonal anti-HIF-1 alpha (ab16066, Abcam)	1/100
HIF-2α: Rabbit monoclonal anti-HIF-2 alpha (D9E3, Cell Signal)	1/200
MPO: Rabbit monoclonal anti-Myeloperoxidase (EPR20257, Abcam)	1/500
CITH3: Rabbit polyclonal anti-Histone H3 (Ab5168, Abcam)	1/500
HMGB1: Rabbit monoclonal anti-HMGB1 (EPR3507, Abcam)	1/500

The detection system avoids the use of streptavidin and biotin, and therefore eliminates non-specific staining, as a result, of endogenous biotin. All steps were performed on the Leica Bond III automated system (Leica Microsystems) with exception of HIF-1α and HIF-2α stains which were performed manually. Tissue sections were deparaffinised (Dewax Solution, AR9222, Leica Biosystems) and antigen retrieval carried out on the instrument for 20 minutes using Heath Mediated (Bond Epitope retrieval Solution 2 (ER2), AR9640, Leica Biosystems).

The slides were incubated with the primary antibody for 15 minutes, post primary for 8 minutes, mixed chromogen (DAB) refine for 10 minutes, and haematoxylin as counter stain for 5 minutes. These incubations were performed at room temperature.

Between incubations sections were washed with buffered Bond washed solution (Wash Solution AR9590, Leica Biosystem). The stained slides were dehydrated on Autostainer (Leica Microsystem, Bannockburn, Illinois) and coverslipped using Leica CV5030 fully automated coverslipper. Known positive tissue section controls were run in parallel with the actual liver core tissue sections. For negative controls, the primary antibody tested was omitted and replaced with Tris buffer. This was done to eliminate false positive results.

2.4 Digital image analysis

2.4.1 Hepatic steatosis quantification

2.4.1.1 Reveal Biosciences

In Chapter 3, hepatic steatosis (HS) was quantified using imageDx™ (RevealBiosciences, USA) artificial intelligence (AI)-based rapid automated image analysis digital assay. Haematoxylin and Eosin (H&E) stained slides digitised a 3DHISTECH PANNORAMIC™ series scanner (Epredia) by RevealBiosciences (USA). The commercially available imageDx™ digital assay (RevealBiosciences, USA) which provides the total percentage of lipid accumulation within an entire H&E stained section and an algorithm derived score (0-3) for HS severity: none=0, mild=1, moderate=2 and severe steatosis=3. This artificial intelligence (AI)-based rapid automated image analysis platform has been co-developed with histopathologists to provide precise, consistent machine and deep learning trained on several thousand image patches and has been validated for human liver tissue. The workflow involves upload of digitised whole slide images (WSI) on the imageDx™ cloud for analysis. This

platform features in-built quality control to identify and exclude debris, artefacts, tears and out-of-focus regions (Figure 2.5) (250).

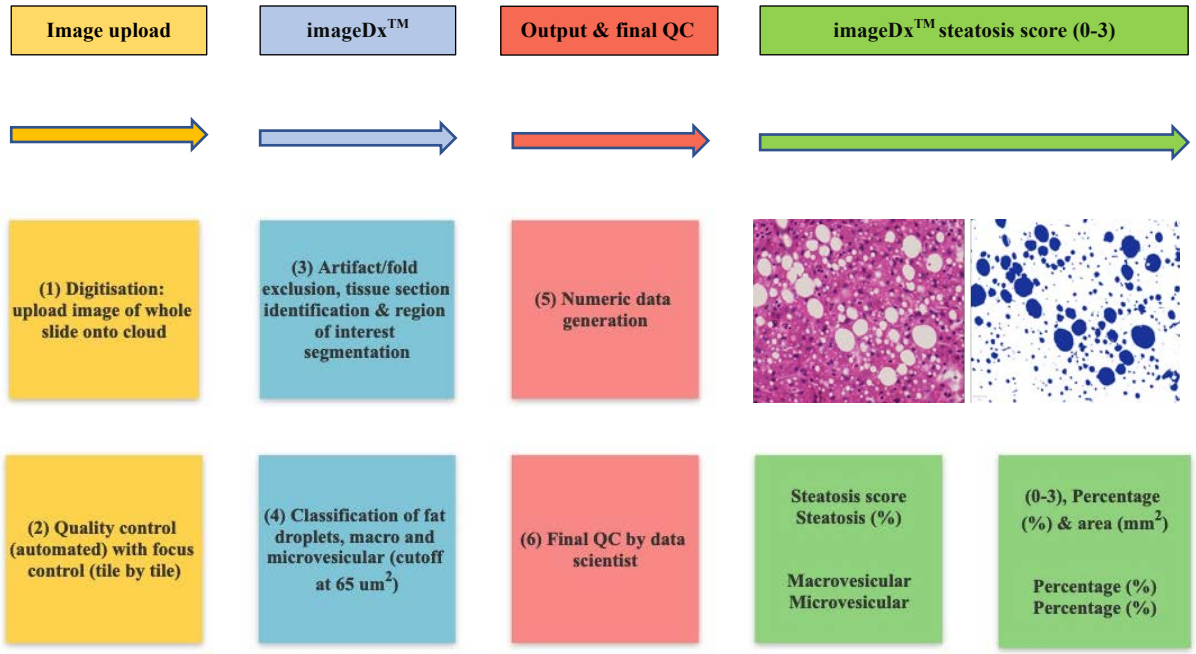

Figure 2.5. imageDx™ workflow quantification of HS. Positive lipid regions (steatotic areas) are identified by overlay of blue mask to produce quantitative outputs including steatosis scores (0-3), % lipid area, total lipid area (mm^2), % microvesicular steatosis, % macrovesicular and mean vesicle size (μm^2).

2.4.1.2 Visiopharm®

In Chapters 4 and 7, in addition to the formal histopathologist report, HS was also quantified using the Visiopharm® AI-based rapid automated image analysis digital assay (Visiopharm® Ltd, Egham, UK). This application is validated for the quantification of small and large droplet macrovesicular steatosis i.e. sd-MaS and ld-MaS (Visiopharm® application 10119, H&E liver steatosis). The H&E stained slides were digitised using the Hamamatsu NanoZoomer 2.0-HT whole slide imager (Hamamatsu UK Ltd, Welwyn Garden City, UK). The Visiopharm® Integrator System (VIS) platform version 2023.01 was used to analyse digitised slides. Image analysis protocols are implemented as Analysis Protocol Packages (APP) in VIS. Several APPs were designed to quantify droplets in H&E slides. Prior to the image analysis, it is important to outline the Region of Interest (ROI), a number of auxiliary APPs were designed to detect ROIs.

The first auxiliary APP runs on the slide using threshold classification that identifies the tissue ROI. The second auxiliary APP runs on the slide using DeepLabv3 network of the VIS AI module that identifies and excludes regions that look similar to fat droplets i.e. liver sinusoids (Figure 2.6A). The droplet detection APP runs on 10X on the H&E slides using the linear Bayesian method of classification that identifies small and large droplets (Figure 2.6B). Several post-processing steps are performed including applying unbiased counting frames to avoid the droplets that are intersecting with neighbouring tile boundaries counted twice (or more) and setting the minimum threshold of 250 square micrometre (μm) for classifying the large droplets. The quantitative output variables obtained from this APP include a described in Table 2.2 and demonstrated in Figure 2.6C:

Table 2.2. Visiopharm® application 10119 (H&E liver steatosis) quantitative output variables

Quantitative output	**Definition**
sd-MaS Count	Number of small-droplets inside the liver tissue
ld-MaS Count	Number of large-droplets inside the liver tissue
Fat Percentage	Total fat percentage
sd Percentage	Percentage of sd-MaS inside the tissue area
ld Percentage	Percentage of ld-MaS inside the tissue area
Percentage sd of Fat	Percentage of sd-MaS of fat
Percentage ld of Fat	Percentage of ld-MaS of fat

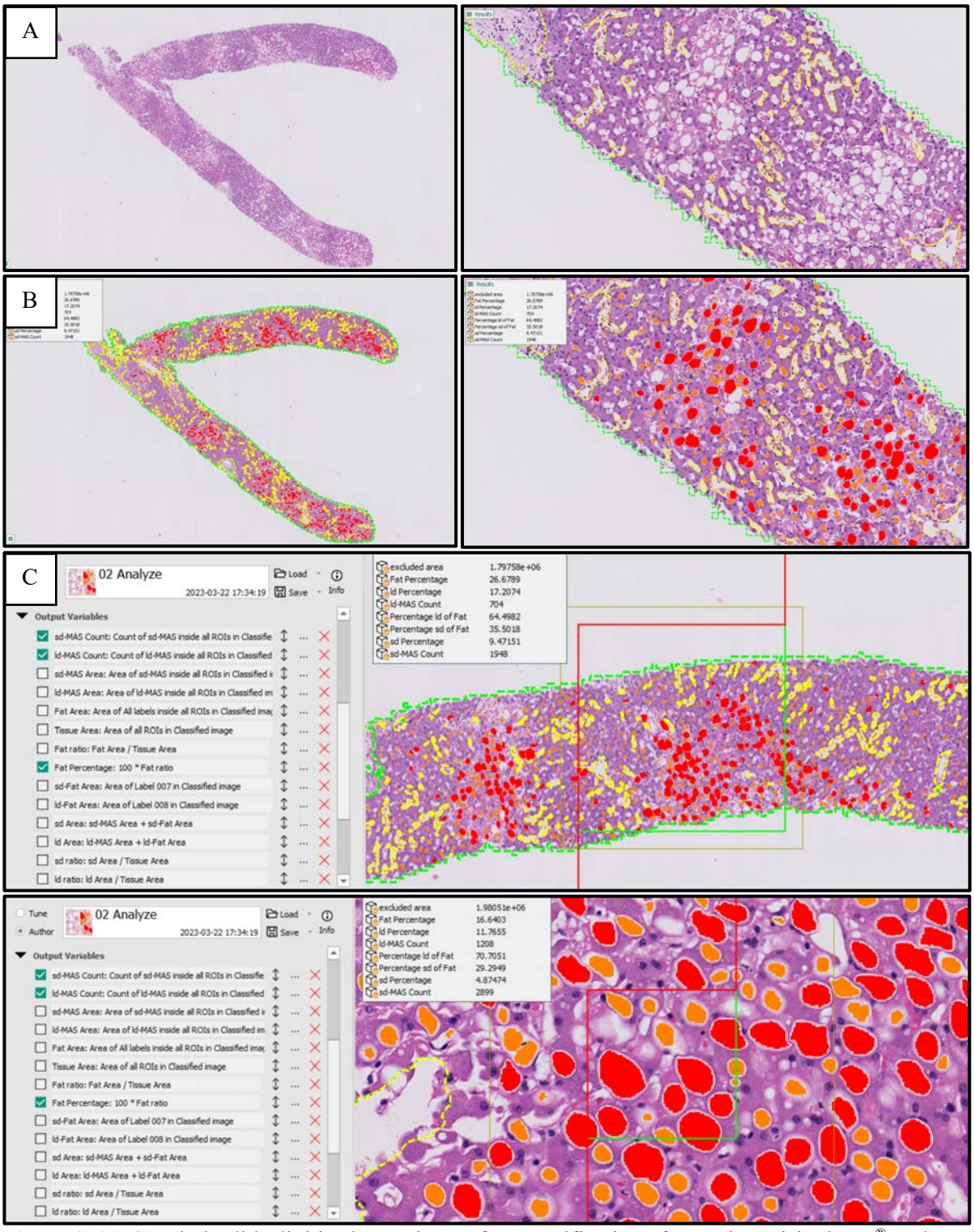

Figure 2.6A-C. Whole slide digitised H&E image for quantification of HS using Visiopharm® AI-based rapid automated image analysis digital assay (application 10119, H&E liver steatosis). The region of interest (ROI) is defined by the green line delineating the whole tissue section (first auxiliary APP) and yellow lines within the ROI delineate segments from the biopsy for exclusion i.e. liver sinusoids (second auxiliary APP) **(A)**. The droplet detection APP (application 10119, H&E liver steatosis) identifies lipid droplets within the whole tissue section and characterises them by size and shape. Large droplet macrovesicular steatosis (ld-MaS) is labelled red and small droplet macrovesicular steatosis (sd-MaS) is labelled orange **(B)**. Post-processing thresholds are applied to distinguish lipid droplets by their size and shape. The quantitative output variables obtained include (but are not limited to) sd-MaS percentage, ld-MaS percentage and total fat percentage **(C)**.

2.4.2 Immunohistochemistry quantification

In Chapter 8, a bespoke immunohistochemistry (IHC) APP was created using the U-Net convolutional neural network of the AI module within Visiopharm® (version 2023.01) to quantify IHC slides at 40x. Following identification of the tissue ROI (as described in section 2.4.1.2) and application of the bespoke IHC APP, several post-processing steps are performed including applying unbiased counting frames to avoid the cells that are intersecting with neighbouring tile boundaries counted twice (or more) (Figure 2.7).

The quantitative output variables obtained from this APP include:

- Positive Cell Count: The number of positive cell inside the liver tissue
- Tissue Area: The area measurement of total liver tissue area
- Positive Cell Density: The number of positive cell divided by the area of total liver tissue area

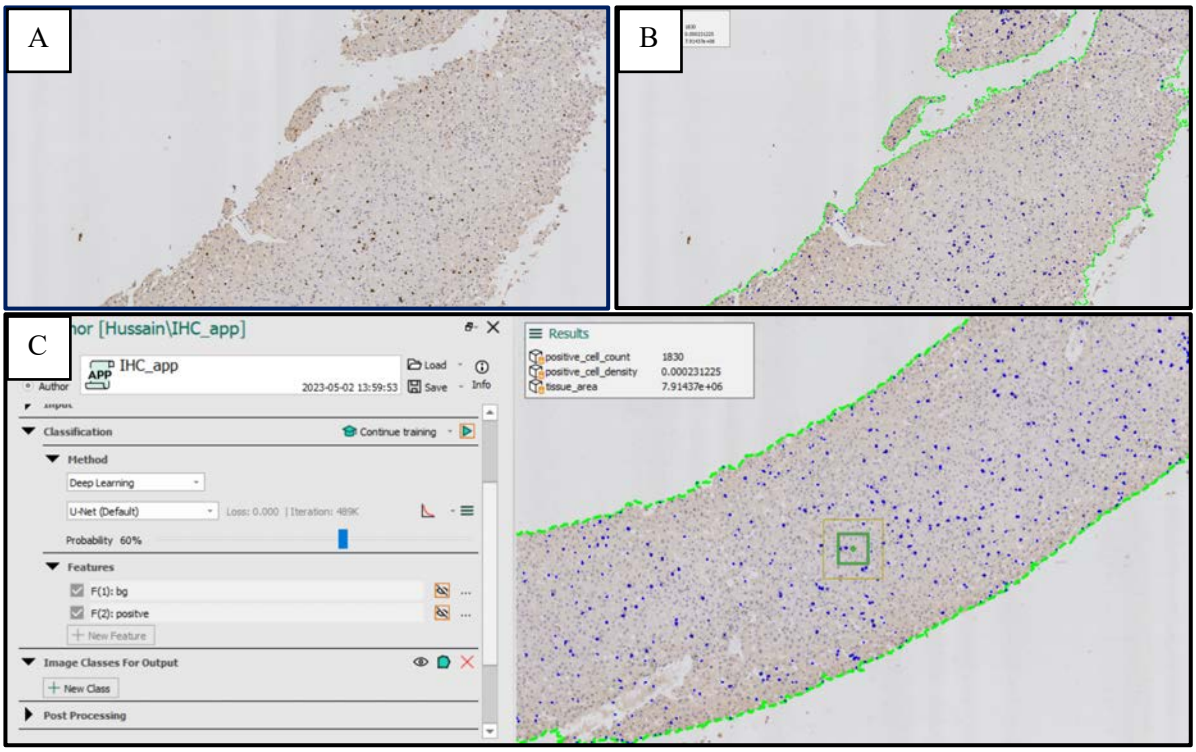

Figure 2.7A-C: Whole slide digitised immunohistochemistry (IHC) image for quantification of positively stained cells. The region of interest (ROI) is defined by the green line delineating the whole tissue section **(A)**. The bespoke IHC Visiopharm® IHC APP identifies positively stained cells within the whole tissue section. The positively stained cells are labelled blue **(B)**. Post-processing thresholds are applied to quantify the overall positive cell count, tissue area and positive cell density (μm^2) **(C)**.

2.5 Perfusate analysis and sampling

During all perfusions described in this thesis, perfusate sampling was performed from the arterial sampling port on the *metra*, located on the shunt between the hepatic artery and IVC. Perfusate samples were either tested immediately after collection on clinical ABL90 Flex or ABL800 Flex Analysers (Radiometer, Crawley, UK) for: pO2, pCO2, pH, haemoglobin (Hb), haematocrit (Hct), sodium (Na), potassium (K), calcium (Ca), lactate and glucose or processed and stored at -80^{o}C for future analysis. Prior to storage, perfusate was centrifuged at 3500rpm for 15 min at room temperature. Supernatant was aspirated and pipetted in 2ml aliquots and initially stored on dry ice and then at -80^{o}C.

2.5.1 Biochemistry

Perfusate samples collected during normothermic machine perfusion (NMP) studies were thawed, vortexed and analysed on a clinical biochemistry analyser via spectrophotometry (Abbott Architect c8000, Abbott diagnostics, Illinois, USA) at the Department of Clinical Biochemistry, John Radcliffe Hospital, Oxford. The relevant biochemical tests pertinent to each chapter are listed in Table 2.3.

Table 2.3. Perfusate biochemistry measurements for NMP studies

Biochemical test category	Chapter 4	Chapter 7	Chapter 8
Hepatocellular enzymes and injury	ALT (IU/L) AST (IU/L)	ALT (IU/L)	ALT (IU/L)
Cholangiocellular	GGT (IU/L) ALP (IU/L) Bilirubin (µmol/L) Bile salts (µmol/L)	X	X
Hepatic lipid metabolism	Total cholesterol (mg/dL) Total triglycerides (mg/dL) ApoB (g/L) 3-OHB (mmol/L)	Total cholesterol (mmol/L) Total triglycerides (mmol/L) 3-OHB (mmol/L)	X
General metabolism	Urea (mmol/L) Insulin (pmol/L)	X	X
Systemic inflammation and metabolic stress	CRP (mg/L)	CRP (mg/L)	X

2.5.2 Fibroblast growth factor 21

In Chapter 4, perfusate FGF-21 was measured by sandwich enzyme-linked immunosorbent assay (ELISA) according to manufacturer instructions (RD191108200R, Oxford Biosystems, Oxford, UK). Briefly, perfusate samples (100 µl in duplicate) were incubated for 1 h at 25°C (room temperature) in a 96-well microtiter plate pre-coated with polyclonal anti-human FGF-21 antibody and placed on an orbital microplate shaker (300 rpm). After washing steps, the level of FGF-21 was quantified by adding 100 µl of biotin-labelled polyclonal anti-human FGF-21 antibody for 1 h at room temperature and placed on an orbital microplate shaker (300 rpm). After another washing, 100 µl streptavidin- HRP conjugate was added to each well. After 30 min of incubation, the last washing step was performed and a peroxidase substrate: 3,3',5,5'-Tetramethylbenzidine (TMB) was added. The colorimetric reaction was stopped after 15 min by adding 100 µ1 of Stop Solution and optical densities of each well were read at 450 nm using a Multiskan™ microplate reader (Thermo Fisher Scientific, Inc). Where the levels remained above the detectable range, repeat analysis was performed in duplicate through multiple serial dilutions.

2.5.3 Cytokine multiplex

In Chapter 7, perfusate plasma samples (100 µl in duplicate) were analysed on the Luminex IS-200™ instrument for cytokines commonly implicated in hepatic IRI (251). A bespoke magnetic Luminex® assay kit (MILLIPLEX® MAP Human Cytokine Panel A, HCYTA-60K, Merck Life Science, LLC, Darmstadt, Germany) containing the analytes: IL-1β, IL-2, IL-6, IL-10 and TNF-α was used according to the manufacturer's instructions for use. Briefly, Luminex® products employ unique proprietary methods to internally colour-code microspheres with two fluorescent dyes. By adjusting the concentrations of these dyes, it is possible to produce distinctly coloured sets of microspheres, ranging from 500-5.6 µm in size for polystyrene microspheres and 80-6.45 µm for magnetic microspheres. Each set is coated with a specific capture antibody. Once an analyte from a sample binds to a bead, a biotinylated detection antibody is added. This is followed by incubation with a Streptavidin-PE conjugate, serving as the reporter molecule, to finalise the reaction on each microsphere's surface.

2.5.4 Extracellular chromatin

In chapter 8, perfusate nucleosomes including H3.1 and H3R8cit were measured using Nu.Q™ ELISA assays (Belgian Volition SRL, Isnes, Belgium) according to the manufacturer's instruction for use. Briefly, plasma samples (20 µl, in duplicate) were incubated at room temperature for 2h in a 96-well microtiter plate with a specific monoclonal antibody targeting either Histone H3.1 or a Histone H3R8cit epitope. Following the washing steps, quantification of nucleosomes levels was determined by addition of 100 µl of a horseradish peroxidase (HRP)-labelled anti-nucleosome antibody (directed to a nucleosome conformational epitope) with incubation for 90 minutes at room temperature. The wells were washed again prior to the addition of peroxidase substrate (TMB). The colorimetric reaction was stopped after 20 min by adding 100 µ1 of Stop Solution and optical densities of each well were read at 450 nm using a Multiskan™ microplate reader (Thermo Fisher Scientific, Inc.) Samples that exceeded the measurable range were further analysed with dilutions at Volition HQ's central lab (Isnes, Belgium) using the DYNEX DS2® automated ELISA system (Dynex Technologies, Denkendorf, Germany).

2.5.5 Indocyanine green

In Chapter 7, indocyanine green (ICG) clearance tests were performed as an adjunct to functional assessment during NMP as described by Liu et al. (238). Following injection of 6.25 ml of 0.1% ICG solution (Verdye™ ICG, Diagnostic Green, GmbH) into the perfusate reservoir, sequential perfusate samples were taken at 1 min, 5 min, 15 min, 30 min, 45 min, 60 min and up to 120 min post-injection. The perfusate serum samples were analysed (100 µl in duplicate) using the CLARIOStar® (BMG LABTECH) microplate reader for fluorescence intensity (FI) of ICG with excitation between 728-743 (728-15) nm and emission between 820-840 (820-20) nm i.e. 728-15/820-20 nm.

2.6 Bile sampling

Bile was collected via a T-tube inserted into the common bile duct. The biochemical analysis was conducted immediately after bile collection using point-of-care blood gas analysers i.e. either the ABL90 Flex or ABL800 Flex Analysers (Radiometer, Crawley, UK). The quantitative outputs included pH, haemoglobin (Hb), bicarbonate and glucose concentrations.

2.7 General statistical methods

All analyses (unless otherwise stated) in this thesis were performed using GraphPad Prism version 10.1.0 for Mac OS X, GraphPad Software, La Jolla California USA. The normality of data distribution for continuous variables was determined using a combination of the D'Agostino-Pearson and Kolmogorov-Smirnov normality tests, supplemented by Q-Q plots and graphical visualisation i.e. histograms. Parametric continuous variables were analysed using the Student's t-test and the Mann-Whitney U test (Wilcoxon rank-sum test) was used for non-parametric continuous variables. For categorical data, the Chi-square (X^2) test was applied. Comparative analyses of more than two groups were performed using one-way ANOVA (Kruskal-Wallis). Perfusion data between two groups were compared using either multiple unpaired t-tests or and mixed effect analysis for repeated measures with post-hoc tukey correction to adjust for multiple comparisons between timepoints. Survival data were analysed using the log-rank test. Pearson r test was used to test for correlation. Continuous variables were reported as either mean ± standard deviation (SD) or median (with range and/or interquartile range). A p value <0.05 was considered statistically significant.

Chapter 3: Prediction of hepatic steatosis prior to deceased donor retrieval

3.1 Introduction

The transplantation of livers with moderate-severe steatosis (>30% large-droplet macrovesicular steatosis, ld-MaS) has been associated with early allograft dysfunction (EAD), primary non-function (PNF) and reduced graft and patient survival (252–255). For this reason, donor livers with HS are frequently declined for transplantation. In addition, donors with a BMI >30kg/m^2 have increased from 23% to 29% in the last decade reflecting the ongoing obesity epidemic (12) and will continue to form a greater proportion of the donor pool. Early identification and optimisation of these organs may become valuable in directing specific interventions to improve utilisation and post-transplantation outcomes.

There are currently no validated methods to determine the degree of HS prior to retrieval. Whilst donor BMI may be a useful predictor of HS (256), other anthropometric measures, clinical risk scores and biochemical tests have not been specifically evaluated in this context. In addition, ultrasonography is an operator dependant procedure and is limited in its ability to quantify HS (89). Cross-sectional imaging including CT and MRI are not compatible with organ donation related time constraints despite providing a more accurate quantification of HS (253,257,258). More recently, the use of hand-held optical spectroscopy devices able to predict >30% ld-MaS in retrieved donor livers have been reported with strong concordance to biopsy results (259,260).

Clinical practice has mainly relied on the retrieval surgeon's macroscopic assessment (which is known to be inaccurate) and in some instances, histopathological evaluation of a donor liver biopsy (89). However, despite being regarded as a gold standard, there are limitations to using biopsies, including histopathologist availability, inter-observer variability, overestimation of ld-MaS in frozen sections and the additional time required to prepare a permanent formalin section (87,89,261). Emerging digital image analysis (DIA) platforms (262) may mitigate some of these concerns by providing rapid 'real time', automated and more sensitive HS quantification of donor biopsies while minimising CIT (263,264).

The hypothesis being explored in this chapter is that pre-retrieval donor predictors including anthropometric measures, clinical risk scores and biochemical tests can facilitate early identification of livers with evidence of HS.

The overall aim of this chapter is to develop a first large scale 'Liver Atlas' of deceased donor livers using samples from the Quality in Organ Donation (QUOD) Bioresource in order to provide additional information to organ retrieval and transplant teams to aide utilisation decisions and avoid unnecessary discards of donor livers. The overall objectives are to:

1. Investigate the incidence of HS in the UK donor pool (quantified using rapid automated DIA);
2. Identify pre-retrieval predictors of HS severity i.e. anthropometric measures, clinical risk scores and biochemical tests;
3. Evaluate the impact of HS severity on organ retrieval, utilisation and post-transplantation outcomes.

3.2 Methods

3.2.1 Study design

In this retrospective study, an unbiased selection of consecutive samples from deceased organ donors was requested from the QUOD bioresource in written application (Project RAP063) and made available following approval of the management board. These samples included pre-retrieval donor bloods and liver biopsy tissue collected over a two-year period between 01/01/2017-31/12/2018. Corresponding donor and recipient demographic, intra-operative and outcome data was obtained from the NHS Blood and Transplant (NHSBT) Registry as part of the QUOD infrastructure.

Whole donor livers (both donation after brain death, DBD and donation after circulatory death, DCD) were included in this study. Donor livers transplanted into recipients that developed primary non-function (PNF) were excluded due to restricted access of these samples from the QUOD bioresource. A total of 1,048 consecutive deceased whole donor livers were identified over the study period. HS was quantified using imageDx^{TM} (RevealBiosciences, USA) artificial intelligence (AI)-based rapid automated image analysis of Haematoxylin and Eosin

(H&E) stained slides. 906 out of 1,048 donor livers had adequate tissue for histological assessment and were included in the final analysis with none (*n*=670, 74%), mild (*n*=102, 11.3%), moderate (*n*=81, 8.9%) and severe steatosis (*n*=53, 5.3%) (Figure 3.1).

There was a full complement of data for donor demographics, recipient demographics, graft survival and patient survival. However, there was a small proportion of missing data for clinical risk scores (Fatty Liver Index, FLI and Hepatic Steatosis Index, HSI), biochemical tests, peri-operative outcomes (ITU stay and renal status post-transplant) and post-transplant complications (vascular, biliary and infection), these are reported in Figure 3.1. There was no imputation for missing data.

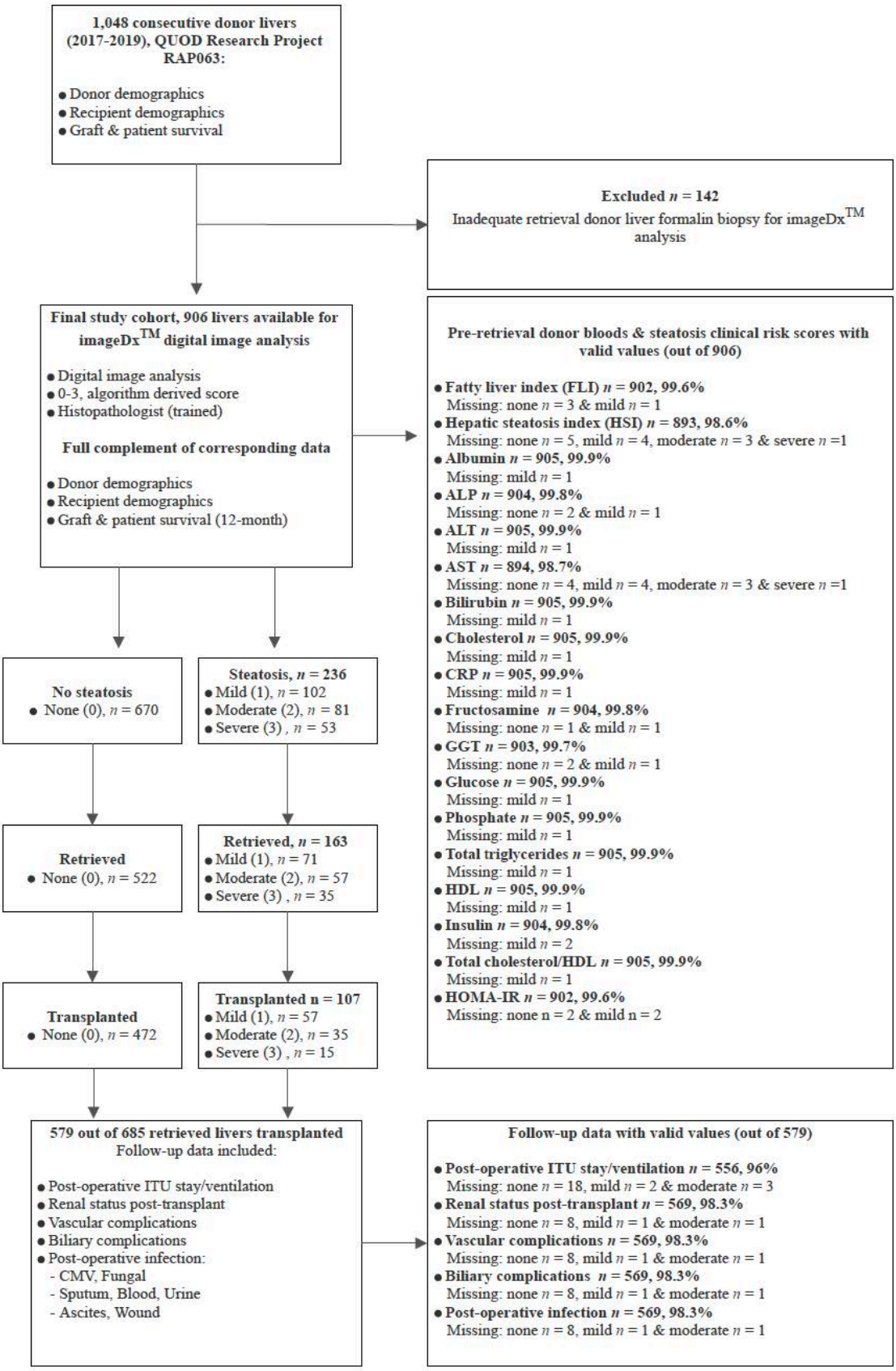

Figure 3.1. Study cohort of 906 donor livers with 579 out of 685 retrieved livers (84.5%) transplanted. Percentage of valid data and missing values for pre-retrieval steatosis predictors (clinical risk indices and biochemical tests), peri-operative outcomes and post-operative complications are reported.

3.2.2 QUOD sample selection and processing

3.2.2.1 Donor blood and biopsy

This study utilised donor blood samples collected in serum separator tubes (SST) prior to commencement of organ retrieval. Samples were processed by QUOD and provided in 0.5ml aliquots per donor liver for analysis on a clinical biochemistry analyser via spectrophotometry (Abbott Architect c8000, Abbott diagnostics, Illinois, USA) at the Department of Clinical Biochemistry, John Radcliffe Hospital, Oxford. The measurements performed included albumin (g/L), alkaline phosphatase (ALP; U/L), aspartate aminotransferase (AST; U/L), alanine aminotransferase (ALT; U/L), gamma-glutamyl transferase (GGT; U/L), bilirubin (µmol/L), total cholesterol (mmol/L), HDL cholesterol (mmol/L), total triglycerides (mmol/L), phosphate (mmol/L), fructosamine (µmol), glucose (mmol/L), insulin (pmol/L), HOMA-IR and c-reactive protein (CRP). The clinical risk scores (FLI and HSI) were derived from biochemical tests and their formulae (265,266):

Fatty Liver Index (FLI) *= e^y / (1 + e^y) × 100, Where y = 0.953 × ln(triglycerides, mg/dL) + 0.139 × BMI, kg/m^2 + 0.718 × ln (GGT, U/L) + 0.053 × waist circumference, cm – 15.745*

Hepatic Steatosis Index (HSI) *= 8 x ALT/AST + BMI (+ 2 if type 2 diabetes yes, + 2 if female)*

The FLI score ranges between 0 and 100 and FLI < 30 (negative likelihood ratio = 0.2) rules out hepatic steatosis and a FLI ≥ 60 (positive likelihood ratio = 4.3) rules in hepatic steatosis. A HSI score of <30.0 rules out hepatic steatosis with sensitivity of 93.1% and a value of >36.0 rules in hepatic steatosis with a specificity of 92.4% (265,266).

The QUOD retrieval donor liver biopsy is routinely taken from segment three of the liver and formalin samples are processed by QUOD into Formalin-Fixed Paraffin-Embedded (FFPE) blocks. These blocks were sectioned, stained for Haematoxylin and Eosin (H&E) and digitised using a 3DHISTECH PANNORAMIC™ series scanner (Epredia) by RevealBiosciences (USA) (250).

3.2.2.2 Steatosis quantification using imageDx™

HS was quantified using the commercially available imageDx™ digital assay (RevealBiosciences, USA) described in Chapter 2 (2.4.1). This artificial intelligence (AI)-based rapid automated image analysis platform has been co-developed with histopathologists to provide precise, consistent machine and deep learning trained on several thousand image patches and has been validated for rodent and human liver tissue (250). Briefly, the quantitative outputs include total lipid %, macrovesicular (MaS) %, microvesicular (MiS) steatosis % and mean vesicle size (μm^2). The total lipid % is the combination of MaS (defined as the presence of intracytoplasmic fat vacuole of >65 μm^2) and MiS (<65 μm^2) rather than the recently published LT specific steatosis reporting Banff consensus guidelines (see chapter to further 1.5.2). Overall, the imageDx™ digital assay also provides a rapid automated, reproducible and objective propriety deep learning algorithm derived score (0-3) of HS severity: none=0, mild=1, moderate=2 and severe steatosis=3.

This algorithm has been recently validated in a NASH mouse model against the conventional histopathologist report (250). In this validation study, the imageDx™ digital assay HS severity score was consistent with the histopathologist-reported HS severity score (0-3). In addition, while the total lipid % followed a similar trend to the histopathologist report, the total lipid % (MaS and MiS) were significantly lower compared to actual percentage reported by the histopathologist e.g. a digital assay-reported value of 15.1% (with HS severity score of 3) corresponded to a histopathologist-reported value of over 67% (despite a consistent steatosis severity score of 3). This finding reflects current literature demonstrating that the actual steatosis percentages obtained from conventional histopathological evaluation are 1.5-4 fold higher than those generated by DIA resulting in its limited use (80,94,267–270). These findings have been taken into consideration in the current study and percentage scores derived from the imageDx™ digital assay have been normalised to conventional histopathology categorisation of HS severity graded 0-3 (Table 1): none, 0: <5%; mild, 1: < 30%; moderate, 2: 30%-60% and; severe 3: >60% (29,30), albeit with the limitations described above (80,81,267,271) using the following min-max normalisation formula:

$$X' = \left(\frac{X - X_{\min}}{X_{\max} - X_{\min}}\right) \times (R_{\max} - R_{\min}) + R_{\min}$$

- X is the original value.
- $X_{\min}$ and $X_{\max}$ are the minimum and maximum values in the original range.
- $R_{\min}$ and $R_{\max}$ are the minimum and maximum values in the new range

To further validate the imageDx™ (RevealBiosciences, USA) software in the present study and context of LT, additional independent histopathological evaluation of histology slides was performed by Professor Alberto Quaglia (Consultant Liver Transplant Histopathologist, Royal Free Hospital, London) who was blinded to the steatosis scores generated by the imageDx™ digital assay. This validation included blinded review of the median and maximum DIA scores (as quantified using the imageDx™ digital assay) for each steatosis category. The degree ld-MaS (defined as a single fat vacuole causing cellular distension, being larger than adjacent non-steatotic/minimally steatotic hepatocytes with nucleus displacement to the hepatocyte periphery) was subsequently reported according to the Banff consensus guidelines for the selection of histology slides described (96).

3.2.3 Statistical analysis

All statistical analysis was performed using SPSS (v.25.001) and GraphPad Prism (9.4.1) software. Distribution of continuous variables was determined using the Kolmogorov-Smirnov test. Due to non-normal distribution, data were expressed as median and interquartile range (IQR). The Chi-square test was used for categorical data and the non-parametric Kruskal-Wallis test was used for continuous data. Multiple comparisons of significant continuous data were performed using Dunn's test. Simple logistic regression analysis was performed to assess the diagnostic accuracy of significant pre-retrieval predictors in predicting moderate-severe from none-mild steatosis. Pre-retrieval predictors with significant likelihood ratios identified on simple logistic regression were further evaluated in a multiple logistic regression model which included BMI, WC, FLI, HSI, GGT, total triglycerides and insulin. A P value of <0.05 was considered statistically significant. Graft and patient survival were reported using Kaplan-Meier curves and statistical significance was determined using the log-rank test. Cox proportional hazards regression analysis was performed to study the effect of HS severity on graft survival adjusting for potential donor confounders (donor type, age, BMI, WC and CIT) and potential recipient confounders (age and BMI).

3.3 Results

3.3.1 Donor demographics

The donor characteristics are summarised in Table 3.1. Donors in all 4 groups were predominately male with a median age over 50 years. Intracranial haemorrhage and hypoxic brain damage were identified as the most common causes of death across groups. The incidence of co-morbid disease including diabetes, hypertension and pre-existing liver disease was higher in donors with HS. The proportion of DCD livers decreased with increasing HS severity (mild, 44.1% vs. moderate, 40.7% vs. severe, 30.2%; $P = 0.808$).

There was a significant difference in mean MaS percentage (quantified using the imageDx™ digital assay) between groups: none=0.2±0.1 (normalised: 1.0±1.0); mild=1.0±0.4 (normalised: 13.0±4.0); moderate=2.0±0.8 (normalised: 43±5.0) and; severe=7.0±3.0 (normalised: 68±8.0); $P < 0.0001$, Table 3.1. Following blinded independent histopathological evaluation (according to the Banff consensus for the reporting of donor liver ld-MaS), the median and maximum histopathological ld-MaS per group as reported by the histopathologist were as follows: none=0% (maximum: 0%); mild=2% (maximum: 25%); moderate=30% (maximum: 40%) and; severe=40% (maximum: 90%). The corresponding imageDx™ digital assay median and maximum total lipid percentage (including percentage MaS and MiS) are shown in Figure 3.2 (slides magnified to 40X).

Table 3.1. Donor demographics

Median [IQR] & Column frequency [%]	None (0) *n*=670	Mild (1) *n*=102	Moderate (2) *n*=81	Severe (3) *n*=53	*P* - value
Age	54 [43-65]	59 [51-66]	56 [51-64]	54 [46-60]	0.016
Donor type					
DBD	412 [61.5]	57 [55.9]	48 [59.3]	37 [69.8]	0.389
DCD	258 [38.5]	45 [44.1]	33 [40.7]	16 [30.2]	
ImageDx™ digital assay					
Macrovesicular (MaS)%[a]	0.2 ±0.1	1.0±0.4	2.0±0.8	7.0±3.0	<0.0001
Total lipid % (MaS + MiS)[a]	0.3±0.2	1.3 ±0.4	2.9±0.7	7.6 ±3.1	<0.0001
Lipid droplet size (μm²)[b]	65 [23.3-193.3]	87 [29.2-215.2]	115 [26.1-260]	161.4 [66-313]	<0.0001
Normalised ImageDx™ digital assay HS percentage					
Macrovesicular (MaS) %[a]	1.0±1.0	13.0±4.0	43±5.0	68±8.0	<0.0001
Total lipid % (MaS + MiS)[a]	1.6±1.0	4.6±1.0	38±5.7	68±7.7	<0.0001
Gender					
Male	344 [51.3]	53 [52]	45 [55.6]	30 [56.6]	0.808
Female	326 [48.7]	49 [48]	36 [44.4]	23 [43.4]	
Donor ethnicity					
White	612 [91.3]	97 [95.1]	75 [92.6]	51 [96.2]	N/A
Asian	15 [2.2]	3 [2.9]	2 [2.5]	-	
Black	17 [2.5]	1 [1]	-	1 [1.9]	
Chinese/Oriental	4 [0.6]	-	1 [1.2]	-	
Mixed	4 [0.6]	-	1 [1.2]	-	
Other	13 [1.9]	-	1 [1.2]	1 [1.9]	
Not reported	2 [0.3]	1 [1]	1 [1.2]	-	
Unknown	3 [0.4]	-	-	-	
Weight (kg)	75 [65-85]	81.75 [70-90]	85 [75-90]	90 [80-100]	0.000
Height (cm)	171 [164-178]	171 [165-176]	170 [163-178]	173 [167-181]	0.333
BMI (kg/m²)	25.5 [22.8-29.1]	28.1 [25.4-30.6]	28.7 [26.6-31.3]	30.7 [25.4-33.4]	0.000
Waist Circumference (cm)	93 [84-103]	102 [95-112]	102 [95-110]	106 [96-118]	0.000
Diabetes	39 [5.8]	11 [10.8]	9 [11.1]	8 [15.1]	0.077
Hypertension	187 [27.9]	35 [34.3]	27 [33.3]	20 [37.7]	0.257
Liver disease	21 [3.1]	5 [4.9]	11 [13.6]	4 [7.5]	<0.0001
Smoking history	439 [65.5]	70 [68.6]	54 [66.7]	40 [75.5]	0.688
Cause of death					
Intracranial haemorrhage	384 [57.3]	57 [55.9]	50 [61.7]	33 [62.3]	N/A
Intracranial thrombosis	28 [4.2]	7 [6.9]	6 [7.4]	3 [5.7]	
Brain tumour	7 [1]	1 [1]	-	1 [1.9]	
Hypoxic brain damage	162 [24.2]	27 [26.5]	18 [22.2]	12 [22.6]	
Intracranial - CVA	16 [2.4]	2 [2]	4 [4.9]	3 [5.7]	
Trauma	27 [4]	3 [2.9]	1 [1.2]	-	
Cardiac arrest	7 [1]	-	-	-	
Myocardial infarction	1 [0.1]	-	-	-	
Pneumonia	1 [0.1]	1 [1]	-	-	
Respiratory failure	4 [0.6]	1 [1]	-	-	
Respiratory - type unclassified	1 [0.1]	-	-	-	
Meningitis	3 [0.4]	-	-	-	
Infections - type unclassified	2 [0.3]	-	-	-	
Acute blood loss	-	-	-	-	
(hypovolaemia)	1 [0.1]	-	1 [1.2]	-	
Other drug overdose	9 [1.3]	-	1 [1.2]	-	
Other	17 [2.5]	3 [2.9]	-	1 [1.9]	
Not reported					
Liver retrieved					
No	148 [22.1]	31 [30.4]	24 [29.6]	18 [34]	0.051
Yes	522 [77.9]	71 [69.6]	57 [70.4]	35 [66]	

[a]Reported as mean ± SD, rather than median [IQR]; [b]Reported a median and range [min-max], rather than [IQR]

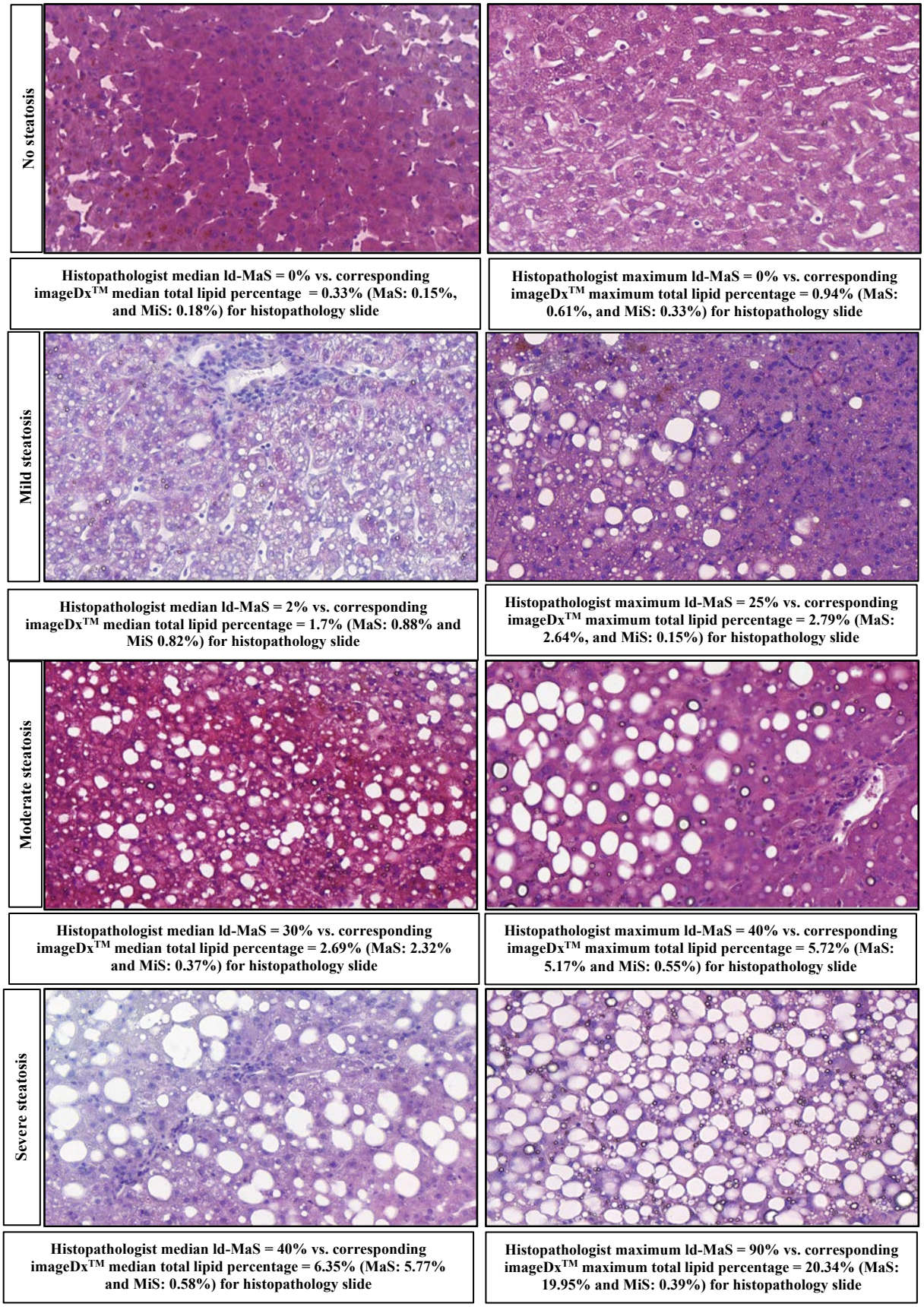

Figure 3.2. Percentage ld-MaS (median and maximum per steatosis category) as reported by the histopathologist vs. corresponding total lipid percentage reported using the imageDx™ digital assay.

There was a significant difference in donor median BMI between groups: none=25.5kg/m^2, interquartile range [IQR] (22.8-29.1); mild=28.1kg/m^2 (25.4-30.6); moderate=28.7kg/m^2 (26.6-31.3); severe=30.7kg/m^2 (25.4-33.4); P = 0.000. This was also reflected in donor median WC: none=93cm (84-103); mild=102cm (95-112); moderate=102cm (95-110); severe=106cm (96-118); P = 0.000. The median FLI also significantly increased with donor HS severity: none=51.3 (21.7-79); mild=71.7 (42.2-88.5); moderate=81.3 (62.2-93.8); severe=86.8 (68.6-95.9); P = 0.000. In addition, a significant difference was also present in the median donor HSI: none=36.2 (31.7-41.3); mild=39.7 (34.8-44); moderate=38 (34.6-42.4); severe=40.9 (34.9-45.2); P = 0.000. Pre-retrieval donor biochemical tests for the 4 groups are summarised in Table 3.2 and demonstrated significant differences in GGT, total triglycerides, insulin and HOMA-IR (P = 0.000, 0.002, 0.000 and 0.002 respectively).

Table 3.2. Pre-retrieval clinical risk scores and biochemical tests

Median [IQR]	**None (0)** ***n*=670**	**Mild (1)** ***n*=102**	**Moderate (2)** ***n*=81**	**Severe (3)** ***n*=53**	***P* - value**
FLI	51.3 [21.7-79]	71.7 [42.2-88.5]	81.3 [62.2-93.8]	86.8 [68.6-95.9]	0.000
HSI	36.2 [31.7-41.3]	39.7 [34.8-44.0]	38 [34.6-42.4]	40.9 [34.9-45.2]	0.000
Albumin (g/L)	25.2 [21.8-29]	25.7 [22.8-29.6]	24.8 [21.4-28.5]	25.9 [20.9-30]	0.486
ALP (IU/L)	71.3 [54.4-99.3]	71.2 [56-88.1]	73.7 [54.3-99.7]	77.6 [60.3-95]	0.922
ALT (IU/L)	29.2 [16.7-64.6]	30.7 [17.8-55.4]	28.1 [16.7-54.0]	47 [29.8-67.8]	0.086
AST (IU/L)	36.5 [21.3-63.7]	30.1 [18.3-55.1]	35.6 [18.7-82.6]	50.4 [27.4-81.9]	0.065
Bilirubin (µmol/L)	5.8 [4.0-9.0]	6.3 [3.9-11.0]	6.0 [3.9-11.1]	6.5 [4.0-9.4]	0.513
Total cholesterol (mmol/L)	3.38 [2.67-4.06]	3.39 [2.75-4.14]	3.45 [2.92-4.07]	3.43 [2.77-4.34]	0.461
CRP (mg/L)	165.1 [102.4-236]	159.3 [113-220.3]	168 [102-265.1]	169.8 [110.9-238]	0.876
Fructosamine (µmol/L)	207.8 [187.7-236]	212.3 [189.6-241.7]	219.6 [189.6-237.9]	221.1 [191.4-254.6]	0.075
GGT (IU/L)	44.6 [21.8-104]	50.3 [24.2-104.7]	73.5 [35-161.8]	84.8 [43.2-230.8]	0.000
Glucose (mmol/L)	7.36 [5.71-9.26]	7.65 [6.14-9.52]	7.05 [6.04-9.77]	8.21 [6.18-10.66]	0.243
Phosphate (mmol/L)	1 [0.78-1.3]	0.98 [0.68-1.24]	1.03 [0.71-1.28]	0.92 [0.69-1.29]	0.493
Total triglycerides (mmol/L)	1.17 [0.8-1.71]	1.42 [0.86-2.22]	1.47 [0.99-2.01]	1.40 [0.94-1.9]	0.002
HDL cholesterol (mmol/L)	0.96 [0.68-1.28]	0.93 [0.62-1.28]	0.90 [0.68-1.17]	0.91 [0.61-1.14]	0.407
Insulin (pmol/l)	124.6 [63.4-255.7]	128.7 [68.6-355.2]	171.7 [66.4-363.2]	247 [136.5-501.6]	0.000
AST/ALT ratio	1.17 [0.77-1.68]	1.02 [0.78-1.47]	1.21 [0.9-1.177]	1.28 [0.85-1.75]	0.081
Total cholesterol/HDL ratio	3.56 [2.57-4.65]	3.49 [2.65-4.83]	3.59 [2.80-4.79]	3.97 [2.89-5.60]	0.091
HOMA-IR	5.92 [2.6-13.5]	6.02 [3.1-17.8]	8.10 [3.3-21.4]	13.9 [5.2-33.4]	0.002

Dunn's test for multiple comparisons demonstrated that BMI, WC and FLI were able to differentiate the presence and absence of HS (across all HS categories). However, of the biochemical tests, only GGT was able to differentiate between HS grades (mild vs. moderate, $P = 0.076$ and mild vs. severe, $P = 0.004$), Figure 3.3.

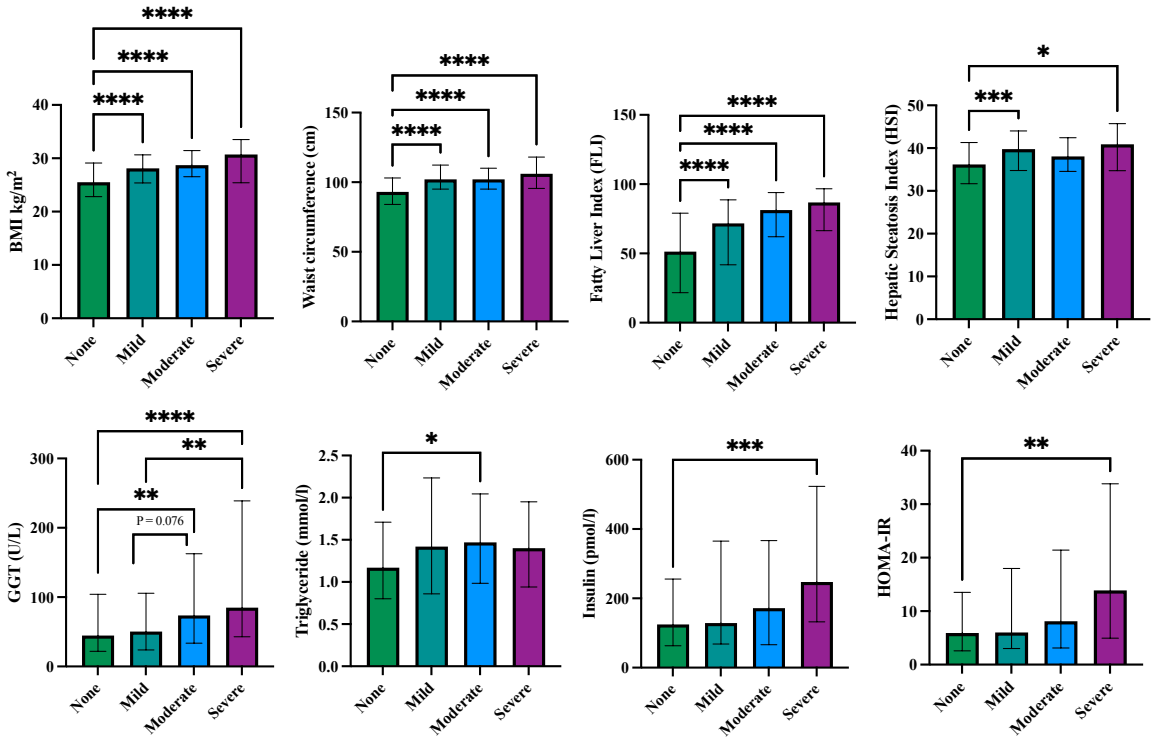

Figure 3.3. Data presented as median and IQR. Dunn's test for multiple comparisons: BMI, WC and FLI were able to differentiate the presence and absence of HS (across all HS categories). Only GGT was able to differentiate between HS grades (mild vs. moderate, $P = 0.076$ and mild vs. severe, $P = 0.004$). * $P \leq 0.05$, ** $P \leq 0.01$, *** $P \leq 0.001$, ***** $P \leq 0.0001$.

Simple logistic regression was performed to assess the diagnostic accuracy of significant pre-retrieval predictors in differentiating moderate-severe from none-mild steatosis: BMI [AUROC: 0.67; $P = 0.000$], WC [AUROC: 0.69; $P = 0.000$], FLI [AUROC: 0.72; $P = 0.000$], HSI [AUROC: 0.58; $P = 0.003$], triglyceride [AUROC: 0.58; $P = 0.004$, GGT [AUROC, 0.64; $P = 0.000$], insulin [AUROC: 0.60, $P = 0.0003$] and HOMA-IR [AUROC: 0.59, $P = 0.001$], see Table 3.3 and Figure 3.4.

Multiple logistic regression demonstrated an AUROC of 0.734 ($P = 0.000$) with a negative predictive power (NPP) of 86.2% and positive predictive power (PPP) of 88.9% for: BMI [OR: 1.07, 95% CI 0.99-1.15; $P = 0.080$], WC [OR: 1.02, 95% CI 0.99-1.04; $P = 0.182$], FLI [OR: 1.02, 95% CI 1.00-1.03; $P = 0.040$], HSI [OR: 0.95, 95% CI 0.91-0.99; $P = 0.009$], GGT [OR:

1.001, 95% CI 1.00-1.002; *P* = 0.041], triglycerides [OR: 1.14, 95% CI 0.96-1.34; *P* = 0.144] and insulin [OR: 1.001, 95% CI 1.00-1.001; *P* = 0.001], see Table 3.3.

Table 3.3. Simple and multiple logistic regression of pre-retrieval steatosis predictors (moderate-severe vs. none-mild steatosis)

Pre-retrieval predictors (moderate-severe vs. none-mild steatosis)	Odds ratio (95% CI)	*P* – value	Log-likelihood ratio	*P* – value	AUROC	*P* – value
Simple logistic regression						
Donor BMI (kg/m²)	1.11 [1.07 to 1.15]	0.000	37.28	0.000	0.67	0.000
WC (cm)	1.04 [1.03-1.06]	0.000	45.92	0.000	0.69	0.000
FLI	1.03 [1.02-1.04]	0.000	66.21	0.000	0.72	0.000
HSI	1.02 [1.00-1.04]	0.017	5.40	0.020	0.58	0.003
Donor GGT (IU/L)	1.002 [1.001-1.003]	0.000	21.38	0.000	0.64	0.000
Donor total triglycerides	1.36 [1.17-1.59]	0.000	17.47	0.000	0.58	0.004
Donor blood insulin (pmol/L)	1.001 [1.00-1.001]	0.012	5.83	0.016	0.60	0.0003
Donor HOMA-IR	1.004 [0.99-1.008]	0.132	2.15	0.142	0.59	0.001
Multiple logistic regression					0.734	0.000
Donor BMI (kg/m²)	1.07 [0.99-1.15]	0.080	-	-	-	-
Donor WC (cm)	1.02 [0.99-1.04]	0.182	-	-	-	-
FLI	1.02 [1.00-1.03]	0.040	-	-	-	-
HSI	0.95 [0.91-0.99]	0.009	-	-	-	-
Donor GGT (IU/L)	1.001 [1.00-1.002]	0.041	-	-	-	-
Donor total triglycerides	1.14 [0.96-1.34]	0.144	-	-	-	-
Donor insulin (pmol/L)	1.001 [1.00-1.001]	0.001	-	-	-	-

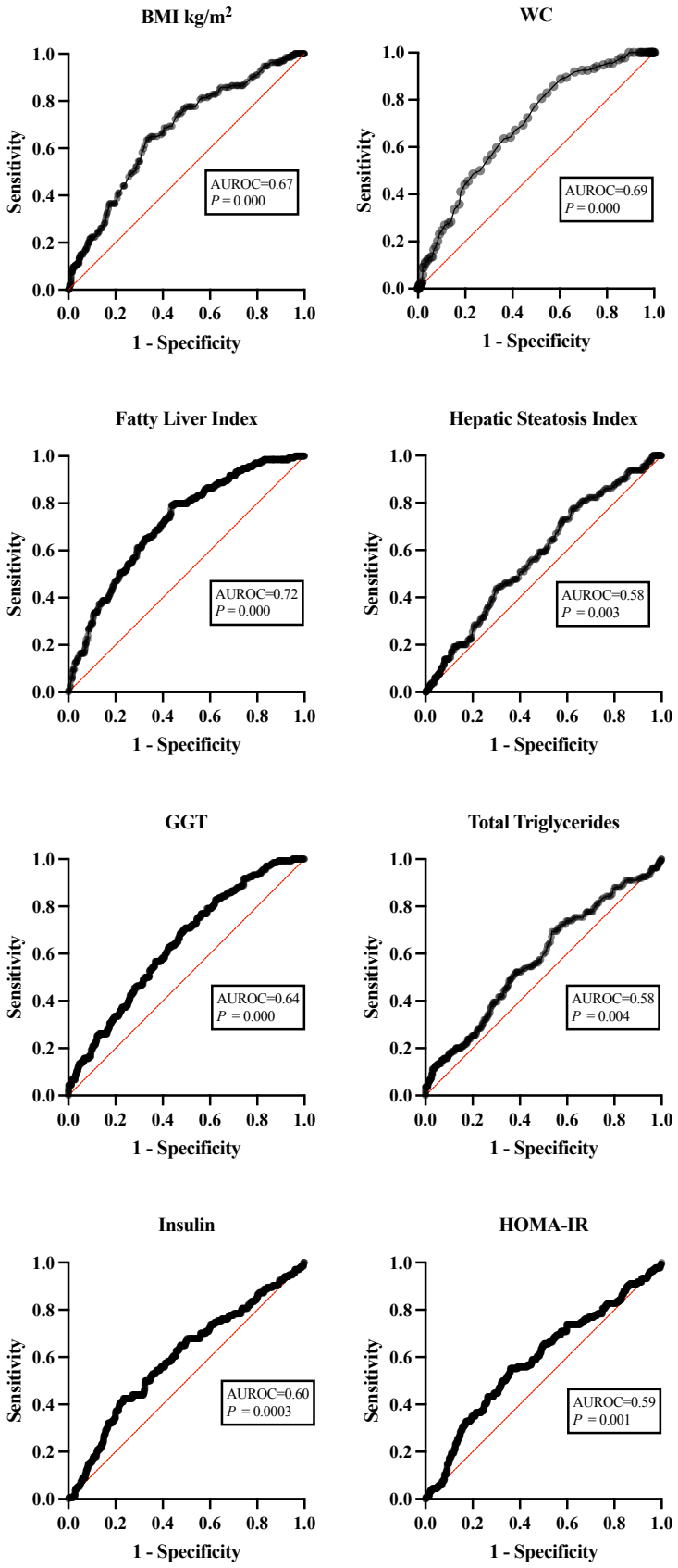

Figure 3.4. AUROCs demonstrating diagnostic accuracy of pre-retrieval predictors of hepatic steatosis (moderate-severe vs. none-mild steatosis)

3.3.2 Retrieved livers

Overall, 685 out of 906 livers (75.6%) were retrieved with the intent of transplantation. Of these, 522 (76.2%) had no steatosis, 71 (10.4%) had mild steatosis, 57 (8.3%) had moderate steatosis and 35 (5.1%) had severe steatosis, $P = 0.051$. There was a poor concordance between the retrieval surgeon's macroscopic assessment and imageDx^{TM} digital assay score (none, 56.9% vs. mild, 43.7% vs. moderate, 40.4% vs. severe, 28.6%; $P = 0.000$). Only a proportion of retrieved livers (579 out of 685, 84.5%) resulted in transplants. The number of transplanted livers decreased with increasing steatosis severity (none, 90.4% vs. mild, 80.3% vs. moderate, 61.4% vs. severe, 42.9%; $P = 0.000$), see Table 3.4. There was a non-significant difference in median cold ischaemia times (CIT) between groups: none=486min (391-593); mild=552min (416-641); moderate=512min (386-607); severe=516min (384-607); $P = 0.240$.

Table 3.4. Retrieval surgeon's macroscopic assessment and proportion of livers transplanted

Median [IQR] & Column frequency [%]	None (0) *n*=522	Mild (1) *n*=71	Moderate (2) *n*=57	Severe (3) *n*=35	*P* - value
Steatosis (Surgeon's assessment)					
No	297 [56.9]	19 [26.8]	9 [15.8]	1 [2.9]	0.000
Yes	224 [42.9]	52 [73.2]	48 [84.2]	33 [94.3]	
Not reported	1 [0.2]	-	-	1 [2.9]	
Steatosis (Surgeon's assessment)					
None	297 [56.9]	19 [26.8]	9 [15.8]	1 [2.9]	0.000
Mild	176 [33.7]	31 [43.7]	14 [24.6]	6 [17.1]	
Moderate	45 [8.6]	17 [23.9]	23 [40.4]	17 [48.6]	
Severe	3 [0.6]	4 [5.6%]	11 [19.3]	10 [28.6]	
Not reported	1 [0.2]	-	-	1 [2.9]	
Liver transplanted					
No	50 [9.6]	14 [19.7]	22 [38.6]	20 [57.1]	0.000
Yes	472 [90.4]	57 [80.3]	35 [61.4]	15 [42.9]	
Cold ischaemia time (minutes)	486 [391-593]	552 [416-641]	512 [386-607]	516 [384-607]	0.240

3.3.3 Recipient characteristics

Recipients were predominately male with a median age over 50 years and livers with HS were transplanted into older recipients: none=55 years (42-62); mild=57 years (45-62); moderate=57 years (47-61); severe=59 years (53-64); $P = 0.373$. Recipients of livers with HS also had a higher BMI: none=26.5kg/m^2, (23.1-30.7); mild=29.2kg/m^2 (24.9-32.6); moderate=28.7kg/m^2 (24.2-32.8); severe=32.9kg/m^2 (30.1-35.6); $P = 0.000$, Table 3.5.

Table 3.5. Recipient demographics

Median [IQR] & Column frequency [%]	None (0) *n*=472	Mild (1) *n*=57	Moderate (2) *n*=35	Severe (3) *n*=15	*P* - value
Age	55 [42-62]	57 [45-62]	57 [47-61]	59 [53-64]	0.373
Gender					
Male	276 [58.5]	43 [75.4]	25 [71.4]	10 [66.7]	0.045
Female	196 [41.5]	14 [24.6]	10 [28.6]	5 [33.3]	
Recipient ethnicity					
White	415 [87.9]	48 [84.2]	27 [77.1]	14 [93.3]	N/A
Asian	28 [5.9]	5 [8.8]	2 [5.7]	1 [6.7]	
Black	13 [2.8]	1 [1.8]	1 [2.9]	-	
Chinese/Oriental	6 [1.3]	1 [1.8]	-	-	
Mixed	-	-	-	-	
Other	9 [1.9]	2 [3.5]	3 [8.6]	-	
Not reported	1 [0.2]	-	2 [5.7]	-	
Weight (kg)	75 [65-91]	85 [74-95]	82 [66-97]	91 [84-103]	0.000
Height (cm)	170 [162-176]	170 [168-175]	170 [162-178]	172 [167-177]	0.607
BMI (kg/m²)	26.5 [23.1-30.7]	29.2 [24.9-32.6]	28.7 [24.2-32.8]	32.9 [30.1-35.6]	0.000
Transplant primary indication					
Primary biliary cirrhosis	37 [7.8]	2 [3.5]	-	-	N/A
Autoimmune chronic active liver disease	16 [3.4]	2 [3.5]	3 [8.6]	1 [6.7]	
Hepatitis B cirrhosis	10 [2.1]	-	1 [2.9]	-	
Primary sclerosing cholangitis	59 [12.5]	3 [5.3]	4 [11.4]	1 [6.7]	
Alpha-1-antitrypsin deficiency	2 [0.4]	1 [1.8]	-	-	
Budd-Chiari syndrome (other)	1 [0.2]	-	-	-	
Cryptogenic cirrhosis	13 [2.8]	1 [1.8]	2 [5.7]	1 [6.7]	
Secondary biliary cirrhosis	4 [0.8]	-	-	-	
Alcohol-associated liver disease	96 [20.3]	16 [28.1]	4 [11.4]	4 [26.7]	
Biliary atresia	4 [0.8]	-	-	-	
Congenital hepatic fibrosis	1 [0.2]	-	-	-	
Wilson's Disease	1 [0.2]	-	-	-	
Hepatitis C cirrhosis	17 [3.6]	5 [8.8]	3 [8.6]	-	
MASLD	44 [9.3]	10 [17.5]	4 [11.4]	4 [26.7]	
Acute hepatic failure - Budd-Chiari syndrome	1 [0.2]	-	-	-	
Acute hepatic failure - other virus	-	1 [1.8]	-	-	
Acute hepatic failure - serologically indeterminate	16 [3.4]	1 [1.8]	1 [2.9]	-	
Acute hepatic failure - Wilson's disease	2 [0.4]	-	-	-	
Acute Hepatic Failure - paracetamol	9 [1.9]	-	-	-	
Acute Hepatic Failure - other drug toxicity	2 [0.4]	-	-	-	
Acute Hepatic Failure – other causes	9 [1.9]	-	-	-	
Hepatocellular carcinoma - cirrhotic	42 [8.9]	6 [10.5]	6 [17.1]	2 [13.3]	
Other metabolic liver disease	3 [0.6]	-	1 [2.9]	-	
Cystic fibrosis	3 [0.6]	-	-	-	
Primary oxalosis	1 [0.2]	-	-	-	
Familial amyloidosis	3 [0.6]	-	-	-	
Polycystic liver disease	14 [3.0]	-	-	-	
Hereditary haemochromatosis	1 [0.2]	-	-	-	
Glycogen storage disease	2 [0.4]	-	-	-	
Progressive familial intrahepatic cholestasis	1 [0.2]	-	-	-	
Crigler-Najjar syndrome	1 [0.2]	-	-	-	
Chronic rejection	4 [0.8]	2 [3.5]	-	1 [6.7]	
Primary non-function	3 [0.6]	1 [1.8]	1 [2.9]	-	
Non-thrombotic infarction	3 [0.6]	-	-	-	
Recurrent disease	7 [1.5]	-	-	-	
Biliary complications	11 [2.3]	1 [1.8]	2 [5.7]	-	
Hepatic artery thrombosis	10 [2.1]	3 [5.3]	1 [2.9]	-	
Early graft dysfunction	2 [0.4]	-	-	-	
Acute vascular occlusion - venous	4 [0.8]	-	-	-	
Other causes	13 [2.8]	2 [3.5]	2 [5.7]	1 [6.7]	
Recipient liver failure grading					
Hyperacute	35 [7.4]	4 [7.0]	2 [5.7]	-	N/A
Acute	15 [3.2]	2 [3.5]	-	-	
Subacute	2 [0.4]	-	-	-	
Not acute	389 [82.4]	48 [84.2]	30 [85.7]	15 [100.0]	
Not reported	31 [6.6]	3 [5.3]	3 [8.6]	-	

The primary indications for transplant in all groups included alcohol-associated liver disease (ALD), metabolic dysfunction-associated steatotic liver disease (MASLD) and hepatocellular carcinoma (cirrhotic). The relative frequency of donor livers (per HS grade) transplanted into recipients with MASLD as the primary indication for transplant was disproportionately highest for livers with severe steatosis (none, 9.3% vs. mild, 17.5% vs. moderate, 11.4% vs. severe, 26.7%), Table 3.5.

3.3.4 Peri-operative outcomes and post-operative complications

A significant difference was noted in the number of days (d) spent in ITU post-transplant with increasing HS severity: none=3d (2-5); mild=2d (2-4); moderate=3d (2-7); severe=5d (3-38); $P = 0.004$. The requirement for transient renal filtration post-transplant also increased with HS severity (none, 10.6% vs. mild, 7.1% vs. moderate, 22.9% vs. severe, 40%; $P = 0.002$). Vascular complications only occurred in livers with no steatosis (hepatic artery thrombosis, 2.5%; portal vein thrombosis, 3.8%; hepatic vein occlusion, 1.1%) and mild steatosis (portal vein thrombosis, 3.8%; hepatic vein occlusion, 1.1%). Haemorrhage requiring re-operation was highest in livers with severe steatosis (26.7%; $P = 0.043$) as was the requirement for anti-fibrinolytic therapy (26.7%; $P = 0.001$). Biliary leaks requiring re-operation were highest in livers with moderate (8.7%) and severe (6.7%) steatosis. Biliary tract strictures within the first 12 months follow-up occurred in 11.4% of livers with moderate steatosis and 6.7% of livers with severe steatosis. Post-operative infection (CMV, fungal, pulmonary and bacteraemia) increased with steatosis severity with bacteraemia being statistically significant across groups (none, 4.9% vs. mild, 7% vs. moderate, 17.1% vs. severe, 20%; $P = 0.003$), see Table 3.6.

Table 3.6. Peri-operative outcomes and post-operative complications

Median [IQR], Column frequency [%] & Missing data [Number, %]		None (0) *n*=472	Mild (1) *n*=57	Moderate (2) *n*=35	Severe (3) *n*=15	*P* - value
Anti-fibrinolytic therapy		57 [12.1]	5 [8.8]	6 [17.1]	4 [26.7]	0.001
Intra-operative death		1 [0.2]	-	-	-	0.157
Number of days ventilated post-transplant [a]		1 [1-2]	1 [1-1]	1 [1-3]	2 [1-4]	0.002
Number of days in ITU post-transplant [a]		3 [2-5]	2 [2-4]	3 [2-7]	5 [3-38]	0.004
Renal status post-transplant						
No or minor renal impairment		359 [76.1]	47 [83.9]	20 [57.1]	7 [46.7]	0.002
Required transient renal filtration		50 [10.6]	4 [7.1]	8 [22.9]	6 [40.0]	
Short-term dialysis		30 [6.4]	1 [1.8]	5 [14.3]	1 [6.7]	
Long-term dialysis		6 [1.3]	-	-	1 [6.7]	
Not reported		19 [4]	4 [7.1]	1 [2.9]	-	
Missing data		8 [1.7]	1 [1.8]	1 [2.9]	-	
Vascular complications	Hepatic artery thrombosis [b]	12 [2.5]	-	-	-	0.239
	Portal vein thrombosis [b]	18 [3.8]	1 [1.8]	-	-	0.256
	Hepatic vein occlusion [b]	5 [1.1]	1 [1.8]	-	-	0.516
	Haemorrhage (reoperation) [b]	46 [9.7]	2 [3.5]	2 [5.7]	4 [26.7]	0.043
Biliary tract leaks						
No leak		434 [91.9]	49 [86]	29 [82.9]	14 [93.3]	0.255
Leak not treated		3 [0.6]	-	-	-	
Leak requiring reoperation		10 [2.1]	1 [1.8]	3 [8.6]	1 [6.7]	
Other radiological intervention		8 [1.7]	2 [3.5]	1 [2.9]	-	
Not reported		9 [1.9]	4 [7]	1 [2.9]	-	
Missing data		8 [1.7]	1 [1.8]	1 [2.9]	-	
Biliary tract stricture [b]		24 [5.1]	2 [3.5]	4 [11.4]	1 [6.7]	0.409
Post-operative infection	CMV [b]	74 [15.7]	2 [3.5]	6 [17.1]	3 [20]	0.168
	Fungal [b]	17 [3.6]	1 [1.8]	2 [5.7]	1 [6.7]	0.538
	Sputum [b]	34 [7.2]	5 [8.8]	4 [11.4]	3 [20.0]	0.091
	Blood [b]	23 [4.9]	4 [7]	6 [17.1]	3 [20]	0.003
	Urine [b]	26 [5.5]	-	-	1 [6.7]	0.086
	Ascites [b]	24 [5.1]	4 [7]	5 [14.3]	1 [6.7]	0.074
	Wound [b]	26 [5.5]	2 [3.5]	2 [5.7]	-	0.296

[a] Missing data and column frequency per steatosis category: none, *n* = 18 (3.8%) vs. mild *n* = 2 (3.5%) vs. moderate *n* = 3 (8.6%) vs. severe *n* = 0 (0%)
[b] Missing data and column frequency per steatosis category: none, *n* = 8 (1.7%) vs. mild *n* = 1 (1.8%) vs. moderate *n* = 1 (2.9%) vs. severe *n* = 0 (0%)

3.3.5 Graft and patient survival

Graft and patient survival rates between groups are demonstrated in Figure 3.5. Differences in death censored graft survival rate at 12 months post-transplant (none, 94.5% vs. mild, 96.5% vs. moderate, 85.7% vs. severe, 86.7%) did not achieve statistical significance ($P = 0.091$). Similarly, differences in patient survival at 12-months (none, 94.1% vs. mild, 93% vs. moderate, 85.7% vs. severe, 86.7%) did not achieve statistical significance ($P = 0.195$). In all groups, biliary complications were the main cause of graft failure and highest in livers with moderate and severe steatosis (40% and 50% respectively). The most common cause of death was multi-system failure in all groups (none, 32.1% vs. mild, 50% vs. moderate, 80% vs. severe, 100%), see Table 3.7. Cox proportional hazard regression analysis identified DCD

donors (HR: 2.35, 95% CI 1.15-4.84; *P* = 0.02) and moderate steatosis (HR: 2.67, 95% CI 1.002-7.11; P = 0.049) as independent predictors of graft survival see Table 3.8.

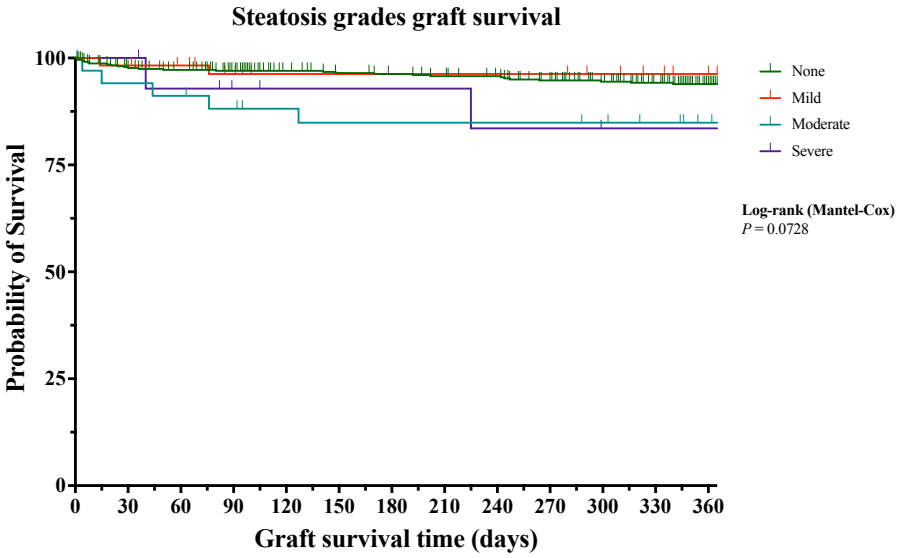

Graft survival time (days)					
Number at risk		**0**	**90**	**180**	**365**
Steatosis	**None (0)**	472	425	388	275
	Mild (1)	57	48	46	37
	Moderate (2)	35	29	27	20
	Severe (3)	15	12	11	9

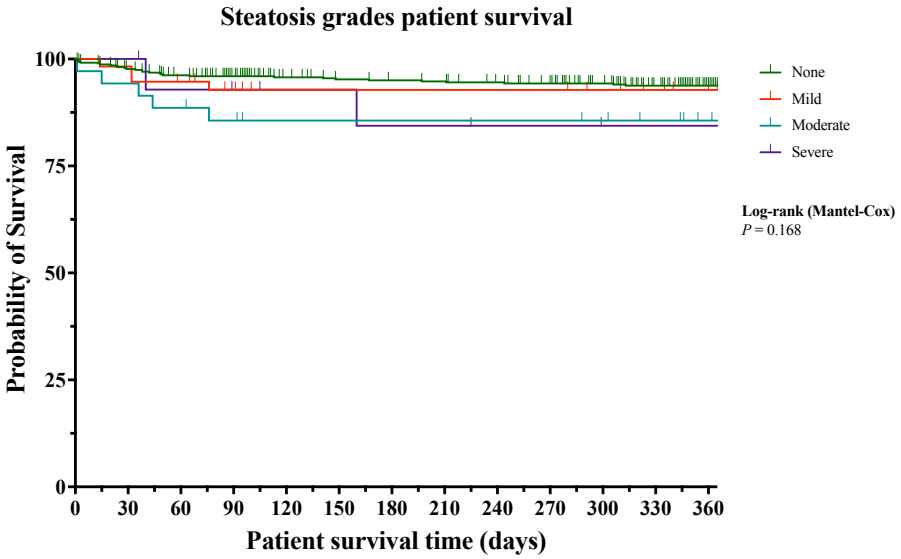

Graft survival time (days)					
Number at risk		**0**	**90**	**180**	**365**
Steatosis	**None (0)**	472	430	393	288
	Mild (1)	57	48	46	37
	Moderate (2)	35	29	28	21
	Severe (3)	15	13	11	9

Figure 3.5. Graft and patient survival (with number at risk) reported using Kaplan-Meier curves. Statistical significance determined using the Log-rank (Mantel-Cox) test

Table 3.7. Graft and patient survival including cause of graft failure and death

Column frequency [%]	None (0) *n*=472	Mild (1) *n*=57	Moderate (2) *n*=35	Severe (3) *n*=15	*P* – value
Death censored 12-month graft survival					
Graft Function	446 [94.5]	55 [96.5]	30 [85.7]	13 [86.7]	0.0907
Graft Failure	26 [5.5]	2 [3.5]	5 [14.3]	2 [13.3]	
Cause of graft failure					
Acute Rejection	1 [3.8]	-	-	-	N/A
Chronic Rejection	0 [0.0]	-	-	-	
Hepatic Artery Thrombosis	4 [15.4]	-	-	-	
Vascular occlusion	2 [7.7]	-	-	-	
Non-thrombotic infarction	1 [3.8]	-	-	-	
Ductopenic rejection	1 [3.8]	-	-	-	
Recurrent disease	-	-	-	-	
Biliary Complications	6 [23.1]	-	1 [20]	1 [50]	
Others	10 [38.5]	1 [50]	2 [40]	1 [50]	
Unknown	1 [3.8]	1 [50]	2 [40]	-	
12-month patient survival					
Patient alive	444 [94.1]	53 [93]	30 [85.7]	13 [86.7]	0.195
Patient dead	28 [5.9]	4 [7]	5 [14.3]	2 [13.3]	
Primary recipient cause of death					
Other causes of cardiac failure	2 [7.1]	-	-	-	N/A
Sudden unexplained cardiac death	1 [3.6]	-	-	-	
Cerebro-vascular accident	-	-	-	-	
Haemorrhage from surgery	-	-	-	-	
Pulmonary infection (bacterial)	1 [3.6]	-	-	-	
Pulmonary infection (viral)	1 [3.6]	-	-	-	
Septicaemia	1 [3.6]	-	-	-	
Cystic liver disease	1 [3.6]	-	-	-	
Liver failure – cause unknown	-	-	-	-	
Renal failure	2 [7.1]	-	-	-	
Recurrent primary disease – benign	-	-	-	-	
Recurrent primary disease – malignant	-	-	-	-	
Therapy ceased for any other reason	-	-	-	-	
Lymphoid malignant (immunosuppressive)	1 [3.6]	-	-	-	
Non-lymphoid malignant disease	1 [3.6]	-	-	-	
Multi-system failure	9 [32.1]	2 [50]	4 [80]	2 [100]	
Donor organ failure	1 [3.6]	-	-	-	
Other identified cause of death	6 [21.4]	1 [25]	1 [20]	-	
Unknown	1 [3.6]	1 [25]	-	-	

Table 3.8. Graft survival: Cox proportional hazard regression analysis using donor and recipient variables

Donor and recipient variables	Hazard ratio (95% CI)	*P* – value
Donor Type (DCD)	2.35 [1.15-4.84]	0.020
Donor age	1.02 [0.99-1.04]	0.243
Donor BMI (kg/m^2)	0.96 [0.85-1.07]	0.461
Donor waist circumference (cm)	1.02 [0.98 to 1.06]	0.379
Mild steatosis	0.59 [0.14 to 2.56]	0.480
Moderate steatosis	2.67 [1.002 to 7.11]	0.049
Severe steatosis	3.09 [0.67 to 14.24]	0.148
Cold ischaemia time (min)	1.00 [0.998-1.002]	0.810
Recipient age	1.01 [0.98 to 1.04]	0.720
Recipient BMI (kg/m^2)	1.03 [0.96 to 1.11]	0.355

3.4 Discussion

3.4.1 Pre-retrieval predictors of donor liver steatosis

There are currently no validated methods to determine the degree of HS prior to retrieval and the accurate identification remains challenging in the setting of deceased donor transplantation. Fedchuk et al. (272) investigated the diagnostic value of clinical risk-scores including the FLI and HSI as predictors of HS using histopathological evaluation as the gold standard. In this study of 324 patients with suspected HS, both the FLI and HSI demonstrated AUROCs of 0.65 for predicting moderate-severe steatosis. In our study cohort, the FLI had an improved accuracy with an AUROC of 0.72 for predicting moderate-severe steatosis while the HSI had a lower diagnostic accuracy with an AUROC of 0.58 compared to that reported by Fedchuk et al (272).

Anthropometric measures have also been investigated as predictors of HS. A large United Network for Organ Sharing (UNOS) registry study identified 1,277 donors that had evidence of moderate-severe steatosis on biopsy. In this study, donors with a BMI >30kg/m^2 were more likely to have >30% ld-MaS (273). In addition, Rodriguez et al. (274) performed a large cross-sectional study of 6,194 patients to develop a predictive model of HS using 14 predictors to identify moderate-severe steatosis determined using liver computed tomography (CT). In the validation cohort, patients with moderate-severe steatosis had a median WC of 108cm [98–118] and mean BMI of 33kg/m^2±7.1, these values are comparable to the findings in our study. The final predictive models of HS included the NAFLD-MESA Index and NAFLD Clinical Index which had better or similar performance to the FLI with AUROCs of 0.83, 0.78 and 0.78 respectively. Whilst Rodriguez et. al did not report individual AUROCs for WC and BMI, we were able to demonstrate limited diagnostic accuracy with AUROCs of 0.69 and 0.67 respectively and a comparable AUROC of 0.72 for FLI.

The use of biochemical tests to predict HS in donors has not been widely reported (275). In our present study, GGT had a higher diagnostic accuracy [AUROC, 0.64; $P = 0.000$] in predicting moderate-severe compared to triglyceride [AUROC: 0.58; $P = 0.004$], insulin [AUROC: 0.60, $P = 0.0003$] and HOMA-IR [AUROC: 0.59, $P = 0.001$]. However, only GGT [OR: 1.001; 1.000-1.002; $P = 0.041$] and insulin [OR: 1.001; 1.000-1.001; $P = 0.001$] were identified as independent predictors of moderate-severe steatosis on multiple logistic regression.

3.4.2 Assessment of donor liver steatosis

The macroscopic assessment of the retrieval surgeon is the mainstay of determining the degree of HS during organ retrieval (276). However, this assessment is known to be inaccurate and remains challenging even when performed by experienced retrieval surgeons (87). This was also evident in our study which demonstrated a poor concordance between the retrieval surgeon's macroscopic assessment and imageDx^{TM} digital assay score, (none, 56.9% vs. mild, 43.7% vs. moderate, 40.4% vs. severe, 28.6%; $P = 0.000$).

The gold standard for HS assessment is the histopathological evaluation of the donor liver biopsy with HS graded 0-3: (none, 0: <5%; mild, 1: < 30%; moderate, 2: 30%-60% and; severe 3: >60%) (267,277). It has been reported that improved accuracy and reproducibility of HS assessment can be achieved by DIA of liver biopsy sections (262,267,268). However, the actual steatosis percentages obtained from conventional histopathological evaluation are 1.5-4 fold higher than those generated by DIA resulting in its limited use (80,94,267–270). Whilst this observation was also apparent in the current cohort (see Table 3.1), steatosis percentages were normalised to conventional histopathological evaluation of HS severity. Overall, the ability of the imageDx^{TM} digital assay to provide a rapid automated, reproducible and objective deep learning algorithm derived score (0-3) of HS severity addressed this limitation (250). In addition, to validate the imageDx^{TM} digital assay against recently published Banff guidelines for histopathological reporting of ld-MaS in donor liver biopsies, an independent histopathologist blinded to the steatosis scores generated by the imageDx^{TM} digital assay provided a histopathological evaluation of the median and maximum DIA scores (as quantified using the imageDx^{TM} digital assay) for each steatosis category (96).

In the setting of organ retrieval, several studies have supported use of portable AI-based platforms including use of smartphones and digital image analysis devices to quantify HS at the point of organ procurement (263,264). Other authors have described hand-held optical spectroscopy devices that are able to accurately predict moderate-severe steatosis (Ld-MaS >30%) in retrieved donor livers as an alternative to liver biopsy (259,260). However, whilst these techniques demonstrate strong concordance with histopathological evaluation, they have only been tested in the setting of pilot studies. In the future, it is therefore possible that a combination of portable rapid automated DIA platforms and optical spectroscopy devices may

facilitate assessment of HS in donor livers. If used in combination with machine perfusion technology, additional benefits can be gained including minimisation of CIT, ex-situ interventions (defatting and siRNAs targeting steatosis related genes) and functional assessment prior to transplantation (278).

3.4.3 Peri-operative and post-transplant outcomes

Overall, the proportion of retrieved livers transplanted decreased with increasing HS severity (none, 90.4% vs. mild, 80.3% vs. moderate, 61.4% vs. severe, 42.9%; $P = 0.000$). Donor livers with HS were disproportionately transplanted into recipients with higher BMIs and those with MASLD as a primary indication for liver transplant. Whilst there is no clinical policy to explain this trend, ascites, a common feature of advanced liver disease, can artificially elevate recipient BMI (by adding significant weight without reflecting actual body fat or lean mass) and can complicate accurate size matching between donor livers and recipients. The findings are comparable to other large cohort studies that highlight these complexities and reflect the increasing problem of MASLD in both the general population and deceased donors (51,277).

Transplantation of donor livers with HS was associated with an unfavourable peri-operative course and more post-operative complications. Haemorrhage requiring re-operation was highest in livers with severe steatosis (26.7%; $P = 0.043$) as was the requirement for anti-fibrinolytic therapy (26.7%; $P = 0.001$). The median duration of ITU stay, requirement for transient renal filtration, post-operative infections, biliary complications (leading to graft failure) and multi-system failure (leading to death) was highest in recipients transplanted with livers of the moderate-severe steatosis category.

There was a trend towards reduction in graft and patient survival for livers with moderate and severe steatosis (85.7% and 86.7% respectively) that did not achieve statistical significance, possibly related to size of the cohort. The only factors found to predict graft survival independently were DCD donors and those with moderate steatosis. Severe steatosis was not identified as an independent predictor graft survival, this is likely due to small proportion of livers transplanted with severe steatosis (n=15). Overall, these findings are comparable to previous studies reporting transplantation of livers with moderate-severe steatosis indicating unfavourable short-term outcomes but similar 12-month survival (279,280). The use of such high-risk livers relies on risk analysis by the implanting surgeon: balancing the risk of a

recipient dying on the waiting list versus the risk incurred by waiting for a more optimal graft (42). One approach to formalise this is the selection of higher-risk livers for lower-risk recipients i.e. 'preferred recipient matching' (defined by MELD 15-34, not on life support and absence of primary biliary cirrhosis) when considering transplantation of donor livers with >30% HS (281). This strategy has been associated with no significant increase in graft loss or mortality compared to transplantation of livers with no HS (281,282). See Figure 3.6 describing proposed utilisation decision-making algorithm.

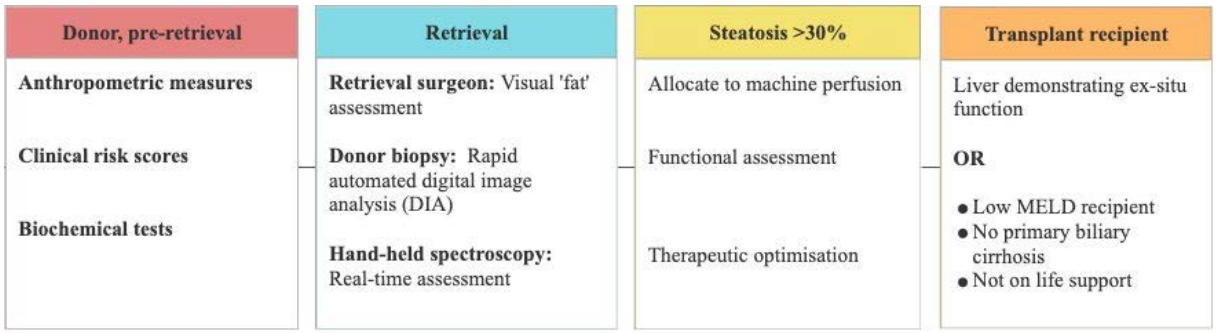

Figure 3.6. Proposed decision-making algorithm for utilisation of donor livers with moderate-severe steatosis

3.4.4 Limitations

This study relies on the use of registry data and, while there was a full complement of donor and recipient outcome data, there was a small proportion of missing data for peri-operative outcomes and post-operative complications. PNF cases were not included due to the scarcity of this event/availability of samples from the QUOD bioresource, and this may limit generalisability of the outcome data. At the time of data extraction, the NHSBT Registry did not routinely collect data on DCD normothermic regional perfusion (NRP) or the use of ex-situ machine perfusion i.e. NMP and therefore the implications of these perfusion modalities on liver discard, utilisation and post-transplantation outcome is unknown. Regarding the study cohort, the majority of donors in our study did not have HS (670 out of 906, 74%) assessed using the imageDx^{TM} digital assay, and this does reflect the incidence of HS in the general population (HS affects 33% of the population) (283). The imageDx^{TM} digital assay addressed the potential limitation of inter-observer variability evident in conventional histopathology. Despite the ability of the imageDx^{TM} digital assay to provide a score of HS severity (0-3), this software was developed before the recent Banff consensus guidelines for reporting HS as described in Chapter 1 (1.5.2) and therefore has similar limitations to previous DIA algorithms in overall steatosis percentages being significantly lower than what would be expected from a

conventional histopathologist report (80,94,267–270). This is evident in the low mean MaS percentages per steatosis category which required normalisation following the imageDx™ digital assay analysis: none=0.2 ±0.1 (normalised: 1.0±1.0); mild=1.0±0.4 (normalised: 13.0±4.0); moderate=2.0±0.8 (normalised: 43±5.0) and; severe=7.0±3.0 (normalised: 68±8.0). To further address this limitation, an independent histopathologist (blinded to the steatosis scores quantified using the imageDx™ digital assay) performed histopathological assessment of the median and maximum DIA scores for each steatosis category based on the recent Banff consensus guidelines for reporting donor HS (96). The histopathologist reported the following median and maximum ld-MaS values for each steatosis category: none = 0% (maximum: 0%), mild = 2% (maximum: 25%), moderate = 30% (maximum: 40%), and severe = 40% (maximum: 90%). These findings are clinically relevant and suggest potential of the imageDx™ digital assay in differentiating between none-mild and moderate-severe steatosis.

Rather than providing a histopathological report for all 906 donor liver biopsies, the histopathological assessment within this study was targeted to assess ability of the imageDx™ digital assay to accurately categorise donor biopsies according to HS severity. In a smaller cohort study, Gambella et al. have recently described and validated an automated and deep-learning algorithm for ld-MaS quantification based on Banff consensus guidelines with a percentage discrepancy of 1.20% (±5.58) when compared to the histopathologist report using 292 donor liver biopsies (284). To ensure clinicians can reliably decide to accept or decline a donor livers for transplantation based on DIA assessments, the algorithms must achieve not only high accuracy but also a low false positive rate. A high rate of false positives could lead to unnecessary organ discards and exacerbate the shortage of donor livers. Therefore, further evaluation of the current cohort using the recently developed algorithm by Gambella et al. and other commercially available DIA platforms is required to provide comparisons and strengthen conclusions from the current results as well as establish thresholds that are both clinically acceptable and feasible within the clinical setting of LT.

3.4.5 Conclusions

This study supports the use of pre-retrieval predictors to enable early identification of donors at high risk of liver steatosis. This complements the use of routine liver biopsy from donors deemed ‘high-risk’ with ‘real-time results’ using DIA platforms, thereby avoiding unnecessary organ discard, guiding utilisation decisions and minimising CIT. Further, transcriptomic

analysis of this cohort is currently being undertaken to map independent signatures associated with HS severity. This may enable targeted ex-situ optimisation with functional assessment prior to transplantation, further improving organ utilisation and outcomes of livers in the moderate-severe steatosis category. This further work is not included and beyond the scope of this thesis.

Chapter 4: Normothermic machine perfusion of steatotic donor transplant livers

4.1 Introduction

Normothermic machine perfusion (NMP) provides a platform to improve outcomes of steatotic donor transplant livers. This is achieved through prevention of the deleterious effects of cooling i.e. static cold storage (SCS), enhanced preservation and reduction in subsequent ischaemia-reperfusion injury (IRI) to which steatotic donor livers have increased susceptibility (126). However, to date, there have been no comprehensive mechanistic studies from large multi-centre randomised clinical trials investigating changes in tissue histology and the perfusate metabolic profile with relation to steatotic donor transplant livers preserved with NMP.

The hypothesis of this chapter is that NMP of steatotic donor transplant livers improves clinical outcomes compared to those preserved with SCS (through reduction in cooling), enhanced preservation (metabolic recovery and repair) and reduction in recipient IRI (through ex-situ reperfusion reconditioning).

The overall aim of this chapter is to characterise longitudinal histological and metabolic changes during perfusion of steatotic donor transplant livers preserved with NMP. The overall objectives are to:

1. Investigate clinical outcomes of recipients transplanted with steatotic livers preserved with NMP and SCS compared to lean counterparts;
2. Investigate the utility of a reproducible automated digital image analysis platform for consistent and accurate assessment of donor liver ld-MaS; and,
3. Compare the mechanistic effect of NMP on steatotic donor livers and lean counterparts through examination of sequential tissue biopsy and perfusate samples

4.2 Methods

4.2.1 Consortium on Organ Preservation in Europe Liver NMP Trial

The COPE liver NMP trial (ISRCTN 39731134) was a phase III randomised clinical trial where donor livers were randomised to continuous NMP using OrganOx *metra*® (1st Generation device, OrganOx Ltd, Oxford, UK) (*n*=121) or SCS alone (*n* =101) across 7 European liver

transplant units (207). Following organ procurement (either standard DBD retrieval or Maastricht III/IV DCD rapid cannulation technique), donor livers randomised to continuous NMP were back-benched and immediately placed on the OrganOx *metra*® device at the donor centre (device-to-donor approach) in order to minimise cold-ischaemia time (CIT) (207). For the purposes of this thesis, the NMP of this clinical trial will be referred to as continuous NMP (cNMP).

4.2.2 Liver core biopsy and perfusate samples

Histological images, proteomic data and cNMP perfusate samples from this Phase III multicentre randomised clinical trial (RCT) comparing efficacy of cNMP to SCS were obtained from the Consortium for Organ Preservation in Europe (COPE, www.cope-eu.org) bioresource, following written application and approval from the management board (Table 4.1). Proteomic analysis of this cohort is described in Chapter 5.

Table 4.1. Samples selected from the COPE bioresource

Sample	Timepoints	Sample ID
Liver core biopsy (digitised H&E & PAS image): 3 samples per liver	Pre-preservation (cNMP or SCS) Post-preservation (cNMP or SCS) Post-reperfusion (in recipient)	LT1 LT2 LT3
Perfusate (collected during NMP): 3 samples per liver	15 min 60 min End (range 4-24h)	P1 P2 P3

Donor livers with evidence of steatosis were identified from the COPE liver database and selected based on the pre-preservation (LT1) H&E biopsy demonstrating evidence of mild (≥ 5% ld-MaS) to severe steatosis (defined by a histopathological score of 1-3). Lean controls were identified and selected based on availability of tissue proteomic and recipient data. A total of 120 donor livers were identified, of these 14 livers were discarded due to steatosis (LT1, ≥ 5% ld-MaS) and 1 steatotic DCD liver (15% ld-MaS) was excluded from the study cohort due to an ABO incompatible transplant following cNMP. The final study cohort comprised of 105 transplanted livers (Table 4.2).

Table 4.2. Final study cohort

Liver phenotype	Preservation	DBD	DCD	Total number	Transplanted livers
Steatotic	**cNMP**				
	Transplanted	16	5	28	21
	Discarded	4	2		
	Excluded	-	1		
Steatotic	**SCS**				
	Transplanted	11	1	20	12
	Discarded	7	1		
Lean	**cNMP**	31	15	46	46
Lean	**SCS**	17	9	26	26

4.2.3 Demographics, preservation data and clinical outcomes

Donor and recipient demographics, preservation data, peri-operative and post-transplantation outcome data was obtained from the COPE clinical database. Data was reported for steatotic livers preserved with cNMP and SCS compared to lean counterparts for each group. The following early outcome data was also reported:

- Evidence of PRS defined by a decrease in mean arterial pressure (MAP) of more than 30% for than one minute during the first five minutes after reperfusion (64,285)
- Post-reperfusion lactate (mmol/L)
- Bilirubin (µmol/L), AST (IU/L), ALT (IU/L), INR, Platelets, Lactate (mmol/L) and Creatinine (µmol/L) on day 1 and 7
- Peak AST (IU/L) in the first 7 days post-transplant
- EAD) defined by presence of any of the following criteria (66):
    - Peak AST >2000 IUL/L in the first 7 days post-transplant
    - Day 7 post-transplant Bilirubin > 172 µmol/L
    - Day 7 post-transplant INR > 1.6
- Evidence of PNF characterised by irreversible liver graft dysfunction necessitating emergency re-transplant during the first 10 days post-transplant and occurring in the absence of immunological or technical causes (207)
- Need for RRT on day 1, 7 and 10 post-transplant
- HDU/ITU stay on day 1, 7 and 10 post-transplant
- Bilirubin (µmol/L), AST (IU/L), ALT (IU/L), INR, and Creatinine (µmol/L) on day 10, day 30, month 6 and month 12 post-transplant
- Graft and patient survival at day 1, day 7, day 10, day 30, month 6 and month 12 post-transplant

4.2.4 Effect of preservation of on steatosis severity, hepatocellular injury and function

4.2.4.1 Histological analysis

To determine the effect of cNMP and SCS on steatosis severity, retrieval/preservation and reperfusion related injury, sequential liver biopsy samples were examined including those taken pre-preservation (LT1), post-preservation (LT2) and post-reperfusion (LT3) in the recipient. Histopathological evaluation of H&E and PAS stained tissue was performed by the study consortium of consultant histopathologists blinded to the randomisation allocation and trained to consensus guidelines for scoring of large droplet macrovesicular steatosis (ld-MaS), small droplet macrovesicular steatosis (sd-MaS), glycogen depletion, congestion, portal oedema, red cells in the space of disse, portal oedema, portal haemorrhage and preservation reperfusion injury (PRI, including preservation related factors in the reperfusion injury following transplantation), (286). The PRI score comprises of small droplet fat, glycogen depletion, neutrophil infiltration, hyper-eosinophillic hepatocytes and necrosis: 0 = nil, 1 = minimal, 2 = mild, 3 = mild to moderate, 4 = moderate, 5 = moderate to severe and 6 = severe, **(Appendix A)**.

In addition to the histopathological steatosis score, digitised images were also analysed using an automated digital image analysis software (Visiopharm application 10119, H&E liver steatosis) (Visiopharm Ltd, Egham, UK) to provide quantitative outputs including total macrovesicular steatosis, ld-MaS and sd-MaS percentage described in Chapter 2.4.1.2. The change in percentage steatosis was compared between groups.

4.2.4.2 Perfusate analysis

To determine the effect of cNMP on ex-situ isolated liver metabolism, biochemical function and hepatocellular injury, sequential perfusate samples collected at 15 min (P1), 60 min (P2) and end of perfusion (P3) were analysed using a clinical biochemistry analyser via spectrophotometry (Abbott Architect c8000, Abbott diagnostics, Illinois, USA) with the exception of FGF-21 which was measured by sandwich enzyme-linked immunosorbent assay (ELISA) according to manufacturer instructions (Oxford Biosystems, Oxford, UK), see Chapter 2.5.1-2. The following perfusate measurements were performed:

- Hepatocellular enzymes and injury:
    - ALT (IU/L)
    - AST (IU/L)
- Cholangiocellular:
    - GGT (IU/L)
    - ALP (IU/L)
    - Bilirubin (μmol/L)
    - Bile salts (μmol/L)
- Hepatic lipid metabolism:
    - Total cholesterol (mg/dL)
    - Total triglycerides (mg/dL)
    - ApoB (g/L)
    - 3-OHB (mmol/L)
- General metabolism:
    - Lactate (mmol/L)
    - Urea (mmol/L)
    - Glucose (mmol/L)
    - Insulin (pmol/L)
- Systemic inflammation and metabolic stress:
    - CRP (mg/L)
    - FGF-21 (ng/L)

4.3 Results

4.3.1 Donor demographics

4.3.1.1 Transplanted donor livers

Donor characteristics of transplanted livers are summarised in Table 4.3. Donors in all 4 groups were predominately male with a mean age over 50 years. There was a significant difference in donor median BMI between groups: Steatotic cNMP=30.56kg/m^2 [IQR] (26.24-35.83); Steatotic SCS=31.58kg/m^2 (26.22-34.04); Lean cNMP=25.47kg/m^2 (22.34-30.07); Lean SCS=26.28kg/m^2 (22.39-30.44); P = 0.005. Donor liver steatosis was associated with co-morbid disease including diabetes, cardiac disease and history of alcohol use. This did not achieve statistical significance.

Table 4.3. Donor demographics

Mean ± SD; Median [IQR]; Column frequency [%]; Missing [Number, %]	**Steatosis cNMP *n*=21**	**Steatosis SCS *n*=12**	**Lean cNMP *n*=46**	**Lean SCS *n*=26**	***P* - value**
Age	52.03 ±12.58	55.92 ±13.04	56.78 ±15.86	53.83 ±14.94	0.631
Age					
<65 years	19 [90.5]	9 [75.0]	33 [71.7]	21 [80.8]	0.370
>65 years	2 [9.5]	3 [25.0]	13 [28.3]	5 [19.2]	
Gender					
Male	14 [66.7]	7 [58.3]	22 [47.8]	17 [65.4]	0.371
Female	7 [33.3]	5 [41.7]	24 [52.2]	9 [34.6]	
Donor type					
DBD	19 [90.5]	9 [75.0]	33 [71.7]	21 [80.8]	0.324
DCD	2 [9.5]	3 [25.0]	13 [28.3]	5 [19.2]	
Ethnicity					
Caucasian	20 [95.2]	12 [100.0]	45 [97.8]	25 [96.2]	N/A
Other	1 [4.8]	-	1 [2.2]	1 [3.8]	
Donor risk index ET	1.65 [1.47-1.93]	1.55 [1.39-1.98]	1.81 [1.50-2.11]	1.94 [1.63-2.49]	0.122
Missing	3 [14.3]	3 [25]	5 [10.86]	4 [15.38]	
Cause of death					
CVA	11 [52.4]	6 [50.0]	27 [58.7]	14 [53.8]	0.912
Hypoxia	5 [23.8]	2 [16.7]	12 [26.1]	6 [23.1]	
Trauma	3 [14.3]	1 [8.3]	3 [6.5]	2 [7.7]	
Other	2 [9.5]	3 [25.0]	4 [8.7]	4 [15.4]	
Weight (kg)	90 [80-105]	86 [75-107.50]	72.5 [60-90]	80 [70-90]	0.005
Height (cm)	175.0 ±10.31	175.5 ±9.95	171.5 ±9.51	172.0 ±7.81	0.360
BMI (kg/m^2)	30.56 [26.24-35.83]	31.58 [26.22-34.04]	25.47 [22.34-30.07]	26.28 [23.39-30.44]	0.005
BMI (kg/m^2)					
<30 kg/m^2	9 [42.9]	5 [41.7]	34 [73.9]	19 [73.1]	0.023
>30 kg/m^2	12 [57.1]	7 [58.3]	12 [26.1]	7 [26.9]	
Diabetes					
No	16 [76.2]	10 [83.3]	39 [84.7]	23 [88.5]	0.227
Yes	5 [23.8]	2 [16.7]	3 [6.5]	2 [7.7]	
Missing	-	-	4 [8.7]	1 [3.8]	
Cardiac disease					
No	12 [57.1]	7 [58.3]	29 [63.0]	19 [73.1]	0.961
Yes	3 [14.3]	2 [16.7]	10 [21.7]	5 [19.2]	
Missing	6 [28.6]	3 [25.0]	7 [15.2]	2 [7.7]	
Smoking history					
No	14 [66.7]	8 [66.7]	31 [67.4]	14 [53.8]	0.685
Yes	7 [33.3]	4 [33.3]	15 [32.6]	12 [46.2]	
Alcohol history					
No	18 [85.7]	9 [75.0]	42 [91.3]	25 [96.2]	0.155
Yes	3 [14.3]	3 [25.0]	3 [6.5]	1 [3.8]	
Missing	-	-	1 [2.2]	-	

4.3.1.2 Discarded donor livers

Donor characteristics of discarded livers are described in Table 4.4.

Table 4.4. Discarded livers

Study arm & discard number	Donor type	Age (years)	BMI (kg/m^2)	ld-MaS (H&E)	DLI (ET)	NMP Bile (ml)	Reason for discard
1: SCS	DBD	54	36.8	15%	1.51	N/A	Macroscopic steatosis
2: SCS	DBD	68.9	28.4	10%	1.85	N/A	60% steatosis (frozen section)
3. SCS	DBD	73	33.0	5%	1.75	N/A	Macroscopic steatosis & lesion
4. SCS	DBD	50.7	32.4	70%	1.38	N/A	60% steatosis (frozen section)
5. SCS	DBD	63.8	33.0	30%	1.69	N/A	Macroscopic steatosis (severe) & size mismatch
6. SCS	DBD	66.1	38.8	20%	-	N/A	Macroscopic steatosis
7. SCS	DBD	30.1	38.0	33%	1.28	N/A	Retrieval biopsy (frozen section): • Fibrosis stage 3 • 55% MiS • 15% ld-MaS
8. SCS	DCD	61.3	31.2	10%	-	N/A	Macroscopic steatosis & poor perfusion
9. cNMP	DBD	61.8	32.8	50%	1.77	Nil	>50% steatosis (frozen section) & peri-portal fibrosis
10. cNMP	DBD	43.1	22.9	30%	1.39	125	Macroscopic steatosis & anaesthetic decision
11. cNMP	DBD	55.4	34.7	34%	1.86	5	Macroscopic steatosis & persistently acidotic with lactate >8mmol/l during NMP
12. cNMP	DBD	65	33.2	10%	1.62	160	Macroscopic steatosis
13. cNMP	DBD	52	43.5	20%	2.30	25	Macroscopic steatosis & persistently acidotic with lactate >6mmol/l during NMP
14. cNMP	DCD	46.2	25.1	60%	1.75	250	Macroscopic serve steatosis & retrieval ALT 2900 IU/L

4.3.2 Pre-preservation donor liver biopsy steatosis quantification

The retrieval surgeon's macroscopic assessment of steatosis overestimated the degree of steatosis severity when compared to the histopathologist report of the pre-preservation (LT1) donor biopsy (Table 4.5).

Table 4.5. Steatosis quantification of LT1 biopsy

Frequency [%]	**Steatosis cNMP *n*=21**	**Steatosis SCS *n*=12**	**Steatosis Discarded *n*=14**	**Lean cNMP *n*=46**	**Lean SCS *n*=26**	***P* - value**
Surgeon's steatosis assessment						
None	1 [4.8]	4 [33.3]	-	15 [32.6]	10 [38.5]	N/A
Mild	7 [33.3]	2 [16.7]	1 [7.1]	21 [45.7]	14 [53.8]	
Moderate	5 [23.8]	4 [33.3]	4 [28.6]	9 [19.6]	2 [7.7]	
Severe	8 [38.1]	2 [16.7]	9 [64.3]	1 [2.2]	-	
Histopathologist steatosis assessment						N/A
None	-	-	-	46 [100]	26 [100]	
Mild	14 [66.7]	9 [75]	10 [71.4]	-	-	
Moderate	6 [28.6]	2 [16.7]	3 [21.4]	-	-	
Severe	1 [4.8]	1 [8.3]	1 [7.1]	-	-	

A full complement of pre-preservation (LT1) histopathology reports were available for steatosis assessment. There was a significant difference in median ld-MaS percentage reported by the histopathologist on the pre-preservation (LT1) biopsy between groups: Steatotic cNMP, 15% and range (5-70%); Steatotic SCS, 10% (5-80%); Steatotic discarded, 25% (5-70%), Lean cNMP, 0.5% (0-4%); Lean SCS, 1% (0-4%); $P < 0.001$ (Figure 4.1A).

Ninety-three livers had a corresponding digitised LT1 biopsy image available for digital image analysis (DIA) and with a significant difference in median ld-MaS percentage also noted between groups: Steatotic cNMP=19, 13.08% (0.10-36.11%); Steatotic SCS=11, 7.37% (0.35-47.2%); Steatotic discarded=9, 8.11% (1.05-35.95%); Lean cNMP=37, 0.16% (0.00-2.54%); Lean SCS=17, 0.19% (0.04-6.784%); $P = 0.000$ (Figure 4.1B). The correlation between digital image analysis and the histopathologist report of ld-MaS was also assessed ($r = 0.81$, $P < 0.001$), (Figure 4.1C).

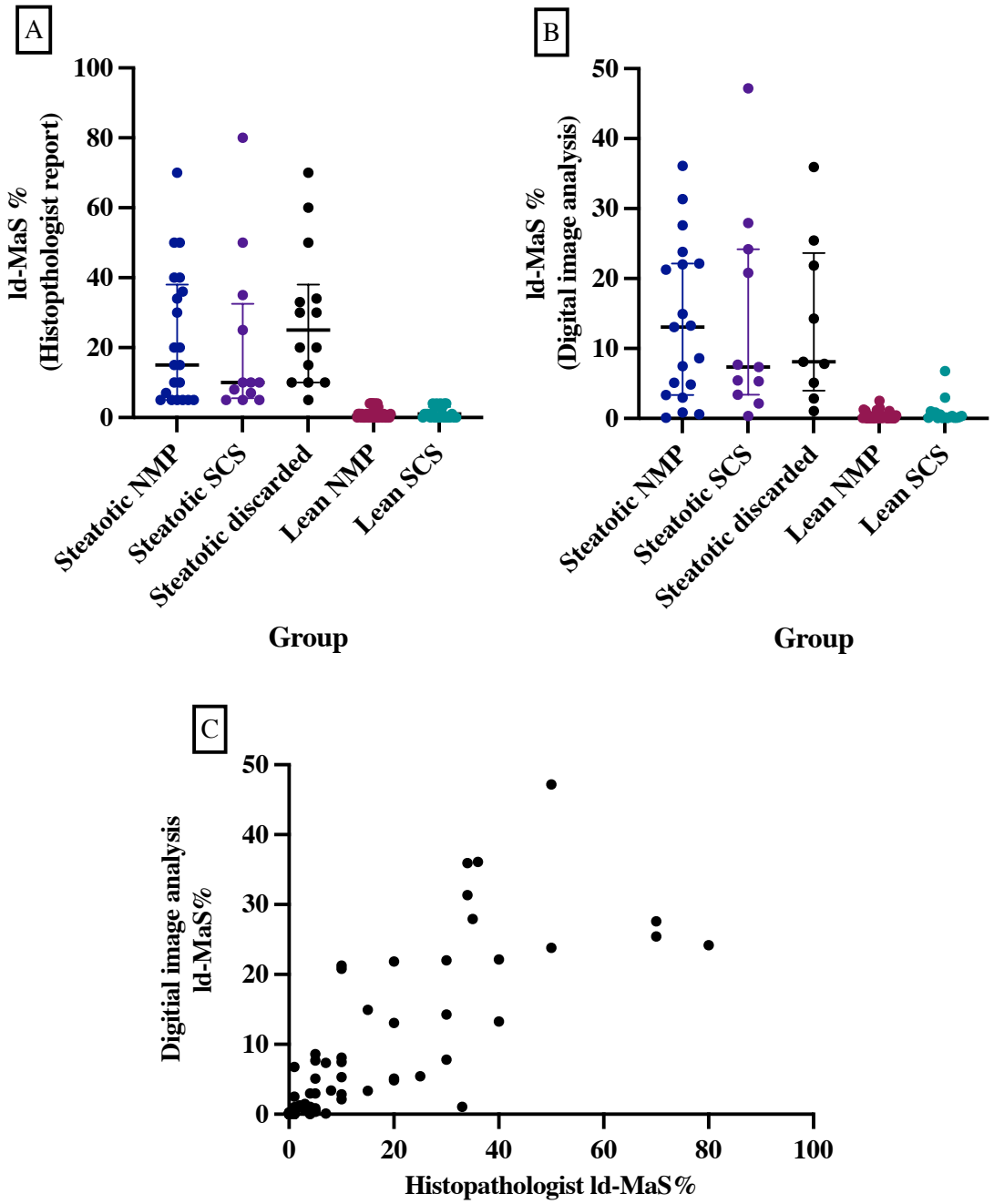

Figure 4.1A-C. The median and IQR are presented for each group. Scatter dot plots demonstrating pre-preservation (baseline) ld-MAS percentage in all groups as quantified by histopathological assessment **(A)** and digital image analysis **(B)**. Correlation between digital image analysis and histopathological assessment of ld-MAS, (r = 0.81, P = 0.000), **(C)**.

4.3.3 Recipient demographics

Recipient demographics are summarised in Table 4.6. Recipients in all 4 groups were predominately male with a mean age over 50 years and a comparable MELD score. There was a non-significant difference in recipient median BMI between groups: Steatotic cNMP=28.98kg/m^2 [IQR] (25.07-36.78); Steatotic SCS=29.30kg/m^2 (25.74-33.70); Lean

cNMP=25.41kg/m^2 (22.48-33.39); Lean SCS=28.03kg/m^2 (24.59-30.63); P = 0.060. The main indication for liver transplant in all 4 groups was Alcoholic Liver Disease (Steatotic cNMP, 33.3% vs. Steatotic SCS, 41.7% vs. Lean cNMP 34.8% vs. Lean SCS, 38.5%).

Table 4.6. Recipient demographics

Median [IQR], Column frequency [%] & Missing data [Number, %]	**Steatosis cNMP *n*=21**	**Steatosis SCS *n*=12**	**Lean cNMP *n*=46**	**Lean SCS *n*=26**	***P* - value**
Age	61.22 [55.07-66.09]	55.53 [50.77-61.06]	54.22 [44.88-61.67]	60.95 [52.68-65.97]	0.060
Gender					
Male	17 [81.0]	9 [75.0]	34 [73.9]	22 [84.6]	0.773
Female	4 [19.0]	3 [25.0]	12 [26.1]	4 [15.4]	
MELD score	14 [11.0-19.0]	11.5 [8.0-17.0]	13.0 [9.0-16.0]	10.5 [8.0-14.0]	0.219
Transplant indication					N/A
NASH	-	1 [8.3]	4 [8.7]	2 [7.7]	
PBC	2 [9.5]	-	5 [10.9]	2 [7.7]	
ALD	7 [33.3]	5 [41.7]	16 [34.8]	10 [38.5]	
HCC (Cirrhosis)	3 [14.3]	3 [25.0]	6 [13.0]	1 [3.8]	
NAFLD	1 [4.8]	1 [8.3]	-	-	
Other	8 [38.1]	2 [16.7]	15 [32.6]	11 [42.3]	
Weight (kg)	86.50 [75.0-107.6]	94.43 [87.53-103.33]	74.55 [63.8-92.8]	80.6 [71.8-96.6]	0.032
Height (cm)	173.0 [164.0-180.0]	176.5 [168.5-183.5]	170.5 [164.0-179.0]	174.5 [167.0-179.0]	0.603
BMI (kg/m^2)	28.98 [25.07-36.78]	29.30 [25.74-33.70]	25.41 [22.48-33.39]	28.03 [24.59-30.63]	0.060
Creatinine (mmol/L)	69.0 [54.0-100.0]	79.0 [51.5-117.5]	66.0 [55.0-89.0]	70.5 [45.0-87.0]	0.449
eGFR	78.53 [59.5-106.1]	93.04 [41.4-104.2]	95.78 [70.8-110.1]	94.48 [79.8-107.2]	0.652
Missing	-	-	1 [2.2]	1 [3.8]	
Bilirubin (µmol/L)	37.0 [16.0-72.0]	18.5 [11.0-35.0]	26.5 [10.0-52.0]	18.0 [13.0-27.0]	0.289
INR	1.40 [1.2-1.7]	1.20 [1.1-1.5]	1.28 [1.17-1.40]	1.26 [1.1-1.4]	0.198

4.3.4 Peri-operative and early post-operative outcomes

Peri-operative outcomes are summarised in Table 4.7. There was a significant reduction in the incidence of post-reperfusion syndrome (PRS) in recipients of Steatotic cNMP livers (14.3%) compared to Steatotic SCS livers (50%), P = 0.0267. There was also a significant reduction in

the incidence of early allograft dysfunction (EAD) in recipients of Steatotic cNMP livers (14.3%) compared to Steatotic SCS livers (66.7%), *P* = 0.002.

Table 4.7. Peri-operative outcomes

Median [IQR ± range], Column frequency [%]	**Steatosis cNMP *n*=21**	**Steatosis SCS *n*=12**	**Lean cNMP *n*=46**	**Lean SCS *n*=26**	***P* - value**
Re-transplant operation					
No	20 [95.2]	12 [100.0]	42 [91.3]	26 [100.0]	0.325
Yes	1 [4.8]	-	4 [8.7]	-	
Operation duration (hours)	5.75 [4.42-7.32]; [2.95-10.27]	6.23 [5.04-6.95]; [4.67-7.67]	5.02 [4.30-6.15]; [3.32-15.42]	5.23 [3.88-6.85]; [2.58-13.12]	0.243
Operative reperfusion time (minutes)	37.0 [26.0-53.0]; [21.0-70.0]	43.0 [34.0-48.5]; [31.0-55.0]	33.5 [24.0-53.0]; [14.0-133.0]	33.5 [28.0-44.0]; [18.0-112.0]	0.521
Evidence of post-reperfusion syndrome					
No	18 [85.7]	6 [50.0]	42 [91.3]	19 [73.1]	0.007
Yes	3 [14.3%]	6 [50.0]	4 [8.7]	7 [26.9]	
Post-reperfusion lactate	3.6 [2.5-4.2]; [1.5-6.1]	4.4 [2.5-6.0]; [2.2-6.9]	3.5 [2.6-4.1]; [1.3-8.7]	3.45 [3.0-4.2]; [2.1-5.7]	0.464
Early allograft dysfunction (EAD)					
No	18 [85.7]	4 [33.3]	42 [91.3]	21 [80.8]	<0.001
Yes	3 [14.3]	8 [66.7]	4 [8.7]	5 [19.2]	

Day 1 post-operative outcomes are summarised in Table 4.8. There was a significant reduction in day 1 median serum AST in recipients of Steatotic cNMP livers (898 IU/L (IQR: 466.0-1355.0)) compared to Steatotic SCS livers (2478.5 IU/L (978-4084.5)); *P* = 0.0270 (Figure 4.2A). Day 1 serum AST in recipients of steatotic cNMP livers (898 IU/L (466.0-1355.0)) was comparable to Lean SCS livers (741 IU/L (476.0-1193.0)); *P* = 0.995 (Figure 4.2B). Day 1 serum AST in recipients of Lean cNMP livers (421 IU/L (238.0-626.5)) was significantly lower than Steatotic cNMP livers (898 IU/L (466.0-1355.0)); *P* = 0.001 (Figure 4.2C). Day 1 serum AST in recipients of Lean SCS livers (741 IU/L (465.0-1419.0)) was significantly higher than Lean cNMP livers (421 IU/L (235.0-633.8)); P = 0.0007 (Figure 4.2D).

There was also a significant reduction in day 1 median serum ALT in recipients of Steatotic cNMP livers (668 IU/L (379.0-1165.0)) compared to Steatotic SCS livers (1524 IU/L (854.5-

2474.5)); P = 0.0390 (Figure 4.2A). Day 1 serum ALT in recipients of steatotic cNMP livers was comparable to Lean SCS livers (557 IU/L (417.0-1063.0)); P = 0.689 (Figure 4.2B). Day 1 serum ALT in recipients of Lean cNMP livers (304.5 IU/L (176.0-486.0)) was significantly lower than Steatotic cNMP livers (668 IU/L (379.0-1165.0)); P = 0.001 (Figure 4.2C). Day 1 serum ALT in recipients of Lean SCS livers (577.0 IU/L (368.5-1122.0)) was significantly higher than Lean cNMP livers (304.5 IU/L (175.3-496.3)); P = 0.0017 (Figure 4.2D). There was a non-significant reduction in the requirement for renal replacement therapy (RRT) in recipients of Steatotic cNMP livers (19%) compared to Steatotic SCS livers (33.3%), P = 0.357.

Table 4.8. Day 1 post-operative outcomes

Mean ± SD, Median [IQR ± range], Column frequency [%] & Missing data [Number, %]		**Steatosis cNMP *n*=21**	**Steatosis SCS *n*=12**	**Lean cNMP *n*=46**	**Lean SCS *n*=26**	***P* - value**
Day 1	**Patient survival**	21 [100.0]	12 [100.0]	46 [100.0]	26 [100.0]	N/A
	Graft survival **Yes** **No**	 21 [100.0] -	 12 [100.0] -	 45 [97.8] 1 [2.2]	 26 [100.0] -	N/A
	Level of care **ITU/HDU** **Ward**	 21 [100.0] -	 12 [100.0] -	 46 [100.0] -	 25 [96.2] 1 [3.8]	N/A
	RRT	4 [19.0]	4 [33.3]	6 [13.0]	3 [11.5]	0.602
	Bilirubin (µmol/L) **Missing**	54.0 [24.0-101.0] -	71.0 [34.5-93.5] -	33.0 [16.0-66.0] 1 [2.2]	39.0 [16.0-73.0] -	0.256
	AST (IU/L) **Missing**	898 [466.0-1355.0] -	2478.5 [978-4084.5] -	421 [238.0-626.5] 6 [13.0]	741 [476.0-1193.0] 1 [3.8]	<0.0001
	ALT (IU/L) **Missing**	668 [379.0-1165.0] 2 [9.5]	1524 [854.5-2474.5] 4 [33.3]	304.5 [176.0-486.0] 8 [17.4]	577 [417.0-1063.0] 9 [34.6]	<0.0001
	INR **Missing**	1.7 [1.4-2.0] -	1.55 [1.3-2.19] -	1.59 [1.3-1.8] 2 [4.4]	1.6 [1.4-1.8] -	0.487
	Lactate (mmol/L) **Missing**	1.5 [1.2-2.4]; [0.6-13.4] 4 [19.04]	2.2 [1.05-2.73]; [0.9-4.1] -	1.5 [1.0-2.0]; [0.5-3.7] 9 [19.6]	1.2 [0.9-2.5]; [0.2-7.4] 4 [15.4]	0.386
	Creatinine **Missing**	100 [78.0-127.0] -	144.5 [120.5-172.5] -	65.0 [54.0-99.0] 1 [2.2]	96.0 [56.0-133.0] -	0.002
	Platelets **Missing**	71.5 [52.0-107.0] 1 [4.8]	68.0 [41.0-83.0] 2 [16.7]	95.0 [67.0-116.0] 1 [2.2]	91.0 [73.0-106.0] 3 [11.5]	0.178

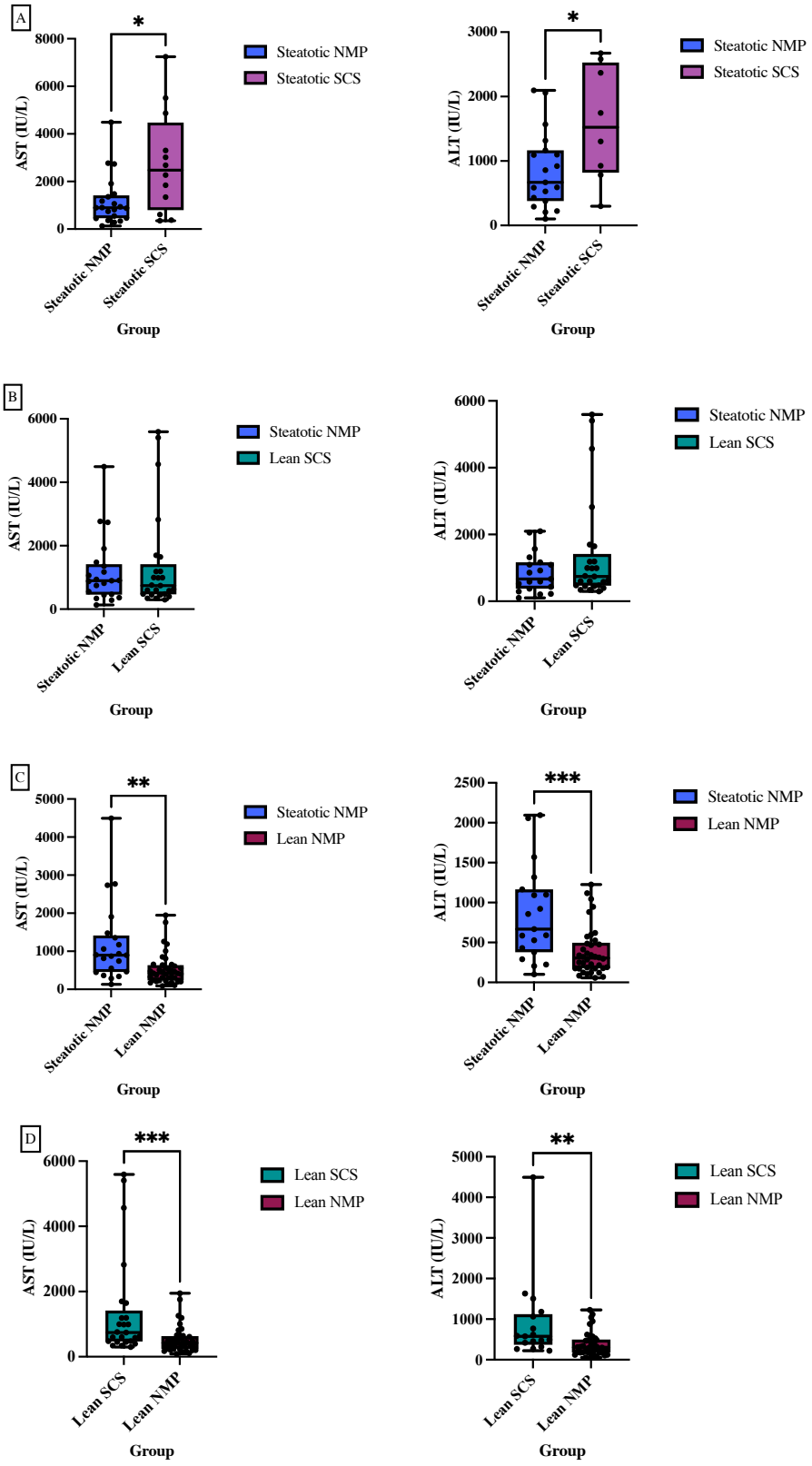

Figure 4.2A-D. Box and whisker plots demonstrating significant reduction in Day 1 serum AST & ALT between Steatotic cNMP and Steatotic SCS livers **(A)**, comparable Day 1 serum AST & ALT between Steatotic cNMP and Lean SCS livers **(B)** and significantly lower AST & ALT between Lean cNMP and Steatotic cNMP livers **(C) and significantly higher AST & ALT between Lean SCS and Lean cNMP livers (D).** Data present as median with IQR and range. *$p \leq$ 0.05, ** $p \leq$ 0.01, *** $p \leq$ 0.001.

Day 7 and 10 post-operative outcomes are summarised in Table 4.9. One liver in the Steatotic cNMP group developed PNF, this was also associated with recipient mortality within the first 7 days post-transplant. Perfusion characteristics of this liver demonstrated persistent acidosis with lactate >4mmol/L throughout perfusion and absence of bile production despite a homogenously perfused appearance of the liver parenchyma.

In addition, there was a significant reduction in median serum peak AST (during first 7 days post-transplant) in recipients of Steatotic cNMP livers (906 IU/L (IQR: 524.0-1417.0)) compared to Steatotic SCS livers (2479 IU/L (1173.0-4476.0)); $P = 0.0126$ (Figure 4.3A). Peak AST in recipients of steatotic cNMP livers (906 IU/L (524.0-1417.0)) was comparable to Lean SCS livers (683.5 IU/L (470.5-1320.0)); $P = 0.649$ (Figure 4.3B). Peak AST in recipients of Lean cNMP livers (407 IU/L (229.5-654.5)) was significantly lower than Steatotic cNMP livers (906 IU/L (524.0-1417.0)); $P < 0.001$ (Figure 4.3C).

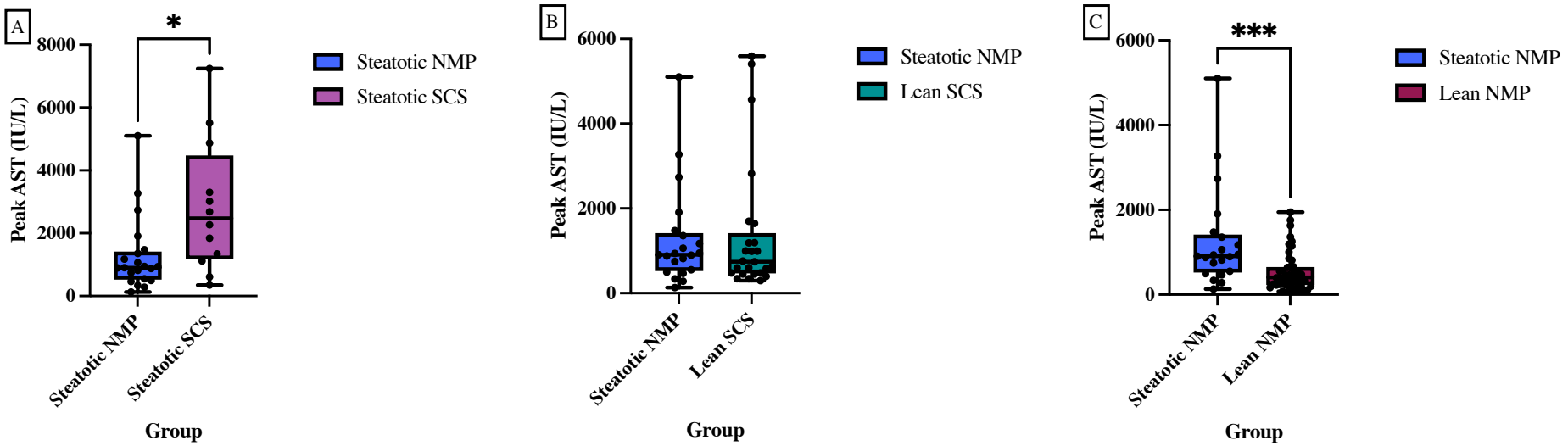

Figure 4.3A-C. Box and whisker plots demonstrating significant reduction peak AST between Steatotic cNMP and Steatotic SCS livers **(A)**, comparable peak AST between Steatotic cNMP and Lean SCS livers **(B)** and significantly lower AST between Lean cNMP and Steatotic cNMP livers **(C)**. Data present as median with IQR and range. *$p \leq$ 0.05, ** $p \leq$ 0.01, *** $p \leq$ 0.001.

Recipients transplanted with both Steatotic cNMP livers and Steatotic SCS livers required continued critical care support (ITU/HDU stay) at post-operative day 10 compared to Lean NMP and SCS livers: Steatotic cNMP (31.6%); Steatotic SCS (33.3%); Lean cNMP (8.7%); Lean SCS (3.8%). There was a significant difference in the requirement for RRT between all 4 groups at post-operative day 10: Steatotic cNMP (10.5%); Steatotic SCS (33.3%); Lean cNMP (2.2%); Lean SCS (11.5%); $P = 0.013$.

Table 4.9. Day 7 and 10 post-operative outcomes

Mean ± SD, Median [IQR ± range], Column frequency [%]		**Steatosis cNMP *n*=21**	**Steatosis SCS *n*=12**	**Lean cNMP *n*=46**	**Lean SCS *n*=26**	***P* - value**
Day 7	**Patient survival**					
	Yes	20 [95.2]	12 [100.0]	46 [100.0]	26 [100.0]	N/A
	No	1 [4.8] [a]	-	-	-	
	Graft survival					
	Yes	20 [95.2]	11 [91.7]	45 [97.8]	26 [100.0]	N/A
	No	1 [4.8] [a]	1 [8.3]	1 [2.2]	-	
	Level of care					
	ITU/HDU	9 [45.0]	7 [58.3]	9 [19.6]	6 [23.1]	0.066
	Ward	10 [50.0]	4 [33.3]	36 [78.3]	19 [73.1]	
	Outpatient	1 [5.0]	1 [8.3]	1 [2.2]	1 [3.8]	
	RRT	3 [15.0]	3 [25.0]	2 [4.3]	3 [11.5]	0.174
Peak AST (IU/L)		906 [524-1417]	2479 [1173-4476]	407 [229.5-654.5]	683.5 [470.5-1320]	<0.0001
Day 10	**Patient survival**					N/A
	Yes	19 [90.5]	12 [100.0]	46 [100]	26 [100.0]	
	No	2 [9.5] [a]	-	-	-	
	Graft survival					
	Yes	19 [90.5]	11 [91.7]	45 [97.8]	26 [100.0]	N/A
	No	2 [9.5] [a]	1 [8.3]	1 [2.2]	-	
	Level of care					
	ITU/HDU	6 [31.6]	4 [33.3]	4 [8.7]	1 [3.8]	0.065
	Ward	10 [52.6]	6 [50.0]	31 [67.4]	20 [76.9]	
	Outpatient	3 [15.8]	2 [16.7]	11 [23.9]	5 [19.2]	
	RRT	2 [10.5]	4 [33.3]	1 [2.2]	3 [11.5]	0.013

[a] Death due to primary non-function (PNF)

4.3.5 Longer-term outcomes

There was a non-significant reduction in graft survival between the 4 groups at post-operative months 6 and 12 (Table 4.10): Steatotic cNMP (90.5%); Steatotic SCS (88.3%); Lean cNMP (93.5%); Lean SCS (100%).

Table 4.10. Longer-term post-operative outcomes

Median [IQR], Column frequency [%] & Missing data [Number, %]		Steatosis cNMP *n*=21	Steatosis SCS *n*=12	Lean cNMP *n*=46	Lean SCS *n*=26	*P* - value
Month 6	**Patient survival**					
	Yes	19 [90.5]	12 [100.0]	45 [97.8]	25 [96.2]	0.443
	No	2 [9.5] [a]	0 [0.0]	1 [2.2]	1 [3.8]	
	Graft survival					
	Yes	19 [90.5]	10 [88.3]	43 [93.5]	26 [100]	0.255
	No	2 [9.5] [a]	2 [16.7]	3 [6.5]	0 [0.0]	
	Bilirubin (µmol/L)	9.0 [4.0-16.0]	11.0 [9.0-12.0]	8 [6.0-14.0]	8.0 [6.0-13.0]	0.793
	Missing	-	3 [25.0]	4 [8.9]	-	
	AST (IU/L)	20.5 [14.0-31.0]	22.0 [17.0-25.0]	28.0 [22.0-37.0]	21.0 [16.0-27.0]	0.156
	Missing	1 [5.3]	5 [41.7.0]	8 [17.8]	3 [12.0]	
	ALT (IU/L)	19.0 [14.0-42.0]	15.0 [13.5-20.0]	25.5 [17.5-43.5]	21.0 [14.0-39.0]	0.244
	Missing	1 [5.3]	4 [33.3]	5 [11.1]	-	
	Creatinine	92.0 [70.0-107.0]	95.0 [80.0-126.0]	88.0 [76.0-105.0]	100.0 [88.0-124.0]	0.336
	Missing	-	3 [25.0]	4 [8.9]	-	
Month 12	**Patient survival**					
	Yes	19 [90.5]	12 [100.0]	45 [97.8]	25 [96.2]	0.443
	No	2 [9.5] [a]	0 [0.0]	1 [2.2]	1 [3.8]	
	Graft survival					
	Yes	19 [90.5]	10 [83.3]	43 [93.5]	26 [100]	0.255
	No	2 [9.5] [a]	2 [16.7]	3 [6.5]	0 [0.0]	
	Bilirubin (µmol /L)	10.0 [4.0-15.5]	12.0 [5.0-13.0]	9.0 [4.0-15.0]	9.0 [6.5-12.0]	0.948
	Missing	3 [15.8]	3 [25.0]	6 [13.3]	1 [4.0]	
	AST (IU/L)	21.0 [19.0-22.0]	25.0 [13.0-38.0]	25.5 [20.0-37.5]	21.0 [15.0-27.0]	0.174
	Missing	7 [36.8]	5 [41.7]	13 [28.9]	6 [24.0]	
	ALT (IU/L)	25.5 [18.5-30.5]	19.5 [12.5-26.0]	24.0 [16.0-36.0]	17.0 [13.0-24.0]	0.111
	Missing	3 [15.8]	4 [33.3]	6 [13.3]	2 [8.0]	
	Creatinine	89.5 [67.0-109.5]	107.0 [96.0-120.0]	90.0 [74.0-106.0]	102.0 [83.5-128.0]	0.188
	Missing	3 [15.8]	3 [25.0]	6 [13.3]	1 [4.0]	

[a] Death due to primary non-function (PNF)

4.3.6 Histological analysis

4.3.6.1 Changes in ld-MaS

Seventeen out of 21 steatotic donor livers preserved with cNMP had a full complement of pre-preservation (LT1), post-preservation (LT2) and post-reperfusion (LT3) biopsy available for comparison of ld-MaS. There was a non-significant reduction in median histopathological ld-

MaS percentage during preservation and post-reperfusion: LT1, 15% and range (5-70%); LT2, 5% (0-35%); LT3, 7% (1-36%); $P = 0.078$. This reduction in ld-MaS was not evident on DIA: LT1, 13.17% (0.10-36.11%); LT2, 13.24% (0.085-37.85); LT3, 9.01% (0.14-43.07%); $P = 0.840$ (Figure 4.4A).

Ten out of 12 steatotic donor livers preserved with SCS had a full complement of pre-preservation (LT1), post-preservation (LT2) and post-reperfusion (LT3) biopsy available for comparison of ld-MaS. There was a non-significant reduction in median histopathological ld-MaS percentage during preservation and post-reperfusion: LT1, 10% and range (5-80%); LT2, 5.5% (1-80%); LT3, 5.5% (2-80%); $P = 0.342$. This reduction in ld-MaS was not evident on DIA: LT1, 6.40% (0.35-47.2%); LT2, 4.52% (0.57-44.44); LT3, 6.27% (0.00-29.89%); $P = 0.889$ (Figure 4.4B).

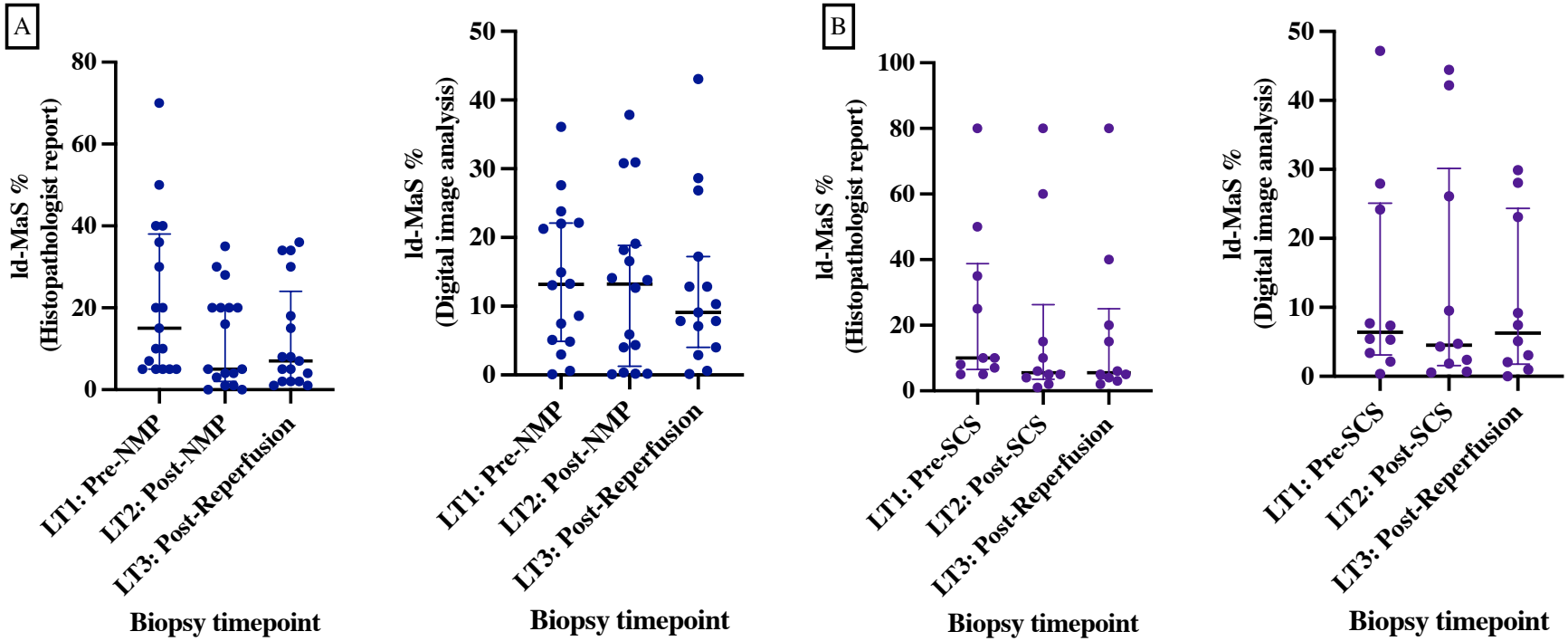

Figure 4.4A-B. Scatter dot plots demonstrating change in ld-MaS in Steatotic cNMP livers **(A)** and Steatotic SCS livers **(B)** on histopathological evaluation and digital image analysis (DIA). The median, IQR and range are presented for each group.

4.3.6.2 Glycogen depletion

There was a non-significant difference in median glycogen depletion percentage between groups pre-preservation (LT1): Steatotic cNMP, 10% and range (0-99%); Steatotic SCS, 10% (0-80%); Lean cNMP, 12.5% (0-100%); Lean SCS, 5.5% (0-80%); $P = 0.538$ (Figure 4.5A). Static cold stored livers had a higher median glycogen depletion percentage at the end of preservation (LT2) compared to NMP preserved livers: Steatotic NMP, 1% and range (0-95%); Steatotic SCS, 24% (0-80%); Lean NMP, 4% (0-90%); Lean SCS, 8% (0-90%); $P = 0.157$ (Figure 4.5B). There was a significant difference between groups post-reperfusion (LT3), livers preserved with cNMP had lower median glycogen depletion percentage compared to livers preserved with SCS: Steatotic cNMP, 30% and range (0-85%); Steatotic SCS, 67.5% (0-90%); Lean cNMP, 10% (0-100%); Lean SCS, 40% (2-100%); $P = 0.0221$ (Figure 4.5C). In addition, Dunn's multiple comparisons test demonstrated a significant difference in glycogen depletion percentage between Lean cNMP and Lean SCS livers, $P = 0.0337$.

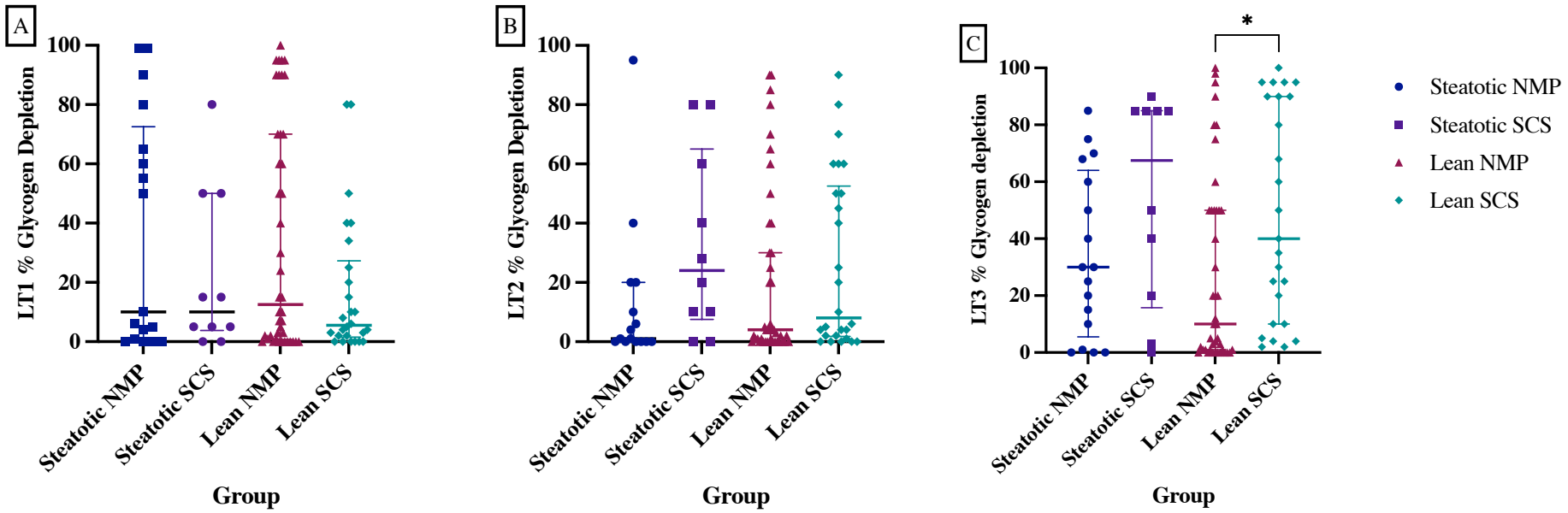

Figure 4.5A-C. Scatter dot plots demonstrating change glycogen depletion percentage for all groups: pre-preservation (LT1) **(A)** post-preservation **(B)** and post-reperfusion **(C)** on histopathological evaluation. The median, IQR and range are presented for each group. *$p < 0.05$.

4.3.6.3 Histological preservation reperfusion injury (PRI)

There was a significant difference in histological PRI scores between groups, Steatotic cNMP livers had comparable median PRI scores (0-6) post-reperfusion (LT3) to Lean SCS livers: Steatotic cNMP, 2 and range (0-5); Steatotic SCS, 4 (0-6); Lean cNMP, 1 (0-6); Lean SCS, 2 (0-5); $P = 0.0463$ (Figure 4.6). In addition, Dunn's multiple comparisons test demonstrated a significant difference in PRI scores between Steatotic SCS and Lean cNMP livers, $P = 0.040$ (Figure 4.6).

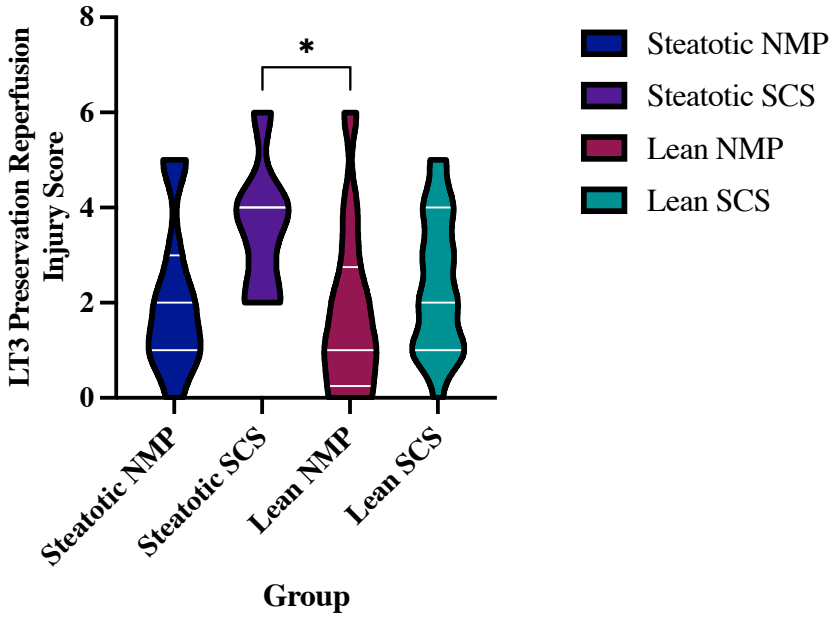

Figure 4.6. Violin plots demonstrating median PRI post-reperfusion for all groups. The median, IQR and range are presented for each group. *$p < 0.05$.

4.3.7 Perfusate analysis

Sequential perfusate samples collected at 15 min (P1), 60 min (P2) and end of perfusion (P3) from all Steatotic cNMP livers (including those not transplanted following NMP) were compared with lean counterparts.

4.3.7.1 Hepatocellular injury

Steatotic cNMP livers demonstrated evidence of a greater degree of hepatocellular injury compared to lean cNMP livers throughout preservation, with a high mean ALT at 15 min (1560.46 ± 1766.04 IU/L vs. 840.40 ± 1560.70 IU/L, $P = 0.0104$) and, at 60 min (1673.50 ± 1758.88 IU/L vs. 993.61 ± 1869.37 IU/L, $P = 0.0035$) and end of preservation (2242.33 ± 2138.77 IU/L vs. 1492.95 ± 2977.11 IU/L, $P = 0.0042$), (Figure 4.7A). This trend was also reflected in perfusate AST at 15 min (2180.63 ± 2130.35 IU/L vs. 1151.71 ± 2206.80 IU/L, $P = 0.0105$) (2348.32 ± 2262.45 IU/L vs. 1313.01 ± 2450.82 IU/L, $P = 0.0145$) and end of preservation (3341.84 ± 2971.30 IU/L vs. 1929.60 ± 3505.02 IU/L, $P = 0.0029$), (Figure 4.7B).

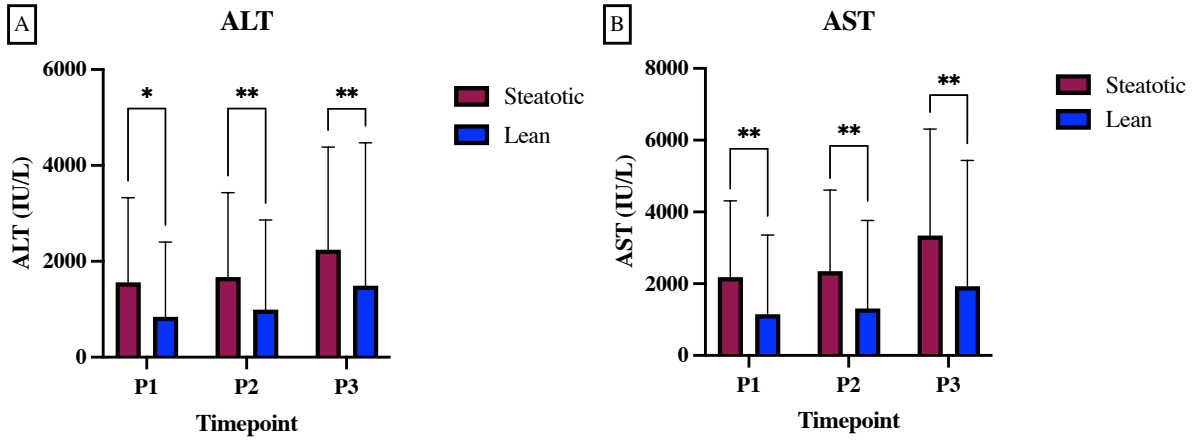

Figure 4.7A-B. Perfusate ALT **(A)** and AST **(B)** in steatotic compared to lean donor livers during cNMP. Data presented as mean ± SD. *$p \leq 0.05$, ** $p \leq 0.01$, *** $p \leq 0.001$.

4.3.7.2 Cholangiocellular

There was no significant difference in perfusate GGT during cNMP in steatotic livers compared to lean counterparts at 15 min ($P = 0.813$) and, at 60 min ($P = 0.672$) and end of preservation ($P = 0.895$), (Figure 4.8A). Similarly, perfusate ALP was comparable between groups at 15 min ($P = 0.159$) and, at 60 min ($P = 0.480$) and end of preservation ($P = 0.677$), (Figure 4.8B). Perfusate bilirubin was comparable between groups 15 min ($P = 0.473$) and, at 60 min ($P = 0.346$) and end of preservation ($P = 0.841$), (Figure 4.8C). Steatotic cNMP livers demonstrated a greater production of bile salts compared to lean livers throughout preservation with a mean bile salt concentration at 15 min (6.49 ± 8.68 µmol/L vs. 4.17 ± 7.47 µmol/L, $P = 0.278$) and, at 60 min (6.99 ± 11.36 µmol/L vs. 4.26 ± 7.43 µmol/L, $P = 0.218$) and end of preservation (81.40 ± 136.01 µmol/L vs. 67.80 ± 113.19 µmol/L, $P = 0.717$), (Figure 4.8D).

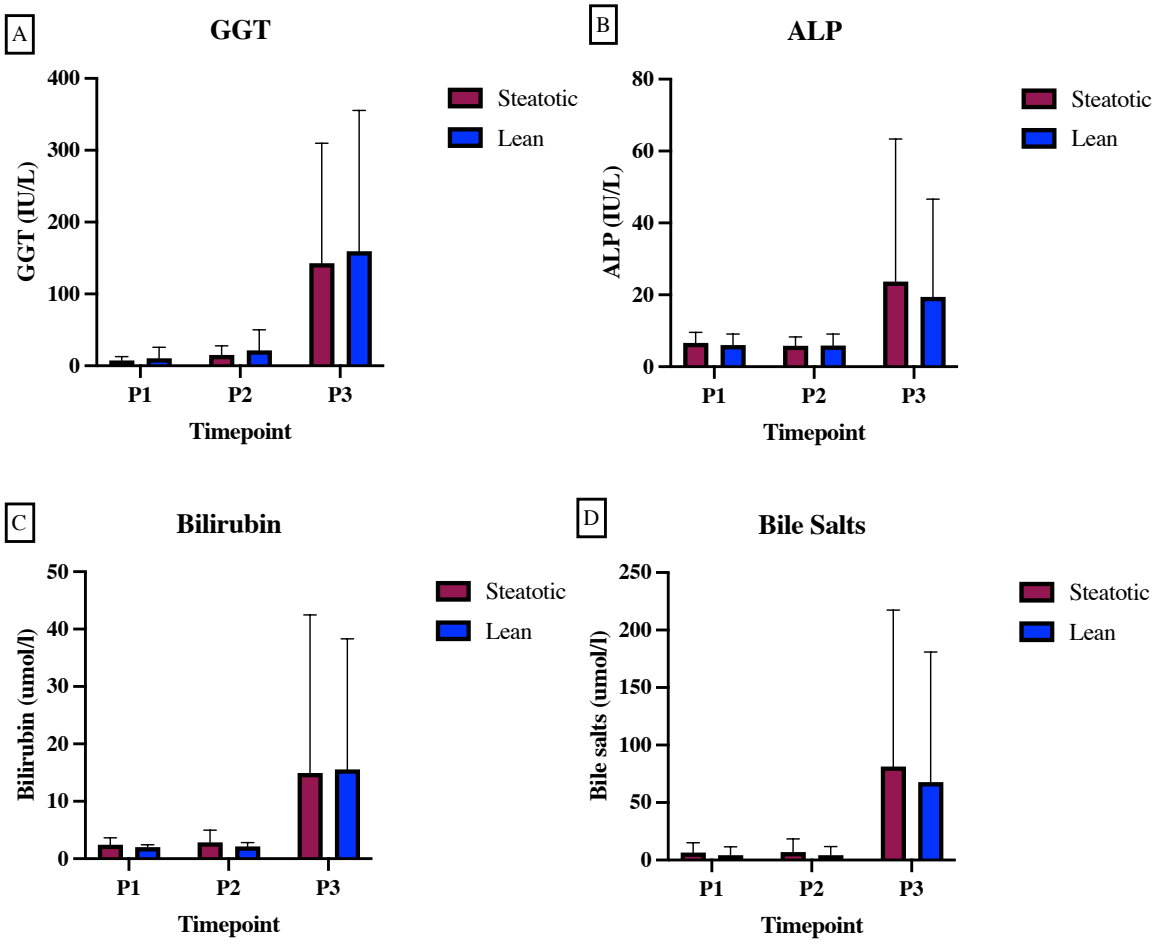

Figure 4.8A-D. Perfusate GGT **(A)**, ALP **(B),** Bilirubin **(C)** and Bile salts **(D)** in steatotic compared to lean donor livers during cNMP. Data presented as mean ± SD.

4.3.7.3 Hepatic lipid metabolism

There was no significant difference in perfusate cholesterol during cNMP in steatotic livers compared to lean counterparts at 15 min (P = 0.219) and, at 60 min (P = 0.536) and end of preservation (P = 0.743), (Figure 4.9A). Steatotic cNMP livers demonstrated greater mobilisation of triglycerides compared to lean livers throughout preservation with a high mean perfusate triglyceride concentration at 15 min (56.37 ± 37.88 mg/dL vs. 30.11 ± 19.83 mg/dL, P = 0.0008) and, at 60 min (61.57 ± 36.80 mg/dL vs. 34.68 ± 19.35 mg/dL, P = 0.001) and end of preservation (149.50 ± 117.63 mg/dL vs. 99.33 ± 58.92 mg/dL, P = 0.052), (Figure 4.9B). There was no significant difference in perfusate ApoB during cNMP in steatotic livers compared to lean counterparts at 15 min (P = 0.458) and, at 60 min (P = 0.995) and end of preservation (P = 0.343), (Figure 4.9C). Steatotic cNMP livers demonstrated greater fatty acid

metabolism compared to lean livers throughout preservation with a high mean perfusate 3-OHB concentration at 15 min (0.27 ± 0.15 mmol/L vs. 0.17 ± 0.09 mmol/L, $P = 0.001$) and, at 60 min (0.48 ± 0.34 mmol/L vs. 0.27 ± 0.14 mmol/L, $P = 0.003$) and end of preservation (1.47 ± 1.30 mmol/L vs. 0.83 ± 1.07 mmol/L, $P = 0.018$), (Figure 4.8D).

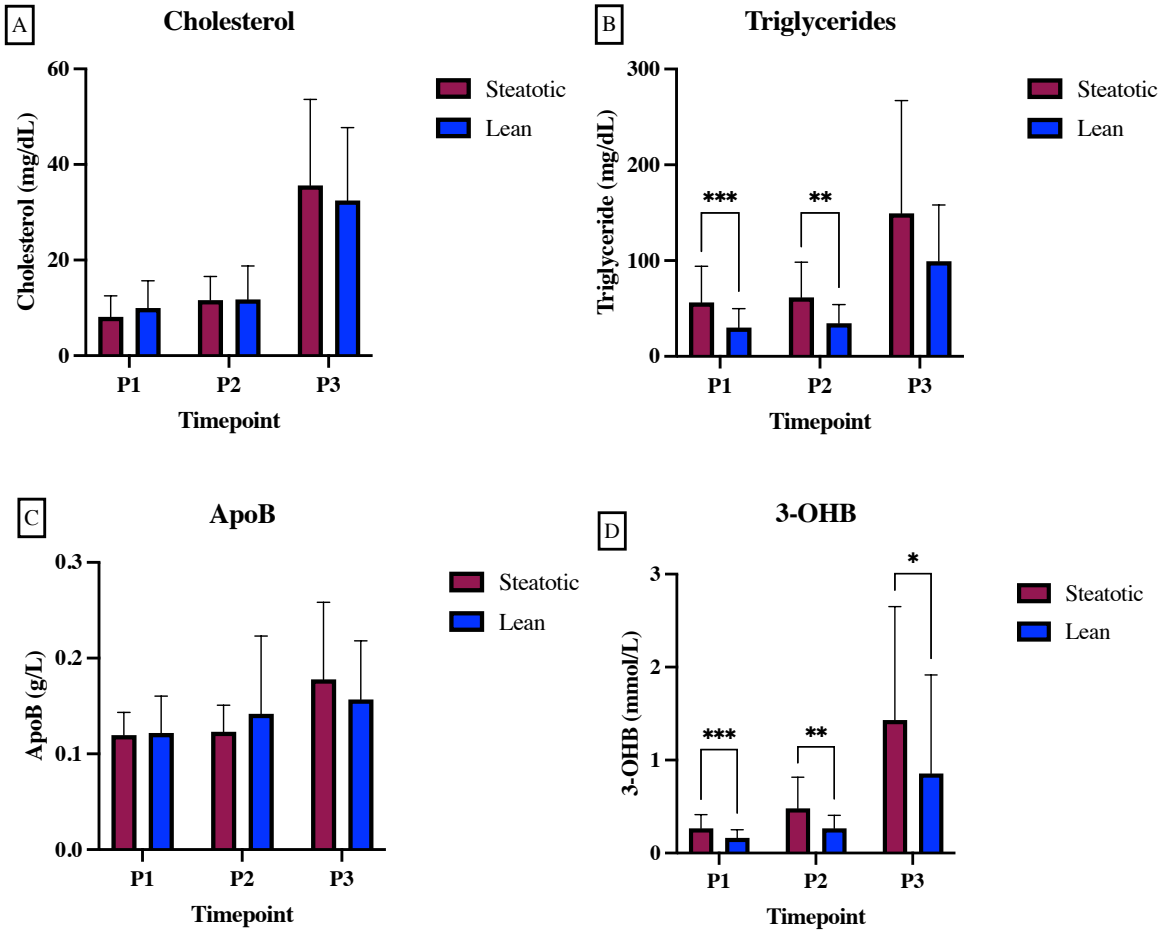

Figure 4.9A-D. Perfusate cholesterol **(A)**, triglycerides **(B),** ApoB **(C)** and 3-OHB **(D)** in steatotic compared to lean donor livers during cNMP. Data presented as mean ± SD. *$p < 0.05$, ** $p < 0.001$, *** $p < 0.0001$.

4.3.7.4 General metabolism

Steatotic cNMP livers demonstrated inferior lactate clearance compared to lean livers throughout preservation with a high mean perfusate lactate concentration at 15 min (9.29 ± 3.91 mmol/L vs. 8.96 ± 4.16 mmol/L, $P = 0.656$) and, at 60 min (4.20 ± 4.60 mmol/L vs. 2.85 ± 2.50 mmol/L, $P = 0.392$) and end of preservation (1.42 ± 2.13 mmol/L vs. 0.73 ± 0.65 mmol/L, $P = 0.601$), (Figure 4.10A). There was no significant difference in urea production during cNMP in steatotic livers compared to lean counterparts at 15 min ($P = 0.735$) and, at 60

min (P = 0.694) and end of preservation (P = 0.546), (Figure 4.10B). Similarly, there comparable glucose metabolism between groups at 15 min (P = 0.653) and, at 60 min (P = 0.810) and end of preservation (P = 0.673), (Figure 4.10C). However, steatotic cNMP livers demonstrated non-significant lower perfusate insulin levels compared to lean livers throughout preservation with a reduction in perfusate insulin concentration at 15 min (1024.67 ± 1521.15 pmol/L vs. 1246.36 ± 1442.97 pmol/L, P = 0.271) and, at 60 min (566.40 ± 967.93 pmol/L vs. 824.95 ± 1107.48 mmol/L, P = 0.143) and end of preservation (1158.60 ± 1397.10 pmol/L vs. 1622.11 ± 1509.32 pmol/L, P = 0.088), (Figure 4.10D).

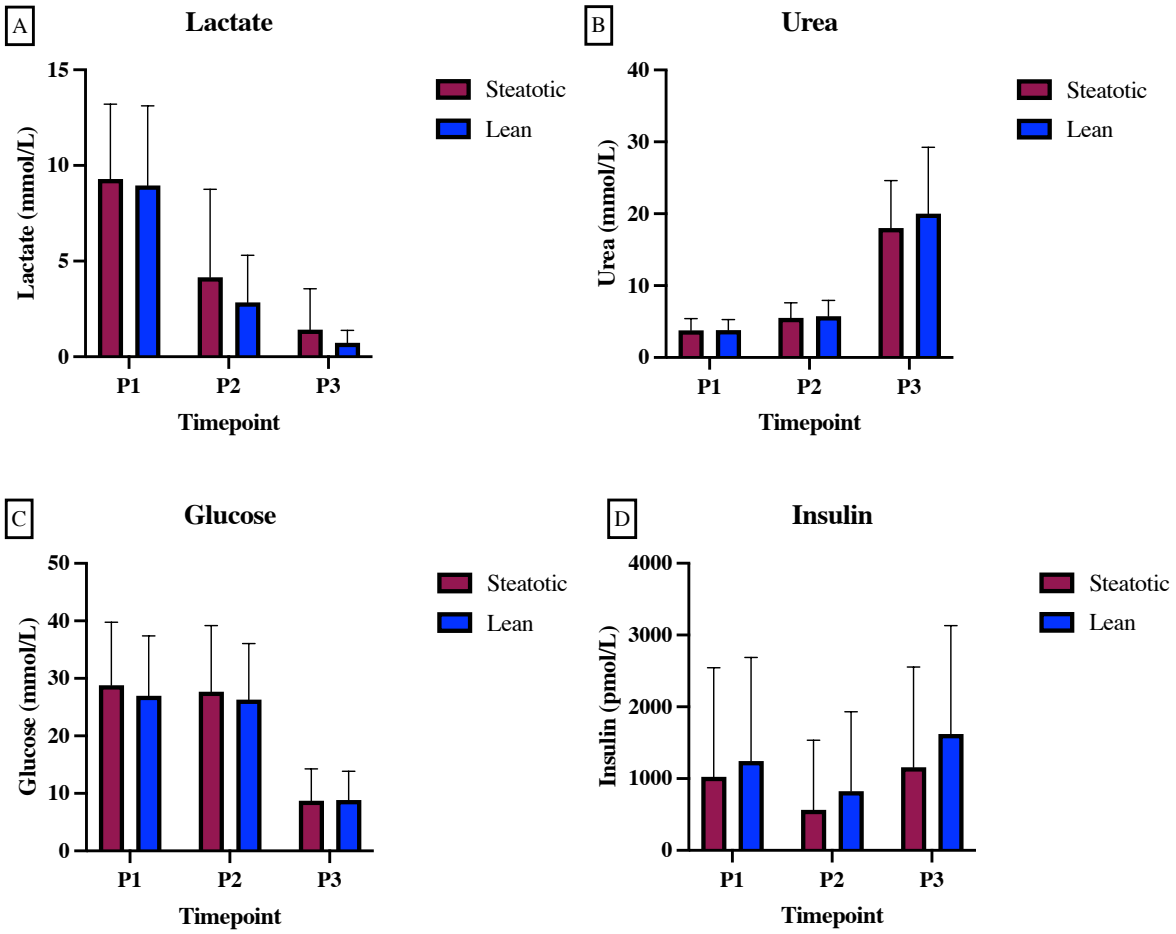

Figure 4.10A-D. Perfusate lactate **(A)**, urea **(B),** glucose **(C)** and insulin **(D)** in steatotic compared to lean donor livers during cNMP. Data presented as mean ± SD.

4.3.7.5 Systemic inflammation and metabolic stress

There was no significant difference in perfusate CRP during cNMP in steatotic livers compared to lean counterparts at 15 min (P = 0.542) and, at 60 min (P = 0.620) and end of preservation (P = 0.603), (Figure 4.11A). Steatotic cNMP livers demonstrated greater FGF-21 release

compared to lean livers throughout preservation with a high mean perfusate FGF-21 concentration at 15 min (9579.71 ± 23403.31 ng/L vs. 7007.63 ± 23276.50 ng/L, $P = 0.173$) and, at 60 min (17742.92 ± 30348.72 ng/L vs. 14974.65 ± 34362.35 ng/L, $P = 0.110$) and end of preservation (376987.0 ± 322046.51 ng/L vs. 234686.29 ± 260028.16 ng/L, $P = 0.116$), (Figure 4.11B).

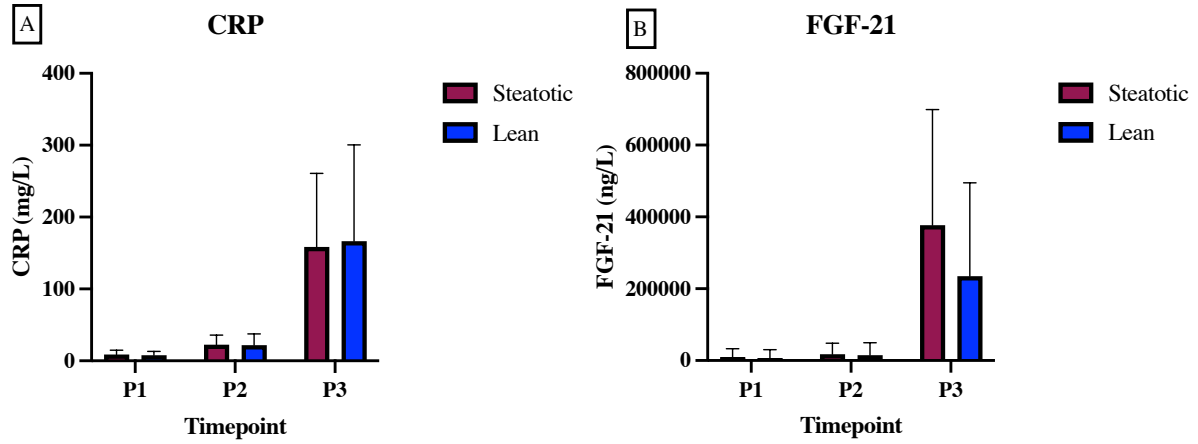

Figure 4.11A-B. Perfusate CRP **(A)** and FGF-21 **(B)** in steatotic compared to lean donor livers during cNMP. Data presented as mean ± SD.

4.4 Discussion

In this chapter, through analysis of clinical data, biological (biopsy) and cNMP perfusate samples from obtained from a Phase III multicentre RCT comparing the efficacy of cNMP to SCS, I have demonstrated the potential clinical benefit of cNMP in the transplantation of steatotic donor livers. I have also explored the utility of digital image analysis to map changes in ld-MaS during perfusion and reperfusion, thereby reducing inter-observer variability of conventional histopathology reports allowing for a more reproducible and accurate quantification of hepatic steatosis. The biochemical analysis of perfusate has identified potential biomarkers associated with metabolic changes occurring during perfusion of steatotic donor livers.

4.4.1 Clinical outcomes

From the data presented, the clinical manifestations of IRI (PRS and EAD) and reduction in peak AST in the first 7 days post-transplant were significantly reduced in steatotic livers preserved with cNMP compared to SCS and were also comparable to lean livers preserved with SCS. Whilst one liver in the Steatotic cNMP group with persistently high lactate (4mmol/L)

throughout perfusion developed PNF (with associated recipient mortality within the first 7 days post-transplant), the overall clinical data suggest the ability of cNMP to reduce the risk profile of steatotic donor livers to that comparable with lean livers preserved with SCS. It can be hypothesised that cNMP allows for ex-situ reperfusion reconditioning (the ability to overcome the 'first hit'), prior to the actual reperfusion in the recipient (the 'second hit', following transplantation). The reason for the success of this reconditioning is likely multifactorial, and related to molecular, biological and cellular changes (see Chapter 5) occurring during cNMP but also influenced by cold ischaemia time (CIT), which was minimised in this cohort due to continuous NMP.

As an alternative approach to cNMP, many centres have adopted a back-to-base approach of NMP post SCS (pSCS-NMP) to facilitate transplant logistics. However, this end-ischaemic approach may provide inferior results as the liver graft may be significantly damaged even after a short period of CIT and result in discard of steatotic livers as demonstrated in a number of end-ischaemic (pSCS-NMP) studies that have included a small proportion of steatotic livers within the overall cohort, Table 4.11.

Table 4.11. Outcomes of pSCS-NMP studies

Author	Number (*n*)	Outcomes
Watson et al., 2018 (227)	1	• Liver described as 'very steatotic' and was accepted for research with no subsequent transplant • Liver demonstrated no glucose metabolism and high ALT of 7542 IU/L at 2 hours of NMP
Ceresa et al., 2019 (210)	1	• Out of the three (9.7%) discarded livers, one liver had histological evidence of 80% MaS. This liver was discarded due to poor lactate clearance, glucose metabolism and lack of bile production.
Mergental et al., 2020 (202)	2	• Out of the 9 (29%) non-transplanted livers, 2 livers had histological evidence of moderate and severe steatosis, respectively. • 7 out of the 9 non-transplanted livers failed to meet the study viability criteria for transplantation. Out of 2 remaining livers, 1 was not transplanted due to poor vessel quality and the other due to donor cancer despite meeting viability criteria for transplantation. • Notably, the livers that did not meet viability criteria were heavier, with increased donor peak AST, longer CIT (550 vs. 452 mins) and a greater proportion (77.8% vs 40.9%) had MaS >30%.
Patrono et al., 2022 (211)	14	• Out of the 14 livers with MaS ≥ 30%, 10 livers (71.4%) resulted in transplantation and of these, 2 (14.3%) developed PNF.

In this present cohort, 22 out of 28 steatotic livers (78.6%) preserved with cNMP resulted in transplants. Of these, 1 steatotic liver was excluded following cNMP due to a subsequent ABO incompatible transplant, resulting in a final cohort of 21 transplanted steatotic livers preserved with cNMP available for recipient outcome analysis. In contrast, only 12 out 20 (60%) livers preserved with SCS resulted in transplants. Overall, steatotic livers preserved with cNMP had comparable graft survival compared to SCS (90.5% vs. 88.3%) and comparable graft survival to lean livers preserved with SCS (90.5% vs. 93.5%). Only lean livers preserved with SCS had 100% graft survival at 12 months. Whilst our cohort of steatotic livers preserved with cNMP also included those with MaS ≤ 30%, the findings suggest higher utilisation of steatotic donor livers compared to the end-ischaemic (pSCS-NMP) study performed by Patrono et al., which resulted in transplantation of 10 out 14 steatotic livers (71.4%) (211).

In support of the findings of our current cohort and addressing the limitations of end-ischaemic NMP, Patrono et al. have published a recent proof-of-concept case describing using upfront NMP (cNMP) of a HCV-positive DBD donor with 70% MaS which fulfilled metrics of ex-situ functional assessment (as prescribed by both the Birmingham and Gronigen criteria). Post-operative recipient follow-up at 6-months demonstrated both graft and patient survival with normal hepatic function and no clinical (or laboratory) evidence of ischaemic cholangiopathy (212).

The potential benefits of preventing ischaemia and complete avoidance of cooling have been explored by He et al., with the first report of successful ischaemia free liver transplantation (IFLT) performed in China of a steatotic DBD donor liver with 85-95% MaS (213). IFLT involves procurement, preservation, and implantation of the donor liver under cNMP without any interruption of blood flow. The subsequent clinical application of this procedure has demonstrated promising results which are detailed in Chapter 1.6.2.

4.4.2 Histological changes

Whilst research FFPE biopsies were taken as part of the study, the results of these were not immediately available and therefore did not influence the decision to transplant. However, the routine use of biopsies with real-time automated results could guide donor liver preservation strategies in future studies, particularly when directed towards livers with moderate-severe steatosis in order to improve utilisation and reduce discard rates. I therefore explored the utility of rapid automated image analysis using Visiopharm® digital image analysis (DIA) software to assess the degree of hepatic steatosis (HS) compared to the histopathologist's report. There was a strong correlation at LT1 (pre-preservation) between histopathologist assessment of ld-MaS and Visiopharm® DIA software ($r = 0.81$, $P < 0.001$).

In previous studies, the main limitation of DIA has been the actual steatosis percentages obtained from conventional histopathological evaluation being 1.5-4 fold higher than those generated by other DIA platforms, resulting in its limited use (80,94,267–270). This limitation was addressed using the Visiopharm® DIA software which provided comparable ld-MaS percentages to that reported by histopathologists. In addition, the effect of NMP and SCS pre-preservation (LT1), post-preservation (LT2) and post-reperfusion (LT3) on percentage of ld-MaS was also assessed. Both preservation techniques demonstrated a reduction in ld-MaS

overtime as reported by the histopathologist. However, use of the Visiopharm® DIA software provided improved accuracy in assessment of ld-MaS and demonstrated no reduction overall in ld-MaS. This finding supports the role of DIA in assessment in sequential biopsies obtained during preservation as means of providing reproducible and accurate quantification of steatosis (284) and potential application in monitoring the effect of pharmacological interventions i.e. defatting during NMP.

The findings of non-reduction in HS following cNMP in our cohort are consistent with those of Liu et al. whose series included 10 discarded human steatotic livers perfused over 24h with no histological reduction in steatosis (219). The inability to reduce HS during cNMP in this study cohort as evidenced by significantly higher post-operative peak AST in recipients of steatotic livers preserved with cNMP compared to lean livers preserved with cNMP support the concept that steatotic livers have a greater susceptibility to hepatocellular injury initiated at the level of parenchymal hepatocytes (115,116,287). Whilst the findings overall suggest a comparable outcome of steatotic livers preserved with cNMP and lean livers preserved with SCS, there is scope for ex-situ optimisation to further reduce the risk profile of steatotic livers preserved with cNMP to that comparable to lean livers preserved with cNMP.

In the current cohort, all livers had similar degrees of median glycogen depletion prior to preservation (LT1), only livers preserved with cNMP had repletion of glycogen at the end of preservation (LT2). However, during recipient reperfusion (LT3) livers preserved with cNMP had lower median glycogen depletion percentage compared to livers preserved with SCS. Under the hypoxic conditions of SCS, glycolysis becomes a pivotal metabolic pathway, essential for maintaining cellular integrity and viability. The cessation of hepatic glycolysis, triggered by either the accumulation of its end products or insufficient glycogen substrate, can lead to cell death (288,289). In a study by Cherid et al., analysis of 62 liver biopsies revealed significant glycogen depletion i.e. 48% in peri-portal regions and 78% overall during cold ischemia, which further exacerbated upon reperfusion (290). This depletion of glycogen plays a critical role in ischemia-reperfusion injury (IRI) and subsequent post-transplantation outcomes, as glycogen reserves are crucial for preserving hepatocellular integrity and function through glucose provision for ATP synthesis. The consumption of glycogen results in ATP depletion, culminating in irreversible cellular damage and necrosis (291).

Several studies have underscored the significance of hepatocellular ATP levels ex-situ and the functionality of post-transplant grafts, indicating a strong association between elevated ATP levels and favourable transplant outcomes (292–294). The differential glycogen storage observed among groups in this study during preservation may elucidate the attenuated reperfusion injury in ischaemia-reperfusion injury (IRI) in livers preserved with cNMP compared to SCS counterparts with improved post operative graft function. In addition, the ability of cNMP to attenuate IRI is also reflected in the histological preservation reperfusion injury (PRI) scores of steatotic livers. Steatotic cNMP livers had comparable median PRI scores (0-6) post-reperfusion (LT3) to Lean SCS livers: Steatotic cNMP, 2 and range (0-5); Steatotic SCS, 4 (0-6); Lean cNMP, 1 (0-6); Lean SCS, 2 (0-5); $P = 0.0463$. These histological findings also correlate with clinical outcomes of steatotic livers preserved with cNMP including reduction in PRS, EAD, peak AST and need for RRT with comparable outcomes to lean livers preserved with SCS.

4.4.3 Perfusate analysis during cNMP

Steatotic livers demonstrated a greater degree of hepatocellular injury (ALT and AST) during cNMP compared to lean counterparts throughout preservation with highest levels at end of perfusion. This finding supports the hypothesis that steatotic livers are susceptible to greater injury initiated at the level of the hepatocytes. Several mechanisms can explain this observation: (i) altered membrane permeability and cellular integrity: fatty infiltration in hepatocytes alters cell membrane stability and permeability, making them more prone to rupture and necrosis under perfusion conditions with release of ALT and AST into the perfusate (115,148); (ii) inflammatory response and hepatocellular damage: steatosis is often associated with a chronic inflammatory state within the liver, characterised by the infiltration of pro-inflammatory cells and cytokines that can exacerbate hepatocellular damage during NMP (116); and; (iii) impaired regenerative capacity: steatotic livers have been shown to possess impaired regenerative capacity, this can result in sustained hepatocellular damage during perfusion (217,295).

An interesting finding was higher mean bile salts at the end of preservation in steatotic livers: end of preservation (81.40 ± 136.01 μmol/L vs. 67.80 ± 113.19 μmol/L, $P = 0.717$). The changes in perfusate bile salts during normothermic perfusion of steatotic livers has not been previously reported. Whilst the mechanism is unknown, it can be hypothesised that the higher

levels of bile salts observed in the perfusate of steatotic livers are attributed to: (i) impaired bile acid transport: steatosis can impair the function of bile acid transporters on including the bile salt export pump (BSEP) and sodium-taurocholate co-transporting polypeptide (NTCP) resulting in altered bile acid dynamics and subsequent release into the perfusate (296,297) and; (ii) enhanced bile acid synthesis: steatotic livers may exhibit enhanced bile acid synthesis as a compensatory mechanism to deal with increased hepatic lipid content (297,298). However, further research is needed to elucidate the precise mechanisms by which steatotic livers exhibit higher levels of bile salts in perfusate, including detailed studies on bile acid transport and metabolism in the context of liver steatosis.

cNMP of steatotic livers resulted in greater mobilisation of triglycerides compared to lean livers at 15 min of perfusion. This is comparable to a previous study by Liu et al. who demonstrated an increase in perfusate TG in steatotic livers preserved over 24 h, however, without a control group, the authors were unable to establish if this effect was greater in steatotic livers (219). In addition, steatotic livers preserved with cNMP demonstrated evidence of greater fatty acid β-oxidation concentration (through ketone body production) compared to lean counterparts. These changes noted in the perfusate can be attributed to the utilisation of an expanded fatty acid reservoir present within the steatotic liver, supplying fatty acyl-CoA for both esterification and oxidation processes.

Although not statistically significant, steatotic livers demonstrated inferior lactate clearance compared to lean livers throughout cNMP. Impaired lactate clearance in steatotic livers during perfusion can be contributed to by a number of factors: (i) mitochondrial dysfunction: impaired oxidative phosphorylation and the efficient use of oxygen for ATP production with greater reliance on anaerobic glycolysis, even in the presence of oxygen (a phenomenon known as the Warburg effect), leading to an increased production of lactate (299,300); (ii) hypoxia: excessive fat accumulation in steatotic livers can lead to structural and functional alterations in the liver microcirculation, potentially causing inadequate oxygen supply to hepatocytes, the resulting hypoxia favours anaerobic glycolysis over oxidative phosphorylation, further increasing lactate production and release during NMP (301) and; (iii) impaired lactate clearance: due to hyperacetylation of lactate clearing enzymes, such as lactate dehydrogenase B (LDHB) (302). However, in the context of normothermic perfusion, it is also important to contextualise lactate measurements with the liver functional reserve compared with the limited

volume of the perfusion circuit i.e. lactate can be cleared at minimal levels of hepatocellular activity (227). Therefore, when considering lactate measurements, the rate of lactate reduction per unit of liver weight might serve as a more accurate indicator of hepatocellular function and elevated lactate levels can also be attributed to trauma or lobar ischemia, due to lactate production in ischaemic segments of the liver (227).

Steatotic livers had similar glucose levels compared to lean livers during cNMP, however, demonstrated lower insulin levels throughout preservation. During the initial stages of normothermic perfusion, liver glycogen levels decrease, indicative of glycogenolysis as the primary source of observed glucose elevation, which also accounts for heightened glucose concentrations in cold storage fluids for anaerobic ATP synthesis (227). This glycogenolytic activity, triggered by glucagon, epinephrine, and other stress hormones, is pronounced during the withdrawal of treatment in Donation after Circulatory Death (DCD) donors and during coning in Donation after Brain Death (DBD) donors, periods marked by elevated hormone levels. Concurrently, lactate conversion to glucose, an oxygen-dependent mechanism, partially contributes to initial perfusate glucose increase (227). A spontaneous reduction in glucose levels during perfusion is likely due to glucose uptake by the liver through the insulin-independent GLUT2 transporter, with subsequent glycogen synthesis, primarily in zone 3. Despite insulin's established roles in inhibiting glycogenolysis and promoting glycogenesis, high glucose levels may override insulin's effects, as evidenced by glycogen synthesis in its absence during normothermic perfusion. In instances where perfusate glucose does not rise during normothermic perfusion suggest either severe hepatocellular damage or a halt in glycogenolysis, potentially from glycogen depletion, with glucose challenge tests proposed to assess metabolic functionality during normothermic perfusion (227).

Steatotic livers preserved with cNMP demonstrated a non-significant increase in Fibroblast Growth Factor 21 (FGF-21) perfusate concentration at the end of preservation compared to lean counterparts. The elevation of FGF-21 (a critical regulator of metabolism and stress response) is likely to reflect the liver's response to ex-situ reperfusion injury and its effort to correct metabolic dysfunctions. This rise may also indicate of the liver's attempt to regulate disrupted lipid metabolism and restore normal function amidst the excessive lipid accumulation. In addition, the function of FGF-21 in hepatocellular protection and repair is

particularly relevant during normothermic perfusion with respect to mitigating cellular damage and facilitating recovery from injury (303).

4.4.4 Conclusions

This chapter provides a comprehensive analysis of clinical data, biopsy samples, and continuous normothermic machine perfusion (cNMP) perfusate from a previously conducted Phase III multicentre randomized controlled trial. Specifically, the data presented have enabled a comparison of the efficacy of cNMP with static cold storage (SCS) for the transplantation of steatotic donor livers. The findings suggest significant clinical benefits of cNMP in reducing ischemia-reperfusion injury (IRI) markers such as post-reperfusion syndrome (PRS) and early allograft dysfunction (EAD), alongside a reduction in peak alanine aminotransferase (AST) levels in the first 7 days post-transplant. I have also highlighted the advantage of digital image analysis in quantifying hepatic steatosis with greater reproducibility compared to conventional histopathology, potentially offering a more objective measure of this important parameter, and improving donor liver assessment during perfusion.

Whilst this chapter is not without limitations, despite the retrospective nature of this study and small sample size, I have been able to provide a detailed insight into steatotic livers preserved with cNMP compared to well matched lean controls with available proteomic data (see Chapter 5). In addition, despite variability in the degree of ld-MaS in steatotic livers, clear differences in hepatic lipid metabolism were observed in comparison to lean livers preserved with cNMP. Biochemical analysis of perfusate has highlighted potential biomarkers indicative of metabolic changes during perfusion, with steatotic livers showing higher levels of hepatocellular injury markers, bile salts, triglycerides, 3-hydroxybutyrate (3-OHB) and FGF-21 as well as lower levels of lactate clearance and perfusate insulin concentrations compared to lean livers. These findings underscore the metabolic challenges faced by steatotic livers during normothermic perfusion and open the potential to pharmacologically optimise fat metabolism and enhance ex-situ function of steatotic liver grafts. I have also identified the need for future clinical trials to compare different preservation techniques (pSCS-NMP, cNMP, and ischemia-free liver transplantation [IFLT]) in order to fully understand the impact of cNMP on steatotic liver risk profiles. In addition, beyond standard normothermic perfusion, these findings provide the basis for pharmacological optimisation (defatting) as adjunct for improving transplantability of steatotic donor livers (see chapter 6).

Chapter 5: The effect of preservation on the proteomic profile of steatotic donor transplant livers

5.1 Introduction

Poor graft function following transplantation of steatotic livers can be attributed to both structural and metabolic abnormalities that increase susceptibility to ischaemic injury during organ procurement, cold storage and following implantation (reperfusion in the recipient). Large droplet macrovesicular (ld-MaS) steatosis results in the compression of adjacent sinusoids, which results in decreased sinusoidal perfusion compared to non-steatotic livers (304). This reduced baseline sinusoidal flow becomes exacerbated following ischaemia-reperfusion injury (IRI) and consequently limits recovery from acute hepatocellular injury (305). Metabolically, steatosis is linked to decreased baseline hepatocyte adenosine triphosphate (ATP) stores, alongside impaired ATP recovery following depletion (306–308). As recovery from IRI relies on ATP-dependent processes, steatotic livers are at risk of inadequate function post-transplantation. Additionally, steatotic hepatocytes exhibit increased sensitivity to oxidative stress (resulting from chronic reductions in antioxidant capacity) and reactive oxygen species (ROS), potentially leading to graft necrosis following liver transplantation (309).

Normothermic machine perfusion (NMP) has demonstrated potential in reducing organ discard rates and early allograft dysfunction (EAD), while achieving comparable graft survival rates to static cold storage (SCS) (310). The ability to use steatotic donor livers without adversely affecting patient outcomes could greatly increase the availability of donor livers (221). NMP presents an opportunity to enhance the quality of steatotic donor livers prior to transplantation. However, the cellular impairments in steatotic livers during NMP are not fully understood, as steatotic liver disease is influenced by a variety of systemic factors, making it challenging to separate these influences from intrinsic hepatocyte abnormalities observed *in vivo* (311).

To gain a comprehensive understanding of the biological, molecular, and cellular alterations occurring during preservation, proteomic profiling of steatotic donor livers may provide valuable insights. This approach enables the detailed characterisation of the proteome within a given sample under specific conditions by identifying and quantifying the proteins present,

often in comparison to a control or standard treatment, thus providing differential expression data (312–314). The differentially expressed proteins (DEPs) identified through this analysis are subsequently examined using bioinformatics tools to determine the biological, molecular, and cellular alterations and biological pathways involved. This subsequent analysis is commonly known as Gene Ontology (GO) enrichment analysis.

Proteomic analysis has been widely applied in drug discovery and biomarker research. However, its utilisation has largely been confined to centres with adequate resources to operate expensive instrumentation and manage substantial bioinformatics data (315). The high cost of such analyses, coupled with the novelty of machine perfusion technology, has led to a scarcity of proteomic studies on livers preserved with NMP (313). To date, no human clinical studies have investigated the proteomic profile of steatotic human livers preserved with continuous NMP (cNMP) that have resulted in transplantation.

This chapter explores the proteomic profile of steatotic donor livers preserved using cNMP and static cold storage (SCS) compared to lean counterparts. The hypothesis of this chapter is that NMP of steatotic donor livers improves preservation and reperfusion characteristics compared to those livers preserved with SCS through activation of biological pathways that favour recovery from retrieval/preservation related injury and improve graft tolerance to IRI.

The aim of this chapter is to investigate the proteomic profile of steatotic donor livers preserved with continuous NMP*. The overall objectives are to:

1. Identify tissue proteomic signatures of steatotic livers preserved with continuous NMP and SCS compared to lean counterparts; and,
2. Identify the impact of preservation technique on proteomic signatures in steatotic livers preserved with NMP and SCS compared to lean counterparts following reperfusion in the recipient

***This work was performed as a collaboration between the COPE consortium and the Target Discovery Institute (University of Oxford, Kessler Group). I was not personally involved in the sample preparation of the COPE liver samples or the LC-MS data analysis. However, I performed the subsequent downstream bioinformatics analysis of donor livers described in this chapter under the post-doctoral supervision of Dr Sadr**

Shaheed (Oxford Transplant Research Group) and Dr Letizia Lo Faro (Oxford Transplant Research Group).

5.2 Methods

Donor livers with evidence of steatosis were identified from the Consortium for Organ Preservation in Europe (COPE) liver database and selected based on the pre-preservation (LT1) H&E biopsy demonstrating evidence of mild (≥ 5% ld-MaS) to severe steatosis (defined by a histopathological score of 1-3). Lean controls were identified and selected based on availability of tissue proteomic and recipient data. The final study cohort comprised of 105 transplanted livers, of these only 92 livers had a full set of pre-preservation (LT1), post-preservation (LT2) and post-reperfusion (LT3) biopsies for proteomic analysis (Table 5.1).

Table 5.1. Number of livers (per phenotype and preservation method) used in the proteomics analysis

Liver phenotype	**Preservation**	**Study cohort, *n*=105**	**Full set of biopsies, *n*=92**
Steatotic	**NMP**	21	18
Steatotic	**SCS**	12	7
Lean	**NMP**	46	46
Lean	**SCS**	26	21

5.2.1 Proteomics analysis

Shotgun proteomics was performed using ion mobility spectrometry (IMS) with liquid chromatography (LC) and tandem mass spectrometry (MS/MS). All samples were analysed using the timsTOF Pro (Bruker) instrument (a time-of-flight mass spectrometer that utilises trapped ion mobility spectrometry) operated in the parallel accumulation-serial fragmentation (PASEF®) scan mode. The sample preparation and LC-MS analysis is described in **Appendix B.**

5.2.1.1 Statistical and bioinformatic analysis

All statistical analyses were conducted using the proDA package (Bioconductor Software Package version 3.14, in R Studio version 1.4.1106) to identify differentially abundant proteins between each group, in label-free mass spectrometry data. Proteins were considered differentially expressed (differentially expressed proteins, DEPs) using $P < 0.05$, with adjusted *p*-values of 5% false discovery rate (FDR, Benjamini-Hochberg method) for multiple

comparisons. Volcano plots were constructed using the SRPlot web-based bio-informatic tool with P-min: 1e-100, fold change cut-off: 1 and P (or FDR) cut-off: 0.05. Protein-protein interaction (PPI) of statistically significant ($P < 0.05$) differentially expressed proteins (DEPs) was performed using the STRING® (version 12.0) online database for PPI maps, bio-informatic Gene-Ontology (GO) and with either general network analysis (when <100 DEPs identified) or Markov Clustering (MCL) Algorithm cluster analysis (with an inflation parameter of 3 when >100 DEPs identified). In addition, over-representation analyses of gene ontology (GO) terms, including the cellular components, biological process and pathway, molecular function, and enriched pathway analysis was performed using FunRich Version 3.1.4; Functional Enrichment Analysis Tool (www.funrich.org).

5.3 Results

Proteomes of tissue biopsy samples collected from steatotic and lean livers preserved with either NMP or SCS were compared between timepoints (LT2, post-preservation vs. LT1, pre-preservation i.e. the preservation period), (Figure 5.1). In addition, proteomes of post-reperfusion biopsies (LT3) from steatotic livers (preserved with NMP or SCS) were compared with lean counterparts (Figure 5.2). Proteins were considered differentially expressed (differentially expressed proteins, DEPs) using $P < 0.05$ unless otherwise stated.

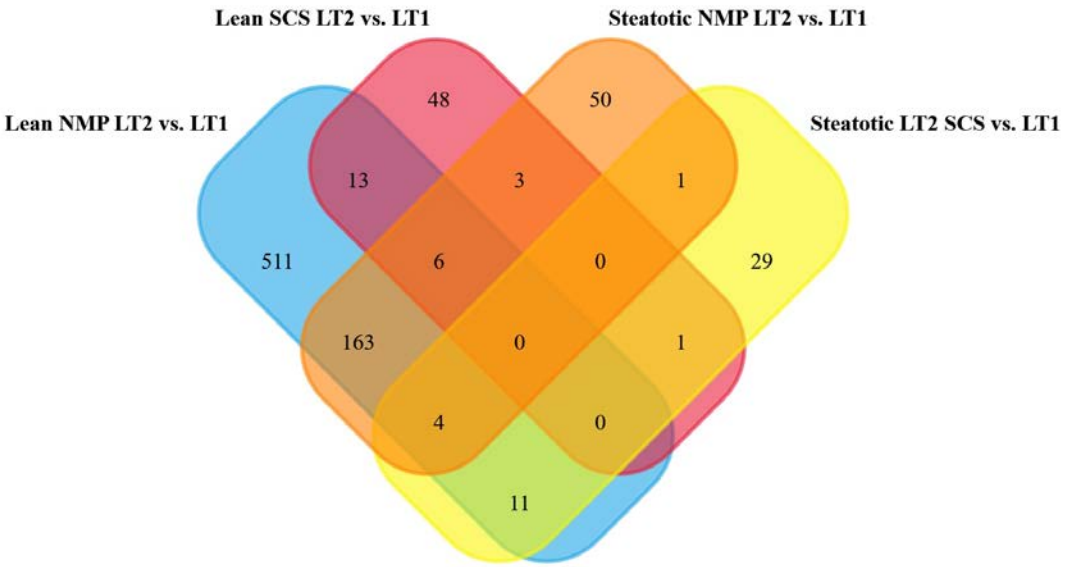

Figure 5.1. Venn diagram demonstrating unique DEPs ($P < 0.05$) over the preservation phase for steatotic and lean livers preserved with either NMP or SCS (LT2 vs. LT1).

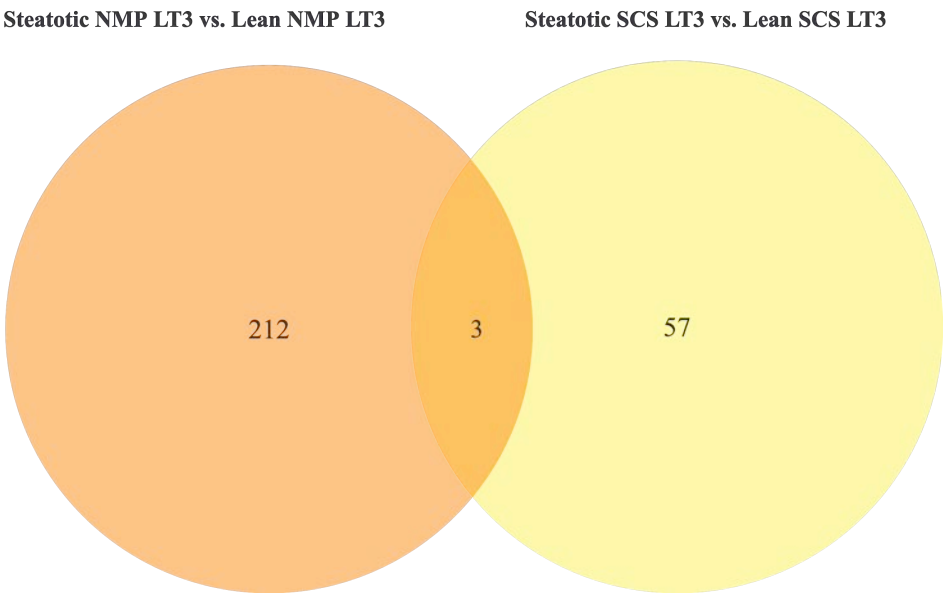

Figure 5.2. Venn diagram demonstrating unique DEPs ($P < 0.05$) at reperfusion (LT3) in steatotic livers (preserved with NMP or SCS) compared with lean counterparts.

5.3.1 Effect of NMP on proteomes of steatotic livers

227 significant ($P < 0.05$) differentially expressed proteins (DEPs) were identified during NMP of steatotic donor livers (LT2, post-preservation vs. LT1, pre-preservation). 144 were upregulated and 83 downregulated. The top 25 most upregulated and downregulated DEPs are demonstrated in Figure 5.3. Of these, the 5 most clinically relevant (based on biological function) upregulated DEPs (with functions related to autophagy, leukocyte adhesion, oxidative phosphorylation and cytoprotection) and downregulated DEPs (with functions related to lipid storage/metabolism and removal of damaged DNA/protein) are described in Table 5.2.

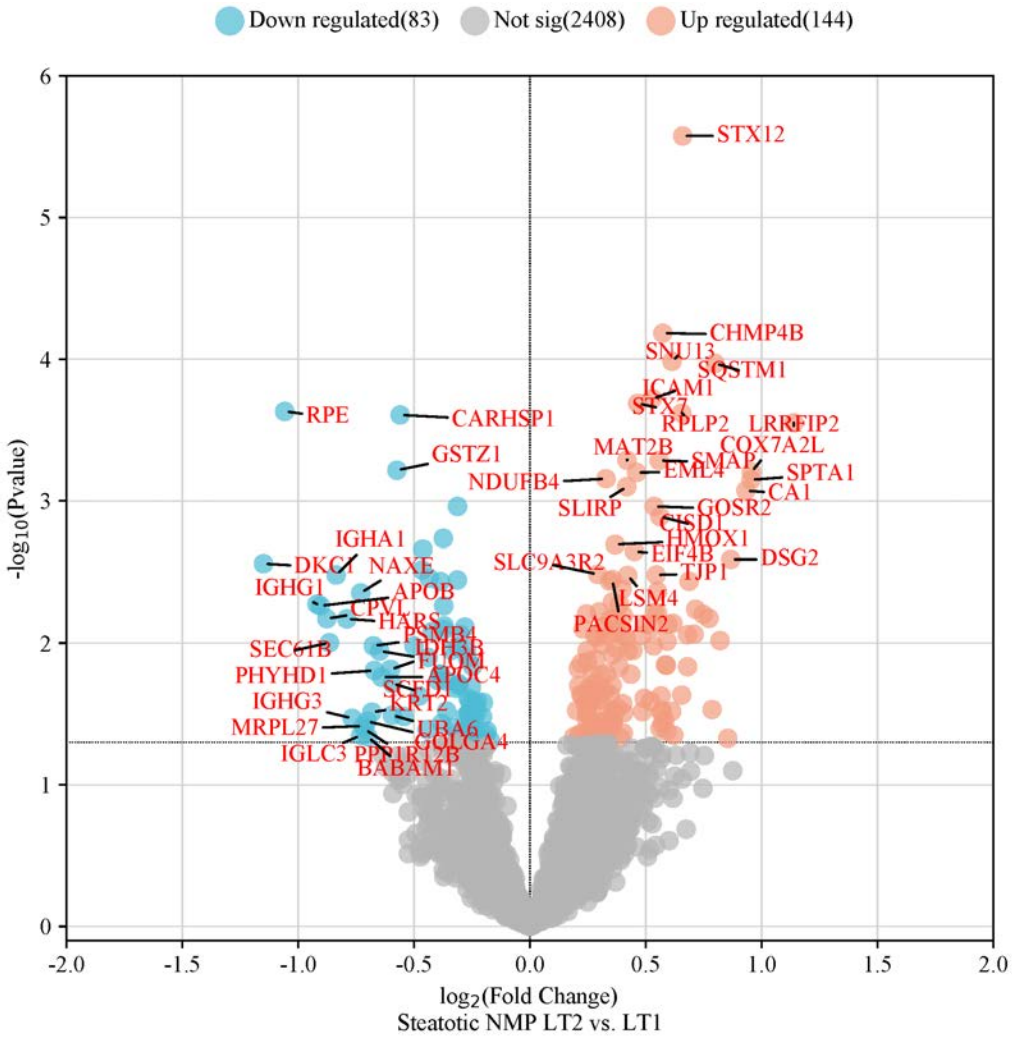

Figure 5.3. The effect of NMP on proteomes of steatotic donor livers. Top 25 upregulated and downregulated proteins are labelled in the plot.

Table 5.2. Clinically relevant upregulated (n = 5) and downregulated proteins (n = 5) during NMP of steatotic donor livers.

Upregulated			
Protein name	Function	Fold change	*P* - value
SQSTM1	Sequestosome-1: Autophagy receptor involved in selective macroautophagy (aggrephagy).	0.799	0.000
ICAM1	Intercellular adhesion molecule 1: Ligand for leukocyte adhesion protein LFA-1 (integrin alpha-L/beta-2).	0.529	0.000
COX7A2L	Cytochrome c oxidase subunit 7A-related protein, mitochondrial: Oxidative phosphorylation, energy metabolism, formation of mitochondrial respiratory super-complex. Part of cytochrome c oxidase VIIa family.	0.956	0.001
NDUFB4	NADH dehydrogenase [ubiquinone] 1 beta subcomplex subunit 4: Transfer of electrons from NADH to the respiratory chain.	0.328	0.001
HMOX1	Haem oxygenase 1: Cleaves haem ring to form biliverdin (which is converted to bilirubin by biliverdin reductase). Cytoprotective role against free haem which is induces cell apoptosis.	0.368	0.002
Downregulated			
Protein name	Function	Fold change	*P* - value
NAXE	NAD(P)HX Epimerase: Protection of cells from reactive oxygen species (ROS). An epimerase in involved in catalyses of R-NAD(P)HX to S-NAD(P)HX (toxic cellular metabolites). Dehydratase NAXD then reconverts S-NAD(P)HX to S-NAD(P)H. Promotes cholesterol efflux to high-density lipoprotein (HDL).	-0.730	0.004
APOB	Apolipoprotein B100: Protein constituent of chylomicrons (ApoB48), LDL (ApoB100) and VLDL (ApoB100). ApoB100 functions as a recognition signal for both the binding and internalisation of LDLs via the ApoB/E receptor.	-0.904	0.005
PSMB4	Proteasome 20S Subunit Beta 4: Degradation of ubiquitinated proteins and removal of misfolded and damaged proteins that could impair cellular function.	-0.676	0.010
APOC4	Apolipoprotein C-IV: Involved in lipoprotein metabolism.	-0.640	0.017
BABAM1	BRISC and BRCA1-A complex member 1: Component of the BRCA1-A complex involved in recognition of 'Lys-63'-linked ubiquitinated histones H2A and H2AX located at DNA lesions sites and targeting the BRCA1-BARD1 heterodimer to sites of DNA damage at double-strand breaks (DSBs).	-0.699	0.046

Protein-protein interaction (PPI) of statistically significant ($P < 0.05$) DEPs was performed using STRING® (version 12.0) online database for PPI maps, bio-informatic and Gene Ontology (GO). MCL cluster analysis demonstrated 51 unique clusters. Of these, the two main clusters (identified by their modularity i.e. more densely connected internally than with the rest of the network and clear separation from other clusters) identified changes in:

- Mitochondrial pathways (Figure 5.4)
- Lipid metabolism, coagulation and immune pathways (Figure 5.5)

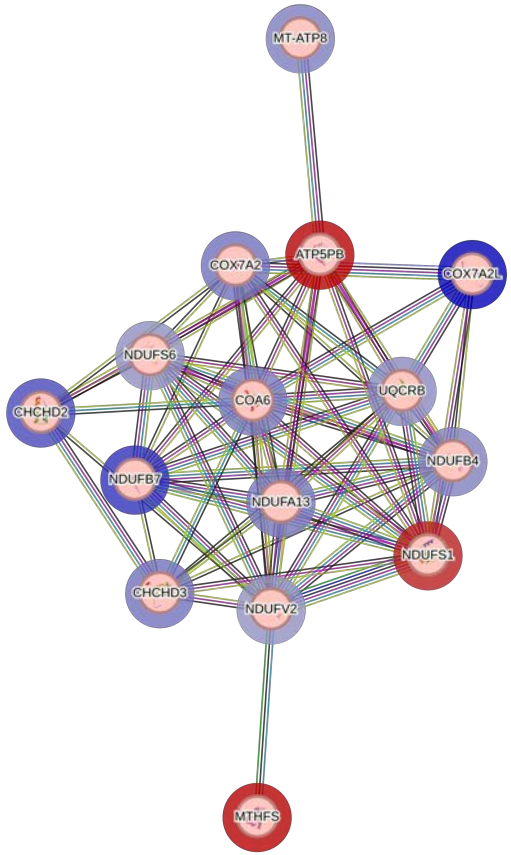

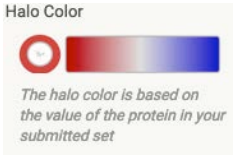

Biological Process (Gene Ontology)

GO-term	description	count in network	strength	false discovery rate
GO:0097250	Mitochondrial respirasome assembly	2 of 11	2.38	0.0106
GO:0042776	Proton motive force-driven mitochondrial ATP synthesis	8 of 64	2.22	2.33e-13
GO:0006120	Mitochondrial electron transport, NADH to ubiquinone	5 of 46	2.15	1.29e-07
GO:0006119	Oxidative phosphorylation	12 of 122	2.11	4.12e-20
GO:0042775	Mitochondrial ATP synthesis coupled electron transport	9 of 92	2.11	2.15e-14
GO:0002082	Regulation of oxidative phosphorylation	2 of 21	2.1	0.0317
GO:0019646	Aerobic electron transport chain	8 of 87	2.08	1.92e-12
GO:0006123	Mitochondrial electron transport, cytochrome c to oxygen	2 of 23	2.06	0.0365
GO:0032981	Mitochondrial respiratory chain complex I assembly	4 of 61	1.94	4.67e-05
GO:0043467	Regulation of generation of precursor metabolites and energy	3 of 131	1.48	0.0313
GO:0007005	Mitochondrion organization	8 of 445	1.37	1.78e-07
GO:0018130	Heterocycle biosynthetic process	9 of 985	1.08	2.89e-06
GO:0019438	Aromatic compound biosynthetic process	9 of 992	1.08	3.00e-06
GO:1901362	Organic cyclic compound biosynthetic process	9 of 1121	1.02	8.44e-06
GO:1901566	Organonitrogen compound biosynthetic process	9 of 1338	0.95	3.68e-05
GO:0044271	Cellular nitrogen compound biosynthetic process	9 of 1494	0.9	8.58e-05
GO:0044281	Small molecule metabolic process	9 of 1645	0.86	0.00019
GO:0065003	Protein-containing complex assembly	7 of 1303	0.85	0.0061
GO:0044237	Cellular metabolic process	13 of 6568	0.41	0.0082

(less ...)

Molecular Function (Gene Ontology)

GO-term	description	count in network	strength	false discovery rate
GO:0008137	NADH dehydrogenase (ubiquinone) activity	5 of 41	2.2	4.02e-07
GO:0015453	Oxidoreduction-driven active transmembrane transporter ac...	6 of 71	2.05	6.99e-08
GO:0009055	Electron transfer activity	6 of 121	1.81	4.02e-07
GO:0015078	Proton transmembrane transporter activity	3 of 126	1.5	0.0414
GO:0016491	Oxidoreductase activity	7 of 731	1.1	0.00022
GO:0022857	Transmembrane transporter activity	8 of 1121	0.97	0.00022

(less ...)

Cellular Component (Gene Ontology)

GO-term	description	count in network	strength	false discovery rate
GO:0000276	Mitochondrial proton-transporting ATP synthase complex, c...	2 of 13	2.31	0.0044
GO:0005747	Mitochondrial respiratory chain complex I	6 of 50	2.2	2.86e-10
GO:0098803	Respiratory chain complex	10 of 90	2.16	2.14e-17
GO:0045277	Respiratory chain complex IV	3 of 27	2.16	0.00012
GO:0070069	Cytochrome complex	4 of 40	2.12	2.96e-06
GO:0005746	Mitochondrial respirasome	9 of 94	2.1	3.38e-15
GO:0005751	Mitochondrial respiratory chain complex IV	2 of 24	2.04	0.0111
GO:0098800	Inner mitochondrial membrane protein complex	12 of 158	2.0	1.04e-19
GO:1990204	Oxidoreductase complex	7 of 124	1.87	3.61e-10
GO:0005758	Mitochondrial intermembrane space	4 of 86	1.79	4.96e-05
GO:1902495	Transmembrane transporter complex	7 of 384	1.38	7.30e-07
GO:0005740	Mitochondrial envelope	14 of 802	1.36	2.30e-16
GO:0098796	Membrane protein complex	13 of 1218	1.15	3.04e-12
GO:0005739	Mitochondrion	15 of 1681	1.07	2.53e-14
GO:0016021	Integral component of membrane	12 of 5670	0.44	0.0045

Figure 5.4. STRING cluster analysis of mitochondrial pathways during NMP of steatotic livers: The upregulation of CHCHD2, CHCHD3, COA6, COX7A2, COX7A2L, MT-ATP8, NDUFA13, NDUFB4, NDUFB7, NDUFS6, NDUFV2, and UQCRB suggests a coordinated response to enhance mitochondrial respiratory capacity and oxidative phosphorylation in the liver, crucial for meeting the metabolic demands of hepatocytes. Downregulation of ATP5PB and NDUFS1 may indicate a shift in metabolic strategy or a response to cellular stress, potentially leading to altered ATP synthesis efficiency. MTHFS downregulation could affect folate metabolism, impacting nucleotide synthesis and repair processes. Blue halo represents upregulation and red halo represents downregulation of protein.

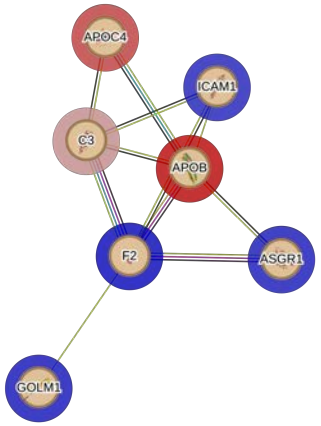

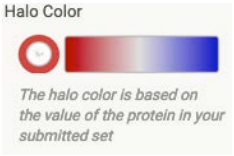

Biological Process (Gene Ontology)

GO-term	description	count in network	strength	false discovery rate
GO:0010884	Positive regulation of lipid storage	3 of 24	2.55	0.0013
GO:0019216	Regulation of lipid metabolic process	4 of 346	1.51	0.0172

Cellular Component (Gene Ontology)

GO-term	description	count in network	strength	false discovery rate
GO:0034361	Very-low-density lipoprotein particle	2 of 20	2.45	0.0198
GO:1905370	Serine-type endopeptidase complex	2 of 26	2.34	0.0198
GO:0034364	High-density lipoprotein particle	2 of 29	2.29	0.0198
GO:0005788	Endoplasmic reticulum lumen	4 of 312	1.56	0.0045
GO:0005615	Extracellular space	6 of 3247	0.72	0.0225
GO:0005576	Extracellular region	7 of 4175	0.67	0.0198

Figure 5.5. STRING cluster analysis of lipid metabolism, coagulation and immune pathways during NMP of steatotic livers: The upregulated proteins GOLM1, F2, ASGR1, and ICAM1 are associated with various aspects of hepatic physiology. GOLM1 is involved in the secretory pathway and is often upregulated in liver diseases, F2 (prothrombin) is central to the coagulation cascade, ASGR1 plays a role in lipoprotein metabolism, and ICAM1 is involved in inflammatory responses. Downregulated proteins such as APOC4 and APOB, both key components in lipid transport and metabolism, along with C3, a central protein in the complement system, suggest alterations in lipid homeostasis and innate immunity. Blue halo represents upregulation and red halo represents downregulation of protein.

5.3.2 Effect of SCS on proteomes of steatotic livers

46 significant ($P < 0.05$) DEPs were identified during SCS of steatotic donor livers (LT2, post-preservation vs. LT1, pre-preservation). 36 were upregulated and 10 downregulated. The top 25 most upregulated and all 10 downregulated DEPs are demonstrated in Figure 5.6. Of these, the 5 most clinically relevant (based on biological function) upregulated DEPs (with functions related to metabolism of fatty acids and protein folding) and downregulated DEPs (with functions related to RAS activation, cellular energy metabolism, succinate dehydrogenase assembly and ATP hydrolysis) are described in Table 5.3.

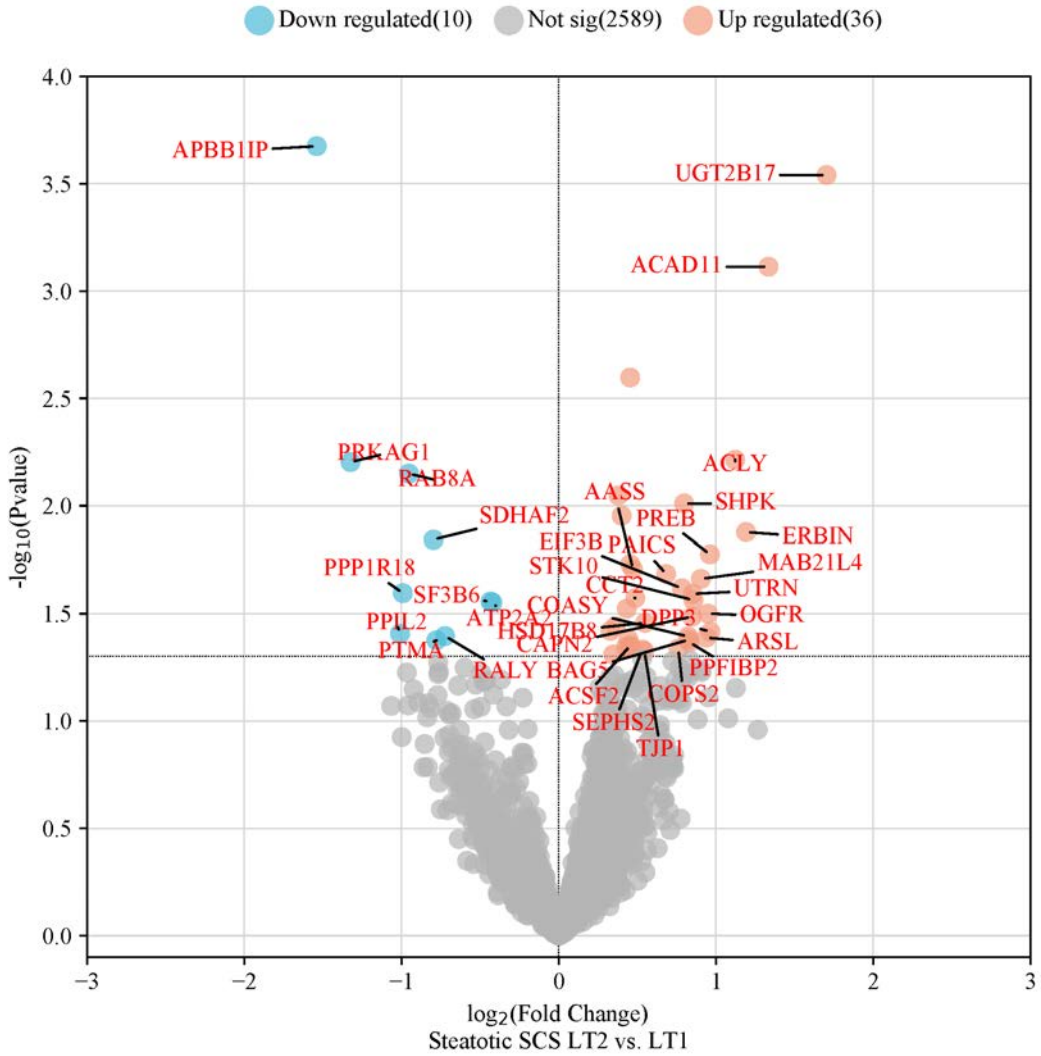

Figure 5.6. The effect of SCS on proteomes of steatotic donor livers. Top 25 upregulated and all 10 downregulated proteins are labelled in the plot.

Table 5.3. Clinically relevant upregulated (n = 5) and downregulated proteins (n = 5) during SCS of steatotic donor livers.

Upregulated			
Protein name	Function	Fold change	*P* - value
ACAD11	Acyl-CoA dehydrogenase family member 11: Maximum activity towards saturated C22-CoA. Role in β-oxidation and metabolism of fatty acids.	1.334	0.001
ACLY	ATP-citrate synthase: Catalyses the cleavage of citrate into oxaloacetate and acetyl-CoA (providing a substrate for *de novo* cholesterol and fatty acid synthesis).	1.122	0.006
CCT2	T-complex protein 1 subunit beta: Molecular chaperone that facilitates the folding of proteins upon ATP hydrolysis.	0.486	0.027
HSD17B8	Estradiol 17-beta-dehydrogenase 8: Role in mitochondrial fatty acid biosynthesis.	0.549	0.035
ACSF2	Medium-chain acyl-CoA ligase ACSF2, mitochondrial: Acyl-CoA synthases, involved in catalysing the first reaction in fatty acid metabolism (through formation of thioester with CoA).	0.456	0.044
Downregulated			
Protein name	Function	Fold change	*P* - value
APBB1IP	Amyloid beta A4 precursor protein-binding family B member 1-interacting protein: Involved in signal transduction (from Ras activation to actin cytoskeletal remodelling). Suppression of insulin-induced promoter activities and mediates Rap1-induced adhesion.	-1.540	0.000
PRKAG1	5'-AMP-activated protein kinase subunit gamma-1: AMP/ATP-binding subunit of AMP-activated protein kinase (AMPK). Regulates cellular energy metabolism in response to reduction in intracellular ATP levels through AMPK related activation of energy producing pathways and inhibition of energy consuming pathways i.e. protein, carbohydrate and lipid biosynthesis.	-1.325	0.006
SDHAF2	Succinate dehydrogenase assembly factor 2, mitochondrial: Assembly of succinate dehydrogenase (SDH, respiratory complex II), a component of both the tricarboxylic acid (TCA) cycle and the mitochondrial electron transport chain.	-0.797	0.014
ATP2A2	Sarcoplasmic/endoplasmic reticulum calcium ATPase 2: A magnesium-dependent enzyme that catalyses the hydrolysis of ATP coupled with cytosolic calcium (Ca^{2+}) translocation to the sarcoplasmic reticulum lumen.	-0.422	0.028
RALY	NA-binding protein Raly: RNA-binding protein that functions as a transcriptional cofactor for cholesterol biosynthetic genes.	-0.724	0.040

Protein-protein interaction (PPI) of statistically significant ($P < 0.05$) DEPs was performed using STRING® (version 12.0) online database for PPI maps, bio-informatic and Gene Ontology (GO). As only 46 DEPs were identified, MCL cluster analysis of pathways was not performed. Instead, general network analysis is demonstrated in Figure 5.7.

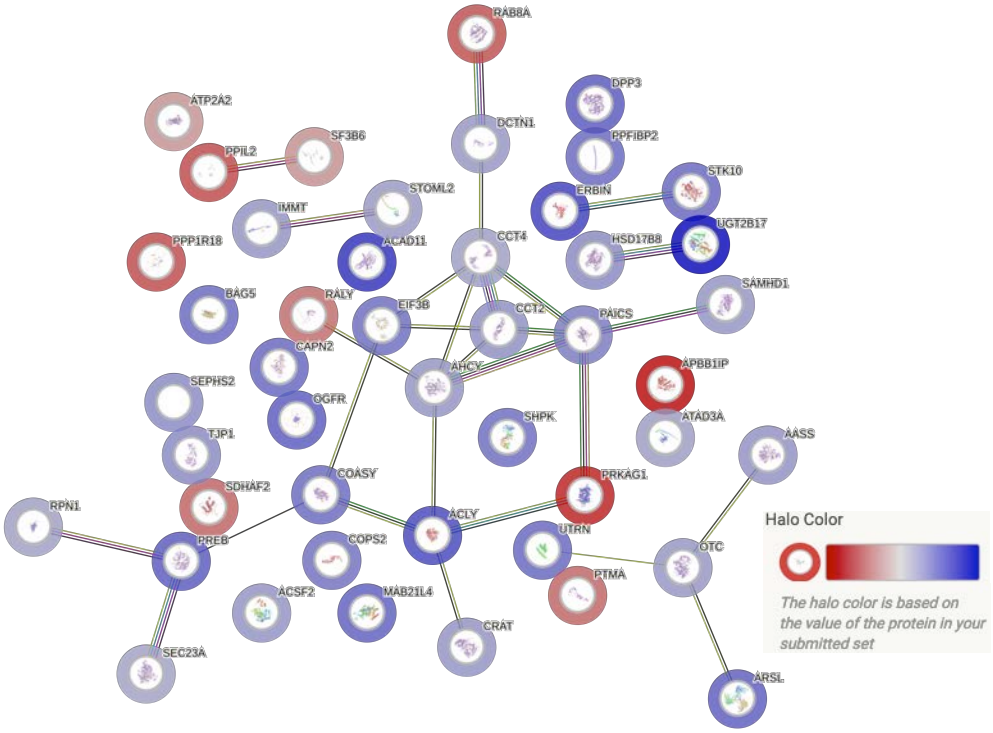

Biological Process (Gene Ontology)

GO-term	description	count in network	strength	false discovery rate
GO:0072521	Purine-containing compound metabolic process	8 of 425	0.91	0.0198
GO:0019752	Carboxylic acid metabolic process	11 of 819	0.76	0.0184
GO:0044281	Small molecule metabolic process	16 of 1645	0.62	0.0080

Molecular Function (Gene Ontology)

GO-term	description	count in network	strength	false discovery rate
GO:0030554	Adenyl nucleotide binding	14 of 1566	0.58	0.0071
GO:0000166	Nucleotide binding	18 of 2168	0.55	0.0038
GO:0017076	Purine nucleotide binding	16 of 1917	0.55	0.0043
GO:0036094	Small molecule binding	19 of 2507	0.51	0.0038
GO:0043168	Anion binding	18 of 2404	0.51	0.0043
GO:0035639	Purine ribonucleoside triphosphate binding	14 of 1834	0.51	0.0340
GO:0032555	Purine ribonucleotide binding	14 of 1903	0.5	0.0416
GO:0003824	Catalytic activity	26 of 5522	0.3	0.0340
				(less ...)

Cellular Component (Gene Ontology)

GO-term	description	count in network	strength	false discovery rate
GO:0005737	Cytoplasm	42 of 12056	0.17	0.0100
GO:0005622	Intracellular anatomical structure	45 of 14891	0.11	0.0423

Figure 5.7. STRING network analysis of upregulated and downregulated proteins during SCS of steatotic donor livers: Upregulated DEPs including UGT2B17, ACAD11, ACLY, CCT2, HSD17B8, and ACSF2 indicate enhanced detoxification, fatty acid β-oxidation, lipid synthesis, protein folding, steroid metabolism, and fatty acid activation, respectively. UGT2B17 has a key role in the glucuronidation pathway required for detoxification. ACAD11 enhances fatty acid β-oxidation, a key process in cellular energy production. ACLY is essential in lipid synthesis, catalysing the conversion of citrate to acetyl-CoA, thereby signifying an increase in lipid biosynthetic activities. CCT2, which is integral to protein folding, indicates an increased requirement for maintaining protein conformation and functionality under stress conditions. Involvement of HSD17B8 in steroid metabolism indicate modifications in hormonal processing pathways. ACSF2, known for its role in activating fatty acids for both synthesis and degradation, reflects adaptive changes in fatty acid metabolism. Downregulated DEPs including APBB1IP, PRKAG1, SDHAF2, ATP2A2, and RALY demonstrates a reduction in cell signalling, energy balance, mitochondrial efficiency, calcium transport and RNA processing. The downregulation of PRKAG1 (a key regulator of AMP-activated protein kinase) and SDHAF2 indicate alterations in energy metabolic pathways and reduction in mitochondrial respiratory efficiency. Downregulation of ATP2A2 indicates disruption of intracellular calcium homeostasis (essential for numerous cellular functions). In addition, downregulation of RALY indicates reduction on RNA metabolism and gene expression.

5.3.3 Effect of NMP on proteomes of lean livers

708 significant ($P < 0.05$) DEPs were identified during NMP of lean donor livers (LT2, post-preservation vs. LT1, pre-preservation). 408 were upregulated and 300 downregulated. The top 25 most upregulated and downregulated DEPs are demonstrated in Figure 5.8. Of these, the 5 most clinically relevant upregulated (functions related to leucocyte adhesion, cytoprotection, HLA, DNA/protein repair and autophagy) and downregulated DEPs (functions related to complement activation, fat metabolism and cytochrome P450 activity) are described in Table 5.4.

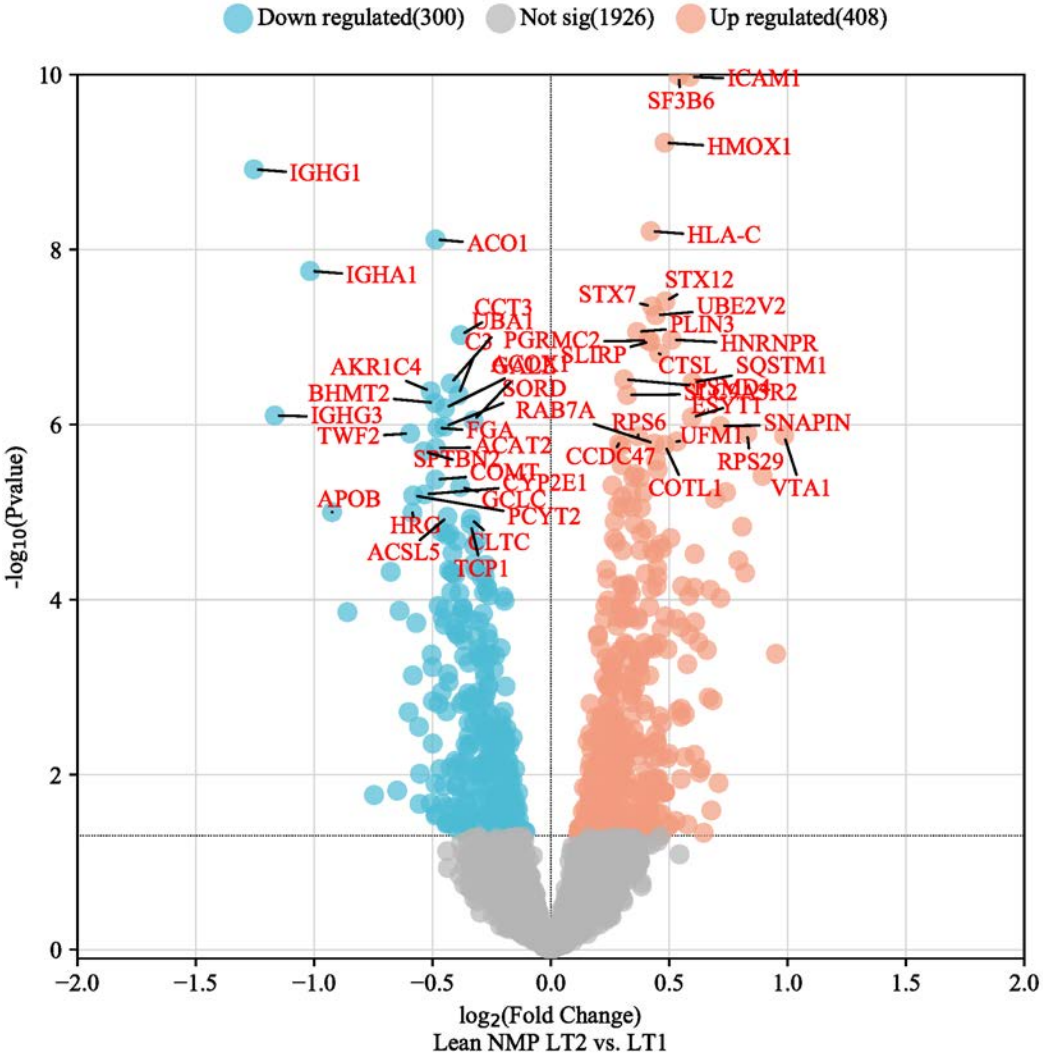

Figure 5.8. The effect of NMP on proteomes of lean donor livers. Top 25 upregulated and downregulated proteins are labelled in the plot.

Table 5.4. Clinically relevant upregulated (n = 5) and downregulated proteins (n = 5) during NMP of lean donor livers.

Upregulated			
Protein name	Function	Fold change	*P* - value
ICAM1	Intercellular adhesion molecule 1: Ligand for leukocyte adhesion protein LFA-1 (integrin alpha-L/beta-2). During leukocyte trans-endothelial migration, ICAM1 engagement facilitates formation of endothelial apical cups through associated ARHGEF26/SGEF and RHOG activation.	0.587	0.000
HMOX1	Heme oxygenase 1: Cleavage of heme ring to form biliverdin (which is subsequently converted to bilirubin by biliverdin reductase). Cytoprotetive effect as free heme sensitises cells to apoptosis.	0.480	0.000
HLA-C	HLA class I histocompatibility antigen, C alpha chain: Anti-viral immunity through interaction with NK cells.	0.422	0.000
PSMD4	26S proteasome non-ATPase regulatory subunit 4: ATP-dependent degradation of ubiquitinated proteins and protein haemostasis (removal of misfolded or damaged proteins). Role in cellular processes including cell cycle progression, apoptosis and DNA damage repair.	0.309	0.000
SQSTM1	Sequestosome-1: Autophagy receptor with role in selective macroautophagy (aggrephagy).	0.598	0.000
Downregulated			
Protein name	Function	Fold change	*P* - value
C3	Complement C3c alpha' chain fragment 1: Activation of complement system (central reaction in classical and alternative complement pathways via processing by C3 convertase). Following activation, C3 binds (via its reactive thioester) to immune aggregates, cell surface carbohydrates and is also chemoattractant to neutrophils.	-0.390	0.000
ACOX1	Peroxisomal acyl-CoA oxidase 1, A chain: Catalyses the desaturation of acyl-CoAs to 2-trans-enoyl-CoAs. Isoform 1 exhibits highest activity against medium-chain fatty acyl-CoAs, with decreasing activity as the chain length increases. Isoform 2 displays a broader substrate range and is active against very long-chain acyl-CoAs.	-0.448	0.000
CYP2E1	Cytochrome P450 2E1: A cytochrome P450 monooxygenase participates in the metabolism of fatty acids, specifically facilitating hydroxylation at the omega-1 position. It demonstrates the greatest catalytic efficiency when acting on saturated fatty acids.	-0.534	0.000
APOB	Apolipoprotein B-100: Primary protein component in chylomicrons (designated as apo B-48), as well as in LDL (apo B-100) and VLDL (apo B-100). Apo B-100 acts as a recognition signal, facilitating the binding and internalization of LDL particles through the apoB/E receptor on cells.	-0.924	0.000
ACSL5	Long-chain-fatty-acid--CoA ligase 5: Catalyses the transformation of long-chain fatty acids into their active acyl-CoA form and facilitates both the synthesis of cellular lipids and degradation through β-oxidation. ACSL5 activates exogenous fatty acids resulting in the production of triacylglycerol for storage within cells.	-0.437	0.000

As there were 708 DEPs that were significantly changed, for PPIs we applied a more restricted *P*-value (using the adjusted *P*-value) to improve the confidence of the MCL clusters. PPIs of statistically significant (adjusted $P < 0.05$) DEPs was performed using STRING® (version 12.0) online database for PPI maps, bio-informatic Gene Ontology (GO) and MCL cluster analysis. MCL cluster analysis demonstrated 99 unique clusters. Of these, four main clusters (identified by their modularity i.e. more densely connected internally than with the rest of the network and clear separation from other clusters) demonstrated changes in:

- Ribosomal pathways (Figure 5.9)
- Anti-inflammatory, coagulation and lipid transport pathways (Figure 5.10)
- Mitochondrial pathways (Figure 5.11)
- Lipid metabolism (Figure 5.12)

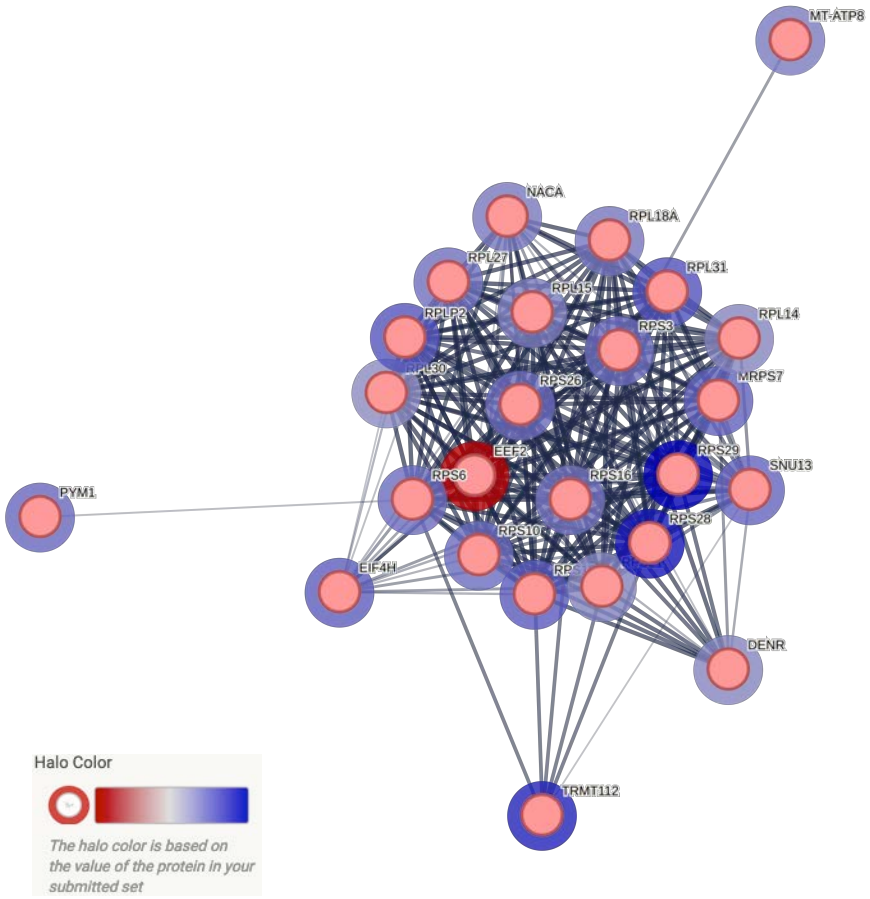

Biological Process (Gene Ontology)

GO-term	description	count in network	strength	false discovery rate
GO:0001731	Formation of translation preinitiation complex	2 of 11	2.16	0.0416
GO:0000028	Ribosomal small subunit assembly	3 of 19	2.09	0.0012
GO:0002181	Cytoplasmic translation	18 of 123	2.06	5.58e-30
GO:0030490	Maturation of SSU-rRNA	5 of 55	1.86	5.64e-06
GO:0042274	Ribosomal small subunit biogenesis	7 of 78	1.85	6.08e-09
GO:0000462	Maturation of SSU-rRNA from tricistronic rRNA transcript (S...	3 of 39	1.78	0.0080
GO:0006412	Translation	21 of 389	1.63	2.60e-28
GO:0006364	rRNA processing	9 of 220	1.51	3.72e-09
GO:0006413	Translational initiation	3 of 75	1.5	0.0438
GO:0042254	Ribosome biogenesis	10 of 299	1.42	1.53e-09
GO:0022618	Ribonucleoprotein complex assembly	6 of 203	1.37	9.37e-05
GO:0022613	Ribonucleoprotein complex biogenesis	12 of 449	1.32	8.40e-11
GO:1901566	Organonitrogen compound biosynthetic process	22 of 1338	1.11	8.82e-20
GO:0044271	Cellular nitrogen compound biosynthetic process	22 of 1494	1.06	8.49e-19
GO:0010467	Gene expression	23 of 2101	0.94	1.70e-17
GO:0044260	Cellular macromolecule metabolic process	23 of 2512	0.86	8.21e-16
GO:0034641	Cellular nitrogen compound metabolic process	25 of 3463	0.75	1.88e-16
GO:0016070	RNA metabolic process	10 of 1550	0.71	0.0042
GO:0019538	Protein metabolic process	22 of 3910	0.65	3.97e-10
GO:0090304	Nucleic acid metabolic process	11 of 2203	0.59	0.0135
GO:0044085	Cellular component biogenesis	13 of 2702	0.58	0.0027
GO:1901564	Organonitrogen compound metabolic process	23 of 4981	0.56	2.25e-09
GO:0006139	Nucleobase-containing compound metabolic process	12 of 2722	0.54	0.0168
GO:0043170	Macromolecule metabolic process	24 of 5781	0.51	2.21e-09
GO:0044238	Primary metabolic process	25 of 7156	0.44	6.29e-09
GO:0071704	Organic substance metabolic process	25 of 7522	0.42	2.03e-08
				(less ...)

Molecular Function (Gene Ontology)

GO-term	description	count in network	strength	false discovery rate
GO:0003735	Structural constituent of ribosome	17 of 169	1.9	8.73e-26
GO:0045296	Cadherin binding	5 of 334	1.07	0.0411
GO:0003723	RNA binding	21 of 1672	1.0	8.03e-16
GO:0003676	Nucleic acid binding	22 of 4003	0.64	9.25e-10

Cellular Component (Gene Ontology)

GO-term	description	count in network	strength	false discovery rate
GO:0098556	Cytoplasmic side of rough endoplasmic reticulum membrane	4 of 5	2.8	4.29e-08
GO:0042788	Polysomal ribosome	7 of 31	2.25	6.58e-12
GO:0022627	Cytosolic small ribosomal subunit	9 of 44	2.21	2.06e-15
GO:0022626	Cytosolic ribosome	16 of 101	2.1	3.23e-27
GO:0005844	Polysome	10 of 65	2.08	4.33e-16
GO:0015935	Small ribosomal subunit	10 of 77	2.01	1.73e-15
GO:0022625	Cytosolic large ribosomal subunit	7 of 56	1.99	2.26e-10
GO:0044391	Ribosomal subunit	17 of 187	1.86	9.27e-26
GO:0005791	Rough endoplasmic reticulum	5 of 81	1.69	8.37e-06
GO:1990904	Ribonucleoprotein complex	19 of 687	1.34	1.95e-20
GO:0005925	Focal adhesion	9 of 416	1.23	2.18e-07
GO:0014069	Postsynaptic density	4 of 324	0.99	0.0434
GO:0005730	Nucleolus	7 of 996	0.74	0.0130
GO:0070062	Extracellular exosome	13 of 2096	0.69	3.44e-05
GO:0030054	Cell junction	13 of 2115	0.69	3.58e-05
GO:0032991	Protein-containing complex	24 of 5506	0.54	2.23e-10
GO:0005829	Cytosol	20 of 5438	0.46	8.91e-06
GO:0043232	Intracellular non-membrane-bounded organelle	19 of 5191	0.46	3.44e-05
GO:0005654	Nucleoplasm	13 of 4169	0.39	0.0426
GO:0005737	Cytoplasm	23 of 12056	0.18	0.0426

Figure 5.9. Cluster analysis of ribosomal pathways during NMP of lean livers: Upregulated DEPs including DENR, EEF2, EIF4H, ribosomal proteins (RPL14, RPL15, RPL18A, RPL27, RPL30, RPL31, RPLP2, RPS10, RPS16, RPS19, RPS21, RPS26, RPS28, RPS29, RPS3) and mitochondrial components (MRPS7, MT-ATP8), indicate enhanced protein synthesis and mitochondrial activity during NMP. This enrichment reflects a response to increased demands for protein production required for metabolic processes and response to cellular stress during NMP. Blue halo represents upregulation and red halo represents downregulation of protein.

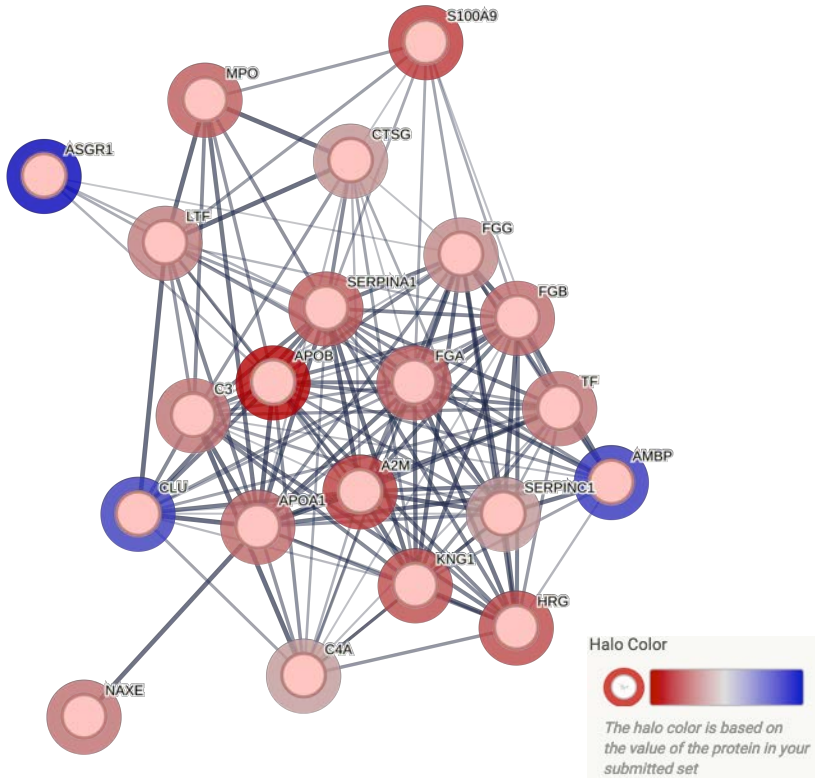

Biological Process (Gene Ontology)

GO-term	description	count in network	strength	false discovery rate
GO:2000257	Regulation of protein activation cascade	2 of 3	2.8	0.0018
GO:0043152	Induction of bacterial agglutination	2 of 6	2.5	0.0041
GO:0031639	Plasminogen activation	3 of 11	2.41	0.00010
GO:2000427	Positive regulation of apoptotic cell clearance	2 of 8	2.37	0.0058
GO:0042730	Fibrinolysis	4 of 19	2.3	3.43e-06

(more ...)

Molecular Function (Gene Ontology)

GO-term	description	count in network	strength	false discovery rate
GO:0070325	Lipoprotein particle receptor binding	3 of 30	1.97	0.0020
GO:0004869	Cysteine-type endopeptidase inhibitor activity	3 of 54	1.72	0.0090
GO:0004866	Endopeptidase inhibitor activity	9 of 177	1.68	6.40e-10
GO:0004867	Serine-type endopeptidase inhibitor activity	5 of 98	1.68	3.31e-05
GO:0008201	Heparin binding	7 of 173	1.58	2.69e-07
GO:0016209	Antioxidant activity	3 of 76	1.57	0.0227
GO:0005539	Glycosaminoglycan binding	8 of 245	1.49	1.14e-07
GO:1901681	Sulfur compound binding	8 of 272	1.44	1.83e-07
GO:0002020	Protease binding	4 of 135	1.44	0.0042
GO:0005102	Signaling receptor binding	13 of 1499	0.91	2.11e-07
GO:0030234	Enzyme regulator activity	10 of 1239	0.88	8.33e-05
GO:0098772	Molecular function regulator activity	11 of 1960	0.72	0.00050
GO:0005515	Protein binding	19 of 7242	0.39	0.00021
GO:0005488	Binding	21 of 12838	0.19	0.0343

(less ...)

Cellular Component (Gene Ontology)

GO-term	description	count in network	strength	false discovery rate
GO:0097013	Phagocytic vesicle lumen	2 of 5	2.57	0.0013
GO:0005577	Fibrinogen complex	3 of 8	2.55	1.17e-05
GO:0034366	Spherical high-density lipoprotein particle	2 of 8	2.37	0.0025
GO:0071682	Endocytic vesicle lumen	4 of 23	2.21	1.20e-06
GO:0042627	Chylomicron	2 of 13	2.16	0.0056
GO:0031093	Platelet alpha granule lumen	8 of 66	2.06	7.11e-13
GO:0072562	Blood microparticle	13 of 118	2.01	5.30e-21
GO:0034364	High-density lipoprotein particle	3 of 29	1.99	0.00033
GO:0034361	Very-low-density lipoprotein particle	2 of 20	1.97	0.0117
GO:0031983	Vesicle lumen	16 of 326	1.66	1.82e-21
GO:0034774	Secretory granule lumen	15 of 321	1.64	7.32e-20
GO:0005788	Endoplasmic reticulum lumen	11 of 312	1.52	7.49e-13
GO:0035578	Azurophil granule lumen	3 of 91	1.49	0.0064
GO:0062023	Collagen-containing extracellular matrix	13 of 407	1.48	6.12e-15
GO:0005775	Vacuolar lumen	4 of 175	1.33	0.0019
GO:0030139	Endocytic vesicle	5 of 338	1.14	0.0014
GO:0009897	External side of plasma membrane	5 of 388	1.08	0.0025
GO:0009986	Cell surface	10 of 894	1.02	6.83e-07
GO:0005769	Early endosome	4 of 411	0.96	0.0350
GO:0070062	Extracellular exosome	20 of 2096	0.95	2.92e-16
GO:0005764	Lysosome	5 of 746	0.8	0.0381
GO:0031410	Cytoplasmic vesicle	16 of 2482	0.78	4.67e-09
GO:0005783	Endoplasmic reticulum	13 of 2021	0.78	1.00e-06
GO:0005576	Extracellular region	21 of 4175	0.67	8.91e-13
GO:0012505	Endomembrane system	19 of 4721	0.58	1.96e-08
GO:0070013	Intracellular organelle lumen	19 of 5660	0.5	5.17e-07

Figure 5.10. Cluster analysis of anti-inflammatory, lipid metabolism and coagulation pathways during NMP of lean livers: Upregulated DEPs including CLU, ASGR1 and AMBP indicate tissue remodelling, glycoprotein clearance and anti-inflammatory responses, respectively. CLU, involved in processes like tissue remodelling and apoptosis in response to cellular stress. ASGR1 is essential in clearing glycoproteins indicating enhancement in liver detoxification processes. AMBP has an anti-inflammatory role, conferring protection against oxidative stress. Conversely, downregulated proteins including A2M, APOA1, APOB, C3 and C4A, CTSG, FGA, FGB, FGG, HRG, KNG1, LTF, MPO, NAXE, S100A9, SERPINA1, SERPINC1, and TF are implicated in various functions including lipid transport and metabolism, immune responses, coagulation, and inflammation. The downregulation of these DEPs reflect alterations in lipid homeostasis, immune function, coagulation pathways, and the overall capacity to respond to inflammation and oxidative stress during NMP. Blue halo represents upregulation and red halo represents downregulation of protein.

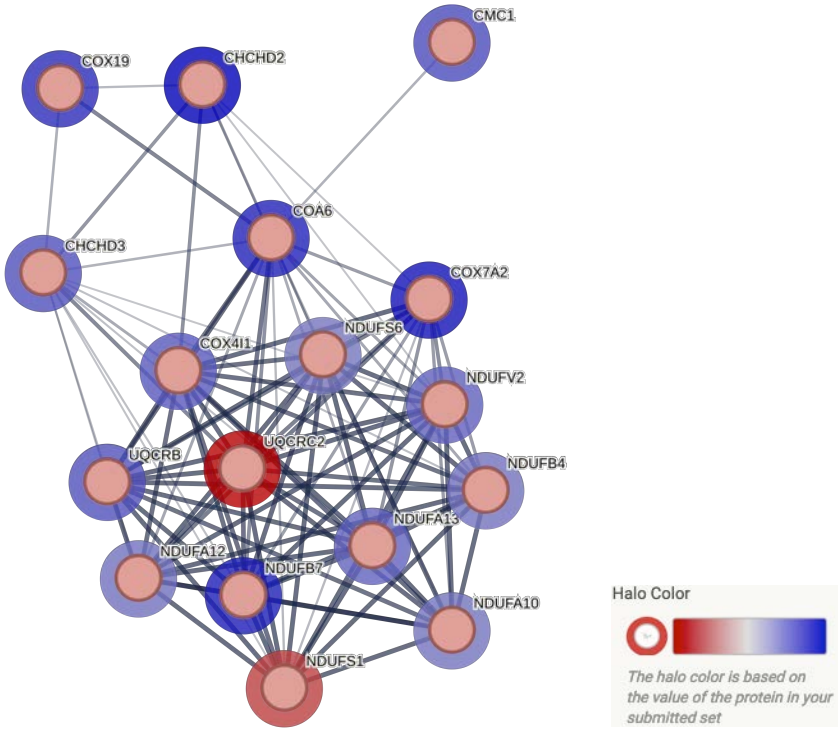

Biological Process (Gene Ontology)

GO-term	description	count in network	strength	false discovery rate
GO:0006122	Mitochondrial electron transport, ubiquinol to cytochrome c	2 of 13	2.25	0.0198
GO:0042775	Mitochondrial ATP synthesis coupled electron transport	12 of 92	2.18	1.14e-20
GO:0006120	Mitochondrial electron transport, NADH to ubiquinone	6 of 46	2.18	1.90e-09
GO:0042776	Proton motive force-driven mitochondrial ATP synthesis	8 of 64	2.16	7.15e-13
GO:0019646	Aerobic electron transport chain	10 of 87	2.12	1.70e-16
GO:0006119	Oxidative phosphorylation	13 of 122	2.09	1.47e-21
GO:0032981	Mitochondrial respiratory chain complex I assembly	6 of 61	2.06	7.44e-09
GO:0033108	Mitochondrial respiratory chain complex assembly	7 of 98	1.92	1.45e-09
GO:0007005	Mitochondrion organization	10 of 445	1.42	5.40e-10
GO:0065003	Protein-containing complex assembly	9 of 1303	0.9	0.00013

(less ...)

Molecular Function (Gene Ontology)

GO-term	description	count in network	strength	false discovery rate
GO:0008137	NADH dehydrogenase (ubiquinone) activity	7 of 41	2.3	1.51e-11
GO:0015453	Oxidoreduction-driven active transmembrane transporter ac...	8 of 71	2.12	5.37e-12
GO:0009055	Electron transfer activity	8 of 121	1.88	4.40e-11
GO:0016491	Oxidoreductase activity	9 of 731	1.15	1.17e-06

Cellular Component (Gene Ontology)

GO-term	description	count in network	strength	false discovery rate
GO:0005747	Mitochondrial respiratory chain complex I	8 of 50	2.27	1.27e-14
GO:0005750	Mitochondrial respiratory chain complex III	2 of 13	2.25	0.0052
GO:0045277	Respiratory chain complex IV	4 of 27	2.23	1.09e-06
GO:0098803	Respiratory chain complex	13 of 90	2.22	4.71e-24
GO:0005746	Mitochondrial respirasome	12 of 94	2.17	1.27e-21
GO:0070069	Cytochrome complex	5 of 40	2.16	3.06e-08
GO:0005751	Mitochondrial respiratory chain complex IV	3 of 24	2.16	0.00012
GO:0098800	Inner mitochondrial membrane protein complex	13 of 158	1.98	1.27e-21
GO:1990204	Oxidoreductase complex	10 of 124	1.97	5.71e-16
GO:0005758	Mitochondrial intermembrane space	5 of 86	1.83	1.08e-06
GO:1902495	Transmembrane transporter complex	10 of 384	1.48	1.77e-11
GO:0005740	Mitochondrial envelope	16 of 802	1.36	4.48e-19
GO:0098796	Membrane protein complex	14 of 1218	1.12	8.84e-13
GO:0005739	Mitochondrion	17 of 1681	1.07	2.14e-16
GO:0016021	Integral component of membrane	13 of 5670	0.42	0.0047

Figure 5.11. Cluster analysis of mitochondrial pathways during NMP of lean livers: Upregulated DEPs including CHCHD2, CHCHD3, CMC1, COA6, COX19, COX4I1, COX7A2, NDUFA10, NDUFA12, NDUFA13, NDUFB4, NDUFB7, NDUFS6, NDUFV2, and UQCRB are implicated in the mitochondrial respiratory chain and oxidative phosphorylation system. These DEPs have important roles in electron transport, ATP synthesis, and overall mitochondrial integrity, indicating an enhanced mitochondrial function and energy production during NMP. Conversely, downregulated DEPs including NDUFS1 (part of complex I) and UQCRC2 (a component of complex III) are essential for efficient electron transport and ATP production. Their reduced expression indicates a complex regulatory mechanism of mitochondrial function during NMP characterised by increased energy requirements during NMP and compensatory responses to cellular stress. Blue halo represents upregulation and red halo represents downregulation of protein.

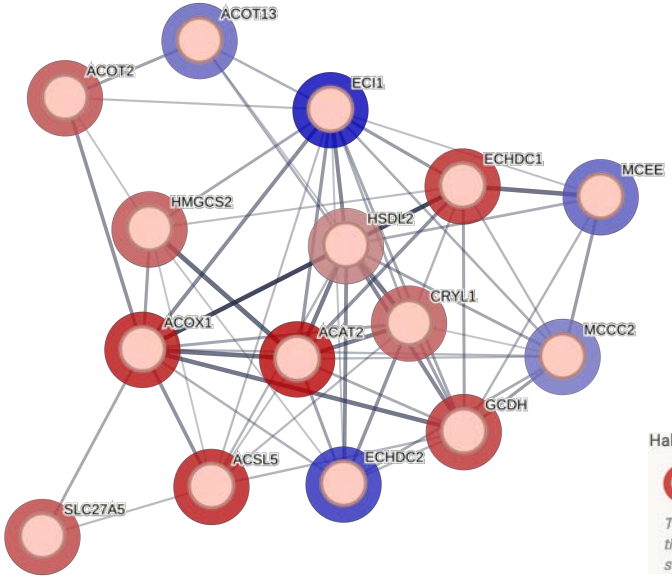

Halo Color

The halo color is based on the value of the protein in your submitted set

Biological Process (Gene Ontology)

GO-term	description	count in network	strength	false discovery rate
GO:0046951	Ketone body biosynthetic process	2 of 6	2.64	0.0058
GO:0006635	Fatty acid beta-oxidation	6 of 60	2.12	6.58e-09
GO:0000038	Very long-chain fatty acid metabolic process	3 of 35	2.05	0.0013
GO:0009062	Fatty acid catabolic process	7 of 85	2.03	4.67e-10
GO:1901570	Fatty acid derivative biosynthetic process	4 of 49	2.03	3.90e-05
GO:0006637	acyl-CoA metabolic process	5 of 88	1.87	4.13e-06
GO:0034032	Purine nucleoside bisphosphate metabolic process	6 of 120	1.82	2.52e-07
GO:0033875	Ribonucleoside bisphosphate metabolic process	6 of 120	1.82	2.52e-07
GO:0046395	Carboxylic acid catabolic process	8 of 225	1.67	2.88e-09
GO:0006631	Fatty acid metabolic process	11 of 325	1.65	6.03e-13
GO:0001676	Long-chain fatty acid metabolic process	3 of 107	1.57	0.0234
GO:0009150	Purine ribonucleotide metabolic process	6 of 390	1.31	0.00016
GO:0019752	Carboxylic acid metabolic process	12 of 819	1.28	6.17e-11
GO:0044255	Cellular lipid metabolic process	12 of 918	1.23	1.01e-10
GO:0006629	Lipid metabolic process	13 of 1210	1.15	6.78e-11
GO:0044281	Small molecule metabolic process	13 of 1645	1.02	1.57e-09
GO:0044238	Primary metabolic process	14 of 7156	0.41	0.0030
GO:0044237	Cellular metabolic process	13 of 6568	0.41	0.0113
GO:0071704	Organic substance metabolic process	14 of 7522	0.39	0.0053

(less ...)

Molecular Function (Gene Ontology)

GO-term	description	count in network	strength	false discovery rate
GO:0004300	enoyl-CoA hydratase activity	3 of 10	2.6	0.00025
GO:0003824	Catalytic activity	15 of 5522	0.55	2.60e-05

Cellular Component (Gene Ontology)

GO-term	description	count in network	strength	false discovery rate
GO:0005759	Mitochondrial matrix	7 of 494	1.27	3.62e-05
GO:0005739	Mitochondrion	11 of 1681	0.93	3.65e-06

Figure 5.12. Cluster analysis of lipid metabolism pathways during NMP of lean livers: Upregulated proteins including ACOT13, ECI1, ECHDC2, MCEE, MCCC2 are mainly involved in the catabolism and processing of fatty acids and organic acids. ECI1 and MCCC2 are key enzymes in fatty acid β-oxidation, a primary pathway for energy production from lipids indicating increased fatty acid catabolic activity. In addition, MCEE is involved in the metabolism of methylmalonic acid, indicative of altered propionate metabolism. Conversely, downregulated DEPs including ACAT2 (ketone body production) and ACOX1 (enzyme involved in peroxisomal fatty acid β-oxidation) indicate a reduction in these lipid metabolism pathways. ACSL5 is essential for the activation of long-chain fatty acids, and its downregulation could signify a decrease in fatty acid utilisation. GCDH and HMGCS2 play roles in amino acid and ketone body metabolism respectively, and their reduced expression may reflect metabolic adaptations during NMP. Overall, these changes suggest a complex reprogramming of metabolic pathways in the liver during NMP as a response to alterations in energy requirements, nutrient availability, or cellular stress. This adaptive response indicates balancing energy production with the need to manage lipid accumulation and mitigate inflammation and cellular injury. Blue halo represents upregulation and red halo represents downregulation of protein.

5.3.4 Effect of SCS on proteomes of lean livers

71 significant ($P < 0.05$) DEPs were identified during SCS of lean donor livers (LT2, post-preservation vs. LT1, pre-preservation). 33 were upregulated and 38 downregulated. The top 25 most upregulated and downregulated DEPs are demonstrated in Figure 5.13. Of these, the 5 most clinically relevant upregulated (functions related to ATP synthesis, NADH dehydrogenase activity, amino acid/lipid degradation, cytoprotection and β-oxidation) and downregulated DEPs (functions related to protein kinase-C activity, nuclear transport, mTORC1 activation and inflammatory cytokine activity) are described in Table 5.5.

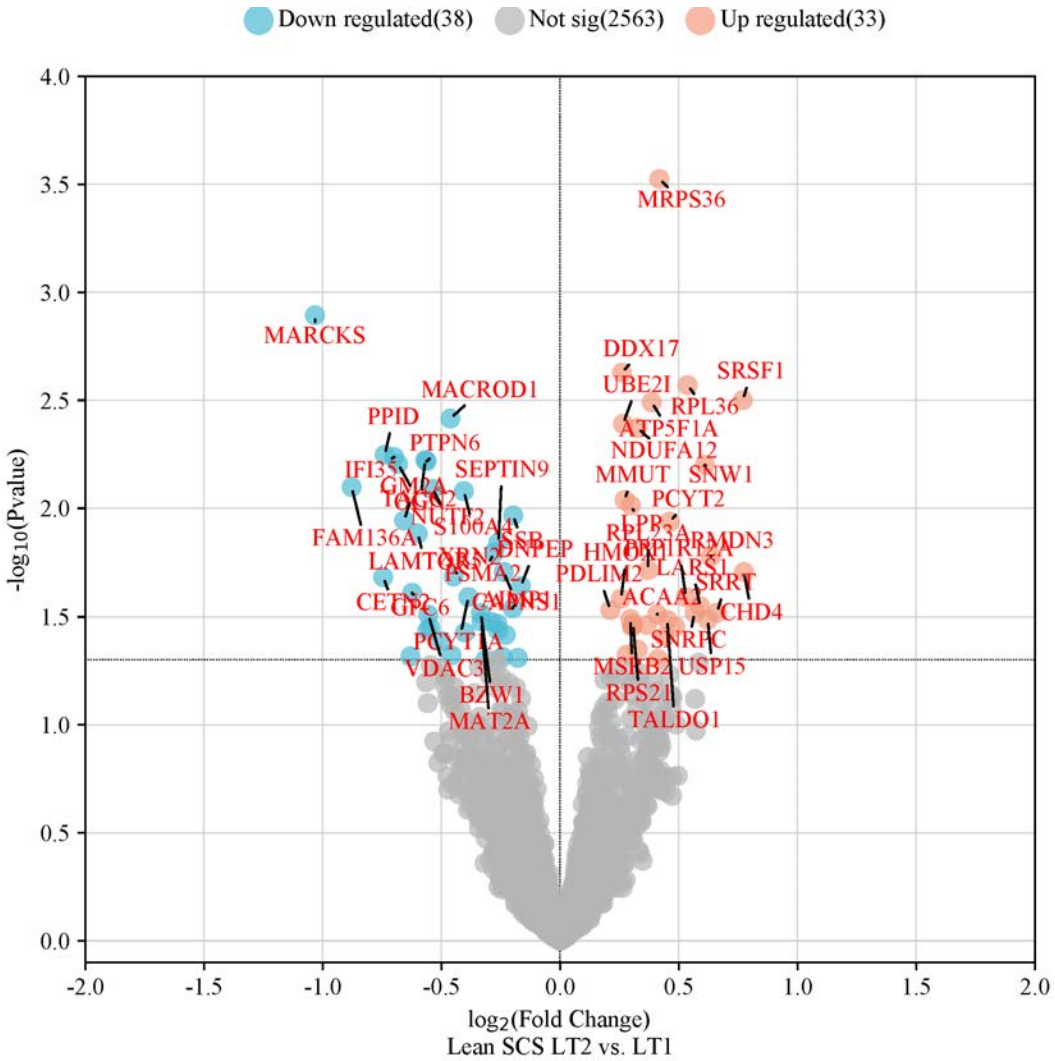

Figure 5.13. The effect of SCS on proteomes of lean donor livers. Top 25 upregulated and downregulated proteins are labelled in the plot.

Table 5.5. Clinically relevant upregulated (n = 5) and downregulated proteins (n = 5) during SCS of lean donor livers.

Upregulated			
Protein name	Function	Fold change	*P* - value
ATP5F1A	ATP synthase subunit alpha, mitochondrial (Complex V): Generates ATP by converting ADP when there is a proton gradient across the membrane. This gradient is established by the electron transport complexes of the respiratory chain.	0.386	0.003
NDUFA12	NADH dehydrogenase [ubiquinone] 1 alpha subcomplex subunit 12: Accessory subunit within the mitochondrial membrane respiratory chain NADH dehydrogenase (Complex I). Complex I facilitates the transfer of electrons from NADH to the respiratory chain.	0.326	0.004
MMUT	Methylmalonyl-CoA mutase, mitochondrial: Participates in the catabolism of various amino acids, odd-chain fatty acids, and cholesterol through the conversion of propionyl-CoA to the tricarboxylic acid cycle.	0.271	0.009
HMOX1	Heme oxygenase 1: Cleavage of heme ring to form biliverdin (which is subsequently converted to bilirubin by biliverdin reductase). Cytoprotetive effect as free heme sensitises cells to apoptosis.	0.256	0.026
ACAA2	3-ketoacyl-CoA thiolase, mitochondrial: Generation of energy from lipid sources, this enzyme is implicated in catalysing the final stage of the mitochondrial β-oxidation pathway - an aerobic metabolic process that converts fatty acids into acetyl-CoA.	0.409	0.031
Downregulated			
Protein name	Function	Fold change	*P* - value
MARCKS	Myristoylated alanine-rich C-kinase substrate: MARCKS represents the primary cellular substrate targeted by protein kinase C. It forms interactions with calmodulin, actin, and synapsin.	-1.033	0.001
MACROD1	ADP-ribose glycohydrolase MACROD1: Eliminates ADP-ribose from aspartate and glutamate residues in proteins featuring a singular ADP-ribose moiety.	-0.463	0.004
NUTF2	Nuclear transport factor 2: Facilitates the translocation of GDP-bound RAN from the cytoplasm to the nucleus, a critical process for RAN's functionality in cargo receptor-mediated nucleocytoplasmic transport.	-0.537	0.008
LAMTOR5	Ragulator complex protein LAMTOR5: As a component of the Ragulator complex, it participates in amino acid detection and the initiation of mTORC1, a signalling complex that stimulates cell growth in response to growth factors, energy status, and amino acids.	-0.600	0.013
AIMP1	Aminoacyl tRNA synthase complex-interacting multifunctional protein: Enhances the catalytic function of cytoplasmic arginyl-tRNA synthase and exhibiting tRNA binding capability. Additionally, it demonstrates inflammatory cytokine activity, plays a negative regulatory role in TGF-beta signalling by stabilizing SMURF2 through direct binding, thereby inhibiting its SMAD7-mediated degradation, and is implicated in glucose homeostasis through the induction of glucagon secretion in response to low glucose levels.	-0.200	0.029

Protein-protein interaction (PPI) of statistically significant ($P < 0.05$) DEPs was performed using STRING® (version 12.0) online database for PPI maps, bio-informatic and Gene Ontology (GO). As only 71 DEPs were identified, MCL cluster analysis of pathways was not performed. Instead, general network analysis is demonstrated in Figure 5.14.

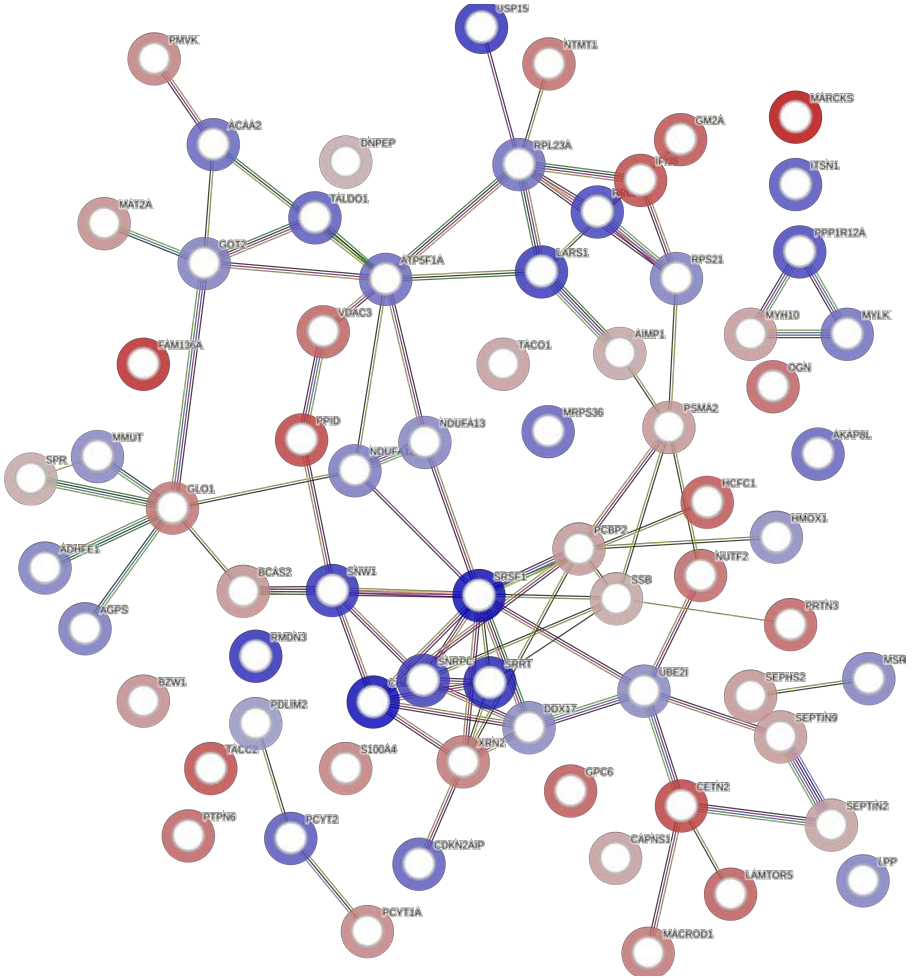

Biological Process (Gene Ontology)

GO-term	description	count in network	strength	false discovery rate
GO:0044237	Cellular metabolic process	45 of 6568	0.29	0.00099
GO:0071704	Organic substance metabolic process	50 of 7522	0.27	0.00029
GO:0044238	Primary metabolic process	47 of 7156	0.27	0.00099
GO:0006807	Nitrogen compound metabolic process	44 of 6643	0.27	0.0020
GO:0009987	Cellular process	67 of 14826	0.1	0.0138

Molecular Function (Gene Ontology)

GO-term	description	count in network	strength	false discovery rate
GO:0003723	RNA binding	22 of 1672	0.57	0.00022

Cellular Component (Gene Ontology)

GO-term	description	count in network	strength	false discovery rate
GO:0032432	Actin filament bundle	6 of 74	1.36	7.93e-05
GO:0001725	Stress fiber	5 of 65	1.34	0.00077
GO:0032153	Cell division site	4 of 70	1.21	0.0117
GO:1990904	Ribonucleoprotein complex	12 of 687	0.69	0.00077
GO:0015629	Actin cytoskeleton	8 of 482	0.67	0.0270
GO:0070062	Extracellular exosome	20 of 2096	0.43	0.0033
GO:0005615	Extracellular space	25 of 3247	0.34	0.0072
GO:0070013	Intracellular organelle lumen	43 of 5660	0.33	1.26e-05
GO:0031981	Nuclear lumen	33 of 4526	0.31	0.00100
GO:0005654	Nucleoplasm	30 of 4169	0.31	0.0037
GO:0005829	Cytosol	38 of 5438	0.29	0.00042
GO:0005634	Nucleus	49 of 7672	0.25	4.36e-05
GO:0032991	Protein-containing complex	33 of 5506	0.23	0.0397
GO:0005737	Cytoplasm	64 of 12056	0.17	1.26e-05
GO:0043231	Intracellular membrane-bounded organelle	63 of 12149	0.16	3.74e-05
GO:0043227	Membrane-bounded organelle	65 of 13188	0.14	7.02e-05
GO:0043229	Intracellular organelle	65 of 13231	0.14	7.46e-05
GO:0005622	Intracellular anatomical structure	70 of 14891	0.12	6.64e-06
GO:0043226	Organelle	66 of 14017	0.12	0.00025

Halo Color

The halo color is based on the value of the protein in your submitted set

Figure 5.14. STRING network analysis of upregulated and downregulated proteins during SCS of lean donor livers: Upregulated DEPs including ATP5F1A and NDUFA12, MMUT, HMOX1, and ACAA2 indicate changes in mitochondrial activity, branched chain amino acid metabolism, response to cellular stress and fatty acid β-oxidation, respectively. In addition, upregulation of ribosomal proteins (RPL23A) and mitochondrial proteins (MRPS36) further indicate increased protein synthesis and mitochondrial function required for energy production and metabolic homeostasis. Other upregulated DEPs including CHD4, SRSF1, SRRT, RMDN3, and USP15 indicate increased gene regulation, RNA splicing, and protein ubiquitination, indicative of dynamic cellular remodelling in response to cellular stress. Downregulated DEPs including MARCKS, MACROD1 and SEPTIN9 indicate modifications in cellular signalling pathways and cytoskeletal dynamics in response to changes in hepatocyte environment or inflammatory stimuli during SCS. Downregulation of NUTF2, LAMTOR5, and AIMP1, implicated in nuclear transport, mTOR signalling, and amino acid metabolism, respectively, indicate a potential downscaling of these metabolic and signalling pathways in response to altered cellular conditions or energy demands during SCS.

5.3.5 Effect of NMP on reperfusion proteomes in steatotic vs. lean donor livers

215 significant ($P < 0.05$) DEPs were identified at reperfusion (LT3) in steatotic livers compared to lean livers preserved with NMP. 44 were upregulated and 171 were downregulated. The top 25 most upregulated and downregulated DEPs are demonstrated in Figure 5.15. Of these, the 5 most clinically relevant upregulated (functions related to β-oxidation, self-nonself discrimination, molecular repair, bile acid amidation and scavenging of damaged nuclear material) and downregulated DEPs (functions related to Ca^{2+} haemostasis, cytochrome c oxidase activity, innate immunity and oxidative stress) are described in Table 5.6.

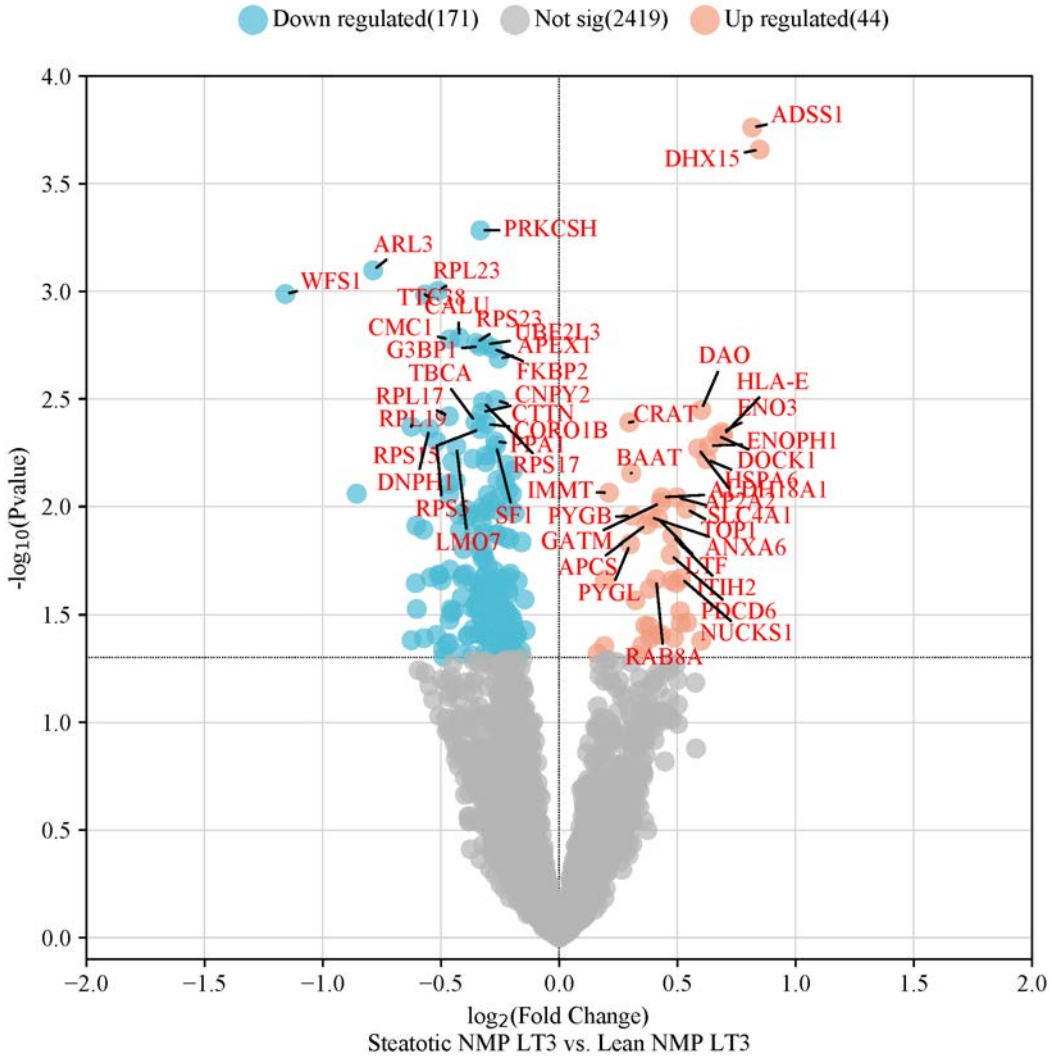

Figure 5.15. The effect of NMP on proteomes at reperfusion (LT3) in steatotic livers compared to lean donor livers. Top 25 upregulated and downregulated proteins are labelled in the plot.

Table 5.6. Clinically relevant upregulated (n = 5) and downregulated proteins (n = 5) at reperfusion (LT3) of steatotic livers preserved with NMP compared to lean donor livers.

Upregulated			
Protein name	Function	Fold change	*P* - value
CRAT	Carnitine O-acetyltransferase: Catalytic function involved in the bidirectional transference of acyl groups between carnitine and coenzyme A (CoA), concurrently modulating the ratio of acyl-CoA to CoA. Also involved on transport of fatty acids for β-oxidation.	0.296	0.004
HLA-E	Soluble HLA class I histocompatibility antigen, alpha chain E: Non-classical major histocompatibility class Ib molecule engages in immune self-nonself discrimination.	0.694	0.005
HSPA6	Heat shock 70 kDa protein 6: Central role in the protein quality control system, overseeing the accurate folding of proteins, the re-folding of misfolded proteins, and the regulation of protein targeting for subsequent degradation.	0.623	0.006
BAAT	Bile acid-CoA:amino acid N-acyltransferase: Catalyses the amidation process in which bile acids (BAs) are conjugated with the amino acids taurine and glycine to form bile salts.	0.304	0.007
APCS	Serum amyloid P-component(1-203): Exhibits the capability to engage with DNA and histones, potentially scavenging nuclear material released from damaged circulating cells.	0.370	0.012
Downregulated			
Protein name	Function	Fold change	*P* - value
WFS1	Wolframin: Regulation of cellular Ca^{2+} homeostasis through modulating the filling state of the endoplasmic reticulum Ca^{2+} store.	-1.159	0.001
CMC1	COX assembly mitochondrial protein homolog: Component of the MITRAC (mitochondrial translation regulation assembly intermediate of cytochrome c oxidase complex) complex. Involved in regulation of cytochrome c oxidase assembly.	-0.463	0.002
RPS23	40S ribosomal protein S23: Integral to the ribosome, a large ribonucleoprotein complex accountable for protein synthesis in the cell. The small ribosomal subunit (SSU) binds to messenger RNAs (mRNAs) and interprets the encoded information by selecting appropriate aminoacyl-transfer RNA (tRNA) molecules.	-0.352	0.002
G3BP1	Ras GTPase-activating protein-binding protein 1: An ATP- and magnesium-dependent helicase with a central role in innate immunity. Involved in the DNA-triggered cGAS/STING pathway by facilitating DNA binding and activation of cGAS. It additionally augments DDX58-induced type I interferon production, likely by assisting DDX58 in sensing pathogenic RNA.	-0.336	0.002
APEX1	DNA-(apurinic or apyrimidinic site) lyase, mitochondrial: Role in the cellular response to oxidative stress, APEX1 exhibits dual major activities involving DNA repair and redox regulation of transcriptional factors. It acts as an apurinic/apyrimidinic (AP) endodeoxyribonuclease in the DNA base excision repair (BER) pathway, specifically addressing DNA lesions induced by oxidative and alkylating agents.	-0.256	0.002

Protein-protein interaction (PPI) of statistically significant ($P < 0.05$) DEPs was performed using STRING® (version 12.0) online database for PPI maps, bio-informatic Gene Ontology (GO) and MCL cluster analysis. MCL cluster analysis demonstrated 55 unique clusters. Of these, the five main clusters (identified by their modularity i.e. more densely connected internally than with the rest of the network and clear separation from other clusters) demonstrated changes in:

- Ribosomal pathways (Figure 5.16)
- RNA splicing pathways (Figure 5.17)
- Immune cell migration pathways (Figure 5.18)
- Glycogen, carbohydrate and energy precursor catabolic processes (Figure 5.19)
- Protein folding and heat shock protein binding processes (Figure 5.20)

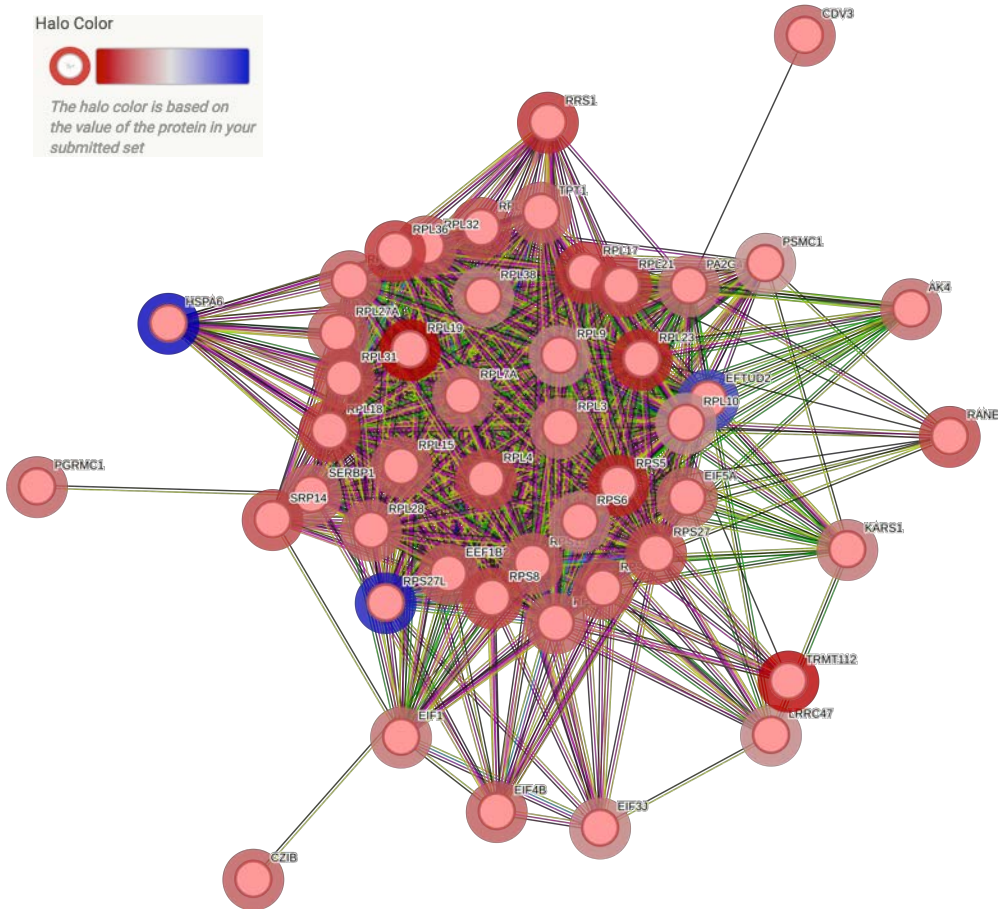

Biological Process (Gene Ontology)

GO-term	description	count in network	strength	false discovery rate
GO:0000028	Ribosomal small subunit assembly	5 of 19	2.03	1.34e-06
GO:0002181	Cytoplasmic translation	28 of 123	1.97	8.96e-44
GO:0000027	Ribosomal large subunit assembly	3 of 25	1.69	0.0151
GO:0042274	Ribosomal small subunit biogenesis	9 of 78	1.68	3.90e-10
GO:0042255	Ribosome assembly	7 of 60	1.68	1.34e-07
				(more ...)

Molecular Function (Gene Ontology)

GO-term	description	count in network	strength	false discovery rate
GO:0003735	Structural constituent of ribosome	27 of 169	1.82	1.18e-38
GO:0019843	rRNA binding	5 of 67	1.49	0.00042
GO:0008135	Translation factor activity, RNA binding	5 of 98	1.32	0.0022
GO:0090079	Translation regulator activity, nucleic acid binding	6 of 121	1.31	0.00034
GO:0045182	Translation regulator activity	7 of 152	1.28	6.61e-05
GO:0003723	RNA binding	39 of 1672	0.98	4.77e-30
GO:0003676	Nucleic acid binding	41 of 4003	0.62	9.54e-19
GO:1901363	Heterocyclic compound binding	44 of 5977	0.48	8.47e-16
GO:0097159	Organic cyclic compound binding	44 of 6050	0.47	1.18e-15
GO:0005488	Binding	47 of 12838	0.18	2.29e-05
				(less ...)

Cellular Component (Gene Ontology)

GO-term	description	count in network	strength	false discovery rate
GO:0022625	Cytosolic large ribosomal subunit	19 of 56	2.14	3.74e-32
GO:0042788	Polysomal ribosome	9 of 31	2.08	8.84e-14
GO:0022626	Cytosolic ribosome	27 of 101	2.04	1.80e-44
GO:0022627	Cytosolic small ribosomal subunit	8 of 44	1.87	8.52e-11
GO:0005844	Polysome	10 of 65	1.8	4.44e-13
GO:0044391	Ribosomal subunit	27 of 187	1.77	3.03e-38
GO:0005791	Rough endoplasmic reticulum	4 of 81	1.31	0.0050
GO:1990904	Ribonucleoprotein complex	32 of 687	1.28	3.09e-32
GO:0005925	Focal adhesion	14 of 416	1.14	1.83e-10
GO:0005730	Nucleolus	11 of 996	0.66	0.0023
GO:0030054	Cell junction	18 of 2115	0.54	0.00013
GO:0005829	Cytosol	41 of 5438	0.49	3.19e-14
GO:0032991	Protein-containing complex	39 of 5506	0.46	5.49e-12
GO:0043232	Intracellular non-membrane-bounded organelle	32 of 5191	0.4	8.55e-07
GO:0070013	Intracellular organelle lumen	25 of 5660	0.26	0.0487
GO:0005634	Nucleus	33 of 7672	0.25	0.0028
GO:0005737	Cytoplasm	46 of 12056	0.19	3.50e-06

Figure 5.16. Cluster analysis of ribosomal pathways during reperfusion (LT3) in steatotic vs. lean donor preserved with NMP: Upregulated DEPs including RPS27L, RPL10 and HSPA6 are important mediators of ribosomal activity and stress response mechanisms. RPS27L and RPL10 (ribosomal components involved in protein synthesis) indicate a selective increase in translational capacity during reperfusion. HSPA6 (a stress-responsive chaperone) indicates an enhanced mechanism for mitigating cellular stress during liver inflammation and injury. Conversely, downregulated ribosomal proteins (RPL15, RPL17, RPL18, RPL18A, RPL19) and mediators of translation initiation and elongation (EIF1, EIF3J, EIF4B, EIF5A) indicate an altered metabolic state characterised by an overall reduction in protein synthesis to conserve energy during cellular stress. In addition, downregulated proteins including AK4 (mitochondrial metabolism) and PGRMC1 (associated with steroid signalling) demonstrate shifts in energy metabolism and hormone response pathways. Blue halo represents upregulation and red halo represents downregulation of protein.

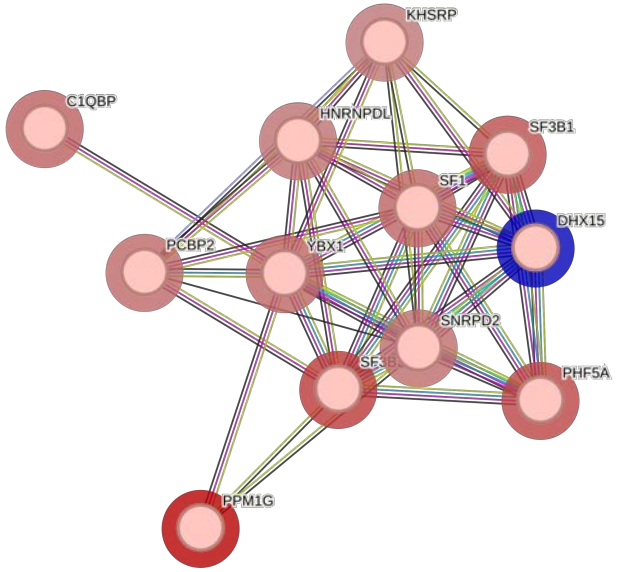

Halo Color

The halo color is based on the value of the protein in your submitted set

Biological Process (Gene Ontology)

GO-term	description	count in network	strength	false discovery rate
GO:1903241	U2-type prespliceosome assembly	4 of 24	2.44	3.14e-06
GO:0000245	Spliceosomal complex assembly	5 of 76	2.03	1.79e-06
GO:0008380	RNA splicing	9 of 370	1.6	8.78e-10
GO:0000375	RNA splicing, via transesterification reactions	6 of 249	1.6	6.54e-06
GO:0006397	mRNA processing	9 of 455	1.51	2.22e-09
GO:0016071	mRNA metabolic process	10 of 611	1.43	8.78e-10
GO:0022613	Ribonucleoprotein complex biogenesis	6 of 449	1.34	0.00010
GO:1903311	Regulation of mRNA metabolic process	4 of 302	1.34	0.0148
GO:0006396	RNA processing	10 of 868	1.28	6.98e-09
GO:0016070	RNA metabolic process	11 of 1550	1.07	2.60e-08
GO:0043170	Macromolecule metabolic process	12 of 5781	0.53	0.00031
GO:0044237	Cellular metabolic process	12 of 6568	0.48	0.0014
GO:0006807	Nitrogen compound metabolic process	12 of 6643	0.47	0.0015
GO:0044238	Primary metabolic process	12 of 7156	0.44	0.0035
				(less ...)

Molecular Function (Gene Ontology)

GO-term	description	count in network	strength	false discovery rate
GO:0003697	Single-stranded DNA binding	3 of 120	1.61	0.0412
GO:0003729	mRNA binding	6 of 326	1.48	4.57e-05
GO:0003723	RNA binding	11 of 1672	1.03	9.31e-08

Cellular Component (Gene Ontology)

GO-term	description	count in network	strength	false discovery rate
GO:0005689	U12-type spliceosomal complex	6 of 28	2.55	3.10e-11
GO:0005686	U2 snRNP	4 of 25	2.42	9.49e-07
GO:0071005	U2-type precatalytic spliceosome	4 of 50	2.12	8.98e-06
GO:0005681	Spliceosomal complex	8 of 197	1.82	5.84e-11
GO:0071013	Catalytic step 2 spliceosome	3 of 90	1.74	0.0025
GO:0016607	Nuclear speck	4 of 420	1.19	0.0093
GO:0016604	Nuclear body	5 of 833	0.99	0.0091
GO:0031981	Nuclear lumen	12 of 4526	0.64	8.98e-06
GO:0005654	Nucleoplasm	11 of 4169	0.64	5.03e-05

Figure 5.17. Cluster analysis of RNA splicing pathways during reperfusion (LT3) in steatotic vs. lean donor preserved with NMP: The upregulation of DHX15 and the downregulation of C1QBP, HNRNPDL, KHSRP, PCBP2, PHF5A, PPM1G, SF1, SF3B1, SF3B2, SNRPD2, and YBX1 indicate adaptations in RNA processing, splicing and cellular metabolism. DHX15 (an RNA helicase) is involved in RNA processing and regulation of gene expression indicating an increase in RNA metabolic activities necessary to adaptation to fluctuating cellular environments. The downregulated DEPs including HNRNPDL, KHSRP, SF3B1, and SF3B2 have central functions in RNA binding and splicing pathways. A reduction in these DEPs could affect a range of RNA molecules and result in alterations in gene expression. A downregulation of C1QBP (involved in mitochondrial function and apoptosis) and PPM1G (involved in RNA splicing and cell cycle regulation) further indicate shifts in mitochondrial metabolism and cell proliferation pathways. Blue halo represents upregulation and red halo represents downregulation of protein.

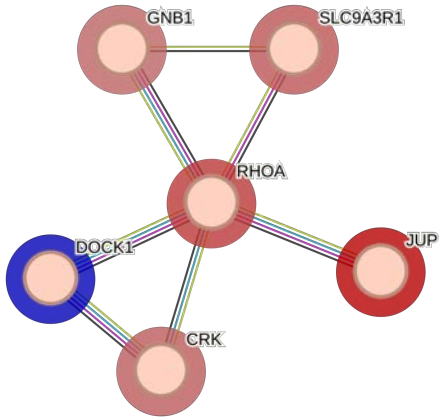

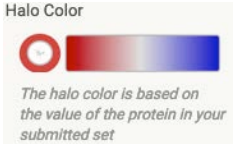

Biological Process (Gene Ontology)

GO-term	description	count in network	strength	false discovery rate
GO:0007191	Adenylate cyclase-activating dopamine receptor signaling p...	2 of 10	2.82	0.0067
GO:0045198	Establishment of epithelial cell apical/basal polarity	2 of 17	2.59	0.0090
GO:0043537	Negative regulation of blood vessel endothelial cell migration	2 of 35	2.27	0.0217
GO:1900026	Positive regulation of substrate adhesion-dependent cell spr...	2 of 45	2.16	0.0289
GO:2000404	Regulation of T cell migration	2 of 49	2.13	0.0334
GO:0099024	Plasma membrane invagination	2 of 60	2.04	0.0429
GO:0014910	Regulation of smooth muscle cell migration	2 of 65	2.0	0.0474
GO:0030010	Establishment of cell polarity	3 of 127	1.89	0.0067
GO:0010811	Positive regulation of cell-substrate adhesion	3 of 128	1.89	0.0067
GO:0008360	Regulation of cell shape	3 of 155	1.8	0.0074
GO:0010810	Regulation of cell-substrate adhesion	4 of 217	1.78	0.0036
GO:2000146	Negative regulation of cell motility	4 of 304	1.64	0.0067
GO:0022604	Regulation of cell morphogenesis	4 of 311	1.63	0.0067
GO:0010632	Regulation of epithelial cell migration	3 of 229	1.63	0.0154
GO:0097305	Response to alcohol	3 of 252	1.59	0.0187
GO:0007264	Small GTPase mediated signal transduction	3 of 273	1.56	0.0217
GO:0016055	Wnt signaling pathway	3 of 284	1.54	0.0232
GO:0030336	Negative regulation of cell migration	3 of 288	1.53	0.0232
GO:0045785	Positive regulation of cell adhesion	4 of 485	1.43	0.0067
GO:0071407	Cellular response to organic cyclic compound	4 of 508	1.41	0.0067
GO:0032970	Regulation of actin filament-based process	3 of 406	1.38	0.0474
GO:0071417	Cellular response to organonitrogen compound	4 of 574	1.36	0.0075
GO:0016477	Cell migration	5 of 903	1.26	0.0067
GO:0030334	Regulation of cell migration	5 of 927	1.25	0.0067
GO:0022603	Regulation of anatomical structure morphogenesis	5 of 920	1.25	0.0067
GO:0010243	Response to organonitrogen compound	5 of 963	1.23	0.0067
GO:1901701	Cellular response to oxygen-containing compound	5 of 1057	1.19	0.0067
GO:0071495	Cellular response to endogenous stimulus	5 of 1103	1.17	0.0067
GO:0007267	Cell-cell signaling	4 of 1079	1.09	0.0390
GO:0071310	Cellular response to organic substance	5 of 2019	0.91	0.0232
GO:0007166	Cell surface receptor signaling pathway	5 of 2040	0.91	0.0234
GO:0048513	Animal organ development	6 of 3246	0.78	0.0121
GO:0007165	Signal transduction	6 of 4714	0.62	0.0484

(less ...)

Molecular Function (Gene Ontology)

GO-term	description	count in network	strength	false discovery rate
GO:0043495	Protein-membrane adaptor activity	2 of 27	2.39	0.0308
GO:0030674	Protein-macromolecule adaptor activity	4 of 322	1.61	0.0053
GO:0019904	Protein domain specific binding	4 of 695	1.28	0.0274
GO:0019899	Enzyme binding	6 of 2084	0.98	0.0053

Cellular Component (Gene Ontology)

GO-term	description	count in network	strength	false discovery rate
GO:0019897	Extrinsic component of plasma membrane	3 of 176	1.75	0.0286
GO:0009898	Cytoplasmic side of plasma membrane	3 of 174	1.75	0.0286
GO:0070062	Extracellular exosome	5 of 2096	0.89	0.0384

Figure 5.18. Cluster analysis of cytoskeletal and immune cell migration pathways during reperfusion (LT3) in steatotic vs. lean donor preserved with NMP: The upregulation of DOCK1 and the downregulation of CRK, GNB1, JUP, RHOA, and SLC9A3R1 indicate adaptations in cellular signalling and cytoskeletal dynamics. DOCK1 (involved in actin cytoskeleton remodelling and cell migration) indicate a response to liver injury or regenerative processes during reperfusion. CRK (involved in cell adhesion and growth signalling pathways), GNB1 (G protein complex involved in cellular signalling) and RHOA (regulation of stress fibre formation) have an important role in maintaining cell structure and mediating signal transduction. The downregulation of these DEPs indicates an alteration in their associated pathways and shift in signal transduction mechanisms. A reduction in JUP and SLC9A3R1 (both involved in cell-cell adhesion and signal transduction) further indicate alterations in cell junction integrity and signalling cascades with potential impact on liver integrity (cellular architecture) in response to physiological stressors. Blue halo represents upregulation and red halo represents downregulation of protein.

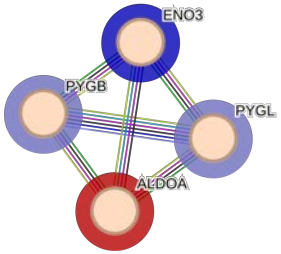

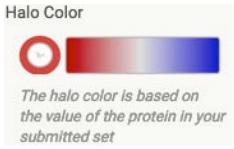

Biological Process (Gene Ontology)

GO-term	description	count in network	strength	false discovery rate
GO:0005980	Glycogen catabolic process	2 of 12	2.91	0.0110
GO:0016052	Carbohydrate catabolic process	4 of 113	2.24	1.85e-05
GO:0006091	Generation of precursor metabolites and energy	4 of 411	1.68	0.0015

Molecular Function (Gene Ontology)

GO-term	description	count in network	strength	false discovery rate
GO:0102499	SHG alpha-glucan phosphorylase activity	2 of 3	3.52	0.0015
GO:0102250	Linear malto-oligosaccharide phosphorylase activity	2 of 3	3.52	0.0015
GO:0008184	Glycogen phosphorylase activity	2 of 3	3.52	0.0015
GO:0030170	Pyridoxal phosphate binding	2 of 54	2.26	0.0468

Cellular Component (Gene Ontology)

GO-term	description	count in network	strength	false discovery rate
GO:0034774	Secretory granule lumen	3 of 321	1.66	0.0356

Figure 5.19. Cluster analysis of glycogen, carbohydrate and energy precursor catabolic pathways during reperfusion (LT3) in steatotic vs. lean donor preserved with NMP: The upregulation of ENO3, PYGL and PYGB with the downregulation of ALDOA indicate adaptations in carbohydrate metabolism and energy production pathways. ENO3 (part of the glycolytic pathway) facilitates the conversion 2-phosphoglycerate to phosphoenolpyruvate resulting in enhanced glycolytic activity. The upregulation of PYGL and PYGB (involved in glycogenolysis) indicating increased conversion of glycogen to glucose-1-phosphate to facilitate heightened glucose demands during reperfusion compared to lean livers. The downregulation of ALDOA (an enzyme responsible for the conversion of fructose-1,6-bisphosphate to glyceraldehyde-3-phosphate and dihydroxyacetone phosphate) suggests a compensatory mechanism in response to increased glycogenolysis. Blue halo represents upregulation and red halo represents downregulation of protein.

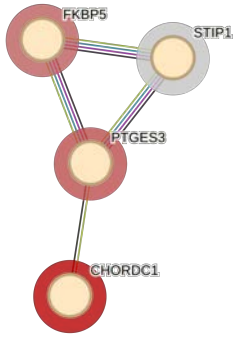

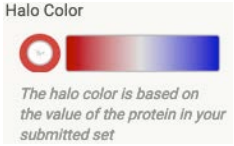

Biological Process (Gene Ontology)

GO-term	description	count in network	strength	false discovery rate
GO:0061077	Chaperone-mediated protein folding	3 of 71	2.32	0.0016
GO:0006457	Protein folding	4 of 215	1.96	0.00023

Molecular Function (Gene Ontology)

GO-term	description	count in network	strength	false discovery rate
GO:0051879	Hsp90 protein binding	3 of 45	2.52	0.00013
GO:0031072	Heat shock protein binding	4 of 126	2.19	8.92e-06

Figure 5.20. Cluster analysis of protein folding and heat shock protein (HSP) binding processes during reperfusion (LT3) in steatotic vs. lean donor preserved with NMP: The downregulation of STIP1, FKBP5 (FK506 Binding Protein 5), PTGES3 and CHORDC1 indicate adaptations in cellular stress response, protein folding mechanisms, and inflammation pathways. STIP1 (co-chaperone interacting with HSP70 and HSP90) facilitates protein folding and stabilisation of protein complexes under stress. Downregulation indicates a reduced capacity for managing misfolded proteins in steatotic livers, potentially affecting cellular homeostasis. Downregulation of FKBP5 (involved in the regulation of glucocorticoid receptor sensitivity) indicates reduced hepatic response to hormonal stimuli and to immunosuppressive therapy i.e. FK506 (Tacrolimus). PTGES3 (involved in steroid hormone receptor activity and protein folding) downregulation indicates alterations in steroid metabolism and reduction in anti-inflammatory gene expression. CHORDC1 (protection against stress-induced apoptosis) downregulation indicates an increase in hepatic apoptosis during reperfusion of steatotic livers compared to lean livers. Blue halo represents upregulation and red halo represents downregulation of protein.

5.3.6 Effect of SCS on reperfusion proteomes in steatotic vs. lean donor livers

60 significant ($P < 0.05$) DEPs were identified at reperfusion (LT3) in steatotic livers compared to lean livers preserved with SCS. 48 were upregulated and 12 were downregulated. The top 25 most upregulated and all 12 downregulated DEPs are demonstrated in Figure 5.21. Of these, the 5 most clinically relevant upregulated (functions related to lipoprotein receptors, hydrolysis of acyl-CoAs, platelet aggregation, respiratory chain and DNA repair) and downregulated DEPs (functions related to metabolism of pteridines, elimination of toxic compounds, N-linked glycosylation, cholesterol biosynthesis and maintenance of sodium (Na^+)/potassium (K^+) gradient across the cell membrane) are described in Table 5.7.

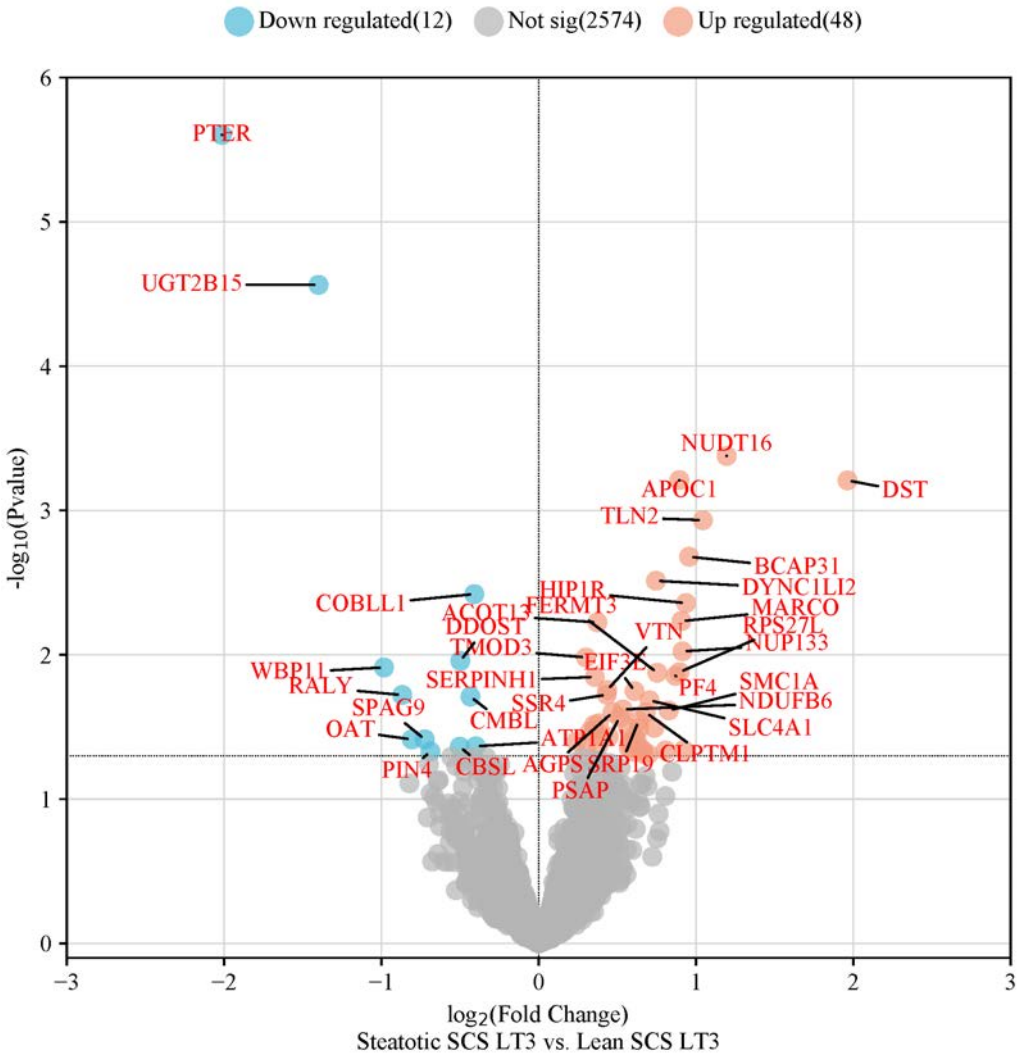

Figure 5.21. The effect of SCS on proteomes at reperfusion (LT3) in steatotic livers compared to lean donor livers. Top 25 upregulated and all 12 downregulated proteins are labelled in the plot.

Table 5.7. Clinically relevant upregulated (n = 5) and downregulated proteins (n = 5).

Upregulated			
Protein name	Function	Fold change	*P* - value
APOC1	Truncated apolipoprotein C-I: Inhibits binding of lipoproteins to low density lipoprotein (LDL) receptor, LDL receptor-related protein and very low-density lipoprotein (VLDL) receptor and inhibits uptake of fatty acids.	0.894	0.001
ACOT13	Acyl-coenzyme A thioesterase 13, N-terminally processed: Acyl-CoA thioesterases constitute an enzyme group responsible for catalysing the conversion of acyl-CoAs into free fatty acids and coenzyme A (CoASH). This enzymatic activity presents a mechanism to control the internal concentrations of acyl-CoAs, free fatty acids and CoASH.	0.373	0.006
PF4	Platelet factor 4, short form: Released during the aggregation of platelets, PF4 counteracts the anticoagulant properties of heparin due to its higher affinity for binding to heparin over the chondroitin-4-sulfate chains found in the carrier molecule. It exhibits chemotactic properties for both neutrophils and monocytes.	0.869	0.014
NDUFB6	NADH dehydrogenase [ubiquinone] 1 beta subcomplex subunit 6: Accessory subunit of the mitochondrial membrane respiratory chain NADH dehydrogenase, also known as Complex I (role not directly related to the catalytic process).	0.534	0.024
SMC1A	Structural maintenance of chromosomes protein 1A: Maintains chromosome cohesion throughout the cell cycle and is actively involved in DNA repair mechanisms.	0.826	0.024
Downregulated			
Protein name	Function	Fold change	*P* - value
PTER	Phosphotriesterase-related protein: Part of the phosphotriesterase family (and metallo-dependent hydrolases superfamily). Function characterised by dependence on metal ions for catalytic activity. The specific function of PTER involves the hydrolysis of phosphotriesters.	-2.014	0.000
UGT2B15	UDP-glucuronosyltransferase 2B15: Role in the conjugation and removal of toxic exogenous substances (xenobiotics) and endogenous compounds.	-1.400	0.000
DDOST	Dolichyl-diphosphooligosaccharide--protein glycosyltransferase 48 kDa subunit: Component of the N-oligosaccharyl transferase (OST) complex. DDOST catalyses the transfer of a high mannose oligosaccharide from a lipid-linked oligosaccharide donor to the asparagine residue found in the Asn-X-Ser/Thr consensus motif in nascent polypeptide chains.	-0.498	0.011
RALY	RNA-binding protein Raly; Functions as a transcriptional co-regulator for genes involved in cholesterol synthesis within the liver.	-0.868	0.019
ATP1A1	Sodium/potassium-transporting ATPase subunit alpha-1: Catalytic unit responsible for driving the hydrolysis of ATP in conjunction with the exchange of sodium and potassium ions across the plasma membrane.	-0.401	0.043

Protein-protein interaction (PPI) of statistically significant ($P < 0.05$) DEPs was performed using STRING® (version 12.0) online database for PPI maps, bio-informatic and Gene Ontology (GO). As only 60 DEPs were identified, MCL cluster analysis of pathways was not performed. Instead, general network analysis is demonstrated in Figure 5.22.

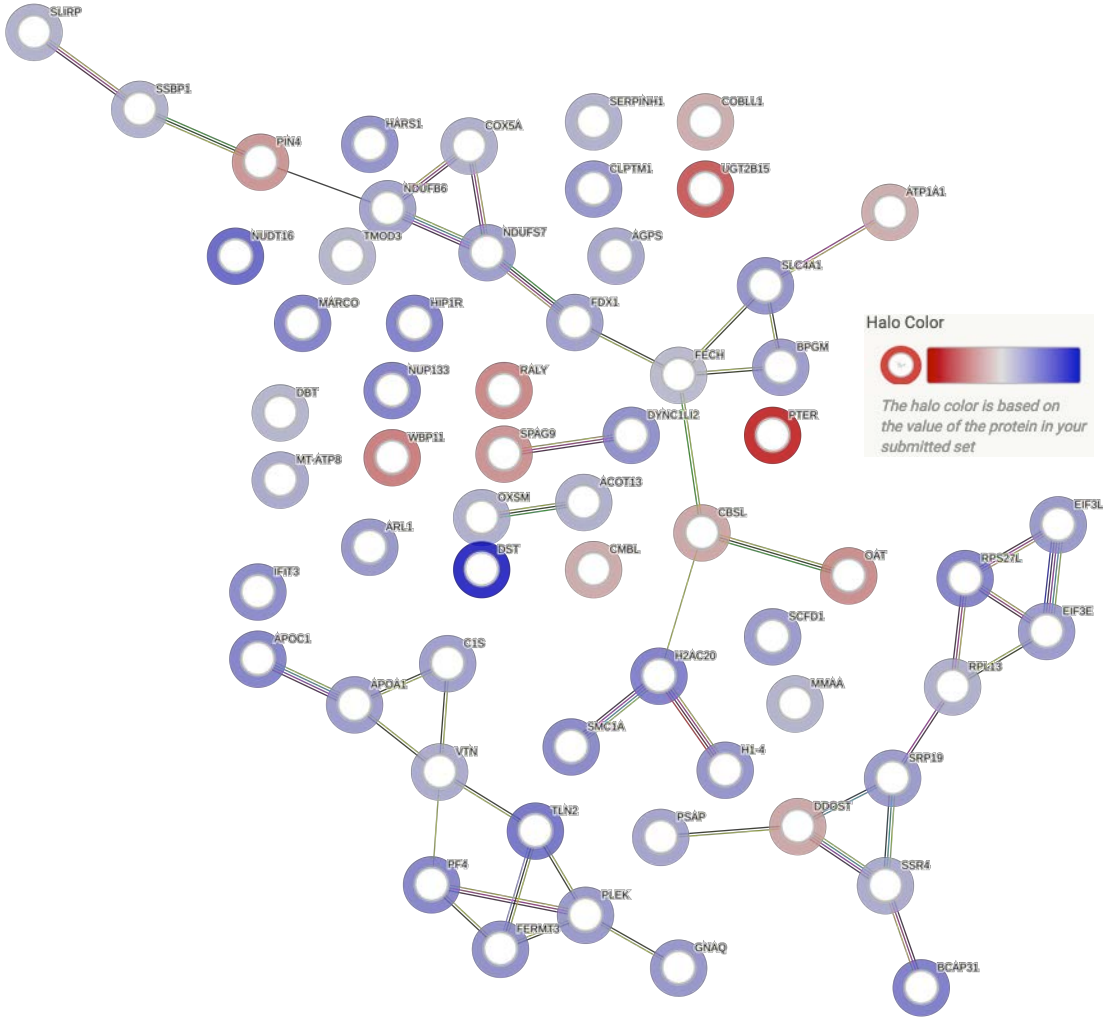

	Molecular Function (Gene Ontology)			
GO-term	description	count in network	strength	false discovery rate
GO:0042803	Protein homodimerization activity	11 of 709	0.71	0.0231
GO:0046983	Protein dimerization activity	14 of 1094	0.62	0.0212

	Cellular Component (Gene Ontology)			
GO-term	description	count in network	strength	false discovery rate
GO:0005759	Mitochondrial matrix	9 of 494	0.78	0.0146
GO:0005739	Mitochondrion	19 of 1681	0.57	0.00070
GO:0031982	Vesicle	25 of 3957	0.32	0.0397
GO:0005737	Cytoplasm	52 of 12056	0.15	0.0146
GO:0043227	Membrane-bounded organelle	54 of 13188	0.13	0.0146
GO:0043226	Organelle	56 of 14017	0.12	0.0146

Figure 5.22. The effect of SCS on proteomic signature at reperfusion (LT3) in steatotic livers compared to lean donor livers. Network analysis of upregulated and downregulated proteins during: Upregulated DEPs including APOC1 and ACOT13, NDUFB6 and MT-ATP8, SMC1A indicate adaptations in lipoprotein transport, mitochondrial activity and genetic stability, respectively. In addition, the upregulation of PF4 (a chemotactic cytokine released by platelets) indicates a pro-thrombotic state and MACRO (scavenger receptor) has an important role in innate immune defence and inflammatory response. Similarly, FERMT3 and SERPINH1 (involved in cellular adhesion and the extracellular matrix) indicate an amplified inflammatory response and tissue remodelling during reperfusion of steatotic livers compared to lean controls. Conversely, the downregulation of PTER and UGT2B15 (essential for detoxification processes) DDOST (involved in N-glycosylation), RALY (associated with RNA processing) and ATP1A1 (essential for maintaining ion gradients) indicate adaptions in various metabolic processes, including detoxification, protein glycosylation, and ion homeostasis. These expression changes reflect the disruption in functional integrity and cellular homeostasis during reperfusion of steatotic livers. Blue halo represents upregulation and red halo represents downregulation of protein.

5.3.7 Effect of preservation technique and steatosis on reperfusion liver biopsy proteomes

Statistically significant DEPs ($P < 0.05$) were compared between two groups to identify differences in proteomic signatures during reperfusion in the recipient (LT3) according to preservation strategy. A total of 212 unique DEPs were identified at reperfusion in steatotic livers preserved with NMP vs. lean livers (Group 1) and 57 unique DEPs were observed in steaotic livers preserved with SCS vs. lean livers (Group 2), 3 DEPs were common between the groups (see Figure 5.2). The change in proteomes within each of these groups is described in sections 5.3.5 and 5.3.6 respectively:

- Group 1: Steatotic NMP LT3 vs. Lean NMP LT3
- Group 2: Steatotic SCS LT3 vs. Lean SCS LT3

Over-representation analyses of gene ontology (GO) terms, including the cellular components, biological process and pathway, molecular function, and enriched pathway analysis was performed using FunRich; Functional Enrichment Analysis Tool (www.funrich.org). A comparison of Group 1 and Group 2 demonstrating the effect of preservation technique and steatosis during reperfusion is demonstrated in Figure 5.23.

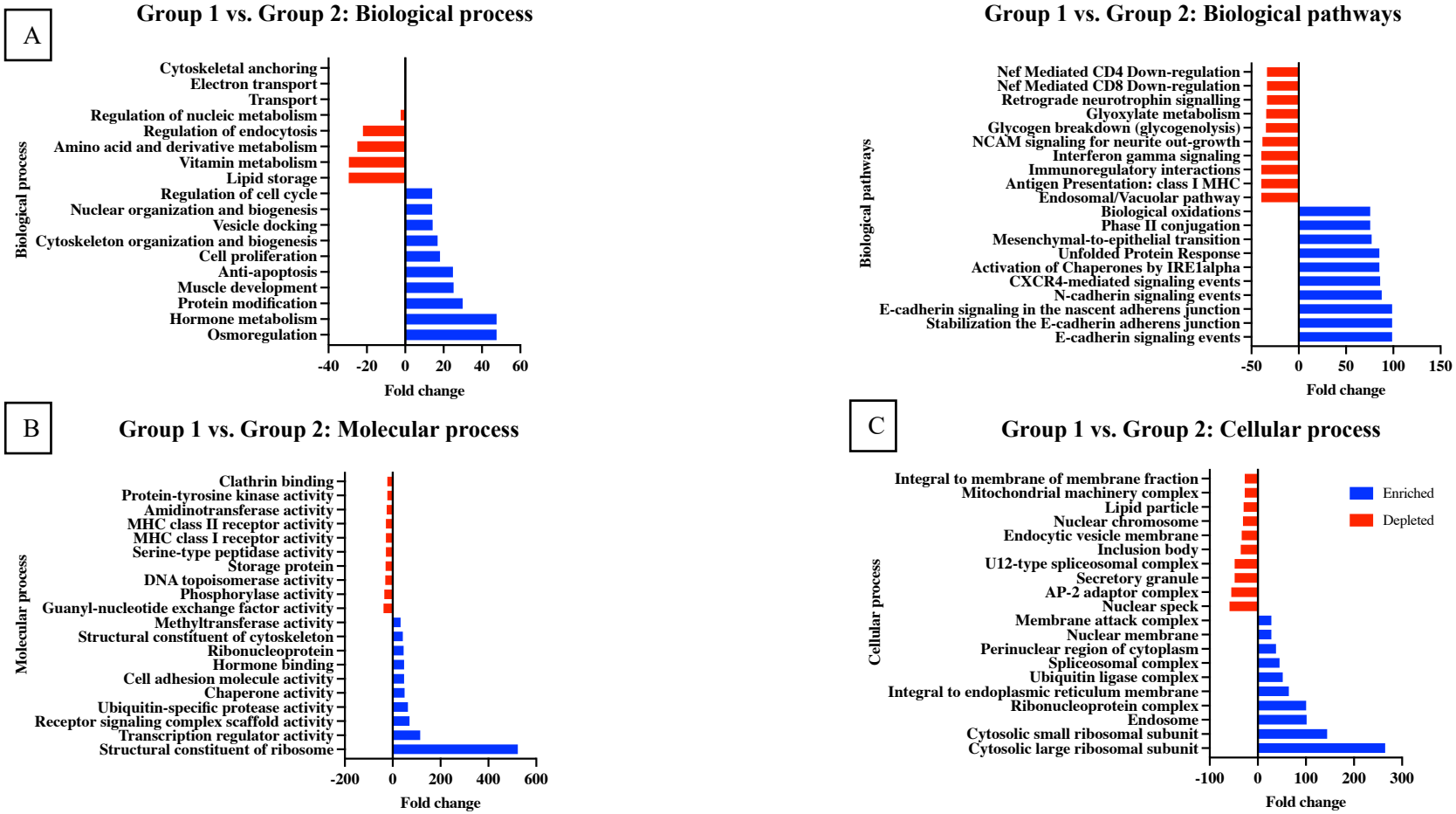

Figure 5.23A-C. The effect of preservation technique and steatosis on reperfusion (LT3) liver biopsy proteome. Significant alterations in biological processes, biological pathways, molecular and cellular components were observed between **Group 1 (Steatotic NMP LT3 vs. Lean NMP LT3)** and **Group 2 (Steatotic SCS LT3 vs. Lean SCS LT3)**. Biological processes and pathways upregulated included those related to protein modification, cell proliferation, cytoskeletal organisation, protein folding/organisation and anti-apoptotic pathways with downregulation of lipid storage, glycogenolysis and immunoregulatory pathways **(A)**. Molecular pathways upregulated included those related to ribosomal stability and chaperone activity with downregulation of MHC Class I and II activity **(B)**. Similarly, cellular pathways upregulated included those related ribosomal and spliceosomal complex, membrane attack complex with downregulation of secretory granules, nuclear chromosome components and mitochondrial machinery complex activity **(C)**.

5.4 Discussion

This chapter investigated the impact of preservation techniques, specifically continuous normothermic machine perfusion (cNMP) and static cold storage (SCS), on the proteomic profiles of steatotic donor livers compared to lean counterparts intended for transplantation. Both cNMP and SCS preservation methods induced significant and progressive alterations in the proteomic profiles of donor livers during the preservation and reperfusion phases. Understanding these proteomic changes is critical for optimising graft outcomes and expanding the donor pool, particularly by enabling the safe utilisation of steatotic livers in transplantation.

Despite increasing integration of NMP into clinical practice, machine perfusion (MP) technologies still represent a relatively new avenue of organ preservation. Consequently, the limited availability of samples and tissue has led to a lack of 'omics' studies related to MP. A systematic review by Lopez et al. on proteomics research in liver transplantation found that none of the included studies examined machine-perfused organs (313). Out of the 12 studies involving human samples, only two analysed liver tissue (316,317). Since this review, two key studies have emerged, focusing on proteomic analysis in liver normothermic machine perfusion (NMP).

The first study, conducted by Laing et al., analysed the proteomic profile of discarded human livers undergoing NMP. The study specifically looked at the effect of administering multipotent adult progenitor cells (MAPC®) to six livers deemed unsuitable for transplantation. These cells were introduced through the portal vein or hepatic artery and their localisation was tracked using immunofluorescence to assess subsequent engraftment. Proteomic analysis of the perfusate aimed to identify proteins related to MAPC® post-therapy, supporting the hypothesis that these cells were modulating the graft. The study identified several unique proteins, such as IL6, ICAM1, TIMP-1, and STIP1, in the treatment group, which were attributed to the introduced cells. However, due to the small sample size, heterogeneity of discarded livers and focus on perfusate (rather than liver tissue) the study did not provide clinically significant insights into the proteomic environment within the graft during NMP (318).

The second study by Ohman et al. performed a comprehensive multi-omics analysis on 12 discarded human livers perfused using NMP. This study compared molecular signatures between livers with adequate and inadequate function (based on predetermined functional criteria). The authors demonstrated that livers with adequate function showed prominent processes of innate immune activation, along with repair mechanisms and autophagy. Conversely, in livers with inadequate function, there was a significant delay in the emergence of proteins related to cellular repair and autophagy. This suggests a correlation between specific molecular processes and the varying outcomes observed during NMP (198).

To date, no human clinical studies have investigated the tissue proteomic profile of steatotic human livers preserved with continuous NMP (cNMP) that have resulted in transplantation. Therefore, the study described within this chapter includes a large cohort of unique samples that have not been previously reported in the literature and represent a clinically relevant group of steatotic livers. Through analysis of the protein expression profiles of cNMP preserved steatotic livers that were successfully transplanted, this chapter provides valuable insights into how NMP affects grafts in a clinical context and serves as an important reference for future studies.

5.4.1 Steatotic livers preserved with continuous NMP (cNMP)

MCL cluster analysis revealed two main clusters (identified by their modularity i.e. more densely connected internally than with the rest of the network and clear separation from other clusters) involving mitochondrial pathways as well as lipid metabolism, coagulation and immune responses. Upregulated mitochondrial proteins (e.g., COX7A2, NDUFA13) enhance respiratory capacity, while downregulated proteins (e.g., ATP5PB, NDUFS1) may reflect a shift in ATP synthesis efficiency or a cellular stress response. In lipid metabolism, the upregulation of GOLM1, coupled with downregulation of lipid transporters like APOC4 and APOB, suggests significant alterations in lipid homeostasis. In addition, the upregulation of ICAM1 and F2 (prothrombin) indicate an inflammatory and hypercoagulable state in steatotic livers preserved with NMP. The down regulation of C3 (complement component 3) suggests a dampened immune response in steatotic livers preserved with NMP.

Among the upregulated DEPs, several proteins of significant clinical relevance (based on biological function) were identified. The upregulation of proteins involved in oxidative phosphorylation (e.g., COX7A2L, NDUFB4) (319,320) suggests enhanced mitochondrial respiratory capacity during cNMP. These proteins are essential for oxidative phosphorylation, which is critical for maintaining energy metabolism in the liver during NMP. These changes suggest that cNMP of steatotic livers may confer protection against mitochondrial dysfunction and oxidative stress in the clinical setting of liver transplantation (321). These findings also align with that of Raigani et al. who performed metabolomic and lipidomic profiling on 8 discarded human livers (steatotic, n = 5 vs. non-steatotic, n = 3) preserved with NMP. The authors demonstrated both steatotic and non-steatotic livers were able to regenerate ATP and maintain similar energy charge ratios, despite clear signs of metabolic deficiencies (322). However, the downregulation of ATP5PB and NDUFS1 (323,324) in steatotic livers preserved with cNMP described within the current chapter suggest a metabolic shift in response to cellular stress that can potentially alter ATP synthesis efficiency suggesting a only a partial resuscitative effect of NMP on steatotic livers.

The upregulation of Intercellular Adhesion Molecule 1 (ICAM1) suggests an increase in leukocyte adhesion, which may play a role in mediating the innate immune responses during perfusion and pro-inflammatory response following ex-situ reperfusion during NMP (325,326). However, the upregulation of HMOX1 and SQSTM1 indicates an enhanced cytoprotective response in steatotic livers preserved with NMP. HMOX1 plays a role in protecting cells from oxidative stress by degrading free heme (327), while SQSTM1 confers protection against lipotoxicity and is involved in autophagy (facilitating the removal damaged cellular components) (328). These results are similar to that reported by Ohman et al. (see above) who demonstrated initial upregulation of innate immune response followed by the activation of autophagy and mechanisms that promote cell survival in adequately functioning discarded human livers preserved with NMP (198). However, the study by Ohman et al. included a small heterogenous cohort of marginal DCD human livers declined for transplantation. In addition, none of the livers actually had steatosis (ld-MaS of >5%) and the livers were all subjected to a varying degree of cold ischaemia with preservation using NMP in a back-to-base approach (pSCS-NMP) (198). It is therefore difficult to draw meaningful conclusions or comparisons when compared to steatotic livers preserved with cNMP described within this chapter.

In addition, the upregulation of F2 (prothrombin) during cNMP of steatotic donor livers was an important finding. Prothrombin (F2) is primarily known for its role in the coagulation cascade, where it is converted into thrombin, a key enzyme in blood clotting. Literature indicates that steatosis is independently linked to endothelial dysfunction with a chronic proinflammatory state that can result in thrombosis. This heightened risk may result from disruptions in multiple aspects of the haemostatic process, including endothelial and platelet dysfunction, alterations in the coagulation cascade, reduced fibrinolytic activity, or a combination of these factors (316,317). In the context of machine perfusion, elevated thrombin generation during perfusion could potentially worsen microcirculatory disturbances in the liver, leading to increased ischaemic injury and biliary complications. This is particularly concerning in steatotic livers, which are already more susceptible to such injuries due to their impaired microcirculation and higher metabolic demands. Recently, Watson et al. reported the impact of fibrin deposits in deceased donor livers undergoing NMP and evaluated the potential role of fibrinolysis during ex-situ liver perfusion. D-dimer levels, indicative of fibrin degradation, were measured in the perfusate of 163 livers after 2 hours of perfusion, including 91 that were subsequently transplanted. The authors demonstrated that D-dimer levels were lowest in livers recovered using in situ normothermic regional perfusion (NRP) and highest in those treated with alteplase, a fibrinolytic agent. A significant correlation was observed between D-dimer levels and cold ischemia duration in livers from DBD donors. Elevated D-dimer levels were associated with reduced transplant survival in non-alteplase-treated livers. Importantly, fibrinolytic treatment with alteplase during NMP resulted in increased D-dimer release, indicating a significant fibrin burden, and was linked to positive transplant outcomes, with 8 out of 9 treated livers remaining free from cholangiopathy (329).These findings suggest that fibrinolytic therapy during NMP could be a valuable strategy to improve transplant outcomes of steatotic donor livers, however, this remains to be investigated.

The downregulation of APOB and APOC4, which are involved in lipid transport, suggests alterations in lipid homeostasis during cNMP. APOB is crucial for the formation and secretion of very low-density lipoproteins (VLDL) in the liver, which are responsible for exporting triglycerides from hepatocytes. When the production or secretion of APOB is disrupted, triglycerides can accumulate within the liver, leading to the development of hepatic steatosis. Anson et al. demonstrated that siRNA-mediated knockdown of ApoB led to elevated hepatic triglycerides and liver steatosis in mice, highlighting the importance of APOB in maintaining

lipid homeostasis and preventing fatty liver disease (330). APOC4 is a relatively underexplored member of the APOC family. Although the APOC4 gene was identified and characterised nearly 25 years ago, it has received limited research focus, possibly due to its plasma concentrations being significantly lower than those of APOC1, APOC2, and APOC3. Like other APOCs, APOC4 is associated with circulating triglyceride-rich lipoproteins (TRLs) and high-density lipoproteins (HDL) (331). There is evidence to suggest that endogenous APOC4 may contribute to increased plasma triglyceride levels. Studies have shown that overexpression of human APOC4 in mice, at levels beyond the normal physiological range, lead to elevated very low-density lipoprotein (VLDL) levels, indicating a potential role in lipid metabolism regulation (332). These findings suggest a metabolic shift that prioritises energy production over lipid storage/haemostasis during NMP of steatotic livers.

The down regulation of Complement component 3 (C3) during cNMP of steatotic donor livers represents an important finding. The complement system is essential in initiating the innate inflammatory response, facilitating both cell-mediated and antibody-mediated defences against pathogens. It also plays a crucial role in sterile tissue injury by responding to damage-associated molecular patterns (DAMPs). The extent and persistence of complement activation are key factors in determining whether inflammation leads to tissue regeneration or destruction after sterile injury. Studies in kidney transplantation have highlighted the significance of complement activation in delayed graft function, a finding supported by rodent models of renal ischemia-reperfusion injury. In the context of liver transplantation, particularly with donor livers exhibiting moderate steatosis, targeting the complement cascade (specifically anaphylatoxins like C3a and C5a) could be a promising strategy to mitigate reperfusion injury and improve graft outcomes. Steatotic livers, burdened by excess lipids, may experience amplified stress responses and increased hepatocyte turnover, further exacerbating complement activation. This activation could contribute to complications such as rejection and thrombosis post-transplantation (333). The results within this chapter therefore highlight the potential of NMP in mitigating complement activation in steatotic donor livers as well as providing a platform for pharmacological modulation of the complement system.

5.4.2 Steatotic livers preserved with SCS

During SCS of steatotic donor livers, there was an upregulation in proteins involved in fatty acid β-oxidation (e.g., ACAD11, ACSF2) (334,335) indicating an increased reliance on fatty

acid metabolism for energy production during SCS. The downregulation of PRKAG1, a key regulator of AMP-activated protein kinase (AMPK), suggests a reduced capacity to respond to cellular stress during SCS. Zaouali et al. investigated the role pharmacological AMPK modulation on autophagy and endoplasmic reticulum (ER) stress in steatotic livers. The addition of melatonin and trimetazidine to the IGL-1 cold preservation solution resulted in enhanced AMPK activation with a reduction in ER stress and enhanced autophagy in livers procured from zucker rats, with improved liver function following ex-situ normothermic reperfusion (336).

Succinate dehydrogenase (SDH), also known as Complex II in the mitochondrial electron transport chain, plays an important role in cellular metabolism. SDH catalyses the oxidation of succinate to fumarate in the tricarboxylic acid (TCA) cycle. This reaction is crucial for the continued production of energy-rich molecules like NADH and FADH2, which are used in the electron transport chain to generate ATP (337). The downregulation of SDHAF2 during the SCS of steatotic livers can impair the proper assembly and function of the succinate dehydrogenase (SDH) complex, resulting in a diminished mitochondrial respiratory capacity and reduced SDH activity. This impairment of the tricarboxylic acid (TCA) cycle decreases ATP production due to disrupted oxidation of succinate to fumarate. The resulting mitochondrial dysfunction exacerbates oxidative stress and energy deficits in steatotic livers, increasing their sensitivity to the process of ischemia-reperfusion injury (IRI) during transplantation.

5.4.3 Lean livers preserved with NMP

MCL cluster analysis revealed four main clusters (identified by their modularity i.e. more densely connected internally than with the rest of the network and clear separation from other clusters) involving ribosomal, anti-inflammatory, mitochondrial and lipid metabolism pathways. The upregulation of ribosomal proteins and mitochondrial components indicates increased protein synthesis and enhanced mitochondrial function, which are essential for energy production and cellular repair during NMP. The modulation of anti-inflammatory and lipid metabolism pathways highlight the metabolic shift to balance energy production, mitigate inflammation and thrombosis, and prevent lipid accumulation, all of which are crucial for maintaining liver function during preservation.

Among the upregulated DEPs, several proteins of significant clinical relevance (based on biological function) were identified, including ICAM1, HMOX1, HLA-C, PSMD4, and SQSTM1. The upregulation of ICAM1 (Intercellular Adhesion Molecule 1) is particularly notable, as it plays a critical role in leukocyte adhesion and trans-endothelial migration. The upregulation of ICAM-1 in both steatotic livers and lean livers preserved during NMP suggests a pro-inflammatory response following ex-situ reperfusion during NMP (325) and monitoring ICAM1 during NMP could be a valuable marker of recovery from (or worsening injury) (326). In addition, similar to steatotic livers preserved with NMP, the upregulation of HMOX1 was evident in lean livers preserved with NMP, thereby confirming the cytoprotective effects of NMP during preservation (338).

Late allograft dysfunction remains a critical issue in liver transplantation, with its underlying mechanisms not fully understood. HLA-C serves as the primary inhibitory ligand for killer immunoglobulin-like receptors (KIRs), which regulate the cytotoxic function of natural killer (NK) cells. HLA-C alleles are categorised into HLA-C1 and HLA-C2 groups, with HLA-C2 providing stronger inhibition of NK cell activation. The upregulation of HLA-C in lean livers preserved with cNMP is an important finding as it highlights potential for immunoregulation/altering the immunogenicity of the liver graft during preservation. Furthermore, Hanvesakul et al. performed a large cohort study of liver transplant recipients, and demonstrated that donor allografts carrying at least one HLA-C2 allele showed significantly reduced histological signs of chronic rejection and graft cirrhosis, along with a 16.2% decrease in graft loss (p = 0.003) (hazard ratio: 2.7, 95% CI 1.4-5.3) and a 13.6% improvement in patient survival (p = 0.01) (hazard ratio: 1.9, 95% CI 1.1-3.3) over 10 years. Notably, transplantation of HLA-C2 homozygous allografts led to a 26.5% reduction in graft loss ($p < 0.001$) (hazard ratio: 7.2, 95% CI 2.2-23.0) compared to HLA-C1 homozygous allografts. These findings underscore the pivotal role of donor HLA-C genotype in liver transplantation outcomes, highlighting the influence of NK cells in chronic rejection. Targeting HLA-C and KIR interactions may offer a promising strategy to enhance long-term graft and patient survival (339).

The increase in PSMD4 (a subunit of the 26S proteasome) and SQSTM1 further supports the idea that NMP promotes cellular homeostasis and autophagy, essential for removing damaged proteins and maintaining cellular integrity during the stress of preservation (198) as also

demonstrated in steatotic livers preserved with NMP which demonstrated an upregulation of SQSTM.

Conversely, the downregulation of proteins such as C3, ACOX1, CYP2E1, APOB, and ACSL5 provides insights into altered metabolic and immune functions during NMP. Similar to steatotic livers preserved with NMP, the downregulation of C3 in lean livers preserved with cNMP indicates a reduction in immune activation, which could be a protective mechanism against excessive inflammation that might otherwise contribute to tissue damage following transplantation (333). The downregulation of ACOX1, ACSL5 and APOB points to altered lipid haemostasis during cNMP of lean donor livers. ACOX1 is a key enzyme in the peroxisomal β-oxidation of fatty acids, and its downregulation suggests a shift away from the catabolism of fatty acids during NMP. This reduction in fatty acid oxidation might be a protective response to prevent the accumulation of reactive oxygen species (ROS) that are typically generated during β-oxidation, thereby minimising oxidative damage to the liver graft (340,341). Recently. Lu et al. demonstrated that ACOX1-mediated β-oxidation in the liver significantly influences inter-organ communication, thereby regulating metabolic homeostasis. Mice with a liver-specific knockout of ACOX1 (Acox1-LKO) exhibited resistance to diet-induced obesity, reduced adipose tissue inflammation and improved systemic insulin sensitivity. These findings position hepatic peroxisomal β-oxidation as a crucial regulator of systemic metabolic balance and suggest that modulation of ACOX1 activity or its substrates could serve as a therapeutic approach for obesity-associated metabolic disorders. ACSL5 is an enzyme critical for the activation of long-chain fatty acids, facilitating their conversion into acyl-CoA, which is essential for lipid metabolism, including both synthesis and β-oxidation of fatty acids. The reduction in ACSL5 and APOB expression during cNMP suggests a metabolic shift in the liver, where there is decreased reliance on the utilisation and breakdown of fatty acids for energy production in lean livers preserved with NMP (330,342)

The downregulation of CYP2E1 points to a decrease in and cytochrome P450 activity. In vitro research indicates that cytochrome P450 enzyme activity can be impacted by hepatic ischemia-reperfusion (IR) injury. Shaik et al. explored how one hour of partial ischaemia, followed by either 3 hours (IR3) or 24 hours (IR24) of reperfusion, affects the metabolism of chlorzoxazone (CZX) and its CYP2E1-mediated metabolite, 6-hydroxychlorzoxazone (HCZX), in rats. After 3 hours of reperfusion, there was a 30% reduction in CZX clearance, though HCZX levels in

plasma were unaffected. However, isolated perfused rat liver (IPRL) experiments showed that IR3 also led to a 70% reduction in HCZX biliary clearance. Microsomal analysis found a 50% decrease in HCZX formation due to reduced enzyme activity, despite no change in CYP2E1 protein levels. This reduction was linked to a 30% decrease in cytochrome P450 reductase activity. After 24 hours of reperfusion, no significant changes were observed in the metabolism of CZX or HCZX. This suggests that metabolism of xenobiotics and endogenous compounds that are substrates for CYP2E1 could be temporarily impaired following surgical procedures that interrupt liver blood flow (343). Whilst this reduction was evident in livers preserved with cNMP, it may be further downregulated with a back-to-base approach (pSCS-NMP, where there is a longer cessation in blood supply) with potential implications on drug metabolism.

5.4.4 Lean livers preserved with SCS

STRING® network analysis provided insights into the complex interactions and pathways affected during SCS of lean livers. The upregulated proteins, such as ATP5F1A, NDUFA12, MMUT, HMOX1, and ACAA2, indicate increased mitochondrial activity, protein synthesis and metabolic homeostasis, suggesting an adaptive response to maintain energy production and cellular integrity during SCS. On the other hand, downregulated proteins like MARCKS, MACROD1, and NUTF2 indicate alterations in signalling pathways and cytoskeletal dynamics, potentially conferring hepatocellular protection to minimise injury during SCS.

Among the upregulated DEPs, several proteins of significant clinical relevance (based on biological function) were identified. The upregulated proteins identified during SCS are primarily involved in critical metabolic processes such as ATP synthesis, NADH dehydrogenase activity, amino acid/lipid degradation, cytoprotection, and fatty acid β-oxidation. These processes are essential for maintaining cellular energy balance and protecting hepatocytes from ischaemic injury during storage.

ATP5F1A is involved in ATP production through oxidative phosphorylation (344). Its upregulation suggests an increased demand for ATP synthesis to maintain cellular homeostasis during the stress of cold storage. NDUFA12 is part of Complex I of the mitochondrial respiratory chain, which is crucial for electron transport and ATP generation. The upregulation of NDUFA12 reflects a heightened mitochondrial activity, possibly as a compensatory mechanism to meet energy demands under the ischaemic conditions of SCS (345). ACAA2

participates in the final step of fatty acid β-oxidation. The acetyl-CoA generated by ACAA2 is then utilised in the tricarboxylic acid (TCA) cycle, contributing to ATP production, or directed towards ketogenesis, especially during periods of low glucose availability. The role of ACAA2 role in fatty acid metabolism is critical for energy production in the liver, particularly during fasting or metabolic stress when the ability to oxidise fatty acids becomes essential for maintaining energy balance (for example in the context of static cold storage, SCS) (346).

MMUT is involved in the breakdown of amino acids and odd-chain fatty acids, indicating increased metabolic activity during SCS to prevent the accumulation of toxic intermediates. This role of MMUT is particularly important during periods of fasting or metabolic stress when the liver needs to efficiently convert stored fats and proteins into energy. Moreover, MMUT helps prevent the accumulation of methylmalonic acid, which can be toxic to cells if it accumulates at high levels (347,348). HMOX1 (Heme oxygenase 1) provides cytoprotection and its upregulation highlights the response to oxidative stress during cold storage (as also observed in steatotic preserved with SCS) (349).

Conversely, the downregulated proteins are involved in pathways such as protein kinase-C activity, nuclear transport, mTORC1 activation and inflammatory cytokine activity. These reductions suggest a potential decrease in signalling pathways, cellular transport, and inflammatory responses during cold storage, which might be a protective mechanism against cold storage-induced injury.

MARCKS is a key protein involved in the regulation of cellular processes such as signal transduction, cell motility and cytoskeletal dynamics. It is one of the major substrates of protein kinase C (PKC), which phosphorylates MARCKS in response to various extracellular signals. MARCKS plays a significant role in modulating actin cytoskeleton dynamics, which is crucial for maintaining the structural integrity of cells and their response to environmental stress (350). During SCS of lean livers, the downregulation of MARCKS indicates a potential reduction in PKC-mediated signalling pathways and cytoskeletal remodelling. This downregulation may be a protective response to minimise cellular stress and prevent over-activation of signalling pathways that could lead to cytoskeletal instability during SCS.

MACROD1 is implicated in the removal of ADP-ribose from proteins, a process important for DNA repair and stress responses (351). Decreased levels of MACROD1 indicate reduced DNA

repair activity during SCS. NUTF2 has an important role in nucleocytoplasmic transport (352). Downregulation of NUTF2 during SCS could be related to energy conservation (and reduced cellular metabolism) during SCS.

LAMTOR5 is involved in mTORC1 signalling, which regulates cell growth in response to nutrient availability (353). During SCS of lean livers, a reduction in LAMTOR5 could be related to a suppression of mTORC1 signalling, likely as a response to the anaerobic and nutrient-deprived conditions characteristic of SCS. The downregulation of LAMTOR5 indicates a metabolic shift from growth and anabolic processes to energy conservation in order to enhance cell survival during SCS.

5.4.5 Reperfusion of steatotic livers preserved with NMP compared to lean donor livers

MCL cluster analysis revealed five main clusters (identified by their modularity i.e. more densely connected internally than with the rest of the network and clear separation from other clusters). These clusters highlight shifts in metabolism, immune response and stress management during reperfusion of steatotic livers preserved with NMP (compared to lean livers) that are critical for determining the success of liver transplantation, particularly in the high-risk category of steatotic donor livers and are described in Table 5.8:

Table 5.8. Reperfusion MCL cluster analysis of steatotic NMP liver vs. lean counterparts

Pathway	**Function**
Ribosomal	The upregulation of specific ribosomal proteins (e.g., RPS27L, RPL10) indicates an increased capacity for protein synthesis and stress response, while the downregulation of others (e.g., RPL15, EIF1) suggests a shift towards energy conservation during reperfusion (354–357).
RNA splicing	The upregulation of RNA helicases like DHX15 indicates enhanced RNA processing activities (358), while downregulation of splicing factors (e.g., SF3B1, HNRNPDL) suggests a reduction in overall RNA splicing efficiency (359,360), possibly impacting gene expression regulation during reperfusion.
Immune cell migration	The upregulation of proteins like DOCK, a key regulator of cytoskeletal dynamics (particularly in the context of cell migration) (361) indicate that steatotic livers actively engage in processes that promote tissue repair and regeneration during reperfusion in the recipient with mobilisation of immune cells to sites of injury. These processes may facilitate the removal of damaged cells and promote hepatocellular regeneration. Conversely, the downregulation of proteins such as CRK and RHOA reflects a complex balancing act during reperfusion. CRK is involved in cell adhesion and growth signalling pathways, while RHOA plays a pivotal role in regulating stress fibre formation and cellular contraction (362,363). The reduced expression of these proteins may indicate a suppression of certain signalling pathways that are usually involved in maintaining cell structure and integrity. This downregulation could lead to decreased cell adhesion and altered signal transduction, potentially compromising the structural integrity of steatotic livers during the stress of reperfusion. The simultaneous upregulation of proteins promoting cell migration and downregulation of those involved in cell adhesion and signalling suggests that while the liver is attempting to repair itself, there may be a trade-off that impacts its overall structural stability. The weakened cell adhesion could make steatotic livers more vulnerable to further hepatocellular injury or impair ability to fully recover from the reperfusion event. This is an important finding especially in steatotic livers where the metabolic and inflammatory burdens are already high.
Glycogen and carbohydrate metabolism	The upregulation of enzymes like ENO3 and PYGL suggests increased glycolytic activity and glycogen breakdown (364,365) which are essential for meeting the energy demands of steatotic livers during reperfusion.
Protein folding and glucocorticoid activity	The downregulation of STIP1 (heat shock protein co-chaperone) indicates a reduced capacity for managing protein misfolding and stress (366,367). This could contribute to cellular dysfunction steatotic livers preserved with NMP following reperfusion. The downregulation of FKBP5 (involved in the regulation of glucocorticoid receptor sensitivity) (368) indicates reduced hepatic response to hormonal stimuli and to immunosuppressive therapy i.e. FK506 (Tacrolimus).

Among the upregulated DEPs, several proteins of significant clinical relevance (based on biological function) were identified. The upregulation of CRAT during reperfusion of steatotic livers preserved with NMP suggests an enhanced capacity for fatty acid β-oxidation (369), which is likely a compensatory response to the excess lipid content in these livers. This metabolic adaptation is crucial for meeting the increased energy demands during reperfusion. The upregulation of HLA-E during reperfusion of steatotic livers preserved with NMP indicate an immunomodulatory effect of NMP. HLA-E is recognised by the CD94/NKG2A receptor on NK cells, which transmits an inhibitory signal that can prevent NK cell-mediated cytotoxicity (370). This may overall contribute to graft tolerance by inhibiting NK cell activity during reperfusion. The upregulation of HSPA6 demonstrate the hepatocellular response to maintain protein homeostasis during injury sustained during reperfusion by promoting the correct folding of proteins and preventing the accumulation of misfolded proteins (371). An important finding was that NMP of steatotic livers results in altered bile metabolism during reperfusion and is characterised by upregulation of BAAT suggesting enhanced bile acid amidation required for bile detoxification processes and maintaining cellular homeostasis (372). In addition, the upregulation of APCS reflects a mechanism for scavenging nuclear debris from damaged cells, which is essential in mitigating inflammation and tissue damage during the critical phase of reperfusion (373).

Conversely, the downregulation of key proteins during reperfusion of steatotic livers indicate only a partial resuscitative effect of NMP in mitigating against IRI compared to lean livers. WFS1 is essential for maintaining calcium homeostasis, when downregulated, leads to increased endoplasmic reticulum stress and a higher likelihood of cell death during reperfusion (374,375). Similarly, the reduced expression CMC1 indicates impaired mitochondrial function, specifically in cytochrome c oxidase assembly, which is essential for energy production and mitigating oxidative stress (376). The downregulation of RPS23 suggests a reduction in protein synthesis (377) as a consequence of IRI. In addition, an important finding was the downregulation of G3BP1. G3BP1 plays a critical role in the formation of stress granules (SGs), which are essential for controlling excessive inflammation and apoptosis triggered by double-stranded RNA. G3BP1 inhibits the entry of p53 into the nucleus, preventing it from binding to the promoter of SLC7A11 thereby reducing hepatocyte ferroptosis during acute liver failure. G3BP1-mediated SGs also protect hepatocytes from apoptosis by inhibiting the hypoxia-inducible factor 1α-endoplasmic reticulum stress pathway. Increased G3BP1 expression correlates with better prognosis in liver failure (378). However, the downregulation

of G3BP1 during reperfusion of steatotic livers preserved with NMP indicate an exacerbated inflammatory response. Furthermore, the downregulation of APEX1 indicates increased sensitivity to oxidative stress during reperfusion with impaired cellular and DNA repair functions (379).

5.4.6 Reperfusion of steatotic livers preserved with SCS compared to lean donor livers

Steatotic livers do not tolerate static cold storage (SCS) and have a heightened sensitivity to the process of IRI (4). Among the upregulated DEPs during reperfusion of steatotic livers preserved with SCS, several proteins of significant clinical relevance (based on biological function) including APOC1, ACOT13, NDUFB6 and PF4 stand out. APOC1, which inhibits lipoprotein binding to receptors such as LDL and VLDL, suggests impaired lipid metabolism and consequent accumulation of intrahepatic triglycerides that could exacerbate hepatocellular injury during reperfusion (380). ACOT13, involved in the hydrolysis of acyl-CoAs, further highlights disruptions in fatty acid metabolism during reperfusion (381). NDUFB6, a subunit of the mitochondrial respiratory chain complex I, indicates mitochondrial response to oxidative stress and energy demands in steatotic livers (compared to lean livers) preserved with SCS (382). PF4, a platelet factor involved in counteracting the anticoagulant properties of heparin which can promote a pro-thrombotic state during reperfusion. The upregulation of PF4 suggests an enhanced risk of thrombosis (383,384) in steatotic livers preserved with SCS. This may exacerbate IRI and complicate post-transplantation outcomes.

Conversely, the downregulated proteins, such as PTER, UGT2B15, and ATP1A1, indicate significant metabolic impairments. PTER, involved in the hydrolysis of phosphotriesters (385), is crucial for detoxification, and its downregulation suggests a reduced capacity to process toxic substances during reperfusion, further aggravating IRI in steatotic compared to lean livers preserved with SCS. UGT2B15, which plays a role in glucuronidation and detoxification (386), further underscores the compromised detoxification processes in steatotic livers preserved with SCS during reperfusion. The reduction in ATP1A1, essential for maintaining ion gradients across the plasma membrane, points to disturbances in ion homeostasis (387), suggest impaired cellular function during reperfusion.

Overall, these proteomic changes indicate that steatotic livers experience more severe metabolic disruptions during reperfusion following SCS than lean livers. The upregulation of

proteins involved in lipid metabolism, mitochondrial function, inflammatory response, and thrombosis, alongside the downregulation of proteins crucial for detoxification and ion homeostasis, highlights the increased sensitivity of steatotic livers to IRI.

5.4.7 Effect of preservation technique and steatosis on reperfusion liver biopsy proteomes

Over-representation analyses of gene ontology (GO) terms demonstrated significant upregulation of biological processes related to protein modification, cell proliferation, cytoskeletal organisation, protein folding, and anti-apoptotic pathways during reperfusion of steatotic livers preserved with NMP. These changes suggest that NMP may help mitigate some of the detrimental effects of steatosis by enhancing cellular repair mechanisms, promoting cell survival, and maintaining cytoskeletal integrity compared to SCS. Moreover, molecular pathways related to ribosomal stability and chaperone activity were also upregulated, indicating an increased need for protein synthesis and proper folding during reperfusion compared to SCS. Conversely, pathways related to lipid storage, glycogenolysis, and immunoregulatory functions were downregulated, which may reflect a shift away from metabolic storage and immune activation towards cellular recovery and stabilisation during reperfusion. However, the downregulation of cellular pathways associated with mitochondrial machinery and secretory granules suggests impaired energy production and diminished secretory functions suggesting that further optimisation, beyond NMP is required to improve outcomes of steatotic donor livers.

5.4.8 Limitations

Several limitations were inherent in this study. The main limitation is the absence of subgroup analysis i.e. DCD (Donation after Circulatory Death) and DBD (Donation after Brain Death), despite their potential biological differences. The duration of normothermic preservation could also have influenced the proteomic profiles of the grafts, with varying levels of protein translation occurring over different preservation times, which may have confounded the results. However, no significant impact of donor type or the length of NMP on the proteomic profiles was identified (when previously explored by our group), therefore supporting the decision not to perform subgroup analysis. The study's relevance is further supported by its focus on a clinically pertinent cohort of livers, using technology consistent with common clinical practice, thereby providing important mechanistic insights into a real-world application. Including a larger cohort of discarded livers, such as those with primary non-function (PNF) or poor

outcomes, could have enhanced the study by allowing for the identification of molecular characteristics linked to graft quality, an area not addressed in this research. However, this study is distinguished by its unbiased observational approach and large sample size, breaks from the more traditional, small-cohort, biomarker-focused proteomics work. Through avoidance of a targeted proteomics approach, which often introduces bias, this research provides a more comprehensive understanding of the proteomic landscape. Unlike previous studies that have relied on easily accessible tissues such as serum, urine, plasma, or perfusate as surrogates for the organ of interest, this work directly accessed graft tissue, offering more accurate insights into the proteomic changes occurring within the liver itself.

5.4.9 Conclusion

This chapter provided a comprehensive analysis of the impact of preservation techniques, specifically continuous normothermic machine perfusion (cNMP) and static cold storage (SCS), on the proteomic profiles of steatotic donor livers compared to their lean counterparts. The findings underscore the significant and progressive alterations in proteomic profiles induced by both cNMP and SCS during the preservation and reperfusion phases, highlighting the critical role of these changes in graft outcomes. Despite the increasing adoption of NMP in clinical practice, the technology remains relatively new, with limited studies focusing on its proteomic effects. The chapter therefore offers valuable insights into how cNMP influences the proteomic environment of steatotic livers, potentially enhancing mitochondrial function, lipid metabolism, and cytoprotective responses while mitigating immune activation and oxidative stress. Moreover, the study identified key differences in the proteomic responses between steatotic and lean livers preserved with cNMP, with steatotic livers exhibiting distinct metabolic challenges during reperfusion. The upregulation of proteins related to lipid metabolism and mitochondrial function in steatotic livers suggests a compensatory mechanism for the heightened metabolic demands during reperfusion. In contrast, SCS preserved steatotic livers demonstrated a greater sensitivity to the process of IRI with dysregulation in lipid metabolism, mitochondrial function, and detoxification processes compared to lean livers. Preservation of steatotic livers with both NMP and SCS resulted in upregulation in pro-thrombotic proteins. Overall, the chapter highlights the potential of cNMP in improving the viability of steatotic donor livers, offering a foundation for future studies aimed at further optimising preservation strategies and expanding the donor pool.

Chapter 6: Defatting of donor transplant livers during normothermic perfusion – a randomised clinical trial: Study protocol for the DeFat study

Liver disease is the third leading cause of premature death in the UK. Transplantation is the only successful treatment for end-stage liver disease but is limited by a shortage of suitable donor organs. As a result, up to 20% of patients on liver transplant waiting lists die before receiving a transplant. A third of donated livers are not judged suitable for transplant, often due to steatosis. Hepatic steatosis, which affects 33% of the UK population, is strongly associated with obesity, an increasing problem in the potential donor pool. We have recently tested defatting interventions during normothermic machine perfusion (NMP) in discarded steatotic human livers that were not transplanted (see Chapter 1, 1.6.3). A combination of therapies including forskolin (NKH477) and L-carnitine to defat liver cells and lipoprotein apheresis filtration were investigated. These interventions resulted in functional improvement during perfusion and reduced the intrahepatocellular triglyceride (IHTG) content. We hypothesise that defatting during NMP will allow more steatotic livers to be transplanted with improved outcomes.

The hypothesis will be tested in a multi-centre randomised clinical trial (the DeFat study), where we will randomly assign 60 livers from donors with a high-risk of hepatic steatosis to either NMP alone or NMP with defatting interventions. We aim to test the safety and feasibility of the defatting intervention, and will explore efficacy by comparing ex-situ and post-reperfusion liver function between the groups. The primary endpoint will be the proportion of livers that achieve predefined functional criteria during perfusion which indicate potential suitability for transplantation. These criteria reflect hepatic metabolism and injury and include: lactate clearance; perfusate pH; glucose metabolism; bile composition; vascular flows; transaminase levels. Clinical secondary endpoints will include: proportion of livers transplanted in the 2 arms, graft function; cell-free DNA (cfDNA) at follow-up visits; patient and graft survival; hospital and ITU stay; evidence of ischemia-reperfusion injury (IRI); non-anastomotic biliary strictures; recurrence of steatosis (determined on MRI at 6 months).

In this first clinical study, the primary objective is to confirm the safety and assess efficacy of the NMP-defatting protocol in steatotic donor livers intended for transplant. The secondary objective is to test the feasibility of the (i) inclusion criteria (false positives & negatives); (ii) delivery of intervention; and; (iii) the study endpoints. These objectives will provide information of likely effect sizes in order to design a subsequent phase III study in the future. The mechanistic studies will be analysed subsequent to the main clinical outcomes. These will be carried out for two broad reasons (i) to identify more sensitive and specific markers of transplantability and; (ii) to understand the process of defatting that leads to a steatotic organ being reconditioned.

This chapter describes the ongoing clinical trial (the DeFat study) outlined above. Whilst no results have been included in this chapter, pertinent sections of the study protocol (v3.3) including the background, rationale, trial design, methods, outcomes (primary, secondary and mechanistic), sample size, recruitment and assignment of the intervention have been replicated verbatim from the study protocol manuscript that I have published as first author, titled: Defatting of donor transplant livers during normothermic perfusion – a randomised clinical trial: Study protocol for the DeFat study. The online link for the full study protocol which includes further information on consent, data collection and management, research sample collection, statistical analysis plan, oversight and monitoring is included in **Appendix C**.

6.1 Background and rationale

Our pre-clinical results in organs retrieved for clinical transplantation but discarded due to steatosis have demonstrated the potential of a novel defatting strategy which forms the basis of the NMP-defatting protocol that is being investigated within the DeFat study (388). Using the commercially-available OrganOx *metra*® device, 18 livers were perfused in the pre-clinical study: 6 using a standard NMP protocol (Group 1); 6 using a circuit including a lipoprotein apheresis filter to remove circulating lipids (Group 2), and 6 using the lipoprotein apheresis filter and pharmacological interventions (Group 3). All livers were perfused over 48 hours.

The first intervention was aimed at reducing the amount of VLDL-TG circulating in the perfusate; these are thought to be pro-inflammatory and might contribute to on-going IHTG accumulation (these can be recycled through the liver). To remove VLDL, a lipoprotein apheresis (DALI® 500) filter (Fresenius Medical Care (UK) Ltd, Huthwaite, UK) was

incorporated into the circuit (Figure 6.1). In clinical practice, this adsorption system is used for patients with severe hyperlipidaemia, refractory to medical therapy (389). The DALI® 500 consists of a matrix of polyacrylate beads, effective for the adsorption of cholesterol, lipoprotein (a) and TGs (389).

Figure 6.1. Lipoprotein apheresis filter connected to the NMP circuit

Following this, we further modified the perfusate to include the following interventions:

- L-carnitine: to increase β-oxidation of fatty acids from the mitochondrial membrane. The perfusate will be supplemented with of L-carnitine 1g/5ml aqueous solution (390–393).
- Forskolin (NKH477, water-soluble forskolin): a glucagon mimetic cAMP activator which results in increased lipolysis of lipid droplets and fatty acid oxidation (394).

- Insulin: infused at a 50% lower concentration than in the OrganOx instructions for use. This reduces the stimulation of *de novo* lipogenesis (DNL), the only source of fatty acid production in the liver during NMP (177).
- Glucose: Glucose acts as a non-lipid precursor for DNL (180). In order to reduce the liver's ability to de novo synthesise fatty acids, the glucose threshold to commence infusion of parenteral nutrition (TPN) infusion was reduced from 10 mmol/L to 5 mmol/L to reduce perfusate glucose concentration.

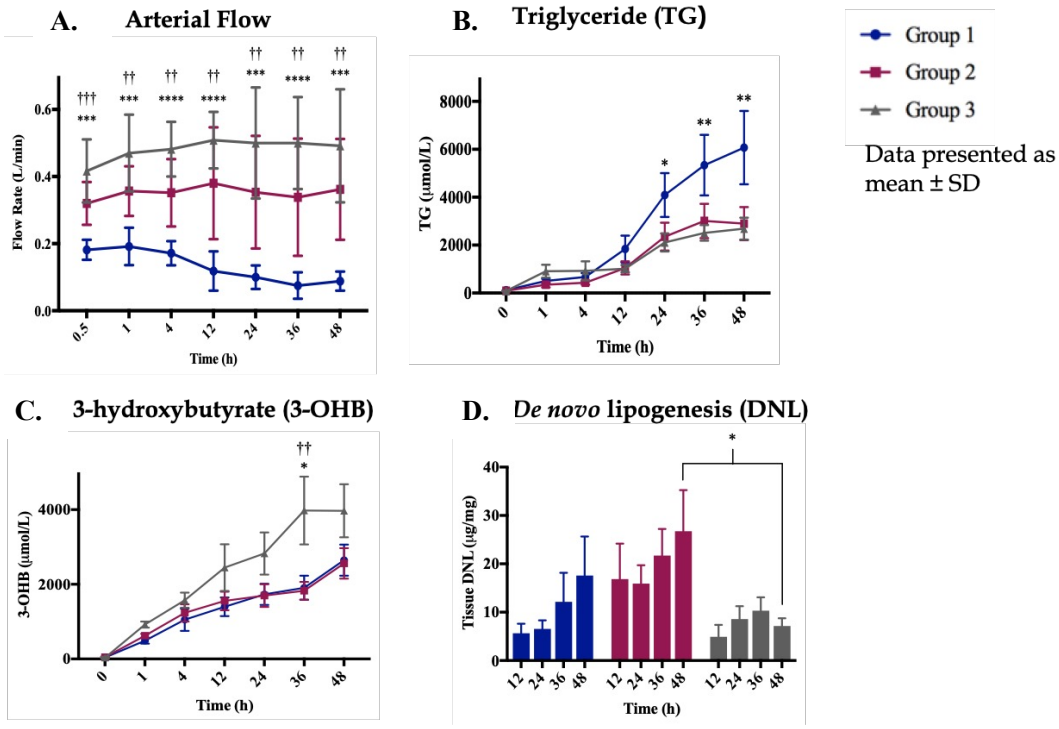

Figure 6.2A-D. Group 1 – NMP alone, Group 2 – filter, Group 3 – filter plus defatting agents

The results described relate to pre-clinical perfusions outside the scope of this thesis. They are included here solely for illustrative purposes, providing context and background for the DeFat clinical trial protocol presented in this chapter. Over 48 hours of perfusion, a significantly increased arterial flow was seen in both intervention groups (Groups 2 and 3) (Figure 6.2A). The lipoprotein apheresis filter (Groups 2 and 3) significantly reduced circulating TG concentrations (Figure 6.2B). 3-OHB measurements showed a significant increase in fatty acid β-oxidation in Group 3, where L-carnitine and forskolin had been added (Figure 6.2C). Significant reduction in intrahepatic DNL (as measured in liver tissue using stable-isotope methodology) was seen in Group 3 (Figure 6.2D). Other functional benefits observed in both Groups 2 and 3 were increased hepatic glycogen production, less rise in perfusate transaminase,

and a reduction in haemolysis (which we previously identified as a marker of ex-situ liver function (207)).

The combination of lipoprotein apheresis filtration and defatting interventions significantly reduced the amount of fat within the liver by 45% at 48 hours. However, the functional improvements were seen much earlier, by 6 hours. From this experimental study, we concluded that a combination of lipoprotein apheresis filtration and perfusate modification reduces hepatic steatosis and improves ex-situ liver function.

The pre-clinical study outlined of ex-situ defatting in discarded human livers has demonstrated, a 'proof of concept' (388): if this translates into clinical practice, it will significantly increase the number of safely-transplantable organs by increasing utilisation of 'marginal' organs. The interventional agents proposed are safe, well-tolerated and available for clinical use (in contrast to previous studies) (217,221). We do not anticipate any systemic side effects following transplantation; first, because the doses are much lower than those used in human studies and, second, because, these agents will be administered ex-situ to livers that are then thoroughly flushed prior to transplant (as per standard practice following NMP) removing the agents from the liver prior to transplantation.

In addition, structural and functional differences were evident after 6 hours of perfusion. These were associated with improved perfusion and biochemical metrics that would have defined these organs as transplantable on current functional criteria. This suggests that 6 hours of perfusion should be the minimum required prior to considering implantation of the organ into the recipient (with a maximum of 24 hours as per OrganOx *metra*® instructions for use).

In the proposed clinical trial (the DeFat study) we intend to enrol livers that have been retrieved for the purpose of transplantation, and that have been identified as high-risk of steatosis. We know that such livers are likely to be discarded after retrieval either because of appearance, histology or unfavourable perfusion metrics on NMP. We will test the targeted defatting protocol described above, using objective measures of function to assess outcomes.

6.2 Trial design

This is a prospective, blinded randomised study, which will test the effect of normothermic defatting of steatotic donor livers. Donor organs meeting enrolment criteria will be randomised, using a 1:1 allocation ratio, using permuted blocks of varying undisclosed size and will be stratified by donor organ type (DBD/DCD). Livers will be perfused using the OrganOx *metra*® NMP device and assigned to either NMP alone (n = 30) or NMP with defatting interventions (n = 30). An interim safety review will be undertaken after perfusion of the first 10 livers.

All recruiting centres have extensive experience in the clinical use of NMP and are current users of the OrganOx *metra*® device. The OrganOx *metra*® is a CE marked normothermic preservation device for use in human liver transplantation. It perfuses the donor liver with blood, oxygen and nutrients, as well as a number of medications, at normal body temperature to replicate physiological conditions and preserve the organ for up to 24 hours. The device provides information as to the haemodynamic, synthetic and metabolic function of the liver during perfusion, which may assist the clinician in assessing the organ's suitability for transplantation. The device is available at all recruiting liver transplant centres.

Perfusions will be supervised by a member of the central trial team. Randomisation (through the web-based service, www.sealedenvelope.com) will be carried out by the trial co-ordinator (clinical research fellow) after inspection of the organ with the transplanting surgeon. Following randomisation, setting up the NMP device will follow standard practice, with addition of the apheresis filter and pharmacological protocol (see below). The presence or absence of the lipoprotein apheresis filter will be blinded through use of a 'dummy' filter covered by a drape. This will prevent the local transplant team (and therefore the patient) from knowing the study allocation. An interim safety review will be undertaken after perfusion of the first 10 livers.

Study visits will align with routine outpatient clinics to avoid extra hospital visits where possible. These will be at post-operative days 1-7, day 30 and, months 3 and 6. At each study visit, details of adverse events, biochemical liver function tests and graft and patient survival will be documented.

The collaboration with the NHSBT Clinical Trials Unit (CTU) will facilitate longer-term (12 month) follow-up of basic parameters (where data is available) beyond the end of the trial and we will request consent to do so. This data will be collected from the UK Transplant Registry (UKTR) held by NHSBT.

Data will be collected into a secure central online electronic database (MACRO) using electronic case report forms. The study will close after the final patient has completed 6 months of follow-up. Longer-term (12 month) follow-up data (beyond the end of the trial) will be collected from the UKTR.

6.3 Methods: Participants, interventions and outcomes

Recruitment will take place at five UK liver transplant centres (Addenbrooke's Hospital, Cambridge; King's College Hospital, London; Queen Elizabeth Hospital, Birmingham; Royal Free Hospital, London; St James's Hospital, Leeds). All of these centres have extensive experience in the clinical use of NMP and are current users of the OrganOx *metra*® device.

6.3.1 Eligibility criteria

The randomised entity in this study is a donor liver, rather than a transplant recipient. Donor livers accepted by each participating transplant centre will be screened for a high likelihood of fatty liver disease at each point of the donor pathway based on: (i) waist circumference (>88 females and >102cm males) or BMI >30kg/m^2 or both at point of acceptance (395) (ii) evidence of macroscopic moderate-severe steatosis identified by the retrieval surgeon (or biopsy result) at point of retrieval.

In addition, any liver offer fast tracked due to moderate-severe steatosis (based on appearance or biopsy result) will also be considered for enrolment (regardless of WC and/or BMI).

The final entry criterion will occur at the point of inspection upon arrival at the transplant hospital: A surgeon from the implanting team will assess the liver to confirm its suitability for inclusion into the trial (based on macroscopic characteristics: colour, texture, rounded edges, size, weight) (87). The objective of this second entry criterion is to reduce the number of false positive (non-fatty) livers enrolled in the trial. Where available, the results of clinical biopsies

demonstrating moderate-severe steatosis (typically >30%) will also be taken into account to assess suitability for randomisation.

The outcomes of livers transplanted during the study will be recorded. Liver transplant recipients will be those on the waiting list in participating centres to whom the livers are offered, and recipients will be consented for use of their data. This study does not alter the normal UK offering process in any way. The inclusion and exclusion criteria are described in Table 6.1:

Table 6.1. Donor and liver transplant recipient inclusion and exclusion criteria

Inclusion criteria	**Exclusion criteria**
Donor Livers: • Donors aged 18 years or over • Offered through the national offering scheme and accepted by participating liver transplant centre • Moderate-severe steatosis: macroscopic characteristics based on colour, texture, rounded edges, size and weight at point of inspection at the transplant hospital to confirm suitability for randomisation. Where available, the results of clinical biopsies demonstrating moderate-severe steatosis (typically >30%) will also be taken into account to assess suitability for randomisation.	Donor Livers: • Donors from outside of the UK • Donor is HIV, hepatitis B or C positive • Cold ischaemia time (CIT) expected to exceed > 10 hours • Macroscopic evidence of fibrosis • Livers undergoing any other form of ex-situ machine preservation • Participating centre cannot offer NMP due to device, logistical or staffing reasons
Liver transplant recipients: • Recipients 18 years of age or above • Elective waiting list at a participating centre • Willing to consent for inclusion into the study and collection and use of their data	Liver transplant recipients: • Receipt of a liver that has not undergone randomisation • Receipt of super urgent transplant for acute liver failure • Receipt of a split liver transplant • Receipt of a multi-organ transplant • Transplanted outside of the participating centres • Contra-indication to MRI e.g. pacemaker

6.3.2 Recruitment

All UK liver offers meeting the inclusion criteria will be eligible for consideration. Offers are managed by NHS Blood and Transplant Hub Operations using the electronic offering system (EOS). Following NHSBT standard practice potential donors are identified by the donor

hospital ITU staff and referred to the specialist nurse for organ donation (SNOD). The SNOD will obtain donor family consent for donation, and/or research samples, arrange any necessary investigations and register the donor with Hub Operations as per standard practice. Liver offering will follow standard NHSBT policy, and offering will not be altered in any way by participation in the study (37).

6.3.2.1 Screening and Eligibility Assessment

Screening of donor livers is described above and the anticipated flow of liver offers through the trial is depicted in Figure 6.3. Randomisation will be undertaken by the trial co-ordinator upon arrival at the recipient liver transplant centre and after inspection of the liver by a surgeon from the implanting team. Where available, the results of clinical biopsies demonstrating moderate-severe steatosis (typically >30%) will also be taken into account to assess suitability for randomisation.

Allocation of organs will not be affected in any way by this study. NHSBT matching runs and in-centre allocation of organs will follow usual practice, irrespective of eligibility for the study.

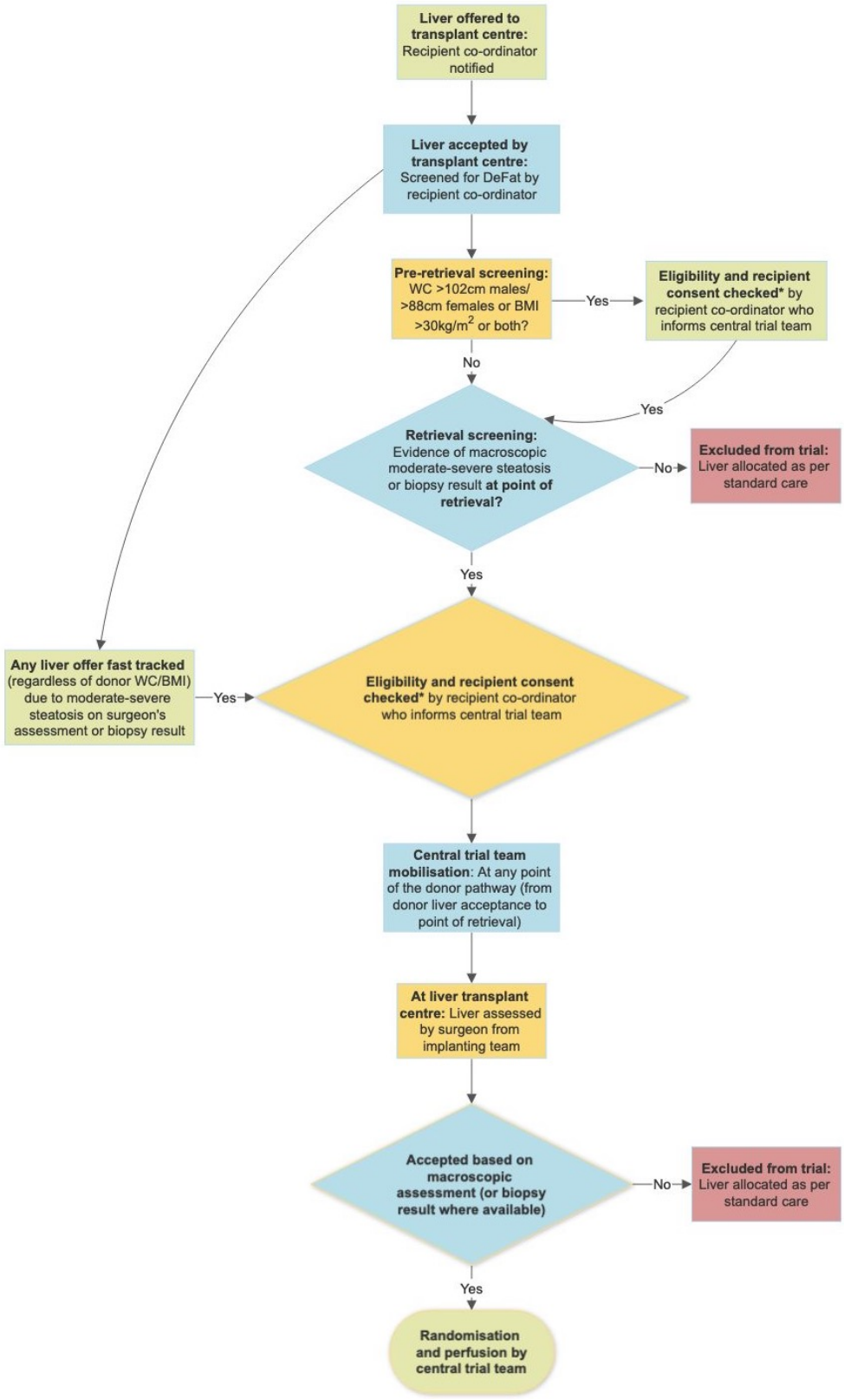

Figure 6.3. Eligibility screening of donor livers and eligible participants for the DeFat study. *Consent refers to evidence of a signed informed consent form, if a patient on the waiting list has indicated intention to consent and has not returned the signed consent form prior to admission for transplant, they will be asked to sign and confirm consent on admission for transplant. Randomisation and perfusion will only be carried out if the informed consent form has been signed.

6.3.3 Interventions

All livers in this study will be perfused using the OrganOx *metra*®. The primary perfusion fluid for the liver comprises packed red blood cells, supplemented by colloid solution (human albumin solution or Gelofusine as per local protocol) to normalise the haematocrit and osmolarity.

Before connection of the liver the blood-based perfusate is supplemented with:

- Antibiotic and antifungal agents as per current local protocols. Heparin (anticoagulant) to prevent thrombosis in the circuit. In clinical use, a half-life of ~90 minutes is assumed; on this basis heparin is also given as a maintenance infusion.
- Sodium bicarbonate (buffer) for adjusting the pH of the perfusate.
- Calcium gluconate/calcium chloride to correct the binding of citrate to calcium

During the perfusion the following are infused at a constant rate:

- Parenteral nutrition solution - a source of amino acids and glucose for liver maintenance.
- Insulin to control the perfusate glucose level
- Heparin to maintain anticoagulation
- A 2% solution of sodium taurocholate in isotonic saline to compensate for loss of bile salts.
- Prostacyclin to optimise micro-perfusion

All solutions required will be attached to the circuit during set-up and before the liver is attached. All solutions are prepared immediately before the organ is attached to the device and contain sufficient solution for 24 hours operation, the intended maximum perfusion time for a liver on the device.

6.3.3.1 NMP (Control Group)

All livers included in the study will undergo NMP using the OrganOx *metra*®, a CE-marked device already in use in liver transplant units in both clinical trials and routine clinical practice (providing special arrangement for consent, governance, audit and research) (207,396).

Livers will be transported on ice to the transplant centre, and those meeting the inclusion criteria will undergo NMP (minimum 6 hours, maximum 24 hours), in accordance with the manufacturer's instructions for use and current local protocols. The procedure for preparing the device for use and placing the organ on the device is described in detail in the instructions for use (IFU) document (L300-0437ReV1.0 RoW Version 25/09/2017). All livers will be perfused with 3 units of donor-type (or O-negative) red blood cells and will be arranged by the recipient surgical team at the recruiting liver transplant centre. The procedure for removing the liver from the device is also described in the IFU. Implantation and reperfusion of the liver proceed as per the usual practice of the implanting centre.

6.3.3.2 NMP with defatting interventions (Study Group)

The study arm of this trial combines the use of a lipoprotein apheresis filter to the normothermic circuit (for a minimum of 6 hours and a maximum of 24 hours), with targeted pharmacological strategies during ex-situ perfusion. Therefore, in addition to NMP, livers randomised to the study group will undergo the defatting protocol developed in our pre-clinical experimental study described in the background/rationale section of this chapter (388). All components of this protocol are licensed for clinical use and include:

- Lipoprotein apheresis filtration (DALI® 500): This is licensed for patients with severe hyperlipidaemia refractory to maximal medical therapy (389).
- L-carnitine (Carnitor, Alfa Sigma): This is licensed for use in primary carnitine deficiency due to inborn errors of metabolism and prevention of L-carnitine deficiency in patients with kidney disease undergoing haemodialysis. It has been shown to increase β-oxidation of fatty acids from the mitochondrial membrane. The perfusate will be supplemented with of L-carnitine 1g/5ml aqueous solution (390–393).
- Forskolin: This is a glucagon mimetic cAMP activator which results in increased lipolysis of lipid droplets and fatty acid oxidation (394). The perfusate will be supplemented with 1 mg of NKH477 (water-soluble version of forskolin: Adehl, Nippon Kayaku) in 2 ml of 0.9% sodium chloride (from a stock solution of 5mg of NKH477 in 10 ml of 0.9% sodium chloride) (397,398).
- Insulin: This will be infused at a 50% lower concentration than in the OrganOx instructions for use. This reduces the stimulation of *de novo* lipogenesis (DNL), the only source of fatty acid production in the liver during NMP (177).

- Glucose: The threshold to infuse parenteral nutrition (TPN) will be reduced from 10 mmol/L to 5 mmol/L. As glucose is a non-lipid precursor for DNL, this will reduce the liver's ability to synthesise fatty acids de novo during perfusion (180).

Normothermic defatting will treat the liver in the ex-situ setting. Following treatment, prior to transplantation, the liver will be flushed with 2L of preservation solution, as per standard NMP practice. The investigational agents will therefore be effectively removed from the liver prior to implantation.

6.3.4 Primary outcome measure

The trial is intended to confirm the safety and assess efficacy of the NMP-defatting protocol in steatotic donor livers intended for transplant. The primary endpoint is the proportion of livers that achieve all of the following functional criteria at 6 hours of perfusion (202,227), as defined by:

- Clearance of lactate to a level < 2.5mmol/L
- Perfusate pH ≥ 7.20
- Evidence of glucose metabolism (spontaneous fall in perfusate glucose)
- Minimum bile pH ≥ 7.5 (if bile produced)
- Bile glucose concentration ≤3 mmol/L or ≥10 mmol less than perfusate glucose
- Hepatic arterial flow ≥ 100ml/min; portal venous flow ≥ 500ml/min
- Perfusate alanine aminotransferase (ALT) < 6000U/L at 6 hours

These objective measures, reflecting both hepatic metabolism and injury, have been derived by experience and a process of consensus amongst current NMP users. These parameters are recognised as a way to discriminate livers with favourable post-transplant outcomes and will be measured at baseline (pre-NMP) and throughout perfusion (1, 2, 4 and 6 hours and end of perfusion) (202,227). Lactate measurements will also be taken at baseline (pre-NMP) and 5 minutes after start of NMP.

These functional criteria are not intended as an instruction to the implanting surgeon, but rather as a consistent endpoint for the trial. The decision as to whether a liver is actually transplanted will remain with the implanting surgeon, who will base this on a number of criteria, including

some that are recipient-related rather than donor organ-related (e.g. the urgency with which the patient needs a transplant may determine the decision).

6.3.5 Secondary outcome measures:

The secondary outcome measures are described in Table 6.2:

Table 6.2. Clinical, histological and imaging secondary outcome measures

Outcome	Measure(s)
Clinical	1. Proportion of livers transplanted in the 2 arms 2. LiMAx (maximum liver function capacity) test performed after 1 hour of liver stabilisation during NMP, repeated at 5 hours and subsequently every 6 hours till the end of perfusion where feasible. If the decision to transplant has been made by 6 hours of NMP, the test will not be repeated. The LiMAx test will allow real time monitoring of CYP1A2 (prominent in functional livers cells and less prominent in damaged cells) and is based on the metabolism of ^{13}C-methacetin. This will enable measurement of liver capacity and functional reserve during perfusion (230). 3. Cell free DNA (cfDNA) measured at baseline (pre-NMP) and during preservation (1, 2, 4 and 6 hours and end of perfusion). Further measurements taken from the recipient peri-operatively (before transplant) and re-perfusion (following liver transplantation). Post-operative samples collected on days 1, 3, 7 and 14 (if the patient is discharged prior to day 14 – a sample will be collected on the day of discharge instead). Outpatient sample collection will align with clinic visits on day 30, month 3 & 6. cfDNA has been correlated with allograft injury, rejection and formation of de novo donor specific antibodies (399). 4. Biochemical liver function in the first 7 days post-transplant: ALT, GGT, INR, Bilirubin and peak serum AST (where AST measurements available) in the first 7 days post-transplant. Peak serum AST is a validated surrogate marker, predictive of PNF as well as graft and patient survival (400). It is also associated with histological evidence of moderate to severe reperfusion injury (105). 5. Model of Early Allograft Function (MEAF) (67): A score (between 0-10) based on bilirubin, INR and ALT within the first 3 post-operative days. 6. Primary non-function (PNF): irreversible graft dysfunction requiring emergency liver replacement during the first 10 days after liver transplantation, in the absence of technical or immunological causes. 7. Post-reperfusion syndrome (PRS) (64): a decrease in mean arterial pressure (MAP) of more than 30% for more than one minute during the first five minutes after reperfusion (64). 8. Need for renal replacement therapy (haemodialysis, haemofiltration, peritoneal dialysis) during the first 7 days post-operatively. 9. Duration of ITU/HDU and hospital stay. 10. Graft survival (defined as a functioning transplant in the absence of death and re-transplantation) at day 7, day 30, month 3, and month 6.

	11. Patient survival at day 7, day 30, month 3 and month 6. In addition, 12-month clinical outcomes (obtained from NHSBT registry) will also be reported: a. Draft and patient survival b. Total number of days in hospital in the last year (excluding transplant admission) c. Total number of re-admissions for: • Recipient infection • Acute rejection • Chronic rejection • Biliary complications • Vascular complications • Disease recurrence • Other reasons d. Transplant related renal dysfunction e. Biochemistry (liver and renal function) 12. The following safety information will be recorded: a. Organ discard rate b. Perfusate culture. At the end of preservation a sample will be taken for microbiological culture. c. Adverse event rates and severity, graded according to the Clavien-Dindo classification (401) during the first 7 days, day 30, month 3 and month 6: • Recipient infection • Biopsy proven acute rejection • Biliary complications (biliary strictures - anastomotic and non-anastomotic, bile duct leaks) • Vascular complications (bleeding, hepatic artery stenosis, hepatic artery thrombosis, portal vein thrombosis) • Reoperation rate d. Technical complications/device failures
Histological & Biochemical	1. Correlation of pre-perfusion donor biopsy (histopathologist's steatosis report) with: a. WC, BMI and clinical risk scores such as the fatty liver index (FLI) and hepatic steatosis index (HSI) (265,272) where relevant data available b. Surgeon's assessment (87) c. Non-invasive pocket-sized micro-spectrometer reading. The device has been developed by SCIO - Consumer Physics (http://www.consumer-physics.com) and is CE marked. It utilises spectroscopy (absorption of near infrared light, 700-1,100nm). The commercially available device is able to quantify composition of foods, estimate body fat levels and identify analgesic agents (260). Readings will be taken sequentially over perfusion (where feasible): at baseline (pre-NMP) and during preservation (1, 6 hours and end of perfusion) to facilitate correlation with post-perfusion (end-NMP) biopsy in addition to the pre-perfusion biopsy. 2. Histological and biochemical evidence of ischaemia -reperfusion injury (IRI):

	a. Histology (formalin fixed paraffin embedded) (388): (i) Neutrophil infiltration & leucocytosis determined using Haematoxylin & Eosin (H&E) stain (ii) Glycogen depletion determined using periodic acid-Schiff (PAS) stain (iii) Lipid peroxidation determined using 4-HNE (4-hydroxynonenal) stain Biopsy samples collected pre-perfusion, post-perfusion and re-perfusion in the recipient (following liver transplantation). b. Cytokine profile implicated in liver transplantation including (251): CXCl8/IL-8, IL-10, IL-2, TNF-a, IFN-γ, IL-13, IL-4, IL-1β, IL-17A and IL-6. Blood samples collected peri-operatively (before transplant) and re-perfusion in the recipient. 3. Histological and biochemical evidence of bile duct injury (BDI) and biliary viability (203) such as: a. Histology (formalin fixed paraffin embedded) biopsy samples pre-perfusion, post-perfusion and following re-perfusion in the recipient. For example, evidence of stromal necrosis, loss/injury to peribiliary glands and vascular lesions. Bile duct biopsies will only be taken if sufficient length on the bile duct and feasible to do so. b. Bile composition measurements (if produced and measured at 1, 2, 4 and 6 hours and end of perfusion) for example: low pH and bicarbonate with high glucose and lactate dehydrogenase (LDH) as indicators of poor biliary viability.
Imaging	1. Biliary strictures (anastomotic and non-anastomotic) determined by MRI scan at month 6 (+/- 1 month) depending on site capacity using MRCP+ (a CE-marked advanced biliary visualisation software by Perspectum Diagnostics) (402). 2. Graft hepatic steatosis determined using multiparametric liver MRI (proton density fat fraction, cT1 and T2* mapping) at 6 (+/- 1 month) depending on site capacity. MRI proton density fat fraction (MRI-PDFF) has demonstrated high diagnostic accuracy in both the detection and grading of hepatic steatosis with histology as a reference standard (403,404). CE-marked software i.e. LiverMultiScan™ developed by Perspectum Diagnostics will aide in the quantification of steatosis.

6.3.6 Mechanistic studies outcome measures

The identification of novel markers could augment current practice by predicting the outcome of each liver with objectivity. The mechanistic studies will test hypotheses based on previous published studies that have investigated markers in the field of NMP and will inform development of functional criteria and optimisation of future defatting protocols, see Table 6.3:

Table 6.3. Mechanistic outcome measures

Outcome	Measure(s)
Steatosis	To measure the effect of the intervention on the histological degree of steatosis: Histological quantification of MaS measured pre-perfusion, post-perfusion, and during re-perfusion in the recipient. We hypothesise that the intervention of defatting will reduce the degree of MaS and severity of NAFLD activity score (405).
Hepatic lipid metabolism	To measure the effect of the intervention on markers on of hepatic lipid metabolism: 1. Perfusate TG, insulin, ketone bodies and cytokines associated with IRI will be measured at baseline (pre-NMP) and during preservation (1,2,4 and 6 hours and end of perfusion). Further measurements taken from the recipient peri-operatively (before transplant) and re-perfusion (following liver transplantation). This will provide insight into changes in intrahepatic lipid handling and inflammation. We hypothesise that the intervention of defatting will 'repartition' intrahepatic fatty acids away from esterification into oxidation pathways leading to a decrease in IHTG and a decrease in IRI-associated cytokine production (251). 2. Perfusate FGF-21 will be measured at baseline (pre-NMP) and during preservation (1,2,4 and 6 hours and end of perfusion). Further measurements taken from the recipient peri-operatively (before transplant) and re-perfusion (following liver transplantation). FGF-21 is a hormone produced in the liver involved in energy homeostasis; its secretion is attributed to metabolic stress. There is evidence that serum FGF-21 is a useful marker for steatosis and correlates with increasing steatosis grade (406). We hypothesise that the defatting intervention will reduce FGF-21.
Transcriptomic, Proteomic & Glycomic	To understand the structural, cellular and metabolic effects of defatting on steatotic livers. Genomic analysis of samples taken pre-perfusion, post-perfusion and following re-perfusion in the recipient: 1. Transcriptomics: A complex signalling cascade regulates metabolic processes within the liver. To understand the effect of NMP and the defatting intervention, genomic analysis of liver tissue will be undertaken. We hypothesise that the defatting intervention will lead to downregulation in pathways related to fat synthesis and inflammation and an upregulation in pathways related to fat disposal. Samples from livers will undergo RNA sequencing of the liver and this will be correlated with clinical outcomes. Changes in gene expression will be mapped with changes occurring in biological pathways, inferring biological changes during NMP. 2. Proteomic and glycomic analysis of perfusate samples taken at baseline (pre-NMP) and during preservation. Further measurements taken from the recipient peri-operatively (before transplant) and re-perfusion (following liver transplantation):

	a. A recent study investigating the use of NMP to increase utilisation of high-risk donor livers, identified protein clusters that were able to discriminate between transplantable and non-transplantable livers (22 out of 31) as well as markers predictive of post-transplant complications (407). We aim to determine the effect of the intervention on protein expression associated with hepatic steatosis, inflammation and IRI. b. Glycomics: The liver perfusate glycome profile may form part of future functional criteria (408). A recent study found that the abundance of a single glycan, agalacto core-alpha-1,6-fucosylated biantennary glycan (NGA2F) was significantly higher in the perfusate of livers that developed PNF. We will test this hypothesis in sequential perfusate samples.

6.3.7 Participant timeline

The proposed study duration is 56 months (01/04/2021 – 30/11/2025): The DeFat study set-up tasks commenced in April 2021 and the study opened for recruitment on the 23rd of February 2023. The anticipated end date for recruitment is the 30th of November 2024 (total recruitment period of 21 months) with 6 month follow-up of the last participant and 6 months analysis/dissemination (close-out) anticipated to be completed by the 30th November 2025 (with a potential further 12 month extension for recruitment currently pending approval from the NIHR). The flow of participants in the study is summarised in Figure 6.4. In addition, all trial procedures are summarised in Table 6.4 (Standard Protocol Items: Recommendations For Interventional Trials, SPIRIT).

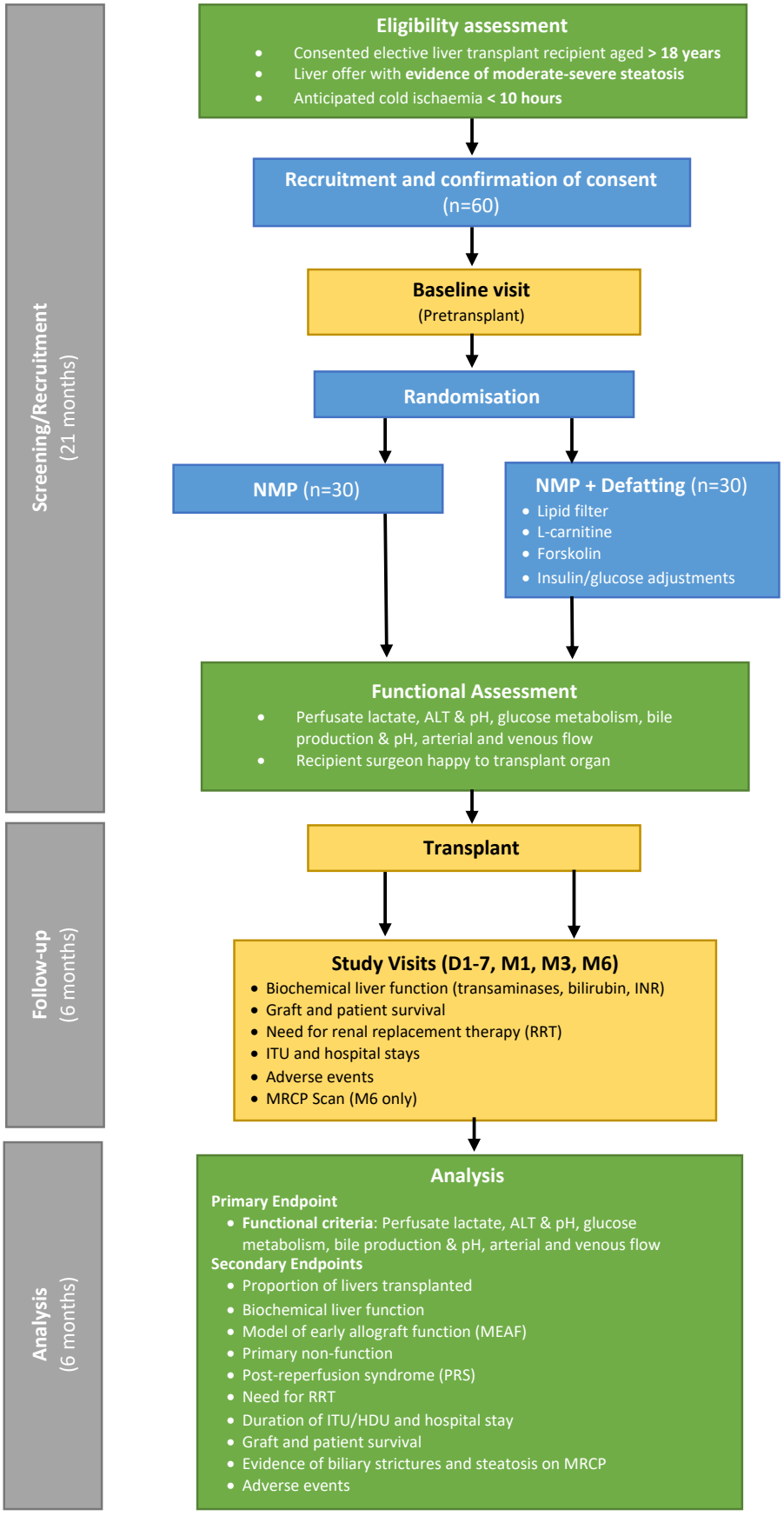

Figure 6.4. Flow of participants through the study. NMP – Normothermic machine perfusion; MRCP – Magnetic Resonance CholangioPancreatography, ALT – Alanine Transaminase

Table 6.4. SPIRIT table of enrolment, interventions, and assessments (schedule of procedures)																			
Activity	**Pre-study Screening**	**Pre-study Baseline**	**Pre-perfusion**	**During & end of perfusion**	**Pre-transplant**	**Post-reperfusion**	**Postoperative**									**Follow-up & Close-out**			
							D1	**D2**	**D3**	**D4**	**D5**	**D6**	**D7**	**D10**	**D14**	**D30**	**M3**	**M6**	**Close-out**
Informed consent	X																		
Meets inclusion/ exclusion criteria	X																		
Randomisation		X																	
Donor & recipient demographics		X																	
Perfusion parameters & samples			X	X	X	X													
cfDNA samples			X	X	X	X	X		X				X		X	X	X	X	
Surgical variables						X													
Serum ALT & AST							X	X	X	X	X	X	X			X	X	X	X
Serum Bilirubin							X	X	X	X	X	X	X			X	X	X	X
Serum GGT							X	X	X	X	X	X	X			X	X	X	X
INR							X	X	X	X	X	X	X			X	X	X	X
Serum lactate*							X	X	X	X	X	X	X						
Primary non-function														X					
Graft survival							X	X	X	X	X	X	X	X		X	X	X	X
Patient survival							X	X	X	X	X	X	X	X		X	X	X	X
Resource use							X	X	X	X	X	X	X	X		X	X	X	X
Safety outcomes						X	X	X	X	X	X	X	X	X		X	X	X	X
MRI (depending on site capacity)																		X	

6.3.8 Baseline donor and recipient assessment

Baseline donor assessments will include donor demographics and blood test results. The following information will be recorded: age, sex, ethnicity, co-morbidities, cause of death, height, weight, BMI, WC, smoking history and alcohol consumption. Donor blood test will include last and peak serum aspartate transaminase (AST), alanine transaminase (ALT), gamma-glutamyl transferase (GGT), serum bilirubin and sodium. Other donor information will include last and fasting triglyceride (TG), if available, evidence of TPN or enteral feed (if information available) and length of ITU stay.

Baseline recipient demographics will include recipient demographic and pre-transplant test results. The following information will be recorded: age, sex, ethnicity, co-morbidities, at the time of transplant (minimum 24 hours of continuous renal replacement therapy) or 2 haemodialysis sessions in the previous week, aetiology of primary liver disease and primary indication of transplant, height, weight, BMI, WC (where available) and smoking history. Pre-transplant recipient blood test will include INR, creatinine, bilirubin and sodium.

6.3.9 Donor timings

These are all routinely collected at the time of retrieval and will be obtained from the NHSBT database.

The parameters to be recorded include:

- Timings:
- Withdrawal of support (DCD donors only)
- Onset of functional warm ischaemia (DCD donors only)
- Cessation of donor circulation (cross clamp or asystole in DCD donors)
- Start of cold perfusion
- Liver removal and placement on ice
- Perfusion solution used for aortic perfusion
- Perfusion solution used for storage and transport
- Degree of steatosis (graded mild, moderate, severe) – surgeon's assessment
- Quality of in-situ perfusion (graded poor, moderate, good)

6.3.10 Preservation parameters

A number of other preservation parameters will be recorded. These are described in Table 6.5:

Table 6.5. Preservation parameters

Preservation parameter	Measurement
NMP duration	• Time of initiation of normothermic machine preservation • Time of cessation of normothermic machine preservation (end flush)
End flush solution	• UW, HTK, other
Perfusion parameters (logged automatically by the NMP device):	• Arterial, and caval pressures (in mmHg) • Arterial, portal and caval flow rates (in L/min) • pO2, pCO2 and pH • Blood temperature (°C), Glucose (mmol/L) and bile production (ml/h)
Perfusate biochemistry	• Perfusate lactate at baseline (pre-NMP), 5 minutes after start of NMP and during preservation (1, 2, 4 and 6 hours and the end of NMP) • Perfusate pH at baseline (pre-NMP) and during preservation (1, 2, 4 and 6 hours and end of NMP) • Perfusate ALT at baseline (pre-NMP) and during preservation (1, 2, 4 and 6 hours and end of NMP) • Glucose levels at baseline (pre-NMP) and during preservation (1, 2, 4 and 6 hours and at the end of NMP) • Bile pH, glucose and bicarbonate (if bile produced) at 1, 2, 4 and 6 hours and at the end of NMP • Bicarbonate use (time and dose of each bolus)
Sampling	• Perfusate at baseline (pre-NMP) and during preservation (1, 2, 4 and 6 hours and end of NMP) • Liver core biopsies taken pre-perfusion and post-perfusion Bile duct biopsies taken pre-perfusion and post-perfusion where feasible i.e. if sufficient bile duct length • At the end of preservation a sample of perfusate/storage solution will be taken for microbiological culture as per standard practice

6.3.11 Operative parameters

These will include:

- Total operative time: defined as time from knife-to-skin to skin closure.
- Time of flush at end of NMP
- Time of liver in body (start of anastomosis)
- Time of reperfusion (portal or arterial, whichever occurs first)
- Portal reperfusion time
- Arterial reperfusion time
- Intraoperative transfusion of blood products measured in units.
- The use of veno-venous bypass or porto-caval shunts
- Type of caval anastomosis (standard end-end, piggyback (end-side or side-side))

6.3.12 Intra-operative outcome assessment

Recipient blood samples (before and after transplant) and post-reperfusion liver biopsy (as well as bile duct biopsy where feasible) will be taken to determine the severity of ischaemia-reperfusion injury (with specific biochemical and histological analyses described in Table 6.2). In addition, changes in mean arterial pressure will be recorded to assess for post-reperfusion syndrome (defined as a decrease in mean arterial pressure of more than 30% for more than one minute during the first five minutes after reperfusion) (64).

6.3.13 Declines and discards

If a decision is made to decline an organ at any point after retrieval (but before randomisation), any donor and preservation data recorded will be kept, and the reason for decline clearly documented in the eCRF. If deemed appropriate by the OTDT Hub, the organ may be offered to other centres on the matching run with liver allocation as per standard of care. If the liver is already on the OrganOx *metra*® device, every attempt should be made to keep it on the device (as per national agreement). If all centres subsequently decline an organ, the organ will be documented as a discard and it will be offered for research or disposed of as per standard procedures.

Data will also be collected for all discards (including reason for discard) from point of randomisation.

6.3.14 Study visits and later outcomes

Following transplantation, patients will be assessed daily by their clinical team and managed according to standard care protocols at the site with clinical information obtained from medical records. Following discharge from hospital, subsequent study visits, where possible, will coincide with routine outpatient appointments. If the recipient is an inpatient, assessment will be made in hospital where appropriate. The study visits will occur on the following dates:

- Study visit 1 – Following transplantation (inpatient stay)
- Study visit 2 - Day 30 (± 2 weeks)
- Study visit 3 – Month 3 (± 1 month)
- Study visit 4 – Month 6 (± 1 month)

The outcome assessments for each study visit are summarised in Table 6.6. Safety outcomes will be graded according to the Clavien-Dindo classification (401), Table 6.7.

Table 6.6. Study outcome measures and participant visits

Endpoint measure	Inpatient stay Study visit 1	Day 30 (± 2 weeks) Study visit 2	Month 3 (± 1 month) Study visit 3	Month 6 (± 1 month) Study visit 4
Biochemical	Days 1-7: • Bilirubin (µmol/l) • GGT (IU/L) • AST (IU/L) / ALT (IU/L) • INR • ALP (IU/L) • Urea (mmol/L) • Creatinine (µmol/l) • Lactate (HDU/ITU) Days 1-3: • MEAF Score	• Bilirubin (µmol/l) • GGT (IU/L) • AST (IU/L) / ALT (IU/L) • INR • ALP (IU/L) • Urea (mmol/L) • Creatinine (µmol/l)	• Bilirubin (µmol/l) • GGT (IU/L) • AST (IU/L) / ALT (IU/L) • INR • ALP (IU/L) • Urea (mmol/L) • Creatinine (µmol/l)	• Bilirubin (µmol/l) • GGT (IU/L) • AST (IU/L) / ALT (IU/L) • INR • ALP (IU/L) • Urea (mmol/L) • Creatinine (µmol/l)
cfDNA	Days 1, 3, 7, 14 or date of discharge	Sample to be taken with routine bloods	Sample to be taken with routine bloods	Sample to be taken with routine bloods
Peri-operative & survival	• Length of stay in (ITU/HDU) (days) • Total length of hospital stay (days) • Requirement for renal replacement therapy • Graft and patient survival at day 7 post-transplant • Primary non-function	• Graft and patient survival at day 30 post-transplant • Requirement for renal replacement therapy (HD, HF, HDF, PD) at any time	• Graft and patient survival at month 3 post-transplant • Requirement for renal replacement therapy (HD, HF, HDF, PD) at any time	• Graft and patient survival at month 6 post-transplant • Protocol MRI Scan (depending on site capacity) • Requirement for renal replacement therapy (HD, HF, HDF, PD) at any time •
Safety	• Recipient infection[a] • Clinically suspected treated rejection • Biopsy-proven acute rejection • Biliary complications[b (i-ii)] • Vascular complications[c (i-vi)] • Reoperation rate • Technical complications and device failures • Any other reported adverse event	• Recipient infection[a] • Biopsy-proven acute rejection • Biliary complications[b (i-ii)] • Vascular complications[c (i-vi)] • Reoperation rate • Technical complications and device failures • Any other reported adverse event	• Recipient infection (CMV infection, fungal infection, post-operative sepsis) • Biopsy-proven acute rejection episodes • Biliary complications[b (i-ii)] • Vascular complications[c (i-vi)] • Reoperation rate • Technical complications and device failures • Any other reported adverse event	• Recipient infection (CMV infection, fungal infection, post-operative sepsis) • Biopsy-proven acute rejection episodes • Biliary complications[b (i)] • Vascular complications[c (i-vi)] • Reoperation rate • Technical complications and device failures • Any other reported adverse event
Immunosuppression	Immunosuppression regimen at day 7 (including doses)	Immunosuppression regimen at day 30 (including doses)	Immunosuppression regimen at month 3 (including doses)	Immunosuppression regimen at month 6 (including doses)

a. **Infection, defined as both clinically diagnosed treated infection and infection with a positive microbiological culture result.**

b. **Biliary complications diagnosed radiologically e.g. a non-protocol MRI or CT scan in clinically symptomatic patient: (i) Biliary strictures - anastomotic and non-anastomotic. Defined as those requiring surgical or radiological intervention and; (ii) Bile duct leaks. Defined as those requiring drainage, refashioning of anastomosis or stenting.**

c. **Vascular complications including: (i) bleeding, defined as bleeding requiring transfusion and/or radiological/surgical intervention; (ii) hepatic artery stenosis, defined as causing graft dysfunction requiring radiological or surgical intervention or resulting in graft loss; (iii) hepatic artery thrombosis, defined as formation of new clot resulting in graft dysfunction or loss, or requiring pharmacological, radiological or surgical intervention; (iv) portal vein thrombosis, defined as formation of new clot resulting in graft dysfunction or loss, or requiring pharmacological, radiological or surgical intervention, (v) portal vein stenosis, defined as causing graft dysfunction requiring radiological or surgical intervention or resulting in graft loss and; (vi) IVC/hepatic vein occlusion, defined as formation of new clot resulting in graft dysfunction or loss, or requiring pharmacological, radiological or surgical intervention.**

Table 6.7. Clavien-Dindo classification of surgical complications (401)

Grade	Definition
I	Any deviation from the normal postoperative course without the need for pharmacological treatment or surgical, endoscopic and radiological interventions.
II	Requiring pharmacological treatment with drugs other than such allowed for grade I complications. Blood transfusions and total parenteral nutrition are also included.
III	Requiring surgical, endoscopic or radiological intervention.
IIIa	Intervention not under general anaesthesia.
IIIb	Intervention under general anaesthesia.
IV	Life-threatening complications (including CNS complications) requiring HDU/ITU management.
IVa	Single organ dysfunction (including dialysis).
IVb	Multi-organ dysfunction.
V	Death of a patient.
Suffix 'd'	If the patient suffers from a complication at the time of discharge, the suffix 'd' (for disability) is added to the respective grade of complication. This label indicates the need for a follow-up to fully evaluate the complication.

Whilst the endpoint for trial participation will be 6 months, patients will also be consented for ongoing follow-up (12 months) by linkage to outcomes recorded by in the NHSBT transplant registry. This will allow the ongoing assessment of resource use (hospital stay and reasons for re-admission), biochemistry results (liver and renal function), transplant related renal dysfunction and longer-term patient/graft survival.

6.4 Sample size

Our preliminary data described above showed that 40% more livers met functional criteria for transplantation where NMP was combined with defatting versus NMP alone (100% vs.60%) (388). However, this is based on a small sample size and the interventions were tested on a very high-risk group of livers that had all been previously discarded. Using the proposed inclusion criteria, a smaller effect size is anticipated. Whilst the present study is not primarily intended to demonstrate efficacy, a sample size of 60 livers (30 per group) will provide greater than 80% power to detect a difference of 30% (from 65% in the control NMP arm) in those meeting criteria for transplantation (at 5% significance): this is a clinically meaningful outcome. This sample size should provide sufficient information for the design of a larger, phase III study to formally test the efficacy of the intervention.

6.5 Recruitment

The annual NHSBT report (2018-19) shows that of 735 adult elective liver transplants, 618 (84%) were performed at the participating liver transplant centres (12). Data from within Eurotransplant show that 23% of livers have moderate to severe steatosis (>30%) on histology (409). This predicts that 142 livers (annually) and 213 livers (over 18 months) with moderate to severe steatosis would be available at the centres participating in this study. Allowing for a 50% recruitment rate, the recruitment of 60 livers in 18 months is feasible (allowing for a small proportion of non-steatotic livers to be inadvertently randomised).

6.6 Assignment of interventions

If the liver is eligible for the study (at the point of organ inspection by a surgeon from the implanting team at the liver transplant centre) or with results of a clinical biopsy, randomisation will be conducted by the trial co-ordinator (clinical research fellow) who will deliver and be unblinded to the intervention.

Once eligibility is confirmed, the central trial team will use an on-line randomisation service (sealedenvelope.com) to allocate the liver to NMP or NMP with defatting interventions. The allocation sequence will be produced by Sealed Envelope and quality checked by the trial statistician.

Donor organs meeting enrolment criteria will be randomised, using a 1:1 allocation ratio, using permuted blocks of varying undisclosed size and will be stratified by donor organ type (DCD/DBD). The randomisation list will only be accessible to the trial statisticians and Sealed Envelope. Randomised livers that are not perfused due to unforeseen reasons will not be replaced. It is anticipated that non-perfusion of a randomised liver will be a very uncommon event.

The DeFat study is a blinded randomised clinical trial. Perfusions will be performed by a member of the central trial team. The trial co-ordinator (clinical research fellow) and/or member of the central trial team will be responsible for enacting the process of randomisation and will be unblinded to the intervention (while the recipients and transplant teams will remain blinded to the intervention). Further information on blinding is included in the full study protocol **(Appendix C)**.

6.7 Discussion

This study addresses the paradox whereby patients die on the liver transplant waiting list whilst less than two thirds of deceased donors (within nationally-agreed offering criteria) result in a transplanted liver in the UK. Poor utilisation of steatotic livers is exacerbated by the globally increasing incidence of obesity and the associated increase in frequency of hepatic steatosis in donors. If the benefit of NMP with ex-situ treatment of steatotic livers are confirmed, NHS practice will be influenced with much greater utilisation of moderately and severely steatotic organs. Evidence that supports this hypothesis is the primary purpose of this study. More broadly, this research has the potential to move NMP into the realm of targeted interventions i.e. ex-situ pharmacological optimisation of a donor organ prior to transplantation.

To date, a total of 22 livers have been randomised, 9 of which have resulted in transplants. In the context of solid organ transplantation, the DeFat study is the first trial of ex-situ pharmacological optimisation during normothermic machine perfusion of the donor liver, and its complexity has created a lot of discussion with the NHSBT Organ and Tissue Donation and Transplantation Team (OTDT) and transplant teams, mainly around the consent requirements and how the study fits within the established NHSBT operational procedures. This has inevitably led to significant challenges during set-up of the study, trial logistics and recruitment at participating centres. A non-exhaustive description of these challenges is detailed below:

Operational challenges: Significant delays during the set-up phase were caused by ongoing discussions with Organ and Tissue Donation and Transplantation (OTDT), Research, Innovation and Novel Technologies Advisory Group (RINTAG) & the Liver Advisory Group (LAG) within NHSBT in regard to ensuring that all the consent and HTA licencing requirements of the study were met and that that the study procedures aligned with the existing offering pathway of the livers for transplant. Additionally, a change in the operational procedures within NHSBT impacted the procedures by which NHSBT CTU contracts with external organisations and this contributed to a further delay.

Impact of the COVID-19 pandemic: The R&D departments of the participating Sites were overwhelmed with the backlog of studies requiring review due to the COVID-19 pandemic and this resulted in inevitable delays in the set-up of the study at the participating sites. Currently all 5/5 Sites are open to recruitment.

Issues with the study specific MRI scan: The set-up of the study was delayed at three sites due to the logistics of performing the study-specific MRI (required at 6 months post-transplant), which required the installation of a specific software. The study-specific MRI is a secondary outcome for this study and issues related to the feasibility of performing this have been largely overcome. However, to avoid further delays to opening to recruitment at the remaining sites, a protocol amendment was submitted clarifying that the scan can be performed depending on site capacity. For example, the study MRI has been outsourced to a site-affiliated contractor at King's College Hospital.

Contract challenges: A change in the operational procedures within the NHSBT has affected the contract between the NHSBT CTU and the randomisation service provider. This also contributed to the overall delay in getting the study started. The contract with the randomisation provider is now in place and the randomisation system was released before the study opened to recruitment.

Site specific challenges: Resource challenges at St James's University Hospital prevented them from progressing with the set-up of the study in a timely manner. Also, there have been issues with the availability of the NMP machine which are currently being resolved with the OrganOx Team. We have kept close contact with the PI during the set-up of the study and have supported them as required following opening of the site for recruitment.

Recruitment issues: Donation and liver transplantation are co-ordinated across the UK, with clear selection and allocation policies; recruitment to the study depends on the number of livers donated and offered via the NHSBT offering pathway and on the principles guiding the offering scheme. The local liver transplant coordinators play an important role to the screening and enrolment of livers to the study, hence any capacity issues in their teams will continue to have an impact on recruitment.

Recipient approach strategy: The local investigators/research teams are expected to approach patients who are on the liver transplant waiting list and give them time to decide about their participation. The REC have advised that the patients should not be approached about the study on the day of transplant and that they should be given enough time to decide without feeling

pressured. The local teams do not know who is going to be called for transplant from the waiting list and for this reason a pool of potential transplant recipients, who are already aware of the study, must be ready to be consented/enrolled to the study at a given time. We have had video calls and in person meetings with the active sites, and we provided guidance and support during the development of their approach strategy. Guidance was based on the principle that the site teams need to identify and prioritise the approach of potential liver recipients on the waiting list who are likely to have a transplant sooner than others (those with a higher Transplant Benefit Score). Hands-on support has also been offered to the sites, where possible and if within our remit.

Consent issues: The consent process for DeFat has encountered challenges that have impacted the trial's recruitment. At several sites, the return of signed consent forms has emerged as a significant issue. The Royal Free Hospital research team has reported some success in improving consent rates through follow-up calls. However, other sites, like Birmingham, are contending with a notably low consent rate of around 20% of trial participants due to logistical difficulties patients face in returning the signed consent forms and staffing issues in performing follow-up calls. Some other factors that potentially have impacted study recruitment, including PI changes at Birmingham and Leeds. Additionally, Birmingham will only randomise DBD livers for the study. To mitigate the challenges around consent, the protocol has been amended to allow greater flexibility to transplant teams and potential participants i.e. the option of remote consent. In addition, each site has been provided with a study manual for the trial containing pertinent information with guidance is outlined to reflect the study protocol.

Mobilisation to sites: Prior to opening each site for recruitment, I have made personal visits to each site to familiarise/introduce myself to the local team and have obtained an NHS-to-NHS letter of access for each site. This is a blinded study, which has required my personal attendance for each liver perfusion to set-up the OrganOx *metra* device according to the randomisation allocation. My attendance and close co-ordination with the local perfusionists and liver transplant teams has ensured the blinding has been maintained throughout the study following randomisation at the recipient centre. In the context of applying a novel intervention in a fast paced and complex process (organ retrieval, perfusion and subsequent transplant), I am in regular communication with site teams to ensure timely mobilisation in order to minimise any delays or impact on cold ischaemia time (CIT).

In certain instances, there have been multiple liver offers at the same time. In these cases, I have been supported by members of the Oxford central trial team (an additional clinical research fellow) to ensure that all perfusions can be attended to maximise recruitment. Each mobilisation is a lengthy process (from the point of arrival of the donor liver at the recipient centre to the point of skin closure in the recipient) which can extend beyond 24 hours: the availability of a trial specific budget for transport to each case has ensured my safe arrival and departure from each site.

Liver enrolment and assessment: The implanting surgeon (or a delegate) is required to complete a trial specific liver and recipient eligibility form to confirm suitability for enrolment. In certain instances, despite physical mobilisation to a participating site a liver is not randomised as it is deemed 'not fatty enough' or is declined for transplant upfront as it is deemed 'too fatty' and therefore high-risk. In order to maximise recruitment, donor livers accepted by each site are screened for a high likelihood of fatty liver disease at each point of the donor pathway (based on anthropometric measures, macroscopic liver appearance and/or clinical biopsy demonstrating moderate-severe steatosis). The final entry criterion for recruiting a liver to the study is the presence of at least moderate or severe steatosis as determined by assessment of the implanting surgeon (or delegate) at the recipient centre (or a clinical biopsy where available) in order to reduce the number of false positive (non-fatty) livers enrolled in the trial.

Surgeon behaviour: There remain anxieties around the transplant of donor livers with moderate-severe steatosis due to the potential implications on recipient outcomes. For this reason, there have been challenges in engaging the wider liver transplant team at each site (beyond the local PI, associate PI and perfusionist) with the clinical trial. The trial has been presented at several local platforms (at sites) and on a national/international level. The personal preferences of clinicians (which have often evolved over many years) is perhaps the most challenging aspect of a clinical trial. Implementing a novel perfusion protocol that necessitates changes in surgeon behaviour can be particularly difficult. Therefore, the protocol was designed with maximum flexibility to minimise disruptions to standard practice with ex-situ liver function as the primary outcome. This flexibility permits the transplanting surgeon to retain the final decision on whether to transplant the liver (i.e. including decision not to

transplant despite all ex-situ functional metrics being met for transplant). These challenges are reflected in low early transplant rates i.e. only 2 livers were transplanted during the first 10 perfusions. However, transplant rates increased with a further 7 livers transplanted after the interim safety review by the DMC (of the first 10 liver perfusions) suggesting an overall change in surgeon behaviour.

6.8 Conclusion

This study explores ex-situ pharmacological optimisation of steatotic donor livers during NMP. If the intervention proves effective, it will allow the safe transplantation of livers that are currently very likely to be discarded (thereby reducing waiting list deaths) and provide data to inform the design a subsequent efficacy trial.

Chapter 7: Hypoxia inducible factor modulation during NMP of human steatotic and extended criteria human livers declined for transplantation

7.1 Introduction

In Chapter 4, I have demonstrated that continuous normothermic machine perfusion (cNMP) improves the preservation of steatotic donor transplant livers compared to static cold storage (SCS). However, cNMP alone does not reduce the degree of hepatic steatosis (HS) during perfusion and steatotic livers exhibit complex metabolic demands compared to lean livers (see Chapter 5). The presence of fat (intrahepatic triglyceride accumulation) negatively impacts post-transplant outcomes and this is evidenced by the more severe ischaemia-reperfusion injury (IRI) observed in steatotic livers compared to lean livers preserved with cNMP. Overall, these findings suggest steatotic livers require further optimisation beyond simply replacing SCS with normothermic perfusion.

To improve outcomes when transplanting livers with higher levels of steatosis than those studied in Chapter 4, it may be crucial to decrease intrahepatic triglyceride accumulation during the preservation process. Our preliminary results point to the potential of a novel defatting strategy in organs retrieved for clinical transplantation but discarded due to steatosis (see Chapter 6) (225). This NMP-defatting protocol is currently being tested in a Phase II randomised clinical trial (the DeFat study) exploring defatting of donor transplant livers during normothermic perfusion in a (pSCS-NMP) back-to-base approach (410). However, it remains unclear whether defatting interventions during NMP (following static cold storage) are sufficient to suppress subsequent IRI in the clinical setting of liver transplantation (LT). Therefore, in addition to these interventions, the modulation of oxygen dependant targeting may further enhance outcomes through amelioration of IRI (a major determinant of graft survival in context of HS). The current chapter builds on pharmacological defatting strategies outlined in Chapter 6 and explores the adjunct of hypoxia inducible factor (HIF) modulation in further optimising steatotic donor livers during NMP.

Hypoxia-inducible factors (HIFs) are cellular oxygen-sensitive transcription factors which have been implicated as the ‘master regulators’ in response to hypoxia through activation of a

number of hypoxia responsive genes. HIF is a heterodimeric complex consisting by an oxygen-destructible HIFα subunit and an oxygen-indestructible HIFβ subunit. During normoxia, HIFα is rapidly degraded by prolyl hydroxylase domain (PHD) enzymes via a von Hippel-Lindau, polyubiquitination, proteasome mediated pathway. However, hypoxia, blocks the PHD activity, promotes HIFα translocation into the nucleus, binds to HIFβ and recruits co-activators to hypoxia responsive elements and regulates several hundred target genes affecting metabolism, vasodilation, erythropoiesis, pH homeostasis, oxygen sensing, and autophagy (154,411)

The HIF-1α isoform has demonstrated a hepatoprotective effect through reduction in lipid synthesis and *de novo* lipogenesis (through suppression of Sterol regulatory element-binding transcription factor 1, Srebp1c) as well as reduction in lipid peroxidation and promotion of fatty acid β-oxidation (154). In the context of IRI, the HIF-1α isoform is involved in reprogramming of cellular metabolism pathways through Glucose transporter 1 (GLUT1), Carbonic anhydrase (CA) and promotes angiogenesis through Vascular Endothelial Growth actor (VEGF) (153).

However, the HIF-2α isoform is reported to activate genes involved in fatty acid synthesis (Srebp1c and Fasn), fatty acid uptake (Cd36) and suppression of genes that regulate fatty acid β-oxidation (PPARα and CPT-1) resulting in progression of lipid accumulation and fibrosis (153,155). Pre-clinical murine studies have demonstrated the benefit of pre-treatment with HIF prolyl-hydroxylase inhibitors and other pharmacological agents including Mangafodipir (a contrast agent) in up-regulation of HIF-1α expression with improved liver graft tolerance to IRI during reperfusion (156,157). This effect has also been demonstrated in steatotic murine livers that received pre-treatment with trimetazidine (an anti-ischaemic drug) through activation of cytoprotective genes i.e. heme oxygenase (HO) associated with HIF-1α (157). However, none of the therapeutic approaches have translated into clinical practice and the effect on human donor steatotic livers has not been investigated.

The hypothesis of this chapter is that NMP with selective pharmacological stabilisation of HIF-1α (achieved through HIF prolyl-hydroxylase inhibition combined with inhibition of HIF-2α dimerisation) and defatting interventions can accelerate reduction in HS and improve graft tolerance to IRI.

The aim of this chapter is to investigate the effects of pharmacological HIF modulation during NMP on discarded steatotic human livers (declined by all UK centres for transplantation). Due to the oxygenated conditions of NMP, pharmacological induction of the HIF pathway is required. The therapeutic agents include Deferoxamine (DFO) and a HIF-2α dimerisation inhibitor (PT2385). DFO is an iron chelator (licensed for clinical use). The reasons to choose this therapeutic agent are three-fold: (i) it has been shown to reduce HS by upregulating proteins related to lipid metabolism; (ii) it both inhibits HIF prolyl-hydroxylases (and thus induces HIF signalling) whilst also reducing free radical production and increasing HIF-1α expression; (iii) it reduces pro-inflammatory cytokines (412). However, DFO can activate both HIF-1α and HIF-2α isoforms and therefore to investigate the effect of HIF-1α alone, the use of a HIF-2α dimerisation inhibitor is necessary. The HIF-2α dimerisation inhibitor (PT2385) has demonstrated beneficial effects in reducing HS and improving insulin sensitivity in murine experiments where obesity was artificially induced with a high-fat diet (413). Importantly, its ability to selectively antagonise HIF-2α in progression of clear cell renal carcinoma (characterised by inactivation of the tumour suppressor gene von Hippel-Lindau and consequent up-regulation of HIF-2α) has been clearly reported in results of a phase 1 dose escalation trial clinical trial (414). The overall objectives are to:

1. Identify dosing schedules for pharmacological HIF modulation during oxygenated normothermic perfusion
2. Optimise methods for liver HIF quantification using IHC, western blots (where frozen tissue available) and correlate this with a downstream HIF dependant target (erythropoietin, EPO)
3. Develop a model of ex-situ ischaemia reperfusion injury (IRI) to compare perfusion outcomes of livers perfused with the established defatting protocol alone (DeFat: described in Chapter 6) and those with the adjunct of defatting and HIF modulation (DeFat-HIF: DFO and PT2385).

7.2 Methods

Between September 2020 and January 2023, 13 discarded human steatotic livers declined by all 7 UK liver transplant centres for transplantation were recruited to this pre-clinical experimental study. Authorisation for research use of the liver was obtained by the specialist nurse in organ donation (SNOD), following NHSBT guidelines. The study was approved by

the London - Riverside Research Ethics Committee (20/PR/0111) and the NHSBT Research, Innovation and Novel Technologies Advisory Group (RINTAG, study reference: 102). All livers included in this studied were retrieved as part of a multi-visceral deceased donor organ retrieval with rapid in-situ cooling (with UW solution), packed and stored on ice (as per standard UK retrieval practice) prior to transportation to the Oxford Transplant Centre (see Chapter 2.2).

7.2.1 Perfusion device

All livers were perfused using the 2nd Generation OrganOx *metra* (OrganOx Ltd, Oxford, UK) NMP device. Following device calibration and priming, donor livers were benched and cannulated as described in Chapter 2.2.

7.2.2 Study design

The study consisted of two phases: (i) HIF modulation dose finding study with a maximum perfusion duration of up to 24h and; (ii) experimental study comparing an established NMP defatting protocol with and without the adjunct of pharmacological HIF modulators in an ex-situ model of simulated liver transplant comprising of an initial NMP duration of 12h with leucodepleted pRBCs, followed by disconnection from the NMP circuit, flush with 2L of cold (UW) preservation solution and reperfusion on the same device using a fresh perfusate comprising of full allogenic whole blood following a short period of warm-ischaemia to simulate implantation (anastomotic time). A total of 13 livers were recruited during the study period. Of these, one liver in the experimental established NMP defatting protocol group did not demonstrate any evidence of metabolic or synthetic liver function and therefore was excluded from further analysis. The final cohort comprised of 12 livers i.e. dose finding study (n = 6) and experimental study (n = 6), see Figure 7.1.

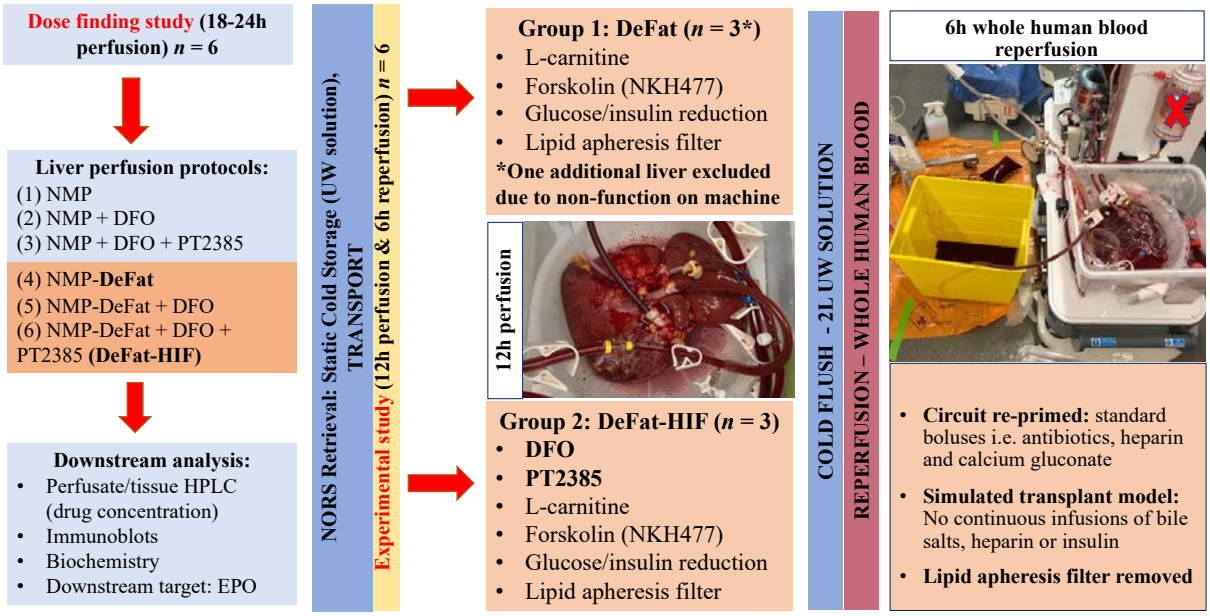

Figure 7.1. Study design outline initial HIF dose finding perfusions and subsequent experimental study comparing the established NMP defatting protocol (DeFat) with the adjunct of pharmacological HIF modulators (DeFat-HIF). Additional functional tests performed during the experimental study included The Maximum Liver Capacity (LiMAx, Humedics GmbH), Monoethylglycinexylidide (MEGX) and Indocyanine green (ICG) clearance tests.

7.2.3 Sampling schedule

A total of six livers were allocated to dose finding perfusions (sampling schedule outlined in Table 7.1) and subsequent livers were perfused as part of the experimental study (sampling schedule outline in Table 7.2).

Table 7.1. Sampling schedule for dose finding perfusions (perfusion duration range 18-24h)

Dose finding perfusions		**Perfusion duration (hours)**										
Sample collection		**0**	**0.5**	**1**	**2**	**4**	**6**	**8**	**12**	**16/18**	**20**	**24**
Tissue	Frozen	x			x	x	x	x	x	x	x	x
	Formalin-fixed	x					x		x			x
Perfusate	Biochemistry	x	x	x	x	x	x	x	x	x	x	x
	Blood gas	x	x	x	x	x	x	x	x	x	x	x
Bile	(if produced)	x	x	x	x	x	x	x	x	x	x	x

Table 7.2. Sampling schedule for experimental perfusions (12h NMP and 6h whole blood reperfusion)

Experimental study: Leucodepleted pRBC perfusion phase		**Perfusion duration (hours)**					
Sample collection		**0**	**0.5**	**1**	**4**	**6**	**12**
Tissue	Frozen	x				x	x
	Formalin-fixed	x				x	x
Perfusate	Biochemistry	x		x	x	x	x
	Blood gas	x	x	x	x	x	x
Bile	(if produced)	x		x	x	x	x
Experimental study: Whole blood reperfusion phase		**Perfusion duration (hours)**					
Sample collection		**0**	**0.5**	**1**	**2**	**4**	**6**
Tissue	Frozen			x			x
	Formalin-fixed			x			x
Perfusate	Biochemistry	x		x	x	x	x
	Blood gas	x	x	x	x	x	x
Bile	(if produced)	x		x	x	x	x

7.2.4 Perfusion protocols

The perfusion protocols for the dose finding perfusions are described in Table 7.3.

Table 7.3. Dose finding perfusion protocols and NMP duration

Perfusion protocol	Description of dose finding perfusion	Perfusion duration (hours)
Liver 1 NMP alone	Standard NMP perfusion protocol (as described throughout this thesis, see Chapter 2.1)	24
Liver 2 Standard NMP with DFO (4h)	Standard NMP protocol (with the addition of DFO at 4h of perfusion)	24
Liver 3 Standard NMP with DFO (4h) + PT2385 (16h)	Standard NMP protocol (with the addition of DFO at 4h of perfusion and PT2385 at 16h of perfusion)	24
Liver 4 DeFat (from commencement of NMP)	NMP defatting protocol with lipoprotein apheresis filter (from the commencement of perfusion, see Chapter 6.1)	18
Liver 5 DeFat + DFO (from commencement of NMP)	NMP defatting protocol with lipoprotein apheresis filter (and addition of DFO from commencement of perfusion)	20
Liver 6 DeFat + DFO + PT2385 (DeFat-HIF from commencement of NMP)	NMP defatting protocol with lipoprotein apheresis filter (and addition of DFO and PT2385 from commencement of perfusion)	24

The pharmacological protocols for the experimental perfusions (both the DeFat and DeFat-HIF group) are summarised in Table 7.4. Briefly, all livers in the DeFat group were perfused as per the established NMP defatting protocol described in Chapter 6.1 and in the DeFat-HIF group, the perfusate was supplemented with the adjunct of pharmacological HIF modulators. In both groups all pharmacological agents were delivered during device priming (prior to commencement of NMP).

Table 7.4. Pharmacological agents delivered in the experimental perfusions

DeFat group	DeFat-HIF group
L-carnitine (Sigma-Aldrich, Dorset, UK): 1 g in 20 ml of 0.9% sodium chloride (B Braun) (390–393)	**DeFat:** L-carnitine, water-soluble forskolin (NKH477) and glucose/insulin reduction as described for the DeFat group
Forskolin: 1 mg of water-soluble forskolin, NKH477 (Cayman Chemical, Michigan, USA) in 2 ml of 0.9% sodium chloride (B Braun) (397,398)	**Deferoxamine (DFO):** DFO, a highly effective iron chelator, was introduced into clinical practice in the 1960s and remains a widely used first-line treatment for patients with iron-overload conditions (412). The concentration of DFO used was 10 mmol/L (extrapolated from previous reported modifications to UW solution) (415) and this equated to a total of 6.6 g (Deferoxamine mesylate, DEMO S.A. Pharmaceutical Industry, Greece) dissolved in 66 ml of 0.9% sodium chloride (B Braun) when applied to the circulating volume of the NMP circuit. This dose was also comparable to that reported in the context of in vivo human studies (416,417).
Insulin: The perfusate was infused at a 50% lower concentration than in the OrganOx instructions for use. This adjustment was made to reduce the stimulation of *de novo* lipogenesis (DNL), the only source of fatty acid production in the liver during NMP (177). The perfusate was supplemented with 100 units of insulin (Actrapid, Novo Nordisk, West Sussex, UK) dissolved in 30 ml of 0.9% sodium chloride (B Braun) and administered at a rate of 1 ml/h. **Glucose:** The threshold to infuse parenteral nutrition (Nutriflex Special, B Braun) was reduced from 10 mmol/L to 5 mmol/L. As glucose is a non-lipid precursor for DNL, this adjustment aimed to reduce the liver's ability to synthesise fatty acids de novo during perfusion (180).	**PT2385:** The dose of the HIF-2α dimerisation inhibitor (PT2385) was extrapolated from a previous *in vivo* human dose escalation trial (414). A total of 100mg of PT2385 (MCE, MedChemExpress) was dissolved in 25 ml of Dimethyl sulfoxide (DMSO, D8418, Sigma-Aldrich) with the aid of water-bath sonication.

Both experimental groups included the addition of a lipoprotein apheresis filter (DALI® 500 filter, Fresenius Medical Care Ltd, Huthwaite, UK). Prior to commencement of perfusion, the filter was primed with 2 L of Gelaspan (B Braun, Sheffield, UK) (389), Figure 7.2.

Figure 7.2. Integration of a lipoprotein apheresis filter into the NMP circuit was achieved using a sterile equal and reducing straight ¼ inch connector with a luer lock (LivaNova UK Ltd, Brockworth, UK) incorporated into the arterial line. A 3-way tap was added to the arterial line to isolate the filter (red). Two additional 3-way taps were attached to the priming port on the IVC line (blue). These connectors enabled priming of the device without disruption by diverting and discarding the priming solution. When the 3-way taps on both the arterial and IVC lines were opened, perfusate flowed through the filter at a rate of 150 ml/min.

7.2.5 Allogenic whole blood reperfusion

All 6 livers in the experimental study were subjected to an ex-situ model of simulated liver transplant which comprised of an initial NMP duration of 12h with leucodepleted human pRBCs, followed by disconnection from the NMP circuit, flush with 2L of cold (UW) preservation solution and reperfusion on the same device using a fresh perfusate comprising of full allogenic whole human blood following a short period of warm-ischaemia to simulate implantation (anastomotic time). The whole blood in the reperfusion phase was supplemented with standard boluses prior to liver connection:

- 10ml of 10% calcium gluconate (B Braun)
- 10,000 IU unfractionated heparin sodium (Wockhardt UK Ltd, Wrexham, UK)

- 750mg of cefuroxime (Flynn Pharma Ltd, Dublin, Ireland)
- 8.4% sodium bicarbonate (B Braun), 30mls for normalisation of perfusate pH prior to connection of the liver and commencement of perfusion

Continuous infusions of heparin, insulin and bile salts were stopped during whole blood reperfusion. However, 0.5mg epoprostonol sodium (Flolan®) (Glaxo, Middlesex, UK) for optimisation of microperfusion was continued at a rate of 1ml/h for the 6 h duration of reperfusion.

7.2.6 Hypoxia inducible factor quantification

The tissue and perfusate concentrations of pharmacological HIF modulators was determined using High Performance Liquid Chromatography (Agilent Technologies, Inc). This analysis was only performed for dose finding Liver 3 which was perfused with the standard NMP protocol with induction of both HIF-1α and HIF-2α (DFO delivered at 4h of perfusion) and sequential selective inhibition of HIF-2α (PT2385 delivered at 16h of perfusion). The tissue and perfusate concentration of each drug (per perfusion timepoint) was then correlated with the presence of HIF-1α and HIF-2α quantified using western blots for the corresponding timepoint. Western blots were performed for all dose finding study livers (except dose finding Liver 4 perfused for 18h using the established NMP defatting protocol: DeFat) and performed for all experimental study livers. Immunohistochemistry (IHC) was also performed for HIF-1α and HIF-2α tissue localisation and to supplement results of the western blots in the dose finding perfusions.

7.2.6.1 HPLC – Tissue concentration

Tissue concentrations of each drug were determined using High Performance Liquid Chromatography (HPLC). Tissue sample preparation and analysis for deferoxamine (DFO alone) and PT2385 is described in Table 7.5.

Table 7.5. DFO and PT2385 tissue concentration measurements

Sample preparation	Method
Tissue drug extraction	DFO and PT2385 drug extraction buffer was prepared in a 1:9 ratio (1ml Acetonitrile and 9mls methanol), a total of 10mls. Then 200 µl of extraction buffer was added to each sample. After mixing, tissue biopsies were homogenised with Prob Sonicator to get a homogenised mixture. The process was performed on ice to avoid the degradation of proteins. After prob sonication, the samples were centrifuged at 13000rpm for 25 mins at 4°C. 170µl supernatant was collected from each sample and dried using SpeedVac (Thermo Fisher Scientific, Inc). The supernatant was extracted and stored at -20°C till further use.
Preparation of standards	1mM each of DFO and PT2385 was prepared from stock solution: • DFO: (i) 50mg/ml = 130mM and; (ii) 1mM = 7.70µl of 50mg/µl + 992.30µl of HPLC water • PT2385: (i) 10mg/ml = 26 mM and; (ii) 1mM = 38.46µl of 10mg/ml + 961.50ul HPLC water 50µl of 1mM DFO, 50µl of 1mM PT2385 and 900µl HPLC water was mixed to create a master mix and a standard set (50µM to 0µM) was subsequently prepared to determine tissue drug concentrations.
High Performance Liquid Chromatography (HPLC)	After drying, samples were resuspended in solvent A (2% Acetonitrile, 0.1% formic acid) and analysed on Agilent 1200 Series HPLC System (Agilent). Equal volume of standard and Samples were applied to C18 (InfinityLab Poroshell 120 EC-C18) column. The separation of extracted compounds were performed at flow rate of 500µl/minute, with linear gradient of 10% solvent B (100% Acetonitrile, 0.1% F.A) to 90% solvent B for 15 minutes, followed by column wash for 2 minutes and column equilibration for 3 minutes. The elution times for DFO and PT2385 were eluted at 7.74 mins and 2.41 mins at 209nm. The HPLC machine was run at A: 2% Acetonitrile & 0.1% F.A. and B: 100% Acetonitrile and 0.1% F.A. The data was analysed manually by using the Agilent Online data analysis software.

7.2.6.2 HPLC – Perfusate concentration

Perfusate drug and drug metabolite concentrations were determined using HPLC. A master mix of seven drugs (100µl, 50µg/ml) was prepared from stock solutions according to the following protocol, Table 7.6:

Table 7.6. Stock solution preparation for master mix

Drugs	**Stock solution preparation (1mg/ml)**
DFO	• Stock 1 (50mg/ml): Dissolve 500mg of drug in 10ml of HPLC water • Stock 2 (1mg/ml): 2ul of stock-1 (50mg/ml) + 98µl HPLC water to get 1mg/ml of DFO • 5µl of Stock 2 (1mg/ml) to prepare the master mix of 50µg/ml
PT2385	• Stock 1 (10mg/ml): Dissolve 10mg of drug in 1ml of 100% DMSO • Stock 2 (1mg/ml): 10ul of stock-1 (10mg/ml) + 90µl of HPLC water to get 1mg/ml of PT2385 • 5µl of Stock 2 (1mg/ml) to prepare the master mix of 50µg/ml
L-carnitine	• Stock 1 (50mg/ml): Dissolve 1g of drug in 20ml of normal saline. • Stock 2 (10mg/ml): 20µl of stock (1g/ml) + 80µl of HPLC water to get 10mg/ml of L-carnitine • Stock 3 (1mg/ml): 10µl of stock (10mg/ml) + 90µl of HPLC water to get 1mg/ml of L-carnitine • 5µl of Stock 3 (1mg/ml) to prepare the master mix of 50µg/ml
NKH477	• Stock 1: (1mg/ml): Dissolve 1mg of drug in 1ml of HPLC water • 5µl of Stock 1 (1mg/ml) to prepare the master mix of 50µg/ml
Lidocaine	• Stock 1 (10mg/ml): original ampoule available as stock solution • Stock 2 (1mg/ml): 10ul of stock-1 (10mg/ml) + 90µl of HPLC water to get 1mg/ml of lidocaine • 5µl of Stock 2 (1mg/ml) to prepare the master mix of 50µg/ml
MEGX (Lidocaine metabolite)	• Stock 1 (25mg/ml): Dissolve 25mg of drug in 1ml of HPLC water • Stock 2 (1mg/ml): 4µl of stock-1 (25mg/ml) + 96µl of HPLC water to get 1mg/ml of MEGX • 5µl of Stock 2 (1mg/ml) to make the master mix of 50µg/ml
ICG	• Stock 1 (1mg/ml): original ampoule available as stock solution • 5µl of Stock 1 (1mg/ml) to make the master mix of 50µg/ml

The master mix (100µl, 50µg/ml) was prepared by mixing 5µl of each drug (at the concentration of 1mg/ml) i.e. a total 35µl with 65µl of HPLC water. A standard set (50µg/ml to 0µg/ml) was subsequently prepared to determine the perfusate drug concentrations.

Perfusate drug extraction buffer was prepared in a 1:9 ratio (1ml Acetonitrile and 9mls methanol), a total of 10mls. Then 800µl of extraction buffer and 100ul of perfusate sample were mixed and stored in in fridge for 1 h, followed by centrifuged at 13000rpm for 25 mins

at 4°C degrees. After centrifuge, 700µl of supernatant was collected and dried using SpeedVac (Thermo Fisher Scientific, Inc). Dried samples were stored in -20°C until further use.

Samples were resuspended in solvent A (2% Acetonitrile, 0.1% formic acid) and analysed on Agilent 1200 Series HPLC System (Agilent). Equal volume of standard and samples were applied to C18 (InfinityLab Poroshell 120 EC-C18) column. The separation of extracted compounds were performed at flow rate of 500µl/minute, with linear gradient of 1% solvent B (100% Acetonitrile, 0.1% F.A) to 20% solvent B for 10 mins and 90% for 2 mins, followed by column wash for 4 mins and column equilibration for 4 mins. The data was analysed manually by using the Agilent data analysis software. The wavelength and elution times for each drug are shown in Table 7.7:

Table 7.7. Elution time and wavelength for detection of pharmacological agents in perfusate

Drug	**Wavelength (nm)**	**Elution time (min)**
DFO	209	9.913
PT2385	209	2.394
L-carnitine	209	1.995
NKH477	209	1.853
Lidocaine	209	10.6
MEGX	209	10.2
ICG	805	14.6

This protocol was developed to allow rapid quantification of drugs delivered (or metabolites i.e. lidocaine to MEGX) during perfusion. However, for the purposes of this thesis, only the perfusate concentrations of DFO and PT2385 are provided in relation to the HIF dose finding experiments. Alternative (more reproducible) protocols were used specifically for ICG, lidocaine and MEGX quantification (see 7.2.11).

7.2.6.3 Immunoblotting

Quantification of tissue HIF-1α and HIF-2α was performed using western blots as described in Table 7.8 and the primary/secondary antibody concentrations are listed in Table 7.9.

Table 7.8. Western blot protocol

Procedure	**Method**
Protein extraction	Protein extraction from tissue biopsies was performed using an 8M urea buffer. The buffer comprised of PIC (with EDTA), 8M urea, 2M thiourea, 0.4% CHAPS, 0.1% SDS, 0.05% sodium deoxycholate in PBS, stored at 4ºC. After mixing, tissue biopsies were homogenised with Prob Sonication to get a homogenised mixture. The process was performed on ice to avoid the degradation of proteins. The samples were then centrifuged at 13000rpm for 25 mins at 4ºC. The supernatant was extracted and stored at -20ºC till further use. The amount of protein recovery from tissue biopsies was estimated by using the Bradford assay (Sigma-Aldrich, Dorset, UK) according to manufacture guidelines. A serial dilution of BSA standard was used to calculate the amount of protein in tissue samples.
Sample preparation	A pre-specified volume of sample (according to concentration) was mixed with 2X volume of SDS gel loading buffer and reduced at 60ºC prior to loading onto the gel. In addition, positive HIF controls were obtained through collaboration with the Hypoxia Biology Group, Nuffield Department of Medicine, University of Oxford. These included the following cell-lines listed in the European Collection of Authenticated Cell Cultures (ECACC), (418,419): • RCC4/VHL_Normoxia (Nx), ECACC 03112703 • RCC4/VHL_Hypoxia (Hx), ECACC 03112703 • RCC4 plus Vector Alone (VA), ECACC 03112702 The renal cell carcinoma (RCC) cell line RCC4 is stably transfected with the plasmid pcDNA3-VHL. This plasmid provides neomycin resistance and expresses the von Hippel-Lindau (VHL) tumour suppressor protein pVHL. The original RCC4 cell line lacks VHL. The RCC4 cell line with the vector alone (ECACC catalogue no. 03112702) serves as a negative control for investigating the effects of pVHL expression from the pcDNA3-VHL plasmid. These modified cells exhibit reduced tumorigenicity compared to cell lines that do not express pVHL (418,419). After loading the samples to each well, proteins were separated on Criterion XT gels, first 20 mins run at 80V and then 150V for 1 h.
Transfer of proteins	The blotting apparatus was assembled in chilled blotting buffer (black side of cast, fibre pad, blotting paper, gel, nitrocellulose membrane, blotting paper, fibre pad, red side of cast) and placed in the tank with blotting buffer (Bio-Rad) with ice. The power supply was attached run at 80V for 1 hour in the cold room.
Blocking	The 0.2µm nitrocellulose membrane (77012, Thermo Fisher Scientific, Inc) was retrieved and washed with TBS-Tween (TBST) x2 and blocked with 5% milk (1g milk in 20ml TBST) for 60 minutes at 4ºC.

Table 7.9. Primary and secondary antibody concentrations

Procedure	Method
Primary antibody application	The primary antibody was prepared to desired dilution in 5% blocking buffer and the membrane was incubated on shaker at 4°C for 48 hours: • **HIF-1α (mouse) 1:250:** 610958, BD Transduction Laboratories™ • **HIF-2α (rabbit) 1:250:** HIF-2α (D9E3) Rabbit mAb #7096, Cell Signaling Technology® • **β-actin (mouse) 1:1000:** mAbcam 8226, Abcam®
Secondary antibody application	After primary antibody incubation the membrane (blots) were washed with TBST (x4 washes 5 minutes each). The secondary antibody to was created to desired dilution in 10ml of the 5% blocking buffer and incubated on shaker for 1 hour under agitation (protected from direct light): • **HIF-1α (mouse) 1:500:** IRDye 680RD Goat anti-mouse IgG 15530535, LI-COR Biosciences, Inc • **HIF-2α (rabbit) 1:500:** IRDye 800CW Goat anti-rabbit IgG: 15570485, LI-COR Biosciences, Inc • **β-actin (mouse) 1:500:** IRDye 680RD Goat anti-mouse IgG: 15530535, LI-COR Biosciences, Inc
Imaging of blots	Following incubation, the blots were washed again with TBST (x4 washes 5 mins each) and rinsed with 1x TBS. The blots were then imaged using the LI-COR imaging system.

7.2.6.4 HIF-1α and HIF-2α immunohistochemistry

Localisation of HIF-1α and HIF-2α was performed using immunohistochemistry (IHC) on selected FFPE sections from the initial HIF dose finding study perfusions. HIF-1α and HIF-2α immunohistochemistry (IHC) analysis was performed using the Visiopharm® AI-based rapid automated image analysis digital assay (Visiopharm® Ltd, Egham, UK) described in Chapter 2.4.2. However, HIF-1α and HIF-2α IHC was not performed for any livers in the experimental study groups due to more quantitative results provided by the immunoblots for these livers.

7.2.7 Histological evaluation

Liver tissue preparation and staining is described in Chapter 2.3. Briefly, FFPE sections were stained with H&E, PAS, Masson's Trichome and Picosirius RED. Histopathological evaluation of histology slides was performed by Professor Alberto Quaglia (Consultant Histopathologist, Royal Free Hospital, London) who was blinded to the perfusion protocols and treatment allocations for each liver. The degree of steatosis was reported according to the Banff

consensus guidelines. The overall report for each biopsy included the degree of large droplet macrovesicular steatosis (ld-MaS), small droplet macrovesicular steatosis (sd-MaS), glycogen depletion and histological preservation reperfusion injury (PRI) score as defined in Chapter 4.2.4 (286).

In addition to the histopathological steatosis score, digitised images were also analysed using an automated digital analysis software (Visiopharm application 10119, H&E liver steatosis) (Visiopharm Ltd, Egham, UK) to provide quantitative outputs including total macrovesicular steatosis, ld-MaS and sd-MaS percentage described in Chapter 2.4.1. The change in percentage steatosis was compared between biopsy timepoints and experimental groups.

For the one liver in the experimental established NMP defatting protocol group that did not demonstrate any evidence of metabolic or synthetic liver function (an outlier, and therefore excluded from the overall analysis), HMBG1, MPO and CITH3 IHC was performed to assess for evidence of damage-associated molecular pattern (DAMP) related injury that could have contributed to ex-situ non-function (as described in Chapter 2.3.8).

7.2.8 Quantifying DNL, total fatty acid composition and tissue triglycerides

Prior to commencement of NMP (and whole blood reperfusions for the experimental study) 200 ml of $^{2}H_2O$ (heavy water, deuterium oxide) was added to the perfusate reservoir prior to commencement of perfusion. The methods for quantification of hepatic *de novo* lipogenesis (DNL) in the perfusate and tissue, measurements of total fatty acid composition and tissue triglycerides are described in **Appendix D**. These measurements are currently pending completion and therefore are outside the scope of this thesis.

7.2.9 Quantifying perfusate Lidocaine and MEGX

7.2.9.1 Mass spectrometry

Samples were prepared for mass spectrometry analysis by pipetting 100 µL of plasma into a polypropylene Amicon® (3Kcutoff) centrifugal filter tube. The sample tubes were capped and centrifuged at 14,000 × g for 15 min at ambient lab temperature. The clear filtrates were transferred to deactivated glass HPLC autosampler vials were stored in -80ºC until further use.

Shotgun LC-MS metabolomics analysis was conducted using a Dionex Ultimate 3000 HPLC System (Thermo Fisher Scientific, Massachusetts, USA) coupled to an Orbitrap Fusion mass spectrometer equipped with a Heated Electrospray Ionization (HESI) source, the methods are described in Table 7.10.

Table 7.10. Methods for mass spectrometry analysis

Procedure	**Method**
Chromatographic separation	Chromatographic separation employed a Hypersil Gold C18 column (150 × 2.1 mm, 1.9 µm; Thermo Fisher Scientific) with gradient elution using mobile phases A (0.1% formic acid in 2% acetonitrile: water, v/v) and B (0.1% formic acid in 90% acetonitrile: water, v/v) at a flow rate of 350 µL/min and a column temperature of 45°C. For each LC-MS run, 5 µL of extracted metabolites dissolved in 20 µL of solvent A were injected. The gradient program initiated at 99% A, decreased to 10% A over 17 min, held at 10% A for 4 min, and reverted to 99% A, maintaining this composition for 5 min.
Mass spectrometry analysis	Mass spectrometry analysis was performed in positive ionization mode. Parameters for positive ionization included a spray voltage of +4.2 kV, sheath gas at 35 arbitrary units, auxiliary gas at 10 arbitrary units, and sweep gas at 2 arbitrary units, with an ion transfer tube and vaporizer temperature of 300°C. MS1 data was acquired at a resolution of 120,000 at m/z 200 with a maximum injection time of 250 ms and AGC target of 5.0 x 10^4. The MS2 of Lidocaine (mz = 235.180) and MEGX (mz = 207.149) fragmentation used higher energy collisional dissociation (HCD) with stepped collision energy (10%, 30%, and 50%), recorded at a resolution of 30,000 at m/z 200.
Raw LC-MS data analysis	All raw LC-MS data analysis was performed on Skyline small molecule software (v24.1). The peak area of Lidocaine (mz = 235.180) and MEGX (mz = 207.149) was extracted from all standards and unknown samples. The standard calibration curve was constructed using Excel, and the unknown concentrations of Lidocaine and MEGX were subsequently quantified by using this calibration curve.

Overall, this comprehensive LC-MS approach enabled robust metabolite profiling and identification, crucial for elucidating metabolic pathways and biomarker discovery in complex biological samples.

7.2.10 Perfusate measurements

7.2.10.1 Blood gas analysis

Perfusate blood gas and biochemistry analysis is described in Chapter 2.5. Briefly, perfusate samples were thawed, vortexed and analysed on a clinical biochemistry analyser via spectrophotometry (Abbott Architect c8000, Abbott diagnostics, Illinois, USA) at the Department of Clinical Biochemistry, John Radcliffe Hospital. The following biochemical measurements were performed:

- Hepatocellular enzymes and injury:
    - ALT (IU/L)
- Hepatic lipid metabolism:
    - Total cholesterol (mmol/L)
    - Total triglycerides (mmol/L)
    - 3-OHB (mmol/L)
- General metabolism:
    - pH
    - Lactate (mmol/L)
    - Glucose (mmol/L)
- Systemic inflammation and metabolic stress:
    - CRP (mg/L)

7.2.10.2 Cytokines

Cytokine multiplex analysis is described in Chapter 2.5.3. For the experimental studies, cytokines (IL-1β, IL-2, IL-6, IL-10 and TNF-α) were measured at 1, 6 and 12h of perfusion and subsequently at 1h and 6h post-whole blood reperfusion.

7.2.11 Bile measurements

Bile (where produced) was measured for pH and glucose concentrations. Bile sampling and measurements are described in Chapter 2.6.

7.2.12 Functional assessment

The ability of each liver to meet functional criteria (indicating suitability for transplantation) was assessed by ex-situ metrics defined by Cambridge (Table 7.11), Birmingham (Table 7.12) and those recently described by Oxford (Table 7.13) in Chapter 6. In addition, to these ex-situ functional metrics, the utility of novel methods to assess ex-situ liver viability including ICG clearance (see Chapter 2.5.5), MEGX and LiMAx tests were performed in the experimental study.

7.2.12.1 Ex-situ functional criteria

A total of three ex-situ functional criteria were utilised to assess ex-situ function for each liver. The ability of each liver to meet these criteria is documented.

Table 7.11. Cambridge NMP criteria for optimal NMP parameters associated with favourable post-transplant outcomes (201). Table reproduced with permission from MDPI (4).

NMP Parameter	Description
Perfusate pH	The ability to maintain perfusate pH > 7.2 (without bicarbonate supplementation exceeding >30 mmol)
Bile pH	A maximum bile pH value > 7.5
Clearance of perfusate lactate	Evidence of a peak reduction in perfusate lactate ≥4.4 mmol/L/kg/h
Metabolism of glucose (perfusate)	Evidence of a reduction in perfusate glucose following 2 h of perfusion OR a glucose value of 10 mmol/L (that also subsequently falls following a challenge 2.5 g of glucose)
Bile glucose concentration	A bile glucose concentration of ≤3 mmol/L OR ≥10 mmol/L less than the perfusate glucose concentration
Hepatocellular injury as demonstrated by perfusate alanine aminotransferase (ALT) level	A perfusate ALT < 6000 IU/L at 2 h of perfusion

Table 7.12. Birmingham NMP criteria as recommended in the 'VITTAL' trial (202). Table reproduced with permission from MDPI (4).

Mandatory NMP Parameter	**Description**
Clearance of perfusate lactate	Evidence of reduction in perfusate lactate ≤2.5 mmol/L
Two or more of the following NMP parameters at 4 h of perfusion	
Perfusate pH	The ability to maintain perfusate pH ≥ 7.3
Glucose	Evidence of glucose metabolism during perfusion
Bile	Evidence of bile production during perfusion
Vascular flows, i.e., hepatic arterial (HA) flow and portal venous (PV) flow	Maintenance of HA flow ≥150 mL/min and PV flow ≥500 mL/min
Macroscopic assessment of donor liver during NMP	Homogenous macroscopic appearance of the liver parenchyma during perfusion

Table 7.13. The DeFat study functional criteria for transplantation (at 6 h of perfusion) (179). Table reproduced with permission from MDPI (4).

NMP Parameter	**Description**
Perfusate pH	The ability to maintain perfusate pH > 7.2
Bile pH	A minimum bile pH value > 7.5 (if bile produced)
Clearance of perfusate lactate	Clearance of lactate to a level <2.5 mmol/L
Metabolism of glucose (perfusate)	Evidence of a reduction in perfusate glucose (spontaneous fall)
Bile glucose concentration	A bile glucose concentration of ≤3 mmol/L OR ≥10 mmol/L lower than the perfusate glucose concentration
Hepatic arterial (HA) flow and portal venous (PV) flow	Maintenance of HA flow ≥100 mL/min and PV flow ≥500 mL/min
Hepatocellular injury as demonstrated by perfusate alanine aminotransferase (ALT) level	A perfusate ALT < 6000 IU/L at 6 h of perfusion

7.2.12.2 ICG

The ICG clearance test (described in Chapter 2.5.5) as described by Liu et al. was performed for the experimental perfusions (238). Briefly, 6.25 ml of 0.1% ICG solution (Verdye™ ICG, Diagnostic Green, GmbH) was injected into the perfusate reservoir at 4 and 10 h during perfusion and subsequently at 4 h during whole blood reperfusion.

Sequential perfusate samples were taken at 1 min, 5 min, 15 min, 30 min, 45 min, 60 min and up to 120 min post-injection. The perfusate serum samples were analysed (100µl in duplicate)

using the CLARIOStar® (BMG LABTECH) microplate reader for fluorescence intensity (FI) of ICG with excitation between 728-743 (728-15) nm and emission between 820-840 (820-20) nm i.e. 728-15/820-20 nm. Data were reported as percentage change in FI from baseline (0 min, pre-injection).

7.2.12.3 Monoethylglycinexylidide (MEGX)

The hepatic conversion of lidocaine to monoethylglycinexylidide (MEGX) was used to assess liver cytochrome P450 system (specifically through CYP3A4) activity during the experimental perfusions (236). A total 4ml of 1% lidocaine solution (as described by Liu et al. (238)) was injected into the perfusate reservoir at 4 and 10h during perfusion and subsequently at 4h during whole blood reperfusion. Sequential perfusate samples were taken 15 and 30 min post-injection.

Stock solutions of lidocaine and MEGX were prepared as described in Table 7.6. A master mix (100µl, 50µg/ml) was prepared by mixing 10µl of lidocaine and MEGX each (at the concentration of 1mg/ml) i.e. a total 20µl with 180µl of HPLC water. A standard set (50µg/ml to 0µg/ml) was subsequently prepared to determine the perfusate drug concentrations. Perfusate analysis of Lidocaine and MEGX was performed by mass spectrometry as described in section 7.2.9 of this chapter.

7.2.12.4 LiMAx

The Maximum Liver Capacity Test (LiMAx test, Humedics GmbH) is described in Chapter 1.7.1 (230–233). This technology was adapted into the set-up of ex-situ liver normothermic machine perfusion during the experimental perfusions and is described in Figure 7.3. An 8ml/kg bolus of 13C-methacetin (4mg/ml, Mohren Apotheke, Germany) was injected into the perfusate reservoir at 1h and 5h of perfusion and subsequently at 5h during whole blood reperfusion and the duration of each test was 60 min. This dosing schedule has been described by Leber et al. in the setting of ex-situ liver perfusion (420). The quantitative outputs included LiMAx curves and LiMAx value was determined using the following formula, adapted from Schurink et al. (234):

DoB_{max}: The maximum delta over baseline kinetics i.e. change in $^{13}CO2$:$^{12}CO2$ ratio

C is a constant: (C= 0.11237)

P: The estimated production rate of CO_2 i.e. 300 mmol/h (per body surface area in m^2)/100 x 17.52 (liver's estimated use of resting energy expenditure) = 52.56

M: The Molar mass of ^{13}C-methacetin (M=166.19 g/mol)

D: The dose of ^{13}C-methacetin dose in mg (½ D)

$$\frac{DoB_{max} * C * P * M}{(½\ D)} = LiMAx\ (\mu g/kg/h)$$

Figure 7.3. The LiMAx FLIP® 4.0 detection device connected to the CO_2 outlet of the OrganOx *metra* oxygenator to allow quantification of the $^{13}CO_2$:$^{12}CO_2$ ratio.

7.3 Results

A total of 13 discarded human livers were recruited during the study period. Of these, 6 livers were perfused as part of a dose finding study to investigate pharmacological HIF modulation during NMP. The subsequent experimental study involved a further 7 perfusions in an ex-situ model of ischaemia-reperfusion injury (IRI). Of these, 4 livers were perfused according to the

established NMP defatting protocol (DeFat) and 3 livers were perfused using the established NMP defatting protocol with the adjunct of pharmacological HIF modulators (DeFat-HIF). One liver in the experimental established NMP defatting protocol (DeFat) group did not demonstrate any evidence of metabolic or synthetic liver function. Whilst perfusion metrics for the ex-situ non-functioning (ENF) liver are described separately, novel functional assessments including ICG clearance, MEGX and LiMAx tests are compared to the experimental DeFat and DeFat-HIF groups to demonstrate the difference between functioning and non-functioning livers. Overall, this liver was an outlier and was therefore excluded from further analysis when comparing the two experimental groups for remaining tissue, perfusate and bile measurement analysis. This ensured valid comparisons were made between the experimental groups. When the primary aim is to investigate the impact of pharmacological interventions on hepatic lipid metabolism, it is essential that all livers exhibit signs of hepatocellular function to ensure that conclusions drawn about the intervention are accurate. Donor demographics, histological evaluation and perfusion characteristics of the non-functioning liver are shown in Table 7.14, Figure 7.4, and Figure 7.5 respectively. Twelve livers were therefore included with 6 livers assigned to dose finding perfusions and 6 assigned to the experimental study. Donor demographics and liver characteristics for these livers are demonstrated in Table 7.15 and 7.16 respectively.

Table 7.14. Donor demographics for non-functioning liver perfused for 12h using the DeFat and reperfused with whole blood for 6h

Age (years)	Gender	Type	BMI (kg/m^2)	Girth (cm)	Cause of death	ALT (IU/L)	Glucose (mmol/L)	CIT (h & min)	Baseline steatosis: Surgeon	Baseline Steatosis: DIA	Baseline Steatosis: Pathology	Liver weight (kg)	Mean vascular flows (artery ml/min & portal L/min)
56	Male	DCD	32.49	112	ICH	72	13.7	20h 13min	Severe	ld-MaS: 39.3% sd-MaS: 10.9% Total: 50.2%	ld-MaS: 40% sd-MaS: 50%	2.3	**Perfusion:** artery 558.3 (±31.3) & portal 1.36 (±0.11) **Reperfusion:** artery 433.3 (±175.1) & portal 0.72 (±0.15)

Abbreviations: ALT, alanine aminotransferase; CIT, cold ischaemia time; DCD, donor after circulatory death; ICH, intracerebral haemorrhage; MaS, macrovesicular steatosis; Ld-MaS, Large droplet macrovesicular steatosis; Sd-MaS, small droplet macrovesicular steatosis.

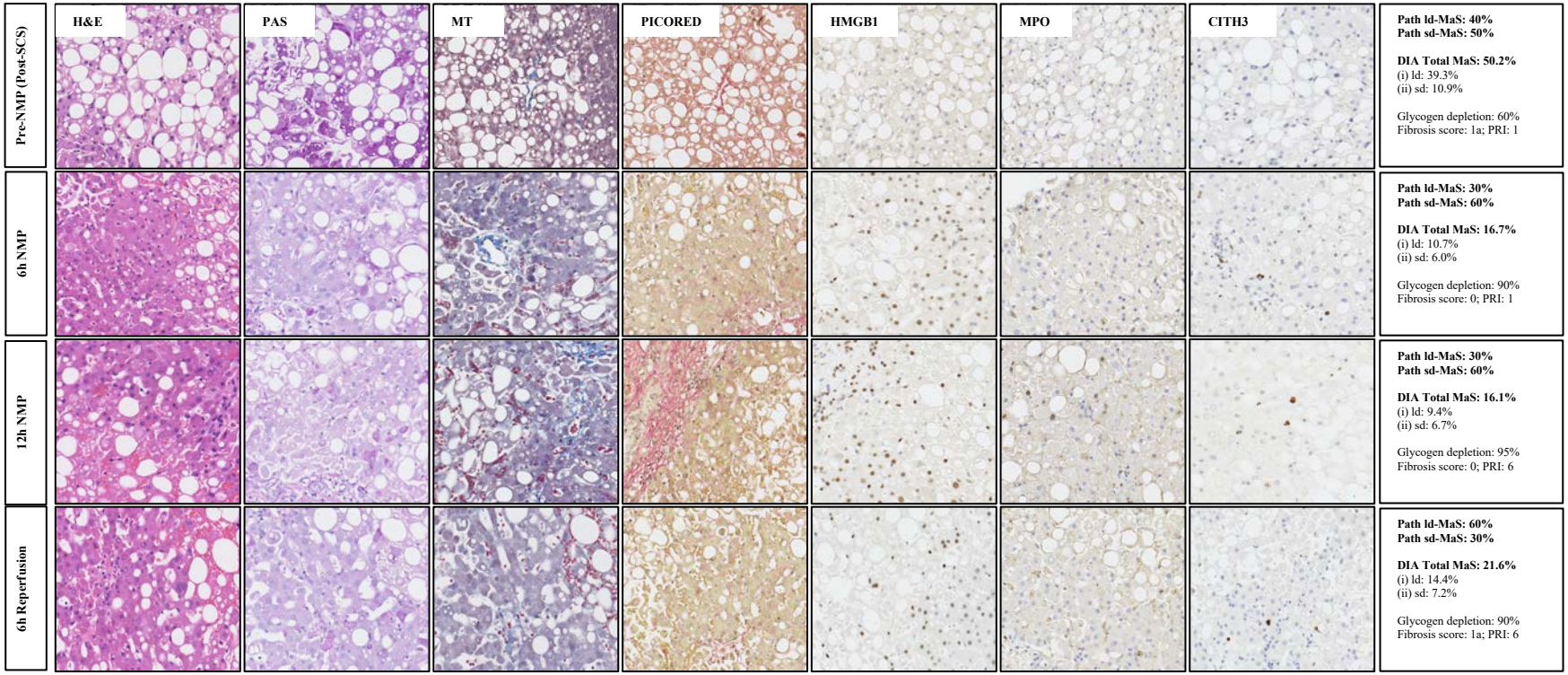

Figure 7.4. Histopathology: H&E, PAS, Masson's Trichome, Picrosirius red, HMGB1, MPO and CITH3 at 0h, 6h, 12h of perfusion and at 6h of reperfusion

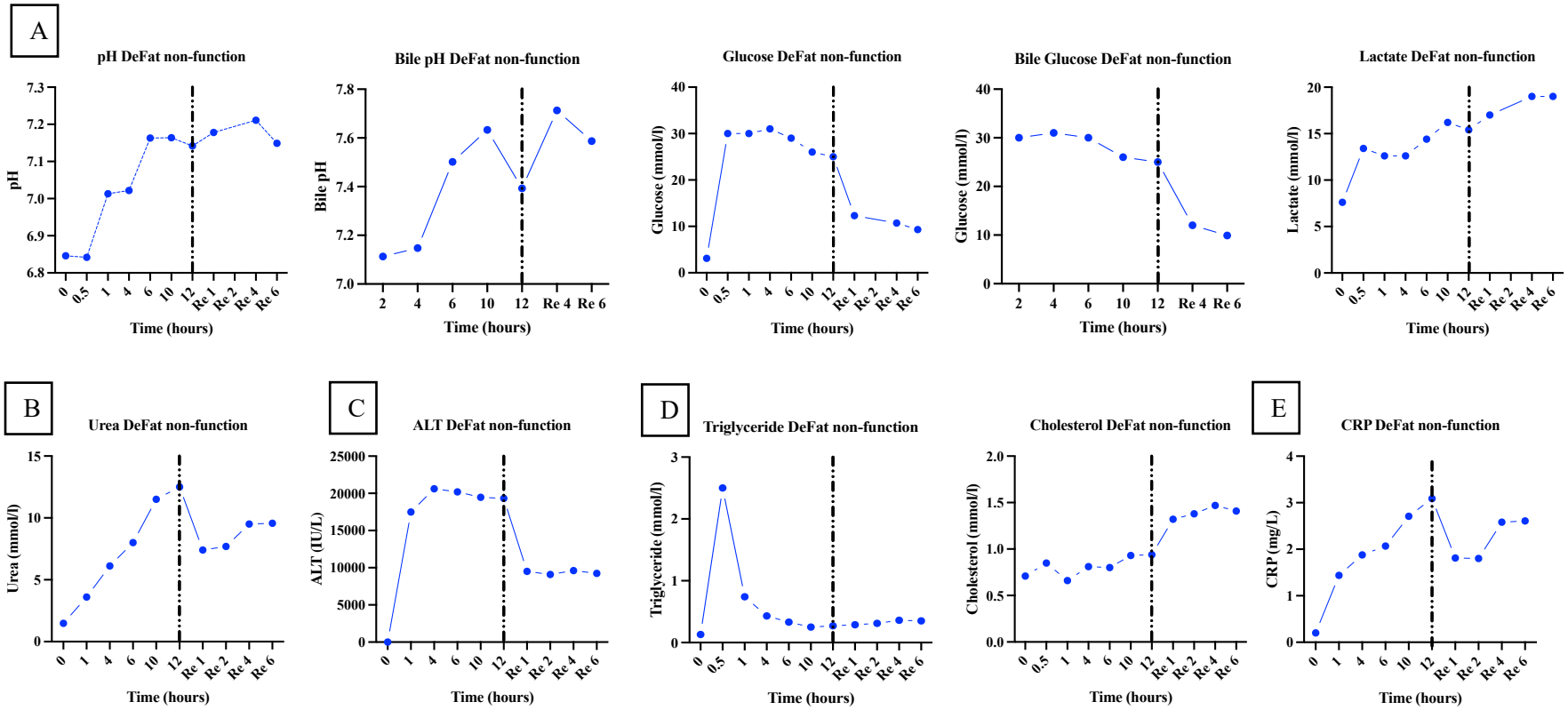

Figure 7.5A-E. Perfusate measurements**:** Low perfusate pH of 6.85 at start of perfusion, 7.14 mmol/l at end of perfusion and 7.15 at end of reperfusion. 30 ml of bicarbonate administered during priming for both the perfusion and reperfusion phases (before liver on board). Total of 230 ml of bicarbonate delivered during perfusion (with 100 ml in the first hour) and only 30 ml delivered during the first hour of reperfusion. Low bile pH of 7.1 at 2h of perfusion, 7.4 at end of perfusion (with 45 ml of bile produced) and 7.6 at end of reperfusion (with 30 ml of bile produced). Slow glucose metabolism during perfusion with value of 25 mmol/l at end of perfusion and 9.3 mmol/l at end of reperfusion (similar trajectory demonstrated in bile glucose values). Increasing lactate during perfusion with value of 15.4 mmol/l at end of perfusion and 19 mmol/l at end of reperfusion **(A)**. Urea production rising during perfusion, reaching peak value of 12.5 mmol/l at end of perfusion and 9.6 mmol/l at end of reperfusion **(B).** Peak in ALT value at 4h of perfusion (19317.7 IU/L) with subsequent decrease at end of reperfusion (9237.8 IU/L) **(C).** Peak in triglyceride value of 0.74 mmol/l at 0.5h of perfusion, decrease at end of perfusion (0.27 mmol/l) and end of reperfusion value of 0.35 mmol/l. Peak cholesterol value at end of perfusion (0.94 mmol/l) and further increase at end of reperfusion (1.41 mmol/l) **(D).** Low CRP values throughout with peak of 3.1 mg/L at end of perfusion and 2.61 mg/L at end of reperfusion. Length of warm ischaemia time (simulated transplant) between the end of perfusion and commencement of reperfusion was 35 min.

Table 7.15. Donor demographics and liver characteristics of livers perfused in the dose finding study

Liver ID	Age (years)	Gender	Type	BMI (kg/m^2)	Girth (cm)	Cause of death	ALT (IU/L)	Glucose (mmol/L)	CIT (h & min)	Baseline steatosis: Surgeon	Baseline Steatosis: DIA	Baseline Steatosis: Pathology	Liver weight (kg)
Liver 1 NMP alone	67	Male	DCD	24.7	92	ICH	14	-	20 h 24 min	Normal (capsular damage)	ld-MaS: 0.15% sd-MaS: 5.15% **Total: 5.3%**	ld-MaS: 0% sd-MaS: 5%	1.65
Liver 2 Standard NMP with DFO (4h)	58	Female	DCD	32	102	ICH	17	9.6	10 h 56 min	Moderate	ld-MaS: 9.2% sd-MaS: 14.5% **Total: 23.7%**	ld-MaS: 20% sd-MaS: 50%	1.56
Liver 3 Standard NMP with DFO (4h) + PT2385 (16h)	57	Male	DCD	31	103	ICH	33	-	14 h 2 min	Mild (capsular damage)	ld-MaS: 1.2% sd-MaS: 3% **Total: 4.2%**	ld-MaS: 5% sd-MaS: 5%	1.70
Liver 4 DeFat (from commencement of NMP)	61	Female	DBD	38	120	Cardiac arrest	65	7.6	11 h 16 min	Moderate	ld-MaS: 13.9% sd-MaS: 25% **Total: 38.9%**	ld-MaS: 30% sd-MaS: 30%	2.0
Liver 5 DeFat + DFO (from commencement of NMP)	75	Male	DBD	26	99	CVA	52	-	11 h 47 min	Mild + stiff (aberrant anatomy)	ld-MaS: 0.3% sd-MaS: 1% **Total: 1.3%**	ld-MaS: 0% sd-MaS: 5%	1.5
Liver 6 DeFat + DFO + PT2385 (DeFat-HIF from commencement of NMP)	56	Female	DBD	25.6	91	ICH	13	13.8	20 h 15 min	Moderate	ld-MaS: 7.9% sd-MaS: 22.7% **Total: 30.6%**	ld-MaS: 10% sd-MaS: 10%	1.56

Abbreviations: ALT, alanine aminotransferase; CIT, cold ischaemia time; DCD, donor after circulatory death; DBD, donation after brain death; ICH, intracerebral haemorrhage; MaS, macrovesicular steatosis; ld-MaS, large droplet macrovesicular steatosis; sd-MaS, small droplet macrovesicular steatosis

Table 7.16. Donor demographics and liver characteristics of livers perfused in the experimental study

Perfusion protocol and warm time between end of NMP, cold flush and commencement of whole blood reperfusion	Age (years)	Gender	Type	BMI (kg/m^2)	Girth (cm)	Cause of death	ALT (IU/L)	Glucose (mmol/L)	CIT (h & min)	Baseline steatosis: Surgeon	Baseline Steatosis: DIA	Baseline Steatosis: Pathology	Liver weight (kg)
DeFat Liver 1 Warm time: 30 min	67	Male	DCD	24.2	94	ICH	22	6.4	17 h 9 min	Mild	ld-MaS: 0.8% sd-MaS: 3.9% **Total: 4.7%**	ld-MaS: 2% sd-MaS: 50%	1.6
DeFat Liver 2 Warm time: 50 min	63	Male	DCD	31.7	115	Hypoxic Brain Injury	62	7.4	11 h 18 min	Moderate	ld-MaS: 16.9% sd-MaS: 4.1% **Total: 21.0%**	ld-MaS: 30% sd-MaS: 10%	2.5
DeFat Liver 3 Warm time: 30 min	77	Male	DBD	25.3	86	ICH	29	7.8	10 h 29 min	Mild (Renal lesion)	ld-MaS: 0.3% sd-MaS: 1.5% **Total: 1.8%**	ld-MaS: 2% sd-MaS: 30%	1.3
DeFat-HIF Liver 1 Warm time: 28 min	60	Female	DCD	33.2	111	CVA	90	6.9	13 h 40 min	Moderate	ld-MaS: 8.1% sd-MaS: 6.4% **Total: 14.5%**	ld-MaS: 5% sd-MaS: 10%	1.5
DeFat-HIF Liver 2 Warm time: 35 min	56	Male	DCD	34.8	118	Hypoxic Brain Injury	69	7.6	11 h 36 min	Moderate	ld-MaS: 24.5% sd-MaS: 4.5% **Total: 29.0%**	ld-MaS: 40% sd-MaS: 20%	2.0
DeFat-HIF Liver 3 Warm time: 15 min	69	Female	DCD	29.4	107	ICH	16	-	13 h 38 min	Moderate	ld-MaS: 0.7% sd-MaS: 2.8% **Total: 3.5%**	ld-MaS: 1% sd-MaS: 40%	2.2

Abbreviations: ALT, alanine aminotransferase; CIT, cold ischaemia time; DCD, donor after circulatory death; DBD, donation after brain death; ICH, intracerebral haemorrhage; MaS, macrovesicular steatosis; ld-MaS, large droplet macrovesicular steatosis; sd-MaS, small droplet macrovesicular steatosis.

Although not statistically significant, the baseline characteristics differed in the experimental groups, with the DeFat-HIF group including donors with a higher-risk profile. The mean age of donors in the DeFat-HIF group was 61.67 ± 6.58 years compared to 69.0 ± 7.21 in the DeFat group. Both the DeFat-HIF and DeFat groups had comparable CIT (778 ± 71.02 min vs. 778.67 ± 218.18 min). Donors in the DeFat-HIF compared to the DeFat group had a higher BMI (32.47 ± 2.77 vs. 27.07 kg/m^2 ± 4.10), waist circumference (112 ± 5.57 cm vs. 98.33 ± 14.98 cm) and pre-retrieval ALT (58.55 ± 38.14 IU/L vs. 37.67 ± 21.36 IU/L). However, the warm time between end of perfusion, flushing of the liver and whole blood reperfusion was shorter in the DeFat-HIF group compared to the DeFat group (26 ± 10.15 min vs. 36.67 ± 11.55 min).

7.3.1 Hypoxia inducible factor quantification: Dose finding study

Quantification of tissue HIF-1α and HIF-2α was performed using western blots as described in Table 7.8 and the primary/secondary antibody concentrations are listed in Table 7.9. Immunohistochemistry (IHC) was also performed for HIF-1α and HIF-2α tissue localisation and to supplement results of the western blots. Perfusate erythropoietin (a downstream target of HIF-2α) measurements were also performed to monitor the effect of PT2385 (a selective HIF-2α dimerisation inhibitor). Western blots, immunohistochemistry and perfusate EPO measurements are demonstrated in Figures below:

- **Liver 1 (NMP alone, control)** 24h duration: Standard NMP perfusion protocol, see Figure 7.6.
- **Liver 2 (NMP + DFO)** 24h duration: Standard NMP protocol (with the addition of DFO at 4h of perfusion), see Figure 7.6.
- **Liver 3 (NMP + DFO + PT2385)** 24h duration: Standard NMP protocol (with the addition of DFO at 4h of perfusion and PT2385 at 16h of perfusion), see Figure 7.7 with tissue and perfusate concentrations of DFO and PT2385 included.
- **Liver 4 (NMP defatting protocol i.e. DeFat)** 18h duration: NMP defatting protocol from the commencement of perfusion, see Figure 7.8.
- **Liver 5 (NMP-DeFat + DFO)** 20h duration: NMP defatting protocol (with addition of DFO from commencement of perfusion), see Figure 7.9.
- **Liver 6 (NMP-DeFat + DFO + PT2385 i.e. DeFat-HIF)** 24h duration: NMP defatting protocol (with addition of DFO and PT2385 from commencement of perfusion), see Figure 7.10.

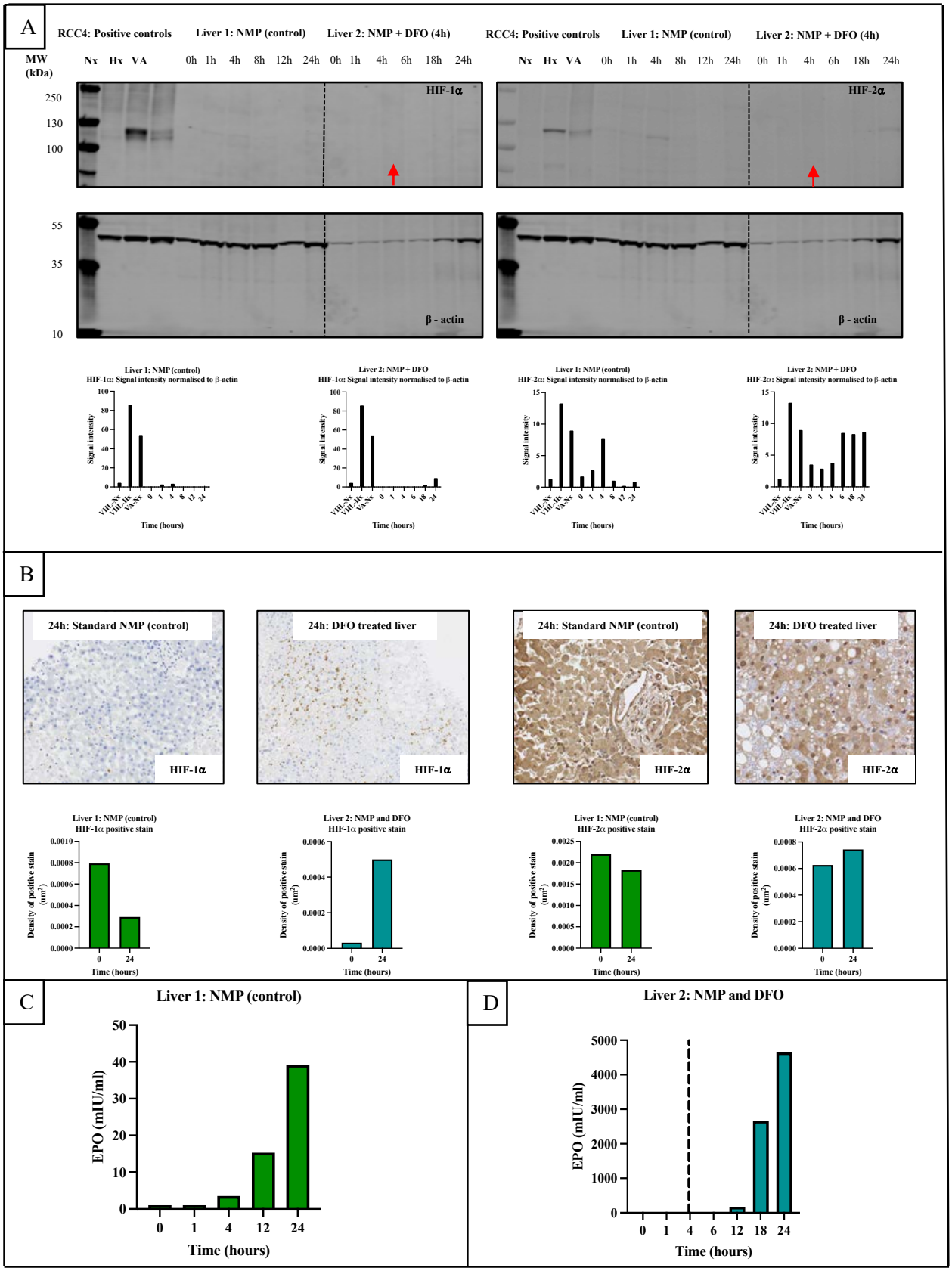

Figure 7.6A-D. Western blot and IHC demonstrating reduction of HIF-1α and HIF-2α expression during standard NMP (Liver 1) and increased expression following delivery of DFO at 4h of perfusion (Liver 2), **(A-B).** Low EPO production (39.2 mIU/ml) at 24h of standard NMP i.e. Liver 1 **(C).** DFO delivered at 4h resulting in high EPO production (4649 mIU/ml) at 24h of perfusion i.e. Liver 2 **(D).**

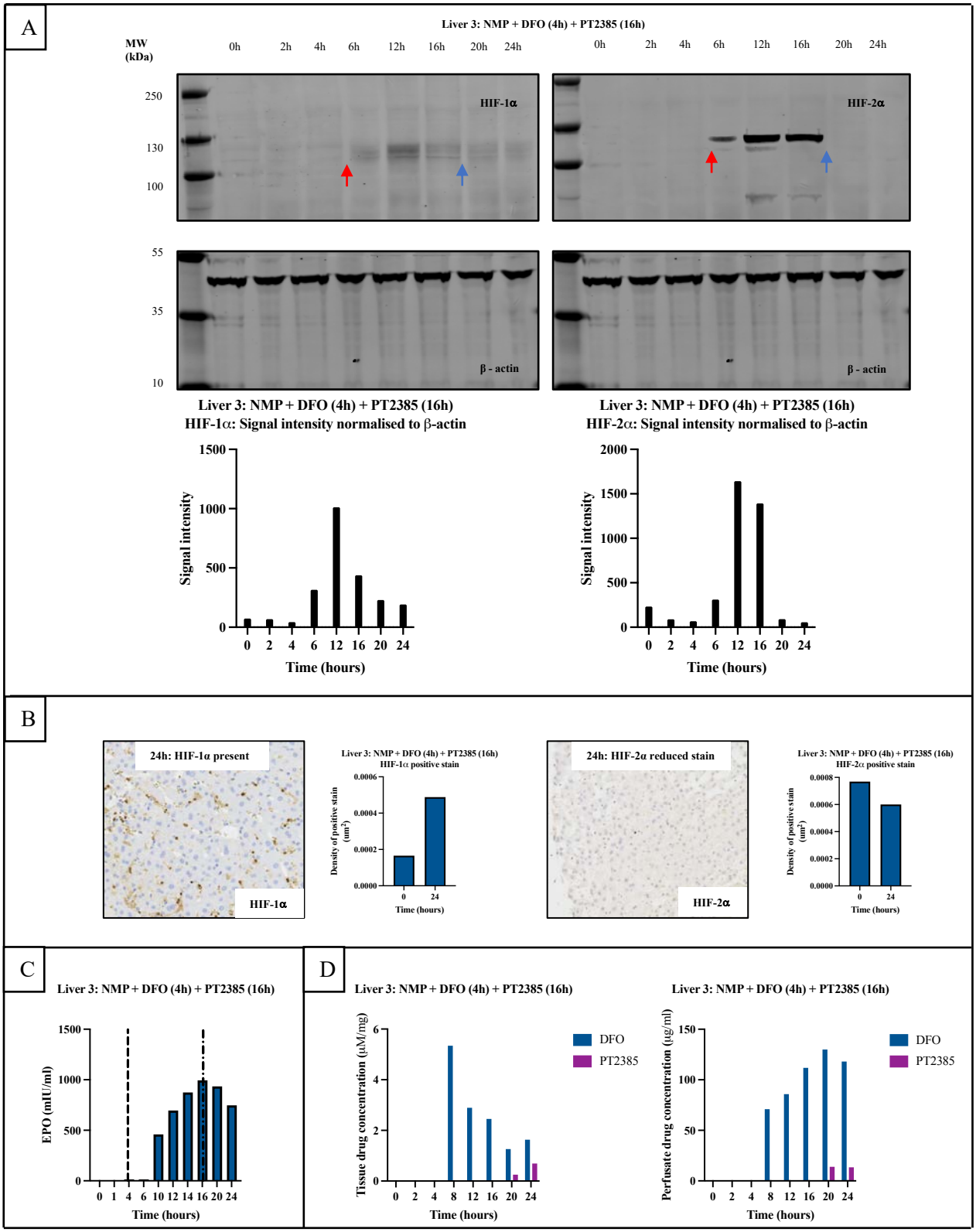

Figure 7.7A-D. Western blot of Liver 3 demonstrating HIF-1α induction (DFO delivered at 4h of NMP) + sequential HIF-2α inhibition (PT2385 delivered at 16h of NMP) **(A).** IHC demonstrating positive HIF-1α stain persisting at 24h of NMP and a reduction in HIF-2α staining **(B).** DFO delivered at 4h resulting in high EPO production (994 mIU/ml) by 16h of NMP. PT2385 delivered at 16h resulting in reduction in EPO (747 mIU/ml) by 24h of NMP **(C).** HPLC measurements: (i) highest DFO tissue concentration at 8h (5.34μM/mg) and perfusate concentration at 20h (129.94μg/ml) and; (ii) highest PT2385 tissue concentration at 24h (0.69μM/mg) and perfusate concentration at 20h (13.97μg/ml) **(D).**

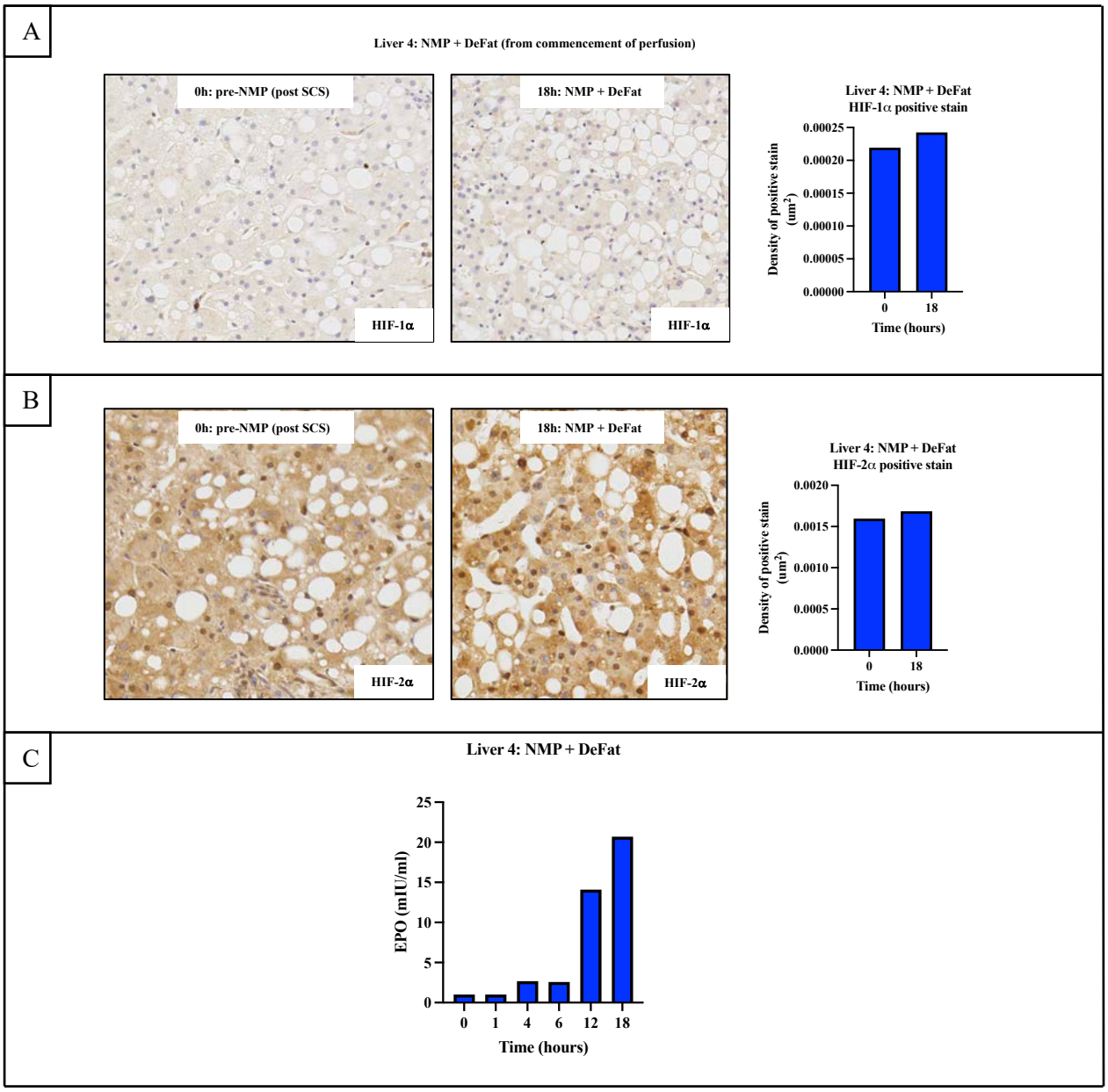

Figure 7.8A-C. IHC of Liver 4 (DeFat) i.e. no delivery of pharmacological HIF modulators. IHC demonstrating similar HIF-1α and HIF-2α positive staining pre-NMP (post-SCS) and at the end of perfusion (18h) **(A-B)**. Low EPO production (in absence of HIF modulators) throughout perfusion with highest EPO measurement at end of perfusion at 18h (20.7mIU/ml) **(C).**

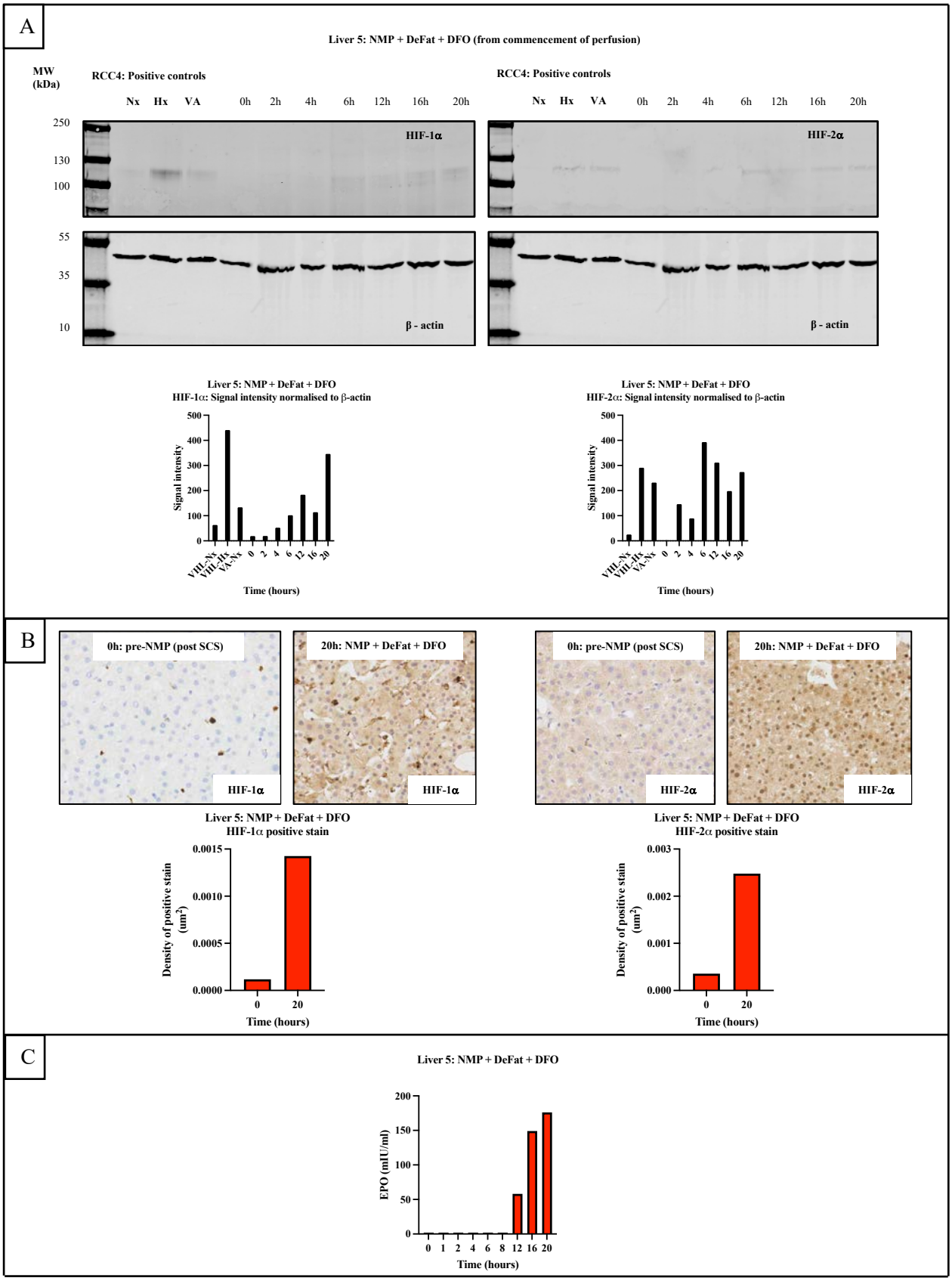

Figure 7.9A-C. Western blot and IHC of Liver 5 (DFO delivered from commencement of perfusion with the established defatting protocol) demonstrating both HIF-1α and HIF-2α induction and positive staining up to the end of NMP (20h) **(A-B).** Perfusate EPO level increasing from 8h and highest (176 mIU/ml) at 20h of NMP **(C).**

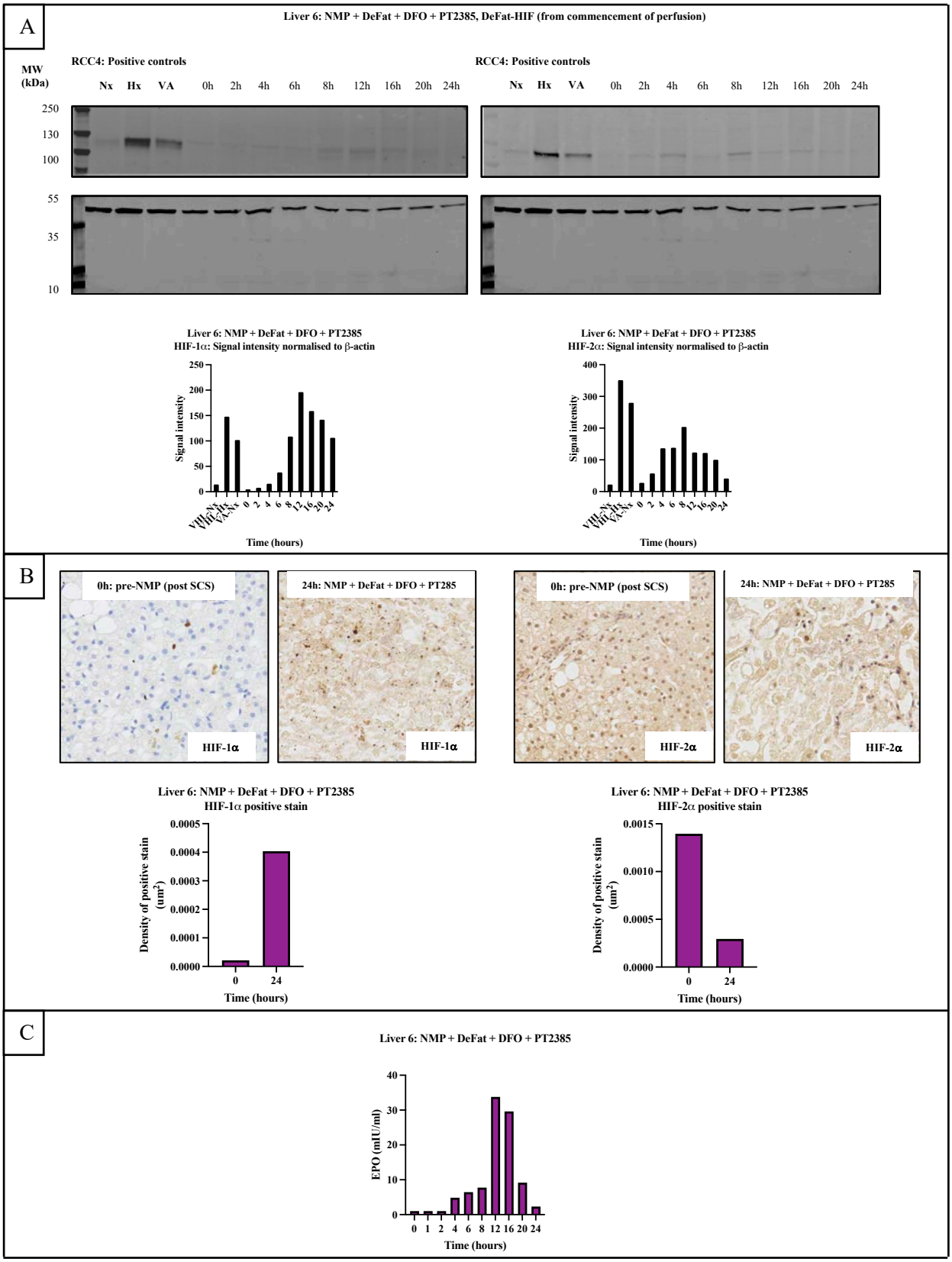

Figure 7.10A-C. Western blot and IHC of Liver 6 (DFO and PT2385 delivered from commencement of perfusion with the established defatting protocol) demonstrating both HIF-1α and HIF-2α induction with persisting HIF-1α and reduction in HIF-2α by end of perfusion i.e. 24h of NMP **(A-B).** Perfusate EPO measurements following similar trajectory to HIF-2α signal intensity and highest at 12h (33.8 mIU/ml) and reduced by 24h (2.33 mIU/ml) **(C).**

7.3.2 Hypoxia inducible factor quantification: Experimental study

Western blots (for HIF-1α and HIF-2α) and perfusate EPO measurements for the DeFat and DeFat-HIF experimental groups are demonstrated in Figure 7.11 and 7.12 respectively.

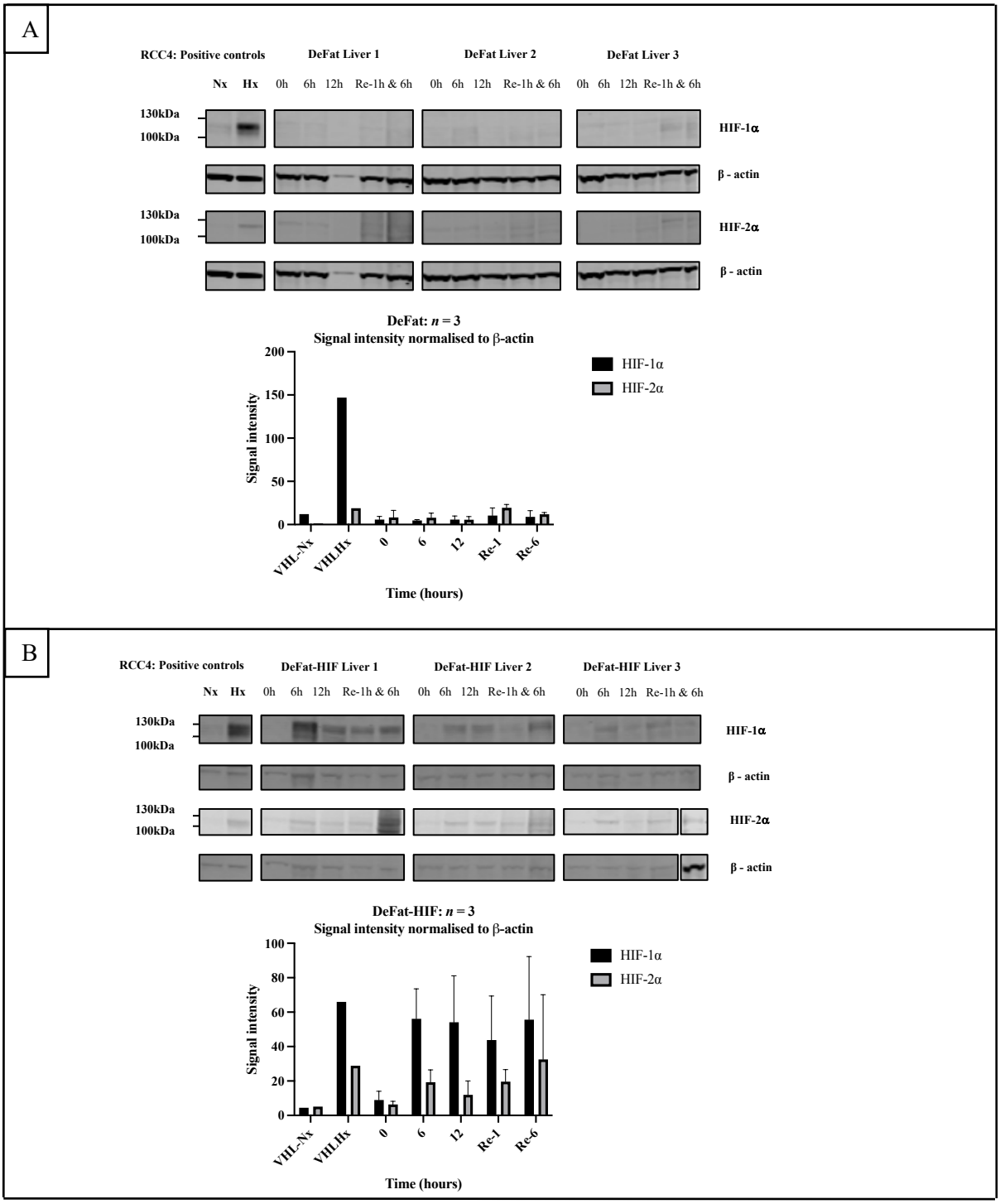

Figure 7.11A-B. Western blots of experimental groups, DeFat (n = 3) and DeFat-HIF (n = 3). DeFat group demonstrating low signal intensity of both HIF-1α and HIF-2α during perfusion (0-12h) with a subsequent increase of both during reperfusion **(A).** DeFat-HIF group demonstrating high signal intensity of HIF-1α (relative to HIF-2α) during perfusion with subsequent increase of both during reperfusion **(B)**.

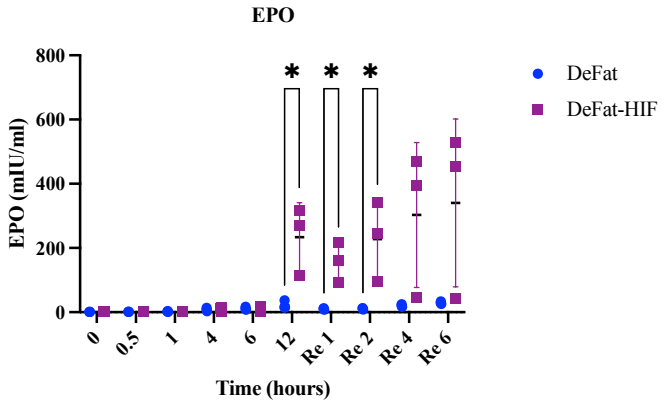

Figure 7.12A-B. Perfusate EPO concentration during perfusion with peak at 12h of perfusion (DeFat-HIF: 233.67 mIU/ml vs. DeFat: 22.37 mIU/ml, $P = 0.028$) and further increase during 6h reperfusion in the DeFat-HIF group (DeFat-HIF: 340.23 mIU/ml vs. DeFat: 29.43 mIU/ml, $P = 0.108$) **(B)**. Multiple unpaired t-tests, data reported as mean ± SD. * $P \leq 0.05$, ** $P \leq 0.01$, *** $P \leq 0.001$ and **** $P \leq 0.0001$.

7.3.3 Histological assessment

7.3.3.1 Dose finding study

Donor demographics and liver characteristics for the dose finding perfusions are described in Table 7.15. Histological assessment for the six livers included in the dose finding study are demonstrated in Figure 7.13 including H&E, PAS and Masson's Trichome stains. Three out of the 6 livers demonstrated a reduction in steatosis following both histopathologist assessment and quantification using Visiopharm® digital image analysis software:

- Liver 2 (Standard NMP with DFO delivered at 4h) demonstrated a reduction in ld-MaS from 20% at baseline to 10% at the end of 24h NMP (as assessed by the histopathologist). Similarly, there was a reduction in Total MaS from 23.7% at baseline to 11.9% at the end of 24h NMP (quantified using Visiopharm® digital image analysis software).
- Liver 3 (Standard NMP with DFO delivered at 4h and PT2385 at 16h) demonstrated a reduction in ld-MaS from 5% at baseline to 0.1% at the end of 24h NMP (as assessed by the histopathologist). Similarly, a reduction in Total MaS from 4.2% at baseline to 1.4% at the end of 24h NMP was observed (quantified using Visiopharm® digital image analysis software).
- Liver 6 (DeFat-HIF: NMP + DeFat + DFO + PT2385 from the commencement of perfusion) demonstrated a reduction in ld-MaS from 10% at baseline to 5% at 12h of

NMP. The 24h biopsy demonstrated marked reduction in steatosis, however, the histopathologist was unable to quantify the degree of steatosis due to concurrent hepatocyte necrosis. The histological appearance was consistent with bacterial/fungal overgrowth suggesting contamination during the perfusion and for this reason, the percentage of steatosis for the 24h biopsy was not reported by the histopathologist. Comparatively, when the steatosis was quantified using the Visiopharm® digital image analysis software, a reduction in Total MaS was demonstrated from 30.6% at baseline to 15.9% at 12h and 7% at the end of 24h NMP. Despite the significant necrosis on the 24h biopsy, the digital image analysis software was able to provide a quantitative output for the percentage of steatosis.

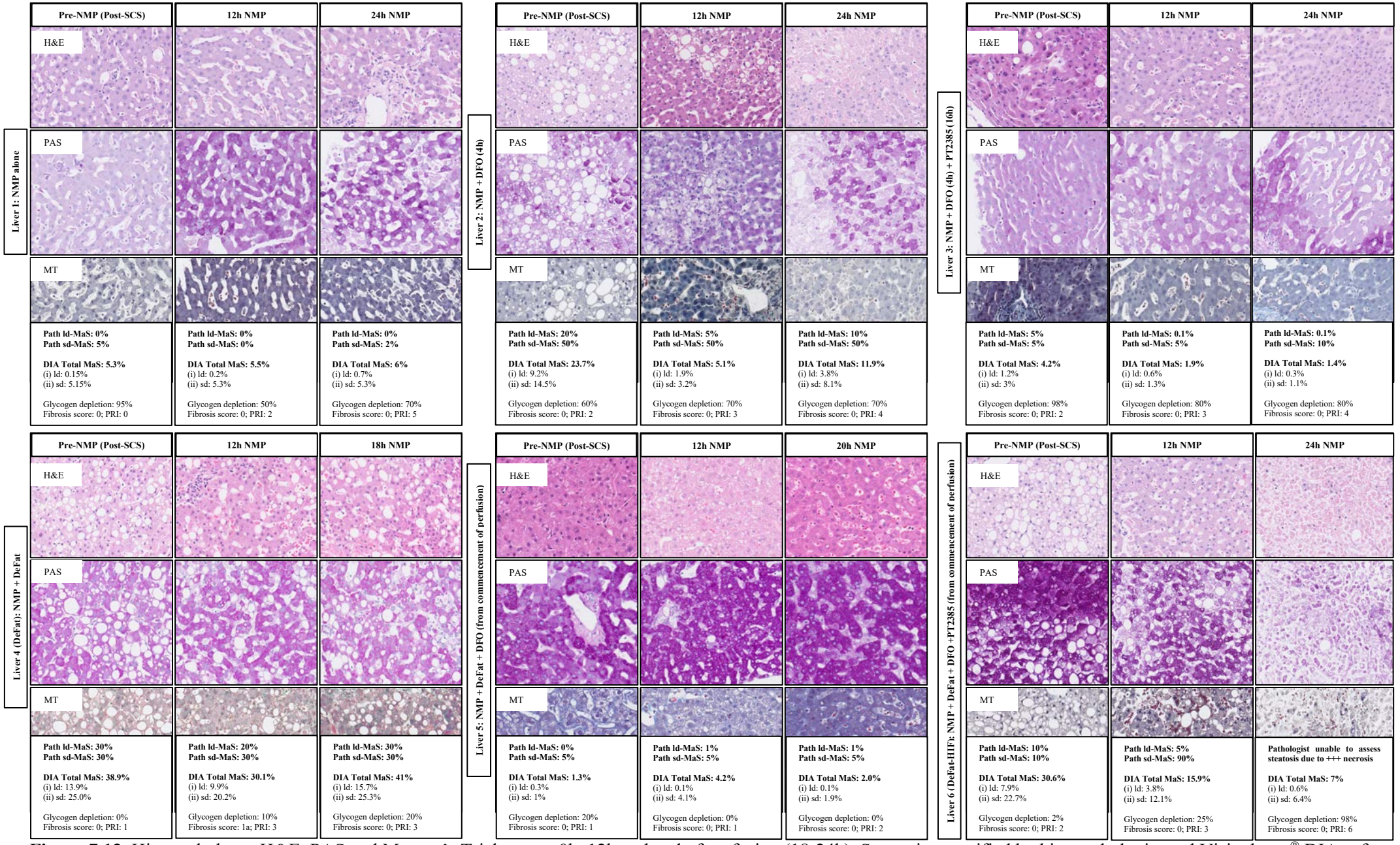

Figure 7.13. Histopathology: H&E, PAS and Masson's Trichome at 0h, 12h and end of perfusion (18-24h). Steatosis quantified by histopathologist and Visiopharm® DIA software

7.3.3.2 Experimental study

Donor demographics and liver characteristics for the experimental study are described in Table 7.16. A non-significant reduction in ld-MaS was demonstrated in the DeFat-HIF group with a reduction in ld-MaS from 15.3 ± 21.5% at baseline to 7.7 ± 10.7% at the end of 6h reperfusion (as assessed by the histopathologist). However, a significant reduction in ld-MaS from 11.1 ± 12.2% at baseline to 4.8 ± 5.9% at the end of 6h reperfusion, $P = 0.0097$ (quantified using Visiopharm® digital image analysis software).

There was no significant difference identified between timepoints in sd-MaS when reported by the histopathologist for both the DeFat and DeFat-HIF group. However, although not significant, changes in sd-MaS quantified using the Visiopharm® digital image analysis software demonstrated increase in sd-MaS in the DeFat-HIF group from 4.6 ± 1.8% at baseline to 8.7 ± 3.8% at 12h of perfusion with a concurrent decrease in sd-MaS from 8.7 ± 3.8% at 12h of perfusion to 4.3 ± 2.3% following 6h of whole blood reperfusion.

There was no significant reduction identified between timepoints in Total MaS when reported by the histopathologist for both the DeFat and DeFat-HIF group. However, changes in Total-MaS quantified using the Visiopharm® digital image analysis software demonstrated a significant reduction in the DeFat-HIF group from 15.7 ± 12.8% at baseline, 15.9 ± 12.4% at 6h and 16.6 ± 10.5% at 12h of perfusion to 8.7 ± 6.2% at 6h of reperfusion ($P = 0.0376$, $P = 0.0301$ and $P = 0.0184$ respectively).

Glycogen depletion between timepoints was similar between the DeFat and DeFat-HIF groups. However, at 6h reperfusion the total percentage of glycogen depletion was higher in the DeFat-HIF group compared to the DeFat group (73.3 ± 37.5% vs 59.7 ± 48.8%; $P = 0.720$).

The change in steatosis (both histopathologist report and Visiopharm® DIA quantification) and glycogen content during perfusion and reperfusion is demonstrated in Figure 7.14. Histological assessment for the three livers included in the DeFat group and three livers in the DeFat-HIF group are demonstrated in Figure 7.15 and 7.16 respectively including H&E, PAS, Masson's Trichome and Picrosirius RED stains.

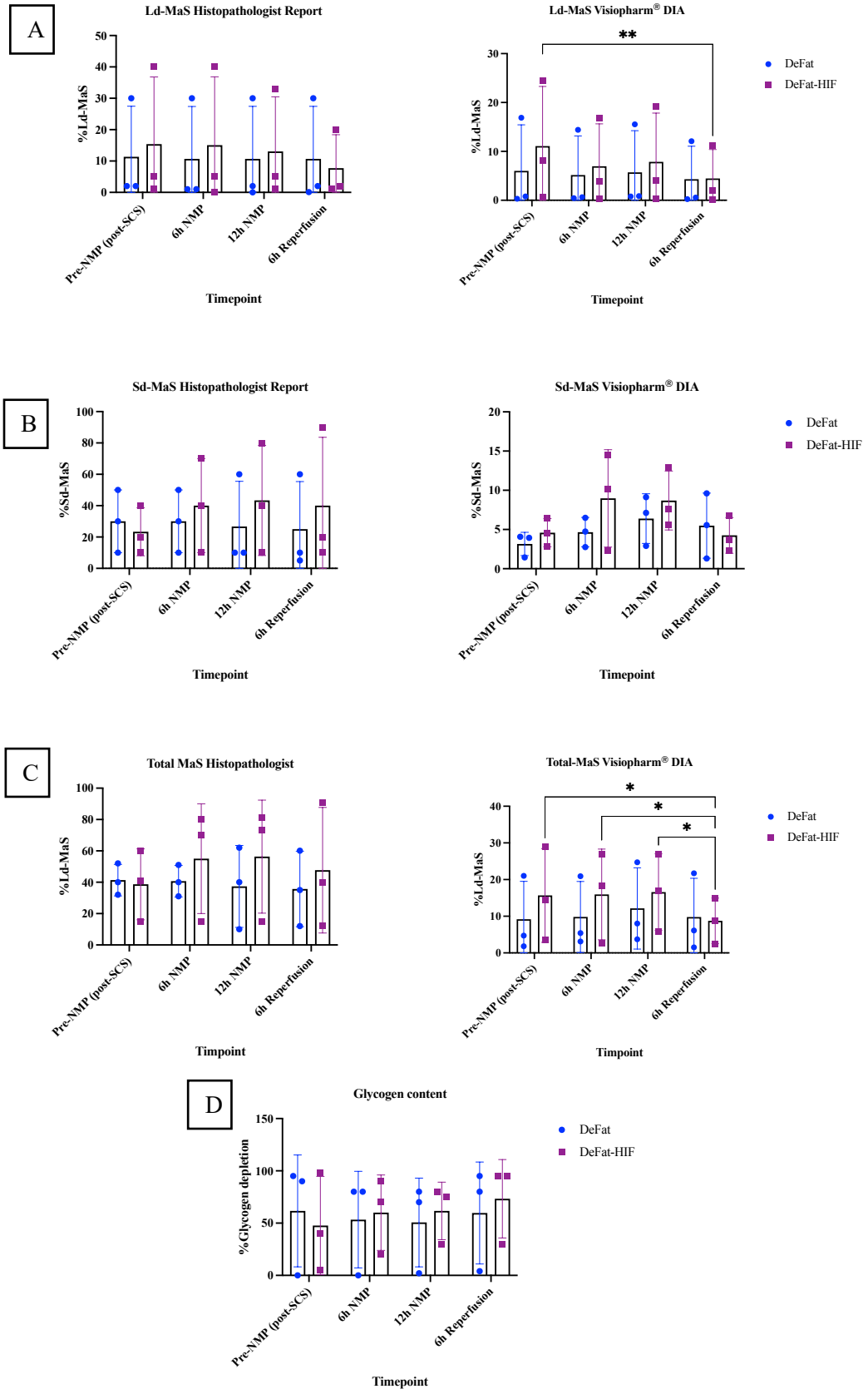

Figure 7.14A-C. Steatosis degree and glycogen content. Multiple unpaired t-tests, data reported as mean ± SD and mixed effect analysis for repeated measures with post-hoc tukey correction to adjust for multiple comparisons between timepoints. * $P \leq 0.05$, ** $P \leq 0.01$, *** $P \leq 0.001$ and **** $P \leq 0.0001$.

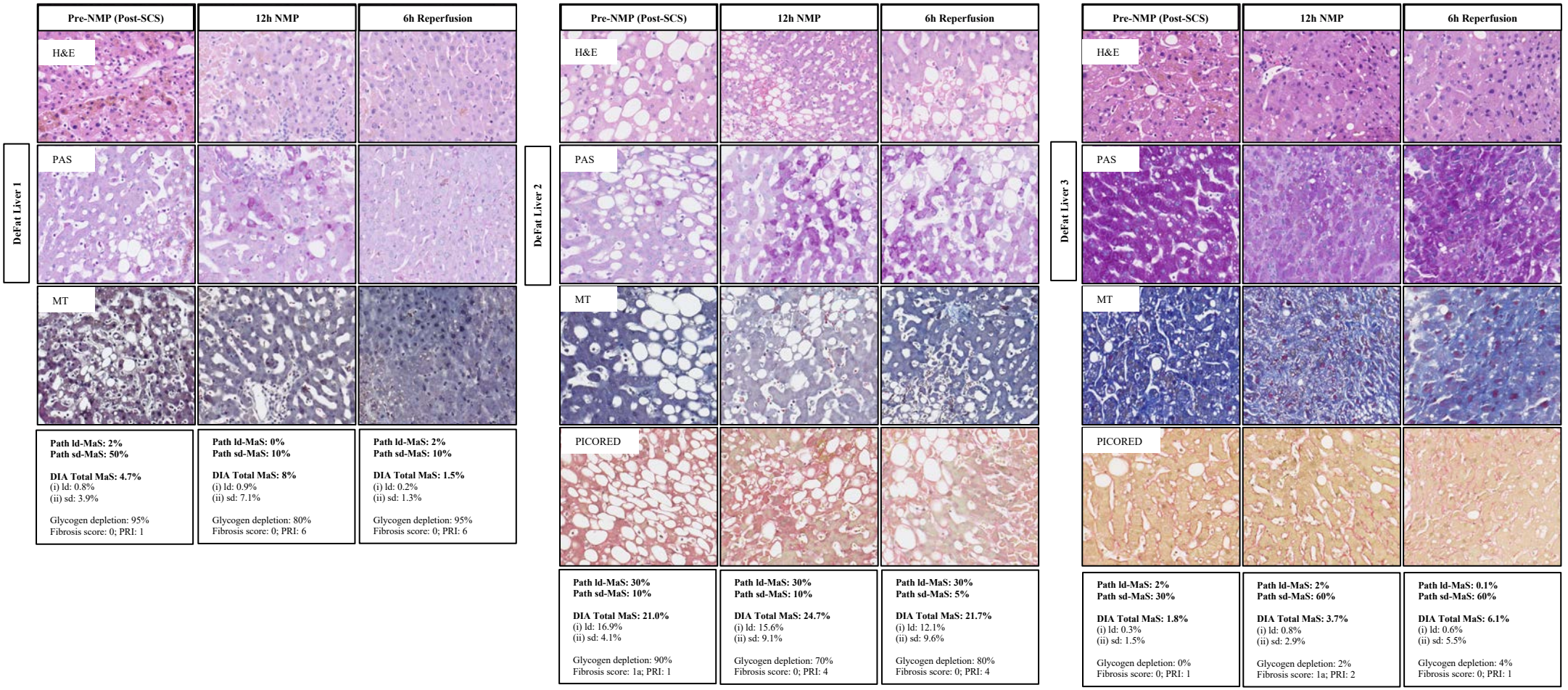

Figure 7.15. Experimental study (Group 1, DeFat): three livers perfused using the established NMP defatting protocol. Histopathology: H&E, PAS, Masson's Trichome and Picrosirius red at 0h, 12h of perfusion and at 6h of reperfusion. Steatosis quantified by histopathologist and Visiopharm® DIA software.

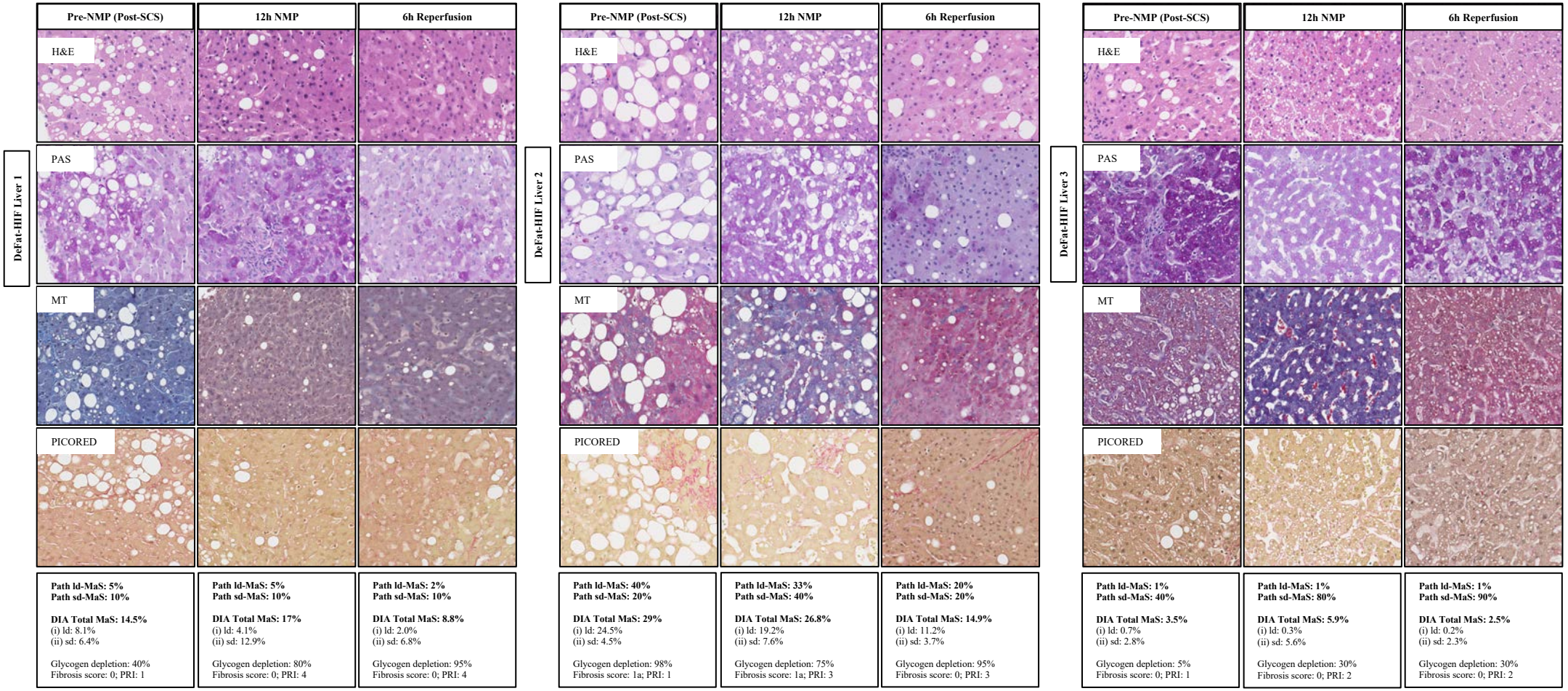

Figure 7.16. Experimental study (Group 2, DeFat-HIF): three livers perfused using the established NMP defatting protocol with the adjunct of pharmacological HIF modulators (DFO and PT2385). Histopathology: H&E, PAS, Masson's Trichome and Picrosirius red at 0h, 12h of perfusion and at 6h of reperfusion. Steatosis quantified by histopathologist and Visiopharm® DIA software.

7.3.4 Perfusate analysis and bile biochemistry: Dose finding study

All 6 livers in the dose finding study demonstrated evidence of glucose metabolism (spontaneous fall in glucose), bile production, lactate clearance and normalisation of pH during perfusion. All livers had comparable ALT measurements of < 6000 IU/L at the end of perfusion, except Liver 6 (DeFat-HIF: DeFat + DFO + PT2385 from commencement of NMP) demonstrated a rise in ALT from 2893.9 IU/L at 6h of perfusion to 14024 IU/L at 24h (end of perfusion). This also correlated with significant necrosis evident on the 24h biopsy and suspected contamination of the perfusion circuit supported by histological features highly suspicious of bacterial/fungal overgrowth as reported by the histopathologist. The perfusate measurements (per liver) from 0h to a maximum of 24h are listed in Table 7.17. The total bicarbonate supplementation, total bile production and where available bile pH and glucose values are listed in Table 7.18.

Table 7.17. Dose finding study biochemical measurements during perfusion

NMP protocol & Biochemical tests		0h	0.5h	1h	6h	12h	18h	20h	24h
Liver 1 NMP alone	**ALT (IU/L)**	6	16772.3	17488.2	11315.2	9598.6	-	-	4415.7
	TG (mmol/L)	0.18	0.21	0.1	0.25	0.42	-	-	0.93
	Chol (mmol/L)	0.24	0.17	0.17	0.38	0.47	-	-	0.64
	3-OHB (mmol/L)	-	-	-	-	-	-	-	-
	pH	6.58	6.80	6.90	7.12	7.14	-	-	7.01
	Lactate (mmol/L)	20.7	8.7	6.31	1.04	1.43	-	-	0.79
	Glucose (mmol/L)	8.4	6.7	8.6	20.9	12.6	-	-	0.6
	Urea (mmol/L)	3.01	3.53	3.94	18.86	25	-	-	38.91
	CRP mg/L	0.2	3.11	4.34	47.44	93.66	-	-	197.76
Liver 2 Standard NMP with DFO (4h)	**ALT (IU/L)**	6	6775.9	5731.7	5474.3	4560.9	4722.8	-	5647.2
	TG (mmol/L)	0.31	1.52	1.34	0.29	0.31	0.64	-	2.05
	Chol (mmol/L)	0.53	0.24	0.43	0.45	0.61	1.0	-	1.36
	3-OHB (mmol/L)	0	0.42	0.44	0.84	0.85	0.79	-	1.65
	pH	6.5	6.41	6.76	7.12	7.11	7.04	-	6.95
	Lactate (mmol/L)	20	7.76	5.96	1.4	2.5	0.8	-	1.1
	Glucose (mmol/L)	11.0	23.1	27	20	13.1	3.3	-	9.1
	Urea (mmol/L)	3.17	2.36	3.07	9.03	9.13	16.7	-	23.98
	CRP mg/L	0.20	1.38	1.69	41.85	148.49	245.88	-	327.39
Liver 3 Standard NMP with DFO (4h) + PT2385 (16h)	**ALT (IU/L)**	6	3103.6	3701.1	3495.2	3777.6	3217	3725.9	4036
	TG (mmol/L)	0.13	0.79	0.57	0.36	0.54	0.44	0.5	0.54
	Chol (mmol/L)	0.39	0.72	0.76	0.74	1.13	1.39	1.69	2.08
	3-OHB (mmol/L)	0.00	0.23	0.44	0.43	0.27	0.43	0.44	0.47
	pH	7.44	7.71	7.36	7.51	7.56	7.43	7.37	7.33
	Lactate (mmol/L)	20.7	15.5	5.53	1.03	0.68	0.73	0.91	1.17
	Glucose (mmol/L)	7.6	10.7	10.8	1.7	0	0	0	0
	Urea (mmol/L)	2.01	0.72	5.62	16.48	28.37	42.38	50.04	61.58
	CRP mg/L	0.20	0.98	3.76	73.74	170.61	225.95	293.19	344.06
Liver 4 DeFat (from commencement of NMP)	**ALT (IU/L)**	6	8605.8	11917.8	7224.2	7181.3	5450.4	-	-
	TG (mmol/L)	0.12	1.53	1.68	0.38	0.51	0.50	-	-
	Chol (mmol/L)	0.18	0.17	0.17	0.25	0.53	0.55	-	-
	3-OHB (mmol/L)	0.01	0.704	0.856	0.979	1.331	1.11	-	-
	pH	7.09	6.90	6.91	7.07	7.15	7.12	-	-
	Lactate (mmol/L)	12.1	8.59	7.95	4.38	1.91	1.69	-	-
	Glucose (mmol/L)	30	37	42	36	31	20.6	-	-
	Urea (mmol/L)	2.23	3.12	4	9.57	19.94	20.77	-	-
	CRP mg/L	0.5	3.17	4.57	11.83	53.73	82.01	-	-
Liver 5 DeFat + DFO (from commencement of NMP)	**ALT (IU/L)**	6.1	788.5	1015.3	1604.5	1249	2488.6	3558.8	-
	TG (mmol/L)	0.11	0.42	0.59	0.75	0.61	0.98	1.45	-
	Chol (mmol/L)	0.32	0.4	0.61	1	0.69	1.1	1.16	-
	3-OHB (mmol/L)	-	-	-	-	-	-	-	-
	pH	7.20	7.28	7.11	7.32	7.25	7.27	7.14	-
	Lactate (mmol/L)	7.1	9.9	9.7	7.1	4.1	4.7	6.1	-
	Glucose (mmol/L)	2.6	29	39	39	27	17.1	10.1	-
	Urea (mmol/L)	1.21	2.97	4.51	11.21	13.76	18.25	19.83	-
	CRP mg/L	0.2	0.4	0.61	1.01	5.2	16.06	25.77	-
Liver 6 DeFat + DFO + PT2385 (DeFat-HIF from commencement of NMP)	**ALT (IU/L)**	16.3	-	2231.1	2893.9	3428.1	-	-	14024
	TG (mmol/L)	0.27	-	0.51	0.49	0.92	-	-	1.08
	Chol (mmol/L)	0.3	-	0.31	0.53	0.88	-	-	2.77
	3-OHB (mmol/L)	0	-	0.24	0.67	1.73	-	-	0.82
	pH	6.88	-	7.13	7.33	7.28	-	-	7.41
	Lactate (mmol/L)	27.0	-	18.95	13.5	8.38	-	-	5.15
	Glucose (mmol/L)	11.5	-	23.2	33	28	-	-	19.2
	Urea (mmol/L)	3.5	-	2.11	3.42	6.77	-	-	10.34
	CRP mg/L	1.29	-	1.29	16.73	40.8	-	-	58.01

Table 7.18. Total bicarbonate supplementation, bile production, bile pH and glucose

NMP protocol & Biochemical tests		0h	0.5h	1h	6h	12h	18h	20h	24h
Liver 1 NMP alone	**pH**	-	-	-	-	-	-	-	-
	Glucose (mmol/L)	-	-	-	-	-	-	-	-
	Total HCO3- supplementation: 30ml								
	Total bile production: 190ml								
Liver 2 DFO (4h)	**pH**	-	-	6.85	7.54	7.50	7.49	-	7.57
	Glucose (mmol/L)	-	-	7	2	3	-	-	5.4
	Total HCO3- supplementation: 70ml								
	Total bile production: 160ml								
Liver 3 DFO (4h) + PT2385 (16h)	**pH**	-	-	-	-	-	-	-	-
	Glucose (mmol/L)	-	-	-	-	-	-	-	-
	Total HCO3- supplementation: 60ml								
	Total bile production: 110ml								
Liver 4 DeFat (from commencement of NMP)	**pH**	-	-	-	7.15	7.33	7.27	-	-
	Glucose (mmol/L)	-	-	-	36	30	20.3	-	-
	Total HCO3- supplementation: 90ml								
	Total bile production: 230ml								
Liver 5 DeFat + DFO (from commencement of NMP)	**pH**	-	-	-	7.66	7.84	-	7.43	-
	Glucose (mmol/L)	-	-	-	28	17.2	-	6.6	-
	Total HCO3- supplementation: 90ml								
	Total bile production: 25ml								
Liver 6 DeFat + DFO + PT2385 (DeFat-HIF from commencement of NMP)	**pH**	-	-	7.22	7.66	-	-	7.33	7.46
	Glucose (mmol/L)	-	-	16.2	15.7	-	-	17.2	16.7
	Total HCO3- supplementation: 210ml								
	Total bile production: 106ml								

7.3.5 Perfusate analysis and bile biochemistry: Experimental study

Sequential perfusate samples were collected during perfusion and reperfusion (with the sampling schedule described in Table 7.2) from all 6 livers perfused in the experimental study i.e. DeFat (n = 3) and DeFat-HIF (n = 3).

7.3.5.1 Hepatocellular injury

DeFat-HIF livers demonstrated a comparable degree of hepatocellular injury when compared to DeFat livers with a high mean ALT at the end of 12h perfusion (5320.9 ± 3048.97 IU/L vs. 5571.83 ± 5059.96 IU/L, P = 0.762) and at the end of 6h reperfusion (6604.27 ± 5578.86 IU/L vs. 3466.27 ± 2264.21 IU/L, P = 0.418), Figure 7.17A.

There was no significant difference in mean perfusate cfDNA concentration at each timepoint between groups. However, significant rise in cfDNA was observed in the DeFat group from 2.52 ± 2.35 µg/ml at 1h of perfusion to 4.90 ± 1.05 µg/ml at the end of 6h reperfusion, P = 0.0379. Similarly, a rise was observed in the DeFat-HIF group from 2.03 ± 1.57 µg/ml at 1h of perfusion to 5.46 ± 1.47 µg/ml at 6h of perfusion, 4.50 ± 0.26 µg/ml at the end of 12h perfusion and 4.46 ± 0.68 µg/ml at 1h of reperfusion (P = 0.0023, P = 0.0294 and P = 0.0329 respectively). Only the DeFat-HIF group demonstrated a non-significant reduction in peak cfDNA concentration of 5.46 ± 1.47 µg/ml at 6h of perfusion to 3.83 ± 1.81 µg/ml at the end of 6h reperfusion, Figure 7.17B.

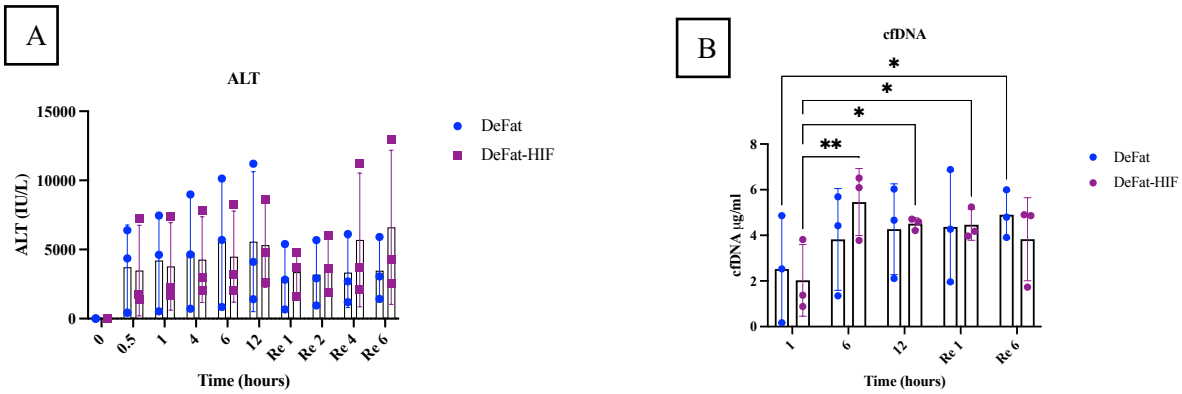

Figure 7.17A-B. Measurements of hepatocellular injury during perfusion and reperfusion. Multiple unpaired t-tests, data reported as mean ± SD and mixed effect analysis for repeated measures with post-hoc tukey correction to adjust for multiple comparisons between timepoints. * $P \leq 0.05$, ** $P \leq 0.01$, *** $P \leq 0.001$ and **** $P \leq 0.0001$.

7.3.5.2 Hepatic lipid metabolism

There was no significant difference in mean perfusate triglyceride concentration at each timepoint between groups. However, the DeFat-HIF group demonstrated a greater degree of triglyceride mobilisation with an increase in perfusate triglyceride was observed between baseline from 0.13 ± 0.04 mmol/L to 0.98 ± 0.58 mmol/L at the end of 12h perfusion, P = 0.0137 and; 0.98 ± 0.44 mmol/L at the end of 6h reperfusion, P = 0.0126. This difference was not observed in the DeFat group, Figure 7.18A.

There was no significant difference in mean perfusate cholesterol concentration at each timepoint between groups. Whilst both groups demonstrated mobilisation of cholesterol during

perfusion and reperfusion, a significant increase was only observed in the DeFat group between timepoints, Figure 7.18B.

There was no significant difference in mean perfusate 3-OHB concentration at each timepoint between groups. However, the DeFat group demonstrated a greater degree of fatty acid β-oxidation with an increase in perfusate 3-OHB observed at 1h of perfusion from 0.52 ± 0.12 mmol/L to 1.72 ± 0.87 mmol/L at the end of 12h perfusion, $P = 0.0030$ and; 1.43 ± 0.43 mmol/L at the end of 6h reperfusion, $P = 0.0267$.

In the DeFat-HIF group, there was also evidence of fatty acid β-oxidation (albeit to a lesser extent) increase in perfusate 3-OHB observed with a perfusate concentration of 0.35 ± 0.09 mmol/L at 1h to 1.39 ± 0.52 mmol/L at the end of 6h reperfusion ($P = 0.0102$). A further increase was observed during reperfusion with a perfusate concentration of 0.54 ± 0.15 mmol/L at 1h reperfusion to 1.39 ± 0.52 mmol/L at the end of 6h reperfusion, $P = 0.0402$. The mean perfusate concentrations of 3-OHB at the end of 6h reperfusion was comparable between the DeFat-HIF and DeFat groups (1.39 ± 0.52 mmol/L vs. 1.43 ± 0.43 mmol/L, $P = 0.930$), Figure 7.18C.

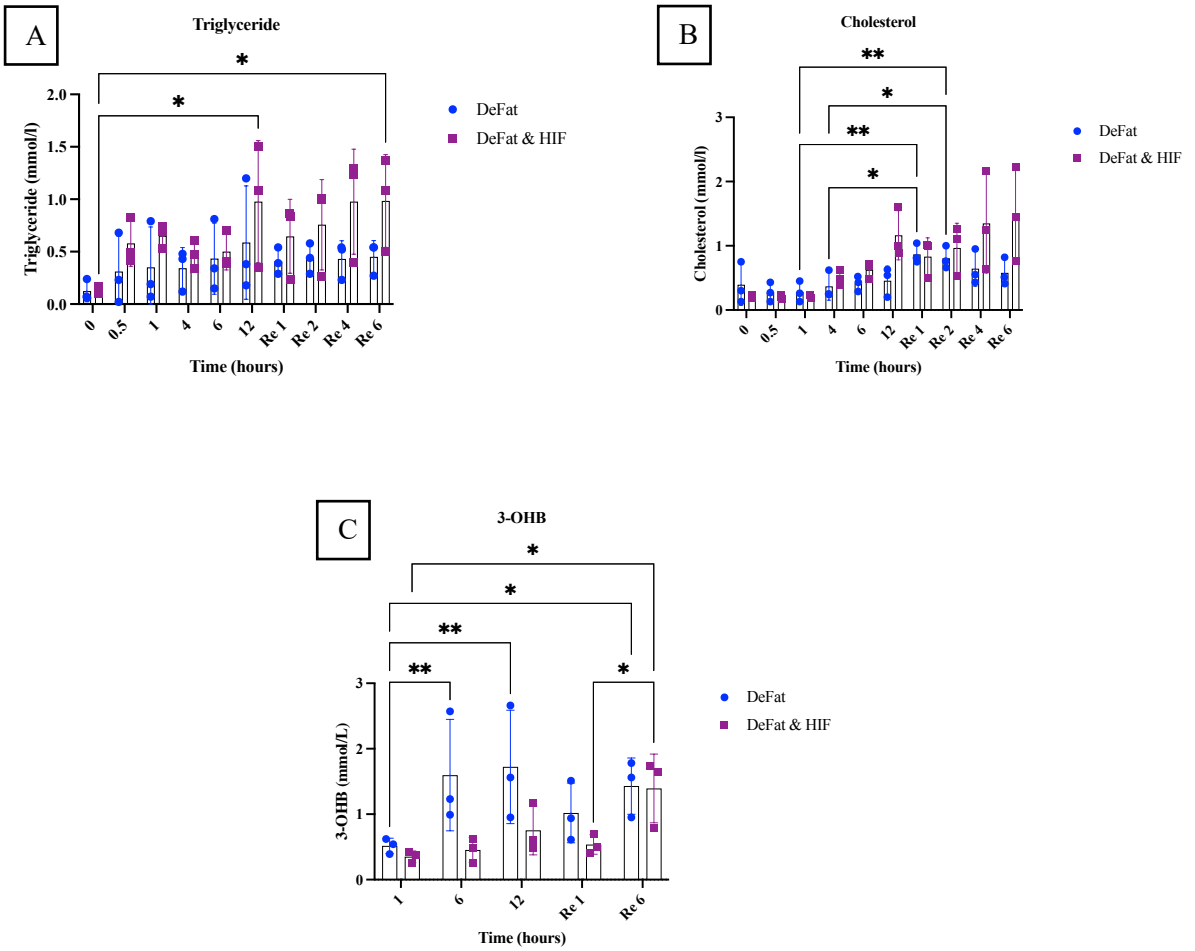

Figure 7.18A-B. Measurements of hepatic lipid metabolism during perfusion and reperfusion. Multiple unpaired t-tests, data reported as mean ± SD and mixed effect analysis for repeated measures with post-hoc tukey correction to adjust for multiple comparisons between timepoints. * $P \leq 0.05$, ** $P \leq 0.01$, *** $P \leq 0.001$ and **** $P \leq 0.0001$.

7.3.5.3 pH maintenance, glucose metabolism and lactate clearance

There was no significant difference in mean perfusate pH at each timepoint between groups. The bile pH followed a similar trend to that of the perfusate pH for both the DeFat and DeFat-HIF groups during perfusion (all livers had a bile pH ≥ 7.5 at 6h of perfusion). However, the 12h end of perfusion bile pH was significantly higher in the in the DeFat-HIF group (7.84 ± 0.11 vs 7.524 ± 0.08, $P = 0.0329$). There was subsequent decrease in bile pH in the DeFat-HIF group from 7.84 ± 0.11 at the end of 12h perfusion to 7.40 ± 0.28 at 4h of reperfusion and 7.61 ± 0.31 at the end of 6h reperfusion. In contrast, the bile pH increased in DeFat group from 7.52 ± 0.08 at the end of 12h perfusion to 7.91 ± 0.03 at 2h of reperfusion and 7.80 ± 0.08 at 4h of reperfusion, Figure 7.19.

The DeFat-HIF group required less perfusate bicarbonate supplementation during perfusion (50 ± 17.32 ml vs 80 ± 45.82 ml, $P = 0.349$) and bicarbonate supplementation for all livers in both groups did not exceed 30 ml during reperfusion. The DeFat-HIF group produced more bile during perfusion (103.33 ± 27.53 ml vs 53.33 ± 25.20 ml, $P = 0.081$) and at reperfusion (63.33 ± 24.66 ml vs 39.0 ± 27.07 ml, $P = 0.313$).

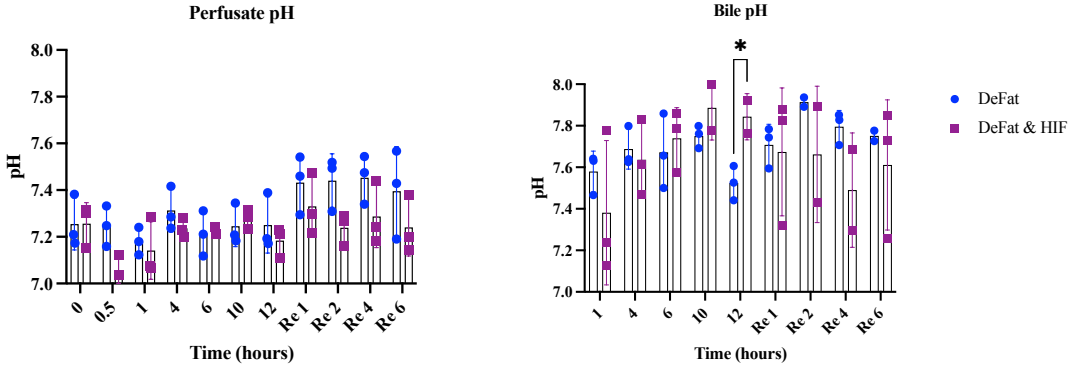

Figure 7.19. Perfusate and bile pH perfusion and reperfusion. Multiple unpaired t-tests, data reported as mean ± S. * $P \leq 0.05$, ** $P \leq 0.01$, *** $P \leq 0.001$ and **** $P \leq 0.0001$.

All livers demonstrated glucose metabolism (spontaneous fall in glucose). There was a comparable mean peak glucose value at 1h of perfusion with a perfusate concentration of 19.53 ± 6.62 mmol/L in the DeFat-HIF group compared to 16.47 ± 10.06 mmol/L in the DeFat group, $P = 0.681$. At 10h of perfusion a significant reduction in glucose was observed with a perfusate concentration of 2.47 ± 2.07 mmol/L in the DeFat-HIF group compared to 12.27 ± 4.07 mmol/L in the DeFat group, $P = 0.0204$.

The greatest reduction in perfusate glucose was observed in the DeFat-HIF from a peak of 19.53 ± 6.62 mmol/L at 1h to 2.43 ± 2.63 mmol/L at the end of 12h perfusion and 3.76 ± 5.33 mmol/L at the end of 6h reperfusion ($P < 0.0001$ and $P = 0.0002$ respectively). There was also a non-significant reduction in perfusate glucose from 16.47 ± 10.06 mmol/L at 1h of perfusion to 11.07 ± 3.73 mmol/L at the end of 12h perfusion and 6.63 ± 6.97 mmol/L at the end of 6h reperfusion in the DeFat group, Figure 7.20A.

The bile glucose concentration followed a similar trend to that of the perfusate bile for both the DeFat-HIF and DeFat groups during perfusion. All livers in the DeFat HIF group had a bile glucose concentration of <3 mmol/L by the end of 12h perfusion compared to one liver in the DeFat group. The greatest reduction in bile glucose was observed in the DeFat-HIF group from

a peak of 16.13 ± 10.04 mmol/L at 1h to 0.97 ± 0.96 mmol/L at the end of 12h perfusion and 3.67 ± 5.46 mmol/L at the end of 6h reperfusion (P = 0.0060 and P = 0.0389 respectively). There was also a non-significant reduction in bile glucose between timepoints during perfusion and reperfusion in the DeFat group, Figure 7.20B.

The starting perfusate lactate concentration was significantly higher in the DeFat-HIF group compared to the DeFat group (14.13 ± 1.67 mmol/L vs. 8.93 ± 2.18, P = 0.0304). However, all livers in both groups cleared lactate to <2.5 mmol/l by 6h of perfusion.

A significant reduction in lactate in the DeFat group from 8.93 ± 2.18 mmol/L from the start of perfusion to 1.0 ± 0.854 mmol/L at 4h of perfusion (P = 0.0487). The perfusate lactate at 1h of reperfusion significantly reduced from 7.47 ± 0.58 to 2.1 ± 1.28 mmol/L at the end of 6h reperfusion (P = 0.0341).

Lactate clearance in the DeFat-HIF group followed a similar trend, with a significant reduction from 14.13 ± 1.67 mmol/L to 1.50 ± 0.265 mmol/L the end of 12h perfusion, P = 0.0389. No significant change was observed at 1h reperfusion and the end of 6h reperfusion. The DeFat-HIF group had a higher 6h end of reperfusion lactate measurement compared to the DeFat group (4.07 ± 3.97 mmol/L vs. 2.1 ± 1.28, P = 0.460), Figure 7.20C.

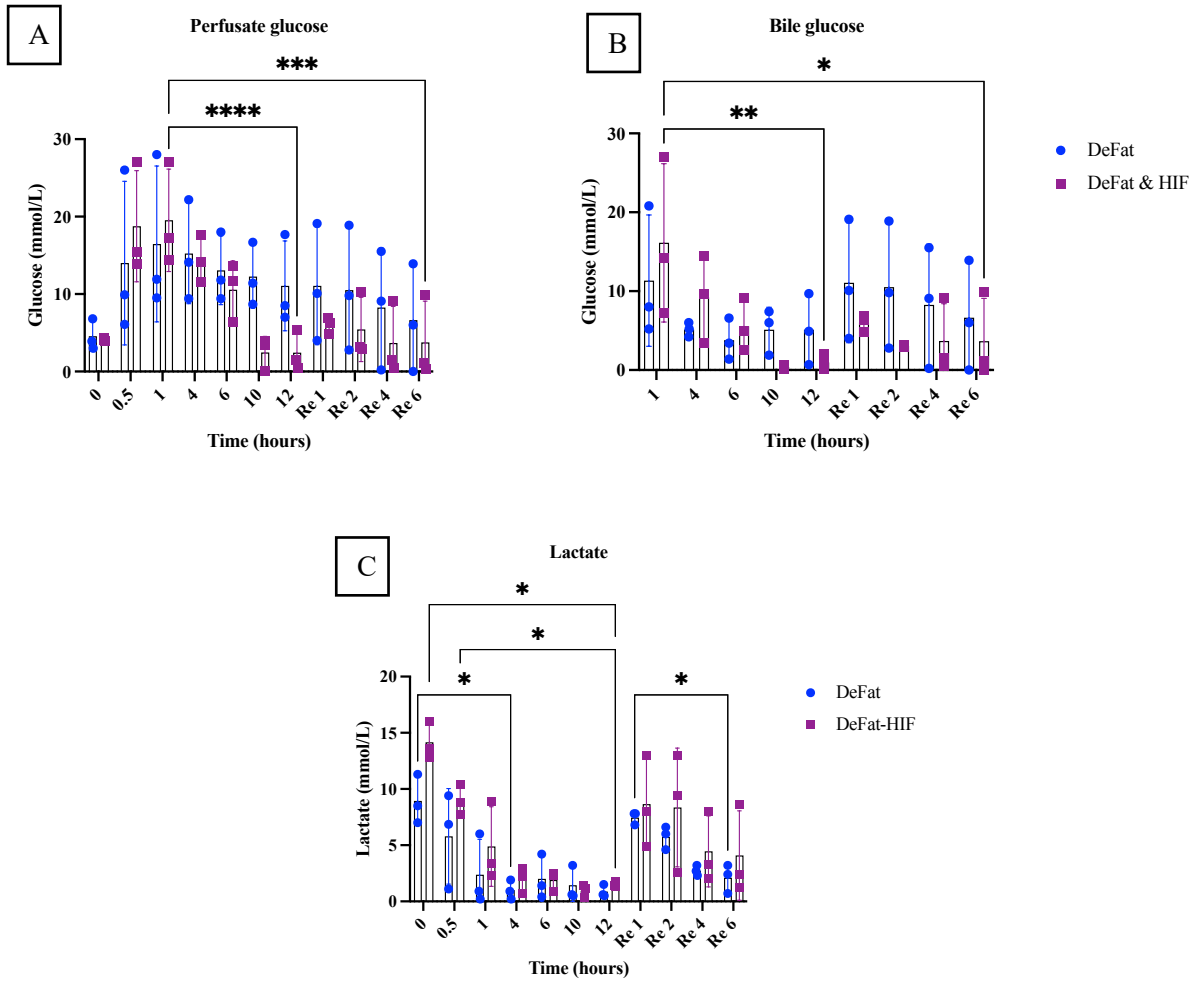

Figure 7.20A-C. Perfusate glucose, bile glucose and lactate clearance during perfusion and reperfusion. Multiple unpaired t-tests, data reported as mean ± SD and mixed effect analysis for repeated measures with post-hoc tukey correction to adjust for multiple comparisons between timepoints. Only selected pairwise comparisons shown for perfusate glucose due to multiple significant differences per timepoint within each group. * $P \leq 0.05$, ** $P \leq 0.01$, *** $P \leq 0.001$ and **** $P \leq 0.0001$.

7.3.5.4 Systemic inflammation (CRP and cytokines)

There was no significant difference in mean perfusate CRP concentration at each timepoint between groups. The DeFat-HIF group demonstrated an increase in perfusate CRP from 8.90 mg/L ± 7.64 at 1h of perfusion to 92.47 ± 61.32 mg/L at the end of 12h perfusion and 84.62 ± 43.64 mg/L at the end of 6h reperfusion ($P = 0.0001$ and $P = 0.0004$ respectfully).

The DeFat group followed a similar trend with a perfusate CRP concentration of 9.41 ± 10.05 mg/L at 1h of perfusion to 70.41 ± 59.67 at the end of 12h perfusion and 59.69 ± 33.70 mg/L at the end of 6h reperfusion ($P = 0.006$ and $P = 0.0360$ respectively), Figure 7.21.

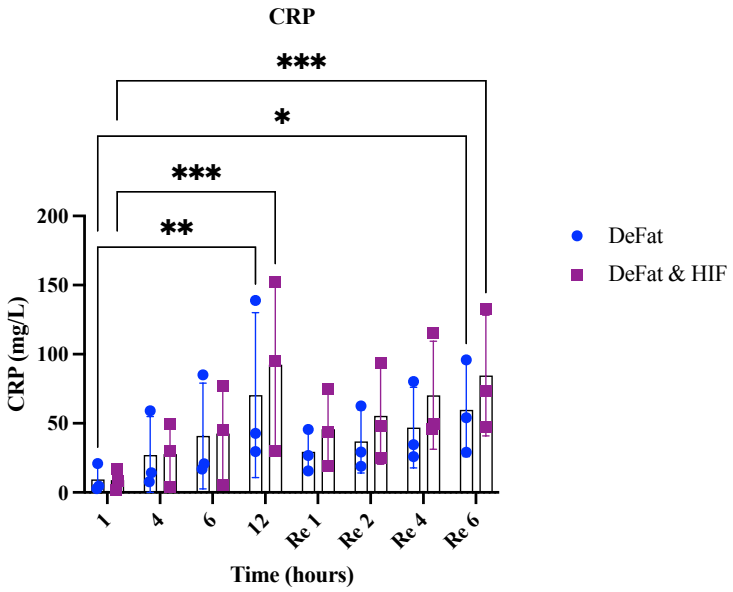

Figure 7.21. Perfusate CRP during perfusion and reperfusion. Multiple unpaired t-tests, data reported as mean ± SD and mixed effect analysis for repeated measures with post-hoc tukey correction to adjust for multiple comparisons between timepoints. * $P \leq 0.05$, ** $P \leq 0.01$, *** $P \leq 0.001$ and **** $P \leq 0.0001$.

The following cytokines were measured during perfusion and reperfusion IL-1β, IL-2, IL-6, IL-10 and TNF-α. A non-significant increase in IL-1β was only observed in the DeFat-HIF group from 2985.01 ± 2649.33 pg/ml at 1h of perfusion to 16268.39 ± 18100.70 pg/ml at end of perfusion at 12h and no significant difference was observed between 1h of reperfusion and at the end of 6h reperfusion. Similarly, a non-significant increase in IL-2 was observed in the DeFat-HIF group from 1.04 ± 0.55 pg/ml at 1h of perfusion to 4.06 ± 0.976 pg/ml at 6h of perfusion and no significant difference was observed between 1h of reperfusion and at the end of 6h reperfusion.

In the DeFat group, a non-significant increase in IL-6 was observed from 12090.14 ± 18175.22 pg/ml at 1h of perfusion to 32541.96 ± 2360.64 pg/ml at 6h of reperfusion and no significant difference was observed between 1h of reperfusion and at the end of 6h reperfusion. In addition, a non-significant increase in IL-10 was observed from 13287.86 ± 20258.85 pg/ml at 1h perfusion to 40844.34 ± 26360.66 at 6h of perfusion and a reduction to 10153.73 ± 9395.10 at 1h of reperfusion. No significant differences in perfusate TNF-α between groups during perfusion and reperfusion, Figure 7.22.

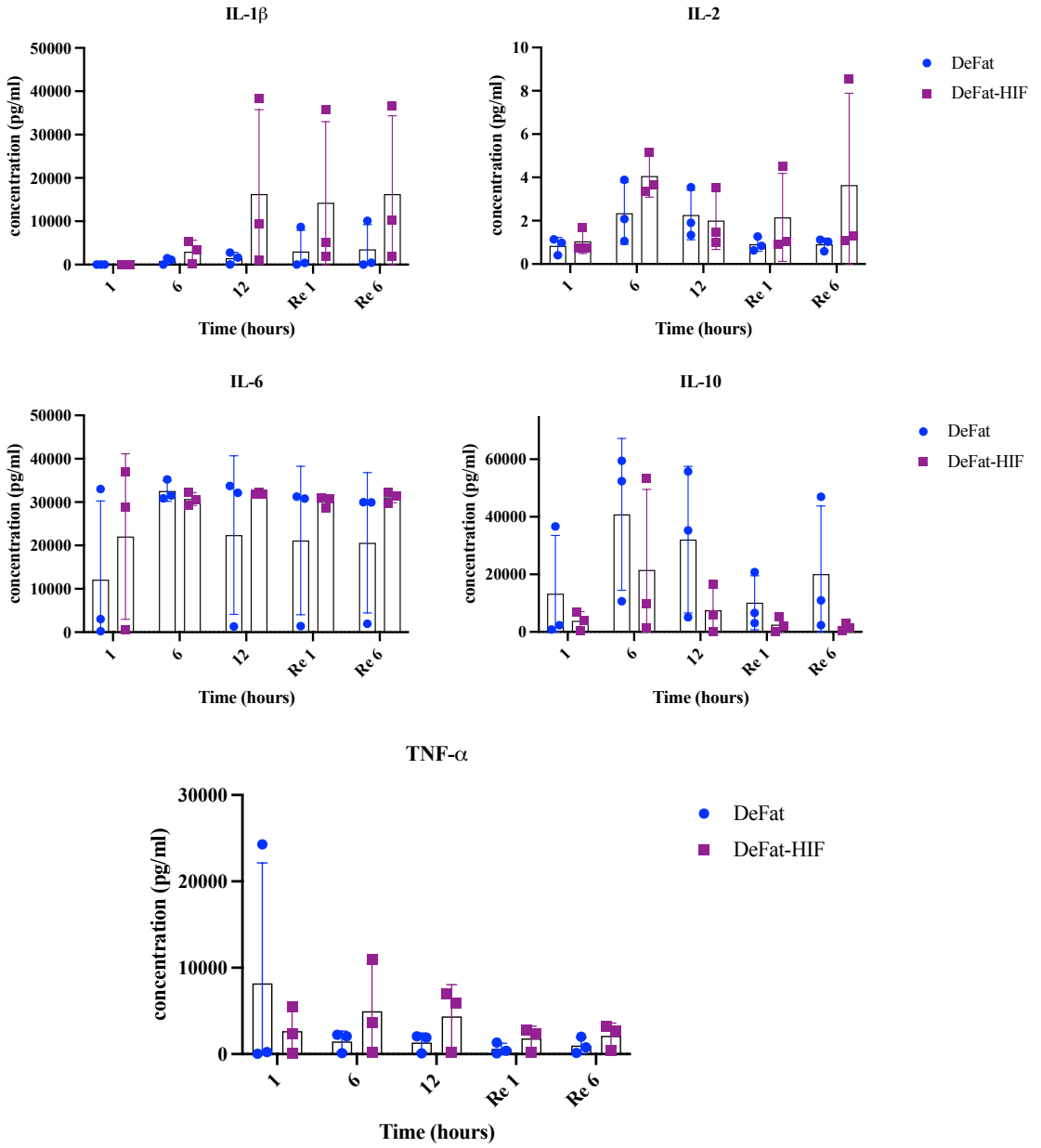

Figure 7.22. IL-1β, IL-2, IL-6, IL-10 and TNF-α during perfusion and reperfusion. Multiple unpaired t-tests, data reported as mean ± SD and mixed effect analysis for repeated measures with post-hoc tukey correction to adjust for multiple comparisons between timepoints. * $P \leq 0.05$, ** $P \leq 0.01$, *** $P \leq 0.001$ and **** $P \leq 0.0001$.

7.3.6 Functional assessment: Dose finding study

7.3.6.1 Flow dynamics

All livers in the dose finding study had a mean arterial flow > 100ml/min and portal flow > 0.5L/min over the course of perfusion, Table 7.19.

Table 7.19. Dose finding study: arterial and portal flows during NMP

NMP protocol		Mean	SD
Liver 1 NMP alone	**Arterial flow (ml/min)**	674.6	65.18
	Portal flow (L/min)	0.96	0.05
Liver 2 DFO (4h)	**Arterial flow (ml/min)**	465.8	64.77
	Portal flow (L/min)	0.89	0.072
Liver 3 DFO (4h) + PT2385 (16h)	**Arterial flow (ml/min)**	345.4	26.06
	Portal flow (L/min)	0.79	0.12
Liver 4 DeFat (from commencement of NMP)	**Arterial flow (ml/min)**	479.1	70.92
	Portal flow (L/min)	0.91	0.12
Liver 5 DeFat + DFO (from commencement of NMP)	**Arterial flow (ml/min)**	288.1	67.03
	Portal flow (L/min)	0.97	0.24
Liver 6 DeFat + DFO + PT2385 (DeFat-HIF from commencement of NMP)	**Arterial flow (ml/min)**	462.9	74.69
	Portal flow (L/min)	1.0	0.22

7.3.6.2 Transplantability criteria

Three livers in the dose finding study met functional criteria for transplantation as described at 4h of perfusion in the VITTAL study. Of these, only one liver met all three functional criteria i.e. Cambridge, Birmingham and Oxford (179,201,202). The ability of each liver in the dose finding study to meet functional criteria for transplantation and specific comments regarding each liver are described in Table 7.20.

Table 7.20. Dose finding study: ability of each liver to meet functional transplantability criteria

Functional criteria determining suitability for transplantation		Criteria met?	Comments
Liver 1 NMP alone	**Watson et al. (Cambridge)**	No	• pH <7.2 • ALT > 6000 IU/L at 2h
	Mergental et al. (VITTAL, Birmingham)	**Yes**	Lactate <2.5mmol/L at 4h and met vascular flows/liver appearance criteria
	Abbas et al. (DeFat, Oxford)	No	• pH <7.2 • ALT > 6000 IU/L at 6h
Liver 2 DFO (4h)	**Watson et al. (Cambridge)**	No	• pH <7.2 • Bile glucose 18.3mmol/l at 4h and 7mmol/l at 6h (bile pH>7.5)
	Mergental et al. (VITTAL, Birmingham)	**Yes**	Lactate <2.5mmol/L at 4h with evidence of glucose metabolism, bile production and met vascular flows/liver appearance criteria
	Abbas et al. (DeFat, Oxford)	No	• pH <7.2 at 6h • Bile glucose only 6.1 mmol/l less than perfusate glucose (although bile pH >7.5)
Liver 3 DFO (4h) + PT2385 (16h)	**Watson et al. (Cambridge)**	**Yes**	Met all parameters
	Mergental et al. (VITTAL, Birmingham)	**Yes**	Met all parameters
	Abbas et al. (DeFat, Oxford)	**Yes**	Met all parameters
Liver 4 DeFat (from commencement of NMP)	**Watson et al. (Cambridge)**	No	• pH <7.2 • Slow reduction in both bile and perfusate glucose • ALT >6000 at 2h
	Mergental et al. (VITTAL, Birmingham)	No	• Lactate 3.46 at 4h, 4.83 at 6h, 1.91 at 12h and 1.69 mmol/l at 18h • pH < 7.3 • Slow metabolism of perfusate glucose 38 at 4h, 36 at 6h, 31 at 12h and 20.6 mmol/l at 18h
	Abbas et al. (DeFat, Oxford)	No	Lactate 4.83 mmol/l at 6h and pH <7.2and slow metabolism of perfuse/bile glucose
Liver 5 DeFat + DFO (from commencement of NMP)	**Watson et al. (Cambridge)**	No	Lactate 10.5 at 2h, 9.5 at 4h, 7.1 at 6h and 6.1 mmol/l at 20h (end of perfusion) and slow metabolism of perfusate/bile glucose
	Mergental et al. (VITTAL, Birmingham)	No	Lactate >2.5mmol/l at 4h and slow perfusate glucose metabolism i.e. 40 mmol/L at 4h (compared to 39 mmol/L 2h)
	Abbas et al. (DeFat, Oxford)	No	• Lactate >2.5mmol/l at 6h • Slow perfusate glucose metabolism i.e. 39 mmol/L at 6h (compared to 39 mmol/L 2h) • Slow bile glucose metabolism
Liver 6 DeFat + DFO + PT2385 (DeFat-HIF from commencement of NMP)	**Watson et al. (Cambridge)**	No	• pH <7.2 • Slow lactate clearance i.e. 17.2 at 2h, 13.9 at 4h, 13.5 at 6h and 5.2 mmol/l at 24h (end of perfusion) • Slow perfusate and bile metabolism
	Mergental et al. (VITTAL, Birmingham)	No	Lactate >2.5mmol/l at 4h and slow perfusate glucose metabolism
	Abbas et al. (DeFat, Oxford)	No	Lactate >2.5mmol/l at 6h and slow perfusate glucose metabolism

7.3.7 Functional assessments: Experimental study

7.3.7.1 Flow dynamics

All livers in the experimental study maintained an arterial flow > 100ml/min and portal flow > 0.5L/min at 6h of perfusion and at the end of 12h perfusion. The mean arterial flow at 1h, 2h and 5h of perfusion in the DeFat-HIF group was significantly higher than the DeFat group (637.41 ± 82.34 ml/min vs. 363.58 ± 55.25 ml/min, $P = 0.00875$; 705.94 ± 11.32 ml/min vs. 430.35 ± 52.58 ml/min, $P = 0.000890$; and 5665 ± 53.36 ml/min vs. 476.10 ± 67.41 ml/min, $P = 0.0186$) with no significant differences at reperfusion. A similar trend was observed for portal flow in the DeFat-HIF group compared to the DeFat group at 6h (1.47 ± 0.45 L/min vs. 0.63 ± 0.51 L/min, $P = 0.102$) with no significant differences at reperfusion, Figure 7.23.

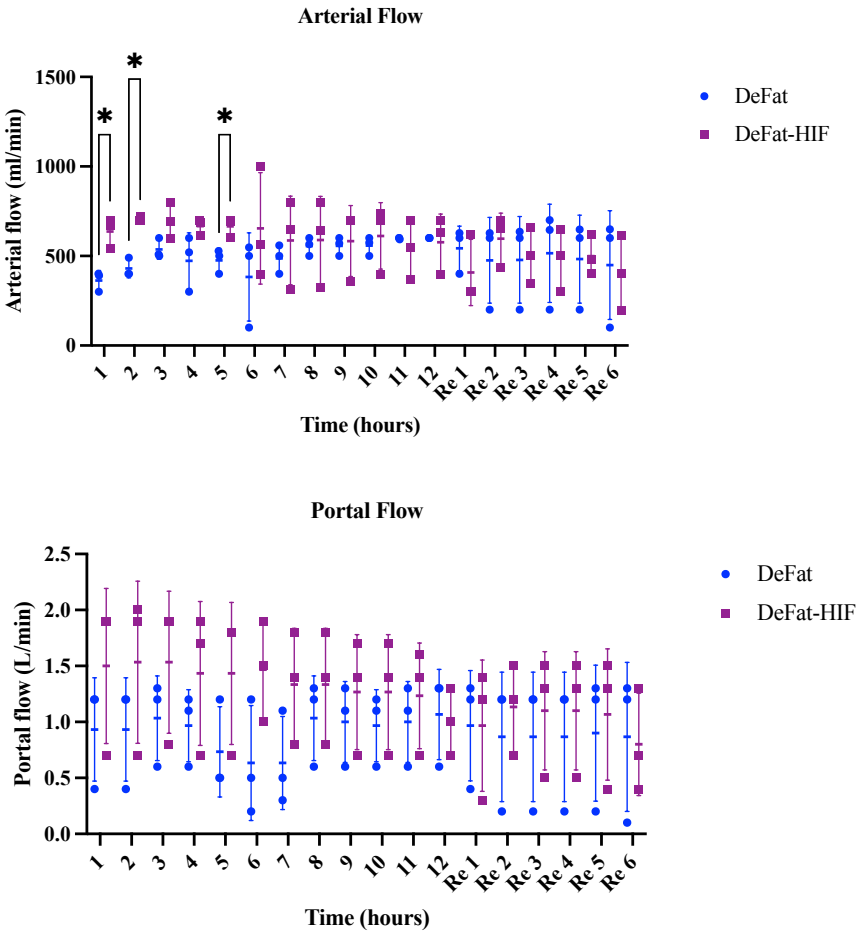

Figure 7.23. Arterial and portal flow during perfusion and reperfusion. Multiple unpaired t-tests, data reported as mean ± SD.

7.3.7.2 Transplantability criteria

All livers met at least one functional criteria for transplantation, 5 out 6 livers met the 4h VITTAL criteria. Only one liver from each group (DeFat Liver 3 and DeFat-HIF Liver 1) met all three functional criteria i.e. Cambridge, Birmingham and Oxford (179,201,202). The ability of each liver in the experimental study to meet functional criteria for transplantation and specific comments regarding each liver are described in Table 7.21.

Table 7.21. Experimental study: ability of each liver to meet functional transplantability criteria

Functional criteria determining suitability for transplantation and baseline (pre-NMP, post-SCS) steatosis degree		Criteria met?	Comments
DeFat Liver 1 **Path ld-MaS: 2%** **Path sd-MaS: 50%** **DIA Total MaS: 4.7%** **(i) ld: 0.8%** **(ii) sd: 3.9%**	**Watson et al. (Cambridge)**	No	Bile glucose concentration not ≤3 mmol/L OR ≥10 mmol/L less than the perfusate glucose concentration. All other parameters met.
	Mergental et al. (VITTAL, Birmingham)	**Yes**	All parameters met (except perfusate pH just under 7.3 i.e. 7.29 at 4h)
	Abbas et al. (DeFat, Oxford)	No	Bile glucose concentration not ≤3 mmol/L OR ≥10 mmol/L less than the perfusate glucose concentration at 6h. All other parameters met.
DeFat Liver 2 **Path ld-MaS: 30%** **Path sd-MaS: 10%** **DIA Total MaS: 21.0%** **(i) ld: 16.9%** **(ii) sd: 4.1%**	**Watson et al. (Cambridge)**	No	ALT at 1, 4 and 6h >6000. All other parameters met.
	Mergental et al. (VITTAL, Birmingham)	**Yes**	All parameters met (except perfusate pH just under 7.3 i.e. 7.24 at 4h)
	Abbas et al. (DeFat, Oxford)	No	ALT >6000, pH 7.12 and lactate 4.2mmol/l at 6h
DeFat Liver 3 **Path ld-MaS: 1%** **Path sd-MaS: 40%** **DIA Total MaS: 3.5%** **(i) ld: 0.7%** **(ii) sd: 2.8%**	**Watson et al. (Cambridge)**	**Yes**	All parameters met
	Mergental et al. (VITTAL, Birmingham)	**Yes**	All parameters met
	Abbas et al. (DeFat, Oxford)	**Yes**	All parameters met
DeFat-HIF Liver 1 **Path ld-MaS: 5%** **Path sd-MaS: 10%** **DIA Total MaS: 14.5%** **(i) ld: 8.1%** **(ii) sd: 8.4%**	**Watson et al. (Cambridge)**	**Yes**	All parameters met
	Mergental et al. (VITTAL, Birmingham)	**Yes**	All parameters met (except perfusate pH just under 7.3 i.e. 7.28 at 4h)
	Abbas et al. (DeFat, Oxford)	**Yes**	All parameters met
DeFat-HIF Liver 2 **Path ld-MaS: 40%** **Path sd-MaS: 20%** **DIA Total MaS: 29%** **(i) ld: 24.5%** **(ii) sd: 4.5%**	**Watson et al. (Cambridge)**	No	ALT at 1, 4 and 6h >6000. Perfusate glucose 6.4 at 6h and 0.1mmol/l at 10h. Bile glucose 4.9 at 6h and 0.1mmol/l at 10h (bile pH >7.5). All other parameters met.
	Mergental et al. (VITTAL, Birmingham)	**Yes**	All parameters met (except perfusate pH just under 7.3 i.e. 7.20 at 4h)
	Abbas et al. (DeFat, Oxford)	No	ALT at 1, 4 and 6h >6000. Perfusate glucose 6.4 at 6h and 0.1mmol/l at 10h. Bile glucose 4.9 at 6h and 0.1mmol/l at 10h (bile pH >7.5). All other parameters met.
DeFat-HIF Liver 3 **Path ld-MaS: 1%** **Path sd-MaS: 40%** **DIA Total MaS: 3.5%** **(i) ld: 0.7%** **(ii) sd: 2.8%**	**Watson et al. (Cambridge)**	**Yes**	Bile glucose of 9.2mmol/l compared to perfusate glucose of 13.6mmol/l at 6h. However, bile glucose of 2mmol/l compared to perfusate glucose of 1.5mmol/l at 12h. Lactate 2mmol/l at 2h (from 13.6 mmol/l at 0h)
	Mergental et al. (VITTAL, Birmingham)	No	Perfusate lactate of 2.9mmol/l at 4h (compared to 2mmol/l at 2h and 2.5mmol/l 6h)
	Abbas et al. (DeFat, Oxford)	No	Bile glucose of 9.2mmol/l compared to perfusate glucose of 13.6mmol/l at 6h. However, bile glucose of 2mmol/l compared to perfusate glucose of 1.5mmol/l at 12h.

7.3.7.3 *ICG clearance*

Indocyanine green (ICG) challenges were performed at 4h of perfusion, 10h of perfusion and at 4h of reperfusion. Serial perfusate samples were taken for a total of 120 min post ICG challenge. Perfusate ICG values were calculated as the percentage change from baseline (0 min, pre-injection of ICG). All livers in the DeFat and DeFat-HIF group demonstrated evidence of ICG clearance with a significant reduction (from a peak value at 1 min) over serial measurements at 15, 30, 60 and 120 min post-injection during the 4h perfusion challenge. The reduction remained significant in the DeFat group following the 4h reperfusion challenge, but was not evident in the DeFat-HIF group. The one liver, that was originally excluded from analysis due to ex-situ non-function (ENF) is shown alongside the DeFat and DeFat-HIF groups for reference purposes only, Figure 7.24A-C.

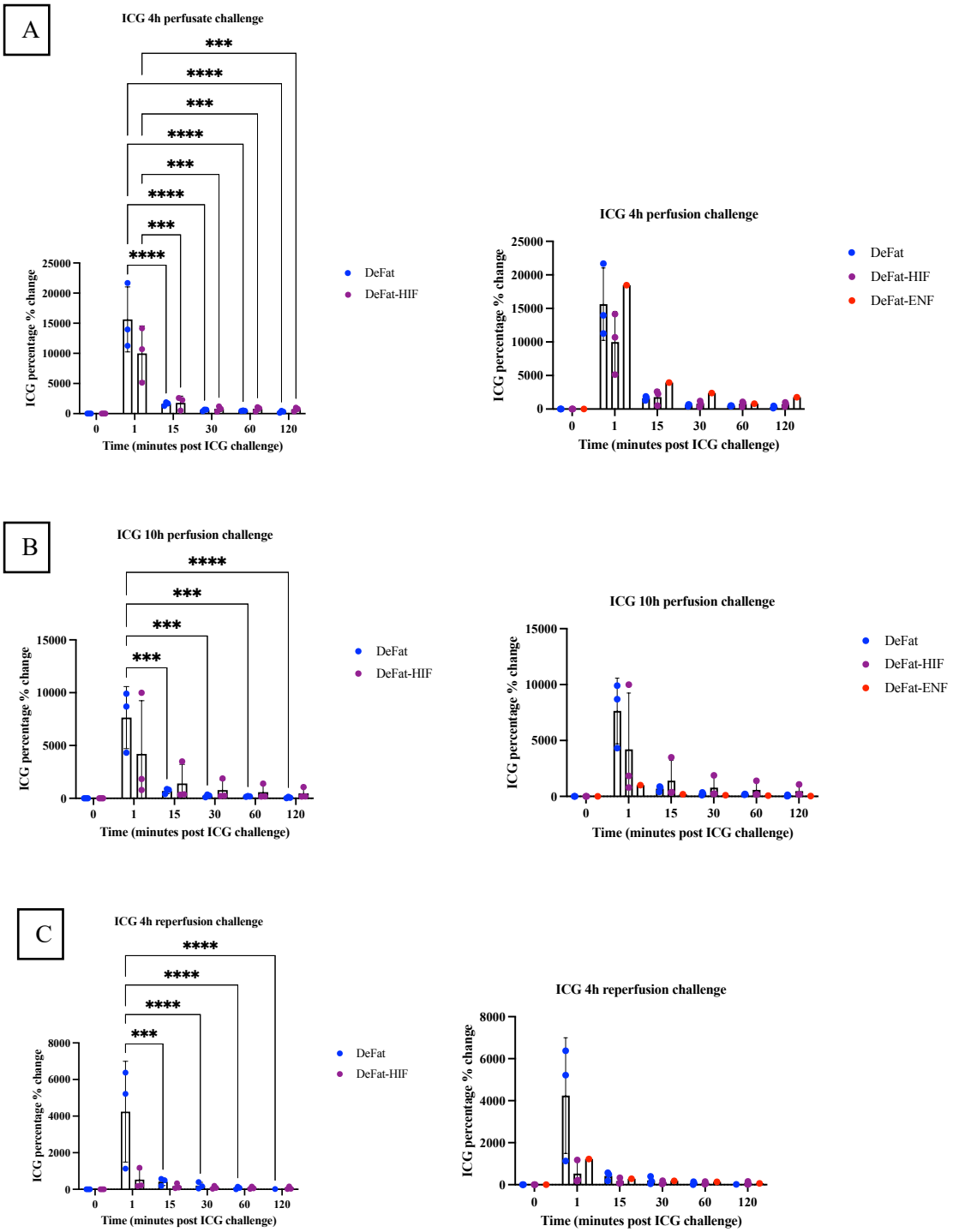

Figure 7.24A-C. Indocyanine green (ICG) challenges during 4h of perfusion **(A)**, 10h of perfusion **(B)** and 4h of reperfusion **(C).** Comparison of DeFat and DeFat-HIF groups (right) and ex-situ non-function liver shown for reference (left). Multiple unpaired t-tests, data reported as mean ± SD and mixed effect analysis for repeated measures with post-hoc tukey correction to adjust for multiple comparisons between timepoints. * $P \leq 0.05$, ** $P \leq 0.01$, *** $P \leq 0.001$ and **** $P \leq 0.0001$.

7.3.7.4 Lidocaine metabolism and MEGX

Lidocaine metabolism was assessed through measurement of its metabolite MEGX. A bolus of Lidocaine was injected at 4h of perfusion, 10h of perfusion and at 4h of reperfusion. Serial

perfusate samples were taken at 15 and 30 min post injection of lidocaine. Perfusate lidocaine and MEGX concentrations were quantified through mass spectrometry analysis.

The lidocaine concentration was significantly higher in the DeFat-HIF group at 15 min and 30 min post injection at the 4h challenge compared to the DeFat group (0.91 ± 0.06 ug/ml vs. 0.45 ± 0.22 µg/ml, P = 0.0268 and; 0.49 ± 0.03 µg/ml vs. 0.17 ± 0.07 µg/ml, P = 0.00165 respectively). However, a significant difference in perfusate lidocaine concentrations between groups was not observed at the 10h perfusion and 4h reperfusion challenge.

All livers in the DeFat and DeFat-HIF group demonstrated evidence of lidocaine metabolism (reduction in perfusate concentration) with a concurrent non-significant increase in perfusate MEGX concentration which was more pronounced in the DeFat group. The one liver, that was originally excluded from analysis due to ex-situ non-function (ENF) is shown alongside the DeFat and DeFat-HIF groups for reference purposes only, Figure 7.25A-C.

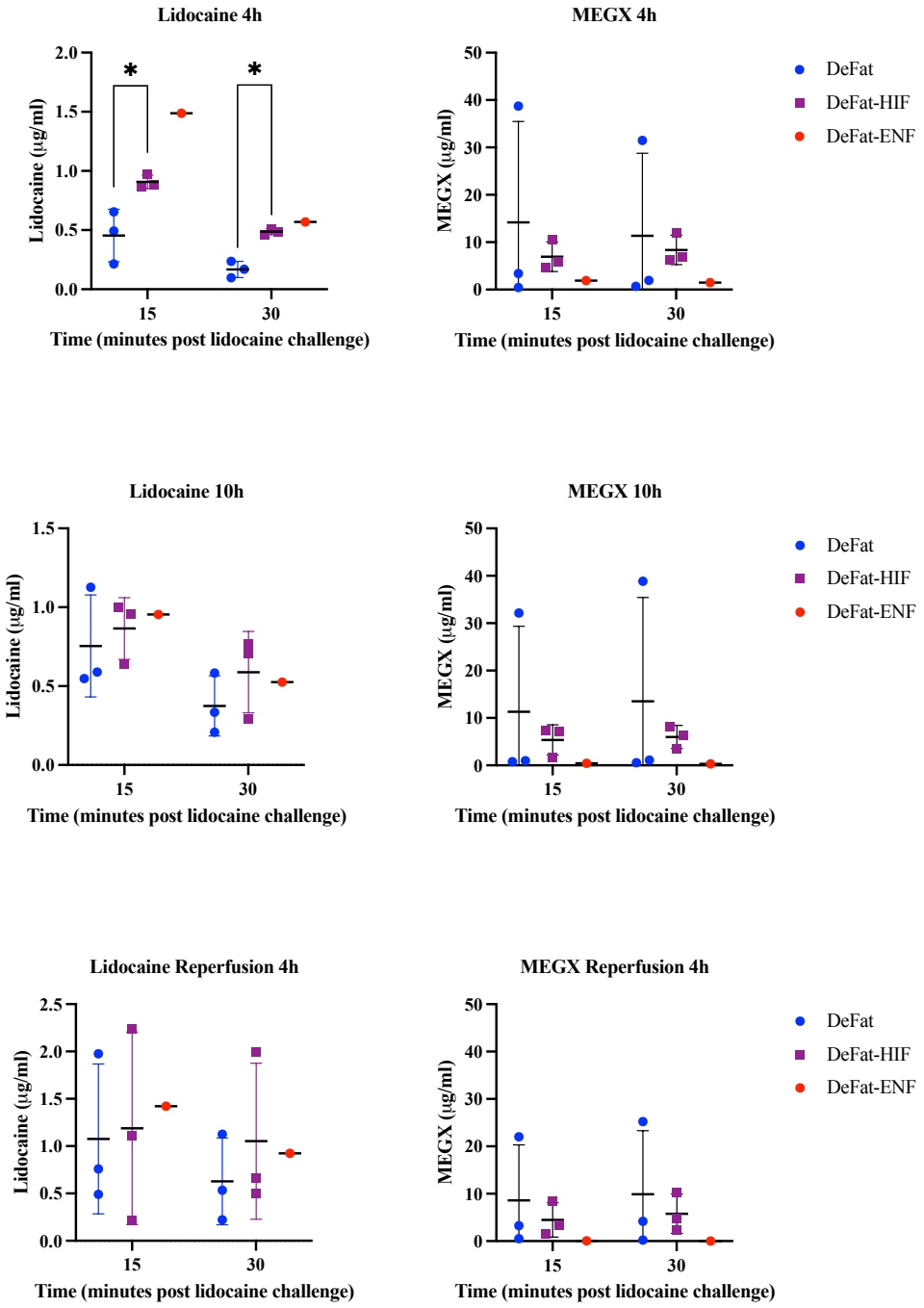

Figure 7.25A-C. Comparison of DeFat and DeFat-HIF groups: Lidocaine challenges during 4h of perfusion **(A)**, 10h of perfusion **(B)** and 4h of reperfusion **(C).** Ex-situ non-function liver (red) shown for reference only. Multiple unpaired t-tests, data reported as mean ± SD. * $P \leq 0.05$, ** $P \leq 0.01$, *** $P \leq 0.001$ and **** $P \leq 0.0001$.

7.3.7.5 LiMAx

^{13}C-methacetin metabolism was assessed using the LiMAx test through connection with the OrganOx *metra.* A bolus of ^{13}C-methacetin was injected at 1h of perfusion, 5h of perfusion and at 5h of reperfusion with metabolism calculated over 60 minutes post injection. Due to device availability at the time of perfusion, the LiMAx test was not performed in DeFat Liver 1 (see Table 7.16). The LiMAx test value in the DeFat-HIF group at 6h was comparable to the DeFat group (280.70 ± 212.06 µg/kg/h vs. 260.10 ± 239.43 µg/kg/h, P = 0.508). However, at the end of 6h reperfusion, there was non-significant reduction in LiMAx value in the DeFat-HIF group compared to the DeFat group (120.71 ± 24.51 µg/kg/h vs. 210.75 ± 119.01 µg/kg/h, $P = 0.261$). Overall, there was no significant difference in LiMAx values between the DeFat-HIF and the DeFat group. The one liver, that was originally excluded from analysis due to ex-situ non-function (ENF) is shown alongside the DeFat ($n = 2$, not possible to perform test for Liver 1) and DeFat-HIF ($n = 3$) groups for reference purposes only, Figure 7.26.

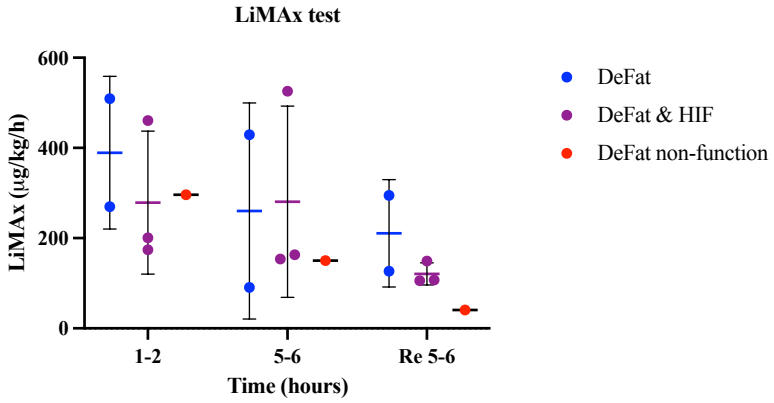

Figure 7.26. Comparison of DeFat and DeFat-HIF groups: ^{13}C-methacetin challenges at 1h of perfusion, 5h of perfusion and 5h of reperfusion**.** Ex-situ non-function liver (red) shown for reference only. Multiple unpaired t-tests, data reported as mean ± SD. * $P \leq 0.05$, ** $P \leq 0.01$, *** $P \leq 0.001$ and **** $P \leq 0.0001$.

7.4 Discussion

This chapter provides substantial evidence to the evolving understanding of the pharmacological optimisation of steatotic livers and the utility of NMP as a therapeutic platform. Hypoxia inducible factors (HIFs) have been implicated in hepatic lipid metabolism. However, the specific isoforms (HIF-1α and HIF-2α) isoforms have contrasting roles. HIF-1α exerts a hepatoprotective effect through reduction in lipid synthesis and enhancement of fatty

acid β-oxidation (154). Conversely, HIF-2α promotes lipid accumulation and fibrosis (153,155). Preclinical studies in murine models have highlighted the potential of pharmacological HIF-1α activation in improving liver graft tolerance to ischaemia-reperfusion injury (IRI), these findings have not yet translated to clinical practice. This chapter is therefore based on the hypothesis that selective pharmacological stabilisation of HIF-1α, combined with inhibition of HIF-2α, could synergistically reduce hepatic steatosis (HS) and improve graft tolerance to IRI.

To explore this hypothesis, I have investigated the role of pharmacological hypoxia inducible factor (HIF) modulation during NMP as an adjunct to an established NMP defatting protocol described in Chapter 6. In the process, I have established dosing schedules of pharmacological HIF modulators and optimised methods to quantify both HIF-1α and HIF-2α. Following the dose finding perfusions, I have developed an ex-situ model of IRI and compared the established NMP-defatting protocol with and without the adjunct of pharmacological HIF modulators. Novel assessments of ex-situ liver function have also been explored within this chapter in order to provide more objective measures of liver function during NMP. Overall, I have demonstrated a reduction in ld-MaS in livers subjected to HIF modulation during NMP (combined with defatting). However, the effect of concurrent HIF modulation in the mitigation of IRI warrants further investigation.

7.4.1 Dose finding study

The pharmacological HIF modulators investigated in this chapter included Deferoxamine (DFO) and PT2385. DFO is a prolyl-hydroxylase inhibitor (PHD) known to activate both the HIF-1α and HIF-2α isoform and has been shown to upregulate pathways involved in lipid metabolism, reduce free radical production and lower pro-inflammatory cytokines (412). PT2385, a selective HIF-2α dimerisation inhibitor that has demonstrated beneficial effects in reducing HS in preclinical murine models (413). However, there have been limited reports of the use of these pharmacological agents in the setting of ex-situ liver machine perfusion.

In the context of SCS, Fukai et al. have reported a modified University of Wisconsin (UW) cold preservation solution containing heavy water (D_2O)-containing buffer, combined with deferoxamine (mDsol) as a novel preservation solution for extended cold preservation (48h) of rat livers. In a model of ex-situ reperfusion, livers preserved with mDsol demonstrated less

hepatocellular injury, improved oxygen consumption, reduced portal resistance and less liver dehydration and swelling during preservation and reperfusion (421). Whilst this study was published after formulation of the original hypothesis presented in this chapter, it supports the addition of heavy water (albeit for the purposes of quantifying DNL) and DFO (as an anti-oxidant) to the pRBCs during NMP.

In the dose finding study presented within this chapter, I perfused 6 discarded human livers with a combination of defatting and HIF modulating pharmacological agents. All livers demonstrated evidence of hepatocellular function with stable pH, clearance of lactate and metabolism of glucose. Livers perfused with NMP and DFO, or a combination of DFO and PT2385 with or without the established NMP defatting protocol, showed a substantial reduction in ld-MaS at 24h of perfusion, despite the noted limitations of bacterial/fungal contamination in one liver i.e. Liver 6 (DeFat-HIF: NMP + DeFat + DFO + PT2385 from the commencement of perfusion).

Immunoblotting of livers perfused with HIF modulating pharmacological agents demonstrated successful upregulation of HIF-1α with suppression of HIF-2α. This was best demonstrated in dose finding Liver 3 where DFO was delivered at 4h of perfusion resulting in induction of both HIF-1α and HIF-2α (with a concurrent increase in perfusate erythropoietin concentration 994 mIU/ml) by 16h of NMP. Following the delivery of PT2385 at 16h of NMP a reduction of Erythropoietin (EPO) to 747 mIU/ml by 24h of NMP was observed with a concurrent reduction in HIF-2α.

EPO is a glycoprotein hormone primarily responsible for regulating erythropoiesis. The liver plays a crucial role in erythropoietin (EPO) production, especially during foetal development and under certain pathological conditions in adults. During foetal and neonatal stages, the liver is the primary site of EPO synthesis, contributing up to 90% of the total EPO production necessary for erythropoiesis during this critical growth period. In adults, while the kidneys assume the dominant role, the liver still retains the capacity to produce about 10-15% of the body's EPO, particularly under hypoxic conditions or when renal function is impaired. Both HIF-1α and HIF-2α can upregulate EPO expression, however, HIF-2α plays a more critical and direct role in this process. HIF-2α is more selectively expressed in tissues involved in erythropoiesis and is the primary regulator of EPO production in the kidneys and liver, the main sites of EPO synthesis. HIF-2α directly binds to the hypoxia-responsive elements (HREs)

in the EPO gene promoter, thereby significantly enhancing EPO transcription under hypoxic conditions (422). In contrast, while HIF-1α also participates in the hypoxic response, its role in EPO regulation is less pronounced compared to HIF-2α (423,424). Overall, the findings presented are the first documented evidence of ex-situ EPO liver production through HIF modulation and the findings suggest that perfusate EPO is a valuable measurement for monitoring selective HIF-2α modulation during NMP.

Recently, Nazzal et al. explored the ferroptosis regulating effect of DFO in a model of ex-situ split normothermic perfusion (using one lobe as a control with concurrent simultaneous perfusion of the treated lobe) demonstrating a reduction in ALT, AST, HO-1, HIF-1α and reduction in iron stain (Perl's Prussian blue) on H&E biopsy (in the lobe treated with deferoxamine over 3h of perfusion). HO-1, HIFα were quantified from tissue biopsy RNA extraction and real-time PCR analysis (425). The reduction in HIFα compared to the control lobe are not consistent with the findings demonstrated in this chapter and the study has several limitations. The authors did not assess tissue biopsies through immunoblotting and did not report the cold-ischaemia time (CIT) of the split liver which can influence hypoxia alone mediated HIF expression. In addition, a perfusion period of 3h may be inadequate to induce HIF in the context of NMP. In the current chapter, a perfusion period of at least 6h following delivery of a 10mmol/L DFO bolus was required to induce HIF supported by immunoblots, IHC and perfusate EPO levels. It is also conceivable, the lower dose of 6mmol/L infusion (rather than a bolus) reported by Nazzal et al. combined with short perfusion duration are responsible for the conflicting results. The higher HO-1, HIFα expression in the control (untreated) lobe may also be related to an ischaemic or under perfused segment as it is unclear why the HIFα expression in the control lobe is almost 8-fold higher compared to normal control liver tissue (used as a standard for both the DFO treated lobe and untreated lobe).

7.4.2 Experimental study

Following completion of the dose finding study, a total of 7 livers were perfused as part of the experimental study. However, one liver in the DeFat group, from a 56 male DCD donor with moderate steatosis on histology (ld-MaS of 40% reported by the histopathologist and 39.3% using DIA) with a CIT of 20h and 13min was identified as an outlier and therefore excluded. The excessive CIT, severity of steatosis and severe hepatocellular injury (peak ALT of 19317.7 IU/L at 4h of perfusion) may have contributed to the ex-situ non function (ENF) and inability

of defatting to salvage this liver. In addition, IHC of FFPE tissue analysis demonstrated increased localisation of HMGBI, MPO and CITH3 over the course of perfusion and reperfusion. When the primary aim is to investigate the impact of pharmacological interventions on hepatic lipid metabolism, it is essential that all livers exhibit signs of hepatocellular function to ensure that conclusions drawn about the intervention are accurate, hence the decision to exclude the single non-functioning liver from the analyses. Whilst this liver was not included in the overall analysis the donor characteristics and perfusion metrics are described separately, and various functional assessments including ICG clearance, MEGX and LiMAx tests are provided alongside the main results for reference purposes only.

A total of 6 livers were therefore included in the experimental study (DeFat, n = 3 and DeFat-HIF, n = 3). All livers recruited to the experimental study were from DCD donors apart from one DBD liver in the DeFat group. Although not statistically significant, the baseline characteristics differed in the two groups, with the DeFat-HIF group including donors with a higher-risk profile i.e. DCD status, high pre-retrieval ALT and high donor BMI. The difference in baseline characteristics highlights the limitations associated with discarded human liver studies mainly related to limited availability of discarded livers for research making it challenging to balance groups for baseline characteristics: the heterogeneity of these livers is a well-known limitation in discarded liver studies. Biological variability among organs means that even with standardised protocols, results may vary significantly. From my experience, the main modifiable factor in reducing the risk profile of discarded human livers is the CIT which was excessive in the liver that did not function but minimised in livers included in the experimental study.

7.4.2.1 HIF quantification

HIF quantification was performed with immunoblots and selective HIF modulation was monitored through perfusate EPO production. In the DeFat-HIF group both DFO and PT2385 with the established defatting protocol were delivered from the commencement of perfusion and an increase HIF-1α relative to HIF-2α expression was observed over the course of 12h perfusion. Comparatively, in the DeFat group (with the absence of HIF modulators) both HIF-1α and to HIF-2α remained low over the 12h perfusion. These results are similar to the dose finding perfusions and support the methodology described within the chapter for HIF quantification.

In addition, the mean concentration of EPO in the DeFat-HIF group after 12 hours of perfusion was >10x lower than that in Liver 2 from the dose-finding study (where DFO alone was delivered at 4 hours of standard NMP). In the dose-finding study, the EPO concentration in the perfusate after 18 hours was 2664 mIU/ml (14 h after drug delivery), compared to the mean 12-hour perfusion measurement in the DeFat-HIF group, which was 233.67 mIU/ml. The observed differences in EPO measurements corroborate earlier dose study findings on the utility of using EPO levels to monitor selective HIF-2α modulation.

Prior to reperfusion, pharmacological agents were thoroughly flushed with 2L of preservation solution and all livers were then reperfused with whole human allogenic blood. In the DeFat-HIF group the relative increase in HIF-1α relative to HIF-2α expression was still apparent following reperfusion (as demonstrated on immunoblots and perfusate EPO measurements) despite flushing the liver and repriming the circuit with fresh perfusate comprising of whole human allogenic blood. It is conceivable, that pharmacological activity of the HIF-modulators persisted even at reperfusion and thereby providing a hepatoprotective effect in this higher-risk cohort. In the DeFat group, whilst there was a small increase in both HIF-1α and HIF-2α expression, it likely related to the period of warm ischaemia between perfusion and reperfusion.

7.4.2.2 Hepatic steatosis quantification

Livers recruited to the DeFat-HIF and DeFat groups had varying degrees of hepatic steatosis on analysis of baseline (pre-NMP) H&E biopsy sections. All biopsies were assessed by a blinded histopathologists as per the Banff guideline recommendations for reporting of HS. In addition, additional assessment was performed using the Visiopharm® digital image analysis (DIA) software. The use of digital image analysis in the context of machine perfusion has several advantages (described in Chapter 3 and 4), primarily to provide automated and consistent results (without interobserver variability and subjectivity of the histopathologist). Whilst livers were accepted for research based on the retrieval surgeon confirming evidence of macroscopic steatosis, retrospective analysis of the baseline biopsy demonstrated discordance between the surgeon's assessment and biopsy result (this has also been highlighted in Chapter 3).

Both the histopathologist and DIA software provided quantification of Total MaS, ld-MaS and sd-MaS. Of these, the most clinically relevant is ld-MaS in the setting of liver transplantation: higher levels of ld-MaS (especially >30%) are associated with poor outcomes (4). A non-significant reduction in ld-MaS was demonstrated in the DeFat-HIF group with a reduction in ld-MaS from 15.3 ± 21.5% at baseline to 7.7% ± 10.7% at the end of 6h reperfusion (as assessed by the histopathologist). When quantified using Visiopharm® digital image analysis software , a significant reduction in ld-MaS from 11.1 ± 12.2% at baseline to 4.8 ± 5.9% at the end of 6h reperfusion, $P = 0.0097$. However, this degree of reduction was not evident in the DeFat group: indeed the findings are comparable to the pre-clinical data supporting the Phase II clinical trial of defatting donor transplant livers described in Chapter 6. In the cohort of livers that were subjected to defatting with lipoprotein apheresis filtration, functional improvements were evident by 6h of perfusion and a histological reduction in steatosis was only apparent at the end of perfusion at 48h.

Therefore, the results presented herein, demonstrated accelerated defatting with the adjunct of HIF modulation during NMP. A comparable study by Boteon et al. has previously described a 'defatting cocktail' comprising of L-carnitine, forskolin, hypericin, scoparone, visfatin and GW501516. Five discarded human livers were perfused using the 'defatting cocktail' and a further 5 with standard NMP for a total of 12h. In the cohort of livers treated with the 'defatting cocktail' there was a reduction in MaS from a median of 31% (10-58%) at baseline to 15% (5-22%) at 12h of perfusion (221). However, a limitation of this study is a lack of assessment of sd-MaS during perfusion.

In the current chapter, there was no significant difference identified between timepoints in sd-MaS when reported by the histopathologist for both the DeFat and DeFat-HIF group. In addition, sd-MaS quantified using the Visiopharm® digital image analysis software demonstrated a non-significant increase in sd-MaS in the DeFat-HIF group from 4.6% ± 1.8 at baseline to 8.7% ± 3.8 at 12h of perfusion with a concurrent decrease in sd-MaS to 4.3% ± 2.3 following 6h of whole blood reperfusion. These findings support the transient nature of sd-MaS which refers to fat vacuoles that are not true ld-MaS i.e. less than half the size of the cell and does not cause displacement of the nucleus. Sd-MaS is known to fluctuate during preservation and at reperfusion and is a transient short-lived process that indicates both liver stress/injury and recovery/regeneration from these processes (96).

7.4.2.3 Glycogen depletion and glucose metabolism

Typically, during normothermic machine perfusion (NMP), elevated perfusate glucose levels are recorded at the onset of perfusion (207,227). This phenomenon is believed to be due to glycogenolysis during static cold storage (SCS), an ATP-independent process (290,426). Additionally, packed red cells, often used in perfusion, contain high glucose levels due to preservation solutions such as citrate-phosphate-dextrose and sodium-adenine-glucose-mannitol (427). At the initiation of NMP, the high circulating glucose levels are expected to inhibit glycogenolysis and promote glycogenesis. In the current study, no significant change in tissue glycogen depletion percentage between 6h and the end of 12h perfusion in the both the DeFat and DeFat HIF groups was observed. However, at 6h reperfusion the total percentage of glycogen depletion was higher (although not significant) in the DeFat-HIF group compared to the DeFat group (73.3% ± 37.5 vs 59.7% ± 48.8; $P = 0.720$). This glycogen depletion (also associated with lower perfusate glucose levels in the DeFat-HIF group) may be explained by the metabolic shift induced by HIF activation characterised by increased glycolytic activity resulting in low perfusate glucose and concurrent glycogenolysis to replenish glucose in order to sustain the glycolytic flux (424,428).

7.4.2.4 Hepatocellular injury

DeFat-HIF livers demonstrated a comparable degree of hepatocellular injury (perfusate ALT) when compared to DeFat livers at the end of 12h perfusion (5320.9 ± 3048.97 IU/L vs. 5571.83 ± 5059.96 IU/L, $P = 0.762$) and a higher (non-significant) perfusate ALT at the end of 6h reperfusion (6604.27 ± 5578.86 IU/L vs. 3466.27 ± 2264.21 IU/L, $P = 0.418$). In contrast, while there was an increase in perfusate cfDNA in both groups, the DeFat-HIF group demonstrated a non-significant reduction in peak cfDNA concentration of 5.46 ± 1.47 μg/ml at 6h of perfusion to 3.83 ± 1.81 μg/ml at the end of 6h reperfusion. Therefore suggesting an added benefit of the DeFat-HIF protocol in dampening the propagation of hepatocellular injury in this ex-situ model of IRI.

7.4.2.5 Hepatic lipid metabolism

Although perfusate triglycerides (TGs) increased over the course of perfusion in both groups, the concentrations remained lower than those observed in six discarded control NMP livers (NMP alone) perfused by Ceresa et al. (who performed the pre-clinical study that supports the

Phase II clinical trial described in Chapter 6, the results of which are included here for reference purposes only). Specifically, at 12 hours of NMP, the triglyceride levels were as follows: DeFat: 0.59 mmol/L ± 0.54; DeFat-HIF: 0.98 mmol/L ± 0.58; and NMP alone: 1.84 ± 1.37 mmol/L. Similarly, perfusate cholesterol concentrations followed a similar trend in both groups and were also lower than those in the six control NMP livers, with perfusate concentrations recorded at: DeFat: 0.46 ± 0.23 mmol/L; DeFat-HIF: 1.16 ± 0.38 mmol/L; and NMP alone: 1.34 ± 0.54 mmol/L at 12 hours of NMP. The lower perfusate concentrations in the experimental groups can be attributed to the lipoprotein apheresis filter.

Hypertriglyceridemia is believed to contribute to lipotoxicity, inducing oxidative stress and a pro-inflammatory response in the liver (429). In a porcine study by Jamieson et al., it was suggested that elevated circulating triglycerides (TG) may have led to excessive hepatic lipid deposition during perfusion (216). Conversely, a murine NMP study by Nagrath et al. reported a 30% reduction in liver fat without the use of defatting agents, achieved by replacing the perfusate hourly (217). In contrast, a study on human livers perfused by Liu et al. observed a significant rise in perfusate TG levels, but found no correlation with ALT, AST, bile production, or histological markers of injury, indicating that increased perfusate TG does not necessarily exacerbate liver injury (219). Consequently, the potential role of lipoprotein apheresis filtration in mitigating lipotoxicity by lowering TG concentrations in the perfusate and enhancing liver function remains uncertain.

However, it is a noteworthy observation in the present study, that following reperfusion with allogenic whole blood (and removal of the lipoprotein apheresis filter) there was a rebound in mobilisation of intracellular TGs into the perfusate with a peak TG concentration of 0.98 ± 0.44 mmol/L in the DeFat-HIF group and 0.45 ± 0.15 mmol/L in the DeFat group at 6h of reperfusion. Similarly, perfusate cholesterol concentration followed a similar trend with a peak concentration of 2.22 ± 0.77 mmol/L in the DeFat-HIF group and 0.41 ± 0.82 mmol/L in the DeFat group at 6h of reperfusion. Overall, the greater mobilisation of TGs in the DeFat-HIF group also corresponded with a histological reduction in ld-MaS observed at the end of whole blood reperfusion.

The perfusate 3-hydroxybutyrate (3-OHB) levels, which serve as a marker for fatty acid β-oxidation, showed no significant difference between the DeFat and DeFat-HIF groups at each timepoint. However, an increase in β-oxidation was observed in both groups (although to a

greater extent in the DeFat group during 12h of perfusion). Despite the initial differences in timing and magnitude of 3-OHB increases between the two groups, their levels converged by the end of the 6-hour reperfusion period ($P = 0.930$), indicating comparable β-oxidation rates ultimately. This suggests that while HIF modulation may alter the temporal dynamics of fatty acid metabolism, it does not significantly alter the overall capacity for β-oxidation.

7.4.2.6 pH, glucose metabolism and lactate clearance

All livers in the DeFat and DeFat-HIF groups maintained stable perfusate pH during perfusion with a bile pH of >7.5 mmol/L at 6h of NMP. Both groups demonstrated significant glucose metabolism, evidenced by a spontaneous decrease in perfusate glucose levels during perfusion and reperfusion. Notably, all livers in the DeFat-HIF group had a low bile glucose concentration of <3 mmol/L at the end of 12h perfusion. Additionally, the DeFat-HIF group required less bicarbonate supplementation and produced more bile compared to the DeFat group.

Lactate levels were initially higher in the DeFat-HIF group but decreased significantly during perfusion. Both groups reduced lactate to <2.5 mmol/L by 6h of perfusion and perfusate lactate concentrations remained low at the end of 12h perfusion. Similarly, both groups had initially higher reperfusion lactate with a subsequent reduction over the course of allogenic whole blood reperfusion. However, at the end of 6h reperfusion the perfusate lactate concentration was higher in the DeFat-HIF group (4.07 ± 3.972 mmol/L vs. 2.1 ± 1.277 mmol/L, $P = 0.460$).

In the context of HIF pharmacological modulation during ex-situ perfusion, HIF activation significantly influences glucose metabolism and lactate clearance. The DeFat-HIF group exhibited a more pronounced reduction in glucose levels, indicating enhanced glycolysis, likely due to HIF-1α's role in upregulating glycolytic enzymes. Both groups effectively cleared lactate during perfusion. However, the higher end reperfusion lactate in the DeFat-HIF group could be attributed to either the effect of glycolytic flux on lactate production or a more pronounced IRI (424,428)

7.4.2.7 Inflammatory pathways

No significant differences were observed in mean perfusate CRP concentrations between the groups at each timepoint. However, both groups showed a significant increase in CRP levels over time. The additional liver that was perfused with the DeFat protocol (but excluded from the overall analysis due to ex-situ non function, ENF) demonstrated very low CRP levels during perfusion and reperfusion. This observation highlights the impact of severe hepatocellular injury on CRP production. Such injury can significantly impair the liver's capacity to produce CRP, as seen in fulminant hepatic failure (430).

Cytokine analysis revealed distinct patterns between groups. The DeFat-HIF group experienced a non-significant increase in IL-1β and IL-2 during the course of perfusion and reperfusion, suggesting an enhanced inflammatory response secondary to the higher-risk donor characteristics of these livers (DCD status, high pre-retrieval donor ALT and metabolic dysfunction). Conversely, the DeFat group showed a non-significant increase in IL-6 and IL-10 levels during perfusion with a subsequent reduction during reperfusion. Whilst there was no reduction in IL-6 in the DeFat-HIF group, a non-significant reduction in IL-10 at reperfusion was observed in the DeFat-HIF group indicating a differing inflammatory profile to the DeFat group. Both groups demonstrated a downward trend in TNF-α levels.

7.4.2.8 Functional assessment

Both the DeFat and DeFat-HIF groups demonstrated ICG clearance during perfusion with a significant reduction (from a peak value at 1 min) over serial measurements at the 4h perfusion challenge. However, only the DeFat group maintained significant clearance during reperfusion (despite better vascular flows in the DeFat-HIF group). All livers in the DeFat and DeFat-HIF group demonstrated evidence of lidocaine metabolism (reduction in perfusate concentration) with a concurrent non-significant increase in perfusate MEGX concentration which was more pronounced in the DeFat group. In addition, higher LiMAx values in DeFat-HIF group were observed at 6h perfusion (compared to the DeFat group) but not at the end of 6h of reperfusion. The overall trend in these functional assessments suggest a more pronounced ischaemia-reperfusion injury (IRI) in the DeFat-HIF group, despite comparable measurements to the DeFat group in the perfusion phase (all livers met at least one functional criteria for transplantation at 6h of perfusion).

These findings are supported by the higher end reperfusion perfusate ALT and lactate levels in the DeFat-HIF group, however, can also be explained by the higher-risk donor characteristics of livers in this group. Despite these findings, the DeFat-HIF livers had lower perfusate cfDNA levels and histological PRI scores at the end of reperfusion suggesting a hepatoprotective effect of HIF modulation in mitigating the propagation of hepatocellular injury in this experimental model.

The additional DeFat liver that was excluded from analysis was shown for reference purposes demonstrating slow ICG clearance, inability to convert lidocaine to MEGX and a lower post whole blood reperfusion LiMAx test value. Whilst the numbers in this study are small, I have highlighted the potential of novel functional assessments during NMP which require validation in the setting of clinical trials.

7.4.3 Limitations

The main limitations of this chapter are related to the small numbers and heterogeneity of discarded livers offered for research. Whilst I have demonstrated the utility of an ex-situ whole blood reperfusion model, the results are difficult to interpret outside the context of clinical liver transplantation and need to be corroborated now in the clinical environment.

7.4.4 Conclusion

I have been able to demonstrate a reduction in steatosis with adjunct of HIF-modulators during NMP. All livers perfused in the experimental study had functional metrics at 6h of perfusion that would have rendered them transplantable. However, the ability of pharmacological HIF modulation during NMP to reduce the magnitude of IRI remains to be elucidated.

Chapter 8: Removal of nuclear DAMPs in an ex-situ model of liver transplantation

8.1 Introduction

In the previous chapter, I demonstrated that during NMP (using leucodepleted blood) and reperfusion (using allogenic whole blood i.e. ex-situ simulated liver transplant) there was an efflux of inflammatory cells including cytokines and cfDNA (a nuclear damage associated molecular pattern, DAMP) into the perfusion circuit thereby suggesting an element of reperfusion injury of extended criteria donor (ECD) livers during ex-situ perfusion (NMP) and following simulation of transplantation.

Damage-associated molecular patterns (DAMPs) are key contributors to inflammation and have an important role in the innate immune response through recruitment of immune cells to sites of injury or infection. However, this protective mechanism can paradoxically lead to harm by triggering an excessive inflammatory response, resulting in tissue damage (431,432). This phenomenon is well-documented in various disease contexts, including transplantation, where DAMPs significantly contribute to reperfusion injury and sterile inflammation (159,399,433). Nuclear DAMPs (including cfDNA, histones, nucleosomes, and HMGB1) are particularly involved in sterile inflammation caused by ischemia-reperfusion in the liver, leading to a self-perpetuating cycle of inflammation that ultimately damages the graft (162,434). In addition, the process of NETosis characterised by the expulsion of DNA proteins (such as elastase and myeloperoxidase) and filaments from neutrophils results in the formation of web-like structures called neutrophil extracellular traps (NETs), which were originally described as a mechanism to facilitate pathogen clearance following entrapment (75). However, clinical studies demonstrate that an increase in circulating cfDNA (as a marker of NETs) is a risk factor for thrombotic disease. Evaluation of thrombi demonstrate presence of cfDNA, VWF, histones and other NET markers. In the context of liver transplantation, it is possible that NETs further propagate IRI by contributing to thrombi formation. Furthermore, the significant role of neutrophils in IRI and cell injury that occur during liver transplantation support this hypothesis (75,399).

Nuclear (chromatin associated) DAMPs are particularly relevant in the context of ex-situ perfusion (a closed circuit) that has limited ability (apart from the liver graft itself) to remove circulating DAMPs and is dependent on an intact reticuloendothelial system which can be compromised in the setting of hepatocellular injury (435).

Recently, a novel extracorporeal column, NucleoCapture® (Santersus, Zurich), has been developed to selectively remove nuclear (chromatin associated) DAMPs from circulation. This technology leverages the unique properties of the recombinant H1.3 protein, a naturally occurring linker histone critical for chromatin packaging within the nucleus. By conjugating H1.3 to porous spherical agarose beads within the column, the system is able to bind and capture components of free extracellular chromatin with high affinity as plasma flows through the column. This approach was initially developed for sepsis, where extracellular chromatin contributes to systemic inflammation, similar to the inflammatory response seen in IRI in solid organ transplantation.

The hypothesis of this chapter is that ex-situ reperfusion induces release of nuclear DAMPs from donor livers during leucodepleted NMP and subsequent whole blood reperfusion that results in the propagation of hepatocellular injury and poor ex-situ function. Herein, I initially describe the incorporation of NucleoCapture® classic column in combination with an apheresis system (Spectra Optia, Terumo) and subsequently using an integrated in-line hemoperfusion NucleoCapture® prototype column connected to the OrganOx *metra* NMP device to facilitate removal of nuclear DAMPs in an ex-situ model of liver transplantation. The focus of this chapter is application of the column in the allogenic whole blood reperfusion phase.

The overarching objective of this chapter was to develop a model of IRI in porcine DCD livers preserved with NMP with removal of DAMPs during allogenic whole blood reperfusion (simulated transplant). The specific aims were to:

1. Assess the ability to integrate NucleoCapture® classic column (with the Spectra Optia, Terumo) into the NMP ex-situ set up
2. Determine if DAMPs can be removed from the perfusate using the NucleoCapture® classic column during ex-situ allogenic whole blood reperfusion on the circuit and establish whether removal of DAMPs reduces the magnitude of IRI (simulated transplant model)*

3. Assess the ability to integrate the in-line hemoperfusion NucleoCapture® prototype column connected directly to the OrganOx *metra* NMP device and apply this continuously both during leucodepleted perfusion (RBCs + plasma) and whole blood allogenic reperfusion
4. Determine if the continuous application of the in-line hemoperfusion NucleoCapture® prototype column results in improved DAMP removal and IRI in a porcine DCD model
5. Validate the findings of the in-line hemoperfusion NucleoCapture® prototype column in a discarded human liver perfusion

***This work was jointly performed with my colleague (Dr Fungai Dengu) who as part of his DPhil focused on the application of the classic column (integrated with the Spectra Optia, Terumo) during the initial leucodepleted NMP (RBCs + plasma) phase (rather than whole blood allogenic reperfusion). As the specific data related to the application of the classic column in the perfusion phase pertain to his DPhil, they are not included in this chapter, however, are summarised in the discussion.**

8.2 Methods

8.2.1 Perfusion device

All livers were perfused using the 2nd Generation OrganOx *metra* (OrganOx Ltd, Oxford, UK) NMP device in a standard fashion. Following device calibration and priming, donor livers were benched and cannulated as described in Chapter 2.2.

8.2.2 Study design

8.2.2.1 Porcine

The study consisted of three groups: (i) **NMP-NMP, *n* = 3:** initial 6h NMP perfusion phase using autologous leucodepleted blood (RBCs + plasma) followed by 6h of allogenic whole blood reperfusion; (ii) **NMP-NC, *n* = 3:** initial 6h NMP perfusion phase using autologous leucodepleted blood (RBCs + plasma) followed by 6h of NucleoCapture® classic treatment (integrated between the Optia Spectra and OrganOx *metra*) during allogenic whole blood reperfusion and; (iii) **hNC-hNC, *n* = 3:** extended perfusion of 12h during both the initial NMP perfusion phase using autologous leucodepleted blood (RBCs + plasma) and the reperfusion

phase using allogenic whole blood with continuous integration of the in-line hemoperfusion NucleoCapture® prototype column to the OrganOx *metra*.

In all cases, the perfusate was comprised of autologous leucodepleted blood (RBCs + plasma) during the initial NMP perfusion phase. Following this, livers were disconnected from the circuit and flushed with 2L of crystalloid and reperfused on the same device using a fresh perfusate comprising of full allogenic (3rd party, ABO compatible) whole blood following 30 min of warm ischaemia to simulate implantation (anastomotic time), Figure 8.1. Liver characteristics i.e. blood group (A/O), macroscopic appearance, along with procurement details (warm and cold ischemia times), perfusion and simulated transplant reperfusion duration were recorded for each liver.

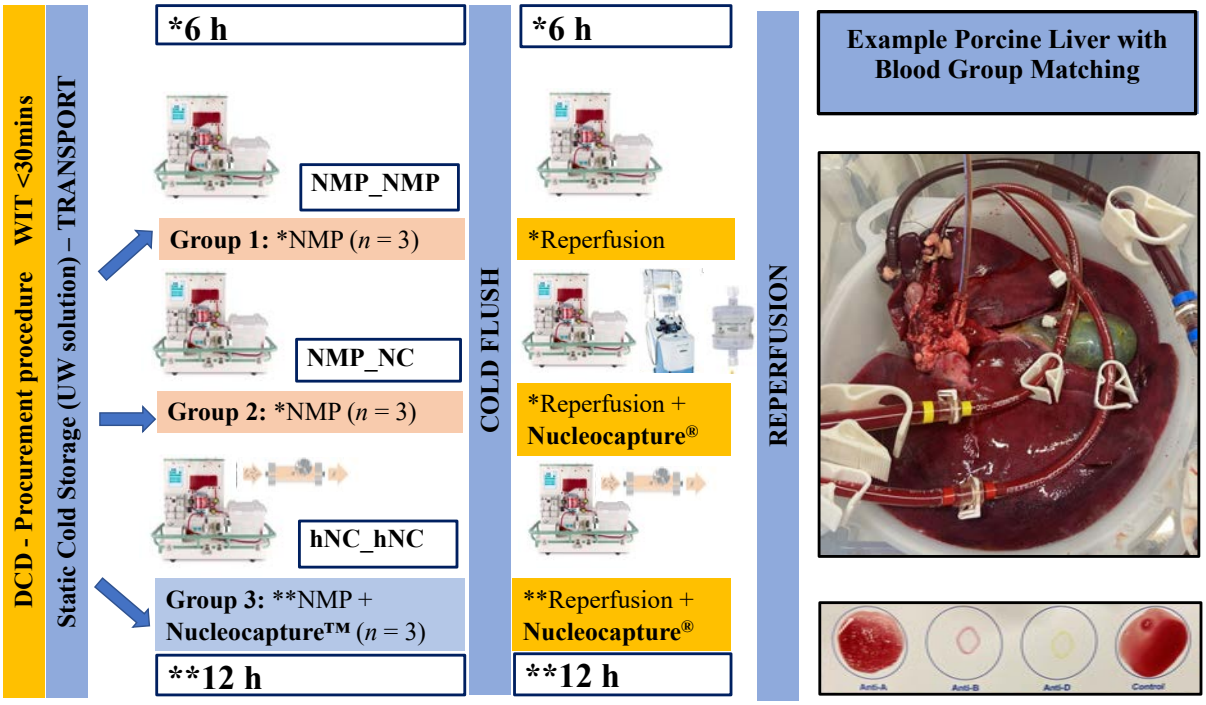

Figure 8.1. Study design outline. Total *n* = 9 DCD Pig livers, 3 groups. Two phases: (i) NMP – autologous RBCs and plasma (leucodepleted) and; (ii) reperfusion (whole blood allogenic (ABO matched) Interventions: NucleoCapture® during reperfusion (Group 2) or both phases (Group 3) compared to standard NMP and reperfusion without column (Group 1). Outcomes: Perfusion haemodynamics, lactate clearance, bile parameters (volume, pH, glucose), perfusate biochemistry and histology.

8.2.3 Animals

Livers were retrieved, flushed, and stored in static cold storage (SCS) for transport. In brief, Sus domesticus pigs weighing 50-70 kg were electrically stunned, exsanguinated (by an

incision across the jugular veins and carotid), cleaned in a 60˚C (140ºF) hot water bath and eviscerated through a thoracoabdominal incision. This protocol replicates donation after circulatory determination of death (DCD) livers and followed guidelines for UK regulated slaughter i.e. compliant with the Welfare of Animals at the Time of Killing (England) Regulations 2015 (WATOK) and EU regulation 1099/2009. Following evisceration, livers were separated from the surrounding viscera, flushed, and preserved in UW® solution for transport. Both autologous and allogenic whole blood were collected in heparinized containers for storage and later preparation in the lab. The process is summarised in Table 8.1.

Table 8.1. Porcine donation after cardiac death donor (DCD) live retrieval protocol.

Procedure	**Method**
Blood collection	Autologous whole blood is collected mixed with 20,000IU of unfractionated heparin sodium (Wockhardt UK Ltd) for storage and subsequent leucodepletion in the lab. Additional ABO compatible from another pig is also collected and stored in the same manner for experiments that involved a 'whole blood' ischaemia-reperfusion component.
Post-exsanguination	Following exsanguination, the pigs are cleaned in a hot water bath at 60ºC (140ºF) over 5 minutes. This is comparable to the 'no-touch' period prior to commencement of the organ retrieval operation in human DCD organ retrieval procedures.
En bloc retrieval	An *en bloc* thoraco-abdominal retrieval is then performed avoid organ injury. The *en bloc* consists of bowel, pancreas, kidneys, spleen, stomach, spleen, liver, diaphragm, oesophagus, heart, lungs, major vessels and trachea.
Portal cannulation and dissection	To minimise warm ischaemia time, the portal vein is rapidly cannulated and flushed with 2L cold heparinized preservation fluid via a soft 18 Fr T-tube (Summit Medical, Cheltenham, UK). This marks the beginning of cold-ischaemia time and facilities dissection of the liver from the *en bloc* (including portal vein, infra-hepatic and supra-hepatic vena cava, bile duct and coeliac aortic patch for the hepatic artery).
Transport	Once the liver is retrieved, it is stored in University of Wisconsin (UW) at 4ºC on ice and transported to the perfusion laboratory prior to NMP.

8.2.4 NucleoCapture technology and integration

NucleoCapture® (Santersus AG, Zurich, Switzerland) is an adsorption column composed of porous, spherical agarose beads with covalently linked recombinant human linker histone (N,N-bismethyonyl-histone H1.3 as a ligand via its N-terminus), Figure 8.2 and Figure 8.3.

This column captures cfDNA, histones, intact nucleosomes and NETs in plasma due to strong binding affinity of the linker histone H1 protein analogue to DNA.

The integration of NucleoCapture® classic column with the Spectra Optia (Terumo) apheresis system into the NMP circuit is illustrated in Figure 8.4. In summary, a connection was established from the bypass line (in-line blood gas sampling line) of the *metra* circuit using a proximal 3-way tap, allowing diversion of blood directly into the Spectra Optia (Terumo) system for centrifugal plasma separation. The plasma then flowed through the NucleoCapture® column before being reconstituted with perfusate and returned to the circuit via a return line attached to a second three-way tap placed distally on the bypass line as illustrated in Figure 8.5. In addition, the connection of the in-line hemoperfusion NucleoCapture® prototype column was established using a 3/8 'Y' connector coming off the centrifugal pump (with a line attached providing inflow into the column) and return from the column via line attached to a 3-way tap feeding back into the soft-shell reservoir as demonstrated in Figure 8.6. A new in-line column prototype was used for each phase i.e. both for perfusion and reperfusion.

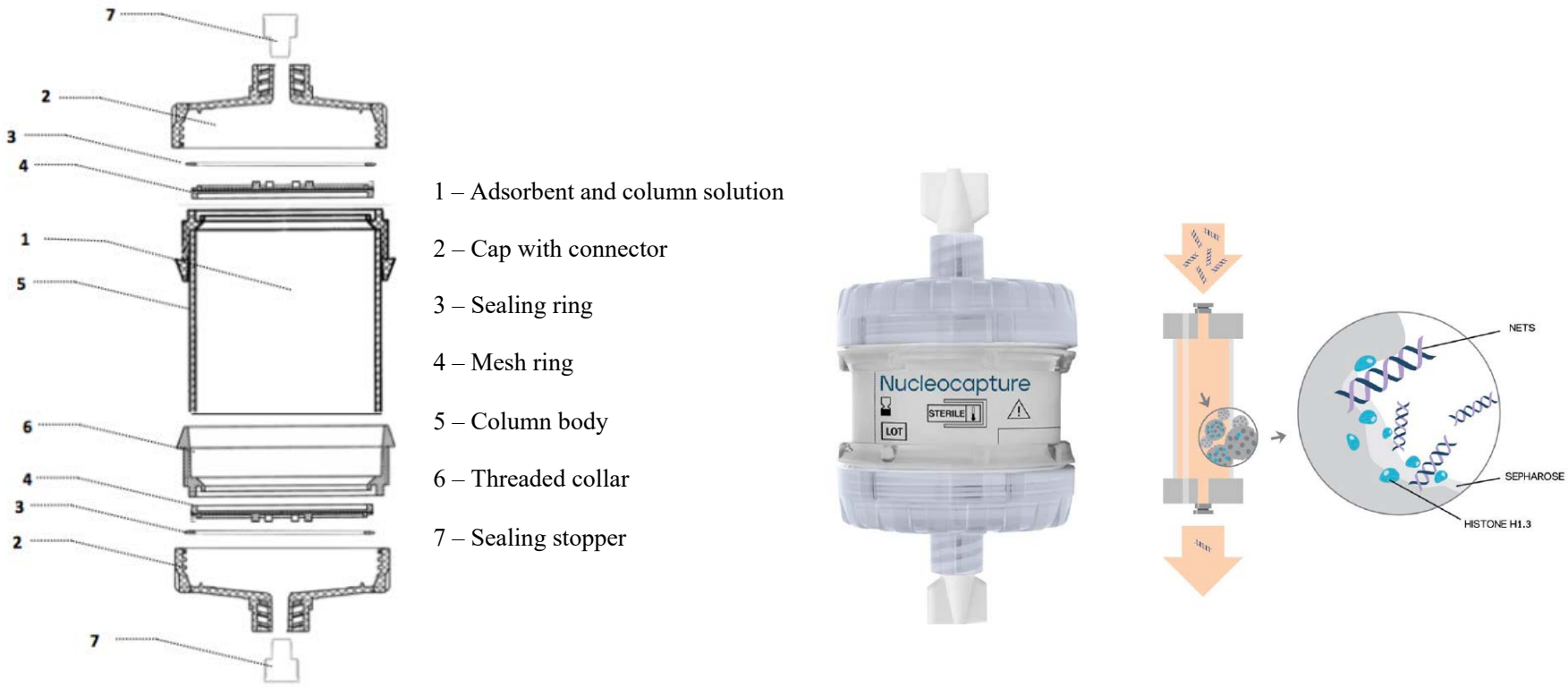

Figure 8.2. Classic NucleoCapture® for connection to Optia Spectra (Terumo). Left: Column components, porous, spherical agarose beads linked with human recombinant histone H1.3 protein (Santersus AG, Zurich, Switzerland). Plasma is separated from the red blood cell-based perfusate using the Spectra Optia (Terumo) apheresis system where it flows through the column and contacts the H1.3-conjugated beads. This interaction effectively binds and removes cell-free DNA, histones, and nucleosomes from circulation. Right: Schematic illustrates the column and beads with trapped/adherent neutrophil extracellular traps (NETs), cfDNA and histones. Linker histone H1 specifically tightly binds nucleosomes with a Kd between 0.022 and 3.3 nM and naked DNA with a Kd value of 5 nM^2.

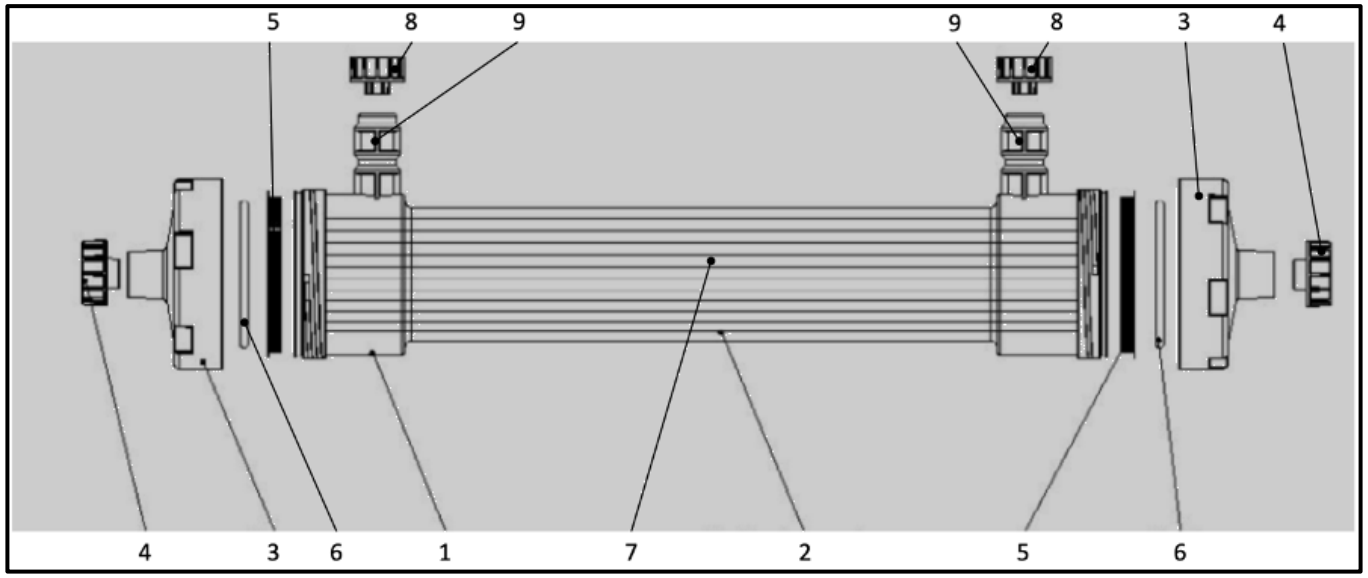

1 - Column housing
2 - Hollow fibre membrane
3 - Blood pot with Twist lock connector
4 - Sealing stopper of blood connector
5 - Sealant
6 - O-ring
7 - Adsorbent beads
8- Sealing stopper of plasma compartment connector
9 - Plasma compartment (technologic) connector

Figure 8.3. In-line hemoperfusion NucleoCapture® prototype column components. The column housing (item 1) with bundle of hollow fibre membrane (item 2), plasma compartment Luer lock connectors (item 9) and blood pots (item 3) with (inlet/outlet) Twist lock connectors provide the structure for the column. The plasma compartment is filled with adsorbent beads in sterile phosphate buffer with 0.01% sodium azide (item 7). The blood ends are plugged with sealing stoppers (item 4). The Twist lock blood connectors are used for the blood circuit line connection. Plasma compartment Luer lock connectors are used for filling of the plasma compartment with adsorbent, tightly closed with sealing stoppers (item 8) and not used during the blood treatment procedure. The adsorbent has granule diameter of 45-165 μm (a mean granule diameter is 90 μm). The pore size of hollow fibre membrane is 0.5 μm; it prevents the passage of the adsorbent from plasma compartment to blood compartment of the column as well as the passage of blood cells from blood compartment of the column to plasma compartment of the column, thus the blood cells do not contact with the adsorbent.

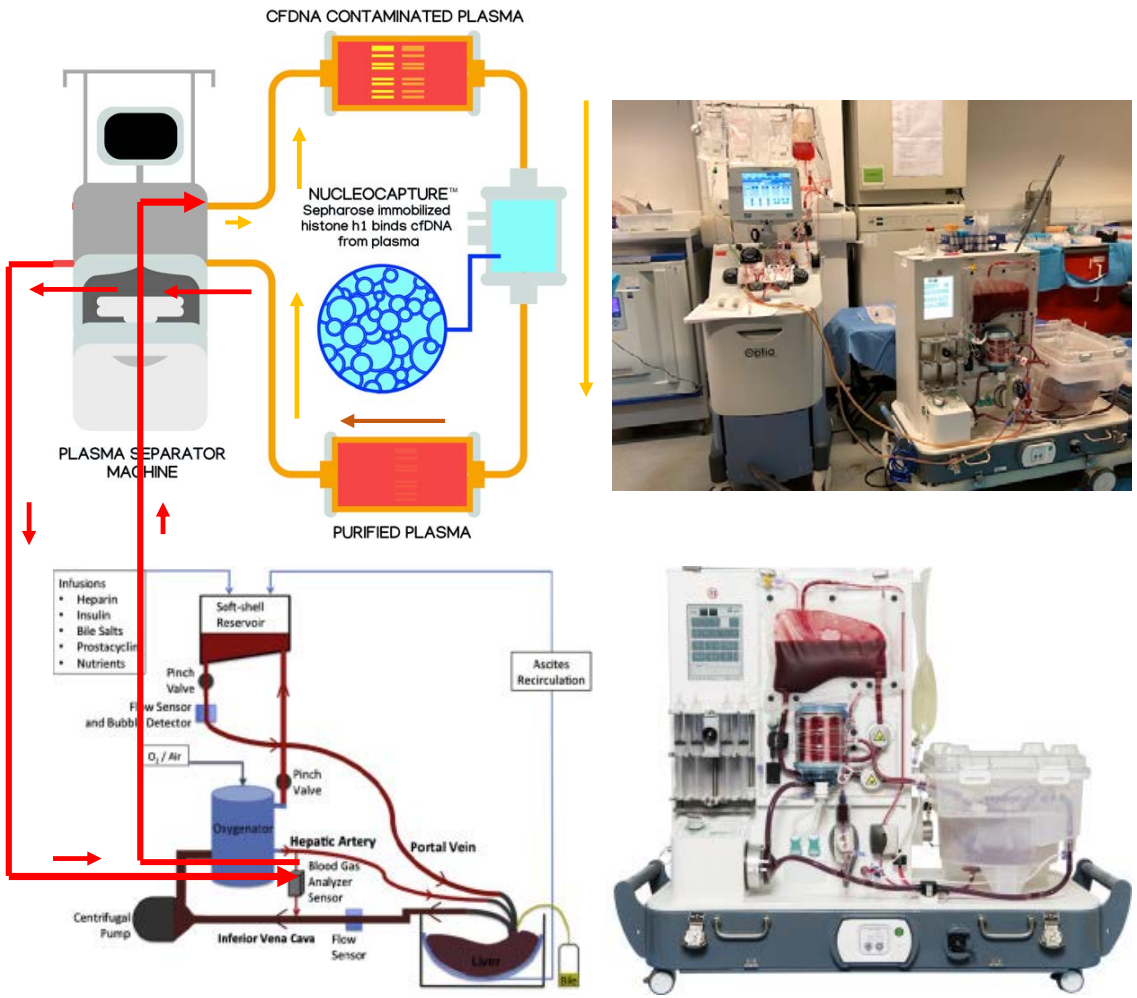

Figure 8.4. Schematic representation demonstrating connection of the OrganOx *metra* to the Spectra Optia (Terumo) apheresis system (plasma separator machine) with the incorporated NucleoCapture® classic column.

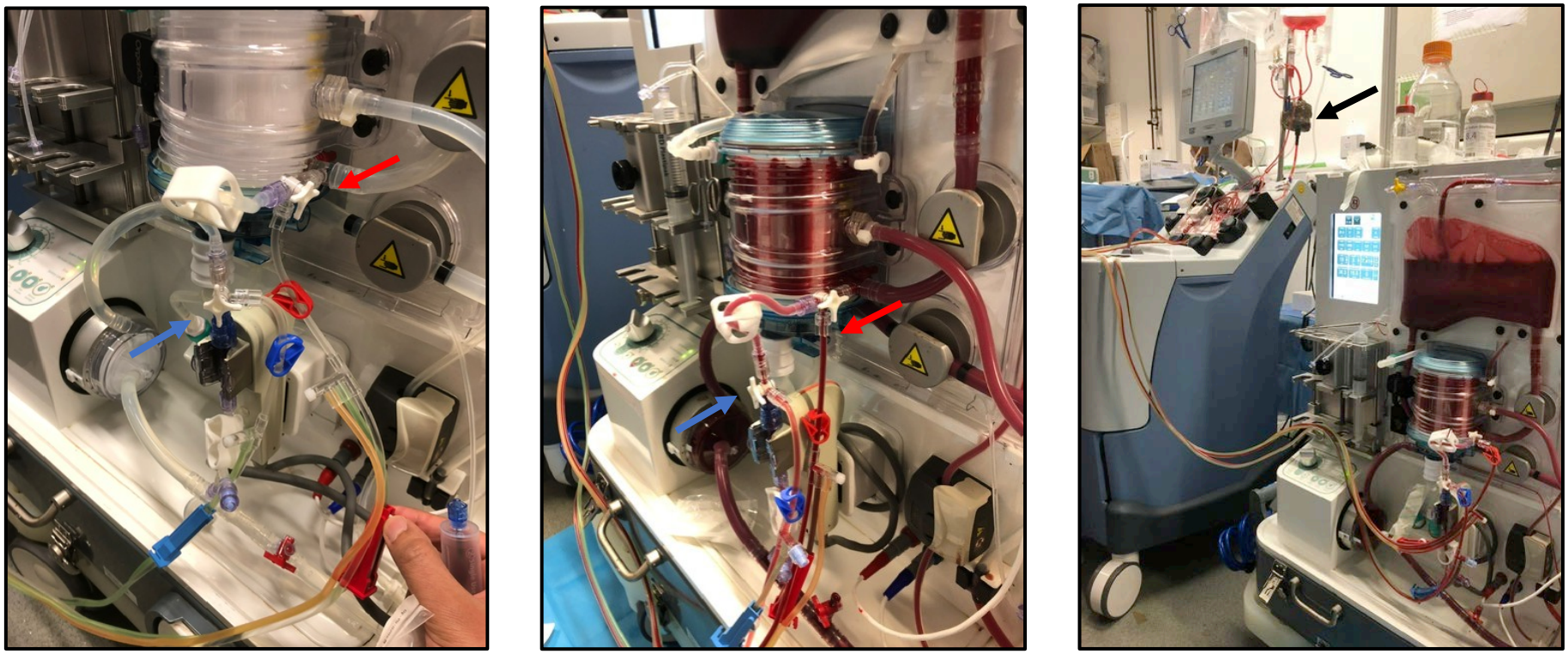

Figure 8.5. Inflow and outflow to Spectra Optia (Terumo) with NucleoCapture® classic column integrated. **Left:** NMP circuit (unprimed) with three-way taps in place to allow blood to leave the OrganOx *metra* (red arrow) and treated perfusate to return (blue arrow) following plasma separation and clearance with NucleoCapture® classic. **Middle:** Primed circuit demonstrating proximal outflow (red) and distal return (blue) of treated perfusate back to the OrganOx *metra.* **Right:** Full connection shown and position of NuceloCapture® classic column on the Spectra Optia (Terumo) device demonstrated (black arrow).

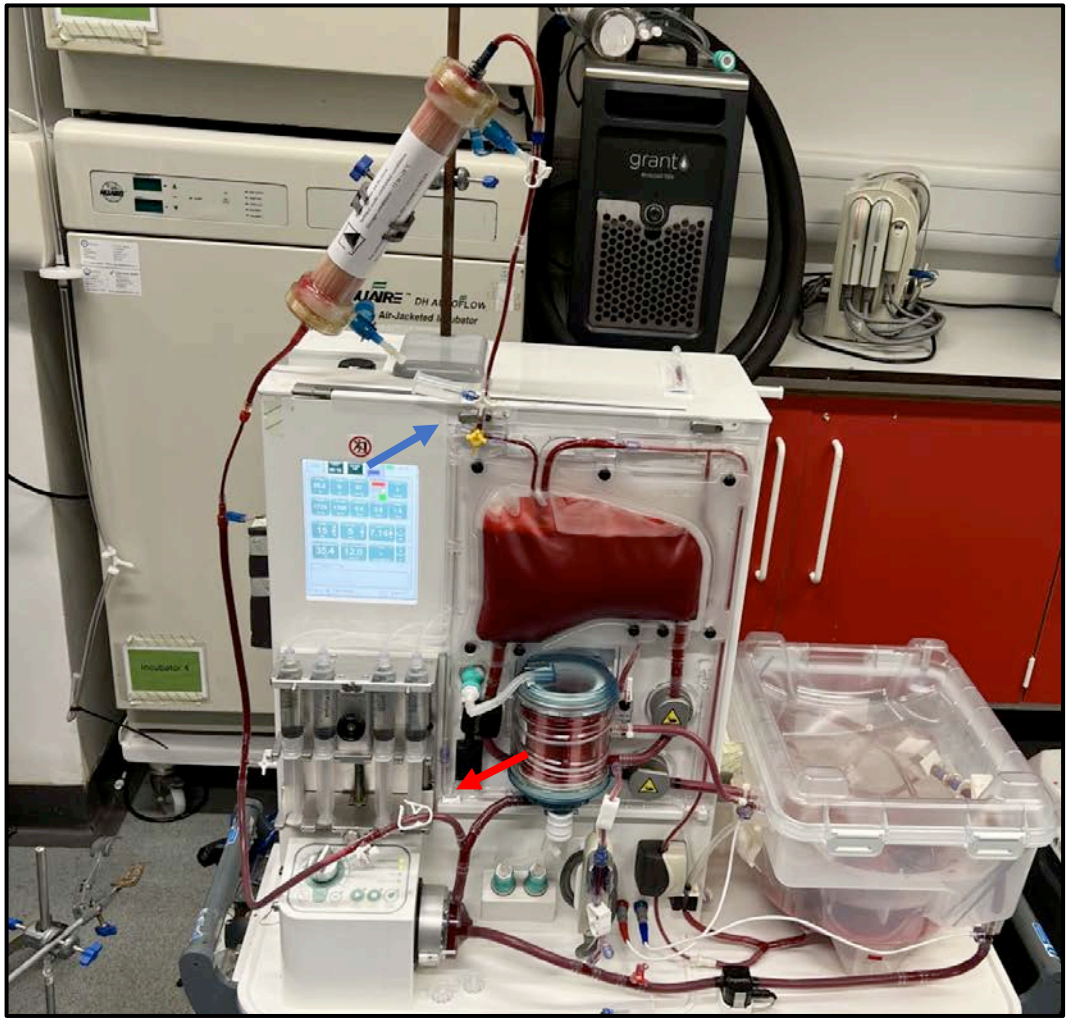

Figure 8.6. Connection of the in-line hemoperfusion NucleoCapture® prototype column established using a 3/8 'Y' connector coming off the centrifugal pump (with a line attached providing inflow into the column, red arrow) and return from the column via line attached to a 3-way tap feeding back into the soft-shell reservoir (blue arrow).

8.2.5 Sampling schedule

The sampling schedule is described in Table 8.2 for all perfusions. An additional 12 h timepoint of samples were collected for the extended in-line hemoperfusion NucleoCapture® prototype perfusions (hNC-hNC group). In addition, matched pre and post-column perfusate samples were taken for all livers.

Table 8.2. Sample schedule (tissue, perfusate and blood gas analysis).

NMP perfusion: Leucodepleted pRBC + plasma perfusion phase		**Perfusion duration (hours)**						
Sample collection		**0**	**0.5**	**1**	**2**	**4**	**6**	**12***
Tissue	Frozen	x					x	x
	Formalin-fixed	x				x	x	x
Perfusate	Biochemistry	x		x	x	x	x	x
	Blood gas	x	x	x	x	x	x	x
Bile	(if produced)	x		x	x	x	x	x
Allogenic reperfusion: Whole blood reperfusion phase		**Perfusion duration (hours)**						
Sample collection		**0**	**0.5**	**1**	**2**	**4**	**6**	**12***
Tissue	Frozen			x			x	x
	Formalin-fixed			x			x	x
Perfusate	Biochemistry	x		x	x	x	x	x
	Blood gas	x	x	x	x	x	x	x
Bile	(if produced)	x		x	x	x	x	x

Additional *12h samples taken for in-line hemoperfusion NucleoCapture® prototype perfusions.

8.2.6 Measurement of DAMPs

The total concentration of cell-free DNA (cfDNA) in the perfusate was quantified using a fluorometric assay with SYTOX® Green Dye (Life Technologies, Cheshire, UK). Fluorescence readings were obtained using a BioTek® Synergy 2 fluorometric plate reader (NorthStar Scientific Ltd, UK), with excitation and emission wavelengths set at 485 nm and 528 nm, respectively. cfDNA concentrations were determined by referencing a λ-DNA standard curve (Fisher Scientific, UK). Extracellular histones were quantified by Western blot analysis, using purified histones as a standard for comparison. These measurements were performed by Dr Jeremy Schofield (under the supervision of Dr Simon Abrams) at the University of Liverpool. The measurement of Nucleosomes (H3.1 and H3R8cit) was performed using Nu.Q™ ELISA assays (Belgian Volition SRL, Isnes, Belgium). These measurements were performed at

Volition HQ's central lab (Isnes, Belgium) using an automated system to measure the samples in triplicate following multiple dilutions, see Chapter 2.5.4. Nucleosome measurements were performed for all livers apart from the in-line hemoperfusion NucleoCapture® prototype perfusions.

8.2.7 Measurement of microclots: amyloidfibrin(ogen) aggregates

Frozen plasma samples were thawed at 37°C for 10 minutes. Microclots were detected by incubating citrated platelet-poor plasma (PPP) with 5 μM Thioflavin T (ThT) for 30 minutes at room temperature, protected from light. A 3 μL aliquot was smeared onto a slide and examined using fluorescence microscopy (Olympus IX83, with excitation at 467-498 nm and emission at 513-556 nm). Five representative fields per sample were imaged at 20x magnification and analysed using Fiji (ImageJ) with the Labkit plugin. A software classifier was trained to identify and quantify microclots based on their number (count per field) and size (pixels per field) (436).

8.2.8 Histology

Several biopsies were taken during perfusion and reperfusion: LT1 (post SCS i.e. pre-NMP), LT2 (end of NMP perfusion phase), LT3 (taken at 1h into whole blood reperfusion) and LT4 (end of whole blood reperfusion).

Two biopsies per timepoint were taken (one for formalin fixation and paraffin embedding and the other snap frozen). FFPE blocks sections were stained for H&E to assess reperfusion injury, PAS stain to assess glycogen depletion and IHC to assess CITH3, HMGB1 and MPO positive stain. Snap frozen biopsies were subsequently stored at -80°C.

All histopathological evaluation of histology slides (apart from IHC) was performed by Professor Alberto Quaglia (Consultant Histopathologist, Royal Free Hospital, London) who was blinded to the perfusion protocols and treatment allocations for each liver. Immunohistochemical assessment of IHC slides was performed using the Visiopharm® digital analysis software which is described in Chapter 2.4.2. These analyses are currently only available for NMP-NMP and NMP-NC groups. The hNC-hNC group is yet to undergo histological evaluation.

8.2.9 Perfusate sampling, blood gas analysis and biochemistry

Perfusate sampling, blood gas analysis and biochemistry analysis is described in Chapter 2.5. Assessment of hepatocellular injury was performed through measurement of perfusate ALT (IU/L).

8.3 Results

The mean procurement, warm ischaemia time (WIT) and cold ischaemia time (CIT) of each group are described in Table 8.3.

Table 8.3. Mean warm and cold ischaemia time per group.

Group	Number, *N*	Warm ischaemia time (WIT), minutes	Cold ischaemia time (CIT), minutes
NMP-NMP	3	17 ± 2.65	258.33 ± 10.60
NMP-NC	3	16.3 ± 4.93	287.67 ± 36.12
hNC-hNC	3	17.7 ± 2.08	276.67 ± 20.82

Warm ischemia time was defined as the period from exsanguination to the start of cold perfusion (during procurement at the slaughterhouse), while SCS was defined as the time from the beginning of cold perfusion (at the slaughter house) to the initiation of NMP in the laboratory. NMP-NMP refers to standard perfusion and reperfusion, NMP-NC refers to NucleoCapture® application (integrated with the Spectra Optia, Terumo) during the reperfusion phase and hNC-hNC refers to the application of the in-line hemoperfusion NucleoCapture® prototype during both perfusion and reperfusion.

8.3.1 Integration of NucleoCapture® into the ex-situ perfusion circuit

All livers were successfully procured, benched, cannulated and perfused without any complications. The warm and cold ischemia times were consistent across all groups (see Table 8.3). During both perfusion and reperfusion, all livers exhibited acceptable perfusion parameters, produced bile and demonstrated a macroscopically uniform appearance. The perfusate pH remained stable throughout the perfusions, with adjustments made using sodium bicarbonate as needed to maintain the pH >7.2. The integration of the Spectra Optia (Terumo) with NucleoCapture® classic column did not have any noticeable impact on the OrganOx *metra* perfusion parameters. Similarly, during the extended perfusions (and reperfusions), the direct integration of in-line hemoperfusion NucleoCapture® prototype column in the hNC-hNC group did not negatively impact perfusion or reperfusion, see Table 8.4.

Table 8.4. Perfusate pH, arterial flow (ml/min) and portal flow (L/min).

Group		Perfusion	Reperfusion
NMP-NMP	**pH**	7.35 ± 0.0109	7.27 ± 0.0851
	Arterial flow (ml/min)	281 ± 20.40	266.5 ± 21.04
	Portal flow (L/min)	0.76 ± 0.11	0.74 ± 0.03
NMP-NC	**pH**	7.27 ± 0.0191	7.28 ± 0.0540
	Arterial flow (ml/min)	297.6 ± 25.60	318.4 ± 28.12
	Portal flow (L/min)	0.73 ± 0.11	0.83 ± 0.05
hNC-hNC	**pH**	7.36 ± 0.0480	7.39 ± 0.0445
	Arterial flow (ml/min)	377.7 ± 87.07	395.2 ± 48.8
	Portal flow (L/min)	0.85 ± 0.04	0.8 ± 0.02

Data presented as mean ± SD

8.3.2 Removal nuclear DAMPs during ex-situ transplant model

The application of NucleoCapture® both with the adjunct of the Spectra Optia (Terumo) during whole blood reperfusion and the in-line hemoperfusion NucleoCapture® prototype during both perfusion (pRBCs + plasma) and allogenic whole blood reperfusion efficiently cleared nuclear DAMPs compared to NMP alone. Perfusate concentrations of cfDNA and extracellular histones were measured in all livers. In addition, nucleosomes/NETs were measured in all livers apart from the in-line hemoperfusion NucleoCapture® experiments (hNC-hNC). These measurements are currently being undertaken and are therefore not included in this thesis.

8.3.2.1 Pre and Post-column clearance of nuclear DAMPs

The application of NucleoCapture® classic during reperfusion with the adjunct of the Spectra Optia (Terumo) demonstrated a significant reduction in cfDNA at 1h of reperfusion (pre-column: 8.16 ± 2.40 µg/ml vs. post-column: 1.39 ± 1.80 µg/ml, $P = 0.0174$) and a clearance of nucleosomes/NETs at 2h of reperfusion (pre-column: 44893.41 ± 14207.02 ng/ml vs. post-column: 7747.28 ± 11530.50 ng/ml, $P = 0.0250$).

A non-significant reduction in extracellular free histones was also observed by 6h of reperfusion (pre-column: 127.44± 27.20 µg/ml vs. post-column: 86.80 ± 36.69 µg/ml, *P* = 0.198), Figure 8.7A. The in-line hemoperfusion NucleoCapture® prototype also demonstrated clearance of nuclear DAMPs (albeit to a lesser extent pre and post-column) and this was most pronounced beyond 6h of perfusion and 6 of reperfusion.

There was a non-significant reduction in cfDNA at 6h of perfusion (pre-column: 2.64 ± 0.99 µg/ml vs. post-column: 2.43 ± 1.05 µg/ml, P = 0.817) and extracellular histones at 6h of perfusion (pre-column: 71.87 ± 63.01 µg/ml vs. post-column: 65.68 ± 76.34 µg/ml, P = 0.919), Figure 8.7B. At 6h of reperfusion, there was a non-significant reduction in cfDNA (pre-column: 0.49 ± 0.24 µg/ml vs. post-column: 0.31 ± 0.04 µg/ml, P = 0.279) and extracellular histones (pre-column: 36.64 ± 31.38 µg/ml vs. post-column: 32.73 ± 38.15 µg/ml, P = 0.897), Figure 8.7C.

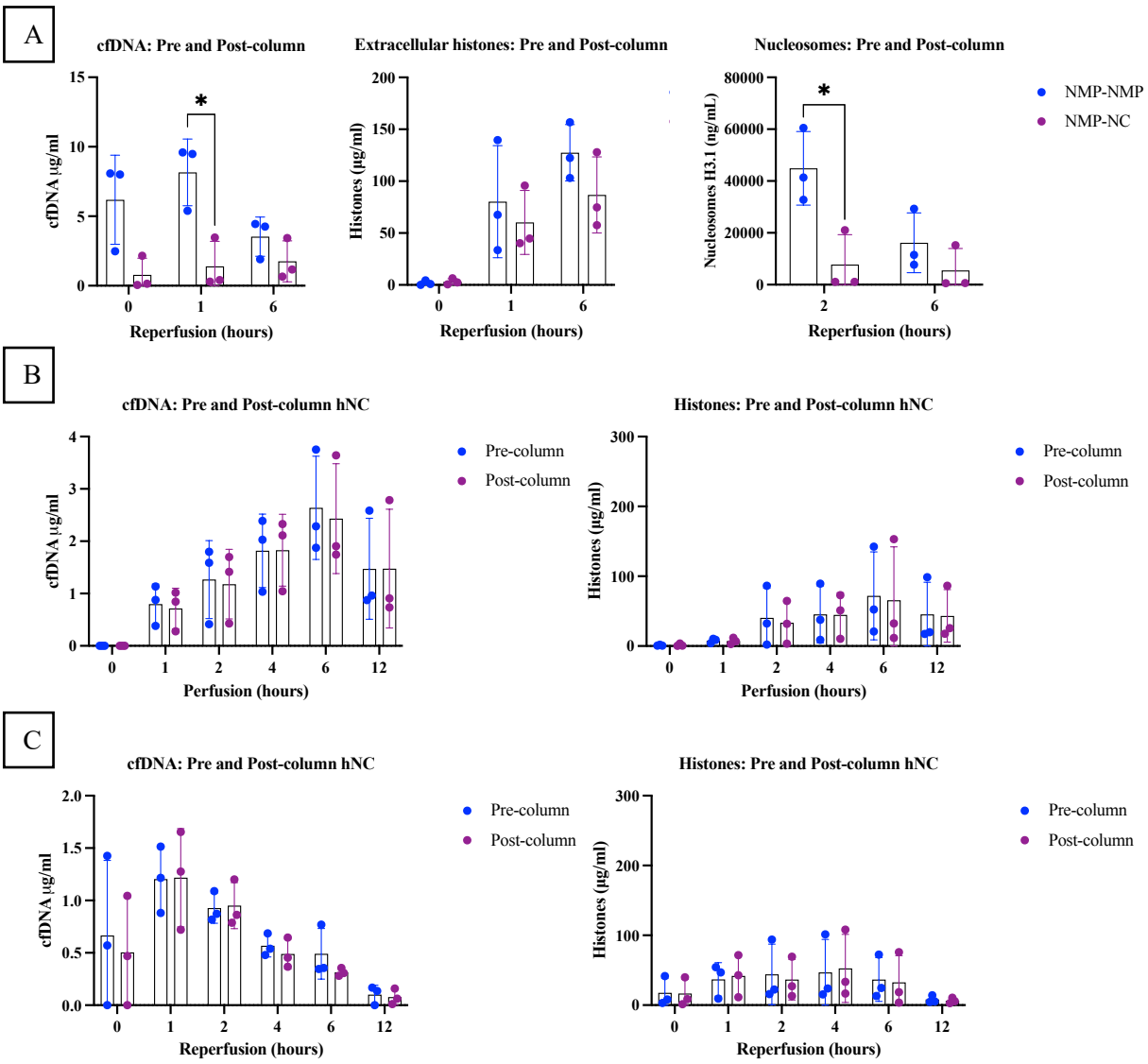

Figure 8.7A-C. Clearance of nuclear DAMPs during 6h of allogenic whole blood reperfusion with integration of the NucleoCapture® classic column with the Spectra Optia (Terumo) and the OrganOx *metra* **(A).** Initial increase in cfDNA and histones with reduction between 6h and 12h using the in-line hemoperfusion NucleoCapture® prototype **(B).** Continued reduction during 12h of allogenic whole blood reperfusion using the in-line hemoperfusion NucleoCapture® prototype **(C).** Multiple unpaired t-tests, data reported as mean ± SD. * $P \leq 0.05$, ** $P \leq 0.01$, *** $P \leq 0.001$ and **** $P \leq 0.0001$.

8.3.2.2 Systemic clearance of nuclear DAMPs

The NMP-NMP and NMP-NC groups were initially perfused for 6h (using autologous pRBC and plasma) and then reperfused for 6h using allogenic whole blood, with integration of the NucleoCapture® classic column and Terumo Optia Spectra only in the NMP-NC group at reperfusion. However, in the hNC-hNC group, the perfusion (and reperfusion) was extended to 12h and there was continuous application of the NucleoCapture® in-line hemoperfusion

column directly attached to the OrganOx *metra* (a new column was attached at reperfusion to avoid saturation).

During the initial perfusion phase, there was an increase in cfDNA in both the NMP-NMP group and NMP-NC group (in the absence of NucleoCapture® technology during the perfusion phase). However, the application of the in-line hemoperfusion NucleoCapture® prototype in the hNC-hNC group resulted in a significant reduction of cfDNA at 6h of perfusion compared to both the NMP-NMP and NMP-NC groups (hNC-hNC: 2.64 ± 0.99 µg/ml vs. NMP-NMP: 15.03 ± 10.30 µg/ml vs. NMP-NC: 34.86 ± 9.37 µg/ml, $P = 0.0287$ and $P < 0.0001$ respectively). This trend was also observed in extracellular histones, with the hNC-hNC group demonstrating a significant reduction at 1h of perfusion (hNC-hNC: 71.87 ± 63.07 µg/ml vs. NMP-NMP: 127.44 ± 27.20 µg/ml, $P = 0.0395$), Figure 8.8.

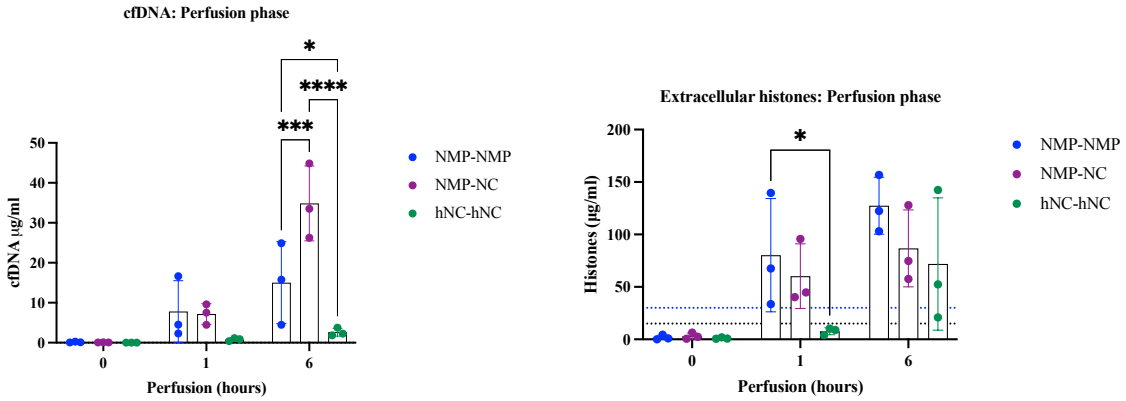

Figure 8.8. Application of the in-line hemoperfusion NucleoCapture® prototype integrated directly into the OrganOx *metra* results in a significant reduction in cfDNA and extracellular histones during perfusion compared to NMP alone. The dotted black line indicates histone levels observed in patients with acute liver failure who did not survive and blue line indicates levels observed in patients that developed graft dysfunction post liver transplant (437,438). Data reported as mean ± SD and mixed effect analysis for repeated measures with post-hoc tukey correction to adjust for multiple comparisons between timepoints. * $P \leq 0.05$, ** $P \leq 0.01$, *** $P \leq 0.001$ and **** $P \leq 0.0001$.

At the end of 6h allogenic whole blood reperfusion, there was a significant decrease in cfDNA in the NMP-NC group and hNC-hNC groups (with the adjunct of NucleoCapture® technology) compared to the NMP-NMP group (NMP-NC: 5.98 ± 4.45 µg/ml and hNC-hNC: 0.49 ± 0.24 µg/ml vs. NMP-NMP: 16.87 ± 3.19 µg/ml, $P = 0.0098$ and $P = 0.003$ respectively), Figure 8.9A. In the hNC-hNC group, where perfusion (and reperfusion) was extended, there was a non-significant reduction in cfDNA between 12h of perfusion and 12h of reperfusion (1.47 ± 0.96 µg/ml vs. 0.10 ± 0.09 µg/ml, $P = 0.070$), Figure 8.9B. Similarly, there was a significant

reduction in extracellular histones in the NMP-NC group and hNC-hNC groups by 6h of reperfusion compared to the NMP-NMP group: NMP-NC: 58.99 ± 12.26 µg/ml and hNC-hNC: 36.64 ± 31.34 µg/ml vs. NMP-NMP: 152.30 ± 16.82µg/ml (P = 0.0015 and P = 0.0001 respectively), Figure 8.9C. In the hNC-hNC group, there was a non-significant reduction in extracellular histones between 12h of perfusion and 12h of reperfusion (45.25 ± 46.21 µg/ml vs. 8.03 ± 5.24 µg/ml, P = 0.237), Figure 8.9D.

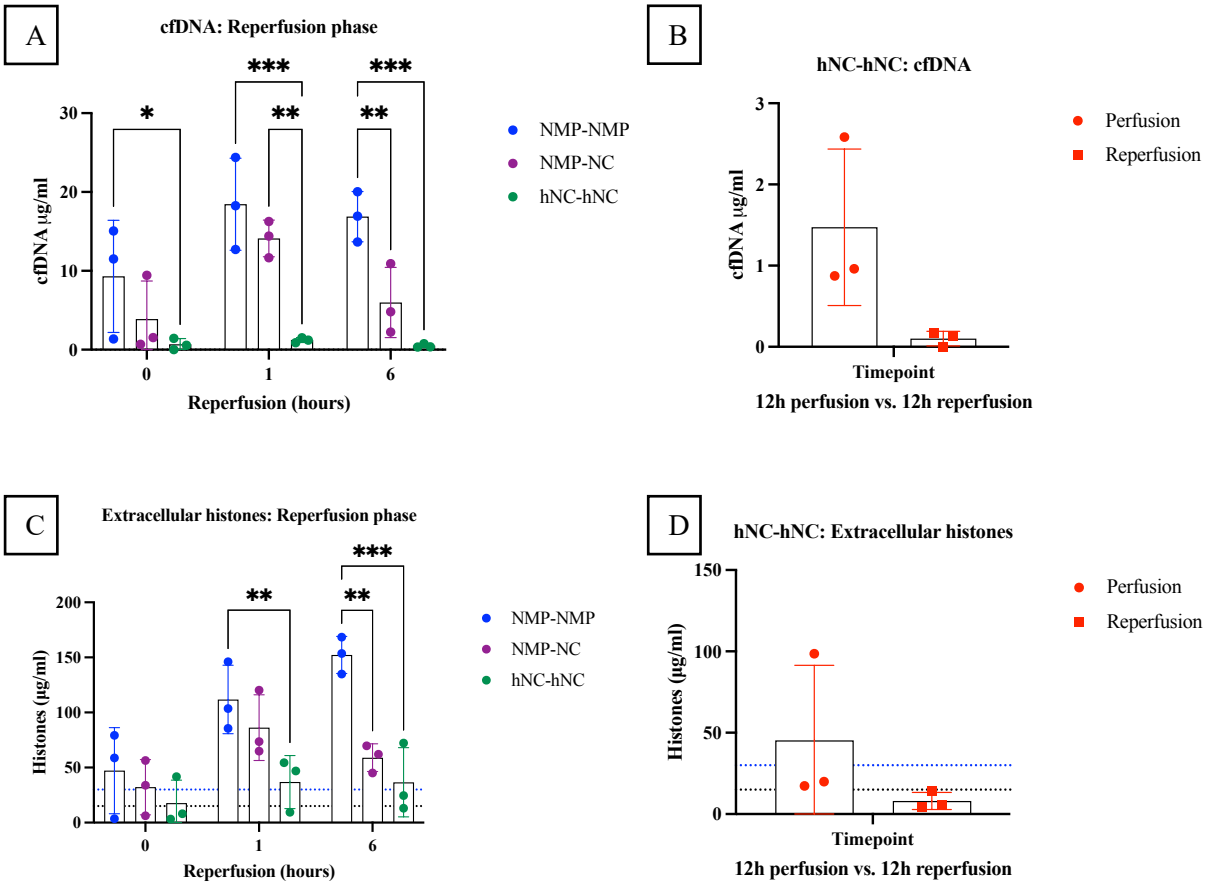

Figure 8.9A-D. Application of both NucleoCapture® classic integrated with the OrganOx *metra* via the Optia Spectra (Terumo) plasma apheresis device (NMP-NC) and the in-line hemoperfusion NucleoCapture® prototype (hNC-hNC) integrated directly into the OrganOx *metra* results in a significant reduction in cfDNA and extracellular histones by 6h of allogenic whole blood reperfusion **(A and C)**. During extended perfusion (and reperfusion) in the hNC-hNC group, a reduction in cfDNA and extracellular histones is also observed between 12h of perfusion and 12h of reperfusion **(B and D)**. The dotted black line indicates histone levels observed in patients with acute liver failure who did not survive and blue line indicates levels observed in patients that developed graft dysfunction post liver transplant (437,438). Multiple unpaired t-tests, data reported as mean ± SD and mixed effect analysis for repeated measures with post-hoc tukey correction to adjust for multiple comparisons between timepoints. * $P \leq 0.05$, ** $P \leq 0.01$, *** $P \leq 0.001$ and **** $P \leq 0.0001$.

Nucleosomes/NETs were only measured in the NMP-NMP and NMP-NC groups. During the initial perfusion phase, there was an increase in Nucleosomes (quantified using the Volition

H3.1 assay) in both the NMP-NMP group and NMP-NC group (in the absence of NucleoCapture® technology during the perfusion phase). Perfusate Nucleosome levels were highest in both groups by 6h of perfusion (NMP-NC: 23561.6 ± 39208.12 ng/ml vs. NMP-NMP: 64256.37 ± 41575.60 ng/ml, P = 0.284). This trend was also observed in NETs (quantified using the Volition H3R8cit assay) with perfusate levels highest by 6h of perfusion (NMP-NC: 591.13 ± 937.72 ng/ml vs. NMP-NMP: 2290.0 ± 1980.56 ng/ml, P = 0.250), Figure 8.10A. During allogenic whole blood reperfusion, there was a significant decrease in Nucleosomes in the NMP-NC group (with the adjunct of NucleoCapture® technology) compared to the NMP-NMP group at 6h of reperfusion (NMP-NC: 15746.0 ± 8138.71 ng/ml vs. NMP-NMP: 108462 ± 29088.84 ng/ml, P = 0.0060). This trend (although not significant) was also demonstrable for perfusate NETs at 6h of reperfusion (NMP-NC: 591.13 ± 937.13 ng/ml vs. NMP-NMP: 2290.0 ± 1980.56 ng/ml, P = 0.250), Figure 8.10B.

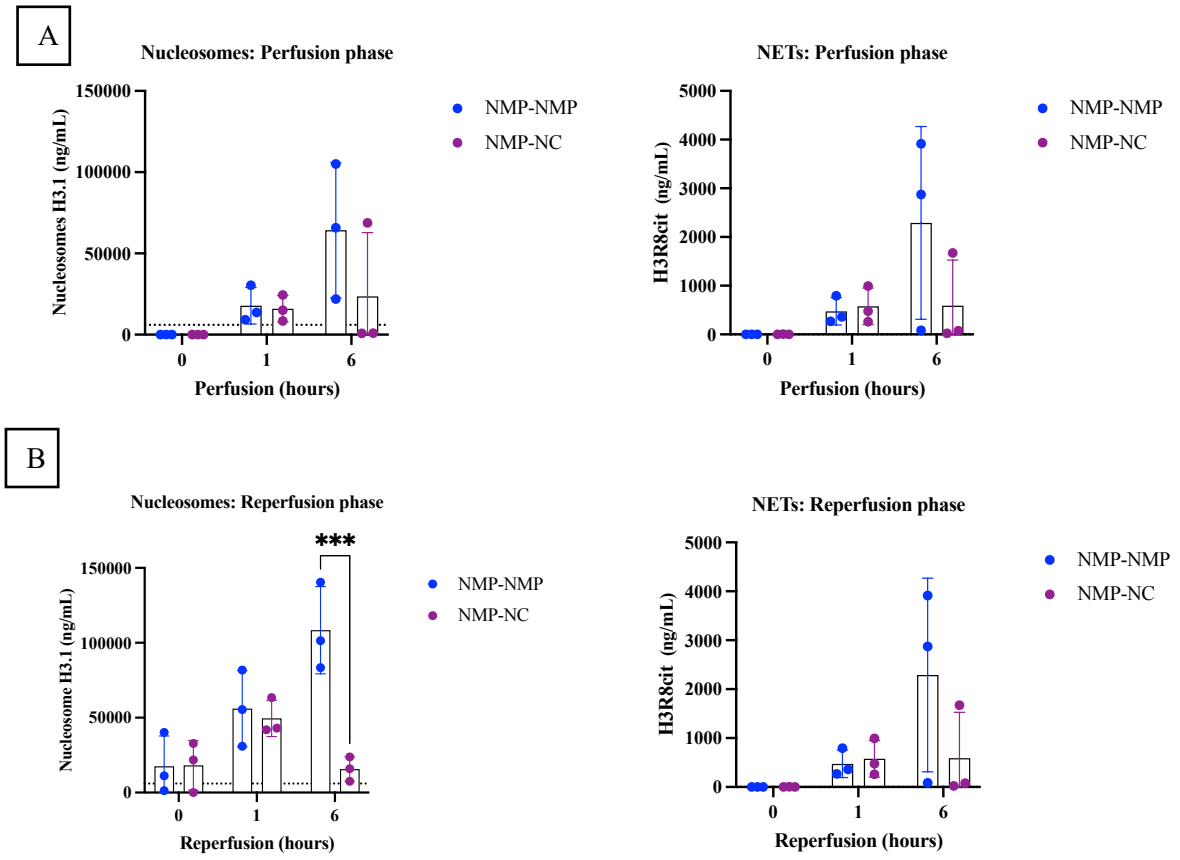

Figure 8.10A-B. The absence of NucleoCapture® integrated with the OrganOx *metra* via the Optia Spectra (Terumo) plasma apheresis device during perfusion results in an increase in both Nucleosomes and Neutrophil Extracellular Traps (NETs) **(A)**. However, with the addition of the NucleoCapture® classic column during whole blood allogenic reperfusion (NMP-NC) there is a significant reduction in Nucleosomes (but not NETs) by 6h of reperfusion **(B)**. The dotted black line indicates Nucleosome levels observed in patients in ICU with COVID who did not survive (439). Multiple unpaired t-tests, data reported as mean ± SD. * $P \leq 0.05$, ** $P \leq 0.01$, *** $P \leq 0.001$ and **** $P \leq 0.0001$.

8.3.3 Reduction in microclots with NucleoCapture®

Application of both the NucleoCapture® classic column integrated with the OrganOx *metra* via the Optia Spectra (Terumo) plasma apheresis device (NMP-NC) and the in-line hemoperfusion NucleoCapture® prototype (hNC-hNC) integrated directly into the OrganOx *metra* resulted in a reduction in microclots as demonstrated in Figure 8.11 and 8.12.

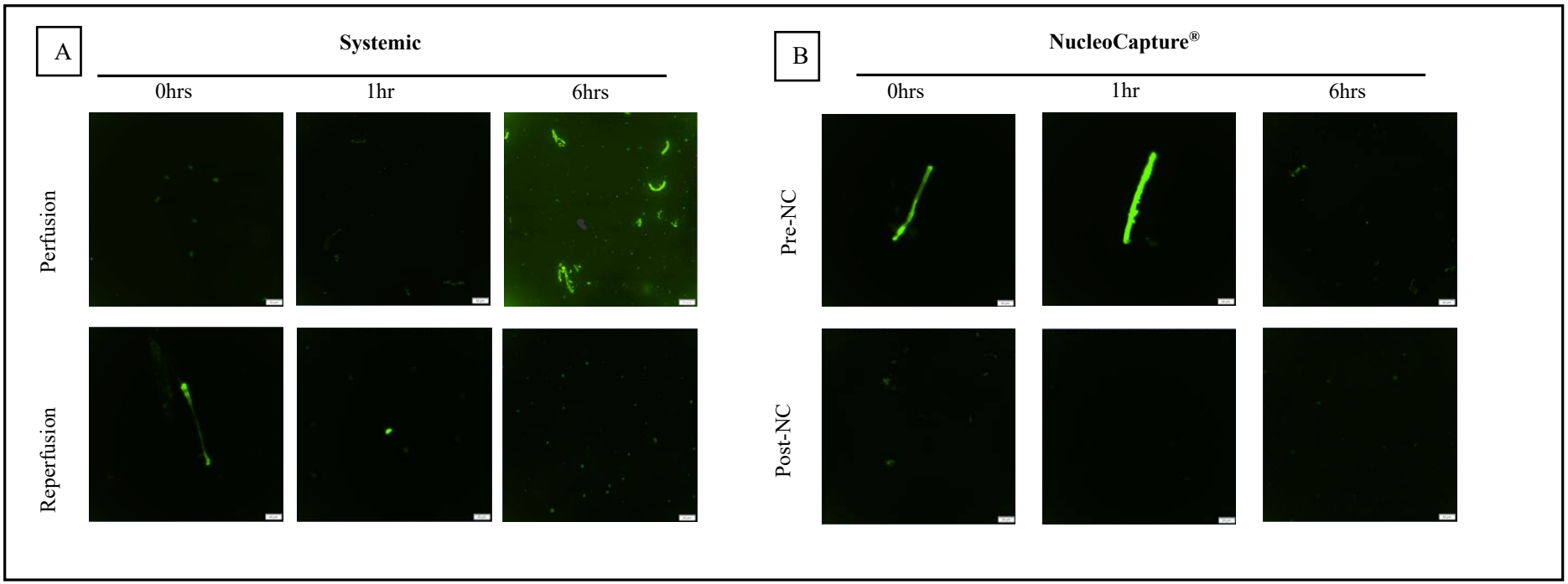

Figure 8.11A-B. Example of an NMP-NC Liver where microclots were assessed by incubating samples with Thioflavin T and viewed under fluorescence microscopy. **Left: Systemic perfusate (top row)** demonstrating an accumulation of microclots during the initial 6h of NMP phase (pRBC + plasma, in the absence of NucleoCapture® technology). Following integration of the NucleoCapture® classic column with the OrganOx *metra* via the Optia Spectra (Terumo) plasma apheresis device during whole blood allogenic reperfusion of the same liver, a reduction in microclots by the end of 6h reperfusion is observed **(bottom row) (A). Right:** Pre-column perfusate samples (up to 6h of reperfusion) are shown in the top row, the post-column samples are shown in the bottom row with successful clearance of microclots **(B).**

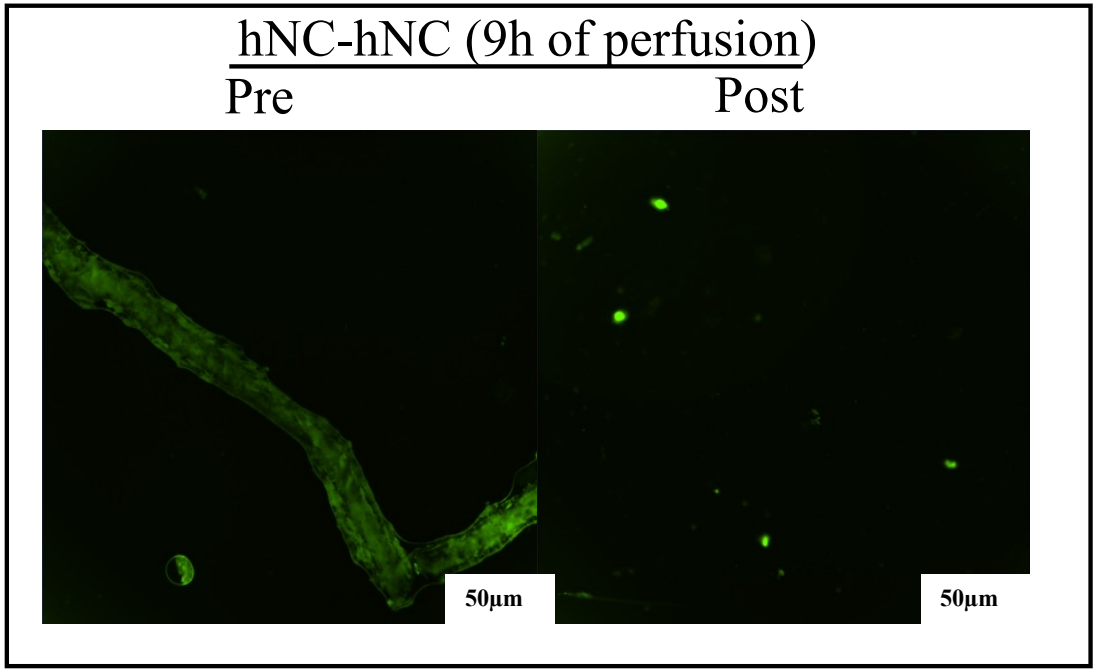

Figure 8.12. Example of liver perfused with the in-line hemoperfusion NucleoCapture® prototype (hNC-hNC) integrated directly into the OrganOx *metra*. Images are representative of the initial NMP perfusion phase (pRBCs + plasma). The perfusate samples (pre and post-column) taken at 9h of NMP demonstrates a reduction in microclots.

8.3.4 Histological assessment

Histological analysis of the livers demonstrated reduced neutrophil infiltration in those treated with NucleoCapture®. Despite this, the overall histological features were comparable across all groups. Notably, any form of NMP, regardless of the inclusion of NucleoCapture®, was associated with glycogen depletion following whole blood allogenic reperfusion (in the absence of insulin). H&E as well as PAS sections for livers perfused in the NMP-NMP and NMP-NC groups are shown in Figure 8.13 and 8.14 respectively. In addition, immunohistochemical (IHC) quantification of DAMPs i.e. CITH3, MPO and HMGB1 (using Visopharm® digital analysis software) is shown in Figure 8.15 demonstrating a reduction in positive staining in the NMP-NC group at the end of reperfusion with NucleoCapture®. Histological sections (H&E, PAS and IHC) for livers perfused in the hNC-hNC group are yet to have histopathological evaluation and are therefore not included in this chapter.

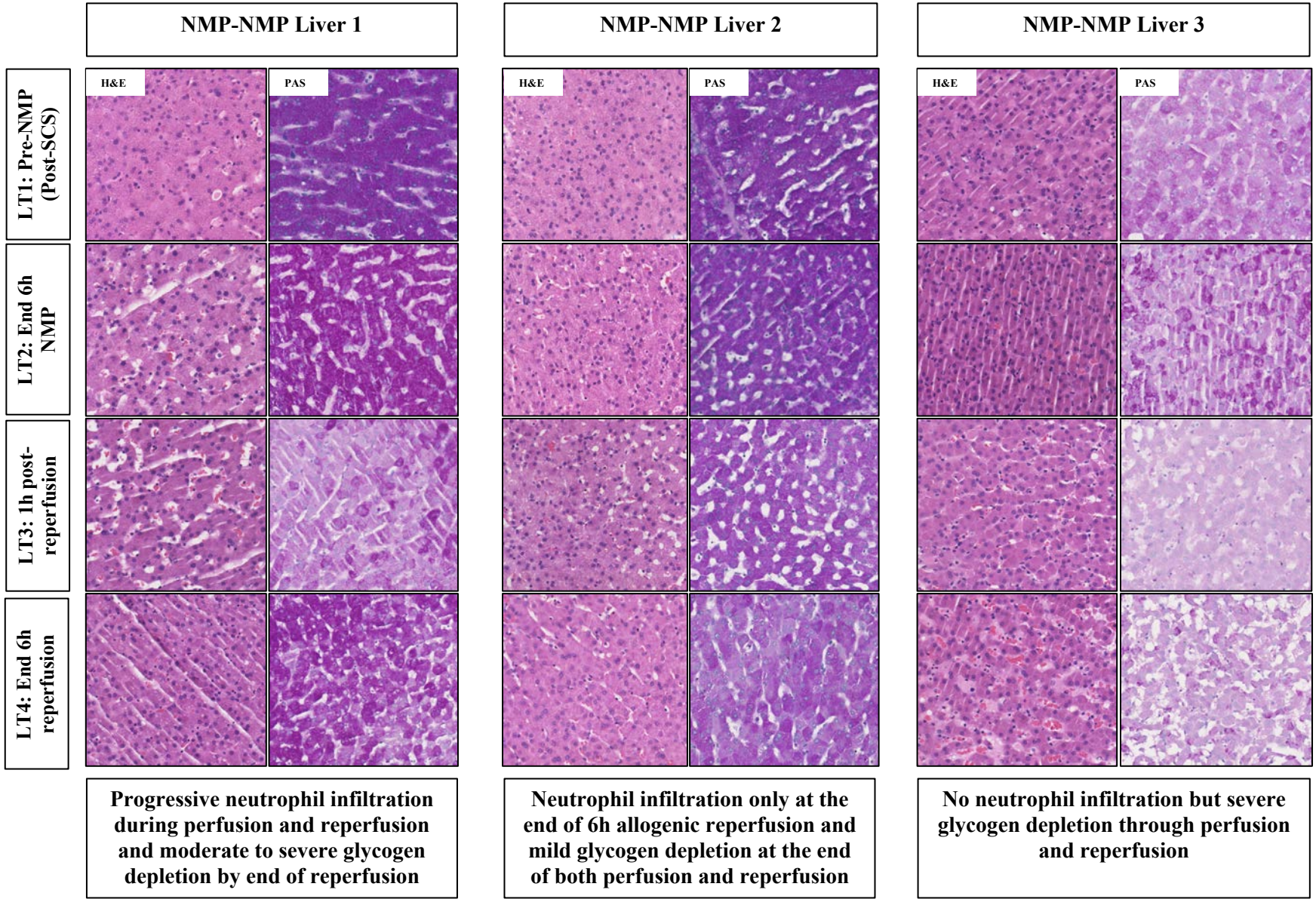

Figure 8.13. Blinded histopathological evaluation of NMP-NMP livers

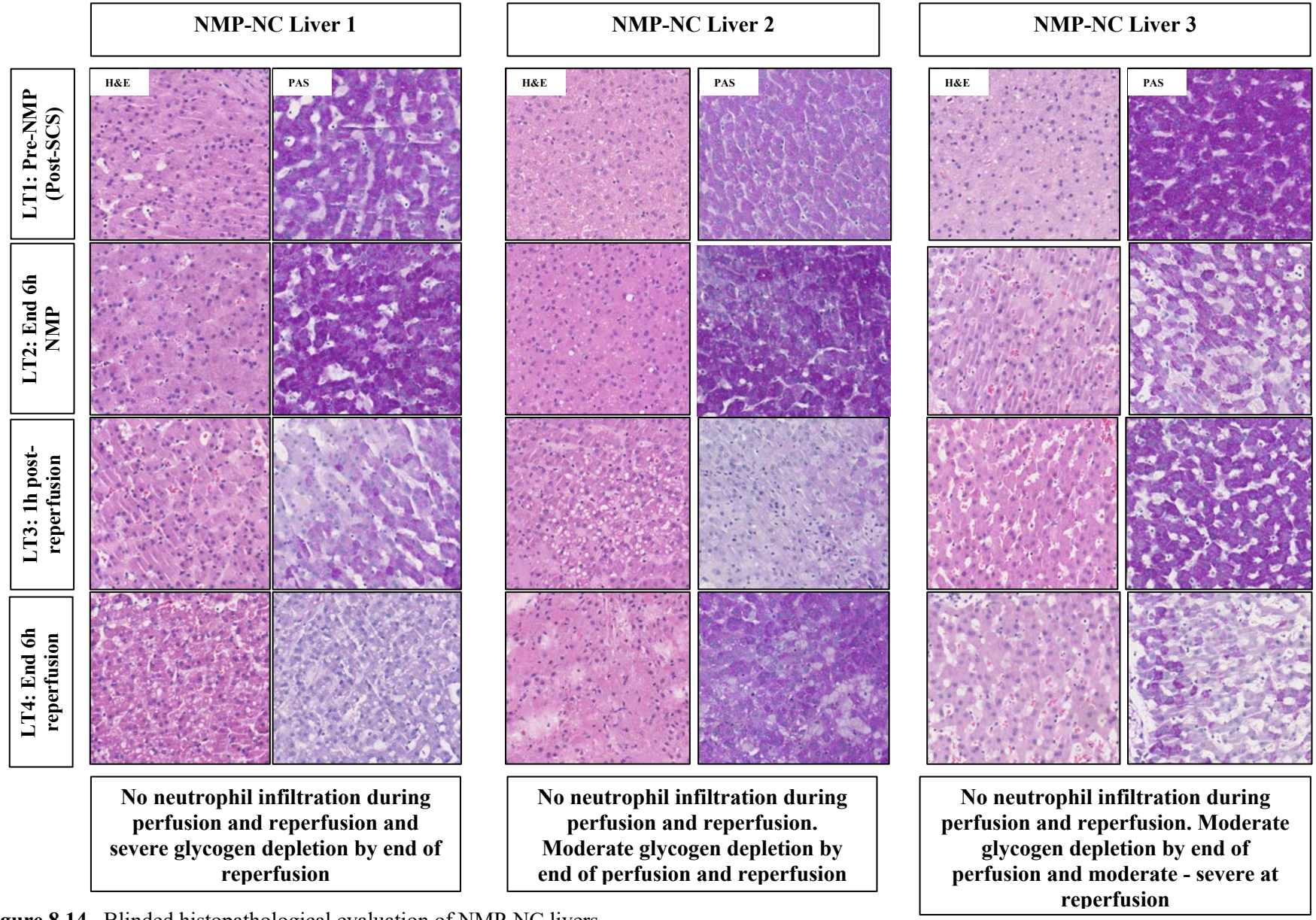

Figure 8.14. Blinded histopathological evaluation of NMP-NC livers

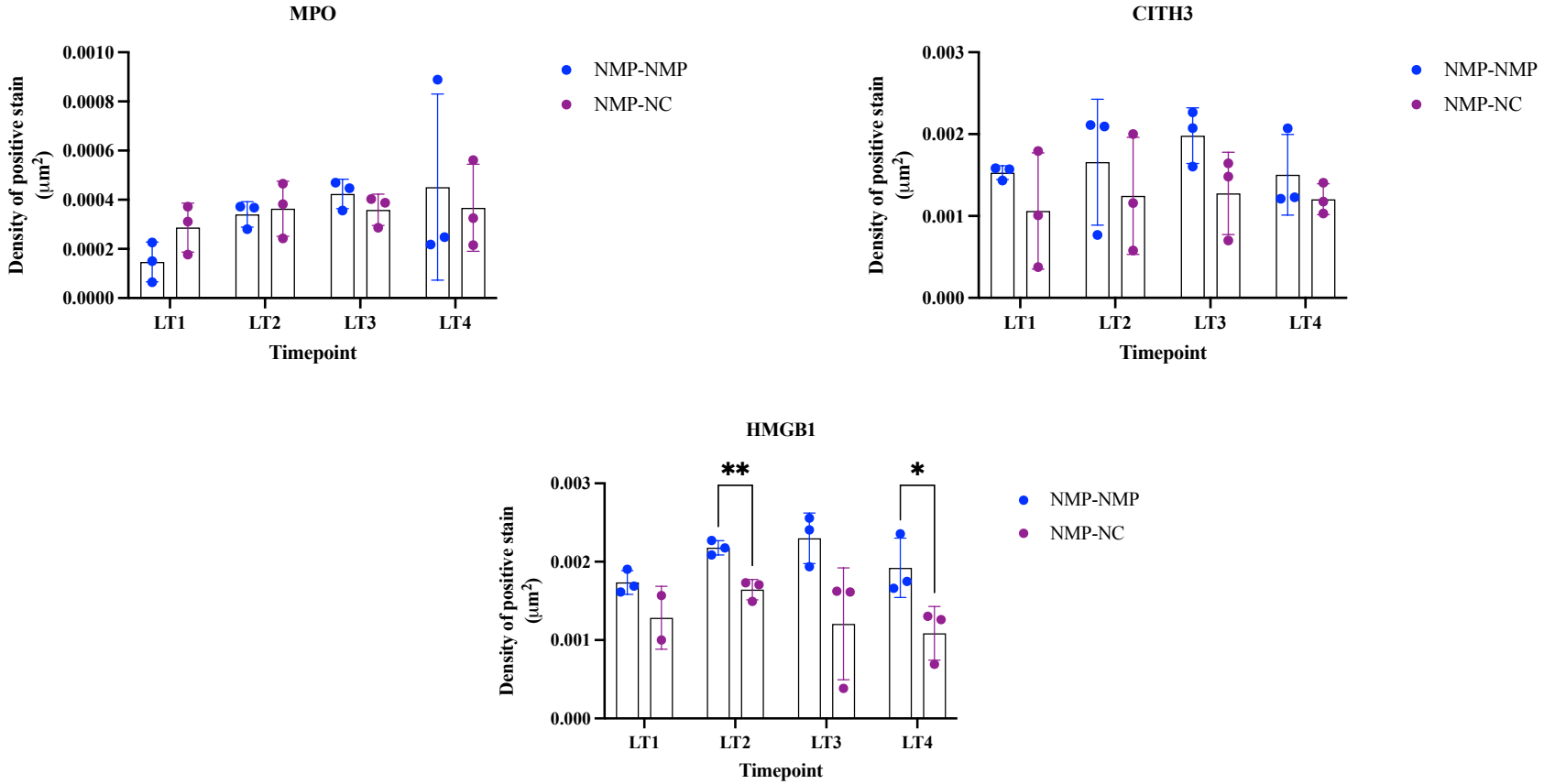

Figure 8.15. LT1 (post SCS, Pre-NMP), LT2 (end of NMP perfusion phase), LT3 (taken at 1h into whole blood reperfusion) and LT4 (end of whole blood reperfusion). Reduction in positive staining for MPO, CITH3 and HMGB1 at the end of reperfusion in the NMP-NC group treated with NucleoCapture®. A significant reduction in HMGB1 stain in the NMP-NC group at the end of both perfusion and reperfusion compared to the NMP-NMP group. Multiple unpaired t-tests, data reported as mean ± SD. * $P \leq 0.05$, ** $P \leq 0.01$, *** $P \leq 0.001$ and **** $P \leq 0.0001$.

8.3.5 Hepatocellular injury

During the initial NMP perfusion phase (with pRBCs + plasma) there was no significant difference between ALT at 6h between groups (NMP-NMP: 260.70 ± 249 IUL; NMP-NC: 307.4 ± 223.74 IU/L and; hNC-hNC: 343.53 ± 409.52 IU/L). This trend in ALT was also observed at 6h of whole blood allogenic reperfusion (NMP-NMP: 215.13 ± 200.80 IUL; NMP-NC: 250.10 ± 105.54 IU/L and; hNC-hNC: 248.1 ± 282.90 IU/L). In the hNC-hNC group, there was a non-significant difference in ALT between 12h of perfusion and 12h of reperfusion (407.60 ± 455.54 µg/ml vs. 422.43 ± 520.88 µg/ml, $P = 0.972$), Figure 8.16.

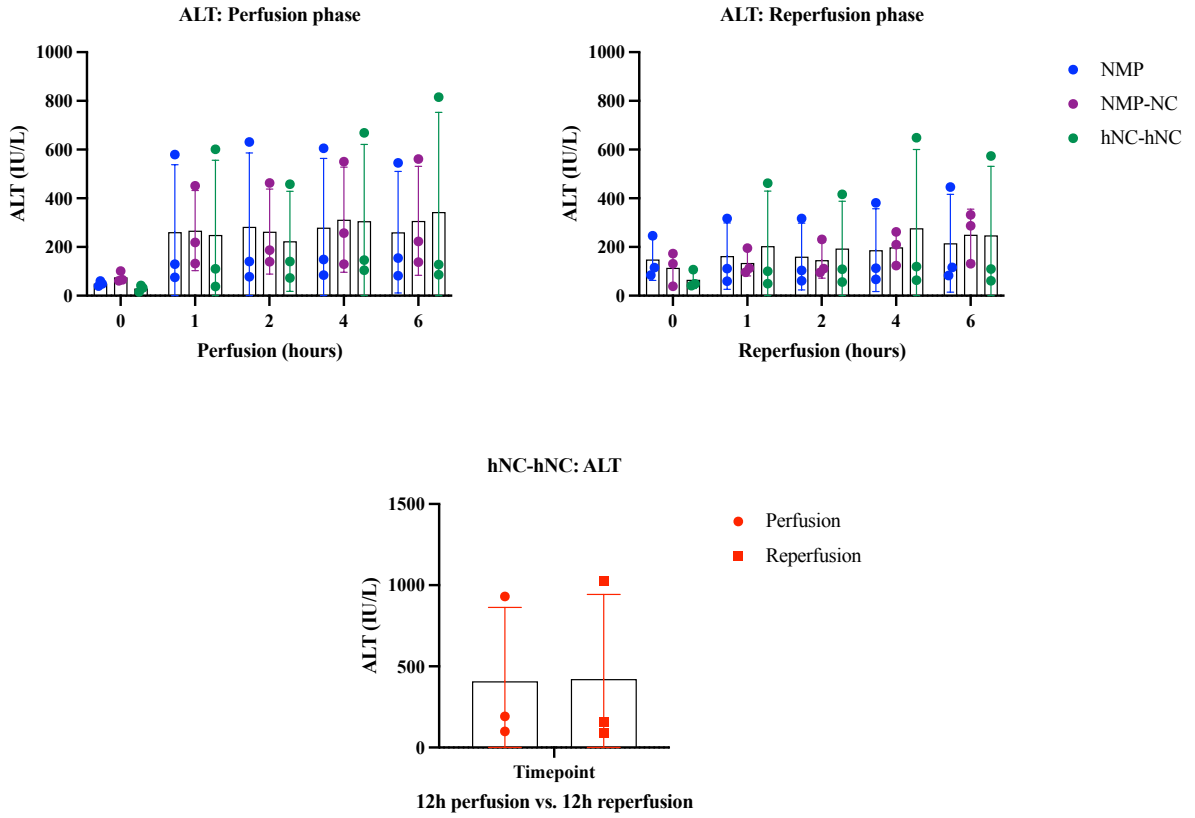

Figure 8.16. Hepatocellular injury quantified through measurement of perfusate ALT (IU/L). No significant difference between timepoints observed. Data reported as mean ± SD, Multiple unpaired t-tests and mixed effect analysis for repeated measures with post-hoc tukey correction to adjust for multiple comparisons between timepoints. * $P \leq 0.05$, ** $P \leq 0.01$, *** $P \leq 0.001$ and **** $P \leq 0.0001$.

8.3.6 Lactate clearance

During the initial NMP perfusion phase (with pRBCs + plasma), although the lactate was higher in the NMP-NC group, there was no significant difference in lactate at 6h between groups (NMP-NMP: 11.67 ± 3.6 mmol/L; NMP-NC: 14.20 ± 9.22 mmol/L and; hNC-hNC: 4.34 ± 5.53 mmol/L). However, at 6h of whole blood allogenic reperfusion the perfusate lactate was lower in the NMP-NC and hNC-hNC groups compared to the NMP-NMP group (NMP-NMP: 11.33 ± 5.66 mmol/L; NMP-NC: 8.23 ± 5.77 mmol/L and; hNC-hNC: 1.87 ± 2.11 mmol/L). In addition, a significant reduction was observed at 1h and 4h of reperfusion in the hNC-hNC group compared to the NMP-NC and NMP-NMP groups ($P = 0.0135$ and $P = 0.0491$ respectively). This reduction in the hNC-hNC group remained significant at 6h of reperfusion compared to the NMP-NMP group ($P = 0.0265$). Overall, in the hNC-hNC group, there was a non-significant decrease in lactate between 12h of perfusion and 12h of reperfusion (2.40 ± 2.52 mmol/L vs. 1.37 ± 1.17 mmol/L, $P = 0.554$), Figure 8.17.

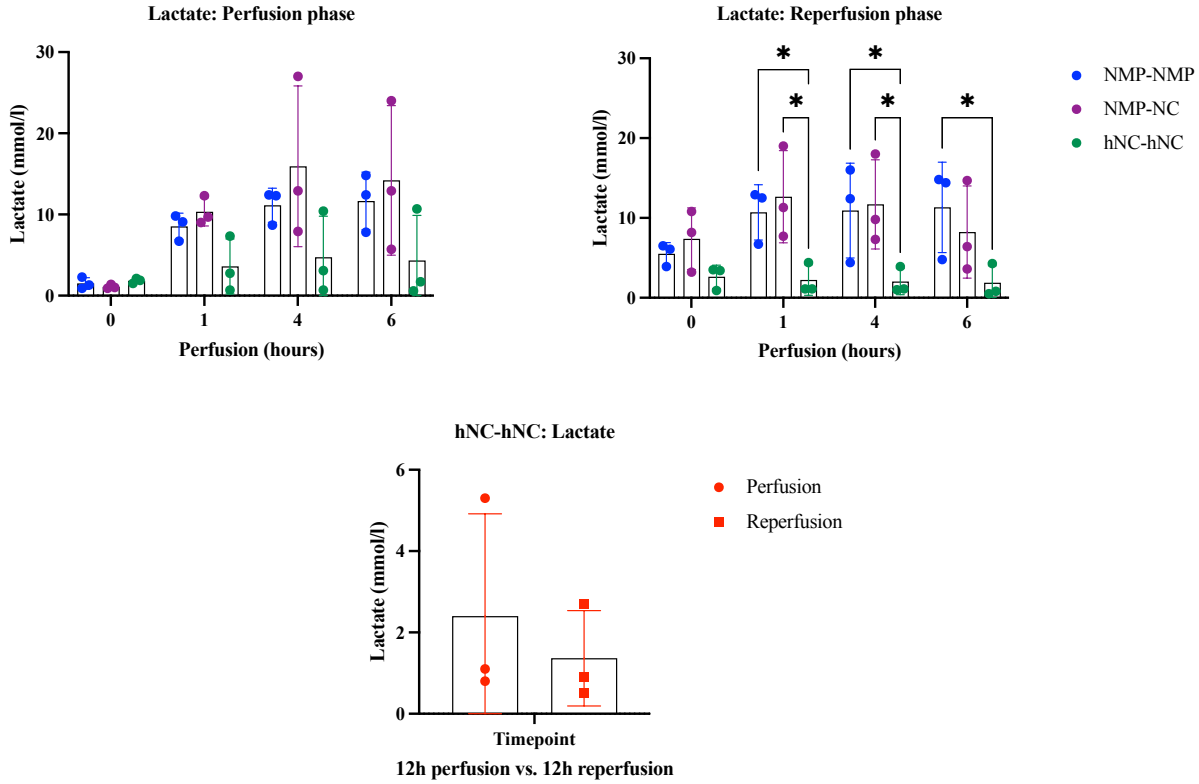

Figure 8.17. A significant reduction in lactate only observed in the hNC-hNC group during whole blood allogenic reperfusion. Data reported as mean ± SD, Multiple unpaired t-tests and mixed effect analysis for repeated measures with post-hoc tukey correction to adjust for multiple comparisons between timepoints. * $P \leq 0.05$, ** $P \leq 0.01$, *** $P \leq 0.001$ and **** $P \leq 0.0001$.

8.3.7 Discarded human liver perfusion with in-line hemoperfusion NucleoCapture®

To confirm the findings of the hNC-hNC group, the in-line hemoperfusion NucleoCapture® prototype column was tested in a discarded human liver during perfusion (total of 12h) and reperfusion (total of 6h). The overall objective of this perfusion was to assess the performance of the in-line hemoperfusion NucleoCapture® prototype column in the clearance of nuclear DAMPs and microclots. The donor details are described in Table 8.5.

Table 8.5. Donor details and liver characteristics

Perfusion protocol and warm time between end of NMP, cold flush and commencement of whole blood reperfusion	Age (years)	Type	CIT (h & min)	Baseline steatosis: Surgeon's assessment	Liver weight (kg)
Human NucleoCapture® Liver 1 Warm time: 42 min	66	DCD	12 h 21 min	Moderate and capsular injury	1.7

The sampling schedule for this human liver perfusion is described in Chapter 7.2.3. However, as with the hNC-hNC perfusions, the pre-column perfusate samples were collected from the IVC line exiting the liver (and therefore also reflect systemic levels). Post-column samples were collected from a three-way tap located on the line exiting the column (prior to drainage into the reservoir), see Figure 8.18. Serial biopsies were taken; however, these are yet to have histopathological evaluation.

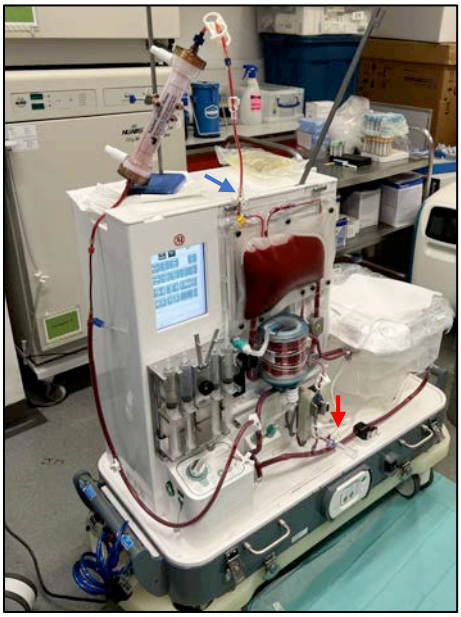

Figure 8.18. Red arrow demonstrates site of sampling for pre-column perfusate, and blue arrow demonstrates post-column site for sample collection.

8.3.7.1 Pre and post-column clearance of nuclear DAMPs

There was no difference in the pre and post-column cfDNA concentrations. However, there was a trend in overall reduction of cfDNA at the end of 12h perfusion (pre-column concentration of 4.82 µg/ml from peak value of 6.06 µg/ml at 6h of perfusion) and further reduction by 6h of allogenic whole blood reperfusion (pre-column concentration of 3.18 µg/ml). This trend was also observed in perfusate extracellular histone concentrations at the end of 12h perfusion (pre-column concentration of 114.52 µg/ml from peak value of 144.62 µg/ml at 4h of perfusion) and a further reduction by 6h of allogenic whole blood reperfusion (pre-column concentration of 34.60 µg/ml). In addition, a reduction in extracellular histones was observed pre and post-column at 4h of perfusion (144.62 µg/ml vs. 89.01 µg/ml) and also during 4h of allogenic reperfusion (43.40 µg/ml vs. 27.08 µg/ml). However, at 6h of perfusion there was an increase in pre and post-column extracellular histone concentrations (101.11 µg/ml vs. 148.99 µg/ml), Figure 8.19.

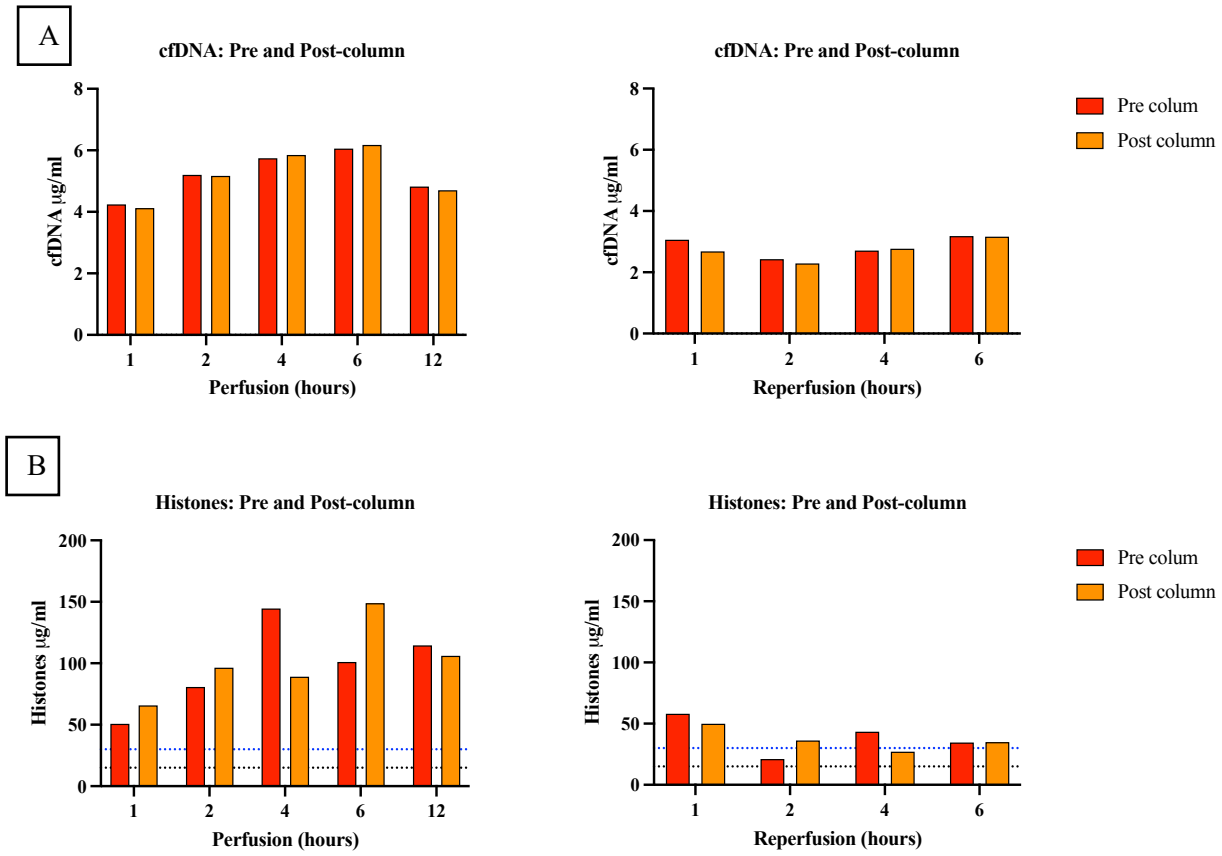

Figure 8.19A-B. Pre-column perfusate samples collected from the IVC line exiting the liver (and therefore also signify systemic levels). Post-column samples collected from three-way tap located on the line exiting the column (prior to drainage into the reservoir). The dotted black line indicates histone

levels observed in patients with acute liver failure who did not survive and blue line indicates levels observed in patients that developed graft dysfunction post liver transplant (437,438).

8.3.7.2 Pre and post-column clearance of microclots

There was an increase in microclots (number/field) progressively during perfusion followed by a reduction during reperfusion (peak of 4.4 at 12h of perfusion with resolution by 6h of whole blood allogenic reperfusion). This trend was also observed in the size of microclots (pixels/field) progressively increasing during perfusion, followed by a reduction during reperfusion (peak of 1517 at 12h of perfusion with resolution by 6h of allogenic whole blood reperfusion). Overall, the column was effective in clearing microclots (pre and post-column) with the greatest clearance seen at 4h of perfusion (number/field: 2 vs. 0.2 and size pixels/field: 268.2 vs. 38.8) and 1h of allogenic whole blood reperfusion (number/field: 1.6 vs. 0.8 and size pixels/field: 398.6 vs. 58.6), see Figure 8.20.

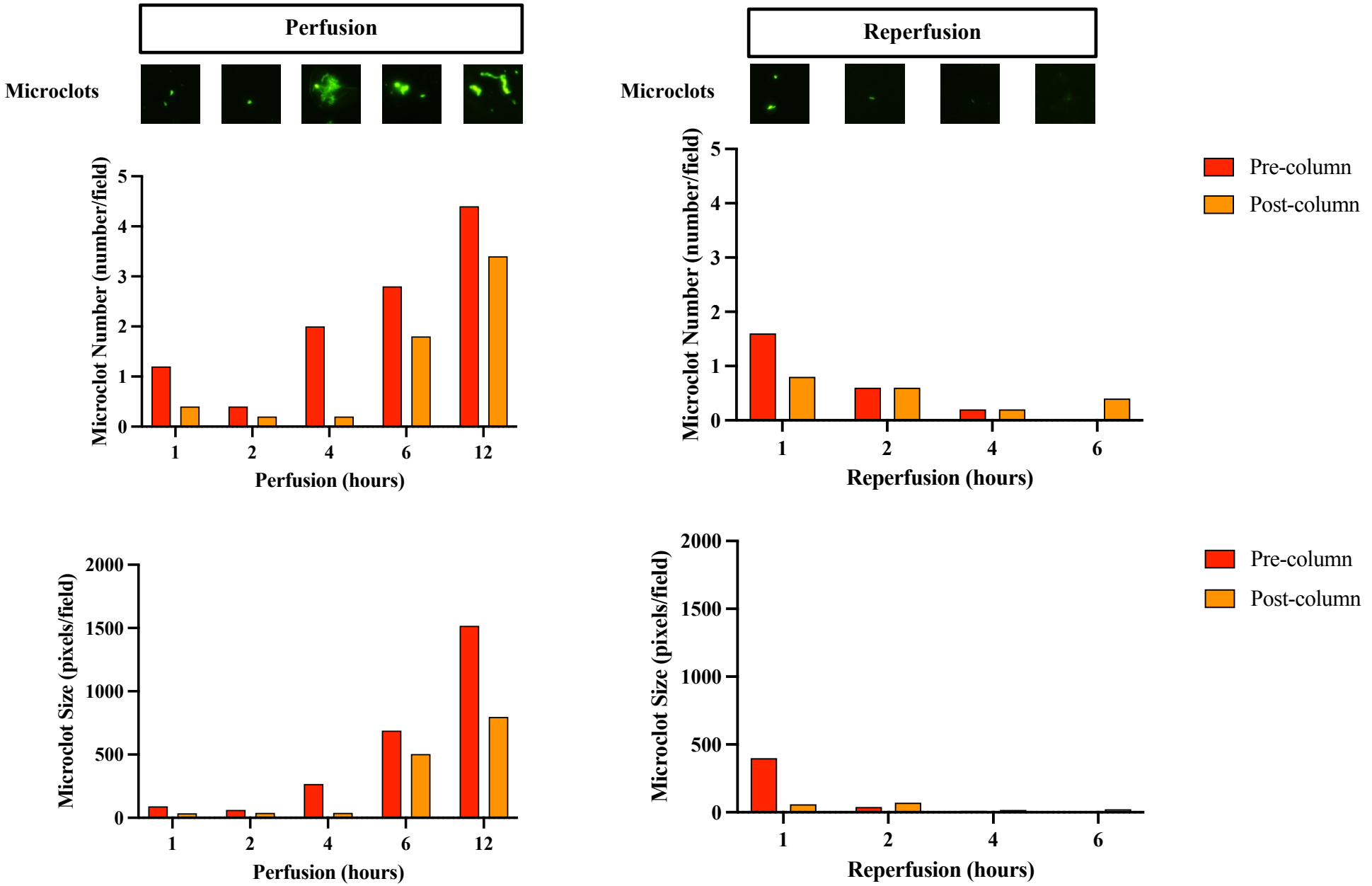

Figure 8.20. Reduction in microclots (number and size) pre and post-column during perfusion and complete resolution of microclots following allogenic whole blood reperfusion.

8.3.7.3 Perfusion parameters

During both perfusion and reperfusion, the liver exhibited acceptable perfusion parameters, the mean perfusion arterial flow was 538.8 ± 51.9 ml/min and reperfusion arterial flow was 470 ± 84.28 ml/min. The portal flows followed a similar trend, the mean perfusion portal flow was 0.83 ± 0.08 L/min and reperfusion portal flow was 0.95 ± 0.14 L/min. In addition, the liver produced bile and demonstrated a macroscopically uniform appearance. The bile pH was 7.43 at 6h and 7.56 at 12h of perfusion (with total bile production of 400 ml during perfusion). Similarly, the bile pH was 7.46 at 1h reperfusion (with total bile production of 80 ml at the end of allogenic whole blood reperfusion). In addition, the perfusate pH remained stable throughout, with adjustments made using sodium bicarbonate as needed to maintain the pH >7.2 (a total of 80 ml given during perfusion and 30 ml during the first 5 min of allogenic whole blood reperfusion). There was clear evidence of glucose metabolism requiring initiation of Nutriflex during perfusion (this was not continued during reperfusion due to simulation of the transplant procedure). The initial ALT was >6000 IU/L during perfusion, with a subsequent decrease at 6h of perfusion and further reduction during allogenic whole blood reperfusion, Figure 8.21.

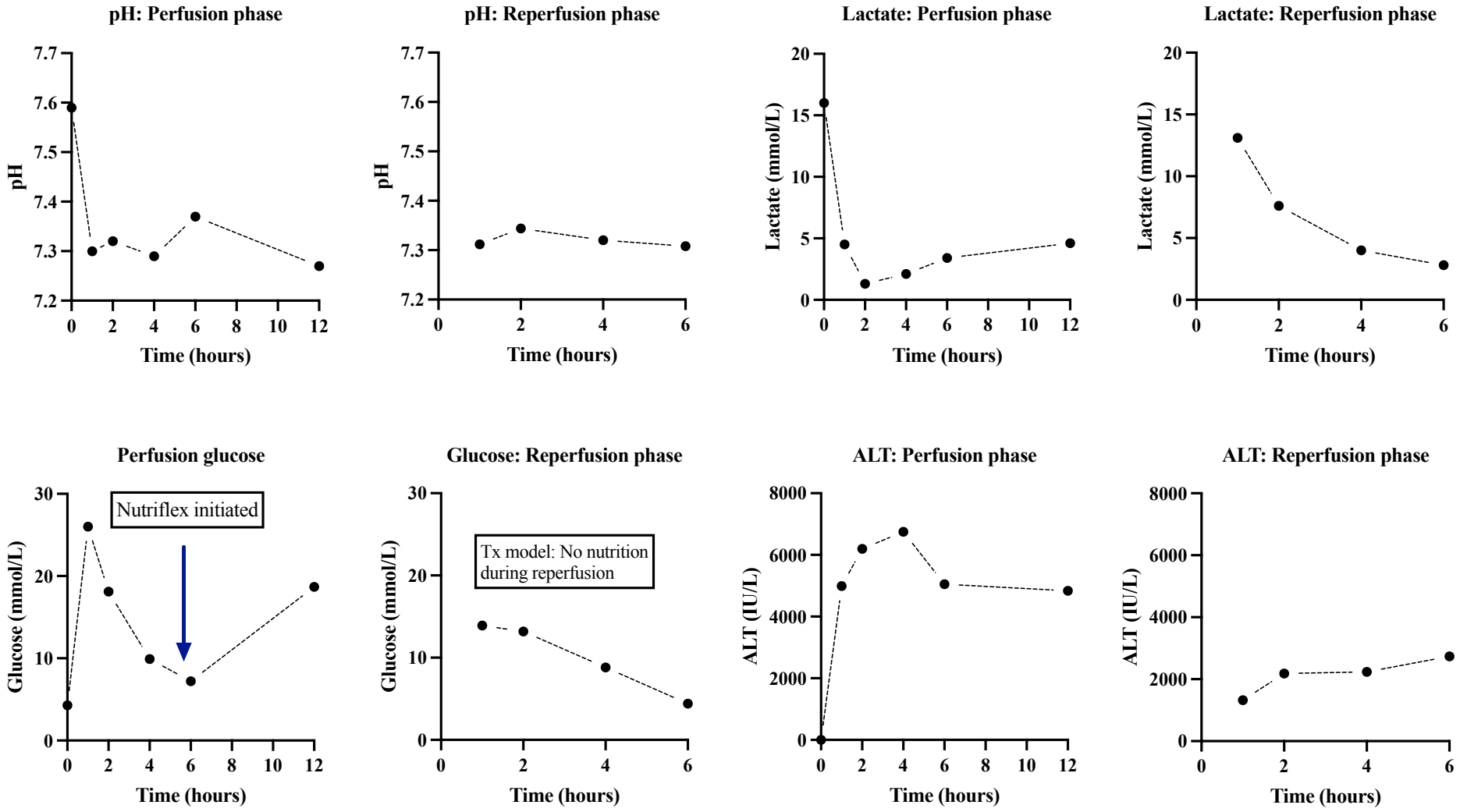

Figure 8.21. Perfusion metrics demonstrating a functioning liver with stable pH, lactate clearance, glucose metabolism and down trending perfusate ALT

8.4 Discussion

Damage-associated molecular patterns (DAMPs) are critical mediators in the innate immune response, serving to recruit immune cells to sites of tissue injury, including during the reperfusion phase of solid organ transplantation (431,432). Although this immune response is intended to protect the host, it can inadvertently result in excessive inflammation and subsequent tissue damage (159,399,433). In the context of NMP, which is increasingly utilised for liver preservation, DAMPs may propagate ex-situ sterile inflammation and therefore exacerbate IRI. The presence of DAMPs, including cfDNA, histones, nucleosomes, and HMGB1, has been strongly associated with suboptimal graft outcomes, primarily due to the inflammatory cascades they trigger (162,434). Furthermore, the significant role of NETs in IRI and cell injury that occur during liver transplantation support this hypothesis (75,399).

8.4.1 Integration of NucleoCapture® in an ex-situ DCD Porcine model of liver transplant

This chapter builds on findings from Chapter 7 that demonstrated an increase in cfDNA (a nuclear DAMP) during NMP and subsequent allogenic whole blood reperfusion in discarded steatotic (and predominately DCD) human livers. The present study involving DCD porcine livers with incorporation of the NucleoCapture® column (both in conjunction with the Spectra Optia or as in-line hemoperfusion column) demonstrated the NucleoCapture® technology was effective in targeting specific molecules such as cfDNA, extracellular histones and intact nucleosomes confirming that the H3.1 protein conjugate to the sepharose beads within the column is highly effective in removing chromatin.

The reduction in these nuclear DAMPs correlated with improved ex-situ liver function, as evidenced by better lactate clearance, reduction in microclots, enhanced vascular flow rates without a significant difference in perfusate ALT levels. The extended 12h application of the in-line hemoperfusion resulted in improved overall clearance of nuclear DAMPs (with lowest perfusate concentrations at the end of reperfusion). The reduction in DAMPs was also confirmed in a discarded human liver perfusion involving the application of the in-line hemoperfusion NucleoCapture® prototype during perfusion and reperfusion.

In addition, specific data regarding the application of NucleoCapture® classic column (integrated with the Spectra Optia, Terumo) in the perfusion phase alone pertain to the DPhil

thesis of my colleague Dr Fungai Dengu and are not included in this chapter but are referenced solely for illustrative purposes. Briefly, the application of NucleoCapture® during the initial 6h of NMP resulted in a pre and post-column reduction in nuclear DAMPs (n = 3) with improved vascular flows and lactate clearance as well as a reduction in hepatocellular injury and perfusate microclot burden compared to NMP alone. However, when these livers where reperfused with allogenic whole blood, there was a rebound and subsequent increase in nuclear DAMPs to a level comparable with initial preservation with NMP alone.

Together, the findings suggest that the application of NucleoCapture® during allogenic whole blood reperfusion or initial autologous leucodepleted perfusion (NMP) can result in DAMP clearance with additional benefits when the column is used in both phases i.e. to prevent rebound of DAMPs during reperfusion. Therefore, the incorporation of NucleoCapture® technology in this context represents a novel and significant step in addressing the inflammatory challenges posed by ex-situ reperfusion (on the machine, first hit) and ischaemia-reperfusion (in the recipient, second hit) injury following transplantation, especially in the context of extended criteria donor (ECD) livers.

Overall, these findings are important as they provide a mechanistic insight into how DAMP removal enhances liver preservation outcomes during NMP and suggest an advantageous role of the technology in a continuous manner i.e. ex-situ to treat the donor liver and attached to the recipient during reperfusion in the clinical setting of liver transplantation. Importantly, incorporation of the NucleoCapture® column into the NMP circuit was both feasible and reproducible, with no negative impact on the perfusion parameters of the OrganOx *metra* device. This is an important finding as it indicates that the addition of the column does not compromise the hemodynamic performance of the NMP system, which is essential for preserving the viability of the liver graft.

8.4.2 NucleoCapture® results in clearance of nuclear DAMPs

Cell-free DNA (cfDNA) and HMGB1

Scheuermann et al. performed a series of perfusions on rat livers and demonstrated an increase in cfDNA and HMGB1 at the end of initial 4h normothermic perfusion (compared to livers perfused at room temperature and sub-normothermic conditions). This occurred despite the use of a leukocyte filter to remove inflammatory cells during perfusion. The increase in cfDNA

and HMGB1 was also demonstrated during a subsequent 2h period of normothermic reperfusion (compared to SCS as a reference group and livers initially perfused at room temperature and sub-normothermic conditions). The results suggest a metabolism and time-dependent accumulation of these DAMPs.

The authors performed an in vitro assay to evaluate the biological activity of DAMPs released during machine perfusion using commercially available TLR reporter cell lines. In this assay, TLR activation was associated with NF-κB activation characterised by secretion of ALP in the cell media. Perfusate samples were incubated with TLR3, TLR4, and TLR9 reporter cell lines, corresponding to extracellular RNA, HMGB1, and cfDNA activation, respectively. End of perfusion perfusate from the normothermic group demonstrated a significantly higher activation of TLR3 and TLR9, with a non-significant trend towards increased TLR4 activation compared to other groups. Similar results were observed after reperfusion, with normothermic perfusion inducing significantly greater TLR3 and TLR9 activation (440).

Whilst this study provides important mechanistic insights, there are several limitations which preclude applicability to a clinical setting and requires validation in a large animal model or on discarded human livers. In addition, the use of a leucocyte filter during the initial perfusion phase may limit the interpretation of the findings as it is an increasingly recognised phenomenon of mobilisation of passenger leucocytes from the liver graft and potential interplay of these in other inflammatory mediators in the ex-situ environment (441,442). In addition, the reperfusion did not necessarily reflect simulation of liver transplantation due to the lack of whole allogenic blood in the perfusate. In contrast, the study described in this chapter with the adjunct of NucleoCapture® technology addresses the majority of these limitations particularly in the ability to remove nuclear DAMPs during short 6h and extended 12h perfusions and reperfusions in a large animal model. Furthermore, the current study also demonstrated a reduction in tissue HMGB1 following allogenic whole blood reperfusion with the integrated NucleoCapture® technology. The results described herein also align with human liver perfusion results published by Cox et al. suggesting that the monitoring cfDNA during NMP is a feasible tool for assessing graft viability, with higher levels indicating potential non-viability of the graft (443).

HMGB1 is a non-histone DAMP and is a nuclear protein that does not contribute to the structural formation of chromatin (as histones do) but instead acts as a dynamic regulator of

DNA function. Upon cellular injury, it is released extracellularly, where it functions as a DAMP by initiating and amplifying inflammatory responses (444). HMGB1, is a widely investigated DAMP in the context of liver transplantation, is released early during NMP, and correlates with traditional markers of hepatocellular injury (AST and GLDH levels) as well as cholangiocyte damage (GGT levels) (445). Ilmakunnas et al. identified HMGB1 as an early indicator of hepatic injury post-transplantation, with levels peaking as early as 10 minutes after portal venous reperfusion, particularly in the caval effluent. Interestingly, HMGB1 kinetics were linked to graft steatosis and postoperative ALT levels, but showed no correlation with IL-6 or TNF-α (446). Additionally, studies have demonstrated that anti-HMGB1 antibodies can protect against ischemia-reperfusion injury (IRI), reducing hepatocellular damage and cytokine release (62,447).

Beetz et al. demonstrated that HMGB-1 and IL-18 levels increase in the perfusate when livers are preserved with prolonged SCS before NMP using autologous whole blood, suggesting their potential as markers of cellular injury during NMP (445). Although HMGB1 is recognised as a key DAMP in liver disease and ischemia-reperfusion injury (IRI) (448,449), its measurement and interpretation are challenging. A significant portion of HMGB1 is bound to IgG complexes, lipids, or DNA/chromatin fragments, making it difficult to detect without sample optimisation. Furthermore, characterising specific HMGB1 isoforms is complex and costly, yet crucial for understanding its inflammatory potential (448). For instance, HMGB1-nucleosome complexes are highly inflammatory, capable of triggering innate immune responses and promoting pro-inflammatory cytokine release from T-cells, as well as influencing adaptive immunity by maturing dendritic cells into more immunogenic antigen-presenting cells (450,451).

Whilst the findings presented within this chapter have demonstrated a reduction in HMGB1 at the end of allogenic whole blood reperfusion with the NucleoCapture® classic column integrated with the Spectra Optia (Terumo) and OrganOx *metra* compared to NMP alone livers. The detection was based on immunohistochemical staining and the results are not without limitation. HMGB1 immunohistochemistry in liver tissue can be limited by technicalities such as antibody cross-reactivity, challenges in distinguishing nuclear and cytoplasmic localisation, variability in staining, sample preparation artifacts and difficulty in detecting different HMGB1 isoforms. Therefore, complementary quantitative methods (i.e. perfusate ELISA) are necessary for more accurate interpretation and reproducibility. Whilst the whole reperfusions described by Beetz et al. did not comprise allogenic (third party) whole blood (and therefore do not

completely reflect an ex-situ transplant model), the findings pertaining to HMGB1 warrant further investigation in perfusate samples collected within the studies described in this chapter. Specifically, the degree to which HMGB1 is bound within nucleosome complexes versus its free form, and whether NucleoCapture® effectively removes either or both forms, is of particular interest.

Extracellular histones and Myeloperoxidase (MPO)

Extracellular histones are key mediators of systemic inflammatory diseases, exhibiting various harmful effects such as direct cytotoxicity, increased vascular permeability, activation of coagulation, platelet aggregation and stimulation of cytokine production (437). In the context of hepatocellular injury, Wen et al. explored the role of extracellular histones in the setting of Acute liver failure (ALF) and demonstrated median plasma histone levels at admission were notably higher in patients at 5.587 μg/ml (IQR: 0.694–7.892) compared to those with chronic liver disease (CLD) at 1.035 μg/ml (IQR: 0.578–1.157) and healthy controls at 0.794 μg/ml (IQR: 0.378–1.136). Moreover, patients with higher histone levels at admission showed increased mortality. There was a significant difference in histone levels between ALF patients who died within 28 days (5.415 μg/ml [IQR: 4.054–7.561]) and those who survived (3.531 μg/ml [IQR: 2.387–5.703], $P = 0.024$). However, there is paucity in the literature exploring the role of extracellular histones in the clinical setting of liver transplantation (437).

Li et al. explored the role of histones in primary graft dysfunction (PGD) following liver transplantation. Blood samples from 58 liver transplant recipients were analysed prior to transplantation and at 24h and 72h post-transplantation. The authors demonstrated a significant increase in extracellular histones immediately after transplantation, peaking at 24 hours and remaining elevated at 72 hours. Patients with PGD had notably higher histone levels compared to those without PGD. These elevated histone levels correlated with other inflammatory markers, including myeloperoxidase (MPO) and S100A8/A9. In vitro experiments demonstrated that post-transplant sera induced cell death in L02 hepatocytes and increased cytokine production in U937 monocytic cells, effects that were mitigated by heparin or an anti-histone antibody. These results suggest that targeting extracellular histones during implantation of the liver graft could be a potential strategy for preventing PGD and improving liver transplant outcomes (438). Overall, no previous studies have demonstrated/quantified extracellular histones during ex-situ perfusion. Therefore, the results presented herein

demonstrate a novel finding of the extracellular histone clearance during NMP and subsequent allogenic whole blood reperfusion with the application of NucleoCapture® technology.

Myeloperoxidase (MPO) is an enzyme primarily found in neutrophils and, to a lesser degree, in monocytes. It has potent bactericidal effects by converting Cl^- and H_2O_2 into hypochlorous acid (HOCl), a strong oxidant. However, excessive production of MPO-derived oxidants has been linked to harmful effects in inflammatory diseases. These oxidants contribute to disease pathology by oxidising biomolecules, thereby increasing inflammation and oxidative stress (452). MPO-DNA complexes are formed when myeloperoxidase (MPO) released by activated neutrophils binds to extracellular DNA. These complexes are key components of neutrophil extracellular traps (NETs) (75,453). In the current study, a reduction (albeit non-significant) in tissue sections stained for MPO was observed at the end of 6h reperfusion with NuceloCapture® integrated with the Spectra Optia (Terumo) and OrganOx *metra* compared to NMP alone livers. Whilst the results suggest an overall trend in DAMP reduction, the results of tissue IHC a subject to similar limitations described for tissue HMGB1 and are useful for localisation of MPO (rather than absolute quantification).

Nucleosomes/NETs and CITH3

Von Meijenfeldt et al. investigated the presence of NET markers in the plasma of liver transplant patients and their association with coagulation activation. Results showed perioperative increases in NET markers, particularly cell-free DNA (cfDNA) and nucleosomes, which peaked after reperfusion. These markers correlated with established coagulation activation indicators. Immunostaining confirmed NETosis in post-reperfusion biopsies. The study suggests that while NETosis occurs during liver transplantation, most circulating DNA likely originates from graft cell death, with cfDNA and nucleosomes potentially influencing the haemostatic rebalance observed in these patients i.e. a more prothrombotic environment following reperfusion in the recipient (75).

In the current study, the measurement of nucleosomes/NETs (H3.1 and H3R8cit) was performed using Nu.Q™ ELISA assays (Belgian Volition SRL, Isnes, Belgium). The H3.1 assay specifically detects nucleosomes that contain histone H3.1, a variant of histone H3. This variant is typically found in NETs, making the H3.1 assay a valuable surrogate marker for the presence of NETs. Thus, by measuring the levels of nucleosomes containing H3.1, the H3.1 assay provides an indirect yet reliable indication of NET formation. The H3R8Cit assay is a

distinct from the H3.1 assay in that it specifically measures citrullinated histone H3, particularly at the arginine 8 position (H3R8). Citrullination is a post-translational modification where the enzyme peptidylarginine deiminase (PAD) converts arginine residues in histone proteins into citrulline. This modification is a hallmark of neutrophil extracellular trap (NET) formation i.e. NETosis.

Measurement of perfusate samples demonstrated a significant increase in Nucleosomes/NETs in livers perfused with NMP alone quantified with the H3.1 assay (64256.36 ± 41575.60 ng/ml during perfusion and 108462.5 ± 29088.84 ng/ml at the end of 6h allogenic whole blood reperfusion). These findings demonstrate pathologically high levels of nucleosomes (H3.1 assay) i.e. >100000 ng/ml in the standard NMP ex-situ set-up when compared to the highest level of 6000 ng/ml in ITU patients with COVID that suffered mortality as reported by Cavalier et al (439). However, when the NucleoCapture® classic column was integrated with the Spectra Optia (Terumo) and the OrganOx *metra* during allogenic whole blood reperfusion, there was systemic and significant reduction in perfusate nucleosomes at the end of reperfusion (15746 ± 8138.71 ng/ml). A similar (non-significant) trend was also observed with the H3R8cit assay. Overall, analysis of the pre and post-column samples demonstrated a significant reduction in H3.1 demonstrable as early as 2h of allogenic whole blood reperfusion. The perfusate findings were also supported by a reduction in CITH3 immunohistochemical stain of liver tissue obtained at the end of NucleoCapture® treatment.

8.4.3 NucleoCapture® is associated with a reduction in amyloidfibrin(ogen) aggregates

Recently, Schofield et al. investigated the presence and clinical significance of amyloid-fibrin(ogen) aggregates, termed microclots, in critically ill patients admitted to the ICU. Microclots were detected in 42.3% of the patients upon admission and were strongly associated with sepsis and adverse outcomes such as disseminated intravascular coagulation (DIC) and increased 28-day mortality. Through proteomic and immunofluorescence analyses, the study confirmed that these microclots contain fibrin(ogen) aggregates (436). Whilst previous studies by Pretorius et al. and Baker et al. identified similar fibrin aggregates in conditions like post-acute sequelae of SARS-CoV-2 infection (PASC) and pulmonary embolism, this research is the first to propose microclots as a potential predictive biomarker in an ICU setting (454,455). The study highlights the need for further research to understand the pathophysiological role of microclots and their formation mechanisms, especially in the context of solid organ

transplantation. Herein, through collaboration with Schofield et al. we have demonstrated presence of microclots during ex-situ perfusion (and allogenic whole blood reperfusion). More importantly we had demonstrated the ability to remove microclots with the application of NucleoCapture® technology in the experimental study involving porcine DCD livers described within this chapter with findings confirmed observed in a discarded human liver perfusion. The measurement of microclots within bile samples collected during perfusions performed within this chapter remains an urgent consideration, with ischaemic cholangiopathy remaining the Achilles heel of DCD liver transplantation (42). The ability of NucleoCapture® to therefore mitigate this complication warrants further investigation.

8.4.4 Comparison with other ex-situ DAMP removal strategies

As NMP continues to be adopted as an advanced preservation technology, most research to date has primarily focused on establishing its efficacy as a preservation method (with advantages in mitigating IRI). More recently, attention has shifted towards exploring NMP's potential as a platform for therapeutic interventions (245,456). However, there has been limited investigation into the molecular and immunological mechanisms at play during NMP (441,442), with even fewer studies attempting to modulate these pathways to optimise graft function and improve transplant outcomes (457,458).

The Toronto group (459) modified their perfusion circuit and perfusate composition to reduce the inflammatory effects of the perfusate through removal of components of whole blood that are known to contribute to IRI: leukocytes, platelets and plasma cytokines. To achieve this, the perfusion circuit was adapted to include an inline leukocyte filtration (Pall LeukoGuard®, Cornwall, UK) and dialysis filtration. In addition, the perfusate was modified to include washed erythrocytes as the oxygen carrier in a 3L Steen solution (XVIVO Perfusion, INC., Goteborg, Sweden), aiming for a 10-12% haematocrit and thereby avoiding a cytokine rich environment. This approach was designed to prevent the negative IRI-related outcomes seen in DCD porcine liver models where SCS was followed by NMP with whole blood-based reperfusion (459). However, the authors did not measure perfusate nuclear DAMPs before and after these modifications, making it difficult to completely assess the impact of these changes on circulating DAMPs and graft performance in this context.

In a recent study by Obara et al. (460), the authors evaluated the performance of DCD pig livers subjected to sub-normothermic machine perfusion (SNMP) with or without early perfusate exchange. This approach aimed to remove inflammatory cytokines that are rapidly produced upon reperfusion (within 5 mins) and may contribute to IRI. However, the use of autologous whole blood in this study limits its broader applicability, as previously highlighted by the Toronto group above (459). Moreover, perfusate exchange introduces a significant dilutional effect, complicating the direct assessment of circulating damage markers. Whilst this exchange likely reduced inflammatory molecules by washing out those generated during reperfusion and diluting those present in the circuit, it also confounds the interpretation of damage marker concentrations in the perfusate. It becomes challenging to distinguish between a true reduction in injury marker generation due to perfusate exchange and the dilution effect itself. In contrast, the study presented within this chapter did not involve perfusate dilution and instead focused on molecules with very short half-lives, such as nucleosomes (4 minutes) and cell-free DNA (15 minutes) (164,461). This approach enabled the samples to more accurately capture real-time events occurring during NMP (closely corresponding with the timing of sample acquisition) and specifically focused on nuclear DAMPs, providing clear evidence on the feasibility of a targeted interventional strategy to remove these inflammatory mediators to improve graft function.

An alternative strategy for optimising perfusate has involved the use of cytokine filtration, specifically employing the CytoSorb® column (CytoSorb 300, CytoSorbents™ Europe GmbH, Berlin, Germany) to selectively remove circulating cytokines. This approach has demonstrated improvements in lung ex vivo lung perfusion (EVLP) and kidney normothermic machine perfusion (NMP) studies (462–464). However, data on cytokine removal in liver NMP is limited. Karangwa et al. (465) conducted a study on DCD liver NMP (perfused for 3.5h) using an acellular, plasma-free perfusion solution containing a bovine haemoglobin-based oxygen carrier, HBOC-201 (Hemopure, HbO2 Therapeutics LLC), followed by autologous whole blood reperfusion (perfused for 2.5h). The livers were randomised to either Cytosorb® filtration or NMP alone during the initial acellular perfusion phase. Whilst the filter was successfully integrated into the Liver Assist (Groningen, the Netherlands) perfusion system without complications, no significant differences in circulating cytokine levels were observed between the groups, nor was there a significant reduction in cytokine levels across the filter. Compared to the study described in this chapter, both the perfusion and reperfusions phases were short and therefore the study lacked data on the performance of Cytosorb® over extended

perfusion. In addition, during perfusion, the use of acellular HBOC-1 may limit the translation of the findings to clinical practice where standard NMP routinely involves the use of pRBC as the primary choice for perfusate. In addition, the authors did not consider integration of the Cytosorb® during the whole blood reperfusion phase, it therefore remains unclear if the column will have any benefit during reperfusion. Furthermore, the liver's unique tolerogenic microenvironment within the liver is also characterised by an anti-inflammatory cytokine expression profile associated with significant post-transplant tolerogenic potential (466–469). There is a possibility that a broad and untargeted cytokine approach to cytokine removal may inadvertently increase graft immunogenicity.

The results presented within this chapter present a novel and distinct approach compared to the studies outlined above with an emphasis on targeting nuclear DAMPs combined with a highly effective intervention (NucleoCapture®) to mitigate reperfusion injury. Compared to cytokines (which are both pro-inflammatory and anti-inflammatory), DAMPs are explicitly pro-inflammatory, making them ideal targets for intervention. This study represents an initial strategy for immunomodulation during NMP and during reperfusion in the recipient. The clinical translation may benefit preservation of ECD donor livers that are particularly sensitive to IRI i.e. livers procured from DCD donors and those with evidence of significant steatosis. Moreover, the application of the column to the recipient during transplantation may provide additional benefits and reduce propagation of graft injury during implantation with a reduction in clinical manifestations of preservation reperfusion injury (including post-reperfusion syndrome, primary allograft dysfunction, primary non-function and need for renal replacement therapy).

8.4.5 Addressing study limitations and expanding the scope

Several limitations should be considered for future research. The primary limitation was the small sample size, which, although adequate to demonstrate significant effects, restricts the generalisability of the findings. Increasing the number of livers perfused in subsequent studies would enhance the robustness of the conclusions and offer a more comprehensive understanding of the impact of NucleoCapture® technology.

The ex-situ model of liver transplantation model (allogenic whole blood reperfusion) presented in the study benefited from total hepatic isolation i.e. without influence of the autonomic

nervous system, hormones and other regulatory molecules that are produced in-vivo. This isolation therefore allowed for a detailed examination of the hepatic response to IRI without external confounding factors. However, it is important to note that this model is not a definitive representation of clinical liver transplantation. A comprehensive evaluation of NucleoCapture® would require assessing its effects on post-transplant survival and graft function. A follow-up study incorporating a porcine transplant model would be crucial in confirming the long-term benefits of DAMP removal during NMP and during reperfusion in the recipient.

Histological analysis demonstrated that glycogen depletion occurred in porcine livers subjected to NMP, irrespective of the integration of NucleoCapture® classic with the Spectra Optia (Terumo) and OrganOx *metra*. This outcome may have been influenced by the absence of insulin infusion in the perfusate composition, which is standard in the OrganOx *metra* perfusion protocol. The rationale for insulin exclusion were related to the relatively short duration of perfusion, and measurable insulin levels already present within both the autologous and allogenic porcine donor blood. However, the findings indicate that while DAMP removal may enhance certain aspects of hepatocellular function, it does not fully alleviate the metabolic stress and demands associated with NMP. Therefore, further perfusions involving the in line hemoperfusion NucleoCapture® prototype employed the standard OrganOx *metra* perfusion protocol (including insulin), histopathological evaluation of these tissue samples is yet to be completed.

8.4.6 Implications for clinical practice and the future of liver preservation

The successful integration and performance of NucleoCapture® technology in this study suggest that targeting nuclear DAMPs during NMP could become a standard practice in liver preservation. As NMP continues to evolve, the inclusion of technologies like NucleoCapture® could significantly reduce the incidence of IRI and improve graft outcomes, particularly for ECD livers that are more vulnerable to preservation-related injury. In addition, the application of this technology during implantation in the recipient (during reperfusion) may further limit the clinical manifestation of PRI. Furthermore, the concept of ex-situ immunomodulation presents new opportunities for therapeutic interventions. The selective removal of pro-inflammatory nuclear DAMPs in combination with other strategies to mitigate injury (including dialysis: to normalise perfusate biochemistry, defatting: to mobilise and filter fat from circulation and thrombolysis: to further reduce microclot burden) may enhance the

findings observed in the current study and can be directly translated to ex-situ perfusion of other solid organs (179,329,459,470).

8.4.7 Conclusion

The findings presented within this Chapter demonstrate that the integration of NucleoCapture® technology into the NMP circuit is not only feasible but also has a role in mitigating hepatocellular injury. Further perfusions include confirmatory studies in discarded human livers with application of the in-line hemoperfusion NucleoCapture prototype®. In parallel, a randomised clinical trial (first in-man) is planned to confirm the preliminary findings in the clinical setting of liver transplantation.

Chapter 9: Overall conclusions and future directions

The success of liver transplantation is critically limited by the availability of suitable donor organs. This has necessitated the use of extended criteria donor (ECD) livers including those procured from donation after circulatory death (DCD) donors and liver grafts with evidence of moderate-severe hepatic steatosis (HS) (3). Whilst static cold storage (SCS) has traditionally been used to preserve livers, ECD livers, in particular those with presence of HS and DCD status do not tolerate SCS and the subsequent ischaemia-reperfusion injury (IRI) that ensues following implantation in the recipient. However, the ever-present need to increase utilisation of ECD livers has prompted liver transplant teams to consider alternative dynamic (non-static) preservation methods to minimise the storage related cold-ischaemic injury and transplantation related IRI to which these livers are susceptible, in order to improve post-transplantation outcomes (1). In this thesis, I have focused on the clinical application of normothermic machine perfusion (NMP) as a therapeutic platform to reduce the risk profile of steatotic and DCD livers.

In an attempt to identify potential clinical risk scores, anthropometric and biochemical and pre-retrieval predictors to facilitate early identification of donors at risk of steatosis, I first performed a large-scale study including analysis of 906 consecutive donor livers from the QUOD bioresource (Chapter 3). The Fatty Liver Index (FLI) demonstrated improved accuracy (AUROC 0.72) for predicting moderate-severe HS compared to previous studies (272), while anthropometric measures, such as BMI and waist circumference, demonstrated limited diagnostic accuracy with AUROCs of 0.69 and 0.67 respectively. Biochemical markers, particularly donor GGT and insulin, were significant independent predictors of moderate-severe HS, underscoring their utility in donor evaluation.

I also explored the utility of digital image analysis (DIA) in providing a rapid, automated and reproducible method of steatosis quantification to address limitations of macroscopic retrieval surgeon's assessment (276) and conventional histopathologist reports, mainly the substantial inter-observer variability in the reporting of HS (80,94,267–270). DIA proved to be a reproducible and rapid automated method for assessing HS severity, addressing variability inherent in conventional histopathology. However, further assessment and validation of this DIA platform is required against algorithms specifically developed according to the Banff consensus for reporting of donor hepatic steatosis (284).

Donor livers with moderate-severe HS were associated with increased peri-operative and post-operative biliary complications, longer ITU stays, and demonstrated trends toward reduced graft and patient survival. These findings underscore the importance of risk stratification, including 'preferred recipient matching' to optimise graft utilisation (281,282). Future directions include integrating portable AI-based tools to facilitate early detection of donor liver steatosis and enable targeted ex-situ interventions i.e. during NMP. These advances aim to reduce organ discard and improve outcomes for high-risk donor livers.

Pre-clinical animal studies have demonstrated the beneficial role of NMP in the preservation of steatotic livers through a reduction intra-hepatic triglyceride content (IHTG) (126,471). In Chapter 4, I explored clinical outcomes of steatotic livers preserved with continuous normothermic machine perfusion (cNMP) compared to SCS and demonstrated a reduction in clinical manifestations of IRI including post-reperfusion syndrome (PRS) and early allograft dysfunction (EAD), with lower peak AST levels in the first seven days post-transplant compared to SCS. Notably, steatotic livers preserved with cNMP exhibited comparable graft survival to lean livers preserved with SCS (90.5% vs. 93.5%), emphasising the potential of cNMP to mitigate the elevated risks traditionally associated with steatotic livers (83,84). I further explored the application of digital image analysis for objective and reproducible quantification of HS, demonstrating strong correlation with histopathology and enabling improved assessment of steatotic livers during perfusion i.e. changes in the degree of HS (which were not observed in this cohort). This finding is consistent with previous studies that demonstrated the mobilisation of fat during NMP but highlighted the need for additional pharmacological interventions to achieve meaningful reductions in HS (217,221).

Biochemical analysis of cNMP perfusate revealed metabolic challenges associated with steatotic livers, including greater hepatocellular injury, impaired lactate clearance and increased mobilisation of triglycerides compared to lean livers preserved with NMP. These findings indicate that, although cNMP offers improved preservation of steatotic livers compared to SCS, it does not fully mitigate the effects of HS compared to lean livers preserved with cNMP. This highlights the potential value of using NMP as a platform for pharmacological interventions aimed at further optimising ex-situ graft function and reducing hepatocellular injury.

Proteomic analysis of this cohort was described in Chapter 5, in order to provide mechanistic insights into the biological, molecular and cellular alterations occurring during preservation and reperfusion. Both cNMP and SCS resulted in significant proteomic changes during preservation and reperfusion, suggesting the potential of cNMP to address the unique metabolic and inflammatory challenges associated with steatotic livers.

Steatotic livers preserved with cNMP demonstrated upregulation of proteins associated with mitochondrial function, cytoprotection, and lipid metabolism, suggesting a compensatory mechanism to mitigate oxidative stress and metabolic dysfunction. However, downregulation of proteins related to ATP synthesis efficiency and immune modulation indicated only partial recovery of these livers during preservation. Notably, cNMP preserved steatotic livers exhibited a pro-inflammatory and pro-thrombotic state. These findings underscore the need for ex-situ strategies to optimise ex-situ lipid metabolism (i.e. defatting) (126,179,221,471) and reduce the pro-inflammatory/thrombotic state (e.g. application of novel technologies to remove damage associated molecular patterns from the perfusate or the adjunct of thrombolysis during NMP) (329).

SCS-preserved steatotic livers demonstrated heightened sensitivity to IRI, with disruptions in lipid homeostasis, mitochondrial function and detoxification pathways. Proteomic profiles indicated metabolic dysregulation and increased susceptibility to oxidative stress, which support the post-transplant outcomes observed in these livers (Chapter 4). Overall, cNMP emerged as a superior technique for preserving steatotic livers. However, further refinement, including pharmacological modulation may be required to further optimise the risk-profile of these livers. These findings underscore the importance of tailoring preservation strategies to donor liver characteristics, offering a foundation for future clinical and mechanistic studies described in Chapters 6 and 7.

In Chapter 6, I described the study protocol for a Phase II multi-centre randomised clinical trial (the DeFat study) that I am currently running. The clinical trial compares a novel defatting strategy, incorporating lipid apheresis filtration and pharmacological interventions (L-carnitine, forskolin: NKH477 with reduction in insulin and glucose infusion). Pre-clinical studies on discarded human livers by our group demonstrated that the application of this strategy during post-static cold storage NMP (pSCS) resulted in improved liver function, enhanced arterial flow, increased mitochondrial β-oxidation and a notable 45% reduction in

intrahepatic triglyceride accumulation by 48h of perfusion in human livers that had been declined for transplantation. This approach addressed the limitations of using NMP alone, which, while beneficial, does not reduce HS to clinically acceptable levels (219,220). The defatting protocol explored in this thesis builds on these findings by utilising clinically approved agents and filtration techniques, thereby facilitating potential clinical translation. The DeFat study aims to validate these findings further in the clinical setting of liver transplantation (179). At present, 22 out of 60 livers have been recruited to this clinical trial. The implications of this study, if the results are positive, will be significant for expanding the donor pool and improving transplant outcomes. By effectively reducing steatosis during preservation, more livers that would otherwise be deemed unsuitable could be transplanted safely, potentially decreasing waiting list mortality. Additionally, enhancing the function of steatotic livers may reduce the incidence of IRI-related complications post-transplantation.

However, whether these interventions during pSCS-NMP can effectively suppress subsequent IRI is yet to be determined. Therefore, this body of research has raised several critical questions warranting further investigation. First, is defatting of steatotic livers essential to improve post-transplant outcomes? Evidence suggests that if recipients overcome the initial severe IRI and avoid primary non-function (PNF), survival rates may be comparable to those of non-steatotic livers (83). Furthermore, post-transplant, intrahepatic fat appears to dissipate rapidly (280). This raises the possibility that enhancing the preservation environment alone, without prioritising fat reduction, might improve outcomes. Given that steatotic livers often exhibit normal biochemical function in donors, it is evident that ischaemia and reperfusion are the primary insults driving adverse outcomes.

An intriguing avenue is whether the risks associated with steatotic liver transplantation could be mitigated by adopting entirely ischemia-free organ donation, preservation, and transplantation techniques, as previously described in Chapter 1.6.2 (3,214,215) and application of this technology is an urgent consideration. Another key question is why some steatotic livers fail to function during NMP and whether these high-risk livers can be salvaged. This failure likely extends beyond the degree of steatosis, potentially involving genetic predispositions or nuanced differences in hepatic lipid metabolism.

Addressing some of these considerations, Chapter 7 introduced the pharmacological modulation of hypoxia-inducible factors (HIFs) with defatting during pSCS-NMP to further enhance outcomes of steaotic livers in a pre-clinical study utilising discarded human livers declined for transplantation demonstrating that selective stabilisation of HIF-1α and inhibition of HIF-2α can synergistically enhance lipid metabolism and influence the magnitude of IRI in an ex-situ model of liver transplantation.

Pharmacological HIF modulation (combined with an established defatting protocol described in Chapter 6) resulted in accelerated defatting in steatotic livers. HIF-1α activation (using deferoxamine, DFO) and HIF-2α suppression (using PT2385) were assessed through immunoblotting and erythropoietin (EPO) quantification, providing the first documented evidence of selective HIF modulation during NMP and utility of perfusate EPO as a potential biomarker for monitoring HIF activity during NMP. This approach facilitated a reduction in ld-MaS and all livers in the experimental groups demonstrated favourable functional metrics that would have rendered them transplantable, not only by currently accepted parameters, but also supported by novel functional assessments including ICG clearance, LiMAx and MEGX tests. These findings suggest the use of these pharmacological adjuncts, can improve the risk profile of steatotic livers preserved with pSCS-NMP (where there is a variable degree i.e. several hours of cold-ischaemia prior to NMP) to comparable or an improved profile of steatotic livers perfused using cNMP (continuous application of NMP following cold flush during retrieval and a brief period of cold ischaemia during preparation of the liver for NMP as described in Chapter 4).

However, the effect of the intervention on mitigating IRI (using the 'ex-situ transplant' model with allogenic whole blood reperfusion) was less conclusive and was perhaps influenced by a higher-risk profile of donor livers compared to livers treated with defatting alone during NMP. An important finding in both experimental groups was the identification of cell-free DNA (cfDNA, a damage-associated molecular pattern) in the perfusate during both perfusion and reperfusion in both groups. This finding suggests that while pharmacological interventions may help achieve functional criteria for transplantation, there are additional complexities that need to be addressed to further dampen the magnitude of IRI i.e. removal of circulating damage-associated molecular patterns (DAMPs) described in Chapter 8. Future research should aim to validate these findings in clinical trials, addressing limitations such as small sample sizes and donor heterogeneity. Exploring extended perfusion protocols (226) and refining functional

assessments (234,236,238,472) could enhance the translational potential of these interventions, ultimately improving outcomes in liver transplantation.

In Chapter 8, I described the critical role of DAMPs in propagating inflammation/injury during liver perfusion and subsequent IRI (using an ex-situ porcine DCD whole blood perfusion model), investigating NucleoCapture® technology as a potential therapeutic approach. DAMPs such as cfDNA, histones, nucleosomes, and HMGB1 are established mediators of sterile inflammation that can propagate injury. By integrating NucleoCapture® technology into the NMP circuit, I demonstrated a significant reduction in these DAMPs, correlating with improved graft function and reduced micro-clot burden during ex-situ allogenic whole blood reperfusion.

Key findings include the effective clearance of cfDNA, extracellular histones and nucleosomes/NETs using NucleoCapture® technology, with evidence of enhanced vascular flow, lactate clearance and reduced microclot formation. Importantly, integrating the column during both NMP and allogenic whole blood reperfusion resulted in a sustained reduction in DAMPs implying benefit in the application of this technology to both the donor liver (ex-situ) and to the recipient (during reperfusion). These results align with and expand upon published descriptions of the accumulation of DAMPs during perfusion and reperfusion. However, the targeted removal of nuclear DAMPs offers a more focused and practical strategy than broader interventions such as cytokine filtration or perfusate exchange (459,460).

The study identifies scope for future research: this includes the need for validation in clinical transplant models and the potential integration of complementary pharmacological strategies, as discussed within this thesis. A planned first-in-human trial will assess the clinical efficacy of NucleoCapture® technology in the clinical setting of liver transplantation. These findings underscore the potential for targeted NMP as a therapeutic platform to transform liver transplantation practices, particularly for ECD livers.

Additional work beyond the scope of this thesis is planned. Transcriptomic analysis of donor liver biopsies (Chapter 3) is being undertaken. This will complement data that has been presented and identify unique transcriptomic signatures in steatotic donor livers that could be potentially targeted with RNA interference (RNAi) during NMP as well as identify therapeutic targets for the treatment of MASLD or MASH. Mechanistic studies for the DeFat study clinical

trial samples described in Chapter 6 (including transcriptomic, proteomic and glycomic analysis) will also be performed for two broad reasons: (i) to identify more sensitive and specific markers of transplantability and; (ii) to understand the process of defatting that leads to a steatotic organ being reconditioned. Metabolomic analysis of perfusate samples from Chapter 7 will be performed to assess the impact of HIF-modulation on cellular energetics through analysis of metabolites involved in energy production pathways (e.g. glycolysis, the tricarboxylic acid (TCA) cycle and oxidative phosphorylation) and provide insights into ATP generation and mitochondrial function. Detailed assessment of *de novo* lipogenesis (DNL) total fatty acid composition and tissue triglycerides through analysis of tissue and perfusate samples will provide insights into the potential benefits of HIF modulation in enhancing the defatting process. The measurement of microclots and DAMPs within bile samples collected during perfusions performed in Chapter 8 is a priority, with ischaemic cholangiopathy remaining the Achilles heel of DCD liver transplantation (42). In this context, investigating the potential of NucleoCapture® to address this complication is important.

The data presented in this thesis highlight the potential of multi-modal strategies to optimise high-risk livers during NMP. The combination of defatting protocols, thrombolysis and the targeted removal of DAMPs can offer a promising approach to improving ex-situ function for transplantation. These interventions must be rigorously validated through clinical trials to establish their impact on transplantation outcomes. Additionally, ischemia-free liver transplantation (IFLT), is a promising alternative and addresses the fundamental challenges associated with transplantation of steatotic livers and those of DCD status by significantly reducing IRI and enhancing post-transplantation outcomes. Demonstrating outcomes comparable to standard criteria donor livers could potentially eliminate concerns surrounding the transplantation of steatotic and DCD livers, marking a significant advancement in the field.

References

1. Abbas SH, Friend PJ. Principles and current status of abdominal organ preservation for transplantation. Surgery in Practice and Science. 2020;3:100020.

2. Posts R. Becoming a living liver donor Why do we need more living liver donors ? [Internet]. 2019. p. 1–10. Available from: https://britishlivertrust.org.uk/becoming-a-living-liver-donor/

3. Chen Z, Wang T, Chen C, Zhao Q, Ma Y, Guo Y, et al. Transplantation of Extended Criteria Donor Livers Following Continuous Normothermic Machine Perfusion Without Recooling. Transplantation. 2022 Jun;106(6):1193.

4. Abbas SH, Ceresa CDL, Pollok JM. Steatotic Donor Transplant Livers: Preservation Strategies to Mitigate against Ischaemia-Reperfusion Injury. International Journal of Molecular Sciences. 2024 Jan;25(9):4648.

5. EASL Clinical Practice Guidelines: Liver transplantation. Journal of Hepatology. 2016 Feb 1;64(2):433–85.

6. Lee WM, Squires RH, Nyberg SL, Doo E, Hoofnagle JH. Acute liver failure: Summary of a workshop. Hepatology. 2008 Apr;47(4):1401–15.

7. Terrault NA, Francoz C, Berenguer M, Charlton M, Heimbach J. Liver Transplantation 2023: Status Report, Current and Future Challenges. Clinical Gastroenterology and Hepatology. 2023 Jul 1;21(8):2150–66.

8. Terrault NA, Pageaux GP. A changing landscape of liver transplantation: King HCV is dethroned, ALD and NAFLD take over! J Hepatol. 2018 Oct;69(4):767–8.

9. Rinella ME, Lazarus JV, Ratziu V, Francque SM, Sanyal AJ, Kanwal F, et al. A multisociety Delphi consensus statement on new fatty liver disease nomenclature. Journal of Hepatology. 2023 Dec 1;79(6):1542–56.

10. Staufer K, Stauber RE. Steatotic Liver Disease: Metabolic Dysfunction, Alcohol, or Both? Biomedicines. 2023 Jul 26;11(8):2108.

11. Nature [Internet]. 2024 [cited 2024 May 7]. Advances in MASLD/NAFLD. Available from: https://www.nature.com/collections/ggfhiijjac

12. NHSBT. Liver Activity. 2018. p. 58–67.

13. Ward ZJ, Bleich SN, Cradock AL, Barrett JL, Giles CM, Flax C, et al. Projected U.S. State-Level Prevalence of Adult Obesity and Severe Obesity. New England Journal of Medicine. 2019 Dec 19;381(25):2440–50.

14. Stepanova M, Kabbara K, Mohess D, Verma M, Roche-Green A, AlQahtani S, et al. Nonalcoholic steatohepatitis is the most common indication for liver transplantation among the elderly: Data from the United States Scientific Registry of Transplant Recipients. Hepatol Commun. 2022 Feb 28;6(7):1506–15.

15. Díaz LA, Ayares G, Arnold J, Idalsoaga F, Corsi O, Arrese M, et al. Liver Diseases in Latin America: Current Status, Unmet Needs, and Opportunities for Improvement. Curr Treat Options Gastroenterol. 2022;20(3):261–78.

16. Yuan L, Hanlon CL, Terrault N, Alqahtani S, Tamim H, Lai M, et al. Portrait of Regional Trends in Liver Transplantation for Nonalcoholic Steatohepatitis in the United States. Am J Gastroenterol. 2022 Mar 1;117(3):433–44.

17. Abouna GM. Organ shortage crisis: problems and possible solutions. Transplant Proc. 2008;40(1):34–8.

18. Wiesner R, Edwards E, Freeman R, Harper A, Kim R, Kamath P, et al. Model for end-stage liver disease (MELD) and allocation of donor livers. Gastroenterology. 2003 Jan;124(1):91–6.

19. Freeman RB, Gish RG, Harper A, Davis GL, Vierling J, Lieblein L, et al. Model for end-stage liver disease (MELD) exception guidelines: results and recommendations from the MELD Exception Study Group and Conference (MESSAGE) for the approval of patients who need liver transplantation with diseases not considered by the standard MELD formula. Liver Transpl. 2006 Dec;12(12 Suppl 3):S128-136.

20. Thuong M, Ruiz A, Evrard P, Kuiper M, Boffa C, Akhtar MZ, et al. New classification of donation after circulatory death donors definitions and terminology. Transpl Int. 2016 Jul;29(7):749–59.

21. Abu-Gazala S, Olthoff KM. Current Status of Living Donor Liver Transplantation in the United States. Annu Rev Med. 2019 Jan 27;70:225–38.

22. Cotter TG, Minhem M, Wang J, Peeraphatdit T, Ayoub F, Pillai A, et al. Living Donor Liver Transplantation in the United States: Evolution of Frequency, Outcomes, Center Volumes, and Factors Associated With Outcomes. Liver Transpl. 2021 Jul;27(7):1019–31.

23. Lamm V, Ekser B, Vagefi PA, Cooper DKC. Bridging to Allotransplantation-Is Pig Liver Xenotransplantation the Best Option? Transplantation. 2022 Jan 1;106(1):26–36.

24. Organ Donation (Deemed Consent) Act 2019 [Internet]. King's Printer of Acts of Parliament; [cited 2024 May 8]. Available from: https://www.legislation.gov.uk/ukpga/2019/7/section/1/enacted

25. Arshad A, Anderson B, Sharif A. Comparison of organ donation and transplantation rates between opt-out and opt-in systems. Kidney Int. 2019 Jun;95(6):1453–60.

26. Moloney G, Sutherland M, Upcroft L, Clark R, Punjabi-Jagdish P, Rienks S, et al. Respect, interaction, immediacy and the role community plays in registering an organ donation decision. PLoS One. 2022;17(1):e0263096.

27. Lomero M, Gardiner D, Coll E, Haase-Kromwijk B, Procaccio F, Immer F, et al. Donation after circulatory death today: an updated overview of the European landscape. Transpl Int. 2020 Jan;33(1):76–88.

28. Miñambres E, Suberviola B, Dominguez-Gil B, Rodrigo E, Ruiz-San Millan JC, Rodríguez-San Juan JC, et al. Improving the Outcomes of Organs Obtained From

Controlled Donation After Circulatory Death Donors Using Abdominal Normothermic Regional Perfusion. Am J Transplant. 2017 Aug;17(8):2165–72.

29. Smith M. Brain death: the United kingdom perspective. Semin Neurol. 2015 Apr;35(2):145–51.

30. Collett D, Friend PJ, Watson CJE. Factors Associated with Short- and Long-term Liver Graft Survival in the United Kingdom: Development of a UK Donor Liver Index. Transplantation. 2017;101(4):786–92.

31. Braat AE, Blok JJ, Putter H, Adam R, Burroughs AK, Rahmel AO, et al. The Eurotransplant donor risk index in liver transplantation: ET-DRI. Am J Transplant. 2012 Oct;12(10):2789–96.

32. ODT Clinical - NHS Blood and Transplant [Internet]. [cited 2024 May 12]. Annual Activity Report. Available from: https://www.odt.nhs.uk/statistics-and-reports/annual-activity-report/

33. Steinbrook R. Organ donation after cardiac death. N Engl J Med. 2007 Jul 19;357(3):209–13.

34. Morrissey PE, Monaco AP. Donation after circulatory death: current practices, ongoing challenges, and potential improvements. Transplantation. 2014 Feb 15;97(3):258–64.

35. Schlegel A, Kalisvaart M, Scalera I, Laing RW, Mergental H, Mirza DF, et al. The UK DCD Risk Score: A new proposal to define futility in donation-after-circulatory-death liver transplantation. Journal of Hepatology. 2018;68(3):456–64.

36. Callaghan CJ, Charman SC, Muiesan P, Powell JJ, Gimson AE, Van Der Meulen JHP. Outcomes of transplantation of livers from donation after circulatory death donors in the UK: A cohort study. BMJ Open. 2013 Aug;3(9):e003287.

37. ODT Clinical - NHS Blood and Transplant [Internet]. [cited 2024 May 9]. Policies and NORS reports. Available from: https://www.odt.nhs.uk/retrieval/policies-and-nors-reports/

38. de Vera ME, Lopez-Solis R, Dvorchik I, Campos S, Morris W, Demetris AJ, et al. Liver transplantation using donation after cardiac death donors: long-term follow-up from a single center. Am J Transplant. 2009 Apr;9(4):773–81.

39. Lee KW, Simpkins CE, Montgomery RA, Locke JE, Segev DL, Maley WR. Factors affecting graft survival after liver transplantation from donation after cardiac death donors. Transplantation. 2006 Dec 27;82(12):1683–8.

40. Muiesan P, Girlanda R, Jassem W, Melendez HV, O'Grady J, Bowles M, et al. Single-center experience with liver transplantation from controlled non-heartbeating donors: a viable source of grafts. Ann Surg. 2005 Nov;242(5):732–8.

41. Abt P, Crawford M, Desai N, Markmann J, Olthoff K, Shaked A. Liver transplantation from controlled non-heart-beating donors: an increased incidence of biliary complications. Transplantation. 2003 May 27;75(10):1659–63.

42. Chan EY, Olson LC, Kisthard JA, Perkins JD, Bakthavatsalam R, Halldorson JB, et al. Ischemic cholangiopathy following liver transplantation from donation after cardiac death donors. Liver Transpl. 2008 May;14(5):604–10.

43. Ghinolfi D, Dondossola D, Rreka E, Lonati C, Pezzati D, Cacciatoinsilla A, et al. Sequential Use of Normothermic Regional and Ex Situ Machine Perfusion in Donation After Circulatory Death Liver Transplant. Liver Transpl. 2021 Feb;27(3):385–402.

44. Álvarez-Mercado AI, Gulfo J, Romero Gómez M, Jiménez-Castro MB, Gracia-Sancho J, Peralta C. Use of Steatotic Grafts in Liver Transplantation: Current Status. Liver Transpl. 2019 May;25(5):771–86.

45. Gao Q, Mulvihill MS, Scheuermann U, Davis RP, Yerxa J, Yerokun BA, et al. Improvement in Liver Transplant Outcomes From Older Donors: A US National Analysis. Ann Surg. 2019 Aug;270(2):333–9.

46. Goldaracena N, Cullen JM, Kim DS, Ekser B, Halazun KJ. Expanding the donor pool for liver transplantation with marginal donors. Int J Surg. 2020 Oct;82S:30–5.

47. Angele MK, Rentsch M, Hartl WH, Wittmann B, Graeb C, Jauch KW, et al. Effect of graft steatosis on liver function and organ survival after liver transplantation. Am J Surg. 2008 Feb;195(2):214–20.

48. Boteon YL, Afford SC. Machine perfusion of the liver: Which is the best technique to mitigate ischaemia-reperfusion injury? World J Transplant. 2019 Jan 16;9(1):14–20.

49. Brunner SM, Junger H, Ruemmele P, Schnitzbauer AA, Doenecke A, Kirchner GI, et al. Bile duct damage after cold storage of deceased donor livers predicts biliary complications after liver transplantation. J Hepatol. 2013 Jun;58(6):1133–9.

50. Farid SG, Attia MS, Vijayanand D, Upasani V, Barlow AD, Willis S, et al. Impact of Donor Hepatectomy Time During Organ Procurement in Donation After Circulatory Death Liver Transplantation: The United Kingdom Experience. Transplantation. 2019 Apr;103(4):e79–88.

51. Croome KP, Mathur AK, Mao S, Aqel B, Piatt J, Senada P, et al. Perioperative and long-term outcomes of utilizing donation after circulatory death liver grafts with macrosteatosis: A multicenter analysis. American Journal of Transplantation. 2020;20(9):2449–56.

52. Foley DP, Fernandez LA, Leverson G, Anderson M, Mezrich J, Sollinger HW, et al. Biliary complications after liver transplantation from donation after cardiac death donors: An analysis of risk factors and long-term outcomes from a single center. Annals of Surgery. 2011 Apr;253(4):817–25.

53. Nair A, Hashimoto K. Extended criteria donors in liver transplantation-from marginality to mainstream. Hepatobiliary Surg Nutr. 2018 Oct;7(5):386–8.

54. Silberhumer GR, Rahmel A, Karam V, Gonen M, Gyoeri G, Kern B, et al. The difficulty in defining extended donor criteria for liver grafts: the Eurotransplant experience. Transpl Int. 2013 Oct;26(10):990–8.

55. Vodkin I, Kuo A. Extended Criteria Donors in Liver Transplantation. Clin Liver Dis. 2017 May;21(2):289–301.

56. Zhai Y, Petrowsky H, Hong JC, Busuttil RW, Kupiec-Weglinski JW. Ischaemia-reperfusion injury in liver transplantation-from bench to bedside. Nature Reviews Gastroenterology and Hepatology. 2013 Feb;10(2):79–89.

57. Chouchani ET, Pell VR, Gaude E, Aksentijević D, Sundier SY, Robb EL, et al. Ischaemic accumulation of succinate controls reperfusion injury through mitochondrial ROS. Nature. 2014;515(7527):431–5.

58. Chouchani ET, Pell VR, James AM, Work LM, Saeb-Parsy K, Frezza C, et al. A unifying mechanism for mitochondrial superoxide production during ischemia-reperfusion injury. Cell Metabolism. 2016;23(2):254–63.

59. Galkin A. Brain Ischemia/Reperfusion Injury and Mitochondrial Complex I Damage. Biochemistry (Mosc). 2019 Nov;84(11):1411–23.

60. Teodoro JS, Da Silva RT, Machado IF, Panisello-Roselló A, Roselló-Catafau J, Rolo AP, et al. Shaping of Hepatic Ischemia/Reperfusion Events: The Crucial Role of Mitochondria. Cells. 2022 Jan;11(4):688.

61. Jiménez-Castro MB, Cornide-Petronio ME, Gracia-Sancho J, Peralta C. Inflammasome-Mediated Inflammation in Liver Ischemia-Reperfusion Injury. Cells. 2019 Sep 23;8(10):1131.

62. Tsung A, Sahai R, Tanaka H, Nakao A, Fink MP, Lotze MT, et al. The nuclear factor HMGB1 mediates hepatic injury after murine liver ischemia-reperfusion. J Exp Med. 2005 Apr 4;201(7):1135–43.

63. Yazdani HO, Geller DA, Tohme S. Spliced CEACAM1: A Potential Novel Biomarker and Target for Ameliorating Liver Ischemia-reperfusion Injury. Transplantation. 2024 Mar 1;108(3):585–7.

64. Hilmi I, Horton CN, Planinsic RM, Sakai T, Nicolau-Raducu R, Damian D, et al. The impact of postreperfusion syndrome on short-term patient and liver allograft outcome in patients undergoing orthotopic liver transplantation. Liver Transplantation. 2008;14(4):504–8.

65. Paugam-Burtz C, Kavafyan J, Merckx P, Dahmani S, Sommacale D, Ramsay M, et al. Postreperfusion syndrome during liver transplantation for cirrhosis: outcome and predictors. Liver Transpl. 2009 May;15(5):522–9.

66. Olthoff KM, Kulik L, Samstein B, Kaminski M, Abecassis M, Emond J, et al. Validation of a current definition of early allograft dysfunction in liver transplant recipients and analysis of risk factors. Liver Transplantation. 2010;16(8):943–9.

67. Pareja E, Cortes M, Hervás D, Mir J, Valdivieso A, Castell JV, et al. A score model for the continuous grading of early allograft dysfunction severity. Liver Transplantation. 2015;21(1):38–46.

68. Agopian VG, Harlander-Locke MP, Markovic D, Dumronggittigule W, Xia V, Kaldas FM, et al. Evaluation of Early Allograft Function Using the Liver Graft Assessment Following Transplantation Risk Score Model. JAMA Surg. 2018 May 1;153(5):436–44.

69. Agopian VG, Markovic D, Klintmalm GB, Saracino G, Chapman WC, Vachharajani N, et al. Multicenter validation of the liver graft assessment following transplantation (L-GrAFT) score for assessment of early allograft dysfunction. Journal of Hepatology. 2021 Apr 1;74(4):881–92.

70. Al-Freah M a. B, McPhail MJW, Dionigi E, Foxton MR, Auzinger G, Rela M, et al. Improving the Diagnostic Criteria for Primary Liver Graft Nonfunction in Adults Utilizing Standard and Transportable Laboratory Parameters: An Outcome-Based Analysis. Am J Transplant. 2017 May;17(5):1255–66.

71. Kulik U, Lehner F, Klempnauer J, Borlak J. Primary non-function is frequently associated with fatty liver allografts and high mortality after re-transplantation. Liver Int. 2017 Aug;37(8):1219–28.

72. Zhang X, Zhang C, Huang H, Chen R, Lin Y, Chen L, et al. Primary nonfunction following liver transplantation: Learning of graft metabolites and building a predictive model. Clin Transl Med. 2021 Jul;11(7):e483.

73. An R, Bai R, Zhang S, Xie P, Zhu Y, Wen J, et al. Blood loss during liver transplantation is a predictor of postoperative thrombosis. Clin Med (Lond). 2022 Sep;22(5):434–40.

74. Channaoui A, Tambucci R, Pire A, de Magnée C, Sokal E, Smets F, et al. Management and outcome of hepatic artery thrombosis after pediatric liver transplantation. Pediatr Transplant. 2021 Aug;25(5):e13938.

75. von Meijenfeldt FA, Burlage LC, Bos S, Adelmeijer J, Porte RJ, Lisman T. Elevated Plasma Levels of Cell-Free DNA During Liver Transplantation Are Associated With Activation of Coagulation. Liver Transplantation. 2018;24(12):1716–25.

76. Hessheimer AJ, Cárdenas A, García-Valdecasas JC, Fondevila C. Can we prevent ischemic-type biliary lesions in donation after circulatory determination of death liver transplantation? Liver Transpl. 2016 Jul;22(7):1025–33.

77. Goussous N, Alvarez-Casas J, Dawany N, Xie W, Malik S, Gray SH, et al. Ischemic Cholangiopathy Postdonation After Circulatory Death Liver Transplantation: Donor Hepatectomy Time Matters. Transplant Direct. 2022 Jan;8(1):e1277.

78. Dong V, Nadim MK, Karvellas CJ. Post-Liver Transplant Acute Kidney Injury. Liver Transpl. 2021 Nov;27(11):1653–64.

79. Todo S, Demetris AJ, Makowka L, Teperman L, Podesta L, Shaver T, et al. PRIMARY NONFUNCTION OF HEPATIC ALLOGRAFTS WITH PREEXISTING FATTY INFILTRATION. Transplantation. 1989 May;47(5):903–5.

80. El-Badry AM, Breitenstein S, Jochum W, Washington K, Paradis V, Rubbia-Brandt L, et al. Assessment of hepatic steatosis by expert pathologists: The end of a gold standard. Annals of Surgery. 2009;250(5):691–6.

81. Hall AR, Dhillon AP, Green AC, Ferrell L, Crawford JM, Alves V, et al. Hepatic steatosis estimated microscopically versus digital image analysis. Liver International. 2013;33(6):926–35.

82. Turlin B, Ramm GA, Purdie DM, Lainé F, Perrin M, Deugnier Y, et al. Assessment of hepatic steatosis: comparison of quantitative and semiquantitative methods in 108 liver biopsies. Liver Int. 2009 Apr;29(4):530–5.

83. Chu MJJ, Dare AJ, Phillips ARJ, Bartlett ASJR. Donor Hepatic Steatosis and Outcome After Liver Transplantation: a Systematic Review. Journal of Gastrointestinal Surgery. 2015;19(9):1713–24.

84. Croome KP, Lee DD, Taner CB. The 'Skinny' on Assessment and Utilization of Steatotic Liver Grafts: A Systematic Review. Liver Transpl. 2019 Mar;25(3):488–99.

85. Wong TCL, Fung JYY, Chok KSH, Cheung TT, Chan ACY, Sharr WW, et al. Excellent outcomes of liver transplantation using severely steatotic grafts from brain-dead donors. Liver Transpl. 2016 Feb;22(2):226–36.

86. Melin C, Miick R, Young NA, Ortiz J, Balasubramanian M. Approach to intraoperative consultation for donor liver biopsies. Arch Pathol Lab Med. 2013 Feb;137(2):270–4.

87. Yersiz H, Lee C, Kaldas FM, Hong JC, Rana A, Schnickel GT, et al. Assessment of hepatic steatosis by transplant surgeon and expert pathologist: A prospective, double-blind evaluation of 201 donor livers. Liver Transplantation. 2013;19(4):437–49.

88. Imber CJ, St Peter SD, Lopez I, Guiver L, Friend PJ. Current practice regarding the use of fatty livers: a trans-Atlantic survey. Liver Transpl. 2002 Jun;8(6):545–9.

89. Rey JW, Wirges U, Dienes HP, Fries JWU. Hepatic Steatosis in Organ Donors: Disparity Between Surgery and Histology? Transplantation Proceedings. 2009;41(6):2557–60.

90. Brunt EM. Surgical assessment of significant steatosis in donor livers: the beginning of the end for frozen-section analysis? Liver Transpl. 2013 Apr;19(4):360–1.

91. Heller B, Peters S. Assessment of liver transplant donor biopsies for steatosis using frozen section: accuracy and possible impact on transplantation. J Clin Med Res. 2011 Jul 26;3(4):191–4.

92. Guido M, Rugge M. Liver biopsy sampling in chronic viral hepatitis. Semin Liver Dis. 2004 Feb;24(1):89–97.

93. Vilgrain V, Ronot M, Abdel-Rehim M, Zappa M, d'Assignies G, Bruno O, et al. Hepatic steatosis: a major trap in liver imaging. Diagn Interv Imaging. 2013;94(7–8):713–27.

94. Li M, Song J, Mirkov S, Xiao SY, Hart J, Liu W. Comparing morphometric, biochemical, and visual measurements of macrovesicular steatosis of liver. Human Pathology. 2011;42(3):356–60.

95. Nativ NI, Chen AI, Yarmush G, Henry SD, Lefkowitch JH, Klein KM, et al. Automated image analysis method for detecting and quantifying macrovesicular steatosis in

hematoxylin and eosin-stained histology images of human livers. Liver Transpl. 2014 Feb;20(2):228–36.

96. Neil DAH, Minervini M, Smith ML, Hubscher SG, Brunt EM, Demetris AJ. Banff consensus recommendations for steatosis assessment in donor livers. Hepatology. 2022;75(4):1014–25.

97. Steggerda JA, Borja-Cacho D, Brennan TV, Todo T, Nissen NN, Bloom MB, et al. A Clinical Tool to Guide Selection and Utilization of Marginal Donor Livers With Graft Steatosis in Liver Transplantation. Transplant Direct. 2022 Feb;8(2):e1280.

98. Dutkowski P, Schlegel A, Slankamenac K, Oberkofler CE, Adam R, Burroughs AK, et al. The use of fatty liver grafts in modern allocation systems: risk assessment by the balance of risk (BAR) score. Annals of surgery. 2012;256(5):861–8.

99. Briceño J, Padillo J, Rufián S, Solórzano G, Pera C. Assignment of steatotic livers by the Mayo model for end-stage liver disease. Transpl Int. 2005 May;18(5):577–83.

100. de Graaf EL, Kench J, Dilworth P, Shackel NA, Strasser SI, Joseph D, et al. Grade of deceased donor liver macrovesicular steatosis impacts graft and recipient outcomes more than the Donor Risk Index. Journal of Gastroenterology and Hepatology (Australia). 2012;27(3):540–6.

101. Deroose JP, Kazemier G, Zondervan P, IJzermans JN, Metselaar HJ, Alwayn IP. Hepatic steatosis is not always a contraindication for cadaveric liver transplantation. HPB (Oxford). 2011 Jun;13(6):417–25.

102. McCormack L, Petrowsky H, Jochum W, Mullhaupt B, Weber M, Clavien PA. Use of severely steatotic grafts in liver transplantation: A matched case-control study. Annals of Surgery. 2007;246(6):940–6.

103. Martin E. K, Allen, England NHS. Annual Report on Liver Transplantation: Report for 2014/2015. Vol. 2016. 2015.

104. Kwong AJ, Kim WR, Lake J, Stock PG, Wang CJ, Wetmore JB, et al. Impact of Donor Liver Macrovesicular Steatosis on Deceased Donor Yield and Posttransplant Outcome. Transplantation. 2023 Feb 1;107(2):405–9.

105. Gaffey MJ, Boyd JC, Traweek ST, Ashraf Ali M, Rezeig M, Caldwell SH, et al. Predictive value of intraoperative biopsies and liver function tests for preservation injury in orthotopic liver transplantation. Hepatology. 1997;25(1):184–9.

106. Karayalcin K, Mirza DF, Harrison RF, Da Silva RF, Hubscher SG, Mayer AD, et al. The role of dynamic and morphological studies in the assessment of potential liver donors. Transplantation. 1994;57(9):1323–7.

107. Ploeg RJ, D'Alessandro AM, Knechtle SJ, Stegall MD, Pirsch JD, Hoffmann RM, et al. Risk factors for primary dysfunction after liver transplantation - A multivariate analysis. Transplantation. 1993;55(4):807–13.

108. Noujaim HM, de Ville de Goyet J, Montero EFS, Ribeiro CMF, Capellozzi VL, Crescentini F, et al. Expanding postmortem donor pool using steatotic liver grafts: a new look. Transplantation. 2009 Mar 27;87(6):919–25.

109. Li J, Liu B, Yan LN, Zuo YX, Li B, Zeng Y, et al. Reversal of Graft Steatosis After Liver Transplantation: Prospective Study. Transplantation Proceedings. 2009;41(9):3560–3.

110. Reddy MS, Bhati C, Neil D, Mirza DF, Manas DM. National Organ Retrieval Imaging System: results of the pilot study. Transpl Int. 2008 Nov;21(11):1036–44.

111. Verran D, Kusyk T, Painter D, Fisher J, Koorey D, Strasser S, et al. Clinical experience gained from the use of 120 steatotic donor livers for orthotopic liver transplantation. Liver Transpl. 2003 May;9(5):500–5.

112. Canelo R, Braun F, Sattler B, Klinge B, Lorf T, Ramadori G, et al. Is a fatty liver dangerous for transplantation? Transplant Proc. 1999;31(1–2):414–5.

113. Ureña MAG, Ruiz-Delgado FC, González EM, Segurola CL, Romero CJ, Garcia IG, et al. Assessing risk of the use of livers with macro and microsteatosis in a liver transplant program. In: Transplantation Proceedings. 1998. p. 3288–91.

114. Selzner N, Selzner M, Jochum W, Amann-Vesti B, Graf R, Clavien PA. Mouse livers with macrosteatosis are more susceptible to normothermic ischemic injury than those with microsteatosis. Journal of Hepatology. 2006;44(4):694–701.

115. Berthiaume F, Barbe L, Mokuno Y, MacDonald AD, Jindal R, Yarmush ML. Steatosis Reversibly Increases Hepatocyte Sensitivity to Hypoxia-Reoxygenation Injury. Journal of Surgical Research. 2009;152(1):54–60.

116. Taneja C, Prescott L, Koneru B. Critical preservation injury in rat fatty liver is to hepatocytes, not sinusoidal lining cells. Transplantation. 1998 Jan 27;65(2):167–72.

117. NERI AA, DONTAS IA, ILIOPOULOS DC, KARATZAS T. Pathophysiological Changes During Ischemia-reperfusion Injury in Rodent Hepatic Steatosis. In Vivo. 2020 May 3;34(3):953–64.

118. Kim JS, Qian T, Lemasters JJ. Mitochondrial permeability transition in the switch from necrotic to apoptotic cell death in ischemic rat hepatocytes. Gastroenterology. 2003 Feb;124(2):494–503.

119. Martins RM, Teodoro JS, Furtado E, Rolo AP, Palmeira CM, Tralhão JG. Recent insights into mitochondrial targeting strategies in liver transplantation. International Journal of Medical Sciences. 2018;15(3):248–56.

120. Hand SC, Menze MA. Mitochondria in energy-limited states: mechanisms that blunt the signaling of cell death. J Exp Biol. 2008 Jun;211(Pt 12):1829–40.

121. Acosta D, Wenzel DG. Injury produced by free fatty acids to lysosomes and mitochondria in cultured heart muscle and endothelial cells. Atherosclerosis. 1974;20(3):417–26.

122. Trauner M, Arrese M, Wagner M. Fatty liver and lipotoxicity. Biochim Biophys Acta. 2010 Mar;1801(3):299–310.

123. Koizumi T, Nakao Y, Kawanishi M, Maeda S, Sugiyama T, Fujita T. Suppression of c-myc mRNA expression by steroid hormones in HTLV-I-infected T-cell line, KH-2. International Journal of Cancer. 1989;44(4):701–6.

124. Sakurada M, Ohkohchi N, Kato H, Koizumi M, Fujimori K, Satomi S, et al. Mitochondrial respiratory function, adenine nucleotides and antioxygenic enzymes in pig liver transplantation. Transplant Proc. 1989 Feb;21(1 Pt 2):1321–2.

125. Fukumori T, Ohkohchi N, Tsukamoto S, Satomi S. Why is fatty liver unsuitable for transplantation? Deterioration of mitochondrial ATP synthesis and sinusoidal structure during cold preservation of a liver with steatosis. Transplant Proc. 1997;29(1–2):412–5.

126. Nativ NI, Maguire TJ, Yarmush G, Brasaemle DL, Henry SD, Guarrera JV, et al. Liver defatting: An alternative approach to enable steatotic liver transplantation. American Journal of Transplantation. 2012;12(12):3176–83.

127. Akhtar MZ, Henderson T, Sutherland A, Vogel T, Friend PJ. Novel approaches to preventing ischemia-reperfusion injury during liver transplantation. Transplant Proc. 2013;45(6):2083–92.

128. Serviddio G, Bellanti F, Tamborra R, Rollo T, Capitanio N, Romano AD, et al. Uncoupling protein-2 (UCP2) induces mitochondrial proton leak and increases susceptibility of non-alcoholic steatohepatitis (NASH) liver to ischaemia-reperfusion injury. Gut. 2008 Jul;57(7):957–65.

129. Shojaie L, Iorga A, Dara L. Cell Death in Liver Diseases: A Review. Int J Mol Sci. 2020 Dec 18;21(24):9682.

130. Gautheron J, Vucur M, Reisinger F, Cardenas DV, Roderburg C, Koppe C, et al. A positive feedback loop between RIP3 and JNK controls non-alcoholic steatohepatitis. EMBO Mol Med. 2014 Aug;6(8):1062–74.

131. Kolachala VL, Lopez C, Shen M, Shayakhmetov D, Gupta NA. Ischemia reperfusion injury induces pyroptosis and mediates injury in steatotic liver thorough Caspase 1 activation. Apoptosis. 2021 Jun;26(5–6):361–70.

132. Hakamada K, Sasaki M, Takahashi K, Umehara Y, Konn M. Sinusoidal flow block after warm ischemia in rats with diet-induced fatty liver. J Surg Res. 1997 Jun;70(1):12–20.

133. Sato N, Eguchi H, Inoue A, Matsumura T, Kawano S, Kamada T. Hepatic microcirculation in Zucker fatty rats. Adv Exp Med Biol. 1986;200:477–83.

134. Teramoto K, Bowers JL, Kruskal JB, Clouse ME. Hepatic microcirculatory changes after reperfusion in fatty and normal liver transplantation in the rat. Transplantation. 1993 Nov;56(5):1076–82.

135. Seifalian AM, Chidambaram V, Rolles K, Davidson BR. In vivo demonstration of impaired microcirculation in steatotic human liver grafts. Liver Transpl Surg. 1998 Jan;4(1):71–7.

136. Ijaz S, Yang W, Winslet MC, Seifalian AM. Impairment of hepatic microcirculation in fatty liver. Microcirculation. 2003 Dec;10(6):447–56.

137. Bioulac-Sage P, Balabaud C, Ferrell L. Lipopeliosis revisited: should we keep the term? Am J Surg Pathol. 2002 Jan;26(1):134–5.

138. Ferrell L, Bass N, Roberts J, Ascher N. Lipopeliosis: fat induced sinusoidal dilatation in transplanted liver mimicking peliosis hepatis. J Clin Pathol. 1992 Dec;45(12):1109–10.

139. Kolios G, Valatas V, Kouroumalis E. Role of Kupffer cells in the pathogenesis of liver disease. World J Gastroenterol. 2006 Dec 14;12(46):7413–20.

140. Koeppel TA, Mihaljevic N, Kraenzlin B, Loehr M, Jesenofsky R, Post S, et al. Enhanced iNOS gene expression in the steatotic rat liver after normothermic ischemia. Eur Surg Res. 2007;39(5):303–11.

141. Tiriveedhi V, Conzen KD, Liaw-Conlin J, Upadhya G, Malone J, Townsend RR, et al. The role of molecular chaperonins in warm ischemia and reperfusion injury in the steatotic liver: A proteomic study. BMC Biochemistry. 2012 Sep 10;13(1):17.

142. Serafín A, Roselló-Catafau J, Prats N, Xaus C, Gelpí E, Peralta C. Ischemic preconditioning increases the tolerance of fatty liver to hepatic ischemia-reperfusion injury in the rat. American Journal of Pathology. 2002;161(2):587–601.

143. Mosbah IB, Roselló-Catafau J, Alfany-Fernandez I, Rimola A, Parellada PP, Mitjavila MT, et al. Addition of carvedilol to University Wisconsin solution improves rat steatotic and nonsteatotic liver preservation. Liver Transplantation. 2010;16(2):163–71.

144. Jaeschke H, Woolbright BL. Current strategies to minimize hepatic ischemia–reperfusion injury by targeting reactive oxygen species. Transplant Rev (Orlando). 2012 Apr;26(2):103–14.

145. Mylonas C, Kouretas D. Lipid peroxidation and tissue damage. In Vivo. 1999;13(3):295–309.

146. Granger DN, Kvietys PR. Reperfusion injury and reactive oxygen species: The evolution of a concept. Redox Biol. 2015 Oct 8;6:524–51.

147. Selzner M, Clavien PA. Fatty liver in liver transplantation and surgery. Seminars in Liver Disease. 2001;21(1):105–13.

148. Nakano H, Nagasaki H, Barama A, Boudjema K, Jaeck D, Kumada K, et al. The effects of N-acetylcysteine and anti-intercellular adhesion molecule-1 monoclonal antibody against ischemia-reperfusion injury of the rat steatotic liver produced by a choline-methionine-deficient diet. Hepatology. 1997;26(3):670–8.

149. Uhlmann D, Gaebel G, Armann B, Ludwig S, Hess J, Pietsch UC, et al. Attenuation of proinflammatory gene expression and microcirculatory disturbances by endothelin A

receptor blockade after orthotopic liver transplantation in pigs. Surgery. 2006 Jan;139(1):61–72.

150. Tsoulfas G, Takahashi Y, Ganster RW, Yagnik G, Guo Z, Fung JJ, et al. Activation of the lipopolysaccharide signaling pathway in hepatic transplantation preservation injury. Transplantation. 2002 Jul 15;74(1):7–13.

151. Boteon YL, Wallace L, Boteon APCS, Mirza DF, Mergental H, Bhogal RH, et al. An effective protocol for pharmacological defatting of primary human hepatocytes which is non-toxic to cholangiocytes or intrahepatic endothelial cells. PLoS ONE. 2018;13(7):e0201419.

152. Zhong Z, Connor H, Stachlewitz RF, Frankenberg M, Mason RP, Lemasters JJ, et al. Role of free radicals in primary nonfunction of marginal fatty grafts from rats treated acutely with ethanol. Mol Pharmacol. 1997 Nov;52(5):912–9.

153. Ju C, Colgan SP, Eltzschig HK. Hypoxia-inducible factors as molecular targets for liver diseases. Journal of Molecular Medicine. 2016;94(6):613–27.

154. Suzuki T, Shinjo S, Arai T, Kanai M, Goda N. Hypoxia and fatty liver. World Journal of Gastroenterology. 2014;20(41):15087–97.

155. Qu A, Taylor M, Xue X, Matsubara T, Metzger D, Chambon P, et al. Hypoxia-inducible transcription factor 2α promotes steatohepatitis through augmenting lipid accumulation, inflammation, and fibrosis. Hepatology. 2011;54(2):472–83.

156. Zhang X, Liu Z, Xiao Q, Zeng C, Lai CH, Fan X, et al. Donor Treatment With a Hypoxia-Inducible Factor-1 Agonist Prevents Donation After Cardiac Death Liver Graft Injury in a Rat Isolated Perfusion Model. Artificial Organs. 2018;42(3):280–9.

157. Guo Y, Feng L, Zhou Y, Sheng J, Long D, Li S, et al. Systematic review with meta-analysis: HIF-1α attenuates liver ischemia-reperfusion injury. Transplantation Reviews. 2015;29(3):127–34.

158. Dery KJ, Kojima H, Kageyama S, Kadono K, Hirao H, Cheng B, et al. Alternative splicing of CEACAM1 by hypoxia-inducible factor-1α enhances tolerance to hepatic ischemia in mice and humans. Sci Transl Med. 2023 Aug 2;15(707):eadf2059.

159. Land WG, Agostinis P, Gasser S, Garg AD, Linkermann A. Transplantation and Damage-Associated Molecular Patterns (DAMPs). Am J Transplant. 2016 Dec;16(12):3338–61.

160. Takeuchi O, Akira S. Pattern recognition receptors and inflammation. Cell. 2010 Mar 19;140(6):805–20.

161. Chen GY, Nuñez G. Sterile inflammation: sensing and reacting to damage. Nat Rev Immunol. 2010 Dec;10(12):826–37.

162. Kang R, Tang D. Nuclear DAMPs in Hepatic Injury and Inflammation. In: Ding WX, Yin XM, editors. Molecules, Systems and Signaling in Liver Injury [Internet]. Cham: Springer International Publishing; 2017 [cited 2024 Mar 1]. p. 133–58. (Cell Death in Biology and Diseases). Available from: https://doi.org/10.1007/978-3-319-58106-4_7

163. Silk E, Zhao H, Weng H, Ma D. The role of extracellular histone in organ injury. Cell Death Dis. 2017 May 25;8(5):e2812.

164. Kustanovich A, Schwartz R, Peretz T, Grinshpun A. Life and death of circulating cell-free DNA. Cancer Biol Ther. 2019;20(8):1057–67.

165. Ni YA, Chen H, Nie H, Zheng B, Gong Q. HMGB1: An overview of its roles in the pathogenesis of liver disease. J Leukoc Biol. 2021 Nov;110(5):987–98.

166. Gowda NM, Wu X, Gowda DC. The Nucleosome (Histone-DNA Complex) Is the TLR9-Specific Immunostimulatory Component of Plasmodium falciparum That Activates DCs. PLoS One. 2011 Jun 8;6(6):e20398.

167. Tsourouktsoglou TD, Warnatsch A, Ioannou M, Hoving D, Wang Q, Papayannopoulos V. Histones, DNA, and Citrullination Promote Neutrophil Extracellular Trap Inflammation by Regulating the Localization and Activation of TLR4. Cell Rep. 2020 May 5;31(5):107602.

168. Wilson AS, Randall KL, Pettitt JA, Ellyard JI, Blumenthal A, Enders A, et al. Neutrophil extracellular traps and their histones promote Th17 cell differentiation directly via TLR2. Nat Commun. 2022 Jan 26;13(1):528.

169. Hu Q, Wood CR, Cimen S, Venkatachalam AB, Alwayn IPJ. Mitochondrial Damage-Associated Molecular Patterns (MTDs) Are Released during Hepatic Ischemia Reperfusion and Induce Inflammatory Responses. PLoS One. 2015;10(10):e0140105.

170. Kobayashi A, Imamura H, Isobe M, Matsuyama Y, Soeda J, Matsunaga K, et al. Mac-1 (CD11b/CD18) and intercellular adhesion molecule-1 in ischemia-reperfusion injury of rat liver. Am J Physiol Gastrointest Liver Physiol. 2001 Aug;281(2):G577-585.

171. Fondevila C, Busuttil RW, Kupiec-Weglinski JW. Hepatic ischemia/reperfusion injury--a fresh look. Exp Mol Pathol. 2003 Apr;74(2):86–93.

172. Oliveira THC de, Marques PE, Proost P, Teixeira MMM. Neutrophils: a cornerstone of liver ischemia and reperfusion injury. Lab Invest. 2018 Jan;98(1):51–62.

173. Nakamura K, Kageyama S, Kupiec-Weglinski JW. The Evolving Role of Neutrophils in Liver Transplant Ischemia-Reperfusion Injury. Curr Transplant Rep. 2019;6(1):78–89.

174. Brinkmann V, Reichard U, Goosmann C, Fauler B, Uhlemann Y, Weiss DS, et al. Neutrophil extracellular traps kill bacteria. Science. 2004 Mar 5;303(5663):1532–5.

175. Cohen JC, Horton JD, Hobbs HH. Human fatty liver disease: old questions and new insights. Science. 2011 Jun 24;332(6037):1519–23.

176. Dowman JK, Tomlinson JW, Newsome PN. Pathogenesis of non-alcoholic fatty liver disease. QJM. 2010 Feb;103(2):71–83.

177. Hodson L, Frayn KN. Hepatic fatty acid partitioning. Current Opinion in Lipidology. 2011;22(3):216–24.

178. Green CJ, Parry SA, Gunn PJ, Ceresa CDL, Rosqvist F, Piché ME, et al. Studying non-alcoholic fatty liver disease: the ins and outs of in vivo, ex vivo and in vitro human models. Horm Mol Biol Clin Investig. 2018 Aug 11;41(1):/j/hmbci.2020.41.issue-1/hmbci-2018-0038/hmbci-2018-0038.xml.

179. Abbas SH, Ceresa CDL, Hodson L, Nasralla D, Watson CJE, Mergental H, et al. Defatting of donor transplant livers during normothermic perfusion-a randomised clinical trial: study protocol for the DeFat study. Trials. 2024 Jun 17;25(1):386.

180. Ameer F, Scandiuzzi L, Hasnain S, Kalbacher H, Zaidi N. De novo lipogenesis in health and disease. Metabolism: Clinical and Experimental. 2014;63(7):895–902.

181. Frayn KN. Metabolic regulation: a human perspective [Internet]. 3rd ed. Chichester, U.K.: Wiley-Blackwell Pub.; 2010 [cited 2024 May 12]. 371 p. Available from: http://www.dawsonera.com/depp/reader/protected/external/AbstractView/S9781444317763

182. Ginsberg HN. Lipoprotein physiology. Endocrinol Metab Clin North Am. 1998 Sep;27(3):503–19.

183. McGarry JD, Foster DW. Regulation of hepatic fatty acid oxidation and ketone body production. Annu Rev Biochem. 1980;49:395–420.

184. Collard CD, Gelman S. Pathophysiology, clinical manifestations, and prevention of ischemia-reperfusion injury. Anesthesiology. 2001;94(6):1133–8.

185. Fuller B, Guibert E, Rodríguez J. Lessons from natural cold-induced dormancy to organ preservation in medicine and biotechnology: From the 'backwoods to the bedside'. Lubzens E, Cerda J, Clark M, editors. Vol. 21, Topics in Current Genetics. Berlin: Springer; 2010. 253–278 p.

186. Ceresa CDL, Davidson BR, Friend PJ, Ploeg RJ. Liver Retrieval and Preservation. In: Neuberger J, Ferguson J, Newsome PN, editors. Neuberger, James Ferguson, James Newsome, Philip N. Chichester: Wiley-Blackwell; 2021.

187. Eghtesad B, Aucejo F, Fung JJ. Preservation solutions in liver transplantation: What are the options? Liver Transplantation. 2006;12(2):196–8.

188. Belzer FO, Sollinger HW, Glass NR, Miller DT, Hoffmann RM, Southard JH. Beneficial effects of adenosine and phosphate in kidney preservation. Transplantation. 1983;36(6):633–5.

189. Belzer FO, Hoffman RM, Miller DT. A new perfusate for kidney preservation. Transplantation Proceedings. 1984;16(1):161–3.

190. Ploeg RJ, Goossens D, Vreugdenhil P, McAnulty JF, Southard JH, Belzer FO. Successful 72-hour cold storage kidney preservation with UW solution. Transplantation Proceedings. 1988;20(1 SUPPL. 1):935–8.

191. Bretschneider HJ, Hubner G, Knoll D, Lohr B, Nordbeck H, Spieckermann PG. Myocardial resistance and tolerance to ischemia: physiological and biochemical basis. Journal of Cardiovascular Surgery. 1975;16(3):241–60.

192. Erhard J, Lange R, Scherer R, Kox WJ, Bretschneider HJ, Gebhard MM, et al. Comparison of histidine-tryptophan-ketoglutarate (HTK) solution versus University of Wisconsin (UW) solution for organ preservation in human liver transplantation - A prospective, randomized study. Transplant International. 1994;7(3):177–81.

193. Tiwari N, Mergental H. Liver Donation and Preservation. In: Neuberger J, Ferguson J, Newsome PN, editors. Liver Transplantation: Clinical Assessment and Management. Chichester: Wiley-Blackwell; 2021.

194. Todo S, Nery J, Yanaga K, Podesta L, Gordon RD, Starzl TE. Extended Preservation of Human Liver Grafts With UW Solution. JAMA: The Journal of the American Medical Association. 1989;261(5):711–4.

195. Roberts MS, Angus DC, Bryce CL, Valenta Z, Weissfeld L. Survival after liver transplantation in the United States: a disease-specific analysis of the UNOS database. Liver Transpl. 2004 Jul;10(7):886–97.

196. Attard J, Sneiders D, Laing R, Boteon Y, Mergental H, Isaac J, et al. The effect of end-ischaemic normothermic machine perfusion on donor hepatic artery endothelial integrity. Langenbecks Arch Surg. 2022 Mar;407(2):717–26.

197. Liu W, Fan Y, Ding H, Han D, Yan Y, Wu R, et al. Normothermic machine perfusion attenuates hepatic ischaemia-reperfusion injury by inhibiting CIRP-mediated oxidative stress and mitochondrial fission. J Cell Mol Med. 2021 Dec;25(24):11310–21.

198. Ohman A, Raigani S, Santiago JC, Heaney MG, Boylan JM, Parry N, et al. Activation of autophagy during normothermic machine perfusion of discarded livers is associated with improved hepatocellular function. Am J Physiol Gastrointest Liver Physiol. 2022 Jan 1;322(1):G21–33.

199. Op den Dries S, Karimian N, Westerkamp AC, Sutton ME, Kuipers M, Wiersema-Buist J, et al. Normothermic machine perfusion reduces bile duct injury and improves biliary epithelial function in rat donor livers. Liver Transpl. 2016 Jul;22(7):994–1005.

200. Jassem W, Xystrakis E, Ghnewa YG, Yuksel M, Pop O, Martinez-Llordella M, et al. Normothermic Machine Perfusion (NMP) Inhibits Proinflammatory Responses in the Liver and Promotes Regeneration. Hepatology. 2019 Aug;70(2):682–95.

201. Watson CJE, Jochmans I. From "Gut Feeling" to Objectivity: Machine Preservation of the Liver as a Tool to Assess Organ Viability. Current Transplantation Reports. 2018;5(1):72–81.

202. Mergental H, Laing RW, Kirkham AJ, Perera MTPR, Boteon YL, Attard J, et al. Transplantation of discarded livers following viability testing with normothermic machine perfusion. Nature Communications. 2020;11(1):2939.

203. Matton APM, De Vries Y, Burlage LC, Van Rijn R, Fujiyoshi M, De Meijer VE, et al. Biliary bicarbonate, pH, and glucose are suitable biomarkers of biliary viability during ex situ normothermic machine perfusion of human donor livers. Transplantation. 2019;103(7):1405–13.

204. Mergental H, Stephenson BTF, Laing RW, Kirkham AJ, Neil DAH, Wallace LL, et al. Development of Clinical Criteria for Functional Assessment to Predict Primary Nonfunction of High-Risk Livers Using Normothermic Machine Perfusion. Liver Transplantation. 2018;24(10):1453–69.

205. Watson CJE, Kosmoliaptsis V, Randle LV, Gimson AE, Brais R, Klinck JR, et al. Normothermic perfusion in the assessment and preservation of declined livers before transplantation: Hyperoxia and vasoplegia-important lessons from the first 12 cases. Transplantation. 2017;101(5):1084–98.

206. Ravikumar R, Jassem W, Mergental H, Heaton N, Mirza D, Perera MTPR, et al. Liver Transplantation After Ex Vivo Normothermic Machine Preservation: A Phase 1 (First-in-Man) Clinical Trial. American Journal of Transplantation. 2016;16(6):1779–87.

207. Nasralla D, Coussios CC, Mergental H, Akhtar MZ, Butler AJ, Ceresa CDL, et al. A randomized trial of normothermic preservation in liver transplantation. Nature. 2018;557(7703):50–6.

208. Ceresa C, Nasralla D, Neil D, Mergental H, Jassem W, Butler A, et al. Oral Presentations. In: Transplant International. 2017. p. 8–164.

209. Markmann JF, Abouljoud MS, Ghobrial RM, Bhati CS, Pelletier SJ, Lu AD, et al. Impact of Portable Normothermic Blood-Based Machine Perfusion on Outcomes of Liver Transplant: The OCS Liver PROTECT Randomized Clinical Trial. JAMA Surgery. 2022;157(3):189–98.

210. Ceresa CDL, Nasralla D, Watson CJE, Butler AJ, Coussios CC, Crick K, et al. Transient Cold Storage Prior to Normothermic Liver Perfusion May Facilitate Adoption of a Novel Technology. Liver Transplantation. 2019;25(10):1503–13.

211. Patrono D, De Carlis R, Gambella A, Farnesi F, Podestà A, Lauterio A, et al. Viability assessment and transplantation of fatty liver grafts using end-ischemic normothermic machine perfusion. Liver Transpl. 2023 May;29(5):508–20.

212. Patrono D, Apostu AL, Rizza G, Cussa D, Barreca A, Limoncelli S, et al. Upfront Normothermic Machine Perfusion for a Liver Graft with Severe Macrovesicular Steatosis: A Proof-of-Concept Case. Transplantology. 2023 Sep;4(3):151–60.

213. He X, Guo Z, Zhao Q, Ju W, Wang D, Wu L, et al. The first case of ischemia-free organ transplantation in humans: A proof of concept. American Journal of Transplantation. 2018 Mar 1;18(3):737–44.

214. Chen M, Chen Z, Lin X, Hong X, Ma Y, Huang C, et al. Application of ischaemia-free liver transplantation improves prognosis of patients with steatotic donor livers – a retrospective study. Transpl Int. 2021 Jul;34(7):1261–70.

215. Guo Z, Zhao Q, Jia Z, Huang C, Wang D, Ju W, et al. A randomized-controlled trial of ischemia-free liver transplantation for end-stage liver disease. Journal of Hepatology. 2023 Aug 1;79(2):394–402.

216. Jamieson RW, Zilvetti M, Roy D, Hughes D, Morovat A, Coussios CC, et al. Hepatic steatosis and normothermic perfusion-preliminary experiments in a porcine model. Transplantation. 2011;92(3):289–95.

217. Nagrath D, Xu H, Tanimura Y, Zuo R, Berthiaume F, Avila M, et al. Metabolic preconditioning of donor organs: Defatting fatty livers by normothermic perfusion ex vivo. Metabolic Engineering. 2009;11(4–5):274–83.

218. Raigani S, Carrol C, Cronin S, Pendexter C. Rosales I, Yarmush M, Uygun K YH. Defatting Steatotic Rat Livers during Ex Situ Normothermic Perfusion Improves Lactate Clearance and Bile Quality - ATC Abstracts. In: 2019 American Transplant Congres [Internet]. 2019. p. 14–7. Available from: https://atcmeetingabstracts.com/abstract/defatting-steatotic-rat-livers-during-ex-situ-normothermic-perfusion-improves-lactate-clearance-and-bile-quality/

219. Liu Q, Nassar A, Buccini L, Iuppa G, Soliman B, Pezzati D, et al. Lipid metabolism and functional assessment of discarded human livers with steatosis undergoing 24 hours of normothermic machine perfusion. Liver Transplantation. 2018;24(2):233–45.

220. Banan B, Watson R, Xu M, Lin Y, Chapman W. Development of a normothermic extracorporeal liver perfusion system toward improving viability and function of human extended criteria donor livers. Liver Transplantation. 2016;22(7):979–93.

221. Boteon YL, Attard J, Boteon APCS, Wallace L, Reynolds G, Hubscher S, et al. Manipulation of Lipid Metabolism During Normothermic Machine Perfusion: Effect of Defatting Therapies on Donor Liver Functional Recovery. Liver Transplantation. 2019;25(7):1007–22.

222. Raigani S, Markmann JF, Yeh H. Rehabilitation of Discarded Steatotic Livers Using Ex Situ Normothermic Machine Perfusion: A Future Source of Livers for Transplantation. Liver Transplantation. 2019;25(7):991–2.

223. Moore LB, Goodwin B, Jones SA, Wisely GB, Serabjit-Singh CJ, Willson TM, et al. St. John's wort induces hepatic drug metabolism through activation of the pregnane X receptor. Proceedings of the National Academy of Sciences of the United States of America. 2000;97(13):7500–2.

224. Glazer RI, Pollock CB, Rodriguez O, Martin PL, Albanese C, Li X, et al. Induction of metastatic gastric cancer by peroxisome proliferator-activated receptorδ activation. PPAR Research. 2010;

225. Ceresa CDL, Nasralla D, Pollok JM, Friend PJ. Machine perfusion of the liver: applications in transplantation and beyond. Nat Rev Gastroenterol Hepatol. 2022 Mar;19(3):199–209.

226. Sousa Da Silva RX, Bautista Borrego L, Lenggenhager D, Huwyler F, Binz J, Mancina L, et al. Defatting of Human Livers During Long-Term e x situ Normothermic Perfusion: Novel Strategy to Rescue Discarded Organs for Transplantation. Ann Surg. 2023 Nov 1;278(5):669–75.

227. Watson CJE, Kosmoliaptsis V, Pley C, Randle L, Fear C, Crick K, et al. Observations on the ex situ perfusion of livers for transplantation. American Journal of Transplantation. 2018;18(8):2005–20.

228. Sutton ME, op den Dries S, Karimian N, Weeder PD, de Boer MT, Wiersema-Buist J, et al. Criteria for Viability Assessment of Discarded Human Donor Livers during Ex Vivo Normothermic Machine Perfusion. PLoS One. 2014 Nov 4;9(11):e110642.

229. Nebert DW, Russell DW. Clinical importance of the cytochromes P450. The Lancet. 2002 Oct 12;360(9340):1155–62.

230. Stockmann M, Lock JF, Malinowski M, Seehofer D, Puhl G, Pratschke J, et al. How to define initial poor graft function after liver transplantation? A new functional definition by the LiMAx test. Transplant International. 2010;23(10):1023–32.

231. Stockmann M, Lock JF, Riecke B, Heyne K, Martus P, Fricke M, et al. Prediction of Postoperative Outcome After Hepatectomy With a New Bedside Test for Maximal Liver Function Capacity. Annals of Surgery. 2009 Jul;250(1):119.

232. Rubin TM, Heyne K, Luchterhand A, Bednarsch J, Vondran FWR, Polychronidis G, et al. Kinetic validation of the LiMAx test during 10 000 intravenous 13C-methacetin breath tests. J Breath Res. 2017 Nov;12(1):016005.

233. Lock JF, Schwabauer E, Martus P, Videv N, Pratschke J, Malinowski M, et al. Early diagnosis of primary nonfunction and indication for reoperation after liver transplantation. Liver Transplantation. 2010;16(2):172–80.

234. Schurink IJ, de Haan JE, Willemse J, Mueller M, Doukas M, Roest H, et al. A proof of concept study on real-time LiMAx CYP1A2 liver function assessment of donor grafts during normothermic machine perfusion. Sci Rep. 2021 Dec 6;11(1):23444.

235. Reichen J. MEGX test in hepatology: The long-sought ultimate quantitative liver function test? Journal of Hepatology. 1993 Jan 1;19(1):4–7.

236. Oellerich M, Armstrong VW. The MEGX test: a tool for the real-time assessment of hepatic function. Ther Drug Monit. 2001 Apr 1;23(2):81–92.

237. Andreeva M, Niedmann PD, Schütz E, Wieland E, Armstrong VW, Oellerich M. Determination of MEGX by HPLC with Fluorescence Detection. Clinical Chemistry. 1997 Jun 1;43(6):1081–3.

238. Liu Q, Nassar A, Farias K, Buccini L, Mangino MJ, Baldwin W, et al. Comparing Normothermic Machine Perfusion Preservation with Different Perfusates on Porcine Livers from Donors after Circulatory Death. American Journal of Transplantation. 2016;16(3):794–807.

239. Majlesara A, Golriz M, Hafezi M, Saffari A, Stenau E, Maier-Hein L, et al. Indocyanine green fluorescence imaging in hepatobiliary surgery. Photodiagnosis Photodyn Ther. 2017 Mar;17:208–15.

240. Levesque E, Saliba F, Benhamida S, Ichaï P, Azoulay D, Adam R, et al. Plasma disappearance rate of indocyanine green: A tool to evaluate early graft outcome after liver transplantation. Liver Transplantation. 2009;15(10):1358–64.

241. Faybik P, Hetz H. Plasma disappearance rate of indocyanine green in liver dysfunction. Transplant Proc. 2006 Apr;38(3):801–2.

242. Tang Y, Han M, Chen M, Wang X, Ji F, Zhao Q, et al. Donor Indocyanine Green Clearance Test Predicts Graft Quality and Early Graft Prognosis After Liver Transplantation. Dig Dis Sci. 2017 Nov;62(11):3212–20.

243. Dondossola D, De Falco S, Kersik A, Maggioni M, Di Girolamo L, Biancolilli O, et al. Procurement and ex-situ perfusion of isolated slaughterhouse-derived livers as a model of donors after circulatory death. ALTEX. 2019 Dec 12;

244. Ceresa CDL, Nasralla D, Jassem W. Normothermic Machine Preservation of the Liver: State of the Art. Current Transplantation Reports. 2018;5(1):104–10.

245. Ceresa CDL, Nasralla D, Coussios CC, Friend PJ. The case for normothermic machine perfusion in liver transplantation. Liver Transplantation. 2018;24(2):269–75.

246. Brockmann JG, Vaidya A, Reddy S, Friend PJ. Retrieval of abdominal organs for transplantation. Br J Surg. 2006 Feb;93(2):133–46.

247. Makowka L, Stieber AC, Sher L, Kahn D, Mieles L, Bowman J, et al. Surgical technique of orthotopic liver transplantation. Gastroenterol Clin North Am. 1988 Mar;17(1):33–51.

248. Lillie RD, Pizzolato P, Donaldson PT. Nuclear stains with soluble metachrome metal mordant dye lakes. The effect of chemical endgroup blocking reactions and the artificial introduction of acid groups into tissues. Histochemistry. 1976 Oct 7;49(1):23–35.

249. McManus JFA. Histological and Histochemical Uses of Periodic Acid. Stain Technology. 1948 Jan;23(3):99–108.

250. Schroen D, Kelly S, Singh M, Wilkinson B, Coley C BCS. Validation of an Off-the-Shelf, Diet-Induced NASH Mouse Model using Digital Whole Slide Scanning of Liver Tissue and Artificial Intelligence-Enabled, Quantitative Histopathological Analysis [Internet]. 2020. Available from: https://www.revealbio.com/post/validation-of-a-nash-mouse-model-white-paper/

251. Sosa RA, Zarrinpar A, Rossetti M, Lassman CR, Naini BV, Datta N, et al. Early cytokine signatures of ischemia/ reperfusion injury in human orthotopic liver transplantation. JCI Insight. 2016;1(20):e89679.

252. Spitzer AL, Lao OB, Dick AAS, Bakthavatsalam R, Halldorson JB, Yeh MM, et al. The biopsied donor liver: Incorporating macrosteatosis into high-risk donor assessment. Liver Transplantation. 2010;16(7):874–84.

253. McCormack L, Dutkowski P, El-Badry AM, Clavien PA. Liver transplantation using fatty livers: Always feasible? Journal of Hepatology. 2011;54(5):1055–62.

254. Adam R, Reynes M, Johann M, Morino M, Astarcioglu I, Kafetzis I, et al. The outcome of steatotic grafts in liver transplantation. In: Transplantation Proceedings. 1991. p. 1538–40.

255. Baccarani U, Isola M, Adani GL, Avellini C, Lorenzin D, Rossetto A, et al. Steatosis of the hepatic graft as a risk factor for post-transplant biliary complications. Clinical Transplantation. 2010;24(5):631–5.

256. Rinella ME, Alonso E, Rao S, Whitington P, Fryer J, Abecassis M, et al. Body mass index as as a predictor of hepatic steatosis in living liver donors. Liver Transplantation. 2001;7(5):409–14.

257. Nickkholgh A, Weitz J, Encke J, Sauer P, Mehrabi A, Büchler MW, et al. Utilization of extended donor criteria in liver transplantation: A comprehensive review of the literature. In: Nephrology Dialysis Transplantation. 2007.

258. Raptis DA, Fischer MA, Graf R, Nanz D, Weber A, Moritz W, et al. MRI: The new reference standard in quantifying hepatic steatosis? Gut. 2012;61(1):117–27.

259. Richards JA, Randle LV, Butler MChir AJ, Martin JL, Fedotovs A, Davies SE, et al. Pilot study of a noninvasive real-time optical backscatter probe in liver transplantation. Transplant International. 2021;34(4):709–20.

260. Golse N, Cosse C, Allard MA, Laurenzi A, Tedeschi M, Guglielmo N, et al. Evaluation of a micro-spectrometer for the real-time assessment of liver graft with mild-to-moderate macrosteatosis: A proof of concept study. Journal of Hepatology. 2019;70(3):423–30.

261. Lo IJ, Lefkowitch JH, Feirt N, Alkofer B, Kin C, Samstein B, et al. Utility of liver allograft biopsy obtained at procurement. Liver Transplantation. 2008;14(5):639–46.

262. Munsterman ID, van Erp M, Weijers G, Bronkhorst C, de Korte CL, Drenth JPH, et al. A Novel Automatic Digital Algorithm that Accurately Quantifies Steatosis in NAFLD on Histopathological Whole-Slide Images. Cytometry Part B - Clinical Cytometry. 2019;96(6):521–8.

263. Cesaretti M, Brustia R, Goumard C, Cauchy F, Poté N, Dondero F, et al. Use of Artificial Intelligence as an Innovative Method for Liver Graft Macrosteatosis Assessment. Liver Transplantation. 2020;26(10):1224–32.

264. Narayan R, Abadilla N, Yang L, Chuan Hsu C, Jensen C, Chen SB, et al. Quantification of Donor Liver Steatosis Using an Unsupervised Artificial Intelligence Platform. Journal of the American College of Surgeons. 2019;229(4):p e151.

265. Bedogni G, Bellentani S, Miglioli L, Masutti F, Passalacqua M, Castiglione A, et al. The fatty liver index: A simple and accurate predictor of hepatic steatosis in the general population. BMC Gastroenterology. 2006;6:1–7.

266. Lee JH, Kim D, Kim HJ, Lee CH, Yang JI, Kim W, et al. Hepatic steatosis index: A simple screening tool reflecting nonalcoholic fatty liver disease. Digestive and Liver Disease. 2010;42(7):503–8.

267. Hall AR, Green AC, Luong TV, Burroughs AK, Wyatt J, Dhillon AP. The use of guideline images to improve histological estimation of hepatic steatosis. Liver International. 2014;34(9):1414–27.

268. Marsman H, Matsushita T, Dierkhising R, Kremers W, Rosen C, Burgart L, et al. Assessment of Donor Liver Steatosis: Pathologist or Automated Software? Human Pathology. 2004;35(4):430–5.

269. Fiorini RN, Kirtz J, Periyasamy B, Evans Z, Haines JK, Cheng G, et al. Development of an unbiased method for the estimation of liver steatosis. Clinical Transplantation. 2004;18(6):700–6.

270. Lee MJ, Bagci P, Kong J, Vos MB, Sharma P, Kalb B, et al. Liver steatosis assessment: Correlations among pathology, radiology, clinical data and automated image analysis software. Pathology Research and Practice. 2013;209(6):371–9.

271. Biesterfeld S, Knapp J, Bittinger F, Götte H, Schramm M, Otto G. Frozen section diagnosis in donor liver biopsies: Observer variation of semiquantitative and quantitative steatosis assessment. Virchows Archiv. 2012;461(2):177–83.

272. Fedchuk L, Nascimbeni F, Pais R, Charlotte F, Housset C, Ratziu V. Performance and limitations of steatosis biomarkers in patients with nonalcoholic fatty liver disease. Alimentary Pharmacology and Therapeutics. 2014;40(10):1209–22.

273. Steggerda JA, Bloom MB, Noureddin M, Brennan TV, Todo T, Nissen NN, et al. Higher thresholds for the utilization of steatotic allografts in liver transplantation: Analysis from a U.S. National database. PLoS ONE. 2020;15(4).

274. Rodriguez LA, Shiboski SC, Bradshaw PT, Fernandez A, Herrington D, Ding J, et al. Predicting Non-Alcoholic Fatty Liver Disease for Adults Using Practical Clinical Measures: Evidence from the Multi-ethnic Study of Atherosclerosis. Journal of General Internal Medicine. 2021;36(9):2648–55.

275. Kyoung KH, Lee SG, Hwang S, Kim KH, Hong SK. Liver Steatosis in Brain-Dead Donors: Progression Pattern and Affecting Factors. Transplantation Proceedings. 2020;52(5):1318–24.

276. Abudhaise H, Luong TV, Watkins J, Fuller BJ, Davidson BR. Reliability and Accuracy of Clinical Assessment and Digital Image Analysis for Steatosis Evaluation in Discarded Human Livers. Transplantation Proceedings. 2019;51(6):1679–83.

277. Alvikas J, Deeb AP, Jorgensen DR, Minervini MI, Demetris AJ, Lemon K, et al. Moderately Macrosteatotic Livers Have Acceptable Long-Term Outcomes but Higher Risk of Immediate Mortality. Transplantation Proceedings. 2021;53(5):1682–9.

278. Lascaris B, de Meijer VE, Porte RJ. Normothermic liver machine perfusion as a dynamic platform for regenerative purposes: What does the future have in store for us? Journal of Hepatology. 2022;77(3):825–36.

279. Wu C, Lu C, Xu C. Short-term and long-term outcomes of liver transplantation using moderately and severely steatotic donor livers a systematic review. Medicine (United States). 2018;97(35):35(e12026).

280. Doyle MBM, Vachharajani N, Wellen JR, Anderson CD, Lowell JA, Shenoy S, et al. Short- and long-term outcomes after steatotic liver transplantation. Archives of Surgery. 2010;145(7):653–60.

281. Jackson KR, Motter JD, Haugen CE, Long JJ, King B, Philosophe B, et al. Minimizing risks of liver transplantation with steatotic donor livers by preferred recipient matching. Transplantation. 2020;104(8):1604–11.

282. Jackson KR, Bowring MG, Holscher C, Haugen CE, Long JJ, Liyanage L, et al. Outcomes after declining a steatotic donor liver for liver transplant candidates in the United States. Transplantation. 2020;104(8):1612–8.

283. Dyson JK, Anstee QM, McPherson S. Non-alcoholic fatty liver disease: a practical approach to diagnosis and staging. Frontline Gastroenterology. 2014;5(3):211–8.

284. Gambella A, Salvi M, Molinaro L, Patrono D, Cassoni P, Papotti M, et al. Improved assessment of donor liver steatosis using Banff consensus recommendations and deep learning algorithms. J Hepatol. 2023 Nov 29;S0168-8278(23)05289-3.

285. Chung IS, Kim HY, Shin YH, Ko JS, Gwak MS, Sim WS, et al. Incidence and predictors of post-reperfusion syndrome in living donor liver transplantation. Clinical Transplantation. 2012;26(4):539–43.

286. Hann A, Osei-Bordom DC, Neil DAH, Ronca V, Warner S, Perera MTPR. The Human Immune Response to Cadaveric and Living Donor Liver Allografts. Front Immunol. 2020 Jun 22;11:1227.

287. Selzner M, RüDiger HA, Sindram D, Madden J, Clavien PA. Mechanisms of ischemic injury are different in the steatotic and normal rat liver. Hepatology. 2000;32(6):1280–8.

288. Dutkowski P, Southard JH, Junginger T. [Liver metabolism during cold ischemic incubation in UW solution in the rat model]. Langenbecks Arch Chir. 1997;382(6):343–8.

289. Quintana AB, Guibert EE, Rodríguez JV. Effect of cold preservation/reperfusion on glycogen content of liver. Concise review. Ann Hepatol. 2005;4(1):25–31.

290. Cherid A, Cherid N, Chamlian V, Hardwigsen J, Nouhou H, Dodero F, et al. Evaluation of glycogen loss in human liver transplants. Histochemical zonation of glycogen loss in cold ischemia and reperfusion. Cell Mol Biol (Noisy-le-grand). 2003 Jun;49(4):509–14.

291. Rosser BG, Gores GJ. Liver cell necrosis: cellular mechanisms and clinical implications. Gastroenterology. 1995 Jan;108(1):252–75.

292. Lanir A, Jenkins RL, Caldwell C, Lee RG, Khettry U, Clouse ME. Hepatic transplantation survival: correlation with adenine nucleotide level in donor liver. Hepatology. 1988;8(3):471–5.

293. Kamiike W, Burdelski M, Steinhoff G, Ringe B, Lauchart W, Pichlmayr R. Adenine nucleotide metabolism and its relation to organ viability in human liver transplantation. Transplantation. 1988 Jan;45(1):138–43.

294. Cywes R, Greig PD, Sanabria JR, Clavien PA, Levy GA, Harvey PR, et al. Effect of intraportal glucose infusion on hepatic glycogen content and degradation, and outcome of liver transplantation. Ann Surg. 1992 Sep;216(3):235–46; discussion 246-247.

295. Yagi S, Hirata M, Miyachi Y, Uemoto S. Liver Regeneration after Hepatectomy and Partial Liver Transplantation. Int J Mol Sci. 2020 Nov 9;21(21):8414.

296. Halilbasic E, Claudel T, Trauner M. Bile acid transporters and regulatory nuclear receptors in the liver and beyond. J Hepatol. 2013 Jan;58(1):155–68.

297. Gottlieb A, Canbay A. Why Bile Acids Are So Important in Non-Alcoholic Fatty Liver Disease (NAFLD) Progression. Cells. 2019 Oct 30;8(11):1358.

298. Wei J, Qiu DK, Ma X. Bile acids and insulin resistance: implications for treating nonalcoholic fatty liver disease. Journal of Digestive Diseases. 2009;10(2):85–90.

299. Rector RS, Thyfault JP, Wei Y, Ibdah JA. Non-alcoholic fatty liver disease and the metabolic syndrome: An update. World J Gastroenterol. 2008 Jan 14;14(2):185–92.

300. Ma YL, Ke JF, Wang JW, Wang YJ, Xu MR, Li LX. Blood lactate levels are associated with an increased risk of metabolic dysfunction-associated fatty liver disease in type 2 diabetes: a real-world study. Frontiers in Endocrinology [Internet]. 2023 [cited 2024 Feb 13];14. Available from: https://www.frontiersin.org/journals/endocrinology/articles/10.3389/fendo.2023.1133991

301. Lu Q, Tian X, Wu H, Huang J, Li M, Mei Z, et al. Metabolic Changes of Hepatocytes in NAFLD. Frontiers in Physiology [Internet]. 2021 [cited 2024 Feb 13];12. Available from: https://www.frontiersin.org/journals/physiology/articles/10.3389/fphys.2021.710420

302. Wang T, Chen K, Yao W, Zheng R, He Q, Xia J, et al. Acetylation of lactate dehydrogenase B drives NAFLD progression by impairing lactate clearance. Journal of Hepatology. 2021 May 1;74(5):1038–52.

303. Fisher FM, Maratos-Flier E. Understanding the Physiology of FGF21. Annu Rev Physiol. 2016 Feb 10;78(1):223–41.

304. Farrell GC, Teoh NC, McCuskey RS. Hepatic microcirculation in fatty liver disease. Anat Rec (Hoboken). 2008 Jun;291(6):684–92.

305. Hasegawa T, Ito Y, Wijeweera J, Liu J, Malle E, Farhood A, et al. Reduced inflammatory response and increased microcirculatory disturbances during hepatic ischemia-reperfusion injury in steatotic livers of ob/ob mice. Am J Physiol Gastrointest Liver Physiol. 2007 May;292(5):G1385-1395.

306. Cortez-Pinto H, Chatham J, Chacko VP, Arnold C, Rashid A, Diehl AM. Alterations in liver ATP homeostasis in human nonalcoholic steatohepatitis: a pilot study. JAMA. 1999 Nov 3;282(17):1659–64.

307. Nair S, P Chacko V, Arnold C, Diehl AM. Hepatic ATP reserve and efficiency of replenishing: comparison between obese and nonobese normal individuals. Am J Gastroenterol. 2003 Feb;98(2):466–70.

308. Veteläinen R, Bennink RJ, van Vliet AK, van Gulik TM. Mild steatosis impairs functional recovery after liver resection in an experimental model. Br J Surg. 2007 Aug;94(8):1002–8.

309. Selzner M, Selzner N, Jochum W, Graf R, Clavien PA. Increased ischemic injury in old mouse liver: an ATP-dependent mechanism. Liver Transpl. 2007 Mar;13(3):382–90.

310. Reiniers MJ, van Golen RF, van Gulik TM, Heger M. Reactive oxygen and nitrogen species in steatotic hepatocytes: a molecular perspective on the pathophysiology of ischemia-reperfusion injury in the fatty liver. Antioxid Redox Signal. 2014 Sep 1;21(7):1119–42.

311. Bessone F, Razori MV, Roma MG. Molecular pathways of nonalcoholic fatty liver disease development and progression. Cell Mol Life Sci. 2019 Jan;76(1):99–128.

312. Anderson NL, Anderson NG. The human plasma proteome: history, character, and diagnostic prospects. Mol Cell Proteomics. 2002 Nov;1(11):845–67.

313. López-López V, Pérez-Sánz F, de Torre-Minguela C, Marco-Abenza J, Robles-Campos R, Sánchez-Bueno F, et al. Proteomics in Liver Transplantation: A Systematic Review. Front Immunol. 2021;12:672829.

314. Traum AZ, Schachter AD. Transplantation proteomics. Pediatr Transplant. 2005 Dec;9(6):700–11.

315. Cho WCS. Proteomics technologies and challenges. Genomics Proteomics Bioinformatics. 2007 May;5(2):77–85.

316. Huang S, Ju W, Zhu Z, Han M, Sun C, Tang Y, et al. Comprehensive and combined omics analysis reveals factors of ischemia-reperfusion injury in liver transplantation. Epigenomics. 2019 Apr;11(5):527–42.

317. Vascotto C, Cesaratto L, D'Ambrosio C, Scaloni A, Avellini C, Paron I, et al. Proteomic analysis of liver tissues subjected to early ischemia/reperfusion injury during human orthotopic liver transplantation. Proteomics. 2006 Jun;6(11):3455–65.

318. Laing RW, Stubblefield S, Wallace L, Roobrouck VD, Bhogal RH, Schlegel A, et al. The Delivery of Multipotent Adult Progenitor Cells to Extended Criteria Human Donor Livers Using Normothermic Machine Perfusion. Front Immunol. 2020;11:1226.

319. Pérez-Pérez R, Lobo-Jarne T, Milenkovic D, Mourier A, Bratic A, García-Bartolomé A, et al. COX7A2L Is a Mitochondrial Complex III Binding Protein that Stabilizes the III2+IV Supercomplex without Affecting Respirasome Formation. Cell Rep. 2016 Aug 30;16(9):2387–98.

320. Parmar G, Fong-McMaster C, Pileggi CA, Patten DA, Cuillerier A, Myers S, et al. Accessory subunit NDUFB4 participates in mitochondrial complex I supercomplex formation. J Biol Chem. 2024 Jan 9;300(2):105626.

321. Shi S, Wang L, van der Laan LJW, Pan Q, Verstegen MMA. Mitochondrial Dysfunction and Oxidative Stress in Liver Transplantation and Underlying Diseases: New Insights and Therapeutics. Transplantation. 2021 Nov;105(11):2362.

322. Raigani S, Karimian N, Huang V, Zhang AM, Beijert I, Geerts S, et al. Metabolic and lipidomic profiling of steatotic human livers during ex situ normothermic machine perfusion guides resuscitation strategies. PLoS One. 2020 Jan 24;15(1):e0228011.

323. ATP5PB ATP synthase peripheral stalk-membrane subunit b [Homo sapiens (human)] - Gene - NCBI [Internet]. [cited 2024 Aug 29]. Available from: https://www.ncbi.nlm.nih.gov/gene/515

324. Elkholi R, Abraham-Enachescu I, Trotta AP, Rubio-Patiño C, Mohammed JN, Luna-Vargas MPA, et al. MDM2 Integrates Cellular Respiration and Apoptotic Signaling through NDUFS1 and the Mitochondrial Network. Molecular Cell. 2019 May 2;74(3):452-465.e7.

325. Clarke G, Mergental H, Hann A, Perera MTPR, Afford SC, Mirza DF. How Machine Perfusion Ameliorates Hepatic Ischaemia Reperfusion Injury. Int J Mol Sci. 2021 Jul 14;22(14):7523.

326. Eshmuminov D, Becker D, Bautista Borrego L, Hefti M, Schuler MJ, Hagedorn C, et al. An integrated perfusion machine preserves injured human livers for 1 week. Nat Biotechnol. 2020 Feb;38(2):189–98.

327. Sodhi K, Douglas WG, Peterson SJ, Dial L, Khawaja IT, Shapiro J, et al. Abstract 397: HMOX1 Ameliorates Fatty Liver and Metabolic Syndrome by Reduction of Hepatic Heme and PGC1a. Hypertension. 2013 Sep;62(suppl_1):A397–A397.

328. Lee DH, Park JS, Lee YS, Han J, Lee DK, Kwon SW, et al. SQSTM1/p62 activates NFE2L2/NRF2 via ULK1-mediated autophagic KEAP1 degradation and protects mouse liver from lipotoxicity. Autophagy. 2020 Nov;16(11):1949–73.

329. Watson CJE, MacDonald S, Bridgeman C, Brais R, Upponi SS, Foukaneli T, et al. D-dimer Release From Livers During Ex Situ Normothermic Perfusion and After In Situ Normothermic Regional Perfusion: Evidence for Occult Fibrin Burden Associated With Adverse Transplant Outcomes and Cholangiopathy. Transplantation. 2023 Jun;107(6):1311–21.

330. Ason B, Castro-Perez J, Tep S, Stefanni A, Tadin-Strapps M, Roddy T, et al. ApoB siRNA-induced Liver Steatosis is Resistant to Clearance by the Loss of Fatty Acid Transport Protein 5 (Fatp5). Lipids. 2011;46(11):991–1003.

331. Hsu CC, Kanter JE, Kothari V, Bornfeldt KE. Quartet of APOCs and the Different Roles They Play in Diabetes. Arteriosclerosis, Thrombosis, and Vascular Biology. 2023 Jul;43(7):1124–33.

332. Allan CM, Taylor JM. Expression of a novel human apolipoprotein (apoC-IV) causes hypertriglyceridemia in transgenic mice. Journal of Lipid Research. 1996 Jan 1;37(7):1510–8.

333. Núñez K, Thevenot P, Alfadhli A, Cohen A. Complement Activation in Liver Transplantation: Role of Donor Macrosteatosis and Implications in Delayed Graft Function. Int J Mol Sci. 2018 Jun 13;19(6):1750.

334. Rashan EH, Bartlett AK, Khana DB, Zhang J, Jain R, Smith AJ, et al. ACAD10 and ACAD11 enable mammalian 4-hydroxy acid lipid catabolism. bioRxiv. 2024 Jan 9;2024.01.09.574893.

335. PubChem. ACSF2 - acyl-CoA synthetase family member 2 (human) [Internet]. [cited 2024 Aug 29]. Available from: https://pubchem.ncbi.nlm.nih.gov/gene/ACSF2/human

336. Zaouali MA, Boncompagni E, Reiter RJ, Bejaoui M, Freitas I, Pantazi E, et al. AMPK involvement in endoplasmic reticulum stress and autophagy modulation after fatty liver graft preservation: a role for melatonin and trimetazidine cocktail. J Pineal Res. 2013 Aug;55(1):65–78.

337. Goetzman E, Gong Z, Zhang B, Muzumdar R. Complex II Biology in Aging, Health, and Disease. Antioxidants (Basel). 2023 Jul 24;12(7):1477.

338. Clatworthy MR, Watson CJE. Understanding the Immunology of Normothermic Machine Perfusion. Transpl Int. 2023;36:11670.

339. Hanvesakul R, Spencer N, Cook M, Gunson B, Hathaway M, Brown R, et al. Donor HLA-C genotype has a profound impact on the clinical outcome following liver transplantation. Am J Transplant. 2008 Sep;8(9):1931–41.

340. Schrader M, Fahimi HD. Peroxisomes and oxidative stress. Biochimica et Biophysica Acta (BBA) - Molecular Cell Research. 2006 Dec 1;1763(12):1755–66.

341. Chen X, Tian M, Sun R, Zhang M, Zhou L, Jin L, et al. SIRT5 inhibits peroxisomal ACOX1 to prevent oxidative damage and is downregulated in liver cancer. EMBO Rep. 2018 May;19(5):e45124.

342. Luo Q, Das A, Oldoni F, Wu P, Wang J, Luo F, et al. Role of ACSL5 in fatty acid metabolism. Heliyon. 2023 Feb 1;9(2):e13316.

343. Shaik IH, Mehvar R. Effects of normothermic hepatic ischemia-reperfusion injury on the in vivo, isolated perfused liver, and microsomal disposition of chlorzoxazone, a cytochrome P450 2E1 probe, in rats. J Pharm Sci. 2011 Dec;100(12):5281–92.

344. ATP5F1A ATP synthase F1 subunit alpha [Homo sapiens (human)] - Gene - NCBI [Internet]. [cited 2024 Aug 30]. Available from: https://www.ncbi.nlm.nih.gov/gene?Db=gene&Cmd=DetailsSearch&Term=498

345. Rak M, Rustin P. Supernumerary subunits NDUFA3, NDUFA5 and NDUFA12 are required for the formation of the extramembrane arm of human mitochondrial complex I. FEBS Letters. 2014 May 2;588(9):1832–8.

346. Eaton S, Bursby T, Middleton B, Pourfarzam M, Mills K, Johnson AW, et al. The mitochondrial trifunctional protein: centre of a β-oxidation metabolon? Biochemical Society Transactions. 2000 Feb 1;28(2):177–82.

347. Methylmalonyl-CoA Mutase - an overview | ScienceDirect Topics [Internet]. [cited 2024 Aug 30]. Available from: https://www.sciencedirect.com/topics/agricultural-and-biological-sciences/methylmalonyl-coa-mutase

348. Gagné J, Manoli I, Harrington E, Smyth S, Hattenbach JD, Sloan JL, et al. 353. 1-13C-Propionate Oxidation as a Measure of Methylmalonyl-CoA Mutase (MUT) Activity in Methylmalonic Acidemia. Molecular Therapy. 2016 May 1;24:S141.

349. Buis CI, van der Steege G, Visser DS, Nolte IM, Hepkema BG, Nijsten M, et al. Heme oxygenase-1 genotype of the donor is associated with graft survival after liver transplantation. Am J Transplant. 2008 Feb;8(2):377–85.

350. Hartwig JH, Thelen M, Rosen A, Janmey PA, Nairn AC, Aderem A. MARCKS is an actin filament crosslinking protein regulated by protein kinase C and calcium-calmodulin. Nature. 1992 Apr 16;356(6370):618–22.

351. Rack JGM, Perina D, Ahel I. Macrodomains: Structure, Function, Evolution, and Catalytic Activities. Annual Review of Biochemistry. 2016 Jun 2;85(Volume 85, 2016):431–54.

352. Stewart M, Kent HM, McCoy AJ. Structural basis for molecular recognition between nuclear transport factor 2 (NTF2) and the GDP-bound form of the ras-family GTPase ran1. Journal of Molecular Biology. 1998 Apr 6;277(3):635–46.

353. Zhang W, Zhuang N, Liu X, He L, He Y, Mahinthichaichan P, et al. The metabolic regulator Lamtor5 suppresses inflammatory signaling via regulating mTOR-mediated TLR4 degradation. Cell Mol Immunol. 2020 Oct;17(10):1063–76.

354. Sun S, He H, Ma Y, Xu J, Chen G, Sun Y, et al. Inactivation of ribosomal protein S27-like impairs DNA interstrand cross-link repair by destabilization of FANCD2 and FANCI. Cell Death Dis. 2020 Oct 13;11(10):1–10.

355. Pollutri D, Penzo M. Ribosomal Protein L10: From Function to Dysfunction. Cells. 2020 Nov 19;9(11):2503.

356. RPL15 ribosomal protein L15 [Homo sapiens (human)] - Gene - NCBI [Internet]. [cited 2024 Aug 30]. Available from: https://www.ncbi.nlm.nih.gov/gene/6138

357. Passmore LA, Schmeing TM, Maag D, Applefield DJ, Acker MG, Algire MA, et al. The Eukaryotic Translation Initiation Factors eIF1 and eIF1A Induce an Open Conformation of the 40S Ribosome. Molecular Cell. 2007 Apr 13;26(1):41–50.

358. Portolés I, Ribera J, Fernandez-Galán E, Lecue E, Casals G, Melgar-Lesmes P, et al. Identification of Dhx15 as a Major Regulator of Liver Development, Regeneration, and Tumor Growth in Zebrafish and Mice. Int J Mol Sci. 2024 Mar 27;25(7):3716.

359. López-Cánovas JL, del Rio-Moreno M, García-Fernandez H, Jiménez-Vacas JM, Moreno-Montilla MT, Sánchez-Frias ME, et al. Splicing factor SF3B1 is overexpressed and implicated in the aggressiveness and survival of hepatocellular carcinoma. Cancer Letters. 2021 Jan 1;496:72–83.

360. Li RZ, Hou J, Wei Y, Luo X, Ye Y, Zhang Y. hnRNPDL extensively regulates transcription and alternative splicing. Gene. 2019 Mar 1;687:125–34.

361. Benson CE, Southgate L. The DOCK protein family in vascular development and disease. Angiogenesis. 2021;24(3):417–33.

362. Birge RB, Kalodimos C, Inagaki F, Tanaka S. Crk and CrkL adaptor proteins: networks for physiological and pathological signaling. Cell Communication and Signaling. 2009 May 10;7(1):13.

363. Zhou X, Zheng Y. Cell Type-specific Signaling Function of RhoA GTPase: Lessons from Mouse Gene Targeting. J Biol Chem. 2013 Dec 20;288(51):36179–88.

364. PubChem. ENO3 - enolase 3 (human) [Internet]. [cited 2024 Aug 30]. Available from: https://pubchem.ncbi.nlm.nih.gov/gene/ENO3/human

365. PYGL glycogen phosphorylase L [Homo sapiens (human)] - Gene - NCBI [Internet]. [cited 2024 Aug 30]. Available from: https://www.ncbi.nlm.nih.gov/gene/5836

366. Beckley SJ, Hunter MC, Kituyi SN, Wingate I, Chakraborty A, Schwarz K, et al. STIP1/HOP Regulates the Actin Cytoskeleton through Interactions with Actin and Changes in Actin-Binding Proteins Cofilin and Profilin. International Journal of Molecular Sciences. 2020 Jan;21(9):3152.

367. Bhattacharya K, Weidenauer L, Luengo TM, Pieters EC, Echeverría PC, Bernasconi L, et al. The Hsp70-Hsp90 co-chaperone Hop/Stip1 shifts the proteostatic balance from folding towards degradation. Nat Commun. 2020 Nov 25;11(1):5975.

368. Voll AM, Meyners C, Taubert MC, Bajaj T, Heymann T, Merz S, et al. Macrocyclic FKBP51 Ligands Define a Transient Binding Mode with Enhanced Selectivity. Angew Chem Int Ed Engl. 2021 Jun 7;60(24):13257–63.

369. Jogl G, Hsiao YS, Tong L. Structure and Function of Carnitine Acyltransferases. Annals of the New York Academy of Sciences. 2004;1033(1):17–29.

370. Lee N, Llano M, Carretero M, Ishitani A, Navarro F, López-Botet M, et al. HLA-E is a major ligand for the natural killer inhibitory receptor CD94/NKG2A. Proc Natl Acad Sci U S A. 1998 Apr 28;95(9):5199–204.

371. Calil IL, Tustumi F, de Sousa JHB, Tomazini BM, Cruz RJ, Saliba GN, et al. What is the role of heat shock protein in abdominal organ transplantation? Einstein (Sao Paulo). 2022 Mar 4;20:eRB6181.

372. PubChem. BAAT - bile acid-CoA:amino acid N-acyltransferase (human) [Internet]. [cited 2024 Aug 30]. Available from: https://pubchem.ncbi.nlm.nih.gov/gene/BAAT/human

373. Wang H, Nie Y, Sun Z, He Y, Yang J. Serum amyloid P component: Structure, biological activity, and application in diagnosis and treatment of immune-associated diseases. Molecular Immunology. 2024 Aug 1;172:1–8.

374. PubChem. WFS1 - wolframin ER transmembrane glycoprotein (human) [Internet]. [cited 2024 Aug 30]. Available from: https://pubchem.ncbi.nlm.nih.gov/gene/WFS1/human

375. Ivask M, Volke V, Raasmaja A, Kõks S. High-fat diet associated sensitization to metabolic stress in *Wfs1* heterozygous mice. Molecular Genetics and Metabolism. 2021 Sep 1;134(1):203–11.

376. Gladyck S, Aras S, Hüttemann M, Grossman LI. Regulation of COX Assembly and Function by Twin CX9C Proteins—Implications for Human Disease. Cells. 2021 Jan 20;10(2):197.

377. RPS23 ribosomal protein S23 [Homo sapiens (human)] - Gene - NCBI [Internet]. [cited 2024 Aug 30]. Available from: https://www.ncbi.nlm.nih.gov/gene/6228

378. Li WY, Wang LW, Dong J, Wang Y. Evaluation of G3BP1 in the prognosis of acute and acute-on-chronic liver failure after the treatment of artificial liver support system. World Journal of Hepatology. 2024 Feb 27;16(2):251–63.

379. Guo N, Chen Y, Zhang Y, Deng Y, Zeng F, Li X. Potential Role of APEX1 During Ferroptosis. Front Oncol [Internet]. 2022 Mar 3 [cited 2024 Aug 30];12. Available from: https://www.frontiersin.org/journals/oncology/articles/10.3389/fonc.2022.798304/full

380. Muurling M, van den Hoek AM, Mensink RP, Pijl H, Romijn JA, Havekes LM, et al. Overexpression of APOC1 in obob mice leads to hepatic steatosis and severe hepatic insulin resistance. J Lipid Res. 2004 Jan;45(1):9–16.

381. Kang HW, Niepel MW, Han S, Kawano Y, Cohen DE. Thioesterase superfamily member 2/acyl-CoA thioesterase 13 (Them2/Acot13) regulates hepatic lipid and glucose metabolism. FASEB J. 2012 May;26(5):2209–21.

382. NDUFB6 NADH:ubiquinone oxidoreductase subunit B6 [Homo sapiens (human)] - Gene - NCBI [Internet]. [cited 2024 Aug 30]. Available from: https://www.ncbi.nlm.nih.gov/gene/4712

383. Morris SM, Chauhan A. The role of platelet mediated thromboinflammation in acute liver injury. Front Immunol [Internet]. 2022 Oct 27 [cited 2024 Aug 30];13. Available from: https://www.frontiersin.org/journals/immunology/articles/10.3389/fimmu.2022.1037645/full

384. Li W, Chi D, Ju S, Zhao X, Li X, Zhao J, et al. Platelet factor 4 promotes deep venous thrombosis by regulating the formation of neutrophil extracellular traps. Thrombosis Research. 2024 May 1;237:52–63.

385. Alimova-Kost MV, Imreh S, Buchman VL, Ninkina NN. Assignment1 of phosphotriesterase-related gene (PTER) to human chromosome band 10p12 by in situ hybridization. Cytogenet Cell Genet. 1998;83(1–2):16–7.

386. Divakaran K, Hines RN, McCarver DG. Human Hepatic UGT2B15 Developmental Expression. Toxicol Sci. 2014 Sep 1;141(1):292–9.

387. ATP1A1 ATPase Na+/K+ transporting subunit alpha 1 [Homo sapiens (human)] - Gene - NCBI [Internet]. [cited 2024 Aug 31]. Available from: https://www.ncbi.nlm.nih.gov/gene/476

388. Ceresa C, Nasralla D, Cornfield T, Clark A, Hook P, Young L, et al. Novel approaches in optimising steatotic livers for transplantation. Transplantation. 2019;103(8):90.

389. Bambauer R, Bambauer C, Lehmann B, Latza R, Schiel R. LDL-apheresis: Technical and clinical aspects. The Scientific World Journal. 2012;2012:314283.

390. Stefanutti C, Vivenzio A, Lucani G, Di Giacomo S, Lucani E. Effect of L-carnitine on plasma lipoprotein fatty acids pattern in patients with primary hyperlipoproteinemia. Clinica Terapeutica. 1998;149(2):115–9.

391. Fernandez C, Proto C. [L-carnitine in the treatment of chronic myocardial ischemia. An analysis of 3 multicenter studies and a bibliographic review]. Clinica terapeutica. 1992;140(4):353–77.

392. Koşan C, Sever L, Arisoy N, Çalişşkan S, Kasapçopur Ö. Carnitine supplementation improves apolipoprotein B levels in pediatric peritoneal dialysis patients. Pediatric Nephrology. 2003;18(11):1184–8.

393. Harper P, Elwin CE, Cederblad G. Pharmacokinetics of bolus intravenous and oral doses of L-carnitine in healthy subjects. European Journal of Clinical Pharmacology. 1988;35(1):69–75.

394. Hermansen K. Forskolin, an activator of adenylate cyclase, stimulates pancreatic insulin, glucagon, and somatostatin release in the dog: Studies in vitro. Endocrinology. 1985;116(6):2251–8.

395. Alberti KGMM, Eckel RH, Grundy SM, Zimmet PZ, Cleeman JI, Donato KA, et al. Harmonizing the metabolic syndrome: A joint interim statement of the international diabetes federation task force on epidemiology and prevention; National heart, lung, and blood institute; American heart association; World heart federation; International. Circulation. 2009;120(16):1640–5.

396. NICE. Ex-situ machine perfusion for extracorporeal preservation of livers for transplantation [Internet]. 2021. p. 1–5. Available from: www.nice.org.uk/guidance/ipg636

397. Baumann G, Felix S, Sattelberger U, Klein G. Cardiovascular effects of forskolin (HL 362) in patients with idiopathic congestive cardiomyopathy - A comparative study with dobutamine and sodium nitroprusside. Journal of Cardiovascular Pharmacology. 1990;16(1):93–100.

398. Bersudsky Y, Kotler M, Shifrin M, Belmaker RH. A preliminary study of possible psychoactive effects of intravenous forskolin in depressed and schizophrenic patients. Journal of Neural Transmission. 1996;103(12):1463–7.

399. Dholakia S, De Vlaminck I, Khush KK. Adding insult on injury: Immunogenic role for donor-derived cell-free DNA? Transplantation. 2020;104(11):2266–71.

400. Glanemann M, Langrehr JM, Stange BJ, Neumann U, Settmacher U, Steinmüller T, et al. Clinical implications of hepatic preservation injury after adult liver transplantation. American Journal of Transplantation. 2003;3(8):1003–9.

401. Dindo D, Demartines N, Clavien PA. Classification of surgical complications: A new proposal with evaluation in a cohort of 6336 patients and results of a survey. Annals of Surgery. 2004;240(2):205–13.

402. Goldfinger MH, Ridgway GR, Ferreira C, Langford CR, Cheng L, Kazimianec A, et al. Quantitative MRCP Imaging: Accuracy, Repeatability, Reproducibility, and Cohort-Derived Normative Ranges. Journal of Magnetic Resonance Imaging. 2020;52(3):807–20.

403. Wilman HR, Kelly M, Garratt S, Matthews PM, Milanesi M, Herlihy A, et al. Characterisation of liver fat in the UK Biobank cohort. PLoS ONE. 2017;12(2):1–14.

404. Qu Y, Li M, Hamilton G, Zhang YN, Song B. Diagnostic accuracy of hepatic proton density fat fraction measured by magnetic resonance imaging for the evaluation of liver steatosis with histology as reference standard: a meta-analysis. European Radiology. 2019;29(10):5180–9.

405. Brunt EM, Kleiner DE, Wilson LA, Belt P, Neuschwander-Tetri BA. Nonalcoholic fatty liver disease (NAFLD) activity score and the histopathologic diagnosis in NAFLD: Distinct clinicopathologic meanings. Hepatology. 2011;53(3):810–20.

406. Tucker B, Li H, Long X, Rye KA, Ong KL. Fibroblast growth factor 21 in non-alcoholic fatty liver disease. Metabolism: Clinical and Experimental. 2019;101:153994.

407. Wallace L, Attard J, Boteon Y, Laing R, Yu J, Perera T, et al. ILTS Annual Congress 2019, Toronto, Cananda, May 15-18, 2019. Transplantation. 2019;103(8):1–491.

408. Verhelst X, Geerts A, Jochmans I, Vanderschaeghe D, Paradissis A, Vanlander A, et al. Glycome Patterns of Perfusate in Livers Before Transplantation Associate With Primary Nonfunction. Gastroenterology. 2018;154(5):1361–8.

409. Moosburner S, Gassner JMGV, Nösser M, Pohl J, Wyrwal D, Claussen F, et al. Prevalence of steatosis hepatis in the eurotransplant region: Impact on graft acceptance rates. HPB Surgery. 2018;2018.

410. ISRCTN - ISRCTN14957538: Normothermic (normal body temperature) machine perfusion to remove fat from donor livers prior to transplantation [Internet]. [cited 2024 Mar 1]. Available from: https://www.isrctn.com/ISRCTN14957538

411. Akhtar MZ, Sutherland AI, Huang H, Ploeg RJ, Pugh CW. The role of hypoxia-inducible factors in organ donation and transplantation: the current perspective and future opportunities. Am J Transplant. 2014 Jul;14(7):1481–7.

412. Xue H, Chen D, Zhong YK, Zhou ZD, Fang SX, Li MY, et al. Deferoxamine ameliorates hepatosteatosis via several mechanisms in ob/ob mice. Annals of the New York Academy of Sciences. 2016;1375(1):52–65.

413. Xie C, Yagai T, Luo Y, Liang X, Chen T, Wang Q, et al. Activation of intestinal hypoxia-inducible factor 2α during obesity contributes to hepatic steatosis. Nature Medicine. 2017;23(11):1298–308.

414. Courtney KD, Infante JR, Lam ET, Figlin RA, Rini BI, Brugarolas J, et al. Phase I dose-escalation trial of PT2385, a first-in-class hypoxia-inducible factor-2a antagonist in patients with previously treated advanced clear cell renal cell carcinoma. Journal of Clinical Oncology. 2018;36(9):867–74.

415. Dutkowski P, De Rougemont O, Clavien PA. Machine perfusion for ‘marginal’ liver grafts. American Journal of Transplantation. 2008;8(5):917–24.

416. Sorond FA, Tan CO, LaRose S, Monk AD, Fichorova R, Ryan S, et al. Deferoxamine, Cerebrovascular Hemodynamics, and Vascular Aging: Potential Role for Hypoxia-Inducible Transcription Factor-1-Regulated Pathways. Stroke. 2015 Sep;46(9):2576–83.

417. Ren X, Dorrington KL, Maxwell PH, Robbins PA. Effects of desferrioxamine on serum erythropoietin and ventilatory sensitivity to hypoxia in humans. J Appl Physiol (1985). 2000 Aug;89(2):680–6.

418. RCC4/VHL [Internet]. [cited 2024 Jun 21]. Available from: https://www.culturecollections.org.uk/nop/product/rcc4vhl

419. RCC4 plus vector alone [Internet]. [cited 2024 Jun 21]. Available from: https://www.culturecollections.org.uk/nop/product/rcc4-plus-vector-alone

420. Leber B, Weber J, Rohrhofer L, Aigelsreiter A, Niedrist T, Stiegler P, et al. Real-Time Assessment of Liver Function During Sub-Normothermic Machine Perfusion by a Non-Invasive 13C Based Test [Internet]. 2022 [cited 2024 Jun 22]. Available from: https://www.researchsquare.com/article/rs-1450501/v1

421. Fukai M, Sakamoto S, Shibata K, Ishikawa T, Kawamura N, Fujiyoshi M, et al. Important Constituents of Heavy Water-containing Solution for Cold Storage and Subsequent Reperfusion on an Isolated Perfused Rat Liver. Transplantation Proceedings. 2024 Jan 1;56(1):223–7.

422. Haase VH. Regulation of erythropoiesis by hypoxia-inducible factors. Blood Rev. 2013 Jan;27(1):41–53.

423. Rankin EB, Biju MP, Liu Q, Unger TL, Rha J, Johnson RS, et al. Hypoxia-inducible factor–2 (HIF-2) regulates hepatic erythropoietin in vivo. J Clin Invest. 2007 Apr 2;117(4):1068–77.

424. Semenza GL. Regulation of Oxygen Homeostasis by Hypoxia-Inducible Factor 1. Physiology. 2009 Apr;24(2):97–106.

425. Nazzal M, Madsen EC, Armstrong A, van Nispen J, Murali V, Song E, et al. Novel NMP split liver model recapitulates human IRI and demonstrates ferroptosis modulators as a new therapeutic strategy. Pediatric Transplantation. 2022;26(2):e14164.

426. Dodero F, Benkoel L, Allasia C, Hardwigsen J, Campan P, Botta-Fridlund D, et al. Quantitative analysis of glycogen content in hepatocytes of human liver allograft after ischemia and reperfusion. Cell Mol Biol (Noisy-le-grand). 2000 Nov;46(7):1157–61.

427. Sümpelmann R, Schürholz T, Thorns E, Hausdörfer J. Acid-base, electrolyte and metabolite concentrations in packed red blood cells for major transfusion in infants. Paediatr Anaesth. 2001 Mar;11(2):169–73.

428. Taylor CT, Scholz CC. The effect of HIF on metabolism and immunity. Nat Rev Nephrol. 2022 Sep;18(9):573–87.

429. Yuan G, Al-Shali KZ, Hegele RA. Hypertriglyceridemia: its etiology, effects and treatment. CMAJ. 2007 Apr 10;176(8):1113–20.

430. Silvestre JP da S, Coelho LM da C, Póvoa PMSR. Impact of fulminant hepatic failure in C-reactive protein? J Crit Care. 2010 Dec;25(4):657.e7-12.

431. Dar WA, Sullivan E, Bynon JS, Eltzschig H, Ju C. Ischaemia reperfusion injury in liver transplantation: Cellular and molecular mechanisms. Liver International. 2019 May;39(5):788–801.

432. Abu-Amara M, Yang SY, Tapuria N, Fuller B, Davidson B, Seifalian A. Liver ischemia/reperfusion injury: processes in inflammatory networks--a review. Liver Transpl. 2010 Sep;16(9):1016–32.

433. Allam R, Darisipudi MN, Tschopp J, Anders HJ. Histones trigger sterile inflammation by activating the NLRP3 inflammasome. Eur J Immunol. 2013 Dec;43(12):3336–42.

434. Liu K, Wang FS, Xu R. Neutrophils in liver diseases: pathogenesis and therapeutic targets. Cell Mol Immunol. 2021 Jan;18(1):38–44.

435. Li P, He K, Li J, Liu Z, Gong J. The role of Kupffer cells in hepatic diseases. Molecular Immunology. 2017 May 1;85:222–9.

436. Schofield J, Abrams ST, Jenkins R, Lane S, Wang G, Toh CH. Microclots, as defined by amyloid-fibrinogen aggregates, predict risks of disseminated intravascular coagulation and mortality. Blood Adv. 2024 May 28;8(10):2499–508.

437. Wen Z, Lei Z, Yao L, Jiang P, Gu T, Ren F, et al. Circulating histones are major mediators of systemic inflammation and cellular injury in patients with acute liver failure. Cell Death Dis. 2016 Sep;7(9):e2391–e2391.

438. Li X, Gou C, Pang Y, Wang Y, Liu Y, Wen T. Extracellular histones are clinically associated with primary graft dysfunction in human liver transplantation. RSC Adv. 9(18):10264–71.

439. Cavalier E, Guiot J, Lechner K, Dutsch A, Eccleston M, Herzog M, et al. Circulating Nucleosomes as Potential Markers to Monitor COVID-19 Disease Progression. Front Mol Biosci. 2021 Mar 18;8:600881.

440. Scheuermann U, Zhu M, Song M, Yerxa J, Gao Q, Davis RP, et al. Damage-Associated Molecular Patterns Induce Inflammatory Injury During Machine Preservation of the Liver: Potential Targets to Enhance a Promising Technology. Liver Transpl. 2019 Apr;25(4):610–26.

441. Lee ACH, Edobor A, Lysandrou M, Mirle V, Sadek A, Johnston L, et al. The Effect of Normothermic Machine Perfusion on the Immune Profile of Donor Liver. Front Immunol. 2022;13:788935.

442. Hautz T, Salcher S, Fodor M, Sturm G, Ebner S, Mair A, et al. Immune cell dynamics deconvoluted by single-cell RNA sequencing in normothermic machine perfusion of the liver. Nat Commun. 2023 Apr 21;14(1):2285.

443. Cox DRA, Lee E, Wong BKL, McClure T, Zhang F, Goh SK, et al. Graft-derived cfDNA Monitoring in Plasma and Bile During Normothermic Machine Perfusion in Liver Transplantation Is Feasible and a Potential Tool for Assessing Graft Viability. Transplantation. 2024 Apr 1;108(4):958–62.

444. Scaffidi P, Misteli T, Bianchi ME. Release of chromatin protein HMGB1 by necrotic cells triggers inflammation. Nature. 2002 Jul;418(6894):191–5.

445. Beetz O, Cammann S, Weigle CA, Sieg L, Eismann H, Johanning K, et al. Interleukin-18 and High-Mobility-Group-Protein B1 are Early and Sensitive Indicators for Cell Damage During Normothermic Machine Perfusion after Prolonged Cold Ischemic Storage of Porcine Liver Grafts. Transpl Int. 2022;35:10712.

446. Ilmakunnas M, Tukiainen EM, Rouhiainen A, Rauvala H, Arola J, Nordin A, et al. High mobility group box 1 protein as a marker of hepatocellular injury in human liver transplantation. Liver Transpl. 2008 Oct;14(10):1517–25.

447. Watanabe T, Kubota S, Nagaya M, Ozaki S, Nagafuchi H, Akashi K, et al. The role of HMGB-1 on the development of necrosis during hepatic ischemia and hepatic ischemia/reperfusion injury in mice. J Surg Res. 2005 Mar;124(1):59–66.

448. Deng M, Scott MJ, Fan J, Billiar TR. Location is the key to function: HMGB1 in sepsis and trauma-induced inflammation. J Leukoc Biol. 2019 Jul;106(1):161–9.

449. Zhao G, Fu C, Wang L, Zhu L, Yan Y, Xiang Y, et al. Down-regulation of nuclear HMGB1 reduces ischemia-induced HMGB1 translocation and release and protects against liver ischemia-reperfusion injury. Sci Rep. 2017 Apr 6;7:46272.

450. Tian J, Avalos AM, Mao SY, Chen B, Senthil K, Wu H, et al. Toll-like receptor 9-dependent activation by DNA-containing immune complexes is mediated by HMGB1 and RAGE. Nat Immunol. 2007 May;8(5):487–96.

451. Urbonaviciute V, Fürnrohr BG, Meister S, Munoz L, Heyder P, De Marchis F, et al. Induction of inflammatory and immune responses by HMGB1-nucleosome complexes: implications for the pathogenesis of SLE. J Exp Med. 2008 Dec 22;205(13):3007–18.

452. Lin W, Chen H, Chen X, Guo C. The Roles of Neutrophil-Derived Myeloperoxidase (MPO) in Diseases: The New Progress. Antioxidants. 2024 Jan;13(1):132.

453. Yazdani HO, Chen HW, Tohme S, Tai S, van der Windt DJ, Loughran P, et al. IL-33 exacerbates liver sterile inflammation by amplifying neutrophil extracellular trap formation. J Hepatol. 2017 Sep 21;S0168-8278(17)32291-2.

454. Pretorius E, Vlok M, Venter C, Bezuidenhout JA, Laubscher GJ, Steenkamp J, et al. Persistent clotting protein pathology in Long COVID/Post-Acute Sequelae of COVID-19 (PASC) is accompanied by increased levels of antiplasmin. Cardiovasc Diabetol. 2021 Aug 23;20(1):172.

455. Baker SR, Halliday G, Ząbczyk M, Alkarithi G, Macrae FL, Undas A, et al. Plasma from patients with pulmonary embolism show aggregates that reduce after anticoagulation. Commun Med (Lond). 2023 Jan 28;3(1):12.

456. Dengu F, Abbas SH, Ebeling G, Nasralla D. Normothermic Machine Perfusion (NMP) of the Liver as a Platform for Therapeutic Interventions during Ex-Vivo Liver Preservation: A Review. J Clin Med. 2020 Apr 7;9(4):1046.

457. Linares-Cervantes I, Kollmann D, Goto T, Echeverri J, Kaths JM, Hamar M, et al. Impact of Different Clinical Perfusates During Normothermic Ex Situ Liver Perfusion on Pig Liver Transplant Outcomes in a DCD Model. Transplant Direct. 2019 Mar 4;5(4):e437.

458. Selzner M, Goldaracena N, Echeverri J, Kaths JM, Linares I, Selzner N, et al. Normothermic ex vivo liver perfusion using steen solution as perfusate for human liver transplantation: First North American results. Liver Transpl. 2016 Nov;22(11):1501–8.

459. Knaak JM, Spetzler VN, Goldaracena N, Boehnert MU, Bazerbachi F, Louis KS, et al. Subnormothermic ex vivo liver perfusion reduces endothelial cell and bile duct injury after donation after cardiac death pig liver transplantation. Liver Transpl. 2014 Nov;20(11):1296–305.

460. Obara H, Morito N, Matsuno N, Yoshikawa R, Nakajo T, Gochi M, et al. Initial perfusate purification during subnormothermic machine perfusion for porcine liver donated after cardiac death. J Artif Organs. 2020 Mar;23(1):62–9.

461. Zeerleder S, Zwart B, Wuillemin WA, Aarden LA, Groeneveld ABJ, Caliezi C, et al. Elevated nucleosome levels in systemic inflammation and sepsis. Crit Care Med. 2003 Jul;31(7):1947–51.

462. Iskender I, Cosgun T, Arni S, Trinkwitz M, Fehlings S, Yamada Y, et al. Cytokine filtration modulates pulmonary metabolism and edema formation during ex vivo lung perfusion. J Heart Lung Transplant. 2017 May 20;S1053-2498(17)31802-8.

463. Ferdinand JR, Hosgood SA, Moore T, Ferro A, Ward CJ, Castro-Dopico T, et al. Cytokine absorption during human kidney perfusion reduces delayed graft function-associated inflammatory gene signature. Am J Transplant. 2021 Jun;21(6):2188–99.

464. Ghaidan H, Stenlo M, Niroomand A, Mittendorfer M, Hirdman G, Gvazava N, et al. Reduction of primary graft dysfunction using cytokine adsorption during organ preservation and after lung transplantation. Nat Commun. 2022 Jul 26;13(1):4173.

465. Karangwa S. Hemostatic system activation and reperfusion injury in liver machine preservation and transplantation of extended criteria donor livers. [Groningen]: University of Groningen; 2021.

466. Feng S. Spontaneous and induced tolerance for liver transplant recipients. Curr Opin Organ Transplant. 2016 Feb;21(1):53–8.

467. Doherty DG. Immunity, tolerance and autoimmunity in the liver: A comprehensive review. J Autoimmun. 2016 Jan;66:60–75.

468. Heymann F, Tacke F. Immunology in the liver--from homeostasis to disease. Nat Rev Gastroenterol Hepatol. 2016 Feb;13(2):88–110.

469. Levitsky J, Feng S. Tolerance in clinical liver transplantation. Hum Immunol. 2018 May;79(5):283–7.

470. Haque O, Raigani S, Rosales I, Carroll C, Coe TM, Baptista S, et al. Thrombolytic Therapy During *ex-vivo* Normothermic Machine Perfusion of Human Livers Reduces Peribiliary Vascular Plexus Injury. Front Surg. 2021 Jan 1;8:644859.

471. Boteon YL, Boteon APCS, Attard J, Mergental H, Mirza DF, Bhogal RH, et al. Ex situ machine perfusion as a tool to recondition steatotic donor livers: Troublesome features of fatty livers and the role of defatting therapies. A systematic review. American Journal of Transplantation. 2018;18(10):2384–99.

472. Lau NS, Ly M, Ewenson K, Toomath S, Ly H, Mestrovic N, et al. Indocyanine green: A novel marker for assessment of graft quality during ex situ normothermic machine perfusion of human livers. Artif Organs. 2024 May;48(5):472–83.

Appendix A: Histological grading of PRI

NEUTROPHILS		HYPEREOSINOPHILIC HEPATOCYTES		NECROSIS
0	NIL	0	NIL	0 nil
1	Very occasional and difficult to find	1	Very occasional	1 minimal (few cells)
2	Readily identifiable – moderate numbers	2	moderate numbers	2 mild (small confluent areas)
3	Extensive	3	extensive	3 mod (circumferential periven)
				4 sev (bridging)

OVERALL GRADE OF PRESERVATION-REPERFUSION INJURY

- Based on small droplet fat, glycogen depletion, neutrophils, hypereosinophilic hepatocytes, hepatocyte necrosis
- Grade and number of the above, max grade of all = severe, mild of one = minimal etc, mild low grade of a couple, moderate intermediate grade of most

0 NIL
1 MINIMAL
2 MILD
3 MILD TO MODERATE
4 MODERATE
5 MODERATE TO SEVERE
6 SEVERE

Appendix B: Sample preparation for LC-MS analysis

Frozen tissue biopsy samples were placed on dry ice. Tissue weight was recorded, and samples (where possible) were cut in half for proteomic analysis and further storage at -80°C for future validation studies, i.e. immunoblotting or Q-PCR.

Tissue samples were placed into 2ml tubes containing zirconia beads and sample lysis was performed using 300 µl RIPA lysis buffer (Pierce™) with phospho-protease inhibitor (Sigma-Aldrich, Dorset, UK) and protease inhibitor (Roche, UK) per 10mg of tissue with subsequent beads-beating homogenisation (Precellys®). Samples were homogenised at 5000Hz (20 sec, 2 cycles) with cooling on dry ice between cycles.

Following tissue homogenisation, samples were centrifuged at 10,000g at 4°C for 5min and supernatant was transferred in new Eppendorf tubes. The BCA assay was used for protein concentration estimation and 50µg of protein per sample were further aliquoted and utilised for reduction, alkylation and SMART digestion. Remaining supernatant was aliquoted and frozen at -80°C for further validation studies.

50µg of protein per sample was adjusted to a final volume of 100µl with 100mM Triethylamonium bicarbonate (TEAB) (Thermo Scientific™). Samples were incubated at 55°C for 1 hour after addition of 5µl of 200mM tris(2-carboxyethyl) phosphine (TCEP) (Sigma-Aldrich, Dorset, UK) for denaturing.

Alkylation was performed using 375mM of Iodoacetamide (IAA) solution. Samples were incubated for 30 min after addition of 5µl of 375mM IAA at room temperature and protected from light. Following incubation, samples were adjusted to 200µl using 90µl of 100mM TEAB prior to the addition of 600µl methanol and 150µl of chloroform. Samples were then vortexed for 30 secs and 450µl of sterile water was added, followed by further vortex for 30 secs and centrifugation at 17,000g for 5 min at room temperature.

The upper aqueous phase was removed without disruption of the precipitate interface. 450µl of methanol was added to the organic phase, vortexed for 30 secs and centrifuged for at 17,000g for 2 min at room temperature. After supernatant removal, the Eppendorf lids was left open to

allow for pellets to dry. Subsequent protein precipitate resuspension was performed using 50µl of 100mM TEAB prior to the use of the SMART Digest ™ Kit.

The SMART digestion tube (Thermo Scientific™) contains 150µl of the SMART digestion buffer (proprietary, containing immobilised trypsin beads). 50µg of protein was added to the SMART digestion tube and incubated on a heat shaker (Eppendorf Themomixer®) at 70°C for 3 hours at 1400 rpm. Following digestion, the tubes were centrifuged for 5 min at 2500g. Resultant supernatant (separated from the beads pellet) and consisting of tryptic peptides was then collected and aliquoted.

Desalting of tryptic peptide digests was performed using the SOLAµ™ Solid Phase Extraction (SPE) Plates (Thermo Scientific™) and a 96-well vacuum manifold. 200µl of 100% acetonitrile (ACN) was added to the SOLAµ™ SPE plates with application of a 96-well vacuum to allow passage of ACN through cartridges (for column conditioning). Cartridge equilibration was performed by addition of 200µl of 0.1% trifluoroacetic acid (TFA, in water) to each well and application of vacuum (the resulting effluent was discarded). Subsequently, digested peptides (200µl) were pipetted onto the plates (without touching of beads) and acidified through addition of 200 µl 1% TFA. Vacuum was applied to enable peptide passage (and binding) to C18 packed in the cartridges, followed by washing with 500µl of 0.1% formic acid (FA) in sterile water to each well and further vacuum application. Collection plates were positioned underneath, and peptides where then eluted through addition of 50µl of 'Buffer B' (65% ACN, 1% FA). The process was repeated using a further 100µl of Buffer B.

Following elution of peptides, samples were dried using a vacuum concentrator (Speed-Vac, Eppendorf). Further sample resuspension was performed with 50µl of 'Buffer A' i.e. 98% MilliQ-H_2O, 2% ACN and 0.1% FA. The resuspended peptide digests were then utilised for mass spectrometry analysis.

A master pool was created by mixing aliquots of all samples to be analysed. High pH fractionation was performed to separate master pool into 100 fractions. Subsequently, 60 fractions (which contained the majority of peptides) were selected to run on the timsTOF Pro in order to create a peptide reference library and a total of 6,185 proteins were identified in such library. During the main sample analysis, 7 samples from the pool were run together with

the 60 master pool fractions and the individual samples to allow for enhanced protein identification in the samples and enable peptide matching between the samples and library.

Shotgun proteomics was performed using ion mobility spectrometry (IMS) with liquid chromatography (LC) and tandem mass spectrometry. All samples were analysed using the timsTOF pro instrument (a time-of-flight mass spectrometer that utilises trapped ion mobility spectrometry) operated in the parallel accumulation-serial fragmentation (PASEF®) scan mode.

Prepared samples were loaded onto Evosep (Evosep, Odense Denmark) tips for timsTOF analyses in PASEF mode as described above.

The LC-MS raw data searches were carried out using MSFragger against the Homo sapiens UniProt database version 2021, which contains 564,918 protein sequences. Trypsin was specified as the protease, and a maximum of two missed cleavages were allowed. The search parameters included carbamidomethylation at cysteine, set as a fixed modification, while oxidation of methionine was set as a variable modification. Proteins identified with only one unique peptide were selected for further analysis. Protein abundance was normalised using the median approach and converted to $\log_2$ for statistical analysis.

Appendix C: The DeFat Study Protocol

Full article accessible via: https://trialsjournal.biomedcentral.com/articles/10.1186/s13063-024-08189-4

STUDY PROTOCOL Open Access

Defatting of donor transplant livers during normothermic perfusion—a randomised clinical trial: study protocol for the DeFat study

Syed Hussain Abbas[1*], Carlo D. L. Ceresa[2], Leanne Hodson[3], David Nasralla[2], Christopher J. E. Watson[4], Hynek Mergental[5,6], Constantin Coussios[7], Fotini Kaloyirou[8], Kerrie Brusby[8], Ana Mora[9], Helen Thomas[10], Daphne Kounali[11], Katie Keen[8], Joerg-Matthias Pollok[2], Rohit Gaurav[4], Satheesh Iype[2], Wayel Jassem[12], M. Thamara PR Perera[5], Abdul Rahman Hakeem[12,13], Simon Knight[1†] and Peter J. Friend[1†]

Abstract

Background Liver disease is the third leading cause of premature death in the UK. Transplantation is the only successful treatment for end-stage liver disease but is limited by a shortage of suitable donor organs. As a result, up to 20% of patients on liver transplant waiting lists die before receiving a transplant. A third of donated livers are not suitable for transplant, often due to steatosis. Hepatic steatosis, which affects 33% of the UK population, is strongly associated with obesity, an increasing problem in the potential donor pool. We have recently tested defatting inter- ventions during normothermic machine perfusion (NMP) in discarded steatotic human livers that were not trans- planted. A combination of therapies including forskolin (NKH477) and L-carnitine to defat liver cells and lipoprotein apheresis filtration were investigated. These interventions resulted in functional improvement during perfusion and reduced the intrahepatocellular triglyceride (IHTG) content. We hypothesise that defatting during NMP will allow more steatotic livers to be transplanted with improved outcomes.

Methods In the proposed multi-centre clinical trial, we will randomly assign 60 livers from donors with a high-risk of hepatic steatosis to either NMP alone or NMP with defatting interventions. We aim to test the safety and feasibil- ity of the defatting intervention and will explore efficacy by comparing ex-situ and post-reperfusion liver function between the groups. The primary endpoint will be the proportion of livers that achieve predefined functional criteria during perfusion which indicate potential suitability for transplantation. These criteria reflect hepatic metabo- lism and injury and include lactate clearance, perfusate pH, glucose metabolism, bile composition, vascular flows and transaminase levels. Clinical secondary endpoints will include proportion of livers transplanted in the two arms, graft function; cell-free DNA (cfDNA) at follow-up visits; patient and graft survival; hospital and ITU stay; evidence of ischemia-reperfusion injury (IRI); non-anastomotic biliary strictures and recurrence of steatosis (determined on MRI at 6 months).

Discussion This study explores ex-situ pharmacological optimisation of steatotic donor livers during NMP. If the inter- vention proves effective, it will allow the safe transplantation of livers that are currently very likely to be discarded, thereby reducing waiting list deaths.

[†]Simon Knight and Peter J. Friend are joint senior authors.

*Correspondence:
Syed Hussain Abbas

Appendix D: Quantifying DNL, Total Fatty Acid Composition and Tissue triglycerides

Prior to commencement of NMP (and whole blood reperfusions for the experimental study) 200 ml of $^{2}H_2O$ (heavy water, deuterium oxide) was added to the perfusate reservoir prior to commencement of perfusion. *In vivo*, deuterium oxide quickly equilibrates with the body water pool, creating a homogenous precursor pool for reactions involving water, such as condensation and hydrolysis. This equilibrium facilitates the investigation of various metabolic processes including hepatic DNL. VLDL triglycerides (TGs) reflect hepatic triglycerides, therefore the incorporation of ^{2}H atoms into VLDL-TG palmitate (originating from intracellular $^{2}H_2O$ or initially incorporated into NADPH or acetyl-CoA) can be used to estimate hepatic DNL. Following lipid extraction using the Folch method, measurement of perfusate and tissue DNL will be performed through the incorporation of deuterium from $^{2}H_2O$ (Finnigan GasBench-II, ThermoFisher Scientific, UK) into perfusate and tissue [2H]-palmitate. The [2H]-palmitate enrichments will be quantified by gas chromatography-mass spectrometry (GC-MS).

Lipid extraction will be performed using the Folch method followed by solute solid phase extraction and methylation. The fatty acid composition will be measured using gas chromatography (GC). Peaks will be identified by comparing retention times with established fatty acid methyl ester standards. Subsequently, the fatty acid compositions (µmol per 100 µmol of total fatty acids (mol%)) will be determined by calculating the area of the corresponding peaks. After determining the fatty acid composition, the total fatty acid concentration (µg/mg of tissue) will be calculated.